Department of
Mineral and Petroleum Resources

RECORD
2001/18

GSWA VINES 1
WELL COMPLETION REPORT
WAIGEN AREA, OFFICER BASIN
WESTERN AUSTRALIA

compiled by S. N. Apak, H. T. Moors
and M. K. Stevens

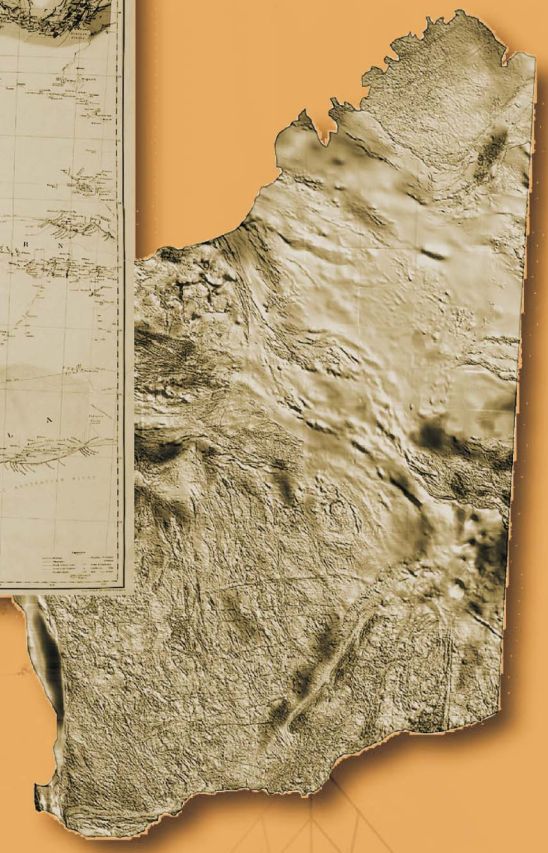

Geological Survey of Western Australia

GEOLOGICAL SURVEY OF WESTERN AUSTRALIA

Record 2001/18

GSWA VINES 1
WELL COMPLETION REPORT
WAIGEN AREA, OFFICER BASIN
WESTERN AUSTRALIA

compiled by
S. N. Apak, H. T. Moors, and M. K. Stevens

with contributions from
K. A. Blundell, K. A. R. Ghori, K. Grey, K. Ooi[1], S. A. Pisarevsky[2], I. Ruddock, J. Sonego[3], and C. Young[3]

[1] Geotechnical Services Pty Ltd (GEOTECH)
[2] Tectonics Special Research Centre, University of Western Australia
[3] PGA Consultants Pty Ltd

Perth 2002

MINISTER FOR STATE DEVELOPMENT
Hon. Clive Brown MLA

DIRECTOR GENERAL
DEPARTMENT OF MINERAL AND PETROLEUM RESOURCES
Jim Limerick

DIRECTOR, GEOLOGICAL SURVEY OF WESTERN AUSTRALIA
Tim Griffin

REFERENCE
The recommended reference for this publication is:
APAK, S. N., MOORS, H. T., and STEVENS, M. K., (compilers), 2002, GSWA Vines 1 well completion report, Waigen area, Officer Basin, Western Australia: Western Australia Geological Survey, Record 2001/18, 32p.

National Library of Australia Card Number and ISBN 0 7307 5715 3

Grid references in this publication refer to the Geocentric Datum of Australia 1994 (GDA94), except on Plate 1, which refers to the Australian Geodetic Datum 1984 (AGD84). Locations mentioned in the text are referenced using Map Grid Australia (MGA) coordinates, Zone 52. All locations are quoted to at least the nearest 100 m.

Published 2002 by Geological Survey of Western Australia

Copies available from:
Information Centre
Department of Mineral and Petroleum Resources
100 Plain Street
EAST PERTH, WESTERN AUSTRALIA 6004
Telephone: (08) 9222 3459 Facsimile: (08) 9222 3444
This and other publications of the Geological Survey of Western Australia are available online through the Department's bookshop at www.mpr.wa.gov.au

Contents

Abstract 1
Introduction 1
Drillhole history 2
General data Vines 1 2
Drilling data Vines 1 4
Logging Vines 1 4
Regional setting 5
Local geology 5
Drillhole geology 8
Stratigraphy 8
Geochronology 8
Palynology 8
Zircon U–Pb dating 11
Palaeomagnetism 12
Petrography 12
Cainozoic 12
?Neoproterozoic to ?Cambrian Vines Formation 13
Unit 6 — 4 to 124.7 m 13
Unit 5 — 124.7 to 301.5 m 13
Unit 4 — 301.5 to 779.2 m 13
Unit 3 — 779.2 to 1228.5 m 15
Unit 2 — 1228.5 to 1632 m 17
Unit 1 — 1632 to 2017.5 m TD 18
Possible correlations 19
Summary 20
Petroleum geology 20
Hydrocarbon shows 21
Source potential and maturity 21
Reservoir character 22
Unit 6 — 4 to 124.7 m 22
Unit 5 — 124.7 to 301.5 m 22
Unit 4 — 301.5 to 779.2 m 22
Unit 3 — 779.2 to 1228.5 m 23
Unit 2 — 1228.5 to 1632 m 23
Unit 1 — 1632 to 2017.5 m TD 23
Summary 23
Seal potential 24
Petrology 24
Facies 24
Provenance 25
Sedimentary provenance 25
Igneous provenance 25
Burial history 26
Anhydrite 26
Barite 26
Mineral potential 27
Contributions to geological knowledge 27
References 30

Appendices

List of Appendices 31
1. Operations report VinesApp1.pdf
2. Vines 1 and Empress 1A thin-section descriptions VinesApp2.pdf
3. Palynology of samples from Vines 1 ..... VinesApp3.pdf
4. Palaeomagnetic study of Vines 1 ..... VinesApp4.pdf
5. Gravity modelling of the Waigen area VinesApp5.pdf
6. Post-petrographic SEM and XRD reports for Vines 1 ..... VinesApp6.pdf
7. Petroleum geochemistry VinesApp7.pdf
8. Log analysis VinesApp8.pdf
9. Routine core analysis VinesApp9.pdf

10. Seal capacity study VinesApp10.pdf
11. Chemical analysis of drillcore from Vines 1 to assess potential for base metals VinesApp11.pdf
12. Well index sheet VinesApp12.pdf

Plates

1. Composite well log VinesPlate1.pdf

Figures

1. Location of petroleum wells and stratigraphic drillholes, Officer Basin 3
2. Major structural elements of the Officer Basin 6
3. Generalized stratigraphy of the Officer Basin 7
4. Vines 1 stratigraphy 9
5. Geological map showing Neoproterozoic and Orodovician outcrops and location of Vines 1 10

GSWA Vines 1 well completion report, Waigen area, Officer Basin, Western Australia

compiled by
S. N. Apak, H. T. Moors, and M. K. Stevens

with contributions from
K. A. Blundell, K. A. R. Ghori, K. Grey, K. Ooi[1], S. A. Pisarevsky[2], I. Ruddock, J. Sonego[3], and C. Young[3]

Abstract

Vines 1 is a vertical stratigraphic drillhole located in the Waigen area of the Officer Basin in Western Australia. It is the first stratigraphic drillhole to be drilled in the Waigen area, and was designed to reveal the stratigraphy and define the petroleum source potential of the Neoproterozoic rocks in this part of the Officer Basin. Vines 1 was continuously cored from 44.5 to 2017.5 m total depth.

Six lithostratigraphic units were intersected (Units 1–6), herein called the Vines Formation. The formation is dominated by sandstone, diamictite, argillaceous siltstone, and claystone, and is characterized mainly by turbidite- and debris flow-dominated successions that were probably deposited on a basin-slope and basin-plain setting. Deposition was essentially continuous, and although several disconformities are present they are not considered to mark significant hiatuses.

All core samples selected for TOC and Rock-Eval analyses have poor oil- and gas-generating potential. Nevertheless, the detection of a drilling-mud gas-show at 1482 m indicates that there is a mature source rock in the region. Sandstones below 1228 m (Unit 1 and Unit 2) have very poor reservoir potential, whereas sandstones between 1228 m and 363 m (Unit 3 and lower part of Unit 4) have fair to poor reservoir potential, and sandstones above 363 m (upper part of Unit 4, Unit 5, and Unit 6) have excellent reservoir potential. Fine-grained diamictites and mudstones have excellent sealing qualities.

The age of the Vines Formation is uncertain. Most palynomorphs recovered from Vines 1 are of mid-Neoproterozoic to earliest Cambrian age and are considered to be reworked, thus implying the succession has a maximum age of latest Neoproterozoic to earliest Cambrian. Palynomorphs of Devonian to Recent age are attributed to contamination. Palaeomagnetic results from oriented drillcore are consistent with a late Neoproterozoic (post c. 600 Ma) to Cambrian age.

KEYWORDS: petroleum potential, stratigraphy, drill hole data, well logs, diamond drilling, source beds, reservoir data, diamictite, turbidite, glacial sediments, Officer Basin

Introduction

The Geological Survey of Western Australia's (GSWA) vertical stratigraphic diamond drillhole Vines 1 is the first drillhole to be drilled in the northwestern margin of the Waigen area of the Officer Basin. The basin was previously divided into sub-basins (e.g. Lennis Sub-basin) that were defined predominantly by potential-field data (Phillips et al., 1985). However, seismic data show that the Officer Basin succession has a mostly

[1] Geotechnical Services Pty Ltd (GEOTECH)
[2] Tectonics Special Research Centre, University of Western Australia
[3] PGA Consultants Pty Ltd

uniform thickness, which gradually thins towards the basin margins. The gravity lows, previously interpreted as sub-basins, actually consist of thicker sedimentary successions that include strata of the underlying pre-Officer Basin, the overlying Gunbarrel Basin, and the Officer Basin. There is no evidence within the Neoproterozoic strata to separate the Waigen area from the rest of the Officer Basin. For this reason, we now refer to the sub-basins as 'areas'.

Vines 1 was drilled as part of GSWA's program to study the petroleum potential of Western Australia's onshore sedimentary basins. The location was chosen to investigate the stratigraphy and to test the petroleum potential of the Neoproterozoic sequences within the Waigen area of the Officer Basin. It was predicted the drillhole would intersect the Neoproterozoic Browne Formation around 1200 m below ground level.

The location of Vines 1 was chosen primarily using existing gravity data and, to a lesser extent, regional aeromagnetic data and surface outcrops. The nearest seismic grid is in the Lennis area, approximately 120 km to the west. The gravity and aeromagnetic data indicate a northwesterly trending structural grain. Vines 1 was drilled on an interpreted structurally simple block, away from faulting.

Vines 1 is located on the COOPER* and VINES (1:100 000) map sheets at latitude 26°42'05"S, longitude 128°15'08"E, approximately 100 km south of the Blackstone Community via the Great South Road (Fig. 1). The well was cored from 44.5 m to the total depth (TD) of 2017.5 m. Flammable gas was registered by hot-wire detector in the drilling mud at 1482 m. The only other evidence for liquid or solid hydrocarbons was at 285 m depth, where a thin section is described as having possible bitumen. A solvent extraction of core at this depth recovered trace hydrocarbons.

Regolith is present between 0 and 4 m. Below this, the drilled section is divided into six lithostratigraphic units: Unit 6 (4 – 124.7 m), Unit 5 (124.7 – 301.5 m), Unit 4 (301.5 – 779.2 m), Unit 3 (779.2 – 1228.5 m), Unit 2 (1228.5 – 1632 m), and Unit 1 (1632 – 2017.5 m). These units are composed of sandstone, diamictite, siltstone, shale, mudstone, and conglomerate, with rare thin carbonate and evaporitic rocks.

The following information related to Vines 1 has been placed in the GSWA statutory petroleum exploration files under reference number S20623: wireline logs at 1:200 and 1:500 scales, porosity and permeability reports, 1:100-scale logging sheets, core photographs, daily drilling reports, petrography report, and a sample list.

The core depths cited within this Record are, unless otherwise specified, those reported by the drillers as modified by the wellsite geologist (core depths). In the composite log (Plate 1), core descriptions are consistent with these core depths; however, all other data including lithologies and analyses have been adjusted to match the wireline log depth.

Drillhole history

General data Vines 1

Location:	Latitude 26°42'04.87"S, Longitude 128°15'07.72"E MGA 425605E, 7046424N (from differential GPS)
Derivation of name:	VINES (1:100 000)
Total depth:	2017.5 m
Date spudded:	4 July 1999

* Capitalized names refer to standard 1:250 000 map sheets unless otherwise indicated

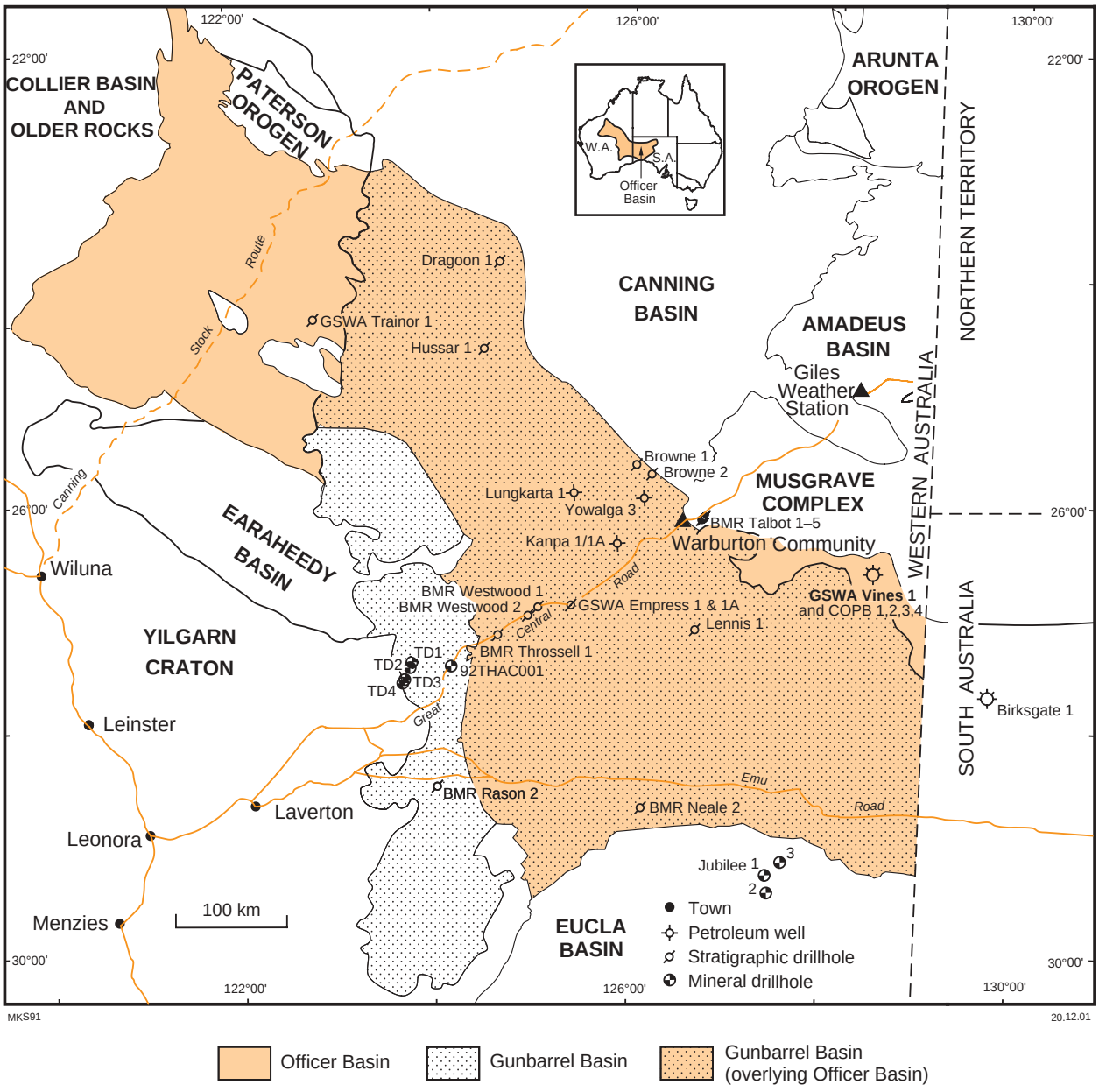

Figure 1. Location of petroleum wells and stratigraphic drillholes in the Officer Basin

Reached 1741.5 m:	17 August 1999
Attempted logging of hole:	19 to 20 August 1999
Commenced NQ drilling:	21 August 1999
Reached TD:	28 August 1999
Logging of hole:	31 August to 2 September 1999
Date completed:	8 September 1999
Elevation:	472 m AHD (from differential GPS)
Status:	Gas show; plugged and abandoned

Drilling data Vines 1

Drilling contractor:	Drillcorp Western Deephole Drilling, 42 Paramount Drive, Wangara, W.A. 6065	
Rig:	UDR 1500 (Rig no. 82)	
Hole size:	0 – 44.5 m	209.5 mm with 177.8 mm casing
	44.5 – 625 m	122.6 mm with PF casing (PQ coring)
	625 – 1741.5 m	96.1 mm with HQ rods as temporary casing (HQ coring)
	1741.5 – 2017.5 m TD	75.7 mm (NQ coring)
Core recovery:	PQ 44.5 – 625 m	(99.7% recovery)
	HQ 625 – 1741.5 m	(100% recovery)
	NQ 1741.5 – 2017.5 m TD	(100% recovery)
Hole deviation:	Maximum of 1° from vertical (Appendix 1; Table 1.2)	

Logging Vines 1

Wireline logs were acquired after the drillhole reached 2017.5 m TD.

Logging contractor:	Reeves Wireline Services, 47 Felspar Street, Welshpool, W.A. 6106	
Logs run:	Dual laterolog, compensated sonic, SP, gamma ray, caliper	625–2018 m
	Density, compensated neutron, gamma ray, caliper	0–2018 m
	Dipmeter, gamma ray, caliper	625–2011 m
	Cement bond, gamma ray	0–620 m

The wireline logs are of very good quality and the hole is virtually within gauge from the casing shoe at 625 m down to 2017.5 m TD. A possible hole washout or open fracture, which has not been recorded by the caliper log, is present at 907 m log depth. Probable zones of mud on one of the dipmeter pads or in possible open fractures are present at 1318 m, 1463 m, 1582 m, and 1734–1740 m log depth (Plate 1). The 1734–1740 m log depth zone, where high dips are calculated, is almost certainly caused by mud on a dipmeter pad, as this is where the hole changes from NQ to HQ size. The depth matching of core to logs is considered good, and where tie points could be established the match was within 0–2 m (Appendix 1).

Regional setting

The Neoproterozoic to Phanerozoic Officer Basin extends for 1500 km from the southeastern flank of the Pilbara Craton in Western Australia, to the central west of South Australia (Fig. 1; Jackson and van de Graaff, 1981; Perincek, 1998). The part of the basin that lies within Western Australia is referred to as the western Officer Basin and in most areas is overlain by a younger depositional succession, the Gunbarrel Basin (Hocking, 1994), which was previously included in the Officer Basin. The Table Hill Volcanics are the lowest part of the Gunbarrel Basin, and are overlain by Palaeozoic and Mesozoic rocks (Hocking, 1994).

The western Officer Basin is dominated by northwest-oriented structural trends. Its largely fault-bounded northern margin is defined by Palaeoproterozoic and Mesoproterozoic igneous and metamorphic rocks of the Musgrave and Rudall Complexes, and by the Anketell–Warri Gravity Ridge (Fig. 2). The western and southern margins of the western Officer Basin are defined as being where Neoproterozoic to Cambrian successions of the Officer Basin have been removed or not deposited (e.g. Kingston Shelf). The adjacent older tectonic units include the Yilgarn and Pilbara Cratons, Albany–Fraser Orogen, and the Earaheedy and Collier and Edmund Basins. The Cainozoic strata of the Eucla Basin conceal parts of the Officer Basin's southern margin.

A detailed account of the palaeogeography and tectonic settings of Neoproterozoic strata throughout Australia can be found in Walter and Veevers (1997) and Walter (2000). Generalized stratigraphy is shown in Figure 3.

Local geology

Cainozoic sediments cover about 75% of the land surface on COOPER. Exposures of bedrock are sparse because of the extensive laterite, colluvium, and aeolian sand cover. Outcrops in the northern part of the map sheet are mostly Mesoproterozoic magmatic and volcanic rocks, which form extensive ranges and hills (Daniels, 1971; Jackson and van de Graaff, 1981). In the central part of the map sheet, scattered large to small outcrops of presumed Neoproterozoic strata are also present. The remaining slightly undulating area to the south consists of scattered outcrops of Early Permian Paterson Formation, and rare outcrops of Table Hill Volcanics and Mesoproterozoic rocks. Potassium–argon dating of the Table Hill Volcanics in Empress 1/1A, which was drilled in the Yowalga area, gave an Early Ordovician age of 484 ± 4 Ma (Stevens and Apak, 1999).

The regional structural features in the area are open west-northwesterly trending anticlines and synclines. Faults are predominantly northeast- and northwest-oriented.

With the exception of three mineral drillholes, Jubilee 1, Jubilee 2, and Jubilee 3, drilled by CRA Exploration in the south of the Waigen area, there was no subsurface control relevant to siting Vines 1. Four waterbores, COPB 1, COPB 2, COPB 3, and COPB 4, were drilled in the vicinity of Vines 1; water was found in COPB 2 (TD 144 m) at the Vines 1 wellsite, COPB 3 (TD 150 m), and COPB 4 (TD 60 m). The nearest petroleum exploration wells (Fig. 1) are Lennis 1 (200 km west-southwest), Kanpa 1A (255 km west), Yowalga 3 (285 km west-northwest), and Birksgate 1 (206 km southeast in South Australia).

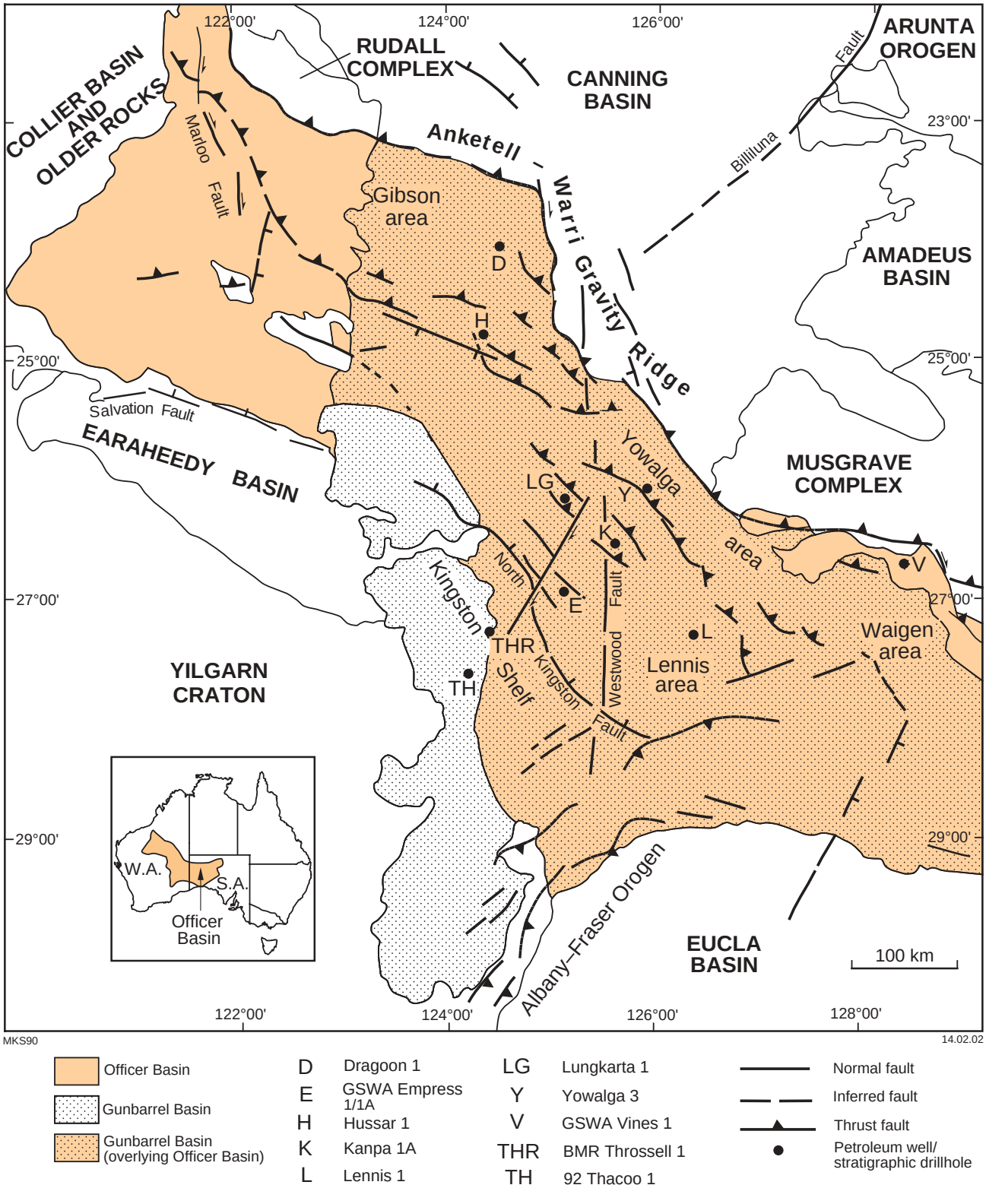

Figure 2. Major structural elements of the Officer Basin and selected wells and drillholes (modified from Perincek, 1996)

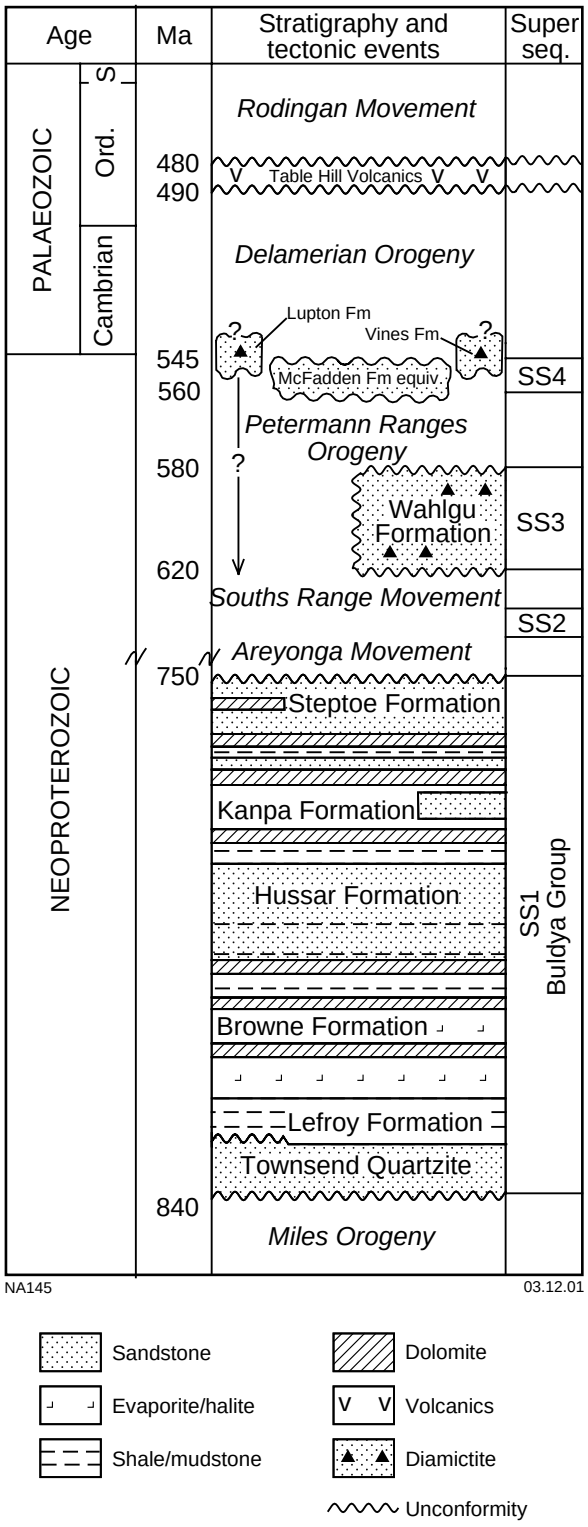

Figure 3. Generalized stratigraphy of the Officer Basin (after Apak and Moors, 2000)

Drillhole geology

Stratigraphy

Vines 1 was spudded in Cainozoic sand and calcrete and intersected the following lithological units: Unit 6 (4 – 124.7 m), Unit 5 (124.7 – 301.5 m), Unit 4 (301.5 – 779.2 m), Unit 3 (779.2 – 1228.5 m), Unit 2 (1228.5 – 1632 m), and Unit 1 (1632 – 2017.5 m TD). These six units are herein referred to as the Vines Formation as no firm correlations can be established with existing lithostratigraphic units in the Officer Basin. The Vines Formation will be formally defined in Grey et al. (in prep.).

A composite log of Vines 1 is presented in Plate 1 and summarized in Figure 4. The age of the Vines Formation is poorly constrained (other than a probable maximum age of latest Neoproterozoic to earliest Cambrian) because of poor biostratigraphic control, the lack of similarity to nearby dated rocks, and the lack of seismic correlation to better dated successions in nearby wells. The following descriptions of the lithological units are derived from cuttings descriptions (0 to 45.5 m) and core logging (45.5 to 2017.5 m). A summary of the petrography of porosity core-plugs and other samples by PGA Consultants Pty Ltd is presented in Appendix 2. Alternatively, a hard-copy version may be viewed in the Department of Minerals and Petroleum Resources library (GSWA statutory petroleum exploration report file, S20623).

Geochronology

Vines 1 is located south of outcropping Neoproterozoic Supersequence 1 strata (Walter et al., 1994), which contains stromatolites identified by K. Grey (GSWA, 2001, written comm.) as *Basisphaera irregularis* and *Baicalia burra*, and north of the Early Ordovician Table Hill Volcanics (Fig. 5). The Officer Basin strata dip regionally to the south and in Vines 1 the average dip is 5° to the south-southwest. Thus, a simplistic interpretation of the controls on age of the Vines Formation is that it is probably younger than the Supersequence 1 (c. 800 Ma) strata to the north, but older than the Table Hill Volcanics. A few stromatolites are present within clasts in the drillcore, but they are too recrystallized to be identifiable and hence do not provide any age constraints.

Palynology

Sixty-two core samples from Vines 1 were submitted for palynological preparation. Regional implications discussed in this section are based on palynology by K. Grey (Appendix 3). The age of the Vines Formation is interpreted to be younger than latest Proterozoic or earliest Cambrian; however, this age remains uncertain because none of the palynomorphs are considered to be in situ. There is extensive reworking and redeposition of older palynomorphs and probable contamination by modern pollen and plant debris. Preservation of recognizable palynomorphs is poor throughout the drillhole. In particular, nearly all specimens recovered above 1632 m are highly fragmented and commonly badly corroded. Those below 1632 m are slightly better preserved and more common, but are also fragmented and corroded.

Four palynological components are recognized, each ranging throughout the drillhole, although several samples are barren.

Component 1 consists of airborne contaminants, dominated by extant pollen grains such as *Pinus*. The thermal maturity of this component is lower than would be expected for pollen grains that are in situ.

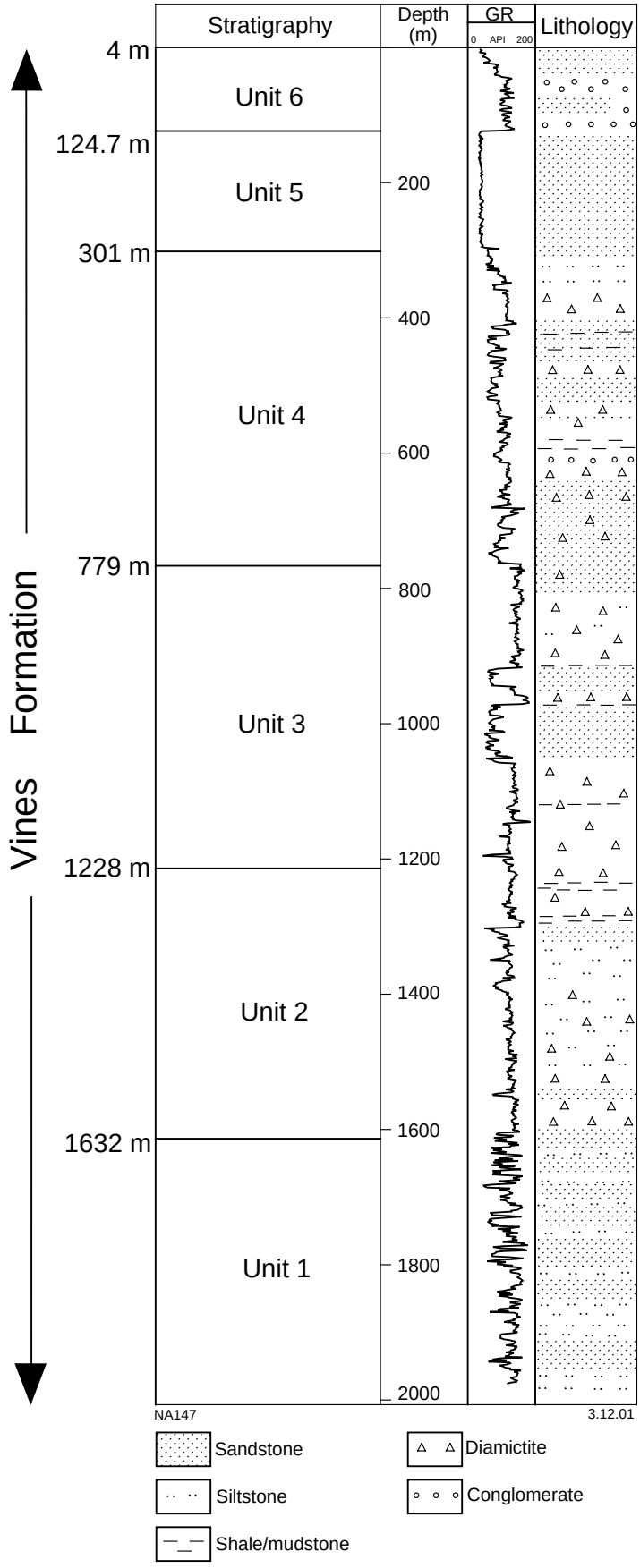

Figure 4. Vines 1 stratigraphy (for lithological description see Plate 1)

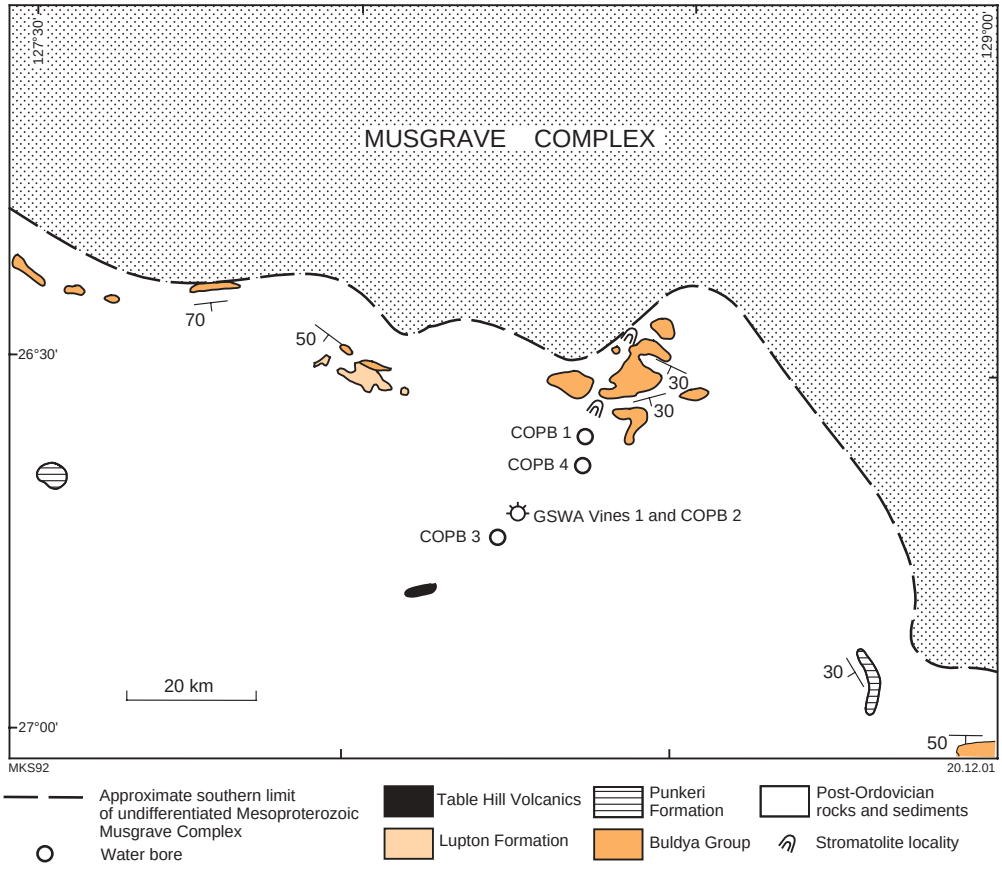

Figure 5. Geological map (Cooper) showing Neoproterozoic and Ordovician outcrops and location of Vines 1 (after Daniels, 1971)

Component 2 comprises plant fragments that also show a low thermal maturity inconsistent with drillhole depth. They may also be airborne contaminants or may have been introduced in the drilling mud. A Devonian age or younger, based on the presence of Component 2, is possible for the Vines Formation, but very unlikely.

Component 3 consists of acritarchs of uncertain age. They are lighter in colour than those unequivocally assigned to Component 4, and have more highly developed excystment structures, indicating that they are probably latest Proterozoic to earliest Cambrian in age. From their taphonomy and preservation, most specimens have been subjected to extensive reworking. They are present throughout the drillhole, except in barren or poorly preserved samples. It is unclear whether the Component 3 acritarchs have been reworked from consolidated or unconsolidated sediments, but their range throughout Vines 1 indicates they are redeposited.

The Component 3 assemblage has been noted (but not described) from the western and eastern Officer Basin and the Georgina Basin (Cotter, 1997, 1999; Gravestock et al., 1997; Grey, 1998; Grey and Cotter, 1996). This assemblage is present in the Narana Formation of the eastern Officer Basin and in the Elkera and Central Mount Stuart Formations of the Georgina Basin. The Mount Stuart Formation contains Ediacara fossils and is therefore latest Neoproterozoic in age. Consequently, the Component 3 assemblage in Vines 1 suggests deposition later than c. 565 Ma based on the estimated age of the Ediacara fossils (Walter et al., 2000).

Only a maximum age can be suggested from the palynomorphs because they are apparently all reworked. However, other limitations suggest an age not much younger than earliest Cambrian. Cambrian and younger successions in drillholes in the eastern Officer Basin commonly contain fossils such as trilobite fragments, sponge spicules, archaeocyathids, and distinctive acritarch species (Gravestock et al., 1997). None of these have been observed in Vines 1, even in the finer grained lithologies near the bottom of the hole that are comparable in lithology to Cambrian or younger rocks in the eastern Officer Basin. In addition, there is no convincing evidence of bioturbation, even in rocks that would normally show such signs in the Phanerozoic. Neither of these points provides conclusive evidence for the age of the Vines 1 succession, but they provide circumstantial evidence for a latest Neoproterozoic to earliest Cambrian age. It should be noted that worldwide, strata containing Component 3 palynomorphs are rare and poorly documented, both taxonomically and stratigraphically.

Component 4 includes palynomorphs diagnostic of a mid-Neoproterozoic age (mid–late Cryogenian, c. 750 to 700 Ma). Component 4 is present in several wells in the Officer Basin in rocks of youngest Supersequence 1 age (Hussar, Kanpa, and Steptoe Formations; Hill et al., 2000), and is documented globally. Specimens are present throughout Vines 1, and, as with Component 3, many samples are fragmented and degraded, indicating extensive reworking. This implies that most of the Vines 1 succession was derived from rocks of mid-Cryogenian age, or younger.

In conclusion, Components 1 and 2 are interpreted as contaminants and have not been taken into consideration in determining the age of the samples. Organic material from Components 3 and 4 has been reworked, based on its severe fragmentation, the presence of fragmented palynomorphs in petrological sections, and poor preservation as a result of corrosion. There is a difference in the quality of preservation, however, between the two assemblages; the older assemblage (Component 4) is very badly corroded, whereas the younger assemblage is less damaged. This may indicate that the older specimens were derived from lithified rocks, whereas the younger specimens may have been derived from unconsolidated sediment.

Many palynomorphs were derived from rocks of the middle Hussar Formation or younger, indicating that mid-Cryogenian to late Cryogenian rocks were exposed and being reworked at the time of Vines Formation deposition. A younger suite of rocks or unconsolidated sediments, probably of latest Proterozoic to earliest Cambrian age, was also exposed at the time of deposition and contributed the Component 3 palynomorphs. Consequently, the Vines 1 succession postdates the youngest Component 3 rocks and is therefore inferred to be latest Neoproterozoic to earliest Cambrian age or younger.

Zircon U–Pb dating

Two samples have been processed to concentrate sedimentary zircon grains for isotopic dating. The first sample (1711.28 – 1713.0 m) is a fine- to coarse-grained sandstone from Unit 1. The second sample (307.84 – 309.29 m) is a medium- to very coarse grained sandstone from Unit 4. Suitable detrital zircon grains were dated by the U–Pb method using a Sensitive High-Resolution Ion Microprobe (SHRIMP). Final results will be reported in Nelson (in prep.) and are summarized below.

GSWA 154880, 1711.3 – 1713.0 m

Twenty-seven analyses were obtained from 27 zircons. Most analyses are concordant or only slightly discordant and indicate a range of $^{207}Pb/^{206}Pb$ dates between c. 950 and 2500 Ma.

The weighted mean $^{206}Pb/^{238}U$ and $^{207}Pb/^{206}Pb$ dates of 973 ± 21 Ma and 1000 ± 80 Ma, respectively, indicated by the six analyses of Group 1, are interpreted as providing maximum times for deposition of the sandstone. Grain 3 is a rounded, elongate, and structureless grain with pitted and abraded terminations. The $^{206}Pb/^{238}U$ date of 915 ± 13 Ma obtained for this grain provides a tentative lower maximum time for host sediment deposition. Source rocks within the western part of Australia having ages matching many of those obtained for the zircons within this sample include the Musgrave Complex and the Albany–Fraser Orogen.

GSWA 154881, 307.8 – 309.3 m

Thirty analyses were obtained from 30 zircons. Most analyses are concordant or only slightly discordant and indicate a range of $^{207}Pb/^{206}Pb$ dates between c. 650 and 1700 Ma.

Grain 8 is an irregular and structureless fragment and part of its surface is rounded and pitted. Grain 23 is a clear, structureless, and euhedral grain with abundant fluid inclusions. The weighted mean $^{206}Pb/^{238}U$ date of 658 ± 8 Ma indicated by the analyses from grains 8 and 23 are interpreted as providing a maximum time for deposition of the sandstone. Source rocks within the western part of Australia having ages matching those of many of the zircons within this sample include the Musgrave Complex and the Albany–Fraser Orogen.

Palaeomagnetism

Core samples between 748 and 2015 m in Vines 1 have been oriented by comparing the dips interpreted from the three-arm dipmeter log with bedding dips visible in the core. A mean palaeomagnetic pole for these rocks is 49.3° latitude and 159.4° ± 14.3 longitude, with the semi-angle of the 95% cone of confidence of 11° (Appendix 4), which is consistent with Australian palaeomagnetic poles from the late Neoproterozoic to Cambrian. This is also consistent with the latest Neoproterozoic to earliest Cambrian maximum age limit inferred by palynological evidence, and therefore suggests that the Vines Formation was deposited during this period.

Petrography

Thin-section petrography by Sonego and Young (Appendix 2) is summarized in **Reservoir character** and **Petrology**. Their descriptions of possible burrows, bioturbation, and phosphate bone fragments have obvious age implications; however, we consider that the apparent bioturbation is soft-sediment deformation, and that there is no firm evidence for biological activity. In particular, we interpret the 'burrow' described from 930 m as a sedimentary clast. Unequivocal evidence of bioturbation has not been found elsewhere in the core.

In summary, no evidence for biological activity or fossils other than palynomorphs is present in the drillcore. Thus, a latest Neoproterozoic to Early Cambrian age remains the preferred interpretation for the Vines Formation.

Cainozoic

The uppermost interval (0–4 m) consists of red, medium- to coarse-grained sandstone and sand (50%), and white calcrete (50%). It is clearly a secondary soil profile, as scattered clasts on the present-day surface are similar to those encountered below this profile.

?Neoproterozoic to ?Cambrian Vines Formation

Unit 6 — 4 to 124.7 m

This unit consists predominantly of sandstone and conglomerate, with minor claystone, siltstone, and limonite. It can be subdivided into the following six intervals:

4–13 m	sandstone (60%), limonite (30%), and siltstone (10%)
13–24 m	dominantly red, fine- to coarse-grained, well-rounded sandstone
24–35 m	dominantly gravel (in the upper half) and sandstone (in the lower half)
35 – 58.9 m	mainly conglomerate and sandstone. Between 39 and 45.5 m there is a coarsening-upward cycle with similar lithologies to those from the overlying unit (24–35 m). Diamond coring commenced in this interval at 44.5 m
58.9 – 65.7 m	coarsening-upward sandstone, grading to conglomerate. The basal 1 m consists of interbedded claystone and sandstone
65.7 – 124.7 m	mainly conglomerate and fine- to coarse-grained sandstone.

The depositional environment of Unit 6 is interpreted as submarine mass-flows. Many of the conglomerates are matrix-supported and could also be described as sandy diamictites. Diamictite is here used as a fabric term for a lithology comprising matrix-supported clasts, in which the clasts and matrix have a large grain-size range. They commonly show vertical fining- or coarsening-upward cycles, imbrication, and cross-bedding. Beds of sandstone and rare thin claystone represent lower energy deposition between higher energy mass-flow events. The matrix of the conglomerates is similar to the clean sandstone intervals between the conglomerates. Below 44.5 m, bedding dips in core are subhorizontal.

Unit 5 — 124.7 to 301.5 m

This unit consists predominantly of sandstone, with minor conglomerate and claystone/argillaceous siltstone. It is transitional into the underlying unit, clearly seen on the gamma-ray log (Plate 1), but for convenience the contact is placed at a sharp-based pebbly sandstone at 301.5 m. Alternatively, the base could be placed at 364 m or 335 m.

The sandstone is red, medium grained, well sorted, with rounded grains and mostly excellent porosity. It is typically massive, but in places shows decimetre- to centimetre-scale cross-bed sets and horizontal lamination.

Because this unit lies between two interpreted submarine mass-flow units (Unit 6 and Unit 4), with no indications of major bathymetric change, a similar depositional environment is proposed. The grain size and fabric is uniform throughout, and the unit shows no indications of change in water depth (energy) that would be expected in a shoreface succession. This uniformity and the absence of erosional contacts also mitigates against a fluvial depositional regime.

The lithological difference between Unit 5 and the underlying Unit 4 is interpreted as a change in the configuration of the basin or a change to a quartz-sand dominated provenance, such as a major fluvial system.

Unit 4 — 301.5 to 779.2 m

Diamictite deposits, interspersed with sand-rich zones and thinner zones of distal turbidites, dominate this unit. The most obvious difference between these diamictites and those below (Unit 3) is the presence of a variety of igneous clasts, reflecting a change in provenance and the unroofing of an igneous complex in the hinterland. The unit comprises numerous sedimentary cycles; each one is at least 10 m thick and commences with a sand-rich zone followed by diamictite. Such cycles are attributed to the changing geometry of the basin as it fills with sediments, or to channel avulsion.

Sand-rich zones may reflect a more distal, deeper position in the basin that, as the basin filled, was displaced by a more proximal slope position and resulting diamictite deposition.

The unit can be subdivided into six lithological intervals, as described below:

301.5 – 362.6 m: predominantly red, fine- to medium-grained, mostly well-rounded and well-sorted sandstone, with lesser conglomerate and rhythmites (here interpreted as distal overbank turbidites). The sandstone is poorly bedded, but in part shows bedding and slumping with dips up to 70°. In particular, between 346.3 and 362.6 m, rhythmites display abundant synsedimentary faulting and slumping, indicative of deposition on a basin slope. Dips of unslumped bedding are typically subhorizontal.

362.6 – 401.8 m: brown diamictite with few clasts and a very argillaceous matrix. Clasts are typically about 2 cm in size and less commonly up to 5 cm. The matrix is more argillaceous than in the lithologies described as conglomerates above 124.7 m. The diamictite contains minor sandstone and argillaceous siltstone horizons.

401.8 – 477.2 m: predominantly sandstone interbedded with lesser diamictite and argillaceous siltstone. The upper part of this interval consists of turbidites that show common slumping and synsedimentary faulting. The sandstone is also disrupted and contorted in parts, interpreted as syndepositional slumping of mass-flow deposits on an unstable slope. Between 362.6 and 477.2 m several coarsening- and fining-upwards cycles are present.

477.2 – 530.3 m: sandstone interbedded with argillaceous diamictite (477.2 – 496 m) and sandy diamictite and diamictite (496 – 530.3 m). The diamictite is grey, mostly massive, and contains a large range of sedimentary and igneous clast types. The sandstone is grey, typically fine grained, and has a fining-upward character. Due to the presence of a clay matrix, these intervals have poor porosity. The sandy diamictite is brown and consists of similar clast types to those in the diamictites above. Some primary porosity, now filled by calcite cement, is present. Based on the gamma-ray log character, the sandstone intervals comprise composites of 1 to 2 m-thick fining-upward beds. Together, the composite cycles show a larger scale fining-upward nature.

530.3 – 619.5 m: argillaceous diamictite in the upper part and sandy diamictite at the base. The upper part (530.3 – 578.7 m) comprises mainly brown and brownish grey diamictite interbedded with minor sandstone and turbiditic argillaceous siltstone. The upper contact of the diamictite is gradational within the overlying sandstone. Clast types within the diamictite vary, but sedimentary rock fragments, in particular dolomites, are common. Some pebbles show facets and striations attributed to glacial action. Sandstone interbedded with the diamictite is brown, fine grained, and massive, and sandstone intervals have an eroded top but a gradational base. The gamma-ray log shows the upper part of this interval to be fairly uniform in grain size, and the lower portion to have scattered fining-upward cycles, each 2 to 3 m thick.

The lower part of this interval (578.7 – 619.5 m) comprises an upper section of claystone with interbedded diamictite, above a lower section of conglomerate or sandy diamictite, and sandstone. The claystone is grey, very silty, and shows soft-sediment deformation with local strong internal contortion. It also contains thin diamictite zones that dip steeply up to 60°, and a sandstone horizon. The diamictite is grey, massive, and has a high clast content.

The lower section is dominated by grey, clast-supported conglomerate containing a sandstone interval at 605.6 to 619.5 m. The sandstone is grey, mainly fine grained, moderately sorted, and grades into underlying conglomerate at the base. It contains ripple structures and flat rip-up clasts at 609.5 m.

619.5 – 779.2 m: predominantly diamictite and sandstone. The upper part (619.5 – 688.8 m) consists of predominantly diamictite, interbedded with minor sandstone and claystone. The diamictite is brown and grey and has a moderate clast content. It contains a large variety of clast types, including igneous, metamorphic, and sedimentary (e.g. dolomite, oolitic dolomite) lithologies. The presence of pyrite within this interval indicates a reducing depositional environment. This is the highest recognized occurrence of pyrite in Vines 1, with the exception of a nodule at 130 m. The sandstone is grey, massive, and has undergone soft-sediment deformation and synsedimentary faulting. Although dipmeter data start at 625 m, dips are scarce in this part of the interval. The best estimate of regional dip is 4–8° towards the south.

The lower part of this interval (688.8 – 779.2 m) is predominantly sandstone. In the upper section, sandstone is interbedded with diamictite and minor conglomerate. The sandstone is grey, in places brown, dominantly fine grained and moderately sorted. It displays soft-sediment deformation, locally strongly contorted slumping with dips of up to 80°, fractures, and local erosive surfaces. On the gamma-ray log, the thin sandstones are stacked in units 15 to 20 m thick, with a typically fining-upwards character. The diamictitic horizons are grey and mostly massive.

On the dipmeter log the sandstone shows cross-bedding with dips of 0–28° towards 250° and 10–20° towards 240°. Two thick sandstone units show slumping (710–720 m, 765–775 m) down a low relief depositional lobe toward 125° and 165°, whereas the upper portion of the sandstone shows additional dips towards 240°.

Unit 3 — 779.2 to 1228.5 m

Unit 3 can be divided into four lithological intervals, as described below:

779.2 – 933.7 m: dominated by diamictite, which is interbedded with minor argillaceous turbiditic siltstone. The diamictite is typically grey, has a sandy silty matrix, a mostly low matrix:clast ratio, and shows soft-sediment deformation. Clast lithologies are typically sedimentary, and less commonly igneous. The wireline logs over this interval have a very uniform character. The dipmeter indicates dips in excess of 30° towards 330° and a supplementary direction of 150°. These dip directions are at right angles to the postulated sedimentary supply direction of 240°. Such dips could be the result of relief over either a depositional lobe or at the foresets of a channel. Structural dip interpreted from the dipmeter is typically low and with a variable azimuth; 3° towards the south being the most common trend.

933.7 – 1075.9 m: an upper and lower sandstone separated by a 30 m section of diamictite and fine-grained turbidites, all of which appear to be part of the same depositional cycle. Structural dip interpreted from the dipmeter log is about 3° towards the southwest.

The upper sandstone (933.7 – 961.3 m) is interbedded with two thin diamictite beds. The sandstone is dominantly grey and brown, medium grained (locally fine grained), poorly sorted, cross-bedded, and argillaceous. In some places the sandstone is conglomeratic and shows extensive soft-sediment deformation. Local scour surfaces and intraformational clasts are common. Diamictite beds are massive and typically have a low to moderate clast content. Wireline logs highlight the sharp contacts at the tops and bases of thick sandstone bodies. This interval was probably deposited as mass flows, infilling a channel cut in a shallow-marine basinal-slope depositional environment . The basal part of the sandstone shows a constant cross-bedding dip of 23° towards 255–285°, whereas in the upper part palaeocurrent azimuths typically dip towards 300°, based on the dipmeter log.

The interval from 961.25 to 988 m is dominated by diamictite (961.25 – 975 m) and silty claystone to argillaceous siltstone (975–988 m). The diamictite is mainly massive with a low to moderate clast content within a silty and sandy matrix. Some clasts are up to 12 cm in size. The argillaceous siltstone consists of extremely contorted strata and includes local erosive surfaces and micro-syndepositional faulting. Wireline logs indicate two coarsening-upward depositional cycles with abrupt tops at 976 and 981 m.

The lower sandstone (988 – 1075.9 m) is interbedded with diamictite and has conglomerate at the base. The sandstone is grey, mainly medium grained, locally fine to medium grained, and bedded to well cross-bedded. It contains argillaceous laminae, soft-sediment deformation, syndepositional faulting with up to 5 mm vertical displacement, and high-angle local scour surfaces suggesting an unstable depositional slope (slump) environment. The sandstone shows both fining-upward and coarsening-upward cycles on the gamma-ray logs. The diamictite is grey and contains highly contorted sandy and silty horizons. It has a mostly moderate to high clast content with clasts to 2 cm in size. From 1060 to 1070.9 m the interval consists of conglomerate and diamictite. The basal conglomerate (1070.9 – 1075.85 m) comprises a variety of clasts of different sizess, including silicified oolite fragments. The sedimentary characteristics indicate a turbiditic depositional environment. This sandy succession is interpreted as having formed by mass-flows down a channel that had eroded a submarine basin-slope, similar to the sand-rich interval above (933.7 – 961.3 m). Dipmeter data do not display any predominant palaeocurrent trends.

The dipmeter data show that this cross-bedded interval has unusual orientations, making Unit 3 distinct from the other units. In particular, most of the dip azimuths are towards the northwest (280°, 300°, 330°, and 350°), whereas a supplementary set exists towards the southeast (115° and 165°). A set towards 055° is also present, the reverse of the 240° direction that is typical of overlying units.

1075.9 – 1214.4 m: mainly diamictite, in part interbedded with either sandstone, argillaceous siltstone, or silty claystone. The diamictite is grey, matrix supported, with a moderate to high content of clasts in a very argillaceous and sandy matrix. Clasts are mostly subangular and up to 15 cm in size. The diamictite has sharp or gradational lower contacts with both the sandstone and argillaceous siltstone throughout this interval. The sandstone and argillaceous siltstone display soft-sediment deformation, local scour surfaces, and syndepositional faulting. Facies and sedimentary characteristics, such as contorted layers within argillaceous siltstone and sandstone and the nature of contacts between these lithologies and diamictite, together suggest a mass-flow depositional environment due to an unstable slope setting. The dipmeter data in the deformed bedding at 1150 m, also indicate that regional dips are distorted at 10° towards 210°. The thin sandstone bed at 1188 m shows dips of 30° towards 120°; however, this is probably due to compaction or slumping, because the base and top surfaces are conformable to the internal dips.

There is a distinct lithological difference between the diamictites above 1214.4 m and those below. Above 1214.4 m the diamictites are more clast rich and the clasts are mostly larger. Dolomite clasts dominate the lower diamictite, and although they are present above 1214.4 m, other sedimentary clasts are less common. The diamictites above 1214.4 m have a uniform character on gamma-ray logs with little change except for cleaner sandstone zones, whereas those below this depth typically show subdivision into several units that mostly fine upwards. This indicates a change in provenance and basin dynamics. The coarser grain size and greater clast concentration above 1214.4 m suggests either a more proximal basin setting, decreased basin subsidence (so that sediment accommodation was less, leading to progradation), or a more elevated hinterland (thereby providing coarser clasts through increased rates of erosion). The latter implies greater rates of tectonic uplift of the hinterland.

1214.4 – 1228.5 m: conglomerate grading into a clast-rich sandy diamictite. Cross-bedding and imbrication of clasts is characteristic of this interval. The clasts are similar to the surrounding diamictites, but with a larger range of sedimentary lithologies.

Unit 2 — 1228.5 to 1632 m

Unit 2 can be divided into six lithological subdivisions, as described below:

1228.5 – 1315 m: matrix-rich diamictite, which between 1244.5 and 1260 m grades into an argillaceous siltstone interpreted as a distal turbidite. Some zones with more abundant clasts are also present. The gamma-ray log shows a number of minor fining-upward cycles. Dipmeter data show a regional dip of 5° towards 200° in the thin-bedded turbidites (with some scatter towards 180°).

1315 – 1356.3 m: predominantly argillaceous siltstone in the upper part, sandstone in the middle, and diamictite in lower part. The argillaceous siltstone is massive, in part diamictitic, and contains common soft-sediment deformation and local scour surfaces. The sandstone is typically medium grained, argillaceous, and in part grades to a pebbly sandstone. The diamictite is massive and has a moderate clast content with a very argillaceous sandy matrix. This facies assemblage was probably deposited in a turbiditic environment. A fining-upwards cycle from 1343 to 1336 m is overlain by a coarsening-upwards cycle visible on the gamma-ray log from 1326 to 1336 m. The dipmeter log suggests the regional dip is 5° towards 190°, but there is some dip-scatter due to contortion of the dewatered sandstone. Dip magnitude ranges from approximately 5 to 18°. Palaeocurrent azimuths interpreted from the dipmeter data are predominantly towards the south.

1356.3 – 1405 m: mainly argillaceous siltstone interbedded with minor sandstone. A minor diamictitic part forms the base of this interval. The argillaceous siltstone is light brown, contains local scour surfaces and abundant soft-sediment deformation. Irregularly shaped leached zones are also common. These zones could be due to several processes, including evaporitic minerals that were leached out, having been subsequently infilled with calcite cement by plastic injection from intersecting calcite-filled fractures during compaction. The gamma-ray log indicates the interval comprises several fining-upward cycles, although a coarsening-upward cycle is present at the top. Dipmeter data suggests regional dip is 8° towards 190°. Some scatter is present, presumably due to soft-sediment deformation.

1405 – 1424.5 m: dominantly grey and brown sandstone, interbedded with minor argillaceous siltstone. The beds show vertically oriented fractures, abundant soft-sediment deformation, and local scour surfaces. In particular, within the lower part of the succession, fining-upward depositional cycles and turbiditic characteristics are present. The gamma-ray log shows a cycle that coarsens upwards to a mid-point at about 1411 m and then fines upwards. The dipmeter records a regional dip of between 5 and 12° towards 180–200°. These dips are most likely due to soft-sediment deformation and fracturing. Palaeocurrent azimuths are predominantly towards the south.

1424.5 – 1540 m: interbedded argillaceous siltstone and diamictite. Argillaceous siltstone beds are grey to brown and contain very fine-grained sandstone layers. Soft-sediment deformation is abundant, and local scour surfaces and fining-upward cycles are common. The sandstone is interpreted as distal turbidite deposits. The presence of well-developed vertical vein-filled fractures up to 5 cm wide are a result of structural movement within this interval.

The diamictite is brown to grey, massive, and has low to moderate clast content with a mainly silty and sandy matrix. It has mostly transitional contacts with

argillaceous siltstone, suggesting a similar mode of emplacement in the same depositional environment. The close association of diamictites with turbiditic sandstone and siltstone beds suggests a subaqueous origin for the diamictites, either by slumping or debris flows on an unstable submarine slope.

1540–1632 m: interbedded diamictite (70%) and argillaceous siltstone and sandstone. The diamictite is grey to dark grey, massive, and has a moderate clast content with a silty and sandy matrix. Clasts are mainly sedimentary and up to 15 cm in size. A partly glacial-derived provenance is indicated by the presence of striated clasts. Contacts are mainly gradational between diamictite and argillaceous siltstone and sandstone. Argillaceous siltstone beds are parallel to wavy bedded and interbedded with sandstone laminae. The siltstone contains cross-bedding, local scour surfaces, and syndepositional faulting with vertical displacements of up to 1 cm. Calcite cement is common, in particular within the sandy horizons. Structural dip interpreted from the dipmeter is about 4° toward the southwest. At 1570 m, palaeocurrent azimuths are predominantly towards the west.

The base of this succession has a sharp contact with the underlying Unit 1; however, there appears to be no evidence for a period of non-deposition, erosion, or weathering at the contact. Sedimentation is therefore believed to have been continuous across this contact.

Unit 1 — 1632 to 2017.5 m TD

Vines 1 terminated within Unit 1 at a depth of 2017.5 m and therefore the nature of Unit 1's base is unknown. The intersected part of the unit comprises repeated cycles of turbidite-dominated sandstone and argillaceous siltstone, and minor interbedded diamictite beds. Unit 1 is sharply overlain by Unit 2 and no significant hiatus is observed in the core between these two units. There are very few sedimentary dips identifiable on the dipmeter, but the regional dip is very consistent at 2–8° towards 195°, with minor variation due to soft-sediment deformation. Palaeocurrent azimuths are predominantly towards the south to southwest.

The unit can be subdivided into three lithological intervals, as described below:

1632–1705 m: interbedded sandstone (60%) and argillaceous siltstone (40%). The sandstone is grey, medium grained, dominantly quartz rich, argillaceous, and is cleaner in the lower part. It shows a slight fining-upward character, from 1650 to 1675 m, and coarsening-upward cycles, in particular from 1685 to 1700 m. The sandstone is mainly massive but is locally cross-bedded with beds inclined up to 15–20° at about 1700 m. Locally developed scour surfaces, overlain by argillaceous siltstone, are common throughout.

The argillaceous siltstone is grey to dark grey, with parallel to wavy bedding, low-relief cross-bedding, and highly contorted bedding from 1667 to 1669 m. It has a sharp contact with overlying sandstone, in places containing scour surfaces. Abundant soft-sediment deformation structures and syndepositional faulting are also present. Graded beds within the siltstone indicate fairly rapid deposition. Both sandstone and argillaceous-dominated intervals were probably deposited as turbidites within a deep marine environment.

1705 – 1866.3 m: predominantly sandstone interbedded with argillaceous siltstone, minor silty claystone, and diamictite. Sedimentary structures within this interval are similar to those above. The bottom 20 m is dominated by argillaceous siltstone, which may represent the basal transgressive event for this interval.

1866.3 – 2017.5 m: comprises two successions, from 1866.3 to 1935 m and from 1935 to 2017.5 m, which are similar to the interval between 1705 and 1866.3 m. Each succession consists of a sandstone-rich upper half and an argillaceous-siltstone-dominated lower half. In particular, from 1866.3 to 1935 m the sandstone beds show a fining-upward cycle throughout. In both successions the sandstone and argillaceous siltstone contains highly contorted beds, indicating a steep depositional slope environment. Minor intraformational erosive surfaces with low-angle contacts (0–10°) between sandstone and argillaceous siltstone are present. Overall, the interval is interpreted to have been deposited by turbidity currents in a slope environment.

Possible correlations

The age of the Vines Formation is poorly constrained but is probably latest Neoproterozoic – Early Cambrian. This is based on palynomorphs of Component 3, which being recycled set a likely maximum age for the Vines Formation.

The lower turbidite-dominated succession (Unit 1; 1631.9 – 2017.5 m) is significantly different from the majority of formations described in both the Officer and Amadeus Basins; turbidites deposited below wave-base are rare in both basins. Correlations based on this unit are therefore difficult. The upper diamictite-dominated succession (Units 2, 3, and 4; 1632 – 301.5 m), however, have some lithological similarities with other conglomeratic and diamictitic strata in the Officer Basin, and conglomerates of the Amadeus Basin. If a latest Neoproterozoic – Early Cambrian or younger age is confirmed for the Vines Formation, then older conglomerates and diamictites can therefore be discounted as possible correlatives. Thus, the two Marinoan diamictite units in the western Officer basin — the Boondawari Formation in the Savory area and the ?Lupton Formation in Empress 1A (redefined as the Wahlgu Formation, Grey et al., in prep.) — can be excluded. Likewise, the Chambers Bluff Tillite of the eastern Officer Basin, although not well constrained, is considered to be Sturtian age (Morton and Drexel, 1997) and can also be excluded.

Coarse clastic units that may be of a similar age to the Vines Formation include: the Lupton Formation, which outcrops in the Vines region, and the McFadden Formation and Durba Sandstone from the Savory area of the western Officer Basin (Williams, 1992); the Punkerri Sandstone and Narana Formation of the Ungoolya Group (Calver and Lindsay, 1998), and units within the Marla Group of the eastern Officer Basin; and the Sir Frederick and the Mount Currie Conglomerates, and the Arumbera Sandstone of the Amadeus Basin (Wells et al., 1970).

The type section of the Lupton Formation is located 31 km to the northwest of Vines 1. In the remeasured type section it comprises 69 m of boulder to pebble diamictite, pebbly sandstone, sandstone, and minor mudstone (Grey et al., 1999), and thus it has some lithological similarities with Units 2, 3, and 4 of the Vines Formation. The age constraints on the Lupton Formation, however, are very poor. The *Baicalia burra* and *Acaciella australica* stromatolite assemblages are present in dolomites of Supersequence 1 strata that outcrop about 35 km east of this type section (Grey et al., 1999), and about 22 km northeast of Vines 1. It can be inferred that these Supersequence 1 (Cryogenian) rocks underlie both the Lupton and Vines Formations, thus setting a maximum age for both formations, but no contacts have been observed to confirm this. The Lower Ordovician Table Hill Volcanics outcrop 33 km south-southeast of the Lupton Formation type section and 17 km southwest of Vines 1, suggesting a minimum age for both the Lupton and Vines Formations. No contacts between these units have been observed, however, and faulting is present immediately north of the Lupton Formation type section. Faulting is inferred to be present near Vines 1 based on gravity data (Appendix 5), indicating that assumptions based on simple

stratigraphic relationships may not be valid. The Permian Paterson Formation is mapped as overlying the Lupton Formation and may set a minimum age. However, these units are lithologically similar, and hence distinguishing them can be problematic. The Paterson Formation has not been directly dated in this area. A correlation between the Vines Formation and the Lupton Formation is therefore possible based primarily on lithological similarities and very limited age constraints.

Until the age of the Sir Frederick Conglomerate is better constrained, there are few grounds to correlate it with the Vines Formation. The Mount Currie Conglomerate, another possible correlative, is a non-marine succession that is interpreted to be the result of uplift associated with the Petermann Ranges Orogeny, and hence possibly of a similar age and tectonic setting to the Vines Formation. The canyon-fill deposits of the Narana Formation are described as fining upwards, which are different to the typically coarsening-upwards and small-scale fining-upwards successions in Vines 1, interpreted as turbiditic deposits on an unstable slope. Consequently, a correlation between these two formations has also not been made. However, as with the Mount Currie Conglomerate (Foreman, 1966), the Narana Formation (Calver and Lindsay, 1998) is interpreted as related to Petermann Ranges Orogeny movements and hence may be of a similar age but different facies to the Vines Formation. Therefore, no lithostratigraphic correlations, other than possibly with the locally outcropping Lupton Formation, can be made at this stage.

Summary

Most of the well intersections in the western Officer Basin are a significant distance from the present basin boundary. Vines 1 was therefore deliberately located near to the northern boundary of the basin, next to the Musgrave Complex. Until further wells are drilled or seismic data is acquired along this boundary, it is impossible to determine the regional extent of the intersected succession. The facies is consistent with tectonic instability along the margin of the Musgrave Complex; however, it is unclear whether any of the diamictite strata that outcrop in places along the southern margin of the Musgrave Complex (mapped as Lupton Formation) are correlatives of Vines 1 diamictites.

The entire drilled sequence is interpreted as a portion of a large basin plain, or slope turbidite-fan, or both. Core descriptions and wireline log patterns indicate beds with abrupt bases and fining-upwards character, typical of such deposits. These beds are stacked into thicker units with a coarsening or fining-upwards character, representing the migration of individual turbidite lobes at the Vines 1 location. The change at 1214.4 m from basin-floor fan deposition to a more proximal slope location is abrupt, and may be a reflection of basin topography.

Overall, the Vines Formation is a coarsening-upwards succession, which suggests that the Vines 1 location became more proximal to the source area throughout its deposition.

Petroleum geology

Petroleum exploration activities in the western Officer Basin are summarized in Phillips et al. (1985), Townson (1985), and Perincek (1998), and the petroleum potential of the eastern Officer Basin (within South Australia) is reviewed in Morton and Drexel (1997).

Mature, but thin, good quality source rocks are recognized from the Browne and Hussar Formations and other Neoproterozoic strata in drillholes NJD 1 and LDDH 1

within the Yowalga and Gibson areas (Ghori, 1998). Fair to good quality reservoirs are noted in the Browne, Hussar, Kanpa, ?Lupton, Lennis, and Paterson Formations from core and log data (Carlsen et al., 1999). Sealing shales are present throughout the Neoproterozoic sedimentary section of the western Officer Basin. The Browne Formation contains thick halite seals throughout much of the basin and is assumed to be present below the base of Vines 1.

Hydrocarbon shows

All core within Vines 1 was inspected for fluorescence under ultraviolet light, and a hot-wire total-gas detector monitored flammable gas levels in the drilling mud below 625 m. This instrument was calibrated so that 1% methane in air gave a reading of 100 units. No oil shows were detected in Vines 1; however, a gas show was recorded whilst drilling at a depth of 1482.9 m. At this depth gas readings rapidly rose from a background range of 20–40 units to 1009 units, fell back to 500 units, rose again in excess of 1000 units and then fell back to 500 units, finally rising again in excess of 1000 units before drilling was stopped. The drillhole was observed for about three hours before the core was carefully recovered. The core had no stain or cut, but a trace of gas could be heard escaping from the core, confirming the show and proving the elevated readings were not an aberration of the gas detector. It is estimated that at the time of the gas show it would take approximately 25 minutes for mud to circulate from the drillbit face to the gas detector (McConachy, D., 2000, written comm.). Given the coring rate was about 2 m/h, the depth of the gas show was about 1482 m. No porosity is visible in thinly interlaminated argillaceous siltstone and very fine-grained sandstone at this depth, and log analysis indicates about 1% porosity. Minipermeameter readings over this zone gave values of less than 0.1 to 0.07 md. Fractures up to 5 cm thick, filled with calcite and quartz, are common in this section of the core. It is assumed that the gas show was sourced from an open fracture in the subsurface as none of the fractures in the core had visible porosity.

A thin-section of a moderately oxidized sandstone from Unit 5 (285 m) exhibits dark-coloured rims around sand grains that are possibly dead oil or bitumen (Appendix 2). Scanning electron microscopy (SEM) imaging did not exclude this dark rim from being bitumen (Appendix 6) and therefore solvent extraction of core at 285 m was conducted and trace hydrocarbons were recovered (Appendix 7). The significance of this hydrocarbon occurrence is unclear and contamination of this porous sandstone during drilling cannot be ruled out. Further work, including producing polished thin-sections is planned.

All sandstones with significant porosity are interpreted as 100% water saturated in the wireline log analysis (Appendix 8).

Source potential and maturity

Fifty-six total organic carbon (TOC) and 10 Rock-Eval analyses were conducted on core samples (Appendix 7). Their organic content ranges from 0.04 to 0.36% and thus no samples can be considered as having source potential. This is confirmed by the low potential yield ($S_1 + S_2$) range of 0.18 to 0.37 mg/g.

Organic petrology and Rock-Eval pyrolysis were used to assess thermal maturity (Appendix 7). Ten samples, between 355 and 1999.2 m, were measured for reflectance and fluorescence and the section is assessed as being late mature for oil generation. Equivalent vitrinite reflectance varies from about 0.8% near 400 m to 1.15 % near the base of the drillhole. There are no obvious jumps in thermal maturity in this limited data set.

The T_{max} production index parameters derived from Rock-Eval pyrolysis suggest that the section is late mature to overmature for oil generation. This interpretation mostly supports the maturity assessment based on organic petrology. However, the maturity based on T_{max} production index parameters may not be reliable due to the low TOC content of the samples.

Maturation modelling has not been undertaken because of the uncertain age of the Vines Formation. The minimum-recorded and estimated present day geothermal gradients are 2.1°C/100 m and 2.4°C/100 m, respectively.

In summary, all potential source rock horizons sampled are lean and hence the source potential of the Vines Formation is very poor. Limited maturity data indicate that the rocks are currently late mature for oil generation.

Reservoir character

Porosity and permeability measurements were conducted on a total of 49 core samples. Mini-probe permeametry (mini-k) was conducted on the surface of the whole core over four zones, including over the gas show at 1482.9 m (Appendix 9). Porosity and permeability analyses were attempted on five core plugs (1473.95 – 1484.3 m) near the gas show, but all were unsuccessful; probably because the clay-rich laminae had become desiccated, causing the core to become brittle. Log analysis was conducted from 45 to 2011.1 m and the calculated porosites are discussed below. All porous beds are interpreted as essentially 100% water saturated (Appendix 8).

Unit 6 — 4 to 124.7 m

No plug porosity and permeability analyses were conducted in this unit.

Calculated log porosity varies from 3 to 25%. These values, however, are fairly unreliable as this section of the hole was cased at the time of logging (Appendix 8) and only the gamma-ray and neutron logs were available. Mini-probe permeametry was conducted from 122.5 to 124.35 m, with five readings at approximately 20 cm intervals. Permeability over this interval ranges from 48 to 64 md.

Based on limited data, this unit has fair to good reservoir potential in parts.

Unit 5 — 124.7 to 301.5 m

Three porosity and permeability analyses were conducted in this unit. Porosity varies from 22.4 to 27.6% and permeability from 95 to 818 md. Calculated log porosity varies from 20 to 32%; however, these values are fairly unreliable as this section of the hole was cased and only the gamma-ray and neutron logs were available. Mini-probe permeametry was conducted from 125.15 to 135.03 m, with 49 readings at approximately 20 cm intervals. Permeability over this interval ranges from 21 to 291 md.

This unit has excellent reservoir potential.

Unit 4 — 301.5 to 779.2 m

Thirteen porosity and permeability analyses were conducted in this unit. Porosity ranges from 4.0 to 23.3% and permeability from less than 0.01 to 928 md. Only four plugs have permeabilities greater than 6 md, these being mostly from the upper part of the

unit where porosity exceeds 20%. A conglomerate sample at 617.5 m, however, has a porosity of 10.7% and permeability of 72 md. Calculated log porosity varies from 0 to 26%; however, values above 625 m are fairly unreliable as this section of the hole was cased and only the gamma-ray and neutron logs were available. Below 625 m there is good agreement between measured and calculated porosities.

This unit has mostly poor reservoir potential, with moderate potential in some zones, particularly near the top of the unit.

Unit 3 — 779.2 to 1228.5 m

Twenty porosity and 19 permeability analyses were conducted in this unit. Porosity ranges from 1.7 to 17.7% and permeability from less than 0.01 to 48 md. Only two plugs have permeabilities of greater than 3 md, both having greater than 15% porosity. Calculated log porosity varies from 0 to 18% and there is fair to good agreement between measured and calculated porosities. Mini-probe permeametry was conducted from 984.51 to 1002.3 m, with 82 readings at approximately 20 cm intervals. Permeability over this interval ranges from less than 0.01 to 0.18 md.

This unit has mostly very poor reservoir potential, with moderate potential in some zones where porosity exceeds 15%.

Unit 2 — 1228.5 to 1632 m

Nine porosity analyses were conducted in this unit (seven at overburden pressure). Porosity ranges from 2.7 to 5.9%. Permeability was able to be measured in seven samples, six of which have less than 0.01 md (at ambient pressure). A sample at 1458.7 m has a permeability of 0.01 md (at overburden pressure). Calculated log porosity varies from 0 to 5% and there is mostly good agreement between measured and calculated porosities.

Mini-probe permeametry was conducted over two zones. The deeper zone, from 1459.58 to 1486.86 m (which includes the gas show at about 1482 m), has 130 readings at approximately 20 cm intervals. Permeability varies from less than 0.01 to 0.09 md. The shallower zone, from 1318.3 to 1331.9 m, had 65 readings recorded at approximately 20 cm intervals, and permeability varies from less than 0.01 to 0.07 md.

This unit has very poor reservoir potential.

Unit 1 — 1632 to 2017.5 m TD

Four porosity and permeability analyses were conducted in this unit. Porosity varies from 2.4 to 4.9% and permeability in all four is less than 0.01 md. Calculated log porosity varies from 0 to 4% and there is good agreement between measured and calculated porosities.

This unit has very poor reservoir potential.

Summary

Overall, Unit 5, which is sandstone dominated, has excellent reservoir potential. Porosity and permeability mostly decrease with increasing depth. Sandstones below 1050 m have less than 10% porosity and sandstones below 1000 m have less than 1 md permeability.

The calculated porosities below 625 m, where open hole logs are available, are mostly in good agreement with measured porosities. However, calculated porosities below 1060 m are in places slightly less than the measured porosities, whereas above 301 m calculated porosities are in places more than the measured porosities.

The mini-probe permeametry was mostly in reasonable agreement with the plug permeabilities. The exceptions are two sandstones at 997.05 m (plug: 48 md versus mini-k: 0.18 md) and 999.65 m (plug: 3.8 md versus mini-k: 0.17 md).

Seal potential

Four porosity and permeability plugs with less than 0.01 md permeability and visually high clay content were analysed by mercury injection to assess their seal capacity (Appendix 10) after SEM imagery confirmed their suitability (Appendix 6). All four samples have excellent seal potential, with one sample from Unit 3 (930.0 m) having a calculated permeability of 0.00003 md and the potential to hold about a 1750 m gas column. The other three samples are from Unit 4 (598.23, 644.0, and 682.0 m). These samples have a calculated permeability range of 0.00003 to 0.00007 md and the potential to hold between a 1730 and 2170 m gas column.

Of the four samples, one is a claystone (598.23 m) and the other three are diamictites. Although the claystone bed is only 4.4 m thick, it is part of an interbedded claystone and diamictite zone that is 20 m thick, which caps a 20 m-thick conglomerate and sandstone interval. The diamictite at 644 m is part of a 31 m-thick unit, whereas the diamictite at 682 m is part of a 10 m-thick unit that caps an interbedded sandstone, diamictite, and conglomerate interval. The diamictite at 930 m is part of a 5.6 m-thick unit, which together with overlying and underlying claystone beds forms a 17 m-thick cap to a 27.5 m-thick (933.7 to 961.2 m) sandstone unit.

The lateral extent of all these potential seals is unknown. However, if the Vines Formation was deposited in a gravity-flow-dominated, relatively deep-water, basin-slope to plain environment as proposed, then the claystone and argillaceous diamictite sealing beds could have significant lateral extent.

Petrology

A summary of the petrography of 62 thin sections of the various lithotypes present in Vines 1 is presented in Appendix 2. The following is a summary of the facies, provenance, and reservoir properties based on the above report, together with a brief review of the thin-section descriptions.

Facies

Based on fabric, the bulk of the sedimentary succession within Vines 1 can be described as diamictite. There are two main components: coarse floating clasts and a fine matrix. The matrix is typically highly argillaceous with silt or sand-sized grains, although above 125 m the matrix lacks clay and is sandy. The clast content ranges from low to high, forming lithologies that range from conglomerate to pebbly silty claystone. The clasts range up to cobble size, and the matrix, excluding the clay content (commonly with a substantial fine carbonate content), contains a wide variety of quartz and lithic grain sizes.

Microscopic features, along with fluidization structures (synsedimentary slumping and faulting) seen in hand specimen, indicate highly water-rich sediments deposited on an unstable basin slope.

Turbidites are commonly associated with the diamictite beds. Individual turbidites range from decimetre- to millimetre-scale thickness, the later present as rhythmites that can be seen in thin section. The thin-section sample at 1478.95 m exhibits numerous individual turbidites that display erosional basal contacts, fining-upward characteristics (locally showing repeated surges), soft-sediment loading and injection, and synsedimentary faulting.

Provenance

A number of provenance-related features are present in the thin sections. For example, quartz grain shape is very much controlled by grain size; the coarser grains are more rounded and have a higher sphericity than the more angular and lower sphericity finer grains. Both grain types, however, can exist in the same sample. This morphology difference may be due to provenance (coarser grains are reworked sediments, whereas angular grains are first-cycle sediments) or distance of transport (coarser material may be sourced from an extensive fluvial system, whereas the fine angular material may be locally derived). The variety of grain sizes and shapes indicates a number of sources as well as two reworked palynological assemblages with different ages (Components 3 and 4, see **Appendix 3**).

Sedimentary provenance

The abundance and composition of sedimentary clasts throughout Vines 1 indicates a provenance dominated by siliciclastic sedimentary rocks, but with consistent associated carbonate rock influx. Some clasts are clearly dolomitized intraclasts (e.g. 1458.53 m) and derived from sediment deposited in the basin, but most are intraclasts, derived from rocks in the hinterland.

The proximity of the source is indicated by the presence of easily weathered materials such as carbonate, argillaceous siltstone, and shale. Although most clasts are well rounded, some are angular with elongate shapes, suggesting minimal transport. Although the carbonate-rich clasts are allogenic, the high carbonate content suggests minimal exposure to a fresh-water environment. A few carbonate clasts are stromatolitic, but the stromatolites are unidentifiable as a result of recrystallization.

Carbonate clasts are absent in the upper 300 m of the section, suggesting either a different provenance or leaching associated with the present-day weathering profile.

Igneous provenance

Two igneous provenances are suggested: a ubiquitous felsic plutonic source, and a mafic volcanic source that became available during deposition of the upper sequence. Both provenances are consistent with lithologies in the Musgrave Complex.

Igneous lithologies are a significant proportion of the clasts in the upper part of the section. They typically constitute over 50% of the clasts above 330 m, but decrease from 30 to 10% between 330 and 800 m, and are absent or rare below 1100 m. This increase up section may indicate the unroofing of an igneous provenance or the commencement of a volcanic phase. The majority of the clasts are described as ‘volcanics’. They are mainly fine grained with common glass, indicative of rapid chilling, and formed either as surface flows or shallow intrusions such as dykes. Both porphyritic and coarser grained varieties are also present.

Coarse feldspar grains are a common accessory in the Vines Formation, and constitute 2 to 3% of the sand-sized component throughout the section. Microcline and K-feldspar dominate, but plagioclase is also consistently present. Most of the feldspar

is fresh, but some saussuritization and leaching is common, even to remnant skeletal outlines.

Burial history

Evidence of substantial compaction due to burial (thin section at 67.8 m) suggests the section penetrated by Vines 1 was originally overlain by a considerable thickness of rocks. Grain contacts are shallow concavo–convex and are interpenetrating. This feature is present not only in labile lithic grains, but also in resistant quartz grains. Unfortunately, because high-matrix lithologies dominate the section, compaction effects are suppressed and a continuous trend can not be discerned. As would be expected, the greatest degree of compaction is in the deepest samples, with severe squeezing of labile grains and interpenetration and solution of more rigid grains. No obvious changes to compaction within these samples could be identified.

Porosity decline is also not a clear indicator of compaction. Although the best porosities are higher up in the section and worst lower down, the highly argillaceous lithologies, diagenetic cementation, and lack of comparable lithologies mask any trends present.

Although substantial quartz solution is indicated by interpenetration of grains, commensurate syntaxial overgrowth is under represented. This is due to the presence of clays — in large amounts as intergranular fill, reducing the space for overgrowth, and as thin rims around quartz grains inhibiting nucleation. Some clear overgrowth, even with crystal terminations, can be seen, but cryptic welding of grains is more common. No quantitative trend is apparent. Hence, the use of quartz overgrowth as an indicator of depth of burial in Vines 1 is impractical.

Anhydrite

Anhydrite is found in three phases within Vines 1: as a replacement of other minerals, as an intergranular-filling cement, and as a void- and fracture-filling medium. The first phase is uncommon, the second phase is present in sandstone lithologies, and the third phase is present in fine-grained distal-turbidite lithologies.

The shallowest occurrence of anhydrite is at 763.7 m, as a local cement in a lithic sandstone. Some crystals have been broken by compaction, suggesting a relatively early emplacement. At 1215 m, anhydrite is a late-stage intergranular cement in a pebbly sandstone. Compaction of clasts took place before early void-filling carbonate, and was followed by later anhydrite cementation. From 1325 m to 1466 m, anhydrite is common as a cement in porous sandstones and as ‘vug’ and fracture fillings in fine-grained argillaceous rocks. The nature of the ‘vugs’ needs further investigation; they may have been passive void fillings or expansive nodular growths. At 1537 m and 1569 m (the deepest occurrence of anhydrite), a carbonate (possibly an algal boundstone) contains fracture- and void-filled anhydrite.

The distribution of anhydrite appears to be controlled by porosity, intergranular in sandstones and mouldic or fractures in tight lithologies, with the anhydrite forming from late basinal brines.

Barite

Although barite is not common in thin sections, many of the SEM samples had fine barite disseminated throughout (see **Appendix 6**).

Mineral potential

Seven drillcore samples were analysed for nine elements (Ag, As, Ba, Co, Cu, Mn, P, Pb, and Zn) to investigate the mineral potential for sedimentary hosted base-metal mineralization (Appendix 11). The values were not encouraging, but this does not necessarily downgrade the mineral potential of the region, as only limited sampling was done and no focusing mechanism for mineralizing fluids was recognized in the drillhole.

Contributions to geological knowledge

Vines 1 is the first drillhole in the Waigen area of the Officer Basin. Investigation of 1973 m of continuous core, together with gravity modelling of the Waigen area was the first significant step to improve the understanding of both chronostratigraphic correlations and petroleum systems of this part of the Officer Basin.

Although Vines 1 lacks precise chronostratigraphic control, it is a key well for understanding the lithostratigraphic development of the western Officer Basin. The age of the Vines Formation is interpreted as no older than the latest Neoproterozoic – earliest Cambrian. This age is based both on palynology, which gives a maximum age of probably latest Neoproterozoic – earliest Cambrian, and palaeomagnetic pole data. As no significant hiatuses are recognized within the Vines Formation, the SHRIMP weighted mean $^{206}Pb/^{238}U$ date of 658 ± 8 Ma indicated by the analyses of two grains from 307.8 – 309.3 m, is interpreted as providing a maximum age for deposition of the formation.

Vines 1 is significant because it intersects a thick Officer Basin succession close to the northern margin of the basin, and may be typical of a zone extending along parts of the northern margin. The sedimentary section represents rapid deposition of over 2 km of submarine diamictites and turbidites in an actively subsiding basin, close to a hinterland that retained pronounced relief throughout its deposition, and minimal chemical weathering probably because of rapid erosion. Data derived from the dipmeter (between 689 and 2010 m) indicate the following trends: Unit 1 (1632 to 2010 m) palaeocurrents are predominantly towards the south to southwest; Unit 2 (1325 to 1570 m) palaeocurrents are predominantly towards the south and west; Unit 3 (lower part from 988 to 1075 m) palaeocurrents display no dominant trend although within the upper part they are typically towards the west or northwest; Unit 4 (from 689 to 779 m) palaeocurrents indicate the dominant transport direction was towards the west-southwest.

The facies associations recognized are attributed to gravity-flow transportation and deposition in a deep (i.e. below storm-wave base) slope to basin-plain environment. On deposition, the sediments were undercompacted and commonly show synsedimentary faulting and folding typical of such an environment. The dominant depositional process was remobilization of mixed clay-rich sediment as debris flows, resulting in a characteristic diamictite lithology. With further mixing and dilution, turbidity currents resulted. Clay-rich and sandy turbidite associations are recognized, with the sandy sediment possibly being the more distal equivalent of the clay-rich sediments. Clay-rich turbidites may be dilute overbank plumes from turbidity currents, tending to be thinly bedded on a millimetre to centimetre scale. Sandy turbidites range in thickness from centimetre to decimetre scale.

The sedimentary succession in Vines 1 represents a record of the sequential unroofing of its hinterland. The oldest part of the succession was sourced from existing

sedimentary rocks. The small size of clasts indicate a distal provenance or the inability of the sedimentary clasts (dominantly dolomite) to survive transportation. The presence of reworked acritarchs of middle- to late-Cryogenian age (c. 750–700 Ma) suggest that the Hussar, Kanpa, and Steptoe Formation equivalents were being reworked from the rising basin margin.

An overall coarsening-upward trend is present in the Vines Formation, reflected by an increase in the number and size of clasts, and the replacement of clay by sand in the diamictite matrix. This trend is probably the result of the coastal margin shifting towards the Vines 1 location as the basin filled. The succession also changes from being dominated by sedimentary clasts at the base to igneous clasts towards the top. A number of individual coarsening-upward trends are embedded within the overall pattern. These may represent basin-filling episodes between pulses of subsidence, or alternatively may reflect episodes of basin hinterland uplift.

Some striated and facetted clasts are present throughout the succession. As this low-relief ornamentation would not survive prolonged transport, it is possible that contemporaneous glacigene sediments were present in the source area. It should be emphasized, however, that the sedimentary rocks in Vines 1 are debris-flow deposits and not tilloidal. A few possible dropstones have been recorded and a weak glacial influence could be implied. However, the finely bedded units are regarded as 'distal' turbidites and not ice-controlled varves (Eyles, N. and C., 2001, written comm.). Glacial processes have probably influenced the supply of large volumes of unweathered clasts to the shoreline before the sediments were redeposited into deeper water. A periglacial environment, reflecting a weak glacial phase or reduction in intensity due to low latitude, is suggested. It is unclear which, if any, of the recognized late Neoproterozoic to Early Cambrian glacial episodes can be correlated with the Vines Formation. The identification of Component 3 palynomorphs suggests that the Vines Formation post-dates both the Sturtian and Marinoan glaciations, which are recognized elsewhere in the Officer Basin.

There is no evidence of any significant sedimentary breaks within the 2 km-thick succession intersected in Vines 1, implying that the rate of sedimentation was probably rapid. The time span represented by these deposits, however, is very poorly constrained. Since the drillhole did not intersect any Supersequence 1 units that are regionally distributed across the basin, there is probably a significant thickness of Officer Basin strata underlying the Vines 1 section. This inference, combined with evidence that a significant thickness of the younger sedimentary pile has been subsequently removed, suggests the Vines Formation represents only a relatively short period of the c. 340 Ma (c. 825–485 Ma) Officer Basin depositional cycle.

Regional correlations of the Vines Formation are uncertain. There are some lithological similarities with the Lupton Formation, which outcrops 31 km northwest of Vines 1; however, the Lupton Formation has poor age constraints. The Sir Frederick Conglomerate of the Amadeus Basin also has very poor age constraints, making a correlation with this unit difficult. The Mount Currie Conglomerate and Arumbera Sandstone of the Amadeus Basin and the canyon-fill deposits of the Narana Formation in the eastern Officer Basin, are both interpreted to have formed during the Petermann Ranges Orogeny. Thus these formations may have been deposited at a similar time and in a similar structural setting to the Vines Formation, but they exhibit different depositional environments and hence are not considered lithostratigraphic correlatives. Likewise, the Early Cambrian Mount Johns Conglomerate Member of the Apamurra Formation may also have been deposited in a similar structural setting to the Vines Formation, but it was deposited in an alluvial-fan environment, which is significantly different to that interpreted for the Vines Formation.

It is unclear if the Vines 1 section was deposited in a zone fringing the northern margin of the western Officer Basin, and therefore its basinal extent and relationship to other facies is unknown. Consequently the regional applicability of the following conclusions is uncertain.

Reservoir facies are present within Vines 1 and may improve in a more distal position. For example, conglomerates and turbidite sandstones should have good primary porosity, with the possibility of some stacked reservoirs. Sandstones like those between 125 and 300 m would make excellent thick reservoir targets.

Excellent reservoir properties are present above 500 m. Below this depth, compaction, matrix clays, and later cements that have occluded the primary porosity, become more common. No significant reservoir rocks are present below 1000 m. However, the major cements comprise relatively soluble anhydrite and carbonate, which could be easily dissolved by meteoric waters or by reactive fluids, perhaps accompanying petroleum migration. Intergranular and fracture porosity could thus be generated, resulting in reservoir properties within some lithologies.

The high-energy slope to basin depositional environment and inferred cold climate was not conducive to high organic productivity, and therefore the source-rock potential of these rocks is low. Whether organic material by-passed the Vines 1 location and was deposited in quieter, more distal positions, is unknown.

The highly argillaceous and very thick nature of many of the diamictites in Vines 1 makes them excellent local seals, as indicated by the change in water salinity in the drillhole at about 1060 m (SP log; Appendix 8). Less argillaceous, more distal equivalents may not be such good seals. No evidence of thick shale beds, which could act as an efficient regional seal, was observed. Claystones are mostly less than 10 m thick and are typically silty and sandy. However, a 4.4 m-thick claystone bed at 598.23 m, which is part of a 20 m-thick zone of interbedded claystone and diamictite, has excellent measured seal potential.

The measured present day geothermal gradient to TD (assuming a surface temperature of 25ºC) is a low 2.1ºC/100 m.

The gas show encountered at 1482.9 m proves the existence of a gas petroleum system within the region, but no suitable trap at the Vines 1 location. The significant fracturing and veining present in the drillcore between about 1425 and 1500 m suggests the gas was probably released from a fracture system. The gas show substantially upgrades the petroleum potential of the Waigen area.

References

APAK, S. N., and MOORS, H. T., 2000, Basin development and petroleum exploration potential of the Yowalga area, Officer Basin, Western Australia: Western Australia Geological Survey, Report 76, 61p.

CALVER, C. R., and LINDSAY, J. F., 1998, Ediacarian sequence and isotope stratigraphy of the Officer Basin, South Australia: Australian Journal of Earth Sciences, v. 45, p. 513–532.

CARLSEN, G. M., APAK, S. N., GHORI, K. A. R., GREY, K., and STEVENS, M. K., 1999, Petroleum potential of the Neoproterozoic Western Officer Basin, Western Australia, based on a source-rock model from Empress-1A: APPEA Journal, v. 39, pt 1, p. 322–341.

COTTER, K. L., 1997, Neoproterozoic microfossils from the Officer Basin, Western Australia: Alcheringa, v. 21, p. 247–270.

COTTER, K. L., 1999, Microfossils from Neoproterozoic Supersequence 1 of the Officer Basin: Western Australia: Alcheringa, v. 23, p. 63–86.

DANIELS, J. L., 1971, Cooper, W.A.: Western Australia Geological Survey, 1:250 000 Geological Series Explanatory Notes, 22p.

FORMAN, D. J., 1966, Regional geology of the south-west margin, Amadeus Basin, central Australia: Australia BMR, Report 87, 54p.

GHORI, K. A. R., 1998, Petroleum generating potential and thermal history of the Neoproterozoic Officer Basin, Western Australia, *in* The Sedimentary Basins of Western Australia 2 *edited by* P. G. PURCELL and R. R. PURCELL: Petroleum Exploration Society of Australia, Symposium, Perth, W.A., 1998, Proceedings, p. 717–730.

GRAVESTOCK, D. I., MORTON, J. G. G., and ZANG, W-L., 1997, Biostratigraphy and correlation, *in* Petroleum Geology of South Australia, Volume 3: Officer Basin *edited by* J. G. G. MORTON and J. F. DREXEL: South Australia Department of Mines and Energy Resources, Report Book 97/19, p. 87–97.

GREY, K., 1998, Ediacarian acritarchs of Australia: Macquarie University, PhD thesis (unpublished).

GREY, K., APAK, S. N., EYLES, C., EYLES, N., STEVENS, M. K., and CARLSEN, G. M., 1999, Neoproterozoic glacigene successions, western Officer Basin, Western Australia: Western Australia Geological Survey, Annual Review 1998–99, p. 74–80.

GREY, K., STEVENS, M. K., APAK, S. N., CARLSEN, G. M., and MOORS, H. T, in prep., Stratigraphic revision of Neoproterozoic rocks of the western Officer Basin: Western Australia Geological Survey.

HILL, A. C., COTTER, K. L., and GREY, K., 2000, Mid-Neoproterozoic biostratigraphy and isotope stratigraphy in Australia: Precambrian Research, v. 100, p. 283–300.

HOCKING, R. M., 1994, Subdivisions of Western Australian Neoproterozoic and Phanerozoic sedimentary basins: Western Australia Geological Survey, Record 1994/4, 84p.

JACKSON, M. J., and van der GRAAFF, W. J. E., 1981, Geology of the Officer Basin, Western Australia: Australia Bureau of Mineral Resources, Bulletin 206, 102p.

MORTON, J. G. G., and DREXEL, J. F., 1997, The petroleum geology of South Australia. Volume 3 — Officer Basin: South Australia Department of Mines and Energy Resources, Report Book, 97/19, 213p.

NELSON, D. R., in prep., Compilation of geochronology data, 2001: Western Australia Geological Survey, Record 2002/2.

PERINCEK, D., 1996, The stratigraphic and structural development of the Officer Basin, Western Australia — a review: Western Australia Geological Survey, Annual Review 1995–96, p. 135–148.

PERINCEK, D., 1998, A compilation and review of data pertaining to the hydrocarbon prospectivity of the Officer Basin: Western Australia Geological Survey, Record 1997/6, 209p.

PHILLIPS, B. J., JAMES, A. W., and PHILIP, G. M., 1985, The geology and hydrocarbon potential of the northwestern Officer Basin: APEA Journal, v. 25, pt 1, p. 52–61.

STEVENS, M. K., and APAK, S. N., (compilers), 1999, GSWA Empress 1 and 1A well completion report, Yowalga Sub-basin, Officer Basin, Western Australia: Western Australia Geological Survey, Record 1999/4, 110p.

TOWNSON, W. G., 1985, The subsurface geology of the western Officer Basin — results of Shell's 1980–1984 petroleum exploration campaign: APEA Journal, v. 25, pt 1, p. 34–51.

WALTER, M. R., (editor), 2000, Neoproterozoic of Australia: Precambrian Research, v. 100, 438p.

WALTER, M. R., GREY, K., WILLIAMS, I. R., and CALVER, C. R., 1994, Stratigraphy of the Neoproterozoic to Early Palaeozoic Savory Basin, Western Australia, and correlation with the Amadeus and Officer Basins: Australian Journal of Earth Sciences, v. 41, p. 533–546.

WALTER, M. R., and VEEVERS, J. J., 1997, Australian Neoproterozoic palaeogeography, tectonics, and supercontinental connections: Australian Geological Survey Organisation, Journal of Australian Geology and Geophysics, v. 17, p. 73–92.

WALTER, M. R., VEEVERS, J. J., CALVER, C. R., GORJAN, P., and HILL, A. C., 2000, Dating the 840–544 Ma Neoproterozoic interval by isotopes of strontium, carbon, and sulfur in seawater, and some interpretative models: Precambrian Research, v. 100, p. 371–433.

WELLS, A. T., FORMAN, D. J., RANFORD, L. C., and COOK, P. J., 1970, Geology of the Amadeus Basin, central Australia: Australia Bureau of Mineral Resources, Bulletin 100.

WILLIAMS, I. R., 1992, Geology of the Savory Basin, Western Australia: Western Australia Geological Survey, Bulletin 141, 115p.

Appendices

(Appendices 2, 6, 9, and 10 are presented as submitted to the Department of Mineral and Petroleum Resources and have not been edited to conform with GSWA house style.)

Appendix 1

Operations report

by M. K. Stevens

(VinesApp1.pdf)

Appendix 2

Vines 1 and Empress 1A thin-section descriptions

by J. Sonego and C. Young, PGA Consultants Pty Ltd

(VinesApp2.pdf)

Appendix 3

Palynology of samples from Vines 1

by K. Grey

(VinesApp3.pdf)

Appendix 4

Palaeomagnetic study of Vines 1

by S. A. Pisarevsky, Tectonics Special Research Centre, University of Western Australia

(VinesApp4.pdf)

Appendix 5

Gravity modelling of the Waigen area

by K. A. Blundell

(VinesApp5.pdf)

Appendix 6

Post-petrographic SEM and XRD reports for Vines 1

by J. Sonego, PGA Consultants Pty Ltd

(VinesApp6.pdf)

Appendix 7

Petroleum geochemistry

by K. A. R. Ghori

(VinesApp7.pdf)

Appendix 8

Log analysis

by M. K. Stevens

(VinesApp8.pdf)

Appendix 9

Routine core analysis

by Geotechnical Services Pty Ltd (GEOTECH)

(VinesApp9.pdf)

Appendix 10

Seal capacity study

by K. Ooi, Geotechnical Services Pty Ltd (GEOTECH)

(VinesApp10.pdf)

Appendix 11

Chemical analysis of drillcore from Vines 1 to assess potential for base metals

by I. Ruddock

(VinesApp11.pdf)

Appendix 12

Well index sheet

(VinesApp12.pdf)

Appendix 1

Operations report

by M. K. Stevens

Drillhole history

Vines 1 is a stratigraphic drillhole in the Officer Basin, drilled for the Geological Survey of Western Australia (GSWA) to test the source-rock potential of Neoproterozoic strata. Vines 1 was drilled by Drillcorp Western Deephole using a UDR 1500 drillrig, and was spudded at 1300 h on Sunday 4 July 1999 and reached a total depth (TD) of 2017.5 m (drillers depth) at 1300 h on Saturday 28 August 1999. The drillhole was continuously cored from 44.5 to 2017.5 m. Time taken to reach to TD was 55 days, 0 hours, and total time was 64 days, 20 hours. Vines 1 was plugged and abandoned at 09:00 h, Tuesday 7 September 1999 (Fig. 1.1).

Vines 1 was geophysically logged by Reeves Wireline who recorded a TD of 2018.8 m during the first and only logging suite carried out from 31 August to 2 September 1999. The logging tools went into PF casing at 625 m.

Water for drilling and camp use was pumped from COPB 2, a waterbore drilled 43 m to the south-southwest of Vines 1, which was completed from 126 to 138 m and produced water from an unnamed sandstone.

Vines 1 was terminated in Officer Basin sedimentary rocks at 2017.5 m. Almost 100% core recoveries were obtained in the PQ, HQ, and NQ cored intervals.

Operations

Drilling shifts: Two 12-hour shifts operated each day (Table 1.1). Shift change was at 06:00 h and 18:00 h.

Drilling crews: Each crew consisted of one driller and two or three driller's offsiders. The drillers were K. Davies, D. Wilson, G. Birkett, and C. Lovrick.

GSWA personnel: Henry Moors, Neil Apak, and Peter Gillies.

Orientation surveys: Hole orientation was monitored during drilling operations at various intervals with an Eastman Single Shot Camera (Table 1.2).

Core recovery: PQ core recovery was approximately 578.5 m of 580.5 m drilled (99.7%). HQ core recovery was approximately 1116.5 m of 1116.5 m drilled (100%). NQ core recovery was approximately 276 m of 276 m drilled (100%).

Time–depth curve: The time–depth curve (Fig. 1.2) shows the progress of the drillhole during drilling. The data are tabulated in Table 1.3.

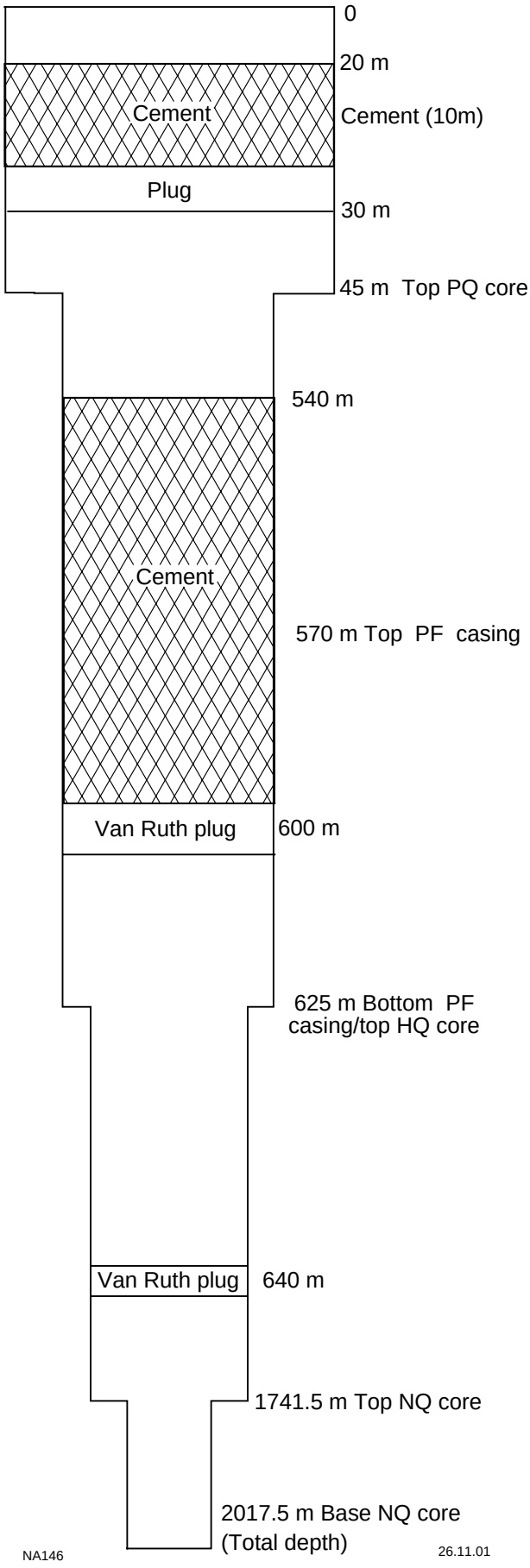

Figure 1.1. Engineering diagram for Vines 1

Table 1.1. Daily drilling summary, Vines 1

Date	*Shift*	*Tine*	*Activity*
4 July 1999	Night	Rotary drilling: 7 h 30 min	**Spud Vines 1 at 1300** h, rotary drill with 215.9 mm, 8.5" rock roller bit to 24 m, run 25.5 m of 177.8 mm, 7" casing (24 m)
		Set up: 2 h	
		Cement casing: 2 h 30 min	
		Pump repairs: 1 h	
5 July 1999	Day	Rotary drilling: 5 h	Rotary drill with 158.8 mm, 6.25" rock roller bit to 30 m (6 m)
		Run and cut 7" casing: 4 h	
		Condition hole: 1 h	
		Rig repairs: 2 h	
	Night	Cut 7" casing: 1 h	Rotary drill with 158.8 mm, 6.25" rock roller bit to 45 m. PQ core 45 to 49.5 m (19.5 m)
		Rotary drilling: 4 h 30 min	
		Prepare to PQ core: 2:30 h	
		PQ core: 2 h 30 min	
		Repairs: 1 h 30 min	
6 July 1999	Day	PQ core: 10 h 30 min	PQ core 49.5 to 67 m (17.5 m)
		Trip for bit change:1 h 30 min	
	Night	PQ core: 11 h	PQ core 67 to 94 m (27 m)
		Trip for bit change: 1 h	
7 July 1999	Day	PQ core: 12 h	PQ core 94 to 112 m (18 m)
	Night	PQ core: 7 h 30 min	PQ core 112 to 118.3 m, PQ3 core 118.3 to 123.5 m (11.5 m)
		Ground problems: 2 h 30 min	
		Trip: 2 h	
8 July 1999	Day	PQ core: 12 h	PQ3 core 123.5 m to 150 m (26.5 m)
	Night	PQ core: 7 h 30 min	PQ core 150 to 163 m (13 m)
		Trip for core in barrel: 2 h 30 min	
		Trip for bit change: 2 h	
9 July 1999	Day	PQ core: 9 h 30 min	PQ3 core 163 m to 187 m (24 m)
		Trip for bit change: 2 h	
		Survey: 30 min	
	Night	PQ core: 11 h 30 min	PQ3 core 187 m to 223 m (36 m)
10 July 1999	Day	PQ core: 12 h	PQ3 core 223 to 271 m (48 m)
	Night	PQ core: 12 h	PQ3 core 271 to 313 m (42 m)
11 July 1999	Day	PQ core: 11 h 30 min	PQ3 core 313 to 340 m (27 m)
		Survey: 30 min	
	Night	PQ core: 5 h	PQ3 core 340 to 349 m (27 m)
		Trip: 3 h 30 min	
		Repairs and service: 3 h 30 min	
12 July 1999	Day	PQ core: 10 h 30 min	PQ3 core 349 to 370 m (21 m)
		Repairs: 1 h 30 min	
	Night	PQ core: 7 h	PQ3 core 370 to 385 m (15 m)
		Pull casing: 2 h	
		Trip: 3 h	
13 July 1999	Day	PQ core: 3 h	PQ3 core 385 to 391 m (6 m)
		Run rods: 4 h	
		Condition hole: 1 h	
		Repairs to hole opener: 4 h	
	Night	PQ core: 9:30 h	PQ3 core 391 to 406 m (15 m)
14 July 1999	Day	PQ core: 11 h	PQ3 core 406 to 427 m (21 m)
		Condition hole: 1 h	
	Night	PQ core: 11 h	PQ3 core 427 to 451 m (24 m)
		Condition hole and meeting: 1 h	
15 July 1999	Day	PQ core: 11 h	PQ3 core 451 to 478 m (27 m)
		Repairs: 1 h	
	Night	PQ core: 11 h 30 min	PQ3 core 478 to 511 m (33 m)
		Condition hole: 30 min	
16 July 1999	Day	PQ core: 11 h	PQ3 core 511 to 538.2 m (27.2 m)
		Survey: 1 h	
	Night	PQ core: 11 h	PQ3 core 538.2 to 562.2 m (24 m)
		Condition hole: 30 min	
		Service: 30 min	
17 July 1999	Day	PQ core: 12 h	PQ3 core 562.2 to 583.2 m (21 m)
	Night	PQ core: 3 h	PQ core 583.2 to 589.2 m (6 m)
		Bit change: 7 h	
		Condition hole: 1 h	
		Repairs: 1 h	

Table 1.1. (continued)

Date	*Shift*	*Tine*	*Activity*
18 July 1999	Day	PQ core: 12 h	PQ core 589.2 to 608.7 m (19.5 m)
	Night	PQ core: 10 h	PQ core 608.7 to 625 m, base of PQ core (16.3 m)
		Core in barrel: 1 h	
		Condition hole: 1 h	
19 July 1999	Day	Trip out: 3 h 30 min	Run and cement PF casing to 624 m (0 m)
		Run casing: 1 h	
		Flush hole: 1 h	
		Cement casing: 4 h	
	Night	Dig cellar: 12 h	(0 m)
20 July 1999	Day	Install BOP: 12 h	(0 m)
	Night	Site cleanup: 10 h	Prepare to HQ core (0 m)
		Service rig: 2 h	
21 July 1999	Day	Standby: 12 h	Waiting on HMQ drill rods (0 m)
	Night	Standby: 7 h	(0 m)
		Trip in: 5 h	
22 July 1999	Day	HQ core: 11 h 30 min	HQ core 625 to 648.5 m (23.5 m)
		Test BOP: 30 min	
	Night	HQ core: 11 h	HQ core 648.5 to 670 m (21.5 m)
		Survey: 1 h	
23 July 1999	Day	HQ core: 11 h 30 min	HQ core 670 to 696.5 m (26.5 m)
		Test BOP: 30 min	
	Night	HQ core: 11 h	HQ core 696.5 to 723.5 m. Note: tube turn-around time 50 minutes (27 m)
		Condition hole: 1 h	
24 July 1999	Day	HQ core: 11 h 30 min	HQ core 723.5 to 750.5 m (27 m)
		Circulate and flush hole: 40 min	
	Night	HQ core: 12 h	HQ core 750.5 to 780.5 m (30 m)
25 July 1999	Day	HQ core: 6 h	HQ core 780.5 to 802 m (21.5 m)
		Bit change: 6 h	
	Night	HQ core: 11 h	HQ core 802 to 823 m (21 m)
		Repair survey camera: 1 h	
26 July 1999	Day	HQ core: 10 h	HQ core 823 to 847 m (24 m)
		Survey: 1 h	
		Repairs: 1 h	
	Night	HQ core: 12 h	HQ core 847 to 871 m (24 m)
27 July 1999	Day	HQ core: 12 h	HQ core 871 to 901 m (30 m)
	Night	HQ core: 4 h 30 min	HQ core 901 to 910 m (9 m)
		Trip out: 3 h 30 min	
		Service and repair: 4 h	
28 July 1999	Day	Trip in: 2 h 30 min	HQ core 910 to 931 m (21 m)
		HQ core: 9 h 30 min	
	Night	HQ core: 12 h	HQ core 931 to 967 m (36 m)
29 July 1999	Day	HQ core: 7 h	HQ core 967 to 982 m (15 m)
		BOP check: 5 h	
	Night	HQ core: 12 h	HQ core 982 to 1006 m (24 m)
30 July 1999	Day	HQ core: 12 h	HQ core 1006 to 1036 m (30 m)
	Night	HQ core: 11 h 30 min	HQ core 1036 to 1072 m (36 m)
		Safety meeting: 30 min	
31 July 1999	Day	HQ core: 12 h	HQ core 1072 to 1096 m (24 m)
	Night	HQ core: 11 h 30 min	HQ core 1096 to 1120 m (24 m)
		Condition hole: 30 min	
1 August 1999	Day	HQ core: 11 h	HQ core 1120 to 1144 m (24 m)
		Survey: 1 h	
	Night	HQ core: 11 h 30 min	HQ core 1144 to 1168 m (24 m)
		Condition hole: 30 min	
2 August 1999	Day	HQ core: 12 h	HQ core 1168 to 1192 m (24 m)
	Night	HQ core: 11 h 30 min	HQ core 1192 to 1213 m (21 m)
		Condition hole: 30 min	
3 August 1999	Day	HQ core: 5 h	HQ core 1213 to 1225 m (12.5 m)
		Bit change: 6 h	
		Condition hole: 1 h	
	Night	HQ core: 11 h 30 min	HQ core 1225.5 to 1252.5 m (27 m)
		Condition hole: 30 min	
4 August 1999	Day	HQ core: 11 h	HQ core 1252.5 to 1270.5 m (18 m)
		Work stuck tube: 1 h	
	Night	HQ core: 11 h 30 min	HQ core 1270.5 to 1288.5 m (18 m)
		Condition hole: 30 min	
		Freeing stuck tube: 35 min	

Table 1.1. (continued)

Date	*Shift*	*Tine*	*Activity*
5 August 1999	Day	HQ core: 11 h 30 min Condition hole: 30 min	HQ core 1288.5 to 1306.5 m (18 m)
5 August 1999	Night	HQ core: 11 h 30 min Condition hole: 30 min	HQ core 1306.5 to 1324.5 m (18 m)
6 August 1999	Day	HQ core: 11 h Repairs: 1 h	HQ core 1324.5 to 1342.5 m (18 m)
	Night	HQ core: 4 h Service rig: 8 h	HQ core 1342.5 to 1351.5 m (9 m)
7 August 1999	Day	HQ core: 12 h	HQ core 1351.5 to 1369.5 m (18 m)
	Night	HQ core: 12 h	HQ core 1369.5 to 1387.5 m (18 m)
8 August 1999	Day	HQ core: 12 h	HQ core 1387.5 to 1411.5 m (24 m)
	Night	HQ core: 12 h	HQ core 1411.5 to 1432.5 m (21 m)
9 August 1999	Day	HQ core: 10 h 30 min Condition hole: 30 min BOP test: 30 min Pull rods for repairs: 30 min	HQ core 1432.5 to 1450.5 m (18 m)
	Night	HQ core: 3 h Repair and service rig: 9 h	HQ core 1450.5 to 1456.5 m, replace rotation unit and wireline (6 m)
10 August 1999	Day	HQ core: 11 h 30 min Condition hole: 30 min	HQ core 1456.5 to 1480.5 m (24 m)
	Night	HQ core: 9 h Condition hole, add KCl and circulate: 3 h	HQ core 1480.5 to 1492.5 m, mud gas show at 1482.9 m, add KCL to mud (12 m)
11 August 1999	Day	HQ core: 10 h Repairs: 1 h BOP training: 30 min BOP test: 30 min	HQ core 1492.5 to 1510.5 m (18 m)
	Night	HQ core: 12 h	HQ core 1510.5 to 1531.5 m (21 m)
12 August 1999	Day	HQ core: 11 h 30 min BOP test: 30 min	HQ core 1531.5 to 1552.5 m (21 m)
	Night	HQ core: 12 h	HQ core 1552.5 to 1573.5 m (21 m)
13 August 1999	Day	HQ core: 12 h	HQ core 1573.5 to 1594.5 m (21 m)
	Night	HQ core: 8 h Condition hole: 1 h 30 min Stuck tube: 2 h 30 min	HQ core 1594.5 to 1606.5 m stuck tube due to sludge (12 m)
14 August 1999	Day	Bit change: 8 h Repairs: 4 h	Repair footclamps (0 m)
	Night	HQ core: 10 h Pull rods: 2 h	HQ core 1606.5 to 1624.5 m rods separated while pulling core off bottom (18 m)
15 August 1999	Day	HQ core: 11 h Condition hole: 30 min Breakout core: 30 min	HQ core 1624.5 to 1645.5 m (21 m)
	Night	HQ core: 11 h Breakout core: 1 h	HQ core 1645.5 to 1666.5 m (21 m)
16 August 1999	Day	HQ core: 10 h Breakout core: 1 h Safety meeting: 1 h	HQ core 1666.5 to 1687.5 m, (21 m)
	Night	HQ core: 11 h Breakout core: 1 h	HQ core 1687.5 to 1708.5 m (21 m)
17 August 1999	Day	HQ core: 12 h	HQ core 1708.5 to 1726.5 m (18 m)
	Night	HQ core: 11 h Breakout core: 1 h	HQ core 1726.5 to 1741.5 m, base of HQ core (15 m)
18 August 1999	Day	Condition hole: 1 h 30 min Trip out: 5 h 30 min Survey: 1 h Standby: 4 h	(0 m)
	Night	Standby: 12 h	Standby for wireline loggers (0 m)
19 August 1999	Day	Wireline logging: 12 h	Wireline logging (0 m)
	Night	Wireline logging: 12 h	Wireline logging (0 m)
20 August 1999	Day	Wireline logging: 12 h	Wireline logging (0 m)
	Night	Wireline logging: 3 h Condition hole: 1 h Run in HQ rods: 6 h Modify BOP: 2 h	Wireline logging, run HQ rods as casing (0 m)
21 August 1999	Day	NQ core: 3 h 30 min Trip in NQ rods: 5 h 30 min	NQ2 core 1741.5 to 1750.5 m (9 m)

Table 1.1. (continued)

Date	*Shift*	*Tine*	*Activity*
		Drill out float shoe: 2 h Condition hole: 30 min BOP test: 30 min	
	Night	NQ core: 12 h	NQ2 core 1750.5 to 1768.5 m (18 m)
22 August 1999	Day	NQ core: 12 h	NQ2 core 1768.5 to 1795.5 m (27 m)
22 August 1999	Night	NQ core: 11 h 30 min Service rig: 30 min	NQ2 core 1795.5 to 1819.5 m (24 m)
23 August 1999	Day	NQ core: 12 h	NQ2 core 1819.5 to 1840.5 m (21 m)
	Night	NQ core: 12 h	NQ2 core 1840.5 to 1861.5 m (21 m)
24 August 1999	Day	NQ core: 12 h	NQ2 core 1861.5 to 1885.5 m (24 m)
	Night	NQ core: 12 h	NQ2 core 1885.5 to 1906.5 m (21 m)
25 August 1999	Day	NQ core: 9 h Seat core tube in barrel: 3 h	NQ2 core 1906.5 to 1921.5 m (15 m)
	Night	NQ core: 12 h	NQ2 core 1921.5 to 1936.5 m (15 m)
26 August 1999	Day	NQ core: 12 h	NQ2 core 1936.5 to 1957.5 m (21 m)
	Night	NQ core: 9 h Seat core tube: 3 h	NQ2 core 1957.5 to 1975.5 m (18 m)
27 August 1999	Day	NQ core: 10 h Seat core tube: 1 h 30 min Repairs: 30 min	NQ2 core 1975.5 to 1990.5 m (15 m)
	Night	NQ core: 10 h Seat core tube: 2 h	NQ2 core 1990.5 to 2008.5 m (18 m)
28 August 1999	Day	NQ core: 6 h	NQ2 core 2008.5 to 2017.5 m, **reached total depth of 2017.5 m at about 16:00 h Saturday 28th August 1999** (9 m)
		Seat core tube: 3 h Freeing rods: 1 h Survey: 1 h Trip out: 1 h	
	Night	Trip out: 6 h Standby: 6 h	Pull NRQ drill rods and standby for wireline loggers
29 August 1999	Day	Pull HMQ rods: 4 h	Pull 500 m of HMQ drill rods (temporary casing)
	Night	Standby: 12 h	
30 August 1999	Day	Standby: 12 h	
	Night	Standby: 12 h	Wireline loggers arrive onsite 21:00 h
31 August 1999	Day	Wireline logging: 12 h	
1 September 1999	Day	Wireline logging: 12 h	
2 September 1999	Day	Wireline logging: 12 h	
3 September 1999	Day	Remove BOP: 2 h 30 min	Set Van Ruth plug at 640 m, cut PF casing at 570 and 540 m but unable to free it
		Pull and cut casing: 15 h 30 min	
4 September 1999	Day	Pull and cut casing: 15 h	Cut PF casing at 510 (twice) 501 and 360 m but unable to free it
5 September 1999	Day	Pull and cut casing: 13 h	Cut PF casing at 360 m but unable to free it, work casing, restore circulation and recover 570 m of PF casing
6 September 1999	Day	Pull casing: 1 h	Reset Van Ruth plug at 630 m, set cement plug 530–630 m, set cement plug 20–30 m
		Freeing rods: 1 h Cementing: 10 h	
7 September 1999	Day	Packing up: 9 h	Install PW standpipe 1.5 m above ground level with well identification plate
		Install stand pipe: 3 h	
8 September 1999	Day	Packing up: 14 h	Pack up and rehabilitate site, lower southern water bore COPB 3300 mm below surface and reweld cap
		Weld cap: 1 h	
9 September 1999	Day	Packing up: 10 h	Pack up and rehabilitate site, demobilize at about 14:00 h to Tjukayirla Roadhouse
		Demobilize: 7 h	
February 2001		Rehabilitation	The PW standpipe marking the surface location of Vines 1 was cut back to ground level and a cap rewelded at ground level under the supervision of M. Hammond

Table 1.2. Hole directional surveys, Vines 1

Depth (m)	*Dip (°)*	*Azimuth (°)*
172	89	000
313	89	005
523	89	359
633.5	89	025
829	89	025
1 144	89	025
1 741.5	89	035
2 017.5	89	028

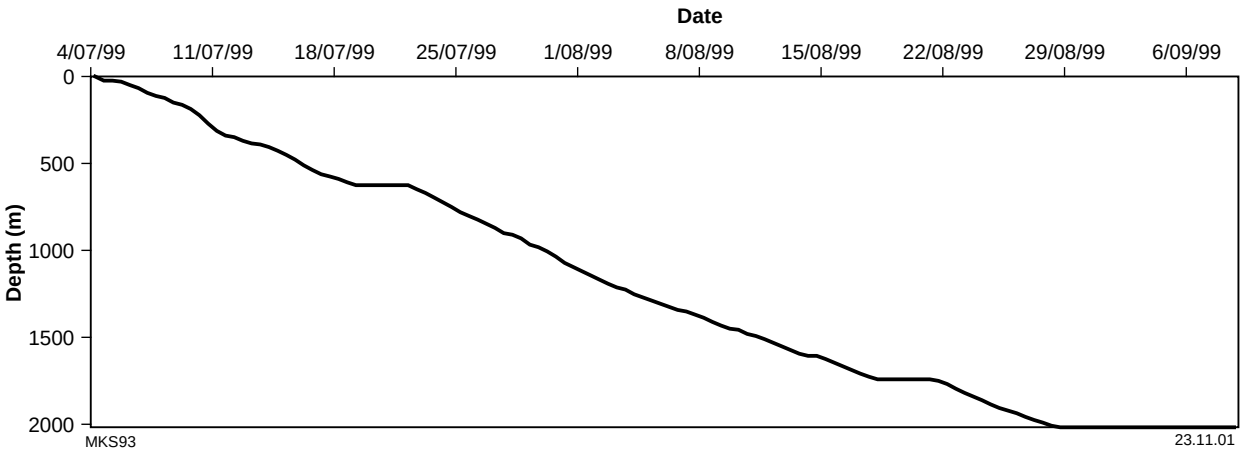

Figure 1.2. Time–depth curve for Vines 1

Table 1.3. Drilling date and depth, Vines 1

Date	*Time*	*Depth (m)*
4 July 1999	0600	0
4 July 1999	1800	-24
5 July 1999	0600	-24
5 July 1999	1800	-30
6 July 1999	0600	-49.5
6 July 1999	1800	-67
7 July 1999	0600	-94
7 July 1999	1800	-112
8 July 1999	0600	-123.5
8 July 1999	1800	-150
9 July 1999	0600	-163
9 July 1999	1800	-187
10 July 1999	0600	-223
10 July 1999	1800	-271
11 July 1999	0600	-313
11 July 1999	1800	-340
12 July 1999	0600	-349
12 July 1999	1800	-370
13 July 1999	0600	-385
13 July 1999	1800	-391
14 July 1999	0600	-406
14 July 1999	1800	-427
15 July 1999	0600	-451
15 July 1999	1800	-478
16 July 1999	0600	-511
16 July 1999	1800	-538.02
17 July 1999	0600	-562.2
17 July 1999	1800	-538.2
18 July 1999	0600	-589.2
18 July 1999	1800	-608.7
19 July 1999	0600	-625
19 July 1999	1800	-625
20 July 1999	0600	-625
20 July 1999	1800	-625
21 July 1999	0600	-625
21 July 1999	1800	-625
22 July 1999	0600	-625
22 July 1999	1800	-648.5
23 July 1999	0600	-670
23 July 1999	1800	-696.5
24 July 1999	0600	-723.5
24 July 1999	1800	-750.5
25 July 1999	0600	-780.5
25 July 1999	1800	-802
26 July 1999	0600	-823
26 July 1999	1800	-847
27 July 1999	0600	-871
27 July 1999	1800	-901
28 July 1999	0600	-910
28 July 1999	1800	-931
29 July 1999	0600	-967
29 July 1999	1800	-982
30 July 1999	0600	-1 006
30 July 1999	1800	-1 036
31 July 1999	0600	-1 072
31 July 1999	1800	-1 096
1 August 1999	0600	-1 120
1 August 1999	1800	-1 144
2 August 1999	0600	-1 168
2 August 1999	1800	-1 192
3 August 1999	0600	-1 213
3 August 1999	1800	-1 225.5
4 August 1999	0600	-1 252.5
4 August 1999	1800	-1 270.5
5 August 1999	0600	-1 288.5
5 August 1999	1800	-1 306.5
6 August 1999	0600	-1 324.5
6 August 1999	1800	-1 342.5
7 August 1999	0600	-1 351.5
7 August 1999	1800	-1 369.5
8 August 1999	0600	-1 387.5
8 August 1999	1800	-1 411.5
9 August 1999	0600	-1 432.5
9 August 1999	1800	-1 450.5
10 August 1999	0600	-1 456.5
10 August 1999	1800	-1 480.5
11 August 1999	0600	-1 492.5
11 August 1999	1800	-1 510.5
12 August 1999	0600	-1 531.5
12 August 1999	1800	-1 552.5
13 August 1999	0600	-1 573.5
13 August 1999	1800	-1 594.5
14 August 1999	0600	-1 606.5
14 August 1999	1800	-1 606.5
15 August 1999	0600	-1 624.5
15 August 1999	1800	-1 645.5
16 August 1999	0600	-1 666.5
16 August 1999	1800	-1 687.5
17 August 1999	0600	-1 708.5
17 August 1999	1800	-1 726.5
18 August 1999	0600	-1 741.5
18 August 1999	1800	-1 741.5
19 August 1999	0600	-1 741.5
19 August 1999	1800	-1 741.5
20 August 1999	0600	-1 741.5
20 August 1999	1800	-1 741.5
21 August 1999	0600	-1 741.5
21 August 1999	1800	-1 750.5
22 August 1999	0600	-1 768.5
22 August 1999	1800	-1 795.5
23 August 1999	0600	-1 819.5
23 August 1999	1800	-1 840.5
24 August 1999	0600	-1 861.5
24 August 1999	1800	-1 885.5
25 August 1999	0600	-1 906.5
25 August 1999	1800	-1 921.5
26 August 1999	0600	-1 936.5
26 August 1999	1800	-1 957.5
27 August 1999	0600	-1 975.5
27 August 1999	1800	-1 990.5
28 August 1999	0600	-2 008.5
28 August 1999	1800	-2 017.5
29 August 1999	0600	-2 017.5
29 August 1999	1800	-2 017.5
30 August 1999	0600	-2 017.5
30 August 1999	1800	-2 017.5
31 August 1999	0600	-2 017.5
31 August 1999	1800	-2 017.5
1 September 1999	1800	-2 017.5
2 September 1999	1800	-2 017.5
3 September 1999	1800	-2 017.5
4 September 1999	1800	-2 017.5
5 September 1999	1800	-2 017.5
6 September 1999	1800	-2 017.5
7 September 1999	1800	-2 017.5

Chemicals consumed

Aqua-Pac, 15 kg	:	169
Aus Det, 25 L	:	53
Cement, 25 kg	:	65
Na bicarbonate, 25 kg	:	5
KCl, 25 kg	:	377
Soda ash, 25 kg	:	120
CR 650, 15 kg	:	71
Flossy salt, 25 kg	:	47
Truck wash, 20 L	:	2
Caustic soda, 25 kg	:	1
Diesel, L	:	200

Note: diesel was only used after completion of wireline logging to help recover the PF steel casing.

Drilling problems

No major difficulties were experienced in the drillhole. In approximate order of occurrence, minor downhole problems included:

- High drillbit wear (PQ H9 bit lasted only 13.5 m);
- Unspecified 'problem ground' while drilling between 112 and 123.5 m (change from PQ to PQ3 coring);
- Stuck tubes during PQ coring from 150 to 163 m required pulling rods to recover core;
- The drillrods became tight in the casing while drilling at about 380 m (problem solved by pulling on casing);
- Approximately 1 hour per day was spent conditioning mud and hole between 406 and 589 m;
- Change to HQ coring at 625 m, with 1 hour spent conditioning hole at about 700 m because mud pump pressure was too high;
- Approximately 0.5 hours per day was spent conditioning mud and hole between 1144 and 1324 m and between 1432 and 1480 m;
- Approximately 3 hours were spent circulating out the gas show detected at 1482.9 m and adding KCl to the mud;
- 3.5 hours were spent freeing a stuck core tube at about 1600 m. The sticking was attributed to 'spin out' in the drill rods caused by excessive solid fines in the mud;
- 2 hours were lost when the drill rods separated at about 1624 m while attempting to break the core off bottom;
- 1 hour was lost each time breaking the core off bottom at about 1650, 1670, 1700 and 1730 m;
- Change to NQ coring at 1741.5 m, with 3 hours lost in three attempts to seat tube in core barrel at about 1910 m;
- 'Broken ground' between about 1921 and 1930 m resulted in short core runs;
- Between 1.5 and 3 hours were lost in each 12-hour shift while attempting to seat the tube in the core barrel between 1957 and 2017.5 m TD;
- The PF casing seated at 624 m was unable to be recovered and cuts at 570, 540, 510 (twice), 501 and 360 m were unsuccessful in freeing the casing;
- After working the casing, re-establishing circulation and adding 200 L of diesel to the mud, 570 m of PF casing was recovered.

Core loss zones

There were no major zones of core loss in the PQ core interval (44.5 – 625 m), the HQ core interval (625 – 1741.5 m), or the NQ core interval (1741.5 – 2017.5 m TD).

Significant zones of core loss (commonly greater than 0.2 m) are: 48.0 m (0.3 m), 81.6 m (0.4 m), 154.1 m (0.8 m), and 605.2 m (0.4 m). The top of the core-loss zone is listed first and is assumed to be from the base of the core run unless there was evidence to the contrary. The estimated core loss is in parentheses.

Depth matching of core to logs

Seventy-three tie points were established between the core and wireline logs (Table 1.4) and a line of best fit was calculated using the equation:

Logger's depth (m) = driller's depth (m) + (0.0016 × driller's depth + 0.3237)

No depth corrections were applied to the lithological column in Plate 1 above 625 m. The depth shift to convert driller's depth to logger's depth below 625 m in Plate 1 was always positive, and may be approximated by the driller's depth and depth increment (Table 1.5). This depth shift may be approximated by the formula:

$$y = 0.0013x - 0.83$$

where x = driller's depth in metres, and y = depth increment in metres.

Table 1.4. Depth matching of core to logs, Vines 1

Core depth (m)	*Log depth (m)*	*Core depth (m)*	*Log depth (m)*
0	0	1 401.2	1 402.0
76	75.7	1 447.7	1 448.7
108.9	108.9	1 465.7	1 466.6
124.7	124.7	1 523.4	1 523.8
302.7	302.8	1 538.5	1 539.6
333.0	333.1	1 577.8	1 578.8
397.0	397.0	1 590.0	1 591.2
423.4	423.5	1 633.3	1 634.3
451.2	451.2	1 640.3	1 641.2
520.7	520.7	1 646.2	1 647.1
530.3	530.3	1 662.2	1 663.8
565.8	565.8	1 672.6	1 673.7
581.0	581.0	1 688.0	1 689.3
620.0	620.0	1 705.0	1 706.5
625.0	625.0	1 741.5	1 742.4
694.4	694.5	1 757.2	1 758.7
723.6	724.1	1 760.6	1 762.2
784.2	784.5	1 803.0	1 804.5
836.5	836.8	1 810.3	1 812.1
924.0	924.4	1 827.5	1 829.3
933.7	934.3	1 830.0	1 831.8
943.5	944.2	1 839.5	1 841.5
961.2	961.6	1 872.3	1 874.0
988.0	988.6	1 877.6	1 878.2
996.0	996.5	1 897.7	1 899.4
1 005.7	1 006.3	1 901.0	1 902.8
1 014.5	1 015.0	1 903.5	1 905.4
1 018.5	1 019.0	1 912.7	1 914.7
1 163.7	1 164.4	1 914.9	1 916.8
1 186.9	1 187.6	1 920.9	1 922.9
1 215.8	1 216.6	1 938.0	1 940.0
1 289.6	1 290.1	1 953.2	1 955.1
1 295.4	1 296.2	1 971.3	1 973.3
1 335.9	1 336.5	1 985.0	1 987.1
1 341.7	1 342.6	1 995.3	1 997.3
1 351.9	1 352.7	2 017.5	2 018.8
1 373.1	1 373.9		

Table 1.5. Depth corrections, Vines 1

Driller's depth (m)	*Increment (m)*
750	0.2
900	0.3
970	0.4
1 005	0.5
1 100	0.6
1 200	0.7
1 300	0.8
1 500	0.9
1 600	1.0
1 675	1.1
1 750	1.3
1 900	1.8
2 017.5	2.0

Appendix 2

PGA CONSULTANTS PTY LTD

VINES-1 & EMPRESS-1A

Thin-section descriptions for 59 thin-sections and 3 polished sections from Vines-1 and 2 thin-sections for Empress-1A*.

JOHN SONEGO & CARL YOUNG

Suite 6, 6 Richardson St,
West Perth, Perth, W.A.
Ph: (08) 9226 3590
Email: jst@highway1.com.au

*Previous petrographic work on Empress 1A included in:
STEVENS, M. K., and APAK, S. N., 1999, GSWA Empress 1 and 1A well completion report, Yowalga Sub-basin, Officer Basin, Western Australia: Western Australia Geological Survey, Record 1994/4, 110p.

CONTENTS

1. INTRODUCTION 7
2. AIMS 7
3. METHODS 7
4. SUMMARY 7
5. MINERALOGY 9
5.1 Conglomerate petrographic results 9
5.1.1 Detrital components 10
5.1.2 Cements and replacement fabrics 11
5.1.3 Structures 12
5.2 Argillaceous siltstone and claystone petrographic results 12
5.2.1 Detrital components 13
5.2.2 Matrix/ Pseudomatrix 14
5.2.3 Cements and replacement fabrics 14
5.2.4 Structures 14
5.3 Diamictite petrographic results 14
5.3.1 Detrital components 15
5.3.2 Matrix/ pseudomatrix 16
5.3.3 Authigenic cements 16
5.3.4 Structures 16
5.4 Sandstone and argillaceous siltstone petrograhic results 16
5.4.1 Detrital components 17
5.4.2 Authigenic cements 18
5.4.3 Structures 18
5.5 Sandstone Petrographic results 18
5.5.1 Detrital components 19
5.5.2 Matrix/ pseudomatrix 21
5.5.3 Authigenic cements 21
5.5.4 Structures 21
6. TEXTURE AND FABRIC 22
6.1 Grain size distribution 22
7. CLAY AND CEMENT VARIATIONS 22
8. DIAGENESIS 23
9. POROSITY 24
10. DISCUSSION AND CONCLUSIONS 24
11. BIBLIOGRAPHY 26
APPENDIX A (Detailed thin-section descriptions) 27
GSWA No. 154867 28
GSWA No. 154844 31
GSWA No. 154843 34
GSWA No. 154842 37
GSWA No. 154866 40
GSWA No. 154841 44
GSWA No. 154865 47
GSWA No. 154864 49
GSWA No. 154863 51
GSWA No. 154838 53
GSWA No. 154837 55
GSWA No. 154862 58
GSWA No. 154861 60
GSWA No. 154835 62
GSWA No. 154834 63
GSWA No. 154860 65
GSWA No. 154859 67
GSWA No. 154858 69
GSWA No. 154833 72
GSWA No. 154857 76
GSWA No. 154830 79
GSWA No. 154829 82

GSWA No. 154828 ..... **85**
GSWA No. 154856 ..... **88**
GSWA No. 154827 ..... **92**
GSWA No. 154826 ..... **95**
GSWA No. 154825 ..... **98**
GSWA No. 154824 ..... **101**
GSWA No. 154823 ..... **104**
GSWA No. 154822 ..... **107**
GSWA No. 154821 ..... **109**
GSWA No. 154820 ..... **112**
GSWA No. 154819 ..... **115**
GSWA No. 154817 ..... **118**
GSWA No. 154853 ..... **121**
GSWA No. 154816 ..... **125**
GSWA No. 154815 ..... **128**
GSWA No. 154814 ..... **131**
GSWA No. 154855 ..... **134**
GSWA No. 154813 ..... **138**
GSWA No. 154812 ..... **142**
GSWA No. 154811 ..... **145**
GSWA No. 154810 ..... **149**
GSWA No. 154869 ..... **152**
GSWA No. 154854 ..... **154**
GSWA No. 154808 ..... **157**
GSWA No. 154807 ..... **161**
GSWA No. 154806 ..... **164**
GSWA No. 154852 ..... **167**
GSWA No. 154851 ..... **170**
GSWA No. 154850 ..... **173**
GSWA No. 154804 ..... **176**
GSWA No. 154803 ..... **179**
GSWA No. 154849 ..... **182**
GSWA No. 154848 ..... **185**
GSWA No. 154802 ..... **188**
GSWA No. 154801 ..... **191**
GSWA No. 154847 ..... **194**
GSWA No. 154846 ..... **198**
GSWA No. 154466 ..... **202**
GSWA No. 154465 ..... **205**
APPENDIX B (Reflective light descriptions) **208**
Polished Section 154862 ..... **209**
Polished section 154856 ..... **209**
Polished section 154860 ..... **209**
APPENDIX C (Photomicrographs) **210**
Sample 154867 (1983.0m) PPL **211**
Sample 154867 (1983.0m) XPL **212**
Sample 154844 (1902.0) XPL **213**
Sample 154844 (1902.0) XPL **214**
Sample 154843 (1815.0m) PPL **215**
Sample 154843 (1815.0m) XPL **216**
Sample 154842 (1713.0m) PPL **217**
Sample 154842 (1713.0m) XPL **218**
Sample 154866 (1665.6m) PPL **219**
Sample 154866 (1665.6m) XPL **220**
Sample 154841 (1656.0m) PPL **221**
Sample 154841 (1656.0m) XPL **222**
Sample 154865 (1569.1m) XPL **223**
Sample 154865 (1569.1m) XPL **224**
Sample 154864 (1537.05m) XPL **225**
Sample 154863 (1478.95m) PPL **226**

Sample 154838 (1473.95m) PPL **227**
Sample 154837 (1469.0m) PPL **228**
Sample 154837 (1469.0m) XPL **229**
Sample 154862 (1465.65m) PPL **230**
Sample 154861 (1463.2m) PPL **231**
Sample 154861 (1463.2m) XPL **232**
Sample 154835 (1458.53m) PPL **233**
Sample 154835 (1458.53m) XPL **234**
Sample 154834 (1410.0m) PPL **235**
Sample 154834 (1410.0m) XPL **236**
Sample 154860 (1395.95m) XPL **237**
Sample 154859 (1383.7m) PPL **238**
Sample 154858 (1372.95m) PPL **239**
Sample 154858 (1372.95m) XPL **240**
Sample 154833 (1325.1m) PPL **241**
Sample 154833 (1325.1m) XPL **242**
Sample 154857 (1227.95m) XPL **243**
Sample 154857 (1227.95m) XPL **244**
Sample 154830 (1215.0m) PPL **245**
Sample 154830 (1215.0m) XPL **246**
Sample 154829 (1212.0m) PPL **247**
Sample 154829 (1212.0m) XPL **248**
Sample 154828 (1100.15m) PPL **249**
Sample 154828 (1100.15m) XPL **250**
Sample 154856 (1076.65m) PPL **251**
Sample 154856 (1076.65m) XPL **252**
Sample 154827 (1070.0m) PPL **253**
Sample 154827 (1070.0m) XPL **254**
Sample 154826 (1062.0m) PPL **255**
Sample 154826 (1062.0m) XPL **256**
Sample 154825 (1050.0m) PPL **257**
Sample 154825 (1050.0m) XPL **258**
Sample 154824 (1000.1m) PPL **259**
Sample 154824 (1000.1m) XPL **260**
Sample 154823 (995.0m) XPL **261**
Sample 154821 (970.0m) PPL **262**
Sample 154821 (970.0m) XPL **263**
Sample 154820 (950.0m) PPL **264**
Sample 154820 (950.0m) XPL **265**
Sample 154819 (939.0m) XPL **266**
Sample 154819 (939.0m) XPL **267**
Sample 154817 (930.0m) PPL **268**
Sample 154817 (930.0m) XPL **269**
Sample 154853 (763.7m) PPL **270**
Sample 154853 (763.7m) PPL **271**
Sample 154816 (749.0m) PPL **272**
Sample 154816 (749.0m) XPL **273**
Sample 154815 (691.0m) PPL **274**
Sample 154815 (691.0m) XPL **275**
Sample 154814 (682.0m) PPL **276**
Sample 154814 (682.0m) XPL **277**
Sample 154855 (677.0m) PPL **278**
Sample 154855 (677.0m) PPL **279**
Sample 154813 (675.0m) PPL **280**
Sample 154813 (675.0m) XPL **281**
Sample 154812 (644.0m) PPL **282**
Sample 154812 (644.0m) PPL **283**
Sample 154811 (617.5m) PPL **284**
Sample 154810 (608.0m) XPL **285**
Sample 154869 (598.23m) PPL **286**

Sample 154854 (559.65m) PPL 287
Sample 154854 (559.65m) XPL 288
Sample 154808 (498.0m) PPL 289
Sample 154808 (498.0m) XPL 290
Sample 154807 (490.05m) PPL 291
Sample 154806 (440.05m) PPL 292
Sample 154806 (440.05m) XPL 293
Sample 154852 (420.1m) PPL 294
Sample 154852 (420.1m) XPL 295
Sample 154851 (360.2m) PPL 296
Sample 154850 (343.44m) PPL 297
Sample 154850 (343.44m) XPL 298
Sample 154804 (327.0m) PPL 299
Sample 154804 (327.0m) XPL 300
Sample 154803 (309.0m) PPL 301
Sample 154803 (309.0m) PPL 302
Sample 154849 (301.65m) PPL 303
Sample 154848 (301.4m) PPL 304
Sample 154848 (301.4m) PPL 305
Sample 154802 (285.0m) PPL 306
Sample 154802 (285.0m) XPL 307
Sample 154801 (133.2m) 308
Sample 154847 (104.55m) PPL 309
Sample 154846 (67.8m) PPL 310
Sample 154846 (67.8m) XPL 311
Sample 154465 (319.0m) PPL 312
Sample 154466 (1060.05m) PPL 313
APPENDIX D (Summary Table of mineralogy) 314

LIST OF TABLES

Table 1. Broad mineralogical classification of samples. 7
Table 2. List of samples provided for thin-sections analysis 8
Table 3. Conglomerate samples and corresponding mineralogical classifications. 9
Table 4. Listing of argillaceous siltstone samples and their mineralogical classification 13
Table 5. Listing of diamictite samples and their corresponding mineralogy. 15
Table 6. Table of sandstone and argillaceous siltstone samples and their corresponding mineralogical classifications 16
Table 7. List of sandstone samples and their respective mineralogical classifications 19
Table 8. Summary of mineralogy in Vines-1 and Empress-1A. 326

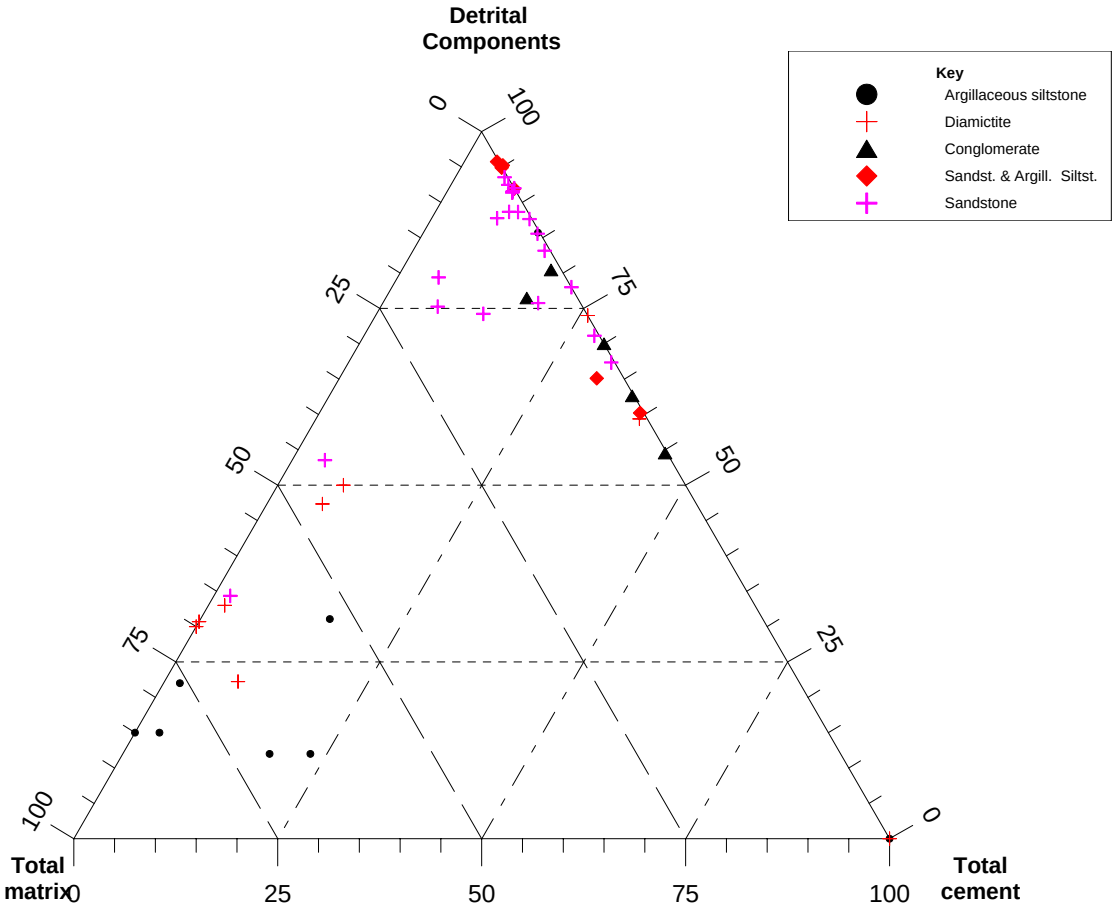
Detrital
Components
Key
Argillaceous siltstone
Diamictite
Conglomerate
Sandst. & Argill. Siltst.
Sandstone
0
100
25
75
50
50
75
25
100
0
Total
matrix
0
25
50
75
100
Total
cement

Figure 1

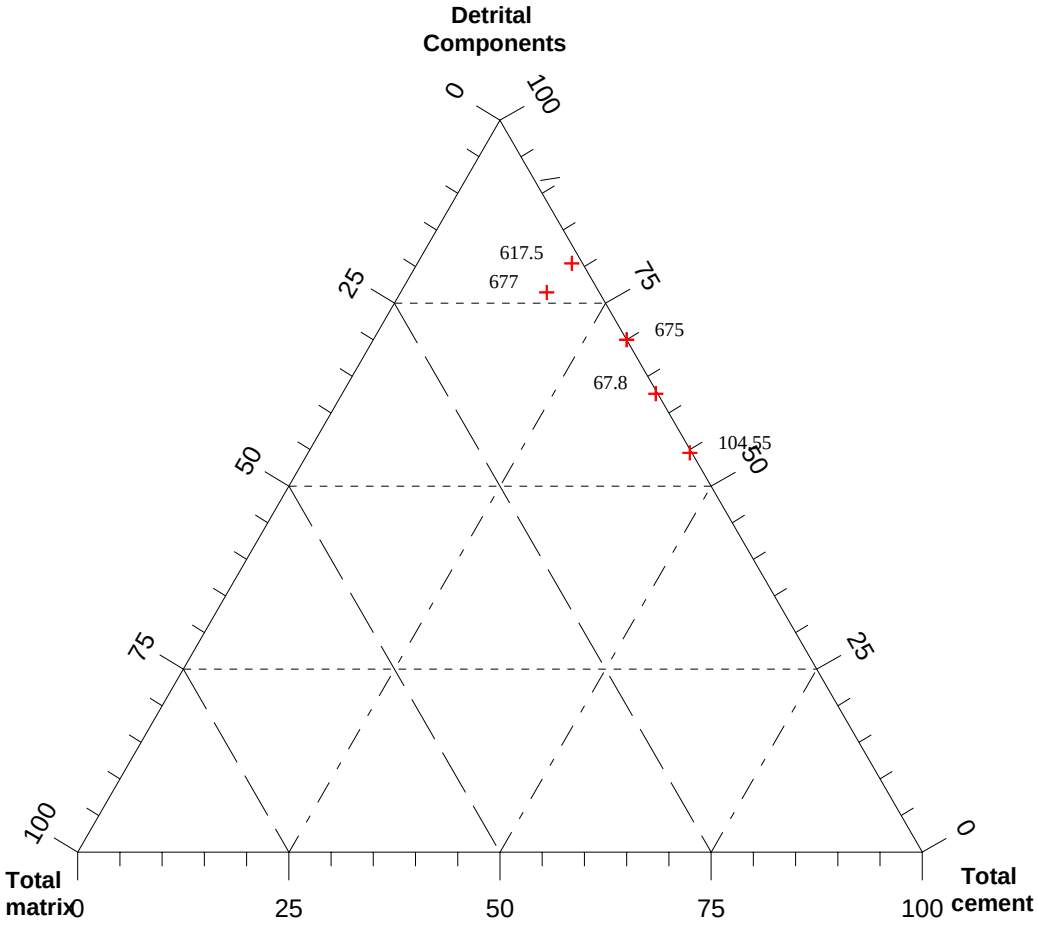
Detrital
Components
0
100
25
75
617.5
677
675
67.8
104.55
50
50
75
25
100
0
Total
matrix
0
25
50
75
100
Total
cement

Figure 2

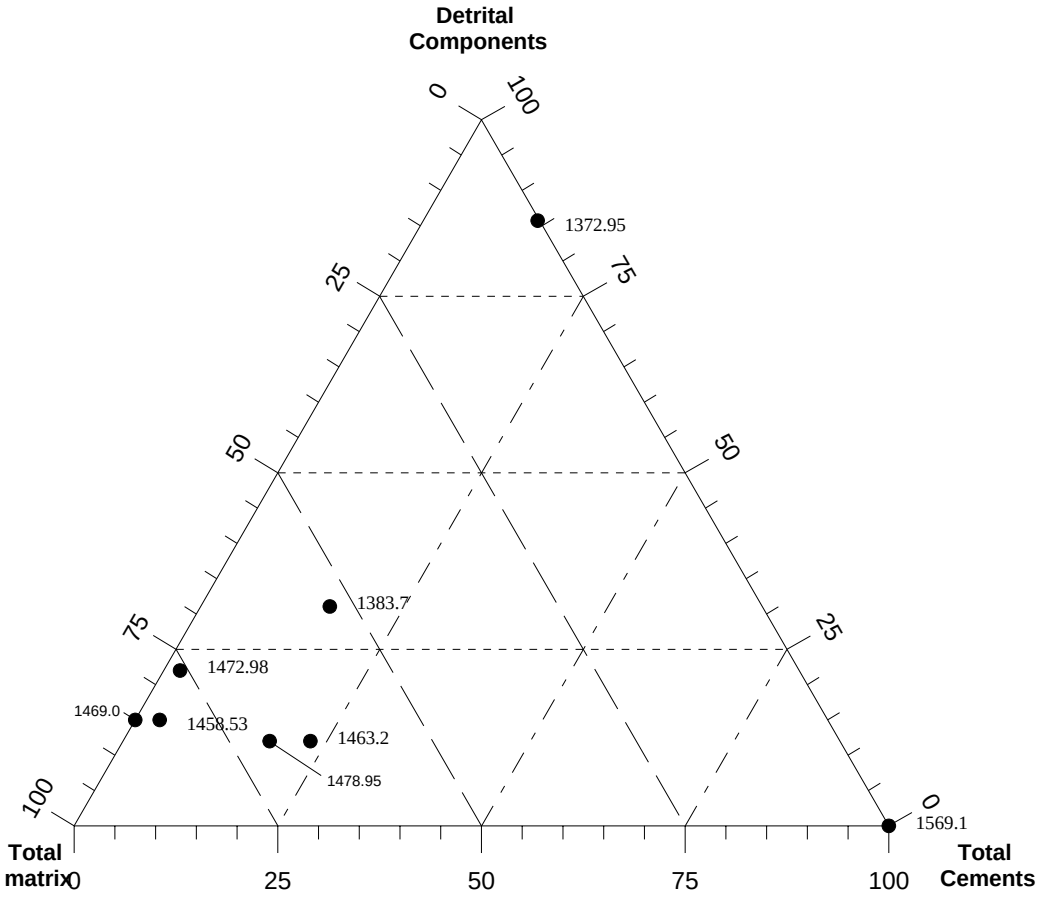
Detrital
Components
0
100
25
75
50
50
75
25
100
0
1372.95
1383.7
1472.98
1469.0
1458.53
1463.2
1478.95
1569.1
Total
matrix
0
25
50
75
100
Total
Cements

Figure 3

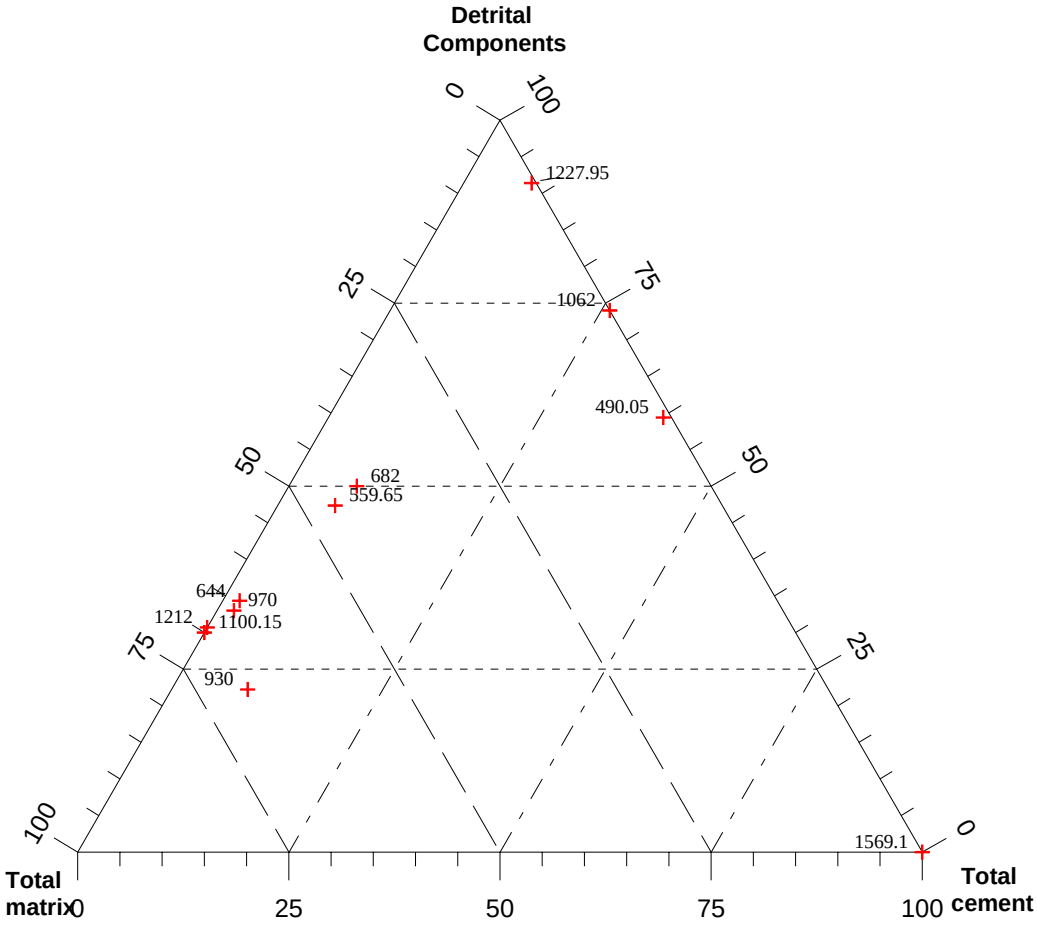
Detrital
Components
0
100
1227.95
25
75
1062
490.05
50
50
682
559.65
644
970
1212
1100.15
75
25
930
100
0
1569.1
Total
matrix
0
25
50
75
100
Total
cement

Figure 4

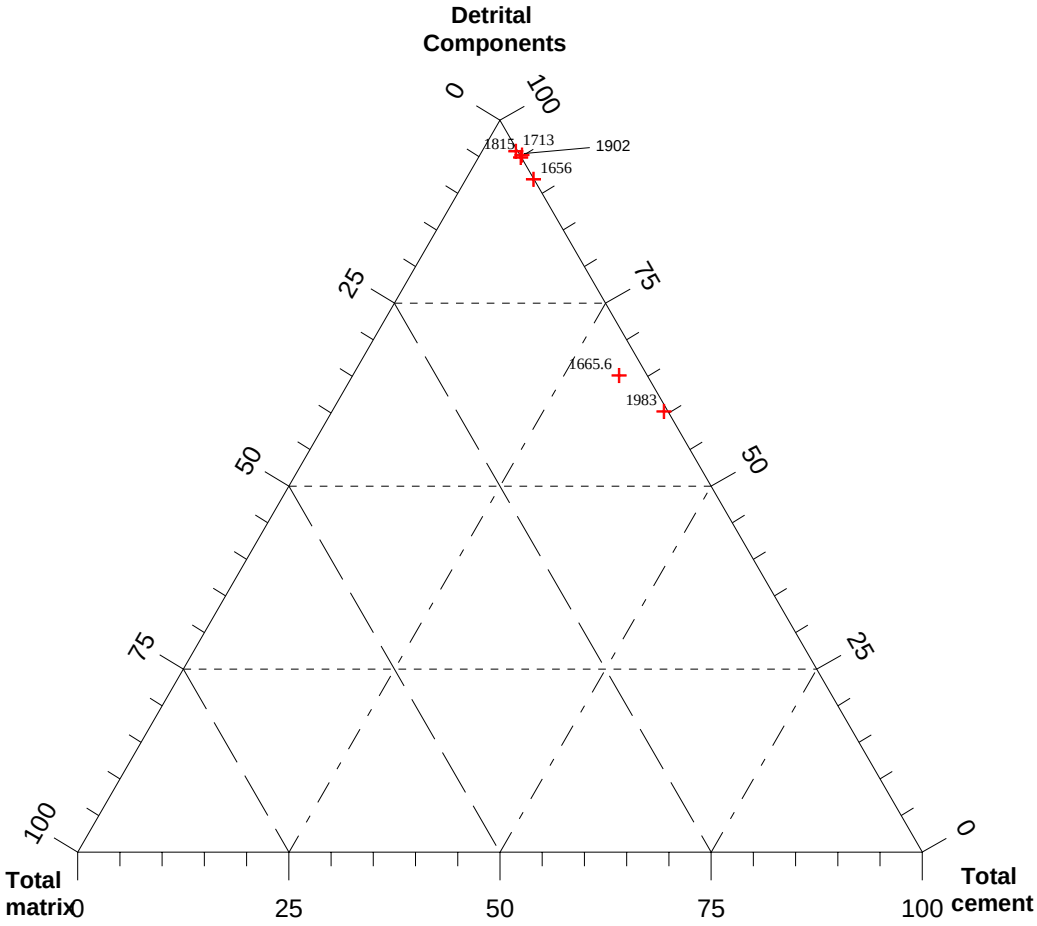
Detrital
Components
0
100
1815
1713
1902
1656
25
75
1665.6
1983
50
50
75
25
100
0
Total
matrix
0
25
50
75
100
Total
cement

Figure 5

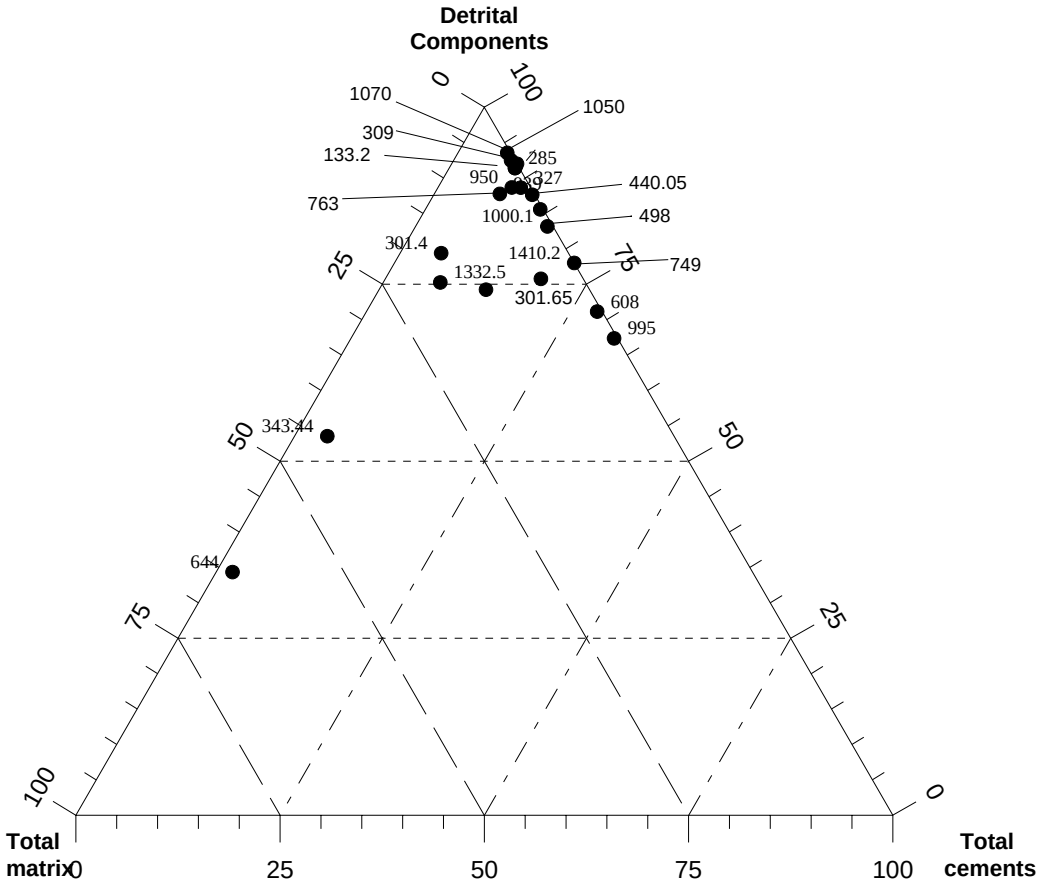
Detrital
Components
0
100
1070
1050
309
133.2
285
950
327
440.05
763
1000.1
498
301.4
1410.2
749
25
75
1332.5
301.65
608
995
343.44
50
50
644
75
25
100
0
Total
matrix
0
25
50
75
100
Total
cements

Figure 6

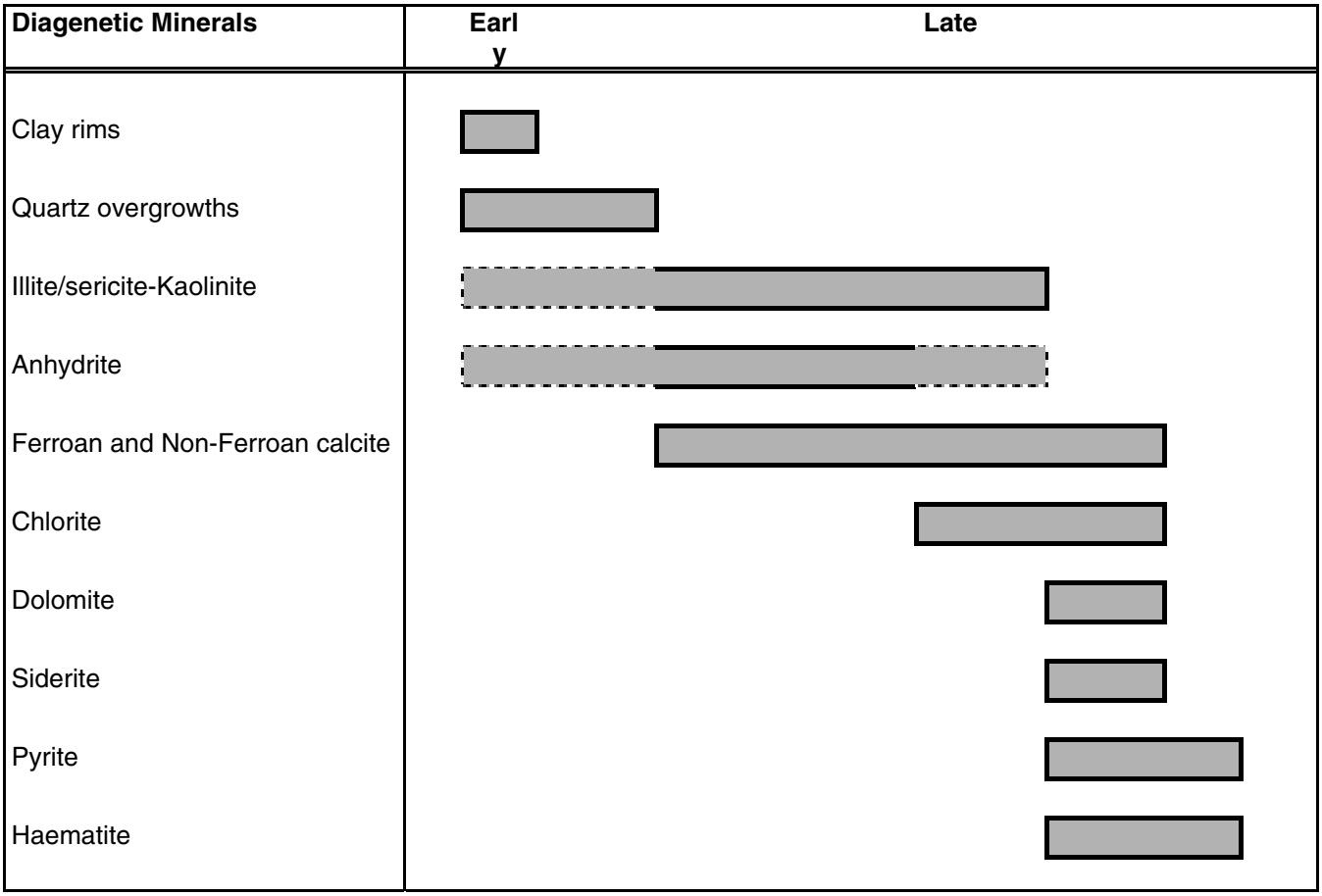

Figure 7

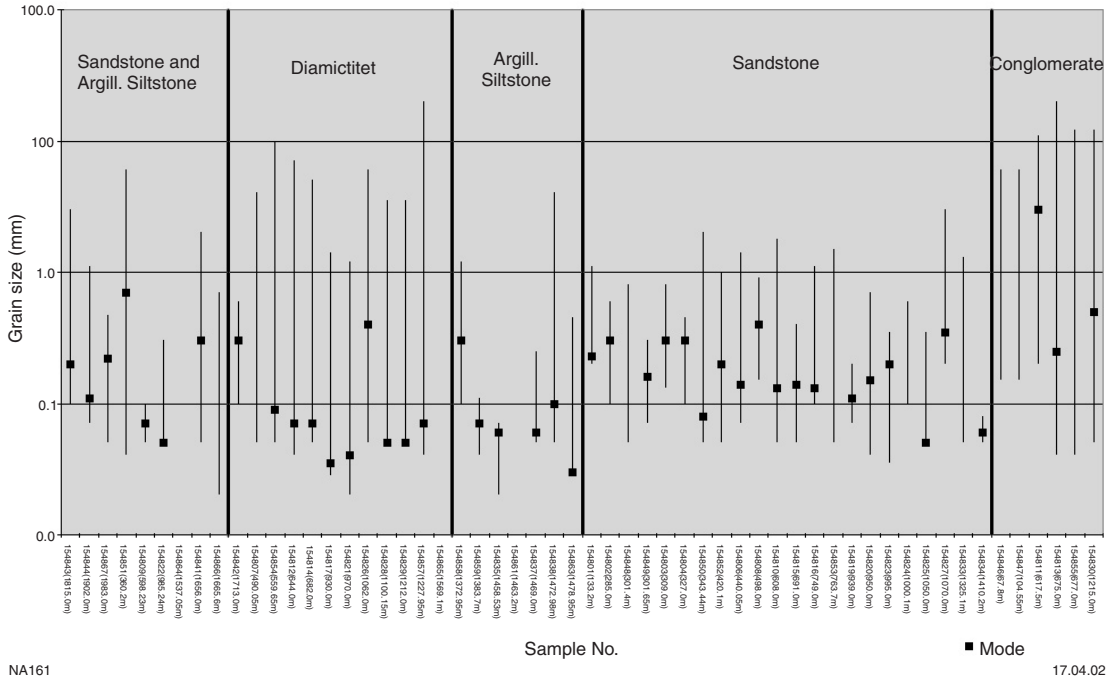

Figure 8

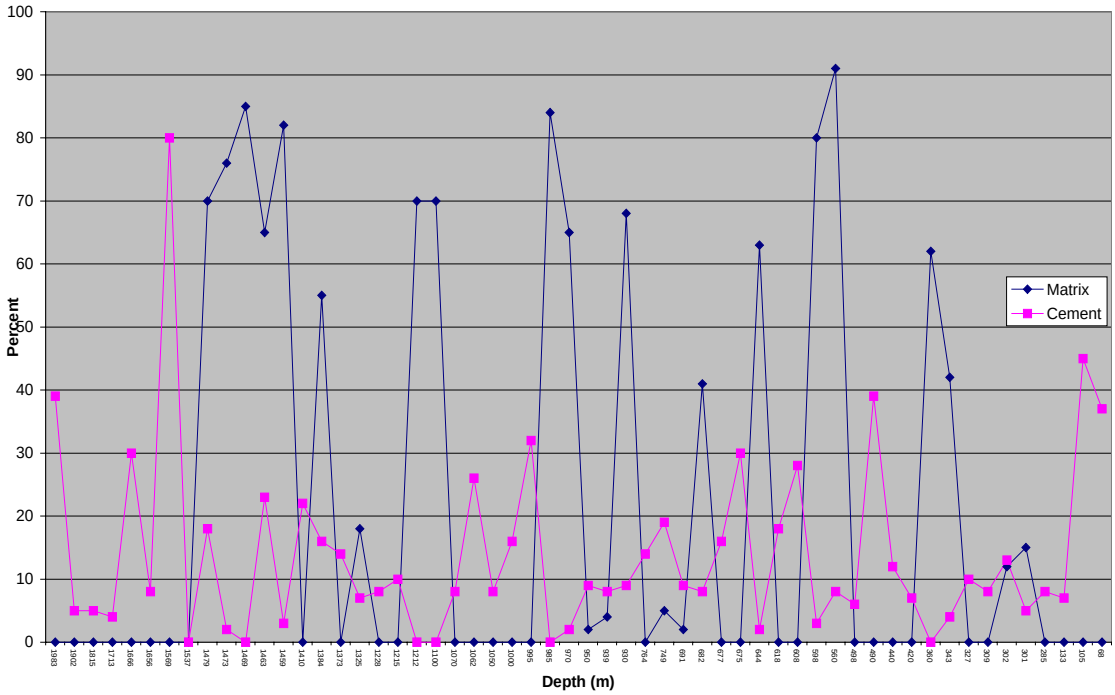

Figure 9

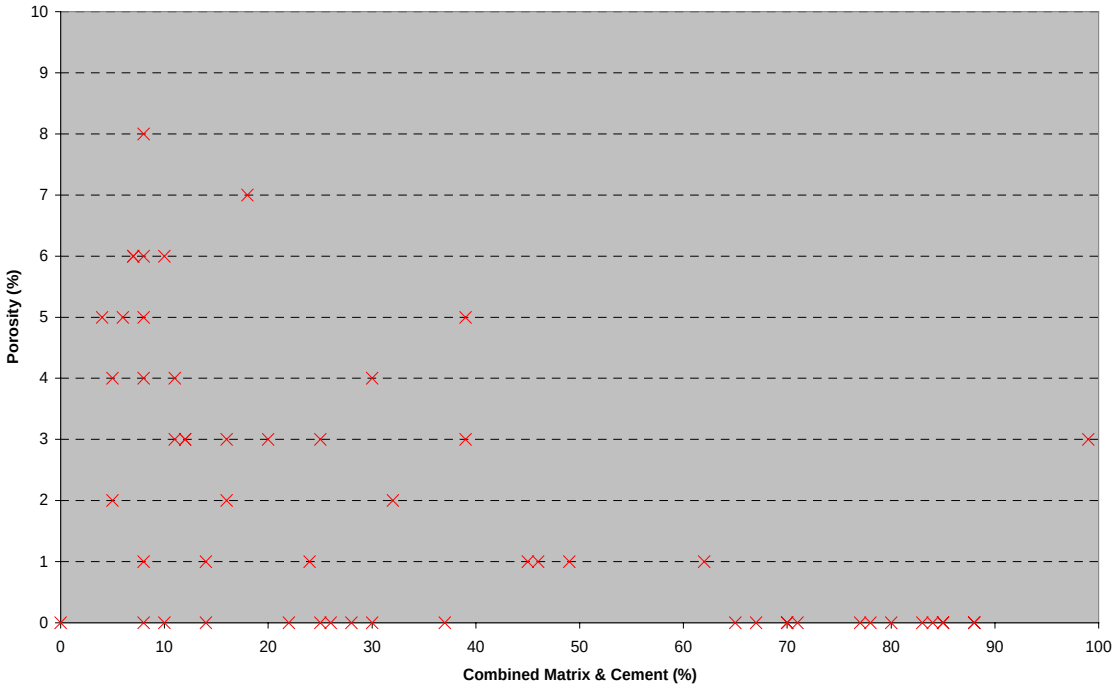

Figure 10

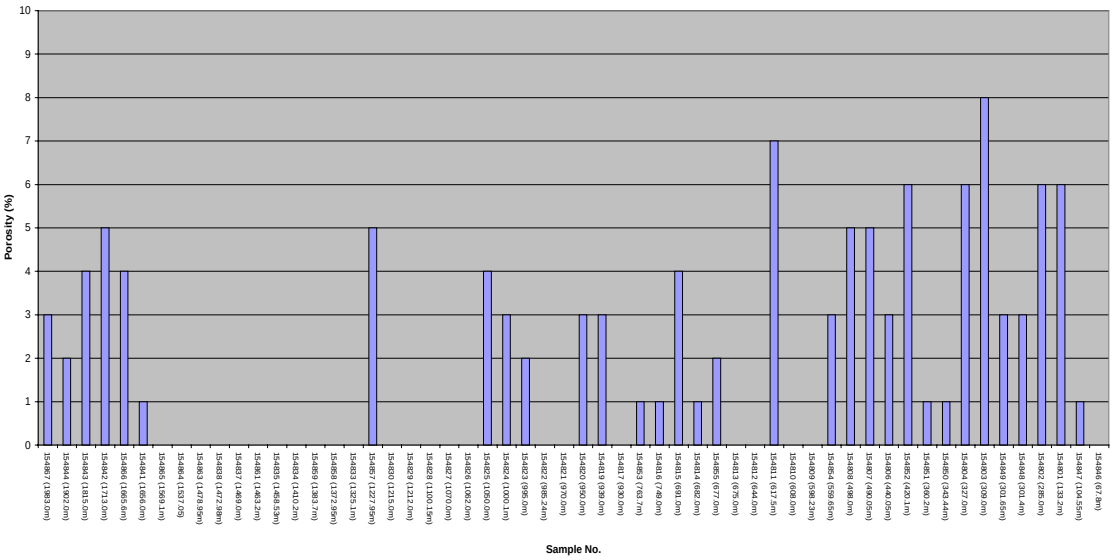

Figure 11

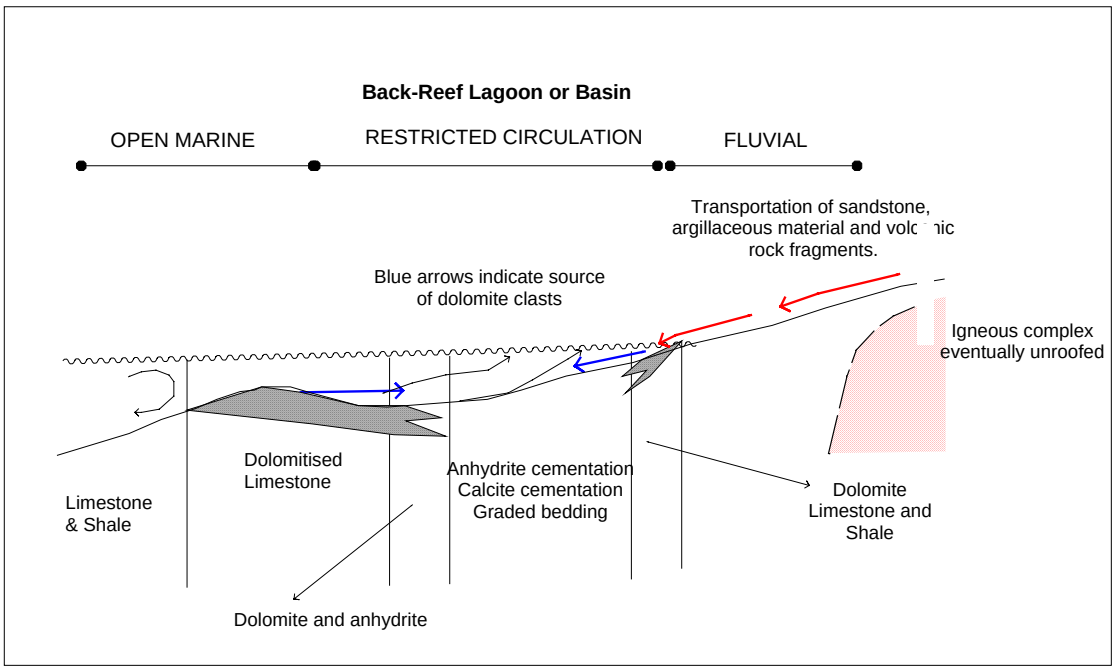

Figure 12

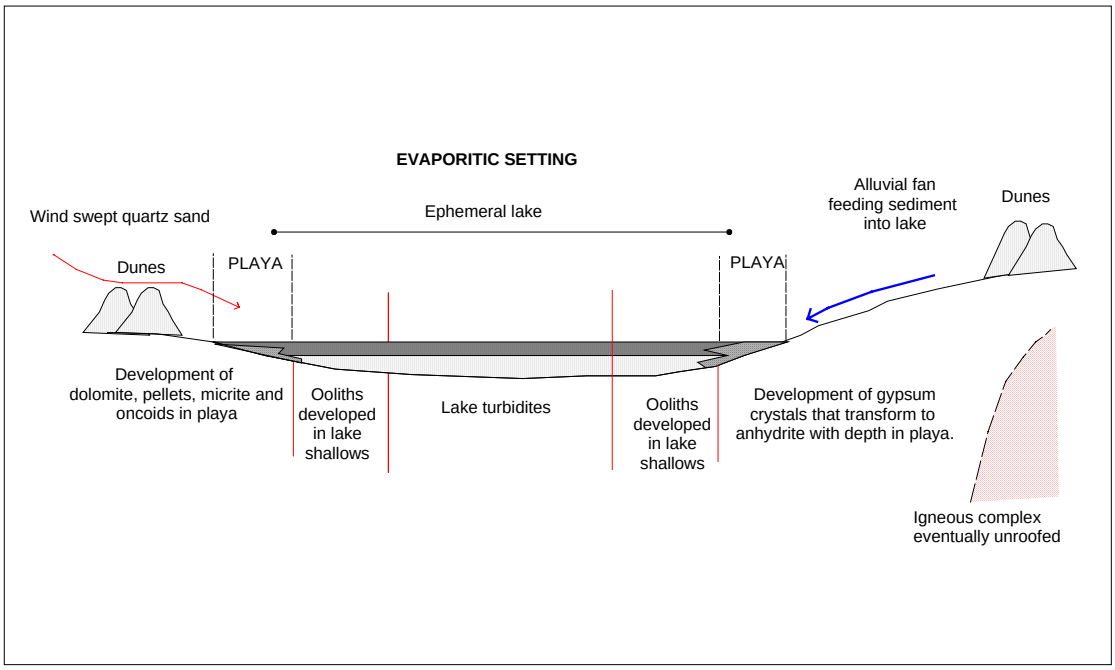
EVAPORITIC SETTING
Wind swept quartz sand
Ephemeral lake
Alluvial fan feeding sediment into lake
Dunes
Dunes
PLAYA
PLAYA
Development of dolomite, pellets, micrite and oncoids in playa
Ooliths developed in lake shallows
Lake turbidites
Ooliths developed in lake shallows
Development of gypsum crystals that transform to anhydrite with depth in playa.
Igneous complex eventually unroofed

Figure 13

1. INTRODUCTION

Sixty four samples were supplied from the Department of Minerals and Energy for thin-section analysis. Samples consisted of a mixture of plugs and core from Vines-1 and Empress 1A. From these samples fifty-nine thin sections and three polished sections were manufactured. These samples were supplied only for brief mineralogical descriptions. All mineralogical percentages provided are estimated through the use of visual estimation charts. No sections in this report were point counted. Due to limitations in microscope resolution the lowest grain size recorded in these samples is 0.02mm. It is important to note that some samples contain a clay-matrix which is sub-microscopic.

2. AIMS

The following report will;

a) Provide a detailed petrographic report and summary of a mixture of 57 plugs and core samples from Vines 1.
b) Provide a brief reflected light description identifying sulphides for three samples: 154856 (1076.75m), 154860 (1395.95m) and 154862 (1465.65m).
c) Observe and comment on sample variations above and below 1076.75m with particular reference to total clay content and porosity between samples
d) Provide two hypothetical models for the deposition of samples.

3. METHODS

A list of samples provided for thin-section analysis is provided in Table 2. All samples were sent to the University of Western Australia for thin section manufacture. Samples were vacuum impregnated and cut into standard 30μm sections by Mr. Frank Nemeth at the University. Sections were stained with Alizarin Red-S and Potassium Ferricyanide under the Dickson (1966) method. This stain is used to distinguish between calcite (red), ferroan calcite (blue), dolomite (no stain), and ferroan dolomite (turquoise). All samples were further stained with blue dye to aid in the identification of porosity.

Mineral percentages were obtained through the visual estimation charts of Harrel (1984). Sorting has been applied from the descriptive terms of Folk and Ward (In: Tucker, 1991). All samples have been named under the classification scheme of Folk (1974).

4. SUMMARY

For simplicity and correlative purposes all samples will be grouped and described in the rock type groupings provided on logs by the Department of Minerals and Energy. All depths listed in the text are core depths. Petrographic samples analysed in this study can be grouped into five general rock types:

a) sandstone and argillaceous siltstone
b) argillaceous siltstone
c) sandstone
d) diamictite
e) conglomerate

In Table 2, samples have been listed with their corresponding rock type grouping and mineralogical classification. Table 1 provides a summary of rock types, and the main mineralogical classifications of samples associated with these rock types.

Table 1. Broad mineralogical classification of samples.

Rock type	Mineralogical classification
Sandstone and argillaceous siltstone	Quartz arenite
Argillaceous siltstone	Micritised mudstone
Sandstone	Quartz arenite, Feldspathic litharenite, sedarenite, lithic wacke
Diamictite	Lithic wacke, sedarenite
Conglomerate	Volcanic arenite, sedarenite

Table 2. List of samples provided for thin-sections analysis

Sample	Depth (m)	Facies	Mineralogical Classification
154867	1983.00	Sandstone and argillaceous siltstone	Quartz arenite
154844	1902.00	Sandstone and argillaceous siltstone	Massive quartz arenite
154843	1815.00	Sandstone and argillaceous siltstone	Laminated quartz arenite
154842	1713.00	Argillaceous siltstone and sandstone	Quartz arenite
154866	1665.60	Argillaceous siltstone and sandstone	Lithic wacke and quartz arenite
154841	1656.00	Argillaceous siltstone and sandstone	Quartz arenite
154865	1569.10	Diamictite	Micritised Mudstone
154864	1537.05	Argillaceous siltstone and diamictite	Micritised Mudstone
154863	1478.95	Argillaceous siltstone	Subhorizontally laminated micrite
154838	1473.95	Argillaceous siltstone	Micritised Mudstone
154837	1469.00	Argillaceous siltstone	Micritised Mudstone
154862	1465.65	Argillaceous siltstone	Micritised Mudstone
154861	1463.20	Argillaceous siltstone	Laminated micritic mudstone
154835	1458.53	Argillaceous siltstone	Micritised Mudstone
154834	1410.20	Sandstone	Quartz arenite
154860	1395.95	Argillaceous siltstone	Micritised mudstone
154859	1383.70	Argillaceous siltstone	Micritised Mudstone
154858	1372.95	Argillaceous siltstone	Micritised Mudstone
154833	1325.10	Sandstone	Interbedded lithic wacke and litharenite
154857	1227.95	Diamictite	Lithic wacke
154830	1215.00	Conglomerate	Lithic wacke
154829	1212.00	Diamictite	Lithic wacke
154828	1100.15	Diamictite	Lithic wacke
154856	1076.65	Conglomerate	Lithic wacke and sedarenite
154827	1070.00	Sandstone	Quartz arenite
154826	1062.00	Conglomerate and diamictite	Sedarenite
154825	1050.00	Sandstone	Laminated quartz arenite
154824	1000.10	Sandstone	Feldspathic litharenite
154823	995.00	Sandstone	Feldspathic litharenite
154822	985.24	Claystone	Claystone
154821	970.00	Diamictite	Lithic wacke
154820	950.00	Sandstone	Quartz arenite
154819	939.00	Sandstone	Feldspathic litharenite
154817	930.00	Diamictite	Lithic wacke
154853	763.70	Sandstone	Sedarenite
154816	749.00	Sandstone	Lithic wacke
154815	691.00	Sandstone	Lithic arkose
154814	682.00	Diamictite	Lithic wacke
154855	677.00	Conglomerate	Sedarenite
154813	675.00	Conglomerate	Lithic wacke and quartz arenite
154812	644.00	Diamictite	Lithic wacke
154811	617.50	Conglomerate	Sedarenite
154810	608.00	Sandstone	Sedarenite
154869	598.69	Claystone	Sedarenite
154854	559.65	Diamictite	Sublitharenite and siltstone
154808	498.00	Sandstone	Quartz arenite
154807	490.05	Diamictite	Sedarenite
154806	440.05	Sandstone	Sedarenite
154852	420.10	Sandstone	Litharenite
154851	360.20	Rhythmites	Lithic wacke
154850	343.44	Sandstone	Lithic wacke and siltstone
154804	327.00	Sandstone	Feldspathic litharenite
154803	309.00	Sandstone	Feldspathic litharenite
154849	301.65	Pebbly Sandstone	Sedarenite
154848	301.40	Sandstone	Litharenite and lithic wacke
154802	285.00	Sandstone	Sedarenite
154801	133.20	Sandstone	Volcanic arenite
154847	104.55	Conglomerate	Volcanic arenite
154846	67.80	Conglomerate	Volcanic arenite
154465	319.0	Sandstone	Quartz arenite
154466	1060.05	Sandstone	Quartz arenite

Apart from the argillaceous siltstone in which all samples are classified petrographically as micritised mudstones, samples from other rock types display some variation petrographically (Table 1). However a dominant classification (shown below) is evident in most of these rock types.

a) Sandstone and argillaceous siltstone- quartz arenite
b) Sandstone- quartz arenite
c) Diamictite- lithic wacke
d) Conglomerate- sedarenite and volcanic arenite.

A ternary plot of total detritals, matrix and cement percentages (Figure 1) for all samples in this study, shows that samples from the same rock types approximately group in the same area on the ternary plot. Argillaceous siltstones plot in the lower left hand corner of the ternary diagram indicating that they contain predominantly matrix (60-85%), with 20 to 35% detrital components and 0 to 24% authigenic cements. Diamictite samples also plot in this vicinity but these samples contain slightly less matrix. Diamictite samples contain between 45 and 70% matrix, 20 to 50% detritals and 0 to 10% cements. Sandstone samples display the widest spread and therefore the greatest compositional variation. These samples mainly plot in the upper right of the ternary diagram but some scattering down the left side of the ternary diagram is evident. As a general observation, these samples are dominated by detrital components (~65-95%), 2 to 30% cements and 0-20% matrix. Conglomerates also plot in the upper right of the diagram. These samples contain between 50 and 75% detrital components, up to 60% matrix (mainly between 0-15%) and up to 33% cement. Finally the sandstone and argillaceous siltstone displays two approximate groupings. The first group consists of approximately 95% detrital components while the second group consists predominantly of a mixture of detrital components and cements. The variations in sample distributions noted will be discussed in further sections of this report.

5. MINERALOGY

In the following section only the dominant mineralogy and structures of samples in their respective rock type groupings will be discussed. The diagenesis and porosity of samples will be discussed in later sections.

5.1 Conglomerate petrographic results

A total of seven samples were analysed from this rock type grouping. These samples and their mineralogical classifications are shown in Table 3 below.

Table 3. Conglomerate samples and corresponding mineralogical classifications.

Sample number	Depth (m)	Mineralogical classification
154830	1215.0	Lithic wacke
154856	1076.65	Sedarenite
154826	1062.0	Sedarenite
154855	677.0	Sedarenite
154813	675.0	Lithic wacke and quartz arenite
154811	617.5	Sedarenite
154847	104.55	Volcanic arenite
154846	67.8	Volcanic arenite

These samples display the widest compositional variation. Samples in this facies have been classified as Sedarenites, lithic wackes and volcanic arenites (Table 1). On observation of individual samples, it is evident that the variations in sample classification reflect differences in rock fragments. As a general rule, samples occurring higher up in the sequence in Vines 1 contain greater volcanic fragments while down sequence samples contain a greater degree of sedimentary rock fragments. No matrix or pseudomatrix component have been identified in any of these samples. Mineralogical components of all samples will be described collectively with references being given to particular samples.

5.1.1 Detrital components

The detrital components of these samples consist predominantly of rock fragments and quartz.

Quartz
Quartz grain percentages are highest in Sample 154830 (1215.0m) where there is approximately 70% quartz. Above this sample quartz percentages range from 5 to 40%. The quartz grain population is dominated by monocrystalline grains with varying percentages of polycrystalline quartz. Quartz grains are angular to sub-rounded and range from coarse silt to medium sand size in most of the samples. Grains are generally poorly sorted and display mainly point contacts.

Feldspar
Feldspar grains are only evident in 154830 (1215.0m), 154856 (1076.65m), 154826 (1062.0m), 154855 (677.0m), 154813 (675.0m) and 154846 (67.80m). Varying percentages of K-feldspar and plagioclase are evident in these samples. Feldspar grains display a similar grain size to quartz grains. Partial dissolution resulting in the vacuolisation of some grains is apparent. Most of these grains have been partially replaced by calcite cements or altered to illite/sericite clays.

Rock fragments
Carbonate clasts
Carbonate clasts are evident in all conglomeritic samples. These clasts form between 2 and 29% of the total rock composition. Clasts are generally sub- to well-rounded and range in size up to pebbles (11mm). They are generally composed of a xenotopic matrix of anhedral to subhedral shaped, very finely to finely crystalline dolomite. Dolomite crystals display planar, curved and sutured contacts. Micritic alteration is evident in most clasts. Most of the micritic patches contained within carbonate clasts consist of equant subhedral to euhedral crystals of microsparite and finer micrite. In some samples patches occasionally contain equant pseudosparic dolomite replacing them indicating that some some aggrading neomorphism of clasts may have occurred. Thin, often discontinuous, isopachous illite/sericite rim is evident coating carbonate clasts in samples 154826 (1062.0m) and 154813 (675.0m). This rim is particularly evident in these samples forming on pressure solution surfaces between clasts.

Ooidal carbonate clasts are evident in samples 154830 (1215.0m), 154856 (1076.65m) and sample 154855 (677.0m). These clasts consist of ooids, 0.1 to 0.3mm in size that have been partially recrystallised by a xenotopic matrix of anhedral to subhedral shaped, very finely to finely crystalline dolomite. Even though ooids have been partially recrystallised their outline has been preserved by a thin micritic rim. Calcite crystals display mainly planar curved and sutured contacts.

Cracking and dissolution and alteration of both types of clasts are not uncommon. Clasts which have been cracked display some alteration or replacement to chert, ferroan calcite or illite/sericite. Chert generally occurs as microsparry accumulations that replace calcite grains.

Sandstone
Sandstone fragments constitute up to 30% of the total rock composition. These fragments are particularly prevalent in samples 154830 (1215.0m), 154856 (1076.65m), 154826 (1062.0m) and sample 154855 (677.0m). Sandstone fragments in these samples range in size up to pebbles (12mm). Sandstone occurring in samples above this point is typically smaller only reaching sizes of granules (2-3mm). Fragments are generally sub-angular to sub-rounded and composed of up to 90% moderately sutured quartz, 1% mica and 9% poikilotopic calcite cement. Nodular pyrite is evident in trace amounts replacing calcite cements and filling intergranular pore space. In sample 154855 (677.0m) sandstone fragments constitute the main detrital component.

Siltstone
Siltstone fragments are evident in most samples. These fragments are composed of varying percentages of silt-sized quartz, mica, illite/sericite and carbonate cements. Mica flakes display in most cases some preferential alignment sub-horizontal to the elongate axis of the fragment. Their shape is often distorted as fragments have been partially squashed into intergranular pore space by mechanical compaction processes. The dark colouration of the illite/sericite clays in these fragments is caused by

the mixture of pyrite and insoluble organic matter. In sample 154830 (1215.0m) a 4mm thick, discontinuous, subhorizontal quartz-rich bed cuts through the centre of a siltstone fragment. This bed consists of well-sutured, coarse-silt sized (0.05mm) quartz that has been partially calcite cemented.

Chert and chalcedony
Chert fragments generally range up to pebble sized. Fragments are generally sub-angular to sub-rounded and composed of patchy microquartz and macroquartz. Alteration of some of these fragments to radiating fibrous crystals of chalcedony and microsparry calcite is evident.

Chalcedony fragments range from trace to 3% in most samples. This type of fragment is only absent in sample 154847 (104.55m). Fragments are generally angular in shape and display a typical chalcedonic texture comprising of radiating fibrous crystals of varying size.

Kaolinite
Kaolinite rock fragments only occur in samples 154830 (1215.0m), 154826 (1062.0m), 154855 (677.0m) and 154813 (675.0m). Kaolinite occurs as sub-rounded to rounded clasts or balls that occupy intergranular pore space. These clasts consist of finely to coarsely crystalline accumulations of kaolinite. Most of the clasts have undergone partial compaction resulting in their expansion of the kaolinite into intergranular pore space.

Shale
The greatest occurrence of shale fragments occurs in samples 154847 (104.5m) and 154846 (67.8m). Below these sample depths, the occurrence of shale fragments is highly variable ranging from nil to 3%. Shale fragments are generally sub-rounded in shape and composed of a dark illite/sericite clay. As in the siltstone fragments this dark colouration is caused by the mixture of pyrite and insoluble organic matter with illite/sericite clays. Partial dissolution and cracking is evident within this fragments. The partial dissociation of some of these fragments has resulted in their alteration to chlorite.

Volcanics
Volcanic fragments are absent or occur in trace amounts in samples 154830 (1215.0m), 154855 (677.0m) and 154813 (675.0m). The main occurrence of these samples is (154811, 154847 and 154846) between the depths of 617.5m and 67.80m. Volcanic fragments in these samples form between 10 and 32% of the total rock composition. The concentration of volcanic rock fragments at shallower depths may be indicative of a change to a more volcanically active environment. Another plausible explanation, is that at greater depths most of the volcanic fragments may have been broken down and completely altered.

Several types of volcanic rock fragments are evident in samples 154811 (617.5m), 154847 (104.5m) and 154846 (67.8m). The most common volcanic rock fragments in these samples are altered alkali basalt and alkali olivine basalt. These fragments are sub-angular to sub-rounded in shape and range up to pebble size. Altered alkali basalts consist of large laths of plagioclase supported by a black cryptocrystalline matrix. Alkali olivine basalts consist of clear feldspar laths, sub-ophitically enclosed by brownish augite laths and opaque pyrite. Partial alteration and replacement of both of these volcanic fragments to chlorite and calcite respectively, is evident. Grain boundaries are often diffuse and fragments have been partially dispersed into intergranular pore space.

Other volcanic rock fragments that characterise sample 154847 (104.5m) are Urtite, Microgranite, Phonolite and undifferentiated volcanics. These rock fragments also range up to pebble size. Urtite grains consist predominantly of large nephline flakes and minor amounts of alkali pyroxene and amphibole. Microgranite rock fragments consist of intergrown quartz and alkali feldspar grains that have a granophyric texture. These grains have been marginally replaced by calcite cements.

5.1.2 Cements and replacement fabrics

Only the main cements and replacement fabrics will be discussed in this section as others have been briefly discussed in the section above.

Non-ferroan calcite
Most non-ferroan calcite occurs as poikilotopic and patchy micro-sparry pore-filling cement and grain/clay replacement. The cement forms highly corrosive contacts with surrounding detrital grains. Non-ferroan calcite occurs as single crystal poikiloptopes or microsparry accumulations of very finely crystalline calcite that fills intergranular pore space, encases clusters of framework grains and replaces clays. This cement also forms highly corrosive contacts with surrounding detrital grains and is often evident marginally replacing framework grains.

Siderite
Trace siderite cementation is only evident in sample 154830 (1215.0m). Siderite cement is evident replacing intergranular pore space and marginally replacing or poisoning detrital grain boundaries. Siderite forms as either single isolated crystals or as small microsparry accumulations.

Illite/sericite
Authigenic illite/sericite is associated with;

a) Micaceous, feldspar grains and volcanic rock fragments that have partially decomposed and dispersed
b) Solution seams or microstylolites
c) Coating detrital grains

Increases in authigenic illite/sericite coincide with the greater occurrence of microstylolites and solution seams along pressure solution surfaces between fragments. Pyrite and insoluble organic matter is often associated with illite/sericite along microstylolites and solution seams giving it a dark colouration. Alteration of feldspars in volcanic fragments has resulted in the formation of illite/sericite cements.

Chlorite
Chlorite mainly forms as a late stage alteration product of clays and feldspars. It is evident particularly in volcanic fragments where it replaces illite/sericite clays. The occurrence of chlorite in samples is variable but it is existent in all samples to some degree.

Anhydrite
Trace amounts of anhydrite are evident in sample 154826 (1062.0m). This cement forms as a massive pore filling cement that fills pores between rock fragments. It generally forms sharp contacts with surrounding detrital grains.

5.1.3 Structures

Most of the samples in this suite are structureless. Only three samples contain any identifiable structures, these are samples 154856 (1076.65m), 154813 (675.0m) and sample 154811 (617.5m). In sample 154813 a sharp sub-vertical contact between a well-sutured quartz arenite and overlying lithic wacke is evident. Sample 154811 is generally massive, however, in places thin, discontinuous, sub-horizontal solution seams and microstylolites are evident. These structures mainly occur on pressure solution surfaces between detrital fragments.

5.2 Argillaceous siltstone and claystone petrographic results

A total of seven samples were analysed from this rock type grouping. These samples and their mineralogical classifications are shown in Table 4 below.

Table 4. Listing of argillaceous siltstone samples and their mineralogical classification

Sample number	Depth (m)	Mineralogical classification
154864	1537.05	Micritised mudstone
154838	1473.95	Micritised mudstone
154837	1469.00	Micritised mudstone
154862	1465.65	Micritised mudstone
154861	1463.20	Micritised mudstone
154835	1458.53	Micritised mudstone
154860	1395.95	Micritised mudstone
154859	1383.70	Micritised mudstone
154858	1372.95	Micritised mudstone
154822	985.24	Claystone
154869	598.23	Lithic wacke
154851	360.20	Lithic wacke

Argillaceous siltstone and claystone samples are the most homogenous. Figure 3 illustrates that these samples are compositionally similar. The only sample that differs considerably is sample 154858 (1372.95m). The greater occurrence of rock fragments in this sample suggests that it may be representative of a thin diamictite bed. Consequently this sample has been described in the diamictite section of this report.

5.2.1 Detrital components

Quartz

Samples range between 10 and 25% quartz. Samples are dominated by angular to sub-rounded monocrystalline quartz that displays a mode grain size of approximately medium silt. Grains are generally poorly-sorted and matrix supported. Grains predominantly display point to concave/convex, grain-grain contacts.

Feldspar

Preservation of feldspar grains is evident in some samples 154863 (1478.95m) and 154837 (1469.0m). These grains are of similar size to quartz grains. Samples are generally dominated by albite varieties. No alteration of these grains is evident.

Rock fragments

Rock fragments are absent in samples 154863 (1478.95m) and 154835 (1458.53m). In all other samples it may range up to 4% of the total mineralogical composition.

Carbonate clasts

Carbonate clasts range up to very coarse sand sized (1.5mm) but display a mode of medium sand (0.3mm). Clasts are generally sub- to well rounded and composed of a xenotopic matrix of anhedral to subhedral shaped very finely to finely crystalline dolomite that displays planar curved and sutured contacts. Some of these clasts display micritisation. Patchy aggrading neomorphism of some of these clasts has resulted in an increase in crystal size.

Sandstone

Sandstone fragments are only evident in sample 154838 (1473.95m). Fragments are predominantly composed of coarse silt sized (0.05mm) quartz grains, mica and poikilotopic calcite cement. In this sample a series of 0.2mm thick, sub-vertical mica-rich illite/sericite seams cut through the fragment.

Chert

Chert grains are generally composed of microcrystalline quartz. These fragments are sub-rounded and display a mode of very fine sand.

5.2.2 Matrix/ Pseudomatrix

Illite/sericite
A complex mixture of cryptocrystalline illite/sericite and micritic mud constitutes up to 52 and 85% of these samples. The micritic mud is composed predominantly of very finely crystalline calcite that occurs as isolated grains and microsparry accumulations that partially replace illite/sericite. The dark colouration of the illite/sericite clays is caused by the accumulation of authigenic pyrite and insoluble organic matter with illite/sericite. The microcrystalline nature of the micrite grains (peloids) in these samples suggests that they are original and not replacement of previous framework grains.

5.2.3 Cements and replacement fabrics

Anhydrite
Anhydrite is evident in samples 154837 (1469.0m), 154862 (1465.65m), 154861 (1463.2m), 154835 (1458.53m), 154860 (1395.95m) and 154859 (1383.7m). It forms mainly as a fracture filling cement, however in sample 154859 it is evident as a massive, partially leached cement that encases framework grains and fills burrows.

Chlorite
Chlorite is evident in sample 154861 (1463.2m) as an alteration product of illite/sericite clays. It defines the tops of sequences in this sample occurring as 0.5mm thick layers that characterise the top of each laminae.

Siderite
Trace siderite cementation is only evident in sample 154859 (1383.7m). Siderite cement is evident replacing intergranular pore space and marginally replacing or poisoning detrital grain boundaries. Siderite forms as either single isolated crystals or as small microsparry accumulations.

5.2.4 Structures

Turbidites
Turbidite beds are evident in samples 154863 (1478.95m), 154861 (1463.2m), 154835 (1458.53m) and 154869 (598.23m). Turbidite samples are generally characterised by fining-upwards laminae. Laminae are typically millimetre thick and consist primarily of graded silt to fine sand sized quartz fining upwards into rippled, convoluted and mildly bioturbated illite/sericite mud. In samples 154861, 154835 and 154859 intense bioturbation and reworking have resulted in the samples having a mottled appearance. A thin chlorite-rich condensed section is evident at the top of each turbidite sequence in sample 154861.

Soft sediment deformation is evident in some of the turbidite samples. In sample 154863 (1478.95m) small flame structures are evident where silt sized quartz has been forced upwards into the overlying laminae.

Micro-faulting
In sample 154863 (1478.95m) a low angle reverse micro-fault is evident. This fault has caused the minor displacement of and the curving of fining-upwards laminae into the fault plane. Traces of micro-fracturing and soft sediment deformation are also evident in sample 154861 (1463.2m).

5.3 Diamictite petrographic results

A total of eleven samples were analysed from this rock type grouping. These samples and their mineralogical classifications are shown in Table 5 below.

Table 5. Listing of diamictite samples and their corresponding mineralogy.

SAMPLE NO	DEPTH	MINERALOGICAL CLASSIFICATION
154865	1569.10	Micritised mudstone
154857	1227.95	Lithic wacke
154829	1212.00	Lithic wacke
154828	1100.15	Lithic wacke
154826	1062.00	Sedarenite
154821	970.00	Lithic wacke
154817	930.00	Lithic wacke
154814	682.00	Lithic wacke
154812	644.00	Lithic wacke
154854	559.65	Sublitharenite and siltstone
154807	490.05	Sedarenite

Apart from samples 154865 (1569.1m), 154826 (1062.0m), 154854 (559.65m) and 154807 (490.05m) this rock type grouping is dominated by lithic wackes. A ternary plot (Figure 4) of total detrital components, matrix and cements shows that the majority of samples group in the bottom left of the ternary diagram and are composed of approximately 55 to 80% matrix, and 15 to 25% detrital grains and cement. Lithic wackes are predominantly composed of quartz, feldspar and rock fragments, supported by a complex mixture of illite/sericite and carbonate mud. Rock fragments common to diamictite samples include: carbonate, chert, kaolinite, chalcedonic silica, chalcedony, shale, sandstone and volcanics.

5.3.1 Detrital components

Quartz

Quartz grains form between 10 and 38% the total composition of these samples. Grains range from coarse silt to coarse sand and are typically angular to sub-rounded and poorly sorted. Grains display mainly point to concave/convex grain-grain contacts.

Feldspar

Varying percentages of albite and other plagioclase varieties dominate these samples. Grains are typically of similar size to quartz grains and do not display any alteration.

Rock fragments

Carbonate clasts

In most samples carbonate clasts range up to granule size. However in sample 154857 (1227.95m) pebble sized fragments are evident. Clasts are generally sub-to well-rounded and consist of a xenotopic matrix of anhedral to subhedral shaped very finely to finely crystalline dolomite. Patchy micritic alteration is evident in most of these clasts. Partial replacement of micrite by non-equant pseudospar indicates that some clasts have undergone aggrading neomorphism.

Ooidal carbonate fragments are evident in samples 154829 (1212.0m), 154812 (644.0m) and 154854 (589.65m). These fragments consist of micritised ooids, 0.1 to 0.3mm in size that have been partially recrystallised by a xenotopic matrix of anhedral to subhedral shaped very finely crystalline dolomite. In some samples clast boundaries have been marginally replaced by secondary calcite cements.

Chert and chalcedony

Fragments range up to very coarse sand (1.1mm) in size. Chalcedonic fragments are typically angular while chert fragments display a rounded to sub-rounded grain shape. Chalcedonic fragments are composed of radiating fibrous crystals of varying size. Chert fragments are mainly composed of microquartz, but megaquartz patches are occasionally evident.

Sandstone

Sandstone fragments are typically sub-rounded to rounded and composed of moderately to well sutured fine sand sized quartz grains that are cemented by chloritised clay and poikliotopic and microsparry calcite cements.

Siltstone
Partial alteration of siltstone fragments has often made them difficult to distinguish from the clay-rich groundmass. Fragments are typically angular to sub-rounded and consist of a mixture of quartz, mica and illite/sericite clay. In some samples quartz and mica flakes display a weak preferential alignment sub-horizontal to the elongate axis of the fragment. Heavy leaching has resulted in the partial leaching and dissolution of these fragments and their incorporation into the surrounding groundmass.

Kaolinite
Kaolinite is only evident in samples 154857 (1227.95m), 154854 (559.65m) and 154858 (1372.95m). Kaolinite occurs mainly as sub-rounded to rounded clasts that occupy intergranular pore space. These clasts consist of finely to coarsely crystalline accumulations of kaolinite that has been partially compacted and as a result have expanded into intergranular pore space.

5.3.2 Matrix/ pseudomatrix

Diamictite samples are bound together by a complex mixture of fine grained illite/sericite clay and micrite. Illite/sericite displays a dark colouration caused by the accumulation of pyrite and insoluble organic matter with illite/sericite clays. Very finely crystalline calcite grains are evident as single crystals or small microsparry accumulations, partially replacing illite/sericite. The matrix and pseudomatrix component of these samples forms between 41 and 70% of total sample composition in samples 154829 (1212.0m), 154828 (1100.15m), 154821 (970.0m), 154817.(930.0m), 154814 (682.0m) and 154812 (644.0m).

5.3.3 Authigenic cements

Pyrite
The main authigenic cement evident in 29 out of 56 samples in Vines 1. Pyrite occurs both in a nodular form and in a massive grain replacement form.
Siderite
It is evident in some samples where it occurs as small microcrystalline accumulations that replace the carbonate mud matrix and marginally coat detrital quartz grains.

5.3.4 Structures

Structurally most diamictite samples are massive. The only structures evident are in samples 154821 (970.0m) and 154817 (930.0m), which display burrow-mottling, and sample 154854 (559.65m), which displays a sharp contact.

Burrows
Burrows are typically 1 to 1.5mm in diameter. Sections through burrows occur as both transverse sections and sub-vertical sections. Burrows are typically filled with medium sand sized quartz that is cemented by poikilotopic calcite, ferroan calcite and siderite. Calcite cement generally occurs as non-equant porphyrotopic calcite.

5.4 Sandstone and argillaceous siltstone petrograhic results

A total of six samples were analysed from this rock type grouping. These samples and their mineralogical classifications are shown in Table 6 below.

Table 6. Table of sandstone and argillaceous siltstone samples and their corresponding mineralogical classifications.

Sample number	Depth (m)	Mineralogical classification
154867	1983.0	Quartz arenite
154844	1902.0	Quartz arenite
154843	1815.0	Quartz arenite
154842	1713.0	Quartz arenite
154866	1665.6	Dominantly quartz arenite
154841	1656.0	Quartz arenite

Apart from samples 154867 (1983.0m) and 154866 (1665.6m) this rock type grouping is dominated by quartz arenites. A ternary plot (Figure 5) of total detrital components, matrix and cement shows that the majority of samples are characterised by high quartz, minor cementation and no observable matrix. Samples 154866 and 154867 contain significantly less quartz and a higher total cement component. The following section will collectively describe the mineralogy of all sections with particular note of the observed differences in sections 154866 and 154867.

5.4.1 Detrital components

Quartz

Excluding samples 154867 (1983.0m) and 154866 (1665.6m) total quartz percentages in other samples ranges between 79 and 83%. The quartz percentages in samples 154866 and 154867 are 43% and 56% respectively. The quartz grain population is dominated by monocrystalline grains with varying percentages of polycrystalline varieties. Grains are predominantly angular to sub-rounded and moderately sorted. In the quartz arenites, pressure solution is evident with most grains displaying concave/convex to well-sutured grain-grain contacts. Point, concave/convex and moderately sutured grain-grain contacts characterise samples 154866 and 154867. Vacuoles or fluid inclusions are evident in most quartz grains. They are defined by dark specks that cut across quartz grains. Traces of thin authigenic silica overgrowths are also apparent on some quartz grain boundaries.

Feldspar

Both K-feldspar (microcline) and plagioclase (albite) are evident in this sample. Feldspar grains display a similar grain size to quartz grains. Most of the grains in samples have undergone partial dissolution and alteration to alteration to kaolinite, sericite and calcite.

Muscovite

Trace muscovite is evident in some samples. Muscovite generally occurs as partially altered bent or broken laths.

Rock fragments

Rock fragments form a minor percentage of all samples. Common rock fragments include carbonate, chert, sandstone, kaolinite, chalcedony, siltstone and shale. In sample 154866 the occurrence of lithoclasts has also been noted.

Carbonate

With the exception of sample 154841(1656.0m) all carbonate clasts in other sample range between medium to very coarse sand. These clasts are generally sub- to well-rounded and composed of a xenotopic matrix of anhedral to subhedral shaped very finely to finely crystalline dolomite that displays planar curved and sutured contacts. Micritic alteration of some of these clasts is evident. Compaction has resulted in some of the grains being deformed and squashed into intergranular pore space.

Sandstone

Traces of sandstone fragments are evident in some of these samples. These fragments are difficult to distinguish from the surrounding host rock as they are compositionally similar. However, quartz grains within these fragments tend to be smaller having a mode of coarse silt. These grains are generally sub-angular to sub-rounded, moderately sorted and cemented by poikilotopic calcite.

Kaolinite

Kaolinite occurs as sub-rounded to rounded clasts. These clasts consist of coarsely to finely crystalline accumulations of kaolinite. Most of the clasts have undergone moderate compaction, which has resulted in their deformation and expansion into intergranular pore space.

Shale

These fragments are typically medium to coarse sand sized and angular to sub-angular in shape. Alteration of some of these fragments to sericite and chlorite is evident.

Chert and chalcedony

Chert fragments generally range up to medium sand sized. Fragments are generally sub-angular to sub-rounded and composed of microquartz with patches of macroquartz. Alteration of some of these fragments to radiating fibrous crystals of chalcedony and microsparry calcite is evident.

Siltstone
Siltstone fragments are mainly composed of illite/sericite with minor percentages of quartz and mica. Mica flakes display some minor preferential alignment sub-horizontal to the elongate axis of the fragment. Grain shape is often distorted as grains have been partially compacted into intergranular pore space.

Lithoclasts
Lithoclasts are only evident in sample 154866 (1665.6m). These lithoclasts consist of a mixture of concentric microquartz and chalcedonic silica. Microquartz is evident as elongate grains varying in size from 0.7mm to 1.1mm. Radiating crystals of chalcedonic silica generally form the cement between these nodules. These crystals increase slightly in size towards the centre of pores.

5.4.2 Authigenic cements

Calcite
Quartz arenite samples contain an average of approximately 5% calcite cement. This percentage is significantly higher in samples 154867 (1983.0m) and 154866 (1665.6m), which contain 8% and 35% respectively. Irrespective of differences in percentages of total calcite cement in samples, fabric and texture of calcite cements is similar for all samples. The cement occurs as single crystal poikilotopes and microsparry accumulations of very finely crystalline calcite that fills intergranular pore space and encases clusters of framework grains. Calcite cement is also evident replacing leached framework grains. Traces of dolomite are often evident marginally replacing calcite cements. Dolomite generally occurs as isolated rhombs and microsparry accumulations.

Authigenic silica
The earliest identifiable cement is quartz overgrowth cement. Most of the cement occurs as single growths on quartz grains but in rare cases triple junctions have been formed. Triple junctions are formed by the mutual interference of individual silica overgrowths.

Ferroan calcite
Ferroan calcite is only evident in samples 154867 (1983.0m) and 154866 (1665.6m). In these samples it mainly forms as small disseminated grains and aggregates that partially fill intergranular pore space and marginally replace carbonate cements and detrital grain boundaries.

Sericite
Sericite is only evident in sample 154866 (1665.6m). The sericitic cement forms approximately 17% of this slide. Partial alteration of sericite to micritic calcite is evident. The cement forms highly corrosive contacts with surrounding detrital grains.

Illite/sericite
Illite/sericite occurs concentrated along thin, sub-horizontal stylolites in sample 154866 (1665.6m) and as sub-rounded grains in sample 154867 (1983.0m). The grains in sample 154867 have undergone some compaction and consequently have been deformed and squashed into intergranular pore space. Illite/sericite cements generally have a dark brown colouration.

5.4.3 Structures

Most of the samples in this grouping are massive. The only samples that display any structures are sample 154843 (1815.0m), which displays weak, discontinuous, sub-horizontal lamination and sample 154866 (1665.6m), which displays a series of thin, wispy, sub-horizontal stylolites. Stylolites are generally concentrated in the more clay-rich portion of sample 154866.

5.5 Sandstone Petrographic results

A total of 21 samples were analysed from this rock grouping. Table 7 shows that sandstone samples consist mainly of quartz arenites, feldspathic litharenites and sedarenite with minor occurrences of lithic wackes and volcanic arenites. Quartz arenites are dominant in sandstones between the depths of 1050-1410.20m, feldspathic litharenites between 939 to 1000.10m and 309-327m, and sedarenites between 440.05-763.70m. A ternary plot of total detrital components, matrix and cement shows that apart from samples 154823 (995.0m), 154812 (644.0m), 154810 (608.0m) and 154850 (343.44m) other samples are composed of 75% or greater detrital components and up to 30% cement. Matrix component is variable, and in most samples it forms only a minor constituent, not reaching higher than

10% of total sample composition. Apart from differences in the overall percentages of detrital components, matrix and cements most samples are compositionally similar. The following section will describe the collective mineralogy of sandstone suite. Particular note will be taken to subtle differences between samples.

5.5.1 Detrital components

Average framework grain composition of sandstones is approximately 60% quartz, 3% feldspar, 4% carbonate clasts and 2% volcanics and trace to 1% heavy minerals and other rock fragments. Other rock fragments consist of a mixture of volcanic and sedimentary rock fragments, they include shale, chert, chalcedony, sandstone, siltstone and kaolinite.

Table 7. List of sandstone samples and their respective mineralogical classifications.

SAMPLE	DEPTH	MINERALOGICAL CLASSIFICATION
154834	1410.20	Quartz arenite
154833	1325.10	Lithic wacke and litharenite
154827	1070.00	Quartz arenite
154825	1050.00	Quartz arenite
154824	1000.10	Feldspathic litharenite
154823	995.00	Feldspathic litharenite
154820	950.00	Quartz arenite
154819	939.00	Feldspathic litharenite
154853	763.70	Sedarenite
154816	749.00	Lithic wacke
154812	644.00	Lithic arkose
154810	608.00	Sedarenite
154808	498.00	Sedarenite
154806	440.05	Sedarenite
154850	343.44	Lithic wacke and siltstone
154804	327.00	Feldspathic litharenite
154803	309.00	Feldspathic litharenite
154849	301.65	Sedarenite
154848	301.40	Litharenite and lithic wacke
154802	285.00	Sedarenite
154801	133.20	Volcanic arenite

Quartz

Apart from samples 154810 (608.0m) and 154850 (343.44m) total quartz percentages in samples range between 50 and 83%. The quartz grain population is dominated by monocrystalline grains with varying percentages of polycrystalline varieties. Quartz grains display a variable grain size mode but in most samples, grain sizes range from coarse silt to coarse sand. Samples 154853 (763.7m), 154824 (1000.1m), 154825 (1050.0m) and 154848 (301.4m) display a bimodal quartz grain size distribution. The bimodal grain size observed in these sections can be attributed to thin, sub-horizontal laminae that contain either a finer or coarser quartz fraction than the surrounding host rock.

Grains are generally sub-angular to sub-rounded. The shape of grains may vary, however, as quartz grain margins have been partially replaced in most samples by authigenic silica, calcite or anhydrite cements. Minor authigenic silica overgrowth cementation is evident in samples 154803 (309.0m), 154823 (995.0m), 154852 (420.1m) and 1554827 (1070.0m). Overgrowth formation has been impeded in samples 154804 (327.0m), 154848 (301.4m) and 154852 (420.1m) by the occurrence of isopachous rims on quartz grain boundaries. In other samples cements have partially to totally overgrown grain margins possibly replacing any overgrowths that may have existed.

The nature of grain-grain contacts is dependant on the percentage quartz; those sample containing higher quartz percentages display point to concave/ convex and moderately to well-sutured grain-grain contacts. Samples containing lower percentages of quartz tend to display mainly point to concave/convex grain-grain contacts with rare moderately sutured grain-grain contacts evident in some samples. Fluid inclusions or vacuoles are evident in most quartz grains. Vacuoles are identified by dark specks that cut across quartz grains.

Feldspars
These samples contain approximately 3% average feldspar. Most of the feldspar population is dominated by albite and other plagioclase feldspars but traces of microcline are evident. Feldspar is dominant in samples 154823 (995.0m), 154852 (420.1m) and 154804 (327.0m), which have all been classified as feldspathic litharenites. In other samples the occurrence of feldspar grains ranges from 0 to 4%. The degree of preservation of feldspar grains in samples varies. Larger grains have undergone partial leaching resulting in vacuolisation and alteration to authigenic kaolinite, sericite and calcite.

Oncoids
Oncoids are evident in two samples, 154833 (1325.1m) and 154823 (995.0m). These samples consist of a concentrically laminated internal quartz grain or phosphate fragment. The identification of these oncoids is often difficult as grains have been partially overgrown by calcite cements.

Rock fragments
Carbonate clasts
Carbonate clasts are evident in most sandstone samples. Clasts are predominantly medium sand sized and sub-angular to well-rounded. The shape of these clasts can vary however depending on the degree of compaction the sample has undergone. In samples that display moderate compaction, carbonate clasts are often cracked and altered and have been dispersed into adjacent intergranular pore space. They are composed of xenotopic matrix of anhedral to subhedral shaped very finely to finely crystalline dolomite that displays planar curved and sutured contacts. Micritic and trace siderite alteration is evident in most clasts. Micritised clasts consist of equant subhedral to euhedral crystals of microsparite and finer micrite which have replaced original dolomite.

Volcanics
The occurrence of volcanic rock fragments in these samples is more prevalent at shallower depths. The majority of volcanic fragments occur 154816 (749.0m) and Sample 154801(133.20m). Below 749m most samples generally contain only trace amounts of volcanic rock fragments. The most common volcanic rock fragment consists of partially altered plagioclase laths supported by mixture of sericite, chlorite and calcite cements and a black undifferentiated cryptocrystalline matrix. Most volcanic fragments display some dissociation and alteration and have expanded into intergranular pore space.

Chert and chalcedony
Chert fragments generally range up to medium sand sized. Fragments are generally sub-angular to sub-rounded and composed of microquartz with patches of macroquartz. Alteration of some of these fragments to radiating fibrous crystals of chalcedony and microsparry calcite is evident.

Siltstone
Siltstone fragments consist predominantly of medium silt sized quartz, mica and illite/sericite. Mica flakes occasionally display a weak preferential alignment, sub-parallel to the elongate axis of the siltstone fragment. These fragments have often been compacted and have expanded into intergranular pore space.

Sandstone
Sandstone fragments are generally angular to sub-rounded in shape. They are composed predominantly of medium to coarse silt sized quartz and mica that has been partially cemented by poikilotopic calcite cement. Mica flakes can display a weak preferential alignment, parallel with the elongate axis of the sandstone fragment. These fragments are often supported by kaolinite that has displays patchy alteration to chlorite and sericite. In some samples these fragments are difficult to distinguish as their margins have been partially replaced by calcite and anhydrite cements.

Kaolinite
Kaolinite occurs as sub-rounded to rounded clasts. These clasts consist of coarsely to finely crystalline accumulations of kaolinite. Most of the clasts have undergone moderate compaction which has resulted in their deformation and expansion into intergranular pore space.

5.5.2 Matrix/ pseudomatrix

Samples classified as quartz arenites and feldspathic litharenites are generally devoid of matrix or pseudomatrix. In most samples that contain a matrix component most of the matrix is contained in thin laminae and beds that cut across samples. Apart from sample 154833 (1325.1m), which contains a micritic carbonate mud pseudomatrix other samples contain a kaolinitic matrix that displays partial alteration to illite/sericite and chlorite. Kaolinite is evident in these samples as finely to coarsely crystalline accumulations that fill intergranular pore space.

5.5.3 Authigenic cements

Calcite
Calcite cementation is absent in 154849 (301.65m), 154848 (301.40m) and 154801 (133.20m) but occurs in all other samples. Sample 154823 (995.0m) displays the greatest calcite cementation. Calcite in samples occurs as single crystal poikilotopes or as a drusy mosaic of finely crystalline calcite that fills intergranular pore space and encases clusters of framework grains. It is also evident as a replacement fabric, partially replacing leached grains. Calcite cements have been partially replaced by isolated rhombs and microsparry dolomite accumulations in some samples.

Ferroan calcite
Ferroan calcite is present in some samples. It mainly occurs as a replacement cement. It is predominantly associated with feldspar grains where it partially replaces grains that have been leached or cracked. Ferroan calcite forms highly corrosive contacts with surrounding detrital grains.

Authigenic silica
The earliest identifiable cement is quartz overgrowth cement. Most of the cement occurs as single growths on quartz grains but in rare cases triple junctions have been formed. These triple junctions are formed by the mutual interference of individual silica overgrowths.

Anhydrite
Anhydrite cementation is mainly evident in samples 154834 (1410.20m) and 154833 (1325.10m) but some anhydrite cementation is evident in sample 154853 (763.70m). Anhydrite cement occurs as separate rectangular crystals or as massive poikilotopic cement encasing framework grains and filling intergranular pore space. The cement has been replaced partially by an equant drusy mosaic of very finely to finely crystalline calcite.
Siderite
Siderite cement is evident replacing intergranular pore space and marginally replacing or poisoning detrital grain boundaries. Siderite forms as either single isolated crystals or as small microsparry accumulations.

Illite/sericite
Illite/sericite has two principle forms of occurrence. It is mainly evident as a replacement of altered grains. These grains have often been compacted and consequentially grains have flowed into intergranular pore space. The second form of occurrence is along thin, discontinuous solution seams and microstylolites. The dark colouration of illite/sericite is generally caused by the concentration of pyrite and insoluble organic matter with illite/ sericite clays.

Haematite
Patchy haematite cementation is evident in samples 154849 (301.65m) and 154848 (301.4m). It mainly forms as a massive pore filling cement that encases clusters of framework grains. It generally forms highly corrosive contacts with surrounding framework grains.

5.5.4 Structures

Laminae and beds
A sub-horizontal lamination is evident in samples 154825 (1050.0m) and 154804 (327.0m). In sample 154825 this lamination is defined by a quartz grain size variation. Laminae are approximately 0.7mm

and consist predominantly of coarse silt sized quartz that has been cemented by authigenic calcite. In sample 154804 laminae tend to be thin and discontinuous . Laminae in this sample are typically 1 to 2mm thick and contain a greater clay concentration.

A 14mm thick lithic wacke bed is evident in sample 154833 (1325.1m). This bed cuts sub-horizontally across the sample. It is defined by a reduction in detrital grain size and increases in the carbonate mud matrix. A small flame structure is evident where the sandstone has been forced up into the lithic wacke bed.

Solution seams
Solution seams are evident in samples 154823 (995.0m) and 154852 (420.1m). These seams tend to be irregular, sub-horizontal and discontinuous. Dewatering has caused the dispersion of some of these seams. The seams are composed of a concentration of coarse silt sized quartz and illite/sericite.

Bleached veins
Samples 154849 (301.65m) and 154848 (301.4m) were marked for special consideration by the Department of Minerals and Energy. In sample 154849 a 3mm thick, vertical haematite-rich vein cuts through the centre of the sample with a 15mm thick alteration halo. It is proposed that this structure possibly formed a vertical micro-fracture. Fluid movement up or down this structure resulted in haematite cementation in the fracture and the bleaching and alteration of the surrounding host rock.

Sample 154848 (301.4m) consists of an interbedded litharenite and lithic wacke. The lithic wacke portion of the slide is defined by concentrations of sericitic clay and by two thin, discontinuous haematite laminae that bound the top and bottom of the bed. The lithic wacke component of this slide has been partially altered to chlorite. It is proposed that fluid movement along this lithic wacke layer has caused the bleaching and deposition of the haematitic crust in this sample.

Soft sediment deformation
Sample 154850 (343.44m) displays a 10mm thick siltstone filled sub-vertical bed. The massive nature of this sandstone bed suggests it was deposited rapidly. There is difficulty in explaining the occurrence of this structure as it is only partially evident. It is proposed that this structure may represent a dilated micro-fault or fracture that has been filled rapidly by a siltstone flow. Another possible explanation is that the structure represents a filled burrow.

6. TEXTURE AND FABRIC

6.1 Grain size distribution

Figure 8 is a grain size distribution plot illustrating the grain size range and mode for samples within their respective rock type groupings. It is important to note that this plot does not take into account matrix material which is too fine to classify petrographically. From this plot a number of interesting inferences can be drawn. As would be expected, conglomerates and diamictite samples display the greatest grain size range. The large range in these samples is the result of a mixture of quartz grains and rock fragments. It is difficult to ascertain a grain size mode for conglomeritic samples but on observation of diamictite samples it is evident that they consist of the lowest observed grain size mode. Samples that characterise diamictites contain an average grain size mode of approximately 0.07mm. This low grain size mode can be attributed to the occurrence of silt sized quartz contained in the matrix/pseudomatrix component of these samples.

Sandstone samples display a grain size distribution that ranges between 0.07mm to about 4mm. These samples display the most uniform grain size distribution out of all the rock type groupings. These samples are dominated by a mode grain size of between 0.2 to 0.4mm. Expectantly, argillaceous siltstone samples contain a low average grain size mode of approximately 0.06mm. Although most argillaceous siltstone samples display a condensed grain size range, the occurrence of an expanded range in some sections reflects the occurrence of larger rock fragments. Finally the argillaceous siltstone and sandstone display a variable grain size range and mode which is reflective of their composition.

7. CLAY AND CEMENT VARIATIONS

The occurrence of matrix and cements in all samples from Vines 1 is given in Figure 9. The trends evident on this figure suggest that the percentage of clay and authigenic cement in a sample is inversely

proportional. In most samples high in clay matrix content, the occurrence of cement is low and visa-versa. The occurrence of scattered clay matrix peaks throughout the well suggests that the variations in the percentage clay matrix are not attributable to depth but are dependent on the rock type. High clay matrix percentages are correlatable to samples occurring in argillaceous siltstone, diamictite and claystone rock type groupings at any depth. Samples low in clay matrix and high in cements are evident between the depths of 1537m and 1983m, 995m to 1070m and 498.0m to 420.1m. All of these samples occur within the sandstone rock type grouping.

8. DIAGENESIS

All samples have been subject to diagenetic processes, which have modified both the detrital grains and pore space. Most samples display a similar diagenetic history. The interpreted timing of diagenetic events is shown in Figure 7.

The earliest diagenetic product observed in these samples is a fine veneer or isopachous rim in samples 154826 (1062.0m), 154813 (675.0m), 154804 (327.0m), 154848 (301.4m) and 154852 (420.1m). These rims are mainly composed of either chlorite, illite/sericite or Fe-oxide clays. Isopachous rims have decreased the occurrence of overgrowth cementation on detrital grains. Authigenic overgrowths on quartz and feldspar grains has developed also relatively early in the diagenetic history, particularly in samples low in matrix components. Some quartz overgrowths are also occasionally evident growing into less competent grains (e.g. carbonate clasts and sandstone fragments).

Anhydrite is interpreted to have occurred relatively early to late in the diagenetic sequence. This cement mainly occurs within sandstones as a pore-filling and poikilotopic cement. It is probable that anhydrite cementation in siltstone pre-dates compaction events. The occurrence of expanded fabrics and felted laths in argillaceous siltstone samples may be indicative of near surface formation. The anhydrite is evident in some argillaceous siltstones expanding and disrupting the detrital fabric of these sediments.

Illite/sericite and kaolinite formation is interpreted to have preceeded anhydrite cementation. These cements are developed locally where detrital grains and rock fragments have undergone dissolution. On replacing framework grains these grains have further expanded into and filled intergranular pore space. The timing of authigenic clay formation is often difficult to distinguish, however, as they tend to have a wide range of formation. These clays have in some samples been replaced by a chlorite clay.

Calcite occurs generally as poikilotopic crystals or as a drusy mosaic of very-finely to finely crystalline calcite that fills intergranular pore space and encases clusters of framework grains. Calcite crystals also commonly replace framework grains or framework grain dissolution sites. In open intergranular pore spaces most drusy calcite display euhedral terminations. The crystals generally display a coarsening from framework grains towards pore centres. The cement generally post-dates overgrowth and anhydrite cementation marginally replacing these cements and growing into pore space that has not been filled. Calcite cements are also evident partially replacing illite/sericite clays in argillaceous siltstones. In these samples it occurs as a very finely crystalline calcite that occurs as isolated grains and microsparry accumulations that partially replace illite/sericite.

Compaction has affected most samples that have remained uncemented by calcite, dolomite and anhydrite. Compaction is particularly prevalent within argillaceous sediments and those sediments high in detrital rock fragments. Deformation of rock fragments, pressure welding and grain to grain suturing is evident in most samples. Other structures that are indicative of compaction include solution seams and thin, wispy stylolites.

Dolomite is pervasive in carbonate clasts and marginally replacing calcite and anhydrite cements in intergranular pore space. In these clasts it mainly occurs as a xenotopic matrix of anhedral to subhedral shaped very finely to finely crystalline dolomite that displays planar curved and sutured contacts. Micritic and trace siderite alteration is evident in most clasts. Micritised clasts consist of equant subhedral to euhedral calcite crystals of microsparite and finer, micrite which has replaced dolomite in these clasts. Small isolated rhombs of dolomite are also evident in some sample partially replacing illite/sericite and the non-selective replacement of dissolved and corroded grains.

Precipitation of late pyrite cement is also evident, filling intergranular pore space and replacing grains and matrix. It mainly occurs both as isolated nodular grains and accumulations that replace illite/sericite clays and fill spaces within dissolved grains and rock fragments.

9. POROSITY

A combined primary and secondary porosity histogram (Figure 11) illustrates that porosity values for Vines 1 and Empress 1A range from 0 to 8%. The histogram also shows that there is an increase in porosity values in samples occurring shallower than 559.65m. Porosity values in these samples, however are reflective of sample composition. Samples that contain higher matrix and/or cement generally contain trace to no porosity (Figure 10). The occurrence of higher porosity values at shallower depths, with exception of samples 154851 (360.20m) and 154850 (343.44m) can be correlatable with cleaner, less matrix and cement-rich samples.

The lack of porosity between the depths of 1569.10m and 1062.0m can be correlated to argillaceous siltstone and diamictite samples. Even though some micro-porosity may be evident in these samples, macro-porosity is absent or extremely poor. The lack of porosity within samples occurring between these depths can be attributed to fine grained micritic cements that have replaced matrix material.

Both primary and secondary porosity is evident in these samples. The most common varieties of pore space in these samples are intergranular porosity (both normal and dissolution enhanced) and oversized pores. Dissolution enhanced porosity is primarily the result of secondary dissolution of feldspars, calcite, anhydrite, rock fragments and unstable grains. In samples occurring shallower than 559.65m there seems only minor evidence of compaction and only partial cementation of samples. This has resulted in the preservation of primary intergranular porosity. Samples with high intergranular porosity can be generally classified as predominantly grain supported with minimal matrix and authigenic cementation.

It is important to note that there is a subtle reduction in porosity of samples with depth which can associated with changes in the microfabric and the degree of lithification of samples. However these changes are only minimal and the occurrence of high porosity values at depth reflect that porosity values are reflective of sample composition.

10. DISCUSSION AND CONCLUSIONS

The mixture of igneous rock fragments, sedimentary rock fragments, sub- to well-rounded quartz grains, anhydrite cements, muddy substrates and red beds indicates that Vines 1 is a multiphase systems. It is important to note, however, that without prior knowledge of palaeogeographic setting and observation macro-scale samples the inferences that will be drawn are only tentative. Two models are proposed for the deposition of sediments in Vines 1. The first model incorporates a back-reef lagoon or basin environment, with influences of shoreward circulating salt water and diluting freshwater streams (Figure 12).

This model is only hypothetical and has some obvious flaws. It is possible that this system was only occasionally connected to a marginal marine or inland sea environment. However the lack of skeletals in samples indicates that in fact the system may not have been connected to an inland sea or marginal marine environment at all.

The occurrence of turbidite-like argillaceous beds and interbedded sandstones indicates that this system was affected by punctuated alluvial processes. Minor fluctuations in sea-level may have caused the system to become fluvially dominated. It is proposed that sandstone beds were deposited during periods in which the fluvial system was dominated by a moderate to high energy regime. The degree of rounding on quartz grains in sandstone beds is indicative of high transportation distances of these grains. The quartz may have been derived from dunes surrounding the area. During periods of waning energy, turbidite-like fining upwards argillaceous beds and laminae would have developed. Shallow water levels and restricted circulation in the back reef lagoon environment would have promoted the development of in situ anhydrite and calcite cements. It is envisaged that sedimentary rock fragments (i.e. dolomite and shale) that are evident in these beds were derived either from the brecciation of patch reef complexes that closed the back reef lagoon or may have been reworked from a pseudomarine

environment in which they formed. The lack of volcanic fragments in samples below 1062m indicates that during deposition of argillaceous beds the hinterland was relatively passive.

At 1062m there is a marked increase in the amount of igneous fragments being introduced into the system. It is possible that fluvial processes resulted in the unroofing of an igneous complex. The alternation of clay-rich and quartz-rich sediments above 1062m may have been caused by fluctuations in both relative sea-level and sediment supply.

The samples examined from 1062m to surface display a mixture of volcanic and sedimentary rock fragments. It is proposed that igneous fragments were transported by fluvial systems into the back-reef lagoon or basin environment. The lack of anhydrite cements indicates that water levels in the back-reef basin would have been significantly higher or the overall hydrogeography changed. The deficiency of igneous fragments in some samples above 1062m may be due to sampling problems. A marked increase in volcanic rock fragments is evident in samples 154847 and 154846 occurring at 104.55m and 67.80m respectively. It is possible that during this period the back-reef lagoon was completely cut off from marine influences and sedimentation into the lagoon was principally terrestrial with streams and rivers, depositing igneous fragments derived from the hinterland.

The second model involves a playa-type environment surrounding an ephemeral lake (Figure 13). This model seemingly provides a slightly better fit than the model described above. It is proposed that semi-arid to arid conditions prevailed during deposition of these sediments. The model is composed of an ephemeral lake that was possibly regional in scale. A modern day analogue would be Lake Grace in Western Australia. Sediment supply and water would have been supplied into the lake by alluvial systems. Drainage within the lake would have been internal.

Quartz-rich sandstones may have been sourced by shifting sand dunes or carried into the lake by high energy streams and rivers. The roundness of quartz grains in samples suggests that they either had high transportation distances or were aeolian in origin. Turbidite-like fining upwards bedding would have been deposited in the deeper parts of the lake as finer clays and silt sized quartz grains held in suspension settled. During periods of moderate to high energy, ooliths may have developed in the lake shallows. It is possible that conditions in the lake during such periods were relatively anaerobic resulting in the development of sulphides. However these sulphides may have developed during burial.

It is proposed that a playa-type setting existed on the lake margins. Low energy water supply with periodic turbulence would have provided an ideal setting for development of dolomite, ooids, micrite, peloids and oncoids. It is uncertain if micritisation is a function of burial. The playa environment with its intermittent water supply would also have provided an ideal setting for the development of gypsum crystals which may have changed to anhydrite crystals during burial. Deformation evident in some micritic limestone samples may have also been caused by the dehydration of primary gypsum or hydration of anhydrite.

The increase in igneous fragments being introduced into the system after 1062m is indicative of increased tectonism resulting in either uplift and erosion or downcutting into an igneous complex by high energy streams or rivers. A possibility is that high energy streams eventually unroofed an igneous complex and transported them into the lake environment. This change may have accompanied an overall change in the hydrogeography of the region.

The models provided in this paper are purely hypothetical. The rationalisation for these models has been achieved through combining the petrographic characteristics of samples and logs. In effect, although they may provide some insight into the depositional settings for Vines 1, it is important to note that these models are two of many models that may be developed.

11. BIBLIOGRAPHY

Choquette, P.W. and Pray, L.C., 1970. Geological nomenclature and classification of porosity in sedimentary carbonates. *Bull. Am. Assoc. Petrol. Geol.*, **54**, 207-250.

Flügel, E. (1982). *Microfacies Analysis of Limestones*. Springer-Verlag Berlin, Heidelberg, 633p.

Folk, R.L. 1959. Practical petrographic classification of limestones. *Bull Am. Assoc. Petrol. Geol*., **43**, 1-38.

Folk, R.L., 1980. *Petrology of Sedimentary Rocks*. Hemphill Publishing Co., Texas.

Greensmith, J.T. (1989). *Petrology of the Sedimentary Rocks*. 7th Ed. University Printing House, Oxford. p 262.

Harrel. J. 1984. A visual comparator for the degree of sorting in thin and plane sections. *Journal of Sedimentary Petrology*, **54**, 646-650.

Morad, S, Ketzer, J.M. & De Ros, L.F., 2000. Spatial and temporal distribution of diagenetic alterations in siliciclastic rocks: implications for mass transfer in sedimentary basins. *Sedimentology*, **47** (Suppl.1), 95-120.

APPENDIX A (Detailed thin-section descriptions)

GSWA No. 154867

Well	VINES-1
Sample number	154867
Sample type	
Depth	1983.0
Unit	
Facies	Sandstone
Sample quality	Sample is in excellent condition.
Brief description	Quartz arenite Sample is predominantly composed of fine sand sized, sub-angular to sub-rounded quartz grains that display point to concave/convex and moderately sutured grain-grain contacts. Detrital grains have been cemented predominantly by a patchy, pseudosparic non-ferroan and ferroan calcite cement. Primary intergranular porosity dominates the sample however some secondary porosity is evident due to the partial leaching and dissolution of feldspar grains.

TEXTURE

Grain size	Range: Coarse silt (0.05mm) to medium sand (0.47mm) Mode: Fine sand (0.22mm)
Sorting	Moderately-sorted.
Grain morphology	Sub-angular to sub-rounded.
Sediment fabric	Grains display point to concave/convex and moderately sutured grain-grain contacts.

MINERALOGY

Tabulated composition (%)	Detrital components		
	Quartz	Monocrystalline	56
		Polycrystalline	Tr
	Muscovite		Tr
	Feldspar	Microcline	1
		Albite	2
	Accessories	Volcanics	Tr
		Zircon	Tr
		Tourmaline	Tr
		Spinel	Tr
		Algae	Tr
	Authigenic cement		
		Calcite	35
		Ferroan calcite	2
		Pyrite	1
		Illite/sericite	1
	Porosity/ Permeability		
		Primary	3
		Secondary	Tr

Detrital components	Quartz Quartz grains range in size from coarse silt (0.05mm) to medium sand (0.47mm) with a mode of fine sand (0.22mm). Grains are sub-angular to sub-rounded, moderately-sorted and display mainly point with occasional concave/convex and moderately sutured grain-grain contacts. Most quartz grain boundaries are irregular due to microcrystalline calcite growths which marginally replace the grains. Feldspar The most common feldspars evident in this sample are albite and to a lesser extent microcline. Feldspar grains display a similar grain size to detrital quartz grains. Smaller grains are typically well preserved while larger grains have undergone partial dissolution or are cracked and altered to calcite. Muscovite Only occurs in the sample in trace amounts. These grains are generally bent and broken.
Matrix/ Pseudomatrix	
Authigenic cement	Calcite Calcite occurs as patchy, cement of varying crystal size. Approximately 30% of the total calcite cement component occurs as a fine pseudosparic cement that encases clusters of framework grains. The remainder occurs as patchy, crystalline/ poikilotopic pore filling cement. The cement forms highly corrosive contacts with surrounding detrital grains, marginally replacing quartz grain boundaries. Ferroan calcite Ferroan calcite occurs as a fine pseudosparic cement. Although its occurrence is limited it has typically formed around detrital grain boundaries where it forms highly corrosive contacts with surrounding detrital grains. Pyrite Pyrite cement occurs in trace amounts filling intergranular pore space. Illite/sericite Illite/sericite occurs in trace amounts as sub-rounded grains of similar shape to detrital grains. The grains have undergone some compactional deformation and have subsequently been deformed and squashed into intergranular pore space. Partial calcite alteration of these grains is also apparent.
Porosity/ Permeability	The majority of the porosity in this sample is primary intergranular porosity. The apparent secondary porosity is the result of partial leaching and vacuolisation of feldspar grains.

DIAGENESIS

Relative timing of events	Microcrystalline calcite and ferroan calcite cementation Pyrite formation
Relative importance of events	

TEXTURAL MATURITY AND INTERPRETATION

Textural maturity	immature
Interpretation	

MINERALOGICAL CLASSIFICATION AND COMMENTS

Mineralogical classification	Quartz arenite
Comments	All mineralogical percentages were obtained through visual estimation.

GSWA No. 154844

Well	VINES-1
Sample number	154844
Sample type	Plug
Depth	1902.0
Unit	
Facies	Sandstone and argillaceous siltstone
Sample quality	The sample is in good condition.
Brief description	Massive quartz arenite This sample consists predominantly of angular to sub-rounded, very fine sand sized quartz grains. Dolomite, siltstone, and shale rock fragments have been partially compacted and are often squashed into intergranular pore space. The sample is cemented by a mixture of poikilotopic and microsparry calcite cements. The porosity is interpreted to be moderate.

TEXTURE

Grain size	Range: Very fine sand (0.07mm) to very coarse sand (1.1mm) Mode: Very fine sand (0.11mm)
Sorting	Moderately sorted
Grain morphology	Angular to sub-rounded
Sediment fabric	Grains display concave/convex to well-sutured grain-grain contacts

MINERALOGY

Tabulated composition (%)	Detrital components		
	Quartz	Monocrystalline	79
	Feldspar	Microcline	Tr
		Albite	2
		Plagioclase	Tr
		Muscovite	Tr
	Rock fragments		
		Carbonate	3
		Chert	Tr
		Kaolinite	3
		Chalcedony	1
		Siltstone	3
		Shale	2
	Accessories	Zircon	Tr
		Tourmaline	Tr
		Spinel	Tr
	Authigenic cement		
		Silica overgrowths	Tr
		Calcite	4
		Pyrite	1
	Porosity/ Permeability		
		Primary	2
		Secondary	Tr

Detrital components	Quartz Quartz ranges from very fine sand (0.07mm) to coarse sand (0.6mm) with a mode of very fine sand (0.11mm). Grains are angular to sub-rounded and moderately sorted. Pressure solution is evident with grains displaying concave/convex to well-sutured grain-grain contacts. Traces of thin authigenic silica overgrowths are apparent on some grain boundaries. Most quartz grains also contain fluid inclusions or vacuoles. Vacuoles are identified by lines of dark specks that cut across quartz grains. Feldspar Feldspar grains are approximately fine sand sized (0.12mm). Several varieties of feldspar are evident these include microcline, albite and plagioclase. Some grains have undergone partial leaching resulting in vacuolisation and alteration to kaolinite. Rock fragments *Carbonate clasts* Carbonate clasts range from medium sand size (0.2mm) to very coarse sand (1.1mm). These clasts are generally sub- to well rounded and composed of xenotopic matrix of anhedral to subhedral shaped very finely to finely crystalline dolomite that displays planar, curved and sutured contacts. Micritic alteration is evident in most of these clasts. Micritised clasts consist of equant subhedral to euhedral calcite crystals of microsparite and finer, micrite which have replaced the original very fine to fine dolomite. Some of these are deformed and have been compacted into intergranular pore space. *Chert* Chert grains are composed of microcrystalline quartz are scattered throughout the sample. These fragments are typically sub-angular to sub-rounded. *Chalcedony* Rare detrital chalcedony fragments are scattered throughout this sample. These fragments range in size from fine sand (0.2mm) to medium sand (0.4mm). Grains are generally angular and occasionally are broken. Grains display typical chalcedonic texture comprising radiating fibrous crystals of varying size. *Shale* These rock fragments are typically medium to coarse sand sized and angular to sub-angular in shape. They are composed predominantly of illite/sericite clay that displays partial alteration to kaolinite. *Kaolinite* Kaolinite occurs in sub-rounded to rounded clasts. These clasts consist of coarsely and finely crystalline accumulations of kaolinite. Most of the clasts have undergone partial compaction resulting in the expansion of the kaolinite into intergranular pore space. *Siltstone* Siltstone fragments range in size from medium sand sized (0.4mm) to very coarse sand (1.1mm). These fragments have irregular grain shapes as they have been compacted into intergranular pore space. The fragments contain predominantly an illite/sericite matrix with minor percentages of quartz and mica flakes. Mica flakes display some minor preferential alignment sub-horizontal to the elongate axis of the fragment. Some of these grains have undergone compactional deformation. Compaction of these grains has resulted in them flowing around adjacent framework grains and into intergranular pore space. Dissolution and alteration of these clasts to kaolinite is evident.

Matrix/ Pseudomatrix	
Authigenic cement	Calcite This sample is partially calcite cemented. Most calcite cement occurs as single crystal poikilotopes or microsparry accumulations of very finely crystalline calcite that fills intergranular pore space and marginally replaces quartz overgrowths. It is also evident growing on pressure solution surfaces between quartz grains. The cement forms highly corrosive contacts with surrounding detrital grains and partially replaces portions of framework grains. Silica overgrowths Trace authigenic silica overgrowths are evident on some quartz grain boundaries. Most of these overgrowth are very thin but occasionally thicker growths are produced at triple junctions between adjacent overgrowths. At these points irregular compromise boundaries are produced by the mutual interference of individual overgrowths. Overgrowths have been marginally replaced by single, poikilotopic calcite cement. Pyrite Pyrite occurs as small isolated nodules and accumulations that fill intergranular pore space and replace clay in some detrital grains.
Porosity/ Permeability	Moderate porosity is visible in this sample. Most of the porosity is primary intergranular porosity but some minor secondary porosity does exist.

DIAGENESIS

Relative timing of events	Mechanical compaction and grain pressure-solution Micritisation of carbonate clasts Calcite cementation Pyrite formation
Relative importance of events	

TEXTURAL MATURITY AND INTERPRETATION

Textural maturity	Mature
Interpretation	

MINERALOGICAL CLASSIFICATION AND COMMENTS

Mineralogical classification	Quartz arenite
Comments	

GSWA No. 154843

Well	VINES-1
Sample number	154843
Sample type	Plug
Depth	1815.0
Unit	
Facies	Sandstone and argillaceous siltstone
Sample quality	The sample is in good condition.
Brief description	Laminated quartz arenite This sample consists predominantly of angular to sub-rounded, fine sand sized quartz interlaminated with thin, discontinuous, sub-horizontal laminae consisting of very fine sand. Carbonate, siltstone, sandstone and shale rock fragments have been partially compacted and are often squashed into intergranular pore space. The sample is mainly calcite cemented but minor siliceous and anhydrite cementation is evident. Visual porosity is good.

STRUCTURES

Structures	Laminated A weak, sub-horizontal, discontinuous lamination is defined by the concentration of very fine sand (0.1mm) sized quartz grains. Laminae are approximately 0.6mm thick.

TEXTURE

Grain size	Range: Very fine sand (0.1mm) to granules (3mm) Mode: Fine sand (0.2mm)
Sorting	Moderately-sorted
Grain morphology	Angular to sub-rounded
Sediment fabric	Grains display concave/convex to well-sutured grain-grain contacts

MINERALOGY

Tabulated composition (%)	Detrital components		
	Quartz	Monocrystalline	80
	Feldspar	Microcline	Tr
		Albite	1
		Plagioclase	Tr
	Rock fragments		
		Carbonate	3
		Chert	Tr
		Kaolinite	2
		Sandstone	2
		Chalcedony	1
		Siltstone	3
		Shale	Tr
	Accessories	Zircon	Tr
		Tourmaline	Tr
		Spinel	Tr
	Authigenic cement		
		Silica overgrowths	1
		Calcite	3
		Siderite	Tr
		Anhydrite	Tr
		Silica	Tr
		Pyrite	Tr

	Porosity/ Permeability Primary 3 Secondary 1
Detrital components	Quartz Quartz ranges from very fine sand (0.1mm) to granules (3mm) with a mode of fine sand (0.2mm). Grains are moderately-sorted, angular to sub-rounded. Pressure solution is evident with grains displaying concave/convex to well-sutured grain-grain contacts. Thin authigenic silica overgrowths are apparent on some grain boundaries. Most quartz grains also contain fluid inclusions or vacuoles. Vacuoles are identified by lines of dark specks that cut across quartz grains. Feldspar Feldspar grains are approximately fine sand sized (0.2mm). Several varieties of feldspar are evident these include microcline, albite and plagioclase. Some grains have undergone partial leaching resulting in vacuolisation and alteration to kaolinite. Rock fragments *Carbonate clasts* Carbonate clasts range from medium sand size (0.2mm) to coarse sand (0.8mm). These clasts are generally sub- to well rounded and composed of xenotopic matrix of anhedral to subhedral shaped very finely to finely crystalline dolomite that displays planar, curved and sutured contacts. Micritic alteration is evident in most of these clasts. Micritised clasts consist of equant subhedral to euhedral calcite crystals of microsparite and finer, micrite which have replaced the original very fine to fine dolomite. Some of these are deformed and have been compacted into intergranular pore space. *Chert* Chert grains are composed of microcrystalline quartz are scattered throughout the sample. These fragments are typically sub-rounded and display a mode of medium sand (0.4mm). *Chalcedony* Rare detrital chalcedony fragments are located throughout this sample. These fragments also have a mode grain size of medium sand (0.4mm). Grains are generally angular and occasionally are broken. Grains display typical chalcedonic texture comprising of radiating fibrous crystals of varying size. *Sandstone* Traces of well-cemented sandstone fragments are also evident in this sample. Although difficult to identify these fragments can be differentiated from the main host rock as they occur as patches of finer grained quartz. Sandstone fragments range up to granules (3mm) in size. They are generally-angular to sub-rounded and composed of up to 94% moderately sutured, coarse silt sized (0.05mm) quartz grains, 1% mica and 5% poikilotopic calcite cement. Advanced pressure solution is evident with grains displaying well-sutured grain-grain contacts. Within the fragment the cement encases clusters of framework grains and fills intergranular pore space. *Shale* These rock fragments are typically medium to coarse sand sized and angular to sub-angular in shape. They are composed of predominantly of illite/sericite clay. *Kaolinite* Kaolinite occurs in sub-rounded to rounded clasts. These clasts consists of coarsely and finely crystalline accumulations of kaolinite. Most of the clasts have undergone partial compaction resulting in their expansion of the kaolinite

	into intergranular pore space. *Siltstone* Traces of medium sand sized (0.4mm) siltstone are evident. These fragments have irregular grain shapes as they have been compacted into intergranular pore space. The fragments contain predominantly an altered kaolinite-rich matrix with minor percentages of quartz and mica flakes.
Matrix/ Pseudomatrix	
Authigenic cement	Silica overgrowths Authigenic silica overgrowths are evident on some quartz grain boundaries. At triple junctions contacts between adjacent overgrowths are irregular compromise boundaries produced by the mutual interference of individual overgrowths. Overgrowths have been marginally replaced by single, poikilotopic calcite cement. Calcite This sample is partially calcite cemented. Most calcite cement occurs as single crystal poikilotopes or microsparry accumulations of very finely crystalline calcite that fills intergranular pore space and marginally replaces quartz overgrowths. It is also evident growing on pressure solution surfaces between quartz grains. The cement forms highly corrosive contacts with surrounding detrital grains and partially replaces portions of framework grains. Siderite Siderite occurs as microcrystalline accumulation and individual grains that marginally replace detrital grains and fills intergranular pore space. Silica Traces of patchy siliceous cementation are evident in this sample. The cement has been partially replaced by late stage anhydrite cementation. Pyrite Nodular pyrite is scattered throughout the sample filling intergranular pore space. There is some concentration of nodular pyrite along quartz-rich laminae.
Porosity/ Permeability	This sample has good visual porosity. There has been some preservation of primary intergranular porosity and the development of some secondary porosity through leaching of detrital grains.

DIAGENESIS

Relative timing of events	Mechanical compaction and grain pressure-solution Micritisation of carbonate clasts Calcite cementation Siderite formation
Relative importance of events	

TEXTURAL MATURITY AND INTERPRETATION

Textural maturity	Immature
Interpretation	

MINERALOGICAL CLASSIFICATION AND COMMENTS

Mineralogical classification	Quartz arenite
Comments	

GSWA No. 154842

Well	VINES-1
Sample number	154842
Sample type	Plug
Depth	1713.0
Unit	
Facies	Argillaceous siltstone and sandstone
Sample quality	Sample is in good condition.
Brief description	Quartz arenite This sample is a relatively clean quartz arenite. It is dominated by angular to sub-rounded medium sand sized quartz grains. These grains have undergone minor pressure solution resulting in the formation of concave/convex to well-sutured grain-grain contacts. Carbonate, chert, and shale clasts have also been deformed and compacted into intergranular pore space. Minor carbonate and siderite cementation is evident. Some primary intergranular porosity is preserved in this sample.

STRUCTURES

Structures	Massive.

TEXTURE

Grain size	Range: Very fine sand (0.1mm) to coarse sand (0.6mm) Mode: Medium sand (0.3mm)
Sorting	Well-sorted
Grain morphology	Angular to sub-rounded
Sediment fabric	Grains display concave/convex to well-sutured grain-grain contacts

MINERALOGY

Tabulated composition (%)	Detrital components		
	Quartz	Monocrystalline	83
		Polycrystalline	1
	Feldspar	Microcline	Tr
		Albite	1
		Plagioclase	Tr
	Rock fragments		
		Carbonate	2
		Chert	1
		Shale	Tr
		Kaolinite	2
	Accessories	Zircon	Tr
		Tourmaline	Tr
	Authigenic cement		
		Calcite	4
		Dolomite	Tr
		Siderite	Tr
	Porosity/ Permeability		
		Primary	4
		Secondary	1

Detrital components	Quartz Quartz ranges from very fine sand (0.1mm) to coarse sand (0.6mm) with a mode of medium sand (0.3mm). Grains are moderately sorted, angular to sub-rounded. Pressure solution is evident with grains displaying concave/convex to well-sutured grain-grain contacts. Thin authigenic silica overgrowths are apparent on some grain boundaries. Most quartz grains also contain fluid inclusions or vacuoles. They are identified as lines of dark specks that cut across quartz grains. Grain boundaries have been marginally replaced by calcite cement. Feldspar Feldspar grains range in size from coarse silt (0.07mm) to medium sand (0.25mm). Several varieties of feldspar are evident these include microcline, albite and plagioclase. Some grains have undergone partial leaching resulting in vacuolisation and alteration to sericite, calcite and kaolinite. Rock fragments *Carbonate clasts* Carbonate clasts range from fine sand size (0.2mm) to coarse sand (0.6mm). These clasts are generally sub- to well rounded and composed of xenotopic matrix of anhedral to subhedral shaped very finely to finely crystalline dolomite that displays planar, curved and sutured contacts. Micritic alteration is evident in some of these clasts. Most of the micritised clasts consist of equant subhedral to euhedral calcite crystals of microsparite and finer, micrite which have replaced the original very fine to fine dolomite. Most of these grains have been deformed and squashed into intergranular pore space. *Chert* Chert grains composed of microcrystalline quartz are scattered throughout the sample. These grains have a mode size of fine sand sized (0.2mm). Some chert grain boundaries are being marginally replaced by calcite cement. *Shale* These rock fragments are typically medium to coarse sand sized and angular to sub-angular in shape. Deformation and alteration of these fragments to kaolinite is evident. *Kaolinite* Kaolinite occurs as sub-rounded to rounded clasts. These clasts consist of coarsely and finely crystalline accumulations of kaolinite. Most of the clasts have undergone partial compaction resulting in their expansion of the kaolinite into intergranular pore space.
Matrix/ Pseudomatrix	
Authigenic cement	Silica overgrowths Authigenic silica overgrowths are evident on some quartz grain boundaries. At triple junctions contacts between adjacent overgrowths are irregular compromise boundaries produced by the mutual interference of individual overgrowths. Overgrowths have been marginally replaced by single, poikilotopic calcite cement. Calcite This sample is partially calcite cemented. Most calcite cement occurs as single crystal poikilotopes or microsparry accumulations of finely to medium crystalline calcite that fills intergranular pore space and marginally replaces quartz overgrowths. It is also evident growing on pressure solution surfaces between quartz grains. The cement forms highly corrosive contacts with surrounding detrital grains and partially replaces portions of framework grains.

	<u>Siderite</u> Siderite occurs as microcrystalline accumulations and individual grains that marginally replace detrital grains and fill intergranular pore space.
Porosity/ Permeability	Porosity in this sample is good. Although most of the porosity has been filled by authigenic cements there is still some pore space that has only partially or has not been subjected to these processes.

DIAGENESIS

Relative timing of events	Mechanical compaction and grain pressure-solution Micritisation of carbonate clasts Calcite cementation Siderite formation
Relative importance of events	

TEXTURAL MATURITY AND INTERPRETATION

Textural maturity	Immature
Interpretation	

MINERALOGICAL CLASSIFICATION AND COMMENTS

Mineralogical classification	Quartz arenite
Comments	

GSWA No. 154866

Well	VINES-1
Sample number	154866
Sample type	Core
Depth	1665.6
Unit	
Facies	Sandstone and argillaceous siltstone
Sample quality	The sample is in good quality.
Brief description	Quartz arenite This sample consists of coarse silt sized quartz supported by a sericitic matrix, interbedded with with a 7mm thick sandstone layer composed predominantly of coarse sand. Quartz grains are sub-angular to rounded, and matrix supported. Visual porosity is poor.

STRUCTURES

Structures	Two structures are evident in this sample. The first is a 7mm thick, sub-horizontal sandstone layer that cuts across the sample. The second is a series of thin, sub-horizontal, illite-sericite filled, wispy stylolites. These stylolites are fabric selective being concentrated mainly in the lithic wacke component of the sample. All stylolites are discontinuous and irregular.

TEXTURE

Grain size	Range: Medium silt (0.02mm) to coarse sand (0.7mm) Mode: Bimodal → Coarse silt (0.05mm) and medium sand (0.4mm)
Sorting	Poorly sorted
Grain morphology	Sub-angular to rounded.
Sediment fabric	Matrix supported. Grains display rare point contacts.

MINERALOGY

Tabulated composition (%)	Detrital components		
	Quartz	Monocrystalline	43
		Polycrystalline	Tr
	Feldspar	Microcline	Tr
		Albite	Tr
	Accessories	Volcanics	Tr
		Zircon	Tr
		Tourmaline	Tr
	Rock Fragments	Lithoclasts	5
		Chert	2
		Sandstone	1
		Chalcedonic quartz	5
		Carbonate	10
	Authigenic cement		
		Calcite	8
		Ferroan calcite	3
		Pyrite	Tr
		Sericite	17
		Illite/sericite	2
	Porosity/ Permeability		
		Primary	1
		Secondary	3

Detrital components	Quartz Quartz displays a bimodal grain size distribution. The smaller quartz fraction ranging from medium silt (0.016mm) to medium sand (0.3mm) with a mode of coarse silt (0.05mm) is located within the lithic wacke host rock. Grains range in shape from angular to sub-rounded and are moderately sorted. Quartz grains are predominantly matrix supported but occasional point and concave/convex grain-grain contacts are apparent. The larger quartz fraction is contained in a 7mm thick, sub-horizontal sandstone layer that cuts through the sample. Quartz within this layer ranges from fine sand (0.13mm) to medium sand (0.4mm) with a mode of medium sand (0.3mm). Grains range in shape from sub-angular to sub-rounded and are moderately-sorted. Most grains display point contacts but occasional concave/convex and moderately sutured grain-grain contacts are evident. Most quartz grains display corrosive grain boundaries. Trace polycrystalline quartz is also evident. Feldspar The most common feldspars evident in this sample are albite and microcline. Most feldspar grains are located in the quartz rich-layer and display a similar grain size to quartz grains within this layer. Rock Fragments *Lithoclasts* These grains could be termed flint, but due to the truncation of microquartz nodules at the grain boundary they have been termed lithoclasts. Lithoclasts consist of a mixture of concentric microquartz and chalcedonic silica. Microquartz is evident as elongate and round grains varying in size from 0.7mm to 1.1mm. These grains predominantly display single-phase growth but occasional multiphase growth on some grains is evident by differences in colouration between successive phases. Chalcedonic silica is typically located between nodules. It mainly occurs as radial-fibrous, pore-filing cement. There is a slight increase in chalcedonic crystal grain size towards the centre of pores. Some microquartz nodules contain high birefringence carbonate grains associated with them. This probably indicates that silica has replaced an original limestone fabric. *Chert* Chert grains composed of microcrystalline quartz are scattered throughout the sample. These grains have an average size of approximately 0.3mm. Some of these chert fragments have patchy carbonate growths associated with them. This possibly indicates replacement by silica of an original limestone fabric. *Sandstone* Traces of irregularly shaped sandstone clasts are evident in this sample. These clasts are composed of fine sand sized, sub-rounded quartz grains and clay. *Chalcedony* Rare detrital chalcedony fragments are located throughout this sample. These fragments range in size from very coarse sand (1.1mm) to granules (2mm). Grains are generally angular and occasionally are broken. Grains display typical chalcedonic texture comprising radiating fibrous crystals of varying size. *Carbonate* Carbonate clasts are granule sized (2-3mm). They display highly irregular boundaries with thin-micritic rims. These clasts consist predominantly of fine dolomite crystals approximately 0.03mm in size.

	In some clasts the dolomite grains are too small to be identified microscopically having been heavily micritised. Partial preservation of grains displaying radial and concentric ooid textures is evident. This ooid texture though has been in most cases been partially lost by neomorphism and micritisation.
Matrix/ Pseudomatrix	
Authigenic cement	Sericite The lithic wacke component of this sample is dominated by a micrtitic sericite cement. A weak, sub-horizontal preferential orientation of mica crystals is evident in this cement. The cement generally forms highly corrosive contacts with surrounding detrital grains. Calcite Authigenic calcite is also evident in the sandstone layer that cuts through the sample. In this layer calcite occurs as a fine pseudosparic cement that fills intergranular pore space and encases clusters of framework grains. Ferroan calcite Ferroan calcite forms as small disseminated grains and aggregates that are prevalent partially growing into pore space and replacing carbonate cements. Ferroan calcite grains display highly corrosive contacts with surrounding grains. Illite/sericite Illite/sericite is concentrated along thin, sub-horizontal stylolites that cut across the sample. The dark colouration of these stylolites is caused by the concentration of insoluble organic matter and pyrite with illite/sericite along these seams.
Porosity/ Permeability	The majority of porosity in this sample is secondary. Evidence for this secondary porosity includes partially dissolved and corroded detrital grains and rock fragments and the occurrence of porosity channels between grains and cements.

DIAGENESIS

Relative timing of diagenetic events	Sericite formation Calcite cementation Micritisation Ferroan calcitisation
Relative importance of events	

TEXTURAL MATURITY AND INTERPRETATION

Textural maturity	Immature
Interpretation	

MINERALOGICAL CLASSIFICATION AND COMMENTS

Mineralogical classification	Interbedded lithic wacke and sandstone
Comments	

GSWA No. 154841

Well	VINES-1
Sample number	154841
Sample type	Plug
Depth	1656.0
Unit	
Facies	Sandstone and argillaceous siltstone
Sample quality	The sample is in good condition.
Brief description	Quartz arenite This sample consists predominantly of well-sutured, medium sand sized quartz grains. Other framework grains include carbonate, siltstone, sandstone and shale. Advanced pressure solution between detrital grains and the growth of poikilotopic and microcrystalline calcite into intergranular pore space has significantly reduced porosity. Some primary intergranular porosity however is interpreted to exist.

STRUCTURES

Structures	Massive.

TEXTURE

Grain size	Range: Coarse silt (0.05mm) to granules (2mm) Mode: Medium sand (0.3mm)
Sorting	Moderately-sorted
Grain morphology	Sub-angular to sub-rounded
Sediment fabric	Grains display concave/convex to well-sutured grain-grain contacts

MINERALOGY

Tabulated composition (%)	Detrital components		
	Quartz	Monocrystalline	81
		Polycrystalline	1
	Feldspar	Microcline	Tr
		Albite	1
		Plagioclase	Tr
	Rock fragments		
		Carbonate	3
		Siltstone	1
		Sandstone	1
		Chert	2
		Chalcedony	1
		Shale	Tr
		Kaolinite	Tr
	Accessories	Zircon	Tr
		Tourmaline	Tr
	Authigenic cement		
		Calcite	8
		Dolomite	Tr
	Porosity/ Permeability		
		Primary	1
		Secondary	Tr

Detrital components	Quartz Quartz ranges from coarse silt (0.05mm) to coarse sand (0.6mm) with a mode of medium sand (0.3mm). Grains are moderately sorted, angular to sub-rounded. Pressure solution is evident with grains displaying concave/convex to well-sutured grain-grain contacts. Thin authigenic silica overgrowths are apparent on some grain boundaries. Most quartz grains also contain fluid inclusions or vacuoles. They are identified as lines of dark specks that cut across quartz grains. Feldspar Feldspar grains range in size from coarse silt (0.07mm) to medium sand (0.25mm). Several varieties of feldspar are evident, these include microcline, albite and plagioclase. Some grains have undergone partial leaching resulting in vacuolisation and alteration to sericite, calcite, kaolinite and chlorite. Rock fragments *Carbonate clasts* Carbonate clasts range from medium sand size (0.2mm) to granules (2mm). These clasts are generally sub- to well rounded and composed of xenotopic matrix of anhedral to subhedral shaped very finely to finely crystalline dolomite that displays planar, curved and sutured contacts. Micritic alteration is evident in some of these clasts. Most of the micritised clasts consist of equant subhedral to euhedral crystals of microsparite and finer micrite which have replaced the original very fine to fine dolomite. The occurrence of patches of non-equant pseudospar replacing micrite in some of the clasts indicates that they may or have undergone partial aggrading neomorphism. *Chert* Chert grains composed of microcrystalline quartz are scattered throughout the sample. These grains have a mode size of medium sand (0.4mm). Some chert grain boundaries are being marginally replaced by calcite. *Chalcedony* Rare detrital chalcedony fragments are located throughout this sample. These fragments also have a mode grain size of medium sand (0.4mm). Grains are generally angular and occasionally are broken. Grains display typical chalcedonic texture comprising of radiating fibrous crystals of varying size. *Sandstone* Traces of well-cemented sandstone fragments are also evident in this sample. Although difficult to identify, these fragments can be differentiated from the main host rock as they occurs as patches of finer grained quartz. Sandstone fragments range up to coarse sand (0.9mm) in size. They are generally sub-angular to sub-rounded and composed of up to 90% moderately sutured, coarse silt sized (0.05mm) quartz grains, 1% mica and 9% poikilotopic calcite cement. Within the fragment the cement encases clusters of framework grains and fills intergranular pore space. *Shale* These rock fragments are typically medium to coarse sand sized and angular to sub-angular in shape. Deformation and alteration of these fragments is evident. Some shale fragments have been partially seriticised and chloritised. *Kaolinite* Kaolinite occurs as sub-rounded to rounded clasts. These clasts consist of coarsely and finely crystalline accumulations of kaolinite. Most of the clasts have undergone partial compaction resulting in their expansion of the kaolinite into intergranular pore space.

	Siltstone Traces of medium sand sized (0.2mm) siltstone are evident. These fragments have irregular grain shapes as they have been compacted into intergranular pore space. The fragments contain predominantly an illite/sericite matrix with minor percentages of quartz and mica flakes. Mica flakes display some minor preferential alignment sub-horizontal to the elongate axis of the fragment.
Matrix/ Pseudomatrix	
Authigenic cement	Silica overgrowths Authigenic silica overgrowths are evident on some quartz grain boundaries. Contacts between adjacent overgrowths are irregular compromise boundaries produced by the mutual interference of individual overgrowths. Overgrowths have been marginally replaced by single, poikilotopic calcite cement. Calcite This sample is partially calcite cemented. Most calcite cement occurs as single crystal poikilotopes or microsparry accumulations of very finely crystalline calcite that fills intergranular pore space and marginally replaces quartz overgrowths. It is also evident growing on pressure solution surfaces between quartz grains.. The cement forms highly corrosive contacts with surrounding detrital grains and partially replaces portions of framework grains.
Porosity/ Permeability	Visual porosity is poor but some primary intergranular porosity is evident.

DIAGENESIS

Relative timing of events	Mechanical compaction and pressure solution Micritisation Neomorphism Calcite cementation
Relative importance of events	

TEXTURAL MATURITY AND INTERPRETATION

Textural maturity	Supermature
Interpretation	

MINERALOGICAL CLASSIFICATION AND COMMENTS

Mineralogical classification	Quartz arenite
Comments	

GSWA No. 154865

Well	VINES-1
Sample number	154865
Sample type	Core
Depth	1569.1
Unit	
Facies	Diamictite
Sample quality	Sample is in good condition.
Brief description	Dismicrite This sample consists predominantly of fine, pseudosparic calcite that has been partially micritised. Calcite crystals are anhedral to subhedral; in shape and display planar, curved and sutured contacts. Porosity is negligible having been totally cemented and filed by anhydrite.

TEXTURE

Grain size	Microcrystalline to micritic
Sorting	Indiscernible
Sediment fabric	Anhedral and subhedral calcite crystals with planar and curved contacts.

MINERALOGY

Tabulated composition	*Grain size/ fabric*	*Percentage*
Primary cement		
Dolomite	microcrystalline	80
Diagenitic cement		
Micrite		15
Authigenic minerals		
Anhydrite		4
Silica		1
Porosity/ Permeability		
Primary		nil
Secondary		nil

Cement	
Diagenetic	Dolomite The sample is dominated by dolomite. Crystals are typically anhedral to subhedral in shape and display planar, curved and sutured contacts. Micrite Spar micritisation is apparent in this section. Alteration of spar particularly around cemented pore spaces has resulted in the precipitation of micrite. Micritic rims also define the outlines of peloids.
Authigenic cement	Anhydrite Anhydrite is interpreted to be a authigenic mineral filling vugular porosity. Pores cemented and filled with anhydrite have highly irregular and diffuse boundaries that have been partially replaced by sparite and micrite.
Porosity/ Permeability	No porosity is evident in this sample as all vugular porosity has been filled and cemented by anhydrite.

DIAGENESIS

Relative timing of events	Anhydrite formation Sparite crystallisation Micritisation

MINERALOGICAL CLASSIFICATION AND COMMENTS

Mineralogical classification	Dismicrite
Comments	

GSWA No. 154864

Well	VINES-1
Sample number	154864
Sample type	Core
Depth	1537.05-1537.15
Unit	
Facies	Argillaceous siltstone
Sample quality	The sample is in good condition.
Brief description	Micritic limestone This sample is predominantly composed of dolomitised micritic mud. It displays some deformation and contorting of layers. The degree of micritisation makes it difficult to distinguish if this is algal or structural. Feint outlines of recrystallised peloids are evident in this sample. Porosity is filled by anhydrite cements.

TEXTURE

Grain size	Microcrystalline to micritic
Sorting	Indiscernible
Sediment fabric	Anhedral and subhedral calcite crystals with planar and curved contacts.

MINERALOGY

Tabulated composition	*Grain size/ fabric*	*Percentage*
Diagenitic cement		
Micrite		95
Authigenic minerals		
Anhydrite		4
Silica		1
Porosity/ Permeability		
Primary		nil
Secondary		nil

Cement *Diagenetic*	Micrite This sample is predominantly composed of a structurally contorted dolomitised micritic mud. Feint outlines of recrystallised peloids are evident in this sample.
Authigenic cement	Anhydrite Anhydrite is interpreted to be a authigenic mineral filling vugular porosity. Pores cemented and filled with anhydrite have highly irregular and diffuse boundaries that have been partially replaced by sparite and micrite.
Porosity/ Permeability	No porosity is evident in this sample as all vugular porosity has been filled and cemented by anhydrite.

DIAGENESIS

Relative timing of events	Anhydrite formation Micritisation

TEXTURAL MATURITY AND INTERPRETATION

Textural maturity	
Interpretation	

MINERALOGICAL CLASSIFICATION AND COMMENTS

Mineralogical	Micritised limestone

classification	
Comments	Two-sections were cut for this sample 64A+B. Sections were looked at described collectively.

GSWA No. 154863

Well	VINES-1
Sample number	154863
Sample type	Core
Depth	1478.95
Unit	
Facies	Argillaceous siltstone
Sample quality	Sample is in excellent condition.
Brief description	Sub-horizontally laminated micrite This sample consists of fining upwards sub-horizontal laminae of varying thickness composed of medium sand sized quartz grading to illite/sericite clays. A reverse micro-fault cuts through the sample. Movement on this fault is defined by the curving of individual laminae into the fault zone. Illite/sericite has been partially replaced by microcrystalline carbonate mud. Visual porosity in this sample is negligible.

STRUCTURES

Structures	Lamination This sample is composed of a series of sub-horizontal laminae of irregular thickness. A fining upwards grading is defined by changes in grain size. The basal section of the laminae are typically composed of very fine to fine sand quartz grains that decrease in size upwards grading eventually into illite/sericite clays and micritic mud. Laminae often display sharp, hummocky tops. Micro-faulting A low angle reverse fault is evident in the top right of this section. This fault displays an angle of approximately 40 to 45°. The sense of movement on this fault is evident from the curving of individual laminae into the fault plane and the minor displacement of these layers. Soft-sediment deformation Small flame structures are evident in this sample. These structures are typically filled with silt-sized quartz that has been forced upwards into the overlying laminae.

TEXTURE

Grain size	Range: Clay to medium sand (0.45mm) Mode: Clay and medium silt (0.03mm)
Sorting	Poorly sorted
Grain morphology	Angular to sub-angular
Sediment fabric	Matrix supported. Grains display occasional point contact.

MINERALOGY

Tabulated composition (%)	Detrital components		
	Quartz	Monocrystalline	10
	Feldspar	Albite	Tr
	Accessories	Mica	Tr
		Pyrite	1
	Rock fragments	Carbonate clasts	1
		Chert	Tr
	Matrix/ Pseudomatrix		
		Dolomite &Illite/sericite	70
	Authigenic cement		
		Dolomite	2
		Carbonate mud	16

	Porosity/ Permeability Primary Nil Secondary Tr
Detrital components	Quartz Quartz grains range in size from medium sand (0.45mm) to medium silt (0.03mm) with a mode of medium silt (0.03mm). Grains are angular to sub-rounded, poorly sorted and are predominantly matrix supported but display rare point contacts. Rock fragments *Carbonate clasts* Carbonate clasts are typically medium sand sized. These clasts are composed of anhedral to subhedral shaped dolomite crystals that display planar, curved and sutured contacts. *Chert* Chert grains are composed of speckled microcrystalline quartz.
Matrix/ Pseudomatrix	Illite/sericite Illite/sericite is the main component of this section. Micritised dolomite mud is also generally associated with illite/sericite rich layers. In some cases the illite/sericite clays encase small clusters of microcrystalline calcite. The dark colouration of these layers is from the pyrite and insoluble organic matter that is associated with it.
Authigenic cement	Dolomite Small isolated rhombohedral dolomite rhombs are scattered throughout the sample replacing carbonate mud and illite/sericite.
Porosity/ Permeability	The secondary porosity evident in this sample is possibly the result of sample plucking during thin-section manufacture.

DIAGENESIS

Relative timing of events	Illite/sericite formation Pyrite formation Carbonate cementation
Relative importance of events	

TEXTURAL MATURITY AND INTERPRETATION

Textural maturity	Immature
Interpretation	

MINERALOGICAL CLASSIFICATION AND COMMENTS

Mineralogical classification	Micrite
Comments	

GSWA No. 154838

Well	VINES-1
Sample number	154838
Sample type	
Depth	1473.95
Unit	
Facies	Argillaceous siltstone
Sample quality	Sample is in reasonable condition but has been slightly fractured during thin section manufacture.
Brief description	Micritised mudstone This sample is a massive lithic wacke composed predominantly of a matrix of partially carbonate cemented, illite/sericite. Minor percentages of sub-angular to sub-rounded, very fine sand sized quartz, carbonate clasts and sandstone fragments also scattered throughout the sample. No visual porosity was noted.

STRUCTURES

Structures	Massive

TEXTURE

Grain size	Range: Coarse silt (0.05mm) to granules (4mm) Mode: Very fine sand (0.1mm)
Sorting	Poorly-sorted
Grain morphology	Angular to sub-rounded
Sediment fabric	Matrix supported

MINERALOGY

Tabulated composition (%)	Detrital components		
	Quartz	Monocrystalline	18
		Polycrystalline	Tr
		Muscovite	Tr
		Glauconite	Tr
	Rock fragments		
		Carbonate	3
		Chert	Tr
		Sandstone	1
	Matrix/ Pseudomatrix		
		Illite/Sericite	76
	Authigenic cements		
		Calcite	2
		Pyrite	Tr
	Porosity/ Permeability		
		Primary	Nil
		Secondary	Nil

Detrital components	Quartz Monocrystalline quartz dominates this sample but trace polycrystalline quartz is also evident. Quartz grains range in size from coarse silt (0.05mm) to medium sand (0.45mm) with a mode of very fine sand (0.1mm). Grains are sub-angular to rounded, poorly-sorted and matrix supported. Rock fragments *Carbonate clasts* Carbonate clasts range from medium sand size (0.2mm) to granules (4mm). These clasts are generally sub- to well rounded and composed of xenotopic matrix of anhedral to subhedral shaped very finely to finely crystalline dolomite that displays planar, curved and sutured contacts. Micritic alteration is evident in most of these clasts. Micritised clasts consist of equant subhedral to euhedral

	crystals of microsparite and finer micrite which have replaced the original very fine to fine dolomite. Patchy aggrading neomorphism resulting in an increase of crystal size is also apparent. A thin, irregularly shaped stylolite is apparent in one of the carbonate clasts. *Chert* Chert grains are composed of microcrystalline quartz are scattered throughout the sample. These fragments are typically sub-rounded and display a mode of very fine sand (0.1mm). *Sandstone* An interlayered sandstone and siltstone fragment is evident in this sample. This fragment is angular and granule sized (3mm). It is approximately composed of up to 94% moderately sutured, coarse silt sized (0.05mm) quartz grains, trace mica and 6% poikilotopic calcite cement. Advanced pressure solution is evident with grains displaying well-sutured grain-grain contacts. Within the fragment the cement encases clusters of framework grains and fills intergranular pore space. A series of 0.2mm thick, parallel mica-rich illite/sericite seams cut through this sample. These seams occur sub-vertical to general sample orientation. They have highly diffuse margins and their dark colouration is caused by concentrations of pyrite and insoluble organic matter with the illite/sercite.
Matrix/ Pseudomatrix	Illite/sericite This sample is dominated by a partially dolomite cemented and illitised, sericitic mud.
Authigenic cement	
Porosity/ Permeability	Nil.

DIAGENESIS

Relative timing of events	Sericitisation Illite formation Micritisation Calcite cementation
Relative importance of events	

TEXTURAL MATURITY AND INTERPRETATION

Textural maturity	Immature
Interpretation	

MINERALOGICAL CLASSIFICATION AND COMMENTS

Mineralogical classification	Micritic mudstone
Comments	SEM or XRD on this sample would aid in the identification of matrix material.

GSWA No. 154837

Well	VINES-1
Sample number	154837
Sample type	Plug
Depth	1469.0
Unit	
Facies	Argillaceous Siltstone
Sample quality	The sample is in good condition but has been cracked during thin-section manufacture.
Brief description	Micritic mudstone This sample consists of a massive lithic wacke containing 15%, angular to sub-rounded, coarse silt sized quartz and a matrix of dolomitised micritic mud and illite/sericite clays. No porosity is visible.

STRUCTURES

Structures	Massive.

TEXTURE

Grain size	Range: Coarse silt (0.05mm) to medium sand (0.25mm) Mode: Coarse silt (0.06mm)
Sorting	Poorly-sorted
Grain morphology	Angular to sub-rounded
Sediment fabric	Matrix supported no contacts between grains evident

MINERALOGY

Tabulated composition (%)	Detrital components		
	Quartz	Monocrystalline	15
	Feldspar	Albite	Tr
	Rock fragments		
		Carbonate	Tr
		Siltstone	Tr
		Phosphate	Tr
	Accessories	Zircon	Tr
	Matrix/ Pseudomatrix		
		Carbonate mud	85
	Authigenic cements		
		Anhydrite	Tr
	Porosity/ Permeability		
		Primary	Nil
		Secondary	Nil

Detrital components	Quartz Quartz ranges from medium silt (0.2mm) to coarse sand (0.5mm) with a mode of medium silt (0.25mm). Grains are angular to sub-rounded and predominantly matrix supported but display point to concave/convex grain-grain contacts. Grain boundaries are highly irregular having been marginally replaced by calcite and siderite cements. Feldspar Feldspar grains display similar grain size to quartz grains. Several varieties of feldspar are evident these include microcline, albite and plagioclase. Rock fragments *Carbonate clasts* Clasts range from medium sand size (0.2mm) to coarse sand (0.8mm). These clasts are generally sub- to well rounded and composed of xenotopic matrix of anhedral to subhedral shaped very finely to finely crystalline dolomite that displays planar, curved and sutured contacts. Micritic alteration is evident in some of these clasts. Most of the micritised clasts consist of equant subhedral to euhedral crystals of microsparite and finer micrite which have replaced the original very fine to fine dolomite. Minor aggrading neomorphism is apparent in some clasts. *Siltstone* These rock fragments are typically medium sand sized (0.4mm). Grains are angular to sub-rounded and consist of varying amounts of coarse silt sized (0.05mm) quartz grains in an illite/sericite matrix. Some grains have been almost completely altered to illite/sericite and are therefore difficult to distinguish from the matrix. *Phosphate* A large black sub-rounded phosphate fragment is evident in this sample. There is no identifiable texture to this grain as it is cryptocrystalline.
Matrix/ Pseudomatrix	Dolomitic mud A complex mixture of dolomite and illite/sericite forms the matrix of this sample. Illite/sericite is interpreted to dominate this sample. It can be differentiated from carbonate mud by its dark colouration. This dark colouration is caused by a mix of pyrite and insoluble organic matter. Dolomite occurs as a micritic cement that replaced or has been replaced by illite/sercite.
Authigenic cement	Anhydrite Trace anhydrite is evident filling a small sub-vertical fracture in this sample.
Porosity/ Permeability	No primary or secondary porosity is visible in this sample.

DIAGENESIS

Relative timing of events	Sericitisation Carbonate cementation Anhydrite formation
Relative importance of events	

TEXTURAL MATURITY AND INTERPRETATION

Textural maturity	Immature
Interpretation	

MINERALOGICAL CLASSIFICATION AND COMMENTS

Mineralogical classification	Micritic mudstone
Comments	

GSWA No. 154862

Well	VINES-1
Sample number	154862
Sample type	Core
Depth	1465.65m
Unit	
Facies	Argillaceous siltstone
Sample quality	The sample is in good condition.
Brief description	Micritic limestone This sample is predominantly composed of dolomitised micritic mud. The degree of micritisation makes it difficult to distinguish if this is algal or structural. Feint outlines of recrystallised peloids are evident in this sample. Porosity is filled by displacive anhydrite cements.

STRUCTURES

Structures	Fault A smalll microfault is evident by a 2mm offset in sub-horizontal dolomite layers in this section.

TEXTURE

Grain size	Microcrystalline to micritic
Sorting	Indiscernible
Sediment fabric	Anhedral and subhedral calcite crystals with planar and curved contacts.

MINERALOGY

Tabulated composition	*Grain size/ fabric*	*Percentage*
Diagenitic cement		
Micrite		89
Authigenic minerals		
Anhydrite		8
Silica		1
Dolomite	0.03mm	2
Porosity/ Permeability		
Primary		nil
Secondary		

Cement *Diagenetic*	Micrite This sample is predominantly composed of a structurally contorted and dolomitised micritic mud. The mud is dolomitic in composition. Feint outlines of recrystallised peloids are evident scattered throughout this sample. Partial aggrading neomorphism is evident with patches of fine pseudospar being locally developed.
Authigenic cement	Anhydrite Anhydrite is interpreted to be a authigenic mineral filling vugular porosity. Anhydrite appears displacive growing into the surrounding micritic matrix. Illite/sericite Illite/sericite is concentrated along irregular sub-horizontal stylolites that cut across the sample. The dark colouration of illite/sericite cements is caused by the concentration of pyrite and insoluble organic matter along these seams. Dolomite Dolomite clasts are approximately medium sand size (0.2mm). These clasts are generally sub- to well rounded and composed of xenotopic matrix of anhedral to

	subhedral shaped very finely to finely crystalline dolomite that displays planar, curved and sutured contacts.
Porosity/ Permeability	No porosity is evident in this sample as all vugular porosity has been filled and cemented by anhydrite.

DIAGENESIS

Relative timing of events	Anhydrite formation Micritisation

TEXTURAL MATURITY AND INTERPRETATION

Textural maturity	
Interpretation	

MINERALOGICAL CLASSIFICATION AND COMMENTS

Mineralogical classification	Micritised limestone
Comments	

GSWA No. 154861

Well	VINES-1
Sample number	154861
Sample type	Core
Depth	1463.2
Unit	
Facies	Siltstone
Sample quality	The sample is in good condition
Brief description	Irregularly laminated fining upwards micrtitic mudstone This sample is defined by a convoluted lamination defined by the alteration of pale, medium sand sized quartz and dark brown and dolomitised micritic mud. Quartz grains are coarse silt sized at the base of the unit and fine upwards and fine upwards to a fine micritic mud. Visual porosity is poor.

STRUCTURES

Structures	Laminated A distinctive striped appearance is evident in this sample caused by the alternation of light and dark layers. Layers typically fine upwards from a dark brown clay at the top, to a pale matrix supported coarse sand sized quartz layer at the base. A thin condensed chlorite-rich lamination is generally evident between the top of one sequence and the beginning of another. Micro-fracturing of layers and soft sediment deformation resulting in the convolution of layers is also evident.

TEXTURE

Grain size	Range: Medium silt (0.02mm) to coarse silt (0.06mm) Mode: Coarse silt (0.05mm)
Sorting	Poorly-sorted
Grain morphology	Angular to sub-rounded
Sediment fabric	Matrix supported. Grains display rare point contacts.

MINERALOGY

Tabulated composition (%)	Detrital components		
	Quartz	Monocrystalline	12
	Rock Fragments		
		Carbonate	Tr
	Matrix/ Pseudomatrix		
		Illite/sericite	65
	Authigenic cement		
		Anhydrite	3
		Chlorite	20
	Porosity/ Permeability		
		Primary	Nil
		Secondary	Tr
Detrital components	Quartz Quartz grains range in size from medium silt (0.02mm) to coarse silt (0.06mm) with a mode of coarse silt (0.05mm). Grains are typically angular to sub-rounded and matrix supported. Some quartz grains display occasional point contacts. Quartz grains fine upwards from the base and eventually are non-existent being replaced by a clay-rich matrix at the top of the sequence.		
Matrix/ Pseudomatrix	Illite/sericite The clay-rich portions of the laminae are filled predominantly with dark, illite/sericite clays mixed with micrite. Illite/sericite units range between 0.8mm to 1.2mm thick but spot thicknesses may be highly irregular. Apart from a few medium silt sized quartz grains randomly scattered throughout the clay-rich		

	matrix most of the clay could be termed cryptocrystalline.
Authigenic cement	Chlorite Chlorite forms both as a sub-horizontal, 0.5mm thick condensed section between successive sequences and as an alteration product replacing the illite/sericite matrix in the more quartz-rich portions of the slide. These thin condensed sections are extremely irregular and display sharp contacts with clay matrix and quartz-rich layers. Altered chlorite tends to replace detrital matrix and encase clusters of framework grains. Most of this alteration is confined to the extent of quartz laminae. Anhydrite Blocky anhydrite typically forms filling fractures. These fractures have no preferred orientation and display some dilation at their centre. The anhydite cement forms highly corrosive contacts with the surrounding matrix.
Porosity/ Permeability	Porosity observed in this section is secondary. It is developed within micro-fractures that are scattered throughout the sample.

DIAGENESIS

Relative timing of events	Anhydrite cementation Chlorite alteration
Relative importance of events	

TEXTURAL MATURITY AND INTERPRETATION

Textural maturity	Immature
Interpretation	

MINERALOGICAL CLASSIFICATION AND COMMENTS

Mineralogical classification	Micritic mudstone
Comments	

GSWA No. 154835

Well	VINES-1
Sample number	154835
Sample type	Core
Depth	1458.53
Unit	
Facies	Argillaceous siltstone
Sample quality	This sample is in good condition.
Brief description	Micritic mudstone This sample is a tubiditic-like siltstone. It consists predominantly of a mottled siltstone composed of sub-angular to sub-rounded very fine sand sized quartz, supported by a matrix of illite/sericite and dolomitised micritic mud. Anhydrite is interpreted to have formed early possibly insitu. No porosity is evident in this sample.

STRUCTURES

Structures	Intensely biturbated turbidites This sample consists of an intensely bioturbated turbidite-like sequence. The degree of bioturbation has given the sample a mottled appearance where it alternates between siltier areas and pure illite/sericite clay.

TEXTURE

Grain size	Range: Medium silt (0.02mm) to very fine sand (0.07mm) Mode: Very fine sand (0.06mm)
Sorting	Poorly-sorted
Grain morphology	Sub-angular to sub-rounded
Sediment fabric	Matrix supported. Grains display occasional point contacts

MINERALOGY

Tabulated composition (%)	Detrital components		
	Quartz	Monocrystalline	15
	Matrix/ Pseudomatrix		
		Illite/sericite	82
	Authigenic cement		
		Anhydrite	1
		Calcite	2
	Porosity/ Permeability		
		Primary	Nil
		Secondary	Nil
Detrital components	Quartz Quartz grains range in size from medium silt (0.02mm) to very fine sand (0.07mm) with a mode of very fine sand (0.06mm). Grains are sub-angular to rounded, poorly-sorted and matrix supported.		
Matrix/ Pseudomatrix	Illite/sericite This matrix is dominated by a dark brown cryptocrystalline illite/sericite clay. The matrix is patchy. Sections of it exist as a mixture of dolomitic mud and illite/sericite pods and other areas are siltier containing quartz impurities.		
Authigenic cement	Anhydrite Trace anhydrite cement is evident and has expanded possibly through dissolution into the adjacent sediment. Calcite Isolated microsparry calcite grains occur replacing the illite/sericite matrix.		
Porosity/ Permeability	No visual porosity is evident in this sample.		

GSWA No. 154834

Well	VINES-1
Sample number	154834
Sample type	Plug
Depth	1410.2
Unit	
Facies	Sandstone
Sample quality	Sample is in good condition.
Brief description	Quartz arenite This sample is dominated by very fine sand sized, angular to sub-rounded quartz that has been cemented by anhydrite. Anhydrite cements have been partially replaced by late stage calcite. Visual porosity is poor.

STRUCTURES

Structures	Soft sediment deformation Minor soft sediment deformation is evident in this sample contorting lamination.

TEXTURE

Grain size	Mode: Coarse silt (0.05) to very fine sand (0.08mm) Mode: Very fine sand (0.06mm)
Sorting	Well-sorted
Grain morphology	Angular to sub-rounded
Sediment fabric	Grains display point to concave/convex and moderately sutured grain-grain contacts

MINERALOGY

Tabulated composition (%)	Detrital components		
	Quartz	Monocrystalline	77
	Feldspar	Microcline	Tr
		Albite	1
		Mica	Tr
		Biotite	Tr
	Accessories	Zircon	Tr
		Tourmaline	Tr
		Organic matter	Tr
	Authigenic cement		
		Calcite	7
		Anhydrite	12
		Illite/sericite	2
		Pyrite	1
	Porosity/ Permeability		
		Primary	Nil
		Secondary	Tr

Detrital components	Quartz Well-sorted, monocrystalline quartz dominates this sample. Quartz grain sizes range from coarse silt (0.05) to very fine sand (0.08mm) with a mode of very fine sand (0.06mm). Grains are angular to sub-rounded and display point to concave/convex and moderately sutured grain-grain contacts. Feldspar Feldspar grains display similar grain size to quartz grains. Several varieties of feldspar are evident these include microcline, albite and plagioclase.
Matrix/ Pseudomatrix	
Authigenic cement	Anhydrite This sample is dominated by anhydrite cement. This cement occurs as separate rectangular crystals or as a massive, poikilotopic cement encasing framework grains and filling intergranular pore space. It has been partially replaced by an equant drusy mosaic of very finely to finely crystalline calcite crystals. Calcite Some of the matrix material and anhydrite cement has been replaced by patchy calcite cement. This cement tends to be replacing sections of the sample in thin discontinuous lenses. Most of this cement occurs as microsparry accumulations of finely to medium crystalline calcite or as rare single crystal poikilotopes. Illite/sericite Most of the illite/sericite is concentrated in thin, discontinuous, sub-horizontal solution seams. These seams are approximately 0.1 to 0.15 mm thick. The dark colouration of these seams is produced by the mixing of pyrite and insoluble organic matter with the illite/sericite. Trace amounts of the illite/sericite are also evident mixed with carbonate cements.
Porosity/ Permeability	Only trace secondary porosity is evident in this sample. This porosity was possibly produced by the leaching and dissolution of anhydrite cement.

DIAGENESIS

Relative timing of events	Mechanical compaction Anhydrite cementation Calcite cementation
Relative importance of events	

TEXTURAL MATURITY AND INTERPRETATION

Textural maturity	Immature
Interpretation	

MINERALOGICAL CLASSIFICATION AND COMMENTS

Mineralogical classification	Quartz arenite
Comments	

GSWA No. 154860

Well	VINES-1
Sample number	154860
Sample type	Core
Depth	1395.95m
Unit	
Facies	Argillaceous siltstone
Sample quality	The sample is in good condition.
Brief description	Micritic limestone This sample is predominantly composed of dolomitised micritic mud. The degree of micritisation makes it difficult to distinguish if this is algal or structural. Feint outlines of recrystallised peloids are evident in this sample. Porosity is filled by displacive anhydrite cements.

TEXTURE

Grain size	Microcrystalline to micritic
Sorting	Indiscernible
Sediment fabric	Anhedral and subhedral calcite crystals with planar and curved contacts.

MINERALOGY

Tabulated composition	*Grain size/ fabric*	*Percentage*
Diagenitic cement		
Micrite		91
Authigenic minerals		
Anhydrite		8
Silica		1
Porosity/ Permeability		
Primary		nil
Secondary		nil

Cement *Diagenetic*	Micrite This sample is predominantly composed of a structurally contorted micritic mud. The mud is dolomitic in composition. Feint outlines of recrystallised peloids are evident scattered throughout this sample. Partial aggrading neomorphism is evident with patches of fine pseudospar being locally developed.
Authigenic cement	Anhydrite Anhydrite is interpreted to be a authigenic mineral filling vugular porosity. Anhydrite appears displacive growing into the surrounding micritic matrix. Illite/sericite Illite/sericite is concentrated along irregular sub-horizontal stylolites that cut across the sample. The dark colouration of illite/sericite cements is caused by the concentration of pyrite and insoluble organic matter along these seams.
Porosity/ Permeability	No porosity is evident in this sample as all vugular porosity has been filled and cemented by anhydrite.

DIAGENESIS

Relative timing of events	Anhydrite formation Micritisation

TEXTURAL MATURITY AND INTERPRETATION

Textural maturity	
Interpretation	

MINERALOGICAL CLASSIFICATION AND COMMENTS

Mineralogical classification	Micritised limestone
Comments	

GSWA No. 154859

Well	VINES-1
Sample number	154859
Sample type	Core
Depth	1383.7
Unit	
Facies	Siltstone
Sample quality	The sample is in good condition.
Brief description	Micritic mudstone This sample is a siltstone consisting predominantly of a partially micritised illite/sericite matrix with minor percentages of coarse silt sized quartz. Visual porosity is extremely poor.

STRUCTURES

Structures	Dewatering structures This sample displays sub-vertical structures filled with anhydrite. Decolouration of the matrix is evident in the vicinity of these structures. They have very irregular and diffuse margins. Dewatering or solution of these structures during burial has caused the generation of small radiating, anhydrite filled sub-horizontal fractures.

TEXTURE

Grain size	Range: Medium silt (0.04mm) to very fine sand (0.11mm) Mode: Coarse silt (0.07mm)
Sorting	Poorly-sorted
Grain morphology	Angular to sub-rounded.
Sediment fabric	Matrix supported. Detrital grains display occasional point to concave/convex grain-grain contacts.

MINERALOGY

Tabulated composition (%)	Detrital components		
	Quartz	Monocrystalline	25
	Glauconite		Tr
	Rock Fragments		
		Carbonate	7
	Matrix/ Pseudomatrix		
		Illite/sericite	52
	Authigenic cement		
		Siderite	1
		Calcite	10
		Anhydrite	5
		Pyrite	Tr
		Silica	1
	Porosity/ Permeability		
		Primary	Nil
		Secondary	Tr
Detrital components	Quartz Quartz grains range in size from medium silt (0.04mm) to very fine sand (0.11mm) with a mode of coarse silt (0.07mm). Grains are typically angular to sub-rounded and matrix supported. Occasional point and concave/convex grain-grain contacts between the quartz grains are evident. Most of the grains have been marginally replaced by calcite and siderite cements, resulting in irregular and diffuse boundaries.		

Matrix/ Pseudomatrix	Illite/sericite The matrix consists predominantly of a massive, dark brown illite/sericite that has been partially micritised. Micirtic crystals occur both as isolated grains and as microsparry accumulations.
Authigenic cement	Anhydrite Blocky anhydrite cement fills fractures within this sample. Most of the anhydrite occurs as partially dissolved, rectangular crystals or as a massive, partially leached cement encasing framework grains. Anhydrite cement in burrows forms highly corrosive contacts with the surrounding illite/sericite matrix. Silica Traces of massive poikliotopic silica cement is evident filling fractures. This cement has been partially replaced by anhydrite.
Porosity/ Permeability	Visual porosity is poor in this sample. Most of the porosity and permeability in this sample is interpreted to be micro and therefore undetectable with a conventional microscope.

DIAGENESIS

Relative timing of events	Anhydrite formation Trace silica cementation Calcite cementation
Relative importance of events	

TEXTURAL MATURITY AND INTERPRETATION

Textural maturity	Immature
Interpretation	

MINERALOGICAL CLASSIFICATION AND COMMENTS

Mineralogical classification	Micritic mudstone
Comments	This sample would warrant SEM work to help in the identification of matrix material and identification of micro-porosity.

GSWA No. 154858

Well	VINES-1
Sample number	154858
Sample type	Core
Depth	1372.95
Unit	
Facies	Argillaceous siltstone
Sample quality	The sample is in good condition
Brief description	Litharenite This sample consists predominantly of sub-angular to sub-rounded, very fine to very coarse sand sized quartz and fragments of carbonate, sandstone and siltstone. Framework grains have been cemented by anhydrite which has been partially replaced by an equant drusy mosaic of very finely to finely crystalline calcite crystals. Porosity is poor as pore space has been filled by anhydite and calcite cements.

STRUCTURES

Structures	Massive.

TEXTURE

Grain size	Range: Very fine sand (0.1mm) to very coarse sand (1.2mm) Mode: Medium sand (0.3mm)
Sorting	Well-sorted
Grain morphology	Sub-angular to sub-rounded
Sediment fabric	Grains display point to concave/convex and moderately sutured grain-grain contacts.

MINERALOGY

Tabulated composition (%)	Detrital components		
	Quartz	Monocrystalline	63
		Polycrystalline	2
	Feldspar	Albite	2
		Plagioclase	1
	Rock fragments		
		Carbonate	7
		Sandstone	4
		Siltstone	3
		Chalcedony	Tr
		Chert	2
		Kaolinite	2
		Ooidal carbonate	Tr
		Algal limestone	Tr
	Accessories	Zircon	Tr
		Tourmaline	Tr
	Authigenic cement		
		Calcite	3
		Anhydrite	10
		Siderite	1
		Silica overgrowths	Tr
	Porosity/ Permeability		
		Primary	Tr
		Secondary	Nil

Detrital components	Quartz Moderately-sorted, monocrystalline quartz dominates this sample. Quartz grain sizes range from very fine sand (0.1mm) to coarse sand (0.6mm) with a mode of medium sand (0.3mm). Grains are sub-angular to rounded. Pressure solution is evident with grains displaying point to concave/convex and weakly sutured grain-grain contacts. Thin authigenic silica overgrowths are apparent on some grain boundaries. Most quartz grains also contain fluid inclusions or vacuoles. They are identified as lines of dark specks that cut across quartz grains. Rock fragments *Carbonate clasts* Carbonate clasts range from medium sand size (0.3mm) to very coarse sand sized (1.5mm). These clasts are generally sub- to well rounded and composed of xenotopic matrix of anhedral to subhedral shaped very finely to finely crystalline dolomite that displays planar, curved and sutured contacts. Micritic alteration is evident in some of these clasts. Most of the micritised clasts consist of equant subhedral to euhedral crystals of microsparite and finer micrite which have replaced the original very fine to fine dolomite. The occurrence of patches of non-equant pseudospar replacing micrite in some of the clasts indicates that they may or have undergone partial aggrading neomorphism. Minor dissolution and vcuolisation of some of these clasts is apparent. Most of the vacuoles created have been cemented by anhydrite. *Ooidal carbonate* Trace ooidal carbonate fragments are evident in this sample. These clasts consist of ooids 0.1 to 0.3mm in size that have been partially recrystallised by a xenotopic matrix of anhedral to subhedral shaped very finely to finely crystalline dolomite that displays planar, curved and sutured contacts. Ooids have a well preserved micritised rim that makes them easily identifiable. Aggrading neomorphism is also apparent in some of these clasts with their centre being replaced by patches of pseudospar. *Sandstone* Traces of well-cemented sandstone fragments are also evident in this sample. These fragments range from medium sand (0.3mm) to coarse sand (0.9mm) size. Fragments are generally sub-angular to sub-rounded and composed of up to 90% moderately sutured, coarse silt sized (0.05mm) quartz grains, 1% mica and 9% poikilotopic calcite cement and trace anhydrite. The cement encases clusters of framework grains and fills intergranular pore space. *Chalcedony* Trace chalcedony fragments are scattered throughout this sample. These fragments range up to coarse sand size (0.6mm). Grains are generally angular and occasionally are broken and display typical chalcedonic texture comprising of radiating fibrous crystals of varying size. *Chert* Chert grains range in size from fine sand (0.14mm) to coarse sand (0.6mm). Most grains are sub-rounded and composed predominantly of microquartz with patches of macroquartz. *Siltstone* Siltstone fragments consist of predominantly of an illite/sericite matrix with trace percentages of medium silt sized quartz and mica. Some of these fragments show an internal anastomosing network of thin, irregular stylolites. Partial dissolution and cracking of these some of these fragments is apparent. Cracks have generally been cemented by anhydrite.

	Kaolinite Kaolinite occurs as sub-rounded to rounded clasts or balls that occupy intergranular pore space. These clasts consist of finely to coarsely crystalline accumulations of kaolinite. Most of the clasts have undergone partial compaction resulting in their expansion of the kaolinite into intergranular pore space.
Matrix/ Pseudomatrix	
Authigenic cement	Silica overgrowths Most of the silica overgrowths are evident at triple junctions between quartz grains. Interference of individual silica overgrowths at triple junctions has produced irregular compromise boundaries. Anhydrite This sample is predominantly anhydrite cemented. Most of the anhydrite occurs as separate rectangular crystals or as a massive, partially leached poikilotopic cement encasing framework grains. It forms highly corrosive contacts with surrounding grains and occasionally replaces detrital grains. Calcite Calcite cement occurs either partially or totally replacing pore filling anhydrite. Calcite generally occurs as an equant drusy mosaic of very finely to finely crystalline crystals and poikiltopic cement. The cement displays a typical pore-filling characteristic increasing in crystal size towards the pore centre. Siderite Siderite occurs as microcrystalline accumulation and individual grains that marginally replace detrital grains and pore-filling cements. Pyrite Pyrite occurs as nodules that partially replace grains and rock fragments.
Porosity/ Permeability	Only trace porosity is evident in this sample. Almost all of the porosity has been filled by anhydrite and calcite cements.

DIAGENESIS

Relative timing of events	Authigenic silica cementation Micritisation of carbonate clasts Anhydrite cementation Calcite cementation Pyrite formation
Relative importance of events	

TEXTURAL MATURITY AND INTERPRETATION

Textural maturity	Immature
Interpretation	

MINERALOGICAL CLASSIFICATION AND COMMENTS

Mineralogical classification	Litharenite
Comments	

GSWA No. 154833

Well	VINES-1
Sample number	154833
Sample type	Plug
Depth	1325.1
Unit	
Facies	Sandstone
Sample quality	The sample is in good condition
Brief description	Interbedded micritic mudstone and litharenite This sample is composed of an interbedded lithic wacke and litharenite. The litharenite is composed of a mixture of anhydrite and calcite cemented coarse sand sized quartz; and carbonate, sandstone, lithoclasts, chert and chalcedony fragments. Some micritic mud is also evident in this unit. The micritic mudstone is dominated by micritic mud and coarse silt sized quartz with lesser amounts of carbonate and chert rock fragments. The contact between the two beds is quite sharp. Visual porosity is extremely poor being replaced by micritic mud, anhydrite and secondary calcite cements.

STRUCTURES

Structures	Bedding This sample consists of a 14mm thick lithic wacke bed that cuts sub-horizontally across it. The bed is defined by a reduction in framework grain size and increases in micritic mud matrix. The grain size mode decreases from medium to coarse sand (0.5mm) in the litharenite, to coarse silt (0.05mm) in the lithic wacke. A flame structure is evident where the sandstone has been forced up into the lithic wacke bed.

TEXTURE

Grain size	Range: Coarse silt (0.05mm) to very coarse sand (1.3mm) Mode: Bimodal→ Coarse silt (0.05mm) to coarse sand (0.5mm)
Sorting	Poorly-sorted
Grain morphology	Sub-angular to sub-rounded
Sediment fabric	Grains display point to concave/convex and moderately sutured grain-grain contacts.

MINERALOGY

Tabulated composition (%)	Detrital components		
	Quartz	Monocrystalline	60
		Polycrystalline	Tr
		Oncoids	Tr
	Rock fragments		
		Carbonate	9
		Lithoclasts	3
		Chert	3
		Chalcedony	Tr
		Chalcedonic quartz	1
		Volcanics	Tr
		Sandstone	Tr
	Matrix/ Pseudomatrix		
		Carbonate mud	18
	Accessories		
		Tourmaline	Tr
		Zircon	Tr
		Spinel	Tr

	Authigenic cement		
		Calcite	2
		Anhydrite	3
		Pyrite	1
		Siderite	1
		Chert	Tr
	Porosity/ Permeability		
		Primary	Nil
		Secondary	Tr
Detrital components	Quartz *Micirite mudstone* Quartz ranges from medium silt (0.2mm) to coarse sand (0.5mm) with a mode of medium silt (0.25mm). Grains are angular to sub-rounded and predominantly matrix supported but display point to concave/convex grain-grain contacts. Grain boundaries are highly irregular having been marginally replaced by calcite and siderite cements. *Litharenite* Quartz ranges from very fine sand (0.1mm) to very coarse sand (0.9mm) with a mode of medium sand (0.4mm). Grains are sub-angular to sub-rounded and display point to concave/convex grain-grain contacts. Oncoid Oncoids range in size from medium sand (0.2mm) to coarse sand (0.6mm). These oncoids consist of a concentrically laminated internal quartz grain or colourless phosphate fragments. They are often difficult to identify as they have been partially replaced and incorporated by calcite cements. Rock fragments **Note:** Most rock fragments occur throughout both lithologies. As a result they have only been described collectively. However a higher percentage of rock fragments has been noted in the sandstone units. An approximate ratio for sandstone to siltstone rock fragments would be 2:1. *Carbonate clasts* Carbonate clasts are evident in both lithologies. Clasts range from medium sand size (0.2mm) to very coarse sand (1.2mm). These clasts are generally sub- to well rounded and composed of xenotopic matrix of anhedral to subhedral shaped very finely to finely crystalline dolomite that displays planar, curved and sutured contacts. Their shape does vary however due to their compaction into intergranular pore space causing them to become elongate or irregularly shaped. Some of these carbonate clasts could be termed allochemical in that they consist of a mixture of medium sand sized quartz grains in a xenotopic matrix of anhedral to subhedral shaped very finely to finely crystalline dolomite that displays planar, curved and sutured contacts. Micritic alteration is evident in some of these clasts. Most of the micritised clasts consist of equant subhedral to euhedral crystals of microsparite and finer, micrite which have replaced the original very fine to fine calcite. Patchy replacement of micrite by non-equant pseudospar is evident in some of the clasts. The change in grain size indicates that almost all clasts have been subjected to some amount of aggrading neomorphism. Rare chert replacement of some grains is also evident. *Lithoclasts* Only evident in litharenite. These grains could be termed flint, but due to the truncation of microquartz nodules at the grain boundary they have been termed lithoclasts. Lithoclasts consist of a mixture of concentric microquartz and chalecedonic silica. Microquartz is evident as elongate and round grains with a mode of fine sand (0.2mm). Chalcedonic silica is typically located between		

	nodules. It mainly occurs as radial-fibrous, pore-filling cement. There is a slight increase in chalcedonic crystal grain size towards the centre of pores. *Chert* Chert grains composed of microcrystalline quartz are scattered throughout the sample. These grains range in size from medium sand (0.3mm) to very coarse sand (1.2mm). Some of these chert fragments have patchy carbonate growths associated with them. This possibly indicates replacement by silica of an original limestone fabric. *Chalcedony* Rare detrital chalcedony fragments are located throughout this sample. These fragments range in size from very coarse sand (1.1mm) to granules (2mm). Grains are generally angular and occasionally are broken. Grains display typical chalcedonic texture comprising of radiating fibrous crystals of varying size. *Volcanics* Trace volcanics are evident in this sample. These rock fragments are of similar size to quartz grains, sub-angular, and consist of large laths of plagioclase feldspar grains. Grain boundaries are highly irregular and diffuse and some volcanic grains display minor dissolution and dispersion into intergranular pore space. Most volcanic fragments have been partially altered to a mixture of sericite, chlorite and carbonate which has destroyed their original fabric. *Sandstone* Traces of well-cemented sandstone fragments are also evident in this sample. These fragments are typically coarse sand sized (0.5mm). Fragments are generally sub-angular to sub-rounded and composed of up to 90% moderately sutured, coarse silt sized (0.05mm) quartz grains, 1% mica and 9% poikilotopic calcite cement. Within the fragment the cement encases clusters of framework grains and fills intergranular pore space.
Matrix/ Pseudomatrix	<u>Carbonate mud</u> Most of this sample is supported by a matrix of micritic mud. The litharenite is interpreted to contain approximately 75% of the total matrix. This mud occurs as a xenotopic fabric of equant, very finely crystalline micrite that occasionally displays fluctuations in grains size to finely crystalline calcite. The dark colouration of this mud may be caused by the mixture of illite/sericite clays with the mud.
Authigenic cement	<u>Anhydrite</u> Anhydrite cement is mainly concentrated in the litharenite but patches of it do exist in the lithic wacke. Most of the anhydrite occurs as separate rectangular crystals or as a massive, poikilotopic cement encasing framework grains. It has been partially replaced by an equant drusy mosaic of very finely to finely crystalline calcite and in rare cases chert cement. <u>Calcite</u> Some of the matrix material and anhydrite cement has been replaced by secondary calcite cement. Most of this cement occurs as microsparry accumulations of medium crystalline calcite or as rare single crystal poikilotopes. <u>Siderite</u> Siderite occurs as microcrystalline accumulation and individual grains that marginally replace detrital grains and pore-filling cements. <u>Pyrite</u> <u>Pyrite occurs as nodules that partially replace grains and rock fragments.</u>
Porosity/ Permeability	Visual porosity is poor in this sample as pore space has been filled by both anhydrite and calcite cements. Rare leaching of the anhydrite cement has produced some trace secondary porosity.

DIAGENESIS

Relative timing of events	Mechanical compaction Micritisation Anhydrite cementation Neomorphism Secondary calcite cementation Pyrite cementation
Relative importance of events	

TEXTURAL MATURITY AND INTERPRETATION

Textural maturity	Mature
Interpretation	

MINERALOGICAL CLASSIFICATION AND COMMENTS

Mineralogical classification	80% Micritic mudstone 20% Litharenite
Comments	

GSWA No. 154857

Well	VINES-1
Sample number	154857
Sample type	Core
Depth	1227.95
Unit	
Facies	Diamictite
Sample quality	The sample is in good condition
Brief description	Lithic wacke This sample is basically composed of a series of rock fragments and very fine to coarse sand sized quartz partially cemented by calcite. The dominant rock fragments include carbonate, siltstone, sandstone and shale. These fragments are up to pebble sized and display point to weakly sutured grain-grain contacts. Quartz grains are mostly located in the intergranular pore space between rock fragments. Visual porosity in this sample is interpreted to be moderate.

STRUCTURES

Structures	Massive

TEXTURE

Grain size	Range: Coarse silt (0.04mm) to pebbles (20mm) Mode: Very fine sand (0.07mm)
Sorting	Poorly-sorted
Grain morphology	Tabular to sub-rounded
Sediment fabric	Framework grains display point to concave/convex point contacts. Internally some grains within fragments may display moderately-sutured grain-grain contacts.

MINERALOGY

Tabulated composition (%)	Detrital components		
	Quartz	Monocrystalline	38
		Polycrystalline	2
	Feldspar	Albite	Tr
		Plagioclase	Tr
	Rock fragments		
		Carbonate	17
		Sandstone	8
		Siltstone	15
		Chalcedony	1
		Chert	3
		Kaolinite	Tr
		Shale	1
	Accessories	Zircon	Tr
		Tourmaline	Tr
	Authigenic cement		
		Calcite	7
		Pyrite	Tr
		Dolomite	1
	Porosity/ Permeability		
		Primary	3
		Secondary	2

Detrital components	Quartz Poorly-sorted, monocrystalline quartz dominates this sample. Quartz grain sizes range from coarse silt (0.05mm) to coarse sand (0.7mm) with a mode of very fine sand (0.07mm). Grains are sub-angular to rounded. Quartz grains are generally matrix supported or cemented. Grains occasionally display point to concave/convex grain-grain contacts. Most quartz grains also contain fluid inclusions or vacuoles. They are identified as lines of dark specks that cut across quartz grains. Rock fragments *Carbonate clasts* Carbonate clasts range up to pebbles (20mm). These clasts are generally sub- to well rounded and composed of xenotopic matrix of anhedral to subhedral shaped very finely to finely crystalline dolomite that displays planar, curved and sutured contacts. Micritic alteration is evident in some of these clasts. Most of the micritised clasts consist of equant subhedral to euhedral dolomite crystals of microsparite and finer micrite which have replaced the original very fine to fine dolomite. The occurrence of patches of non-equant pseudospar replacing micrite in some of the clasts indicates that they may or have undergone partial aggrading neomorphism. Aggrading carbonate crystals may reach sizes of 0.05mm or finely crystalline. Some minor pyrite alteration of these clasts is also evident. Thin, discontinuous wispy stylolites are evident in one of the clasts. These stylolites display no preferred orientation ranging form sub-vertical to sub-horizontal. Illite/sericite, pyrite and insoluble organic matter is concentrated along the stylolites. Thin micritic rims are sometimes evident on the outside of these fragments. *Sandstone* Traces of well-cemented sandstone fragments are also evident in this sample. These fragments range from coarse sand (0.5mm) to pebble (6mm) sized. Fragments are generally sub-angular to sub-rounded and composed of up to 80% moderately sutured, coarse silt sized (0.05mm) quartz grains, 1% mica and muscovite and 19% poikilotopic calcite cement. Mica flakes display a weak preferential orientation sub-horizontal to the elongate axis of the sandstone fragment. The cement encases clusters of framework grains and fills intergranular pore space. A thin, discontinuous pyrite-rich sub-horizontal lamination is evident in some of these fragments. *Chert* These grains range in size from medium sand (0.3mm) to very coarse sand (1.2mm). Chert fragments are typically composed of microquartz with patches of megaquartz. *Chalcedony* Rare detrital chalcedony fragments are located throughout this sample. These fragments range in size from very coarse sand (1.1mm) to granules (2mm). Grains are generally angular and occasionally are broken. Grains display typical chalcedonic texture comprising of radiating fibrous crystals of varying size. *Siltstone* Angular to sub-rounded siltstone fragments range up to pebble size (6mm). These fragments generally composed of 30% medium silt sized quartz grains, 5% mica and 65% sericite. Quartz and mica flakes display some minor preferential alignment sub-horizontal to the elongate axis of the fragment. Heavy leaching and dissolution and cracking of these grains is evident. Some leached fragments display partial dolomitisation, and pyrite replacement and large secondary pores. Thin, discontinuous illite/sericite-rich styolilisation

	surfaces are evident in some of these fragments. *Kaolinite* Kaolinite occurs as sub-rounded to rounded clasts or balls that occupy intergranular pore space. These clasts consist of finely to coarsely crystalline accumulations of kaolinite. Most of the clasts have undergone partial compaction resulting in their expansion of the kaolinite into intergranular pore space.
Matrix/ Pseudomatrix	Sericite Dissolution and dispersion of some of the clay-rich rock fragments has resulted in the patchy accumulation of some detrital clays in intergranular pore space.
Authigenic cement	Calcite Calcite generally occurs as an equant drusy mosaic of very finely to finely crystalline crystals. The cement displays a typical pore-filling characteristic increasing in crystal size towards the pore centre. Partial replacement of framework grain boundaries by very finely crystalline calcite is evident in this sample.
Porosity/ Permeability	Porosity in this sample is good. Minor compactional deformation of rock fragments and only partial calcite cementation of intergranular pore space has resulted in good preservation of primary pore space. Leaching and vacuolisation of some rock fragments has also resulted in the development of moderate secondary porosity.

DIAGENESIS

Relative timing of events	Mechanical compaction Grain dissolution Calcite cementation Pyrite replacement
Relative importance of events	

TEXTURAL MATURITY AND INTERPRETATION

Textural maturity	Immature
Interpretation	

MINERALOGICAL CLASSIFICATION AND COMMENTS

Mineralogical classification	Lithic wacke
Comments	

GSWA No. 154830

Well	VINES-1
Sample number	154830
Sample type	Plug
Depth	1215.0
Unit	
Facies	Conglomerate
Sample quality	Sample is in good condition
Brief description	Pebbly quartz arenite This sample consists predominantly of sub-angular to sub-rounded, medium to coarse sand sized quartz, and medium sand to pebble sized fragments of carbonate, sandstone and siltstone. Framework grains have been cemented by anhydrite which has been partially replaced by an equant drusy mosaic of very finely to finely crystalline crystals. Trace secondary porosity has been produced by the minor dissolution of anhydrite, but overall porosity is extremely poor.

STRUCTURES

Structures	Massive

TEXTURE

Grain size	Range: Coarse silt (0.05mm) to pebbles (12mm) Mode: Medium to coarse sand (0.5mm)
Sorting	Moderately-sorted
Grain morphology	Sub-angular to sub-rounded
Sediment fabric	Grains display point, concave/convex and well-sutured grain-grain contacts

MINERALOGY

Tabulated composition (%)	Detrital components		
	Quartz	Monocrystalline	70
		Polycrystalline	2
	Feldspar	Albite	Tr
		Plagioclase	Tr
	Rock fragments		
		Carbonate	4
		Sandstone	6
		Siltstone	3
		Phosphate	1
		Chalcedony	Tr
		Chert	2
		Kaolinite	2
		Metaquartz	Tr
	Accessories	Zircon	Tr
		Tourmaline	Tr
	Authigenic cement		
		Calcite	3
		Anhydrite	7
		Pyrite	Tr
		Siderite	Tr
		Dolomite	Tr
		Silica overgrowths	Tr
	Porosity/ Permeability		
		Primary	Nil
		Secondary	Tr

Detrital components	Quartz Moderately-sorted, monocrystalline quartz dominates this sample. Quartz grain sizes range from coarse silt (0.05mm) to coarse sand (0.5mm) with a mode of medium to coarse sand (0.5mm). Grains are sub-angular to rounded. Pressure solution is evident with grains displaying concave/convex to well-sutured grain-grain contacts. Thin authigenic silica overgrowths are apparent on some grain boundaries. Most quartz grains also contain fluid inclusions or vacuoles. They are identified as lines of dark specks that cut across quartz grains. Rock fragments *Carbonate clasts* Carbonate clasts range from medium sand size (0.2mm) to granules (4mm). These clasts are generally sub- to well rounded and composed of xenotopic matrix of anhedral to subhedral shaped very finely to finely crystalline dolomite that displays planar, curved and sutured contacts. Micritic alteration is evident in some of these clasts. Most of the micritised clasts consist of equant subhedral to euhedral dolomite crystals of microsparite and finer, micrite which have replaced the original very fine to fine calcite. The occurrence of patches of non-equant pseudospar replacing micrite in some of the clasts indicates that they may or have undergone partial aggrading neomorphism. *Ooidal carbonate* Trace ooidal carbonate fragments are evident in this sample. These clasts consist of ooids 0.1 to 0.3mm in size that have been partially recrystallised by a xenotopic matrix of anhedral to subhedral shaped very finely to finely crystalline dolomite that displays planar, curved and sutured contacts. Ooids have a well preserved micritised rim that makes them easily identifiable. Aggrading neomorphism is also apparent in these clasts with micrite being partially replaced by patches of pseudospar. *Sandstone* Traces of well-cemented sandstone fragments are also evident in this sample. These fragments range from coarse sand (0.5mm) to pebble (12mm) sized. Fragments are generally sub-angular to sub-rounded and composed of up to 90% moderately sutured, coarse silt sized (0.05mm) quartz grains, 1% mica and 9% poikilotopic calcite cement. The cement encases clusters of framework grains and fills intergranular pore space. The large pebble fragment also has traces of coarse sand sized fragments incorporated in it. These clasts include carbonate and metaquartz. *Chalcedony and chert* Trace chalcedony fragments are scattered throughout this sample. These fragments range in size from medium (0.2mm) to very coarse sand (1.1mm). Grains are generally angular and occasionally are broken and display typical chalcedonic texture comprising of radiating fibrous crystals of varying size. Chert grains are generally sub-rounded to round and are composed of microquartz. *Siltstone* An irregularly shaped, granule sized (4mm) siltstone fragment is evident in this sample. The fragment contains approximately 70% medium silt sized quartz grains, 5% mica, 20% illite/sericite and 5% carbonate cement. Quartz and mica flakes display some minor preferential alignment sub-horizontal to the elongate axis of the fragment. A 4mm thick, sub-horizontal quartz-rich bed cuts through the centre of this fragment. This bed consists of well-sutured, coarse silt sized (0.05mm) quartz that has been partially calcite cemented. The bed is discontinuous and thins to

	one end of the fragment. *Kaolinite* Kaolinite occurs as sub-rounded to rounded clasts or balls that occupy intergranular pore space. These clasts consist of finely to coarsely crystalline accumulations of kaolinite. Most of the clasts have undergone partial compaction resulting in their expansion of the kaolinite into intergranular pore space.
Matrix/ Pseudomatrix	
Authigenic cement	Silica overgrowths Only trace silica overgrowths are evident on quartz grains. Most of the silica overgrowths are evident at triple junctions between quartz grains. Interference of individual silica overgrowths has produced irregular compromise boundaries. Anhydrite This sample is predominantly anhydrite cemented. Most of the anhydrite occurs as separate rectangular crystals or as a massive, partially leached poikilotopic cement encasing framework grains. Calcite Calcite cement occurs either partially or totally replacing pore filling anhydrite. Calcite generally occurs as an equant drusy mosaic of very finely to finely crystalline crystals. The cement displays a typical pore-filling characteristic increasing in crystal size towards the pore centre. Siderite Siderite occurs as microcrystalline accumulation and individual grains that marginally replace detrital grains and pore-filling cements. Pyrite Pyrite occurs as nodules that partially replace grains and rock fragments.
Porosity/ Permeability	Visual porosity is poor in this sample, pore space has been filled by both anhydrite and calcite cements. Rare leaching of the anhydrite cement has produced some trace secondary porosity.

DIAGENESIS

Relative timing of events	Authigenic silica cementation Micritisation of carbonate clasts Anhydrite cementation Calcite cementation Pyrite formation
Relative importance of events	

TEXTURAL MATURITY AND INTERPRETATION

Textural maturity	Mature
Interpretation	

MINERALOGICAL CLASSIFICATION AND COMMENTS

Mineralogical classification	Quartz arenite
Comments	

GSWA No. 154829

Well	VINES-1
Sample number	154829
Sample type	Plug
Depth	1212.0
Unit	
Facies	Diamictite
Sample quality	The sample is in good condition
Brief description	Lithic wacke This sample consists of angular to sub-rounded, coarse silt sized quartz and carbonate, siltstone, sandstone and shale fragments supported by a matrix of carbonate mud and illite/sericite. Ferroan calcite, siderite and micrite alteration of carbonate clasts is evident. Visual porosity is negligible.

STRUCTURES

Structures	Massive

TEXTURE

Grain size	Range: Coarse silt (0.05mm) to granules (3.5mm) Mode: Coarse silt (0.05mm)
Sorting	Poorly-sorted
Grain morphology	Angular to sub-rounded
Sediment fabric	Matrix supported. Rare point contacts between framework grains are occasionally evident.

MINERALOGY

Tabulated composition (%)	Detrital components		
	Quartz	Monocrystalline	25
		Mica	1
	Feldspar	Microcline	Tr
		Albite	Tr
		Oncoid	Tr
	Rock Fragments		
		Carbonate	2
		Ooidal carbonate	Tr
		Siltstone	1
		Chalcedony	Tr
		Sandstone	1
		Shale	1
	Matrix/ Pseudomatrix		
		Illite/sericite + Carbonate Mud	70
	Authigenic cement		
		Pyrite	Tr
	Porosity/ Permeability		
		Primary	Nil
		Secondary	Nil
Detrital components	Quartz Quartz grains range in size from coarse silt (0.05mm) to very fine sand (0.07mm) with a mode of coarse silt (0.05mm). Grains are angular to sub-rounded and predominantly matrix supported although rare point contacts do exist between grains. Oncoid A medium sand sized (0.2mm) sized oncoid is evident in this sample. This oncoid consists of a concentrically laminated internal quartz grain or colourless phosphate fragment.		

	Rock fragments *Carbonate clasts* Several types of carbonate clasts are evident in this sample. The main carbonate clasts range in size from very coarse sand (1.5mm) to granules (3mm). Grain boundaries are irregular. Clasts consists of xenotopic matrix of anhedral to subhedral shaped very finely to finely crystalline dolomite that displays planar, curved and sutured contacts. Some of the clasts have been replaced by ferroan calcite, micrite and siderite. The replacement of these grains by these authigenic minerals tends to be patchy. Most of the micritised clasts consist of equant subhedral to euhedral calcite crystals of microsparite and finer micrite which have replaced the original very fine to fine dolomite. The second type of carbonate clast is typically smaller having a mode of medium sand (0.3mm). These clasts are rounded to sub-rounded in shape and consist of a porphyrotopic matrix of anhedral to subhedral shaped, finely to medium crystalline dolomite. Many of these clasts contain recrystallised peloids. Only one ooidal carbonate fragment is evident in this sample. This clast consists of ooids 0.1 to 0.3mm in size that have been partially recrystallised by a xenotopic matrix of anhedral to subhedral shaped very finely to finely crystalline dolomite that displays planar, curved and sutured contacts. Ooids have a well preserved micritised rims that makes them easily identifiable. Trace amounts of up to medium sand sized (0.3mm) quartz are also evident in this clast. These grains have often been overgrown by dolomite. *Chalcedony and chert* Trace chalcedony fragments are scattered throughout this sample. These fragments range in size from medium (0.2mm) to very coarse sand (1.1mm). Grains are generally angular and occasionally are broken and display typical chalcedonic texture comprising of radiating fibrous crystals of varying size. Chert grains are generally sub-rounded to round and are composed of microquartz. *Sandstone* Traces of well-cemented sandstone fragments are also evident in this sample. These fragments are coarse sand sized (0.6mm) and angular to sub-angular in shape. They are composed predominantly of well-sutured, coarse silt sized quartz grains and mica that is supported by a sertiticised matrix that has been partially cemented by a poikilotopic calcite cement. Mica flakes and quartz grains display a weak preferential orientation sub-parallel to the long axis of the sandstone fragment. Fragment boundaries are often extremely gradational and have been replaced by the host matrix of illite/sericite and dolomite. *Siltstone* These rock fragments are typically coarse sand sized (0.4mm). Grains are typically angular to sub-rounded and consist of varying amounts of very fine sand sized (0.12mm) quartz grains and mica in an illite/sericite matrix. Mica flakes display some minor preferential alignment. Some grains have been almost completely altered to illite/sericite. *Shale* These rock fragments range from medium sand (0.3mm) to coarse sand (0.9mm)in size. Grains are sub-angular to sub-rounded in shape. One of these clasts displays an irregular, wispy stylolisation and soft sediment deformation. Stylolites are filled with a dark brown clay which is interpreted to be illite/sericite with concentrations of pyrite and insoluble organic residue.

Matrix/ Pseudomatrix	Carbonate mud A complex mixture of micrite and illite/sericite forms the matrix of this sample. Illite/sericite is interpreted to dominate this sample. It can be differentiated from micrite by its dark colouration. This dark colouration is caused by a mix of pyrite and insoluble organic matter. Carbonate mud occurs as a xenotopic fabric of equant, very finely crystalline calcite that has replaced or has been replaced by illite/sercite.
Authigenic cement	Pyrite Pyrite occurs as nodules that partially replace grains and rock fragments.
Porosity/ Permeability	Visual porosity is nil.

DIAGENESIS

Relative timing of events	Seriticisation Carbonate cementation Pyrite formation
Relative importance of events	

TEXTURAL MATURITY AND INTERPRETATION

Textural maturity	Immature
Interpretation	

MINERALOGICAL CLASSIFICATION AND COMMENTS

Mineralogical classification	Lithic wacke
Comments	

GSWA No. 154828

Well	VINES-1
Sample number	154828
Sample type	
Depth	1100.15
Unit	
Facies	Diamictite
Sample quality	The sample is in good condition.
Brief description	Lithic Wacke This sample is dominated by a mixture consisting of illite/sericite and micritic mud. Quartz occurs as angular to sub-rounded, coarse silt sized grains. All detritals are evident floating in the micritic matrix. Other constituents include medium sand sized to pebble sized carbonate, siltstone and sandstone rock fragments. Visual porosity is negligible in this sample.

STRUCTURES

Structures	Massive

TEXTURE

Grain size	Range: Coarse silt (0.05mm) to granules (3.5mm) Mode: Coarse silt (0.05mm)
Sorting	Poorly-sorted
Grain morphology	Angular to sub-rounded
Sediment fabric	Matrix supported. Rare point contacts between framework grains are occasionally evident.

MINERALOGY

Tabulated composition (%)	Detrital components		
	Quartz	Monocrystalline	25
	Rock Fragments		
		Carbonate	2
		Siltstone	1
		Chert	Tr
		Chalcedony	Tr
		Sandstone	1
		Mica	1
	Accessories	Organic matter	Tr
	Matrix/ Pseudomatrix		
	Illite/sericite + Carbonate Mud		70
	Authigenic cement		
		Pyrite	Tr
	Porosity/ Permeability		
		Primary	Nil
		Secondary	Nil

Detrital components	Quartz Quartz grains range in size from coarse silt (0.05mm) to very fine sand (0.07mm) with a mode of coarse silt (0.05mm). Grains are angular to sub-rounded and predominantly matrix supported although rare point contacts do exist between grains. Rock fragments *Carbonate clasts* Carbonate clasts range in size from medium sand (0.3mm) to granules (3mm). The margins of some of the larger grains are coated in a thin micritic rim. Clasts consist of xenotopic texture of anhedral to subhedral shaped very finely to finely crystalline dolomite that displays planar, curved and sutured contacts. In some clasts patchy replacement by micrite and/or siderite, chert and chalcedony is evident. Most of the micritised clasts consist of equant subhedral to euhedral crystals of microsparite and finer micrite which have replaced the original very fine to fine dolomite. Siliceous replacement of these carbonate clasts is only evident in a couple of the grains. The chert or chalcedony in these grains is extremely patchy. Replacement is most intensive at grain margins. The occurrence of recrystallised peloids is also sometimes evident in these fragments. *Chalcedony* Trace chalcedony fragments are scattered throughout this sample. These fragments range in size from medium (0.2mm) to very coarse sand (1.1mm). Grains are generally angular and occasionally are broken and display typical chalcedonic texture comprising of radiating fibrous crystals of varying size. These chalcedonic fragments occasionally have been replaced by a fine microcrystalline chert. *Sandstone* Traces of well-cemented sandstone fragments are also evident in this sample. These fragments are typically granular in size (2-3mm) and angular to sub-angular in shape. They are composed predominantly of well-sutured, coarse silt sized quartz grains and mica that is supported by a sertiticised matrix that has been partially cemented by a poikilotopic calcite cement. Mica flakes display a weak preferential orientation sub-parallel to the long axis of the sandstone fragment. Sandstone fragments have been partially deformed by compactional processes. This has resulted in grain boundaries being difficult to identify. Boundaries are often extremely gradational and have been replaced by the host matrix. *Siltstone* These rock fragments are typically medium sand sized (0.25mm. Grains are angular to sub-angular and consist of varying amounts of very fine sand sized (0.12mm) quartz grains and mica in a illite/sericite matrix. Mica flakes display some minor preferential alignment. Grains have often been partially to totally incorporated into the host rock and therefore only thin ghost-like outlines of fragment boundaries are evident. *Shale* These rock fragments range from medium sand (0.3mm) to pebble size (5mm). Grains are sub-angular to sub-rounded in shape. A 0.7mm thick sub-horizontal quartz rich-bed cuts across one of the larger shale fragments. The margins of shale fragments are very irregular.
Matrix/ Pseudomatrix	Carbonate mud A complex mixture of micrite and illite/sericite forms the matrix of this sample. Carbonate mud occurs as a xenotopic fabric of equant, very finely crystalline calcite that has replaced or has been replaced by illite/sercite. The two muds are

	aphanocrystalline and therefore they are difficult to separate out microscopically. The matrix material forms highly corrosive contacts with surrounding detrital grains.
Authigenic cement	Pyrite Pyrite mainly forms as small nodules and accumulations that replace carbonate mud.
Porosity/ Permeability	Primary and secondary porosity is negligible in this sample.

DIAGENESIS

Relative timing of events	Calcite cementation Secondary carbonate cementation (siderite + micrite) Silicification Kaolinite replacement Chlorite alteration Pyrite formation
Relative importance of events	

TEXTURAL MATURITY AND INTERPRETATION

Textural maturity	Immature
Interpretation	

MINERALOGICAL CLASSIFICATION AND COMMENTS

Mineralogical classification	Lithic wacke
Comments	

GSWA No. 154856

Well	VINES-1
Sample number	154856
Sample type	
Depth	1076.75m
Unit	
Facies	Conglomerate
Sample quality	Sample is in excellent condition.
Brief description	This sample contains a dolomitised micritic mudstone and a sedarenite separated by a sharp, sub-horizontal contact. The mudstone portion of this slide is predominantly composed of a partially dolomitised, illite/sericite mud. Coarse silt sized quartz grains are also evident scattered throughout. The sedarenite portion of the slide consists of angular to sub-rounded, medium sand sized quartz and carbonate, siltstone, sandstone lithic, and shale fragments supported by carbonate, dolomite and pyrite cements. Visual porosity is negligible.

STRUCTURES

Structures	Contact A sub-horizontal contact is evident cutting across this sample separating a micritised mudstone and a sedarenite.

TEXTURE

Grain size	Range: Coarse silt (0.03mm) to pebbles (6mm) Mode: Fine sand (0.22mm)
Sorting	Poorly-sorted.
Grain morphology	Angular to sub-rounded.
Sediment fabric	Grains mainly display point contacts with occasional concave/convex and weakly sutured grain-grain contacts.

MINERALOGY

Tabulated composition (%)	Detrital components		
	Quartz	Monocrystalline	45
	Mica		Tr
	Feldspar	Microcline	Tr
		Albite	2
		Sphalerite	2
	Rock fragments		
		Chalcedonic silica	3
		Shale	2
		Carbonate	3
		Ooidal carbonate	1
		Sandstone	4
		Siltstone	2
	Accessories	Zircon	Tr
	Authigenic cement		
		Calcite	11
		Pyrite	10
		Illite/sericite	15
	Porosity/ Permeability		
		Primary	Nil
		Secondary	Tr

Detrital components	Quartz Quartz grains range in size from coarse silt (0.03mm) to pebbles (6mm) with a mode of fine sand (0.22mm). Grains are sub-angular to sub-rounded, moderately-sorted and display mainly point with occasional concave/convex and weakly sutured grain-grain contacts. Most quartz grain boundaries are irregular due to microcrystalline calcite growths which marginally replace the grains. Feldspar The most common feldspars evident in this sample are albite and to a lesser extent microcline. Feldspar grains display a similar grain size to detrital quartz grains. Smaller grains are typically well preserved while larger grains have undergone partial dissolution or are cracked and altered to calcite. Mica Only occurs in the sample in trace amounts. Micas show no preferential alignment and occur mainly in siltier sections of the slides. Sphalerite A pebble sized (8mm) sphalerite grain is evident in this sample. This grain is opaque and displays a highly irregular and diffuse grain margin. Rock fragments *Carbonate clasts* Carbonate clasts range from medium sand size (0.2mm) to coarse sand (0.8mm). These clasts are generally sub- to well rounded and composed of xenotopic matrix of anhedral to subhedral shaped very finely to finely crystalline dolomite that displays planar, curved and sutured contacts. Micritic alteration is evident in most of these clasts. Micritised clasts consist of equant subhedral to euhedral calcite crystals of microsparite and finer, micrite which have replaced the original very fine to fine dolomite. Occasional clasts have been completely micritised. Micritised clasts range up to 1mm in size. These clasts contain sub-angular, silt sized (0.05mm) quartz grains incorporated within them. Most quartz grains have been marginally replaced by the micritic dolomite. *Ooidal carbonate* These clasts consist of ooids 0.1 to 0.3mm in size that have been partially recrystallised by a xenotopic matrix of anhedral to subhedral shaped very finely to finely crystalline dolomite that displays planar, curved and sutured contacts. Trace siliceous cementation of these ooids is also evident Ooids have a well preserved micritised rim that makes them easily identifiable. Disseminated pyrite is evident in scattered throughout these clasts. Pyrite is interpreted to be late stage overgrowing dolomite cements. *Lithoclasts* These grains could be termed flint, but due to the truncation of microquartz nodules at the grain boundary they have been termed lithoclasts. Lithoclasts consist of a mixture of concentric microquartz and chalecedonic silica. Microquartz is evident as elongate and round grains with a mode of medium sand (0.5mm). Chalcedonic silica is typically located between nodules. It mainly occurs as radial-fibrous, pore-filling cement. There is a slight increase in chalcedonic crystal grain size towards the centre of pores. *Sandstone* Traces of well-cemented sandstone fragments are also evident in this sample. These fragments are typically very coarse sand sized (1.2mm). Fragments are generally sub-angular to sub-rounded and composed of up to 90% moderately sutured, very fine sand sized (0.08mm) quartz grains, 1% mica and 9%

	poikilotopic calcite cement. Within the fragment the cement encases clusters of framework grains and fills intergranular pore space. In one sandstone fragment a xenotopic matrix of anhedral to subhedral shaped medium crystalline dolomite that displays planar, curved and sutured contacts in evident filling intergranular pore space. Dolomite crystals display highly corrosive contacts with surrounding detrital grains. *Siltstone* Angular to sub-rounded siltstone fragments range up to pebble size (6mm). These fragments generally composed of 35% medium silt sized quartz grains and 65% sericite. Quartz and mica flakes display some minor preferential alignment sub-horizontal to the elongate axis of the fragment. Heavy leaching and dissolution and cracking of these grains is evident. Some leached fragments display partial dolomitisation, and pyrite replacement. A weak, sub-horizontal alignment of disseminated pyrite is evident in this fragment. Thin, discontinuous illite/sericite-rich styolilisation surfaces are evident in some of these fragments.
Matrix/ Pseudomatrix	Dolomitic mud This sample displays an irregular contact between a between a conglomerate and a siltstone. The siltstone component of the slide is dominated by a complex mixture of dolomite and illite/sericite. The dark colouration of this sample is caused by pyrite occurrence. Dolomite generally occurs as a sub-microscopic cement growing into and displacing matrix clays.
Authigenic cement	Calcite Calcite mainly occurs in the conglomerate section of the slide. Calcite occurs as patchy, cement of varying crystal size. Most of the calcite occurs as a fine pseudosparic cement that encases clusters of framework grains. The remainder occurs as patchy, crystalline pore filling cement. The cement forms highly corrosive contacts with surrounding detrital grains, marginally replacing quart grain boundaries. Pyrite Pyrite is evident filling intergranular pore space. It forms both as microcrystalline aggregates and disseminated grains that replace pore space cements and marginally replace detrital grains. Illite/sericite Illite/sericite is mainly concentrated in the thin sub-horizontal stylolites that cut across the sample.
Porosity/ Permeability	Visual porosity in this sample is negligible. Only trace secondary porosity is evident which is due to the partial dissolution of intergranular cements.

DIAGENESIS

Relative timing of events	Calcite cementation Dolomite cementation Pyrite formation
Relative importance of events	

TEXTURAL MATURITY AND INTERPRETATION

Textural maturity	immature
Interpretation	

MINERALOGICAL CLASSIFICATION AND COMMENTS

Mineralogical classification	Litharenite
Comments	All mineralogical percentages were obtained through visual estimation.

GSWA No. 154827

Well	VINES-1
Sample number	154827
Sample type	Core
Depth	1070.0
Unit	
Facies	Conglomerate
Sample quality	The sample is in good condition.
Brief description	Quartz arenite This sample consists predominantly of medium sand sized quartz that has undergone partial pressures solution resulting in the development of convave/convex to well-sutured grain-grain contacts. Most rock fragments have been squashed into intergranular pore space and altered either by kaolinite, chlorite or calcite cement. Poikilotopic calcite cement is evident filling into intergranular pore space and marginally replacing sutured quartz grains and their authigenic overgrowths. Visual porosity in this sample is extremely poor.

STRUCTURES

Structures	Massive

TEXTURE

Grain size	Range: Fine sand (0.2mm) to granules (3mm) Mode: Medium sand (0.35mm)
Sorting	Well-sorted
Grain morphology	Sub-angular to sub-rounded
Sediment fabric	Grains display concave/convex to well-sutured grain-grain contacts

MINERALOGY

Tabulated composition (%)	Detrital components		
	Quartz	Monocrystalline	83
		Polycrystalline	Tr
	Feldspar	Albite	Tr
		Plagioclase	Tr
	Rock fragments		
		Sandstone	2
		Carbonate	2
		Siltstone	1
		Shale	1
		Kaolinite	3
		Chert	Tr
		Volcanic	Tr
	Accessories	Zircon	Tr
		Tourmaline	Tr
	Authigenic cement		
		Siderite	2
		Calcite	5
		Authigenic silica	1
		Pyrite	Tr
	Porosity/ Permeability		
		Primary	Tr
		Secondary	Nil

Detrital components	Quartz Moderately-sorted, monocrystalline quartz dominates this sample. Quartz grain sizes range from fine sand (0.2mm) to coarse sand (0.5mm) with a mode of medium sand (0.35mm). Grains are sub-angular to sub-rounded. Pressure solution is evident with grains displaying concave/convex to well-sutured grain-grain contacts. Thin authigenic silica overgrowths are apparent on some grain boundaries. Most quartz grains also contain fluid inclusions or vacuoles. They are identified as lines of dark specks that cut across quartz grains. Rock fragments *Siltstone* These rock fragments are typically coarse sand sized and angular to sub-angular in shape. They consist predominantly of coarse silt sized quartz grains, mica and illite/sericite. A thin irregular lamination is evident in some of these fragments defined by the concentration of illite/sericite, pyrite and insoluble organic matter. Fragments have often been squashed and partially compacted into intergranular pore space. *Sandstone* Traces of well-cemented sandstone fragments are also evident in this sample. These fragments are typically granular in size (2-3mm) and angular to sub-angular in shape. They are composed predominantly of well-sutured, coarse silt sized quartz grains and mica that has been partially cemented by a poikilotopic calcite cement. Mica flakes display a weak preferential orientation sub-parallel to the long axis of the sandstone fragment. Sandstone fragments have been partially deformed by compactional processes. This has resulted in grain boundaries being highly irregular and diffuse with partial alteration evident. *Shale* These rock fragments are typically medium sand sized (0.25mm) and sub-angular to sub-rounded in shape. Deformation and alteration of these fragments is evident. Most of these grains have been compacted. Compaction of these grains has resulted in them flowing around adjacent framework grains and into intergranular pore space. Dissolution and alteration of these clasts to sericite, kaolinite and chlorite is evident. *Kaolinite* Kaolinite occurs as sub-rounded to rounded clasts or balls that occupy intergranular pore space. These clasts consist mainly of a finely crystalline accumulations of kaolinite. Most of the clasts have undergone partial compaction resulting in the expansion of the kaolinite into intergranular pore space. Compaction of these grains has often made their grain boundaries difficult to identify. *Carbonate clasts* Carbonate clasts are typically fine sand sized (0.2mm). Clasts are mainly sub-rounded to rounded in shape but elongate and irregularly shaped grains are evident. The shape of these grains is due to compactional deformation resulting in grains being squashed and expanded into intergranular pore space. The internal constituents of clasts consist of xenotopic matrix of anhedral to subhedral shaped medium crystalline dolomite that displays planar, curved and sutured contacts. Some clasts have been partially leached and dissolved and replacement of some of these clasts is evident. Common replacement minerals include secondary poikilotopic calcite cement, siderite or micrite. *Chert* Chert fragments displaying similar grain size to quartz grains are scattered throughout the sample. Chert grains are composed of microquartz.

	Volcanics Only one volcanic rock fragment was noted in this sample. This rock fragment is of similar size to carbonate clasts. It is sub-angular and consist of large laths of plagioclase feldspar grains. Grain boundaries are highly irregular and diffuse and some volcanic grains display minor dissolution and dispersion into intergranular pore space. Most volcanic fragments have been partially altered to a mixture of kaolinite, sericite and chlorite, which has destroyed their original fabric.
Matrix/ Pseudomatrix	
Authigenic cement	Silica overgrowths Authigenic silica overgrowths are evident on most quartz grain boundaries. Contacts between adjacent overgrowths are irregular compromise boundaries produced by the mutual interference of individual overgrowths. Overgrowths have been marginally replaced by single, poikilotopic calcite cement. Calcite This sample is partially calcite cemented. Most calcite cement occurs as single crystal poikilotopes or microsparry accumulations of very finely crystalline calcite that fills intergranular pore space and marginally replaces quartz overgrowths or grows on pressure solution surfaces between quartz grains. The cement forms highly corrosive contacts with surrounding detrital grains and partially replaces portions of framework grains. Siderite Siderite mainly occurs in pore filling aggregate form. Microcrystalline accumulations of siderite are evident in this sample filling pore space and marginally replacing detrital grains. The siderite forms highly corrosive contacts with surrounding detrital grains. Pyrite Pyrite mainly occurs as a late stage diagenetic cement. It fills intergranular pore space and occasionally replaces clay material in the sample.
Porosity/ Permeability	Visual porosity is extremely poor in this sample. Porosity has been reduced by mechanical compaction and authigenic silica and calcite cementation.

DIAGENESIS

Relative timing of events	Quartz overgrowth cementation Compactional deformation resulting in pressure solution Seriticisation Kaolinite replacement Calcite cementation Pyrite formation
Relative importance of events	

TEXTURAL MATURITY AND INTERPRETATION

Textural maturity	Mature
Interpretation	

MINERALOGICAL CLASSIFICATION AND COMMENTS

Mineralogical classification	Quartz arenite
Comments	

GSWA No. 154826

Well	VINES-1
Sample number	154826
Sample type	Core
Depth	1062.0
Unit	
Facies	Conglomerate and diamictite
Sample quality	The sample is in good condition
Brief description	Sedarenite This sample is dominated by rock fragments. The main rock fragments evident in this sample are carbonate, sandstone and volcanics with chert, chalcedony and shale occurring to as lesser extent. Framework grains display point to concave/convex and moderately sutured grain-grain contacts. The sample has been partially cemented by poikilotopic and finely to tmedium crystalline calcite, kaolinite and chlorite. Visual porosity in this sample is extremely poor.

STRUCTURES

Structures	Massive

TEXTURE

Grain size	Range: Coarse silt (0.05mm) to pebbles (6mm) Mode: Medium sand (0.4mm)
Sorting	Very-poorly sorted
Grain morphology	Sub-angular to sub-rounded
Sediment fabric	Grains display point to concave/convex and moderately sutured grain-grain contacts.

MINERALOGY

Tabulated composition (%)	Detrital components		
	Quartz	Monocrystalline	8
		Polycrystalline	Tr
	Feldspar	Albite	Tr
		Plagioclase	2
	Rock fragments		
		Sandstone	10
		Carbonate	18
		Siltstone	6
		Shale	5
		Chert	4
		Kaolinite	2
		Chalcedony	3
		Volcanic	16
	Accessories	Zircon	Tr
		Tourmaline	Tr
	Authigenic cement		
		Ferroan Calcite	1
		Calcite	11
		Anhydrite	1
		Phosphate	1
		Chlorite	3
		Kaolinite	6
		Illite/sericite	3
	Porosity/ Permeability		
		Primary	Tr
		Secondary	Tr

Detrital components	Quartz Quartz grains are predominantly medium sand sized (0.4mm). They are sub-rounded to rounded and display concave/convex to moderately sutured grain-grain contacts. Some grains display highly corrosive contacts and have been marginally replaced by calcite cements. Vacuolisation of some quartz grains is evident. Vacuoles are defined by dark specks. Margins of some grains display embayments and contain small zircon inclusions. Feldspar Feldspar grains range in size from very fine sand (0.13mm) to medium sand (0.3mm). Several varieties of feldspar are evident these include microcline, albite and plagioclase. Some grains have undergone partial leaching and dissolution and alteration by authigenic calcite. Rock fragments *Carbonate* Carbonate clasts range up to granule size. These clasts consist of a xenotopic texture of anhedral to subhedral very finely to finely crystalline dolomite. Patchy alterations to micrite is evident in some clasts. Clasts generally display a sub-angular shape but some grains have been squashed and consequentially are more elongate in shape. A 0.22mm thick illite/sericite coating is evident on most clasts. It is also evident on pressure solution surfaces between carbonate rock fragments. *Volcanics* These grains range up to granule size (2.2mm). They are typically composed of large feldspar laths that display some leaching and dissolution and augite crystals. Grains have been cemented by chlorite and pyrite that occurs as isolated grains or accumulations filling intergranular pore space. Late stage calcite cementation is evident in most fragments replacing chlorite and feldspar laths. In some fragments feldspar laths have been partially dissolved resulting in the formation of trace secondary porosity. Zoning of feldspar grains is evident in some fragments. *Shale* Shale fragments are sub-rounded in shape and composed of dark illite/sericite clay. Some fragments have been partially cracked and alteration to chlorite is evident on fracture margins. *Chalcedony* Chalcedony fragments range up to granule size (3mm). Fragments are sub-angular and defined by a chalcedonic texture composed of radiating crystals of varying size. Minor leaching and alteration of these fragments to microsparry calcite is evident. *Chert* Chert grains range up to pebble size (7mm). They are typically angular to sub-rounded and composed of a patchy mixture of micro- and macrosparry quartz. Iron staining is evident in some fragments. Leaching and alteration to chalcedony and microsparry calcite is sometimes evident. *Siltstone* Siltstone fragments are composed predominantly of dark illite/sericite clay with traces of coarse silt sized quartz and mica. The dark colouration of these fragments is caused by the mixture of pyrite and insoluble organic matter with illite/sericite clays. The shape of these fragments varies as they have been squashed into intergranular pore space.

	Sandstone Sandstone fragments are difficult to distinguish from the host rock as calcite cement has almost totally replaced the margins of these fragments and partially replaced them internally. These fragments are typically sub-rounded and composed of coarse silt sized quartz and mica supported in a kaolinitic and chloritic matrix. *Kaolinite* Some detrital kaolinite is evident ion this sample. Kaolinite generally occurs as sub-rounded balls that are composed of coarsely crystalline kaolinite.
Matrix/ Pseudomatrix	
Authigenic cement	Kaolinite Coarsely crystalline kaolinite typically forms as framework grain sized patches that fill intergranular pore space. Kaolinite is possibly formed as an alteration product of detrital grains. In some cases detrital kaolinite clasts may have been squashed into intergranular pore space. Calcite This sample is partially calcite cemented. Most of the calcite cement occurs as single crystal poikilotopes or as microsparry accumulations of very finely to medium crystalline calcite that fills intergranular pore space and replaces clusters of framework grains. Anhydrite Trace amounts are evident as massive pore filling cement that fills pores between rock fragments. Illite/sericite Illite/sericite forms in thin sub-horizontal seams that occur along pressure solution surfaces between fragments.
Porosity/ Permeability	Visual porosity is poor in this sample.

DIAGENESIS

Relative timing of events	Illite/sericite formation Kaolinite formation Chlorite alteration Anhydrite cementation Calcite cementation
Relative importance of events	

TEXTURAL MATURITY AND INTERPRETATION

Textural maturity	Immature
Interpretation	

MINERALOGICAL CLASSIFICATION AND COMMENTS

Mineralogical classification	Sedarenite
Comments	

GSWA No. 154825

Well	VINES-1
Sample number	154825
Sample type	Plug
Depth	1050.0
Unit	
Facies	Sandstone
Sample quality	The sample is on good condition
Brief description	Laminated Quartz arenite This sample is characterised by an ill-defined, sub-horizontal quartz lamination. The lamination can only be defined by a variation in quartz grain sizes. Laminae contain predominantly sub-angular to sub-rounded, coarse silt sized quartz that has been selectively compacted. The host rock is characterised by sub-angular to sub-rounded, fine sand sized quartz (0.2mm). Carbonate, shale, chert and chelcedonic rock fragments are evident in varying amounts in this sample. Fragments have been compacted and squashed into intergranular pore space. The sample has been partially cemented by calcite. Visual primary and secondary porosity is good.

STRUCTURES

Structures	Laminae This sample consists of a weakly laminated sandstone. Laminae are highly irregular but can be broadly classified as sub-horizontal. The laminae are up to 0.7mm thick and composed predominantly of coarse silt sized (0.05mm) quartz that display point, concave/convex and well-sutured grain-grain contacts. Quartz grains are well cemented by authigenic calcite cements. As the laminae consist of a similar mineralogical suite to the host rock their boundaries are often difficult to distinguish. These laminae can only be defined by a reduction in the quartz grain mode size and a reduction in pore space. Selective compaction along these seams is evident.

TEXTURE

Grain size	Range: Coarse silt (0.05mm) to medium sand (0.35mm) Mode: Coarse silt (0.05mm)
Sorting	Moderately sorted
Grain morphology	Sub-angular to sub-rounded
Sediment fabric	Grain display point, concave/convex and well sutured grain-grain contacts.

MINERALOGY

Tabulated composition (%)	Detrital components		
	Quartz	Monocrystalline	76
	Feldspar	Microcline	Tr
		Albite	2
		Plagioclase	3
		Muscovite	Tr
	Rock fragments		
	Carbonate	Calcite	3
		Shale	1
		Chert	Tr
		Chalcedony	Tr
		Kaolinite	2
	Accessories	Zircon	Tr
		Tourmaline	Tr
	Authigenic cement		
		Calcite	6
		Chlorite	1

		Kaolinite	1
		Siderite	1
		Pyrite	Tr
	Porosity/ Permeability		
		Primary	4
		Secondary	Tr
Detrital components	Quartz A bimodal grain size distribution is evident in this sample. Quartz grain size ranges from coarse silt (0.05mm) to medium sand (0.35mm) with an overall sample mode of coarse silt (0.05mm). The finer quartz fraction with a mode of coarse silt (0.05mm) is concentrated in thin lenses. These quartz grains are sub-angular to sub-rounded in shape and display point to concave/convex and well-sutured grain-grain contacts. The larger quartz fraction occurs in the host rock. This quartz fraction has a mode of fine sand (0.2mm). Grains are typically sub-angular to sub-rounded and also display point, concave/convex and well-sutured grain-grain contacts. Even though the host rock is dominated by fine sand sized quartz these areas tend to be a mixture of both quartz grain sizes. Feldspar Feldspar grains range in size from coarse silt (0.07mm) to medium sand (0.25mm). Several varieties of feldspar are evident these include microcline, albite and plagioclase. Some grains have undergone partial leaching resulting in vacuolisation and alteration to sericite, calcite, kaolinite and chlorite. Rock fragments *Carbonate* Carbonate clasts are typically fine sand sized (0.2mm). Clasts are mainly sub-rounded to rounded in shape but elongate and irregularly shaped grains are evident. The shape of these grains is due to compactional deformation resulting in grains being squashed and expanded into intergranular pore space. The internal constituents of clasts consist of xenotopic matrix of anhedral to subhedral shaped medium crystalline dolomite that displays planar, curved and sutured contacts. Some clasts have been partially leached and dissolved and replacement of some clasts is evident. Common replacement minerals include secondary poikilotopic calcite cement, siderite or micrite. *Chert* Chert fragments displaying similar grain size to quartz grains are scattered throughout the sample. Chert grains are composed of microquartz. *Chalcedony* Only trace chalcedony is evident in this sample. These fragments display similar grain size to quartz grains. Grains are generally angular and occasionally are broken and display typical chalcedonic texture comprising of radiating fibrous crystals of varying size. *Kaolinite* Kaolinite occurs as sub-rounded to rounded clasts or balls. These clasts consist mainly of a finely crystalline accumulation of kaolinite. Most of the clasts have undergone partial compaction resulting in their expansion of the kaolinite into intergranular pore space. Compaction of these grains has often made their grain boundaries difficult to identify. *Shale* These rock fragments are typically fine sand sized (0.2mm) and sub-angular to sub-rounded in shape. Deformation and alteration of these fragments is evident.		

	Some of these grains have undergone compactional deformation. Compaction of these grains has resulted in them flowing around adjacent framework grains and into intergranular pore space. Dissolution and alteration of these clasts to kaolinite and/or chlorite is evident.
Matrix/ Pseudomatrix	
Authigenic cement	Calcite This sample is partially calcite cemented. Most calcite cement occurs as single crystal poikilotopes or microsparry accumulations of very finely crystalline calcite that fills intergranular pore space and encases clusters of framework grains. The cement forms highly corrosive contacts with surrounding detrital grains and partially replaces portions of framework grains. Siderite Siderite mainly occurs in pore filling aggregate form. Microcrystalline accumulations of siderite are evident in this sample filling pore space and marginally replacing detrital grains. The siderite forms highly corrosive contacts with surrounding detrital grains. Pyrite Pyrite mainly occurs as a late stage diagenetic cement. It fills intergranular pore space and occasionally replaces clay material in the sample.
Porosity/ Permeability	Visual porosity in this sample is good with framework grains displaying only minor compaction thereby maintaining intergranular pore space. Secondary porosity is also evident. Most of this porosity is the result of leaching and dissolution of detrital grains but oversized pores may indicate that some of this porosity is due to grain plucking during thin-section manufacture.

DIAGENESIS

Relative timing of events	Mechanical compaction Calcite cementation Authigenic kaolinite formation Chloritisation Pyrite formation
Relative importance of events	

TEXTURAL MATURITY AND INTERPRETATION

Textural maturity	Supermature
Interpretation	

MINERALOGICAL CLASSIFICATION AND COMMENTS

Mineralogical classification	Quartz arenite
Comments	

GSWA No. 154824

Well	VINES-1
Sample number	154824
Sample type	Plug
Depth	1000.1
Unit	
Facies	Sandstone
Sample quality	Sample is in good condition
Brief description	Calcite cemented feldspathic litharenite This sample consists of angular to sub-rounded, very fine sand sized quartz grains and carbonate, shale and chert rock fragements cemented by a poiklilotopic and finely crystalline calcite cement. Primary and secondary porosity is poor in this sample having been replaced by authigenic cements.

STRUCTURES

Structures	Weakly laminated.

TEXTURE

Grain size	Range: Very fine sand (0.1mm) to coarse sand (0.6mm) Mode: Bimodal→ Very fine sand (0.12mm) and medium sand (0.3mm)
Sorting	Poorly-sorted
Grain morphology	Sub-angular to rounded
Sediment fabric	Grains display point to concave convex and well-sutured grain-grain contacts

MINERALOGY

Tabulated composition (%)	Detrital components		
	Quartz	Monocrystalline	55
		Polycrystalline	Tr
	Feldspar	Microcline	1
		Albite	3
		Plagioclase	2
		Muscovite	Tr
	Rock fragments		
	Carbonate	Calcite + Siderite	5
		Metaquartz	Tr
		Shale	2
		Chert	4
		Chalcedony	1
		Shale	2
		Volcanic	2
		Sandstone	1
		Kaolinite	3
	Accessories	Zircon	Tr
		Tourmaline	Tr
	Authigenic cement		
		Calcite	12
		Ferroan calcite	1
		Dolomite	2
		Chlorite	1
	Porosity/ Permeability		
		Primary	2
		Secondary	1

Detrital components	Quartz A bimodal grain size distribution is evident in this sample. Quartz grain size ranges from very fine sand (0.1mm) to coarse sand (0.6mm). The finer quartz fraction with a mode of very fine sand (0.12mm) is concentrated in thin lenses. These quartz grains are sub-angular to sub-rounded in shape and display point to concave/convex and well-sutured grain-grain contacts. The larger quartz fraction occurs in the host rock. This quartz fraction has a mode of medium sand (0.3mm). Grains are typically sub-angular to sub-rounded and also display point, concave/convex and well-sutured grain-grain contacts. Feldspar Feldspar grains range in size from very fine sand (0.13mm) to medium sand (0.3mm). Several varieties of feldspar are evident these include microcline, albite and plagioclase. Some grains have undergone partial leaching and dissolution and alteration by authigenic calcite, kaolinite and chlorite cements. Rock fragments *Carbonate* Carbonate clasts range from fine sand (0.15mm) up to medium sand (0.3mm) size. Clasts are mainly sub-rounded to rounded in shape but elongate and irregularly shaped grains are evident. The shape of these grains is due to compactional deformation resulting in grains being squashed and expanded into intergranular pore space. The internal constituents of clasts consist of xenotopic matrix of anhedral to subhedral shaped medium crystalline dolomite that displays planar, curved and sutured contacts. Some clasts have been partially leached and dissolved and replacement of some clasts is evident. Common replacement minerals include secondary poikilotopic calcite cement, siderite or micrite with occasional kaolinite of chlorite occluding secondary porosity. In some clasts, feint outlines of recrystallised peloids are evident. *Siderite clasts* Siderite clasts are predominantly very fine sand sized (0.1mm). These clasts are typically sub-rounded. They consist of an accumulation of very finely crystalline siderite. Siderite clasts form highly corrosive contacts with surrounding detrital grains. *Chert* Chert fragments displaying similar grain size to quartz grains are scattered throughout the sample. Chert grains consist internally of a mixture of micro- and megaquartz. *Chalcedony* These fragments display similar grain size to quartz grains. Grains are generally angular and occasionally are broken and display typical chalcedonic texture comprising of radiating fibrous crystals of varying size. *Volcanics* These rock fragments are of similar size to quartz grains, sub-angular and consist of large laths of plagioclase feldspar grains. Grain boundaries are highly irregular and diffuse and some volcanic grains display minor dissolution and dispersion into intergranular pore space. Most volcanic fragments have been partially altered to a mixture of kaolinite, sericite and chlorite which has destroyed their original fabric.

	Shale These rock fragments are typically medium sand sized and sub-angular to sub-rounded in shape. Deformation and alteration of these fragments is evident. Some of these grains have undergone compactional deformation. Compaction of these grains has resulted in them flowing around adjacent framework grains and into intergranular pore space. Dissolution and alteration of these clasts to kaolinite and/or chlorite is evident. *Sandstone* These fragments consist predominantly of fine sand sized sub-angular to sub-rounded quartz. Quartz grains are supported by a matrix consisting of finely crystalline authigenic calcite. *Kaolinite* Kaolinite occurs as sub-rounded to rounded clasts. These clasts consists of coarsely and finely crystalline accumulation of kaolinite. Most of the clasts have undergone partial compaction resulting in their expansion of the kaolinite into intergranular pore space.
Matrix/ Pseudomatrix	
Authigenic cement	Calcite (Ferroan and non-ferroan) This sample is partially calcite cemented. Most calcite cement occurs as patchy, single crystal poikilotopes or microsparry accumulations of very finely crystalline calcite that fills intergranular pore space and encases clusters of framework grains. The cement forms highly corrosive contacts with surrounding detrital grains and partially replaces portions of framework grains. Dolomite Dolomite occurs as isolated, medium crystalline (0.07mm) rhombs that replace calcite.
Porosity/ Permeability	Visual porosity in this sample is good. Primary porosity, although reduced by compaction and calcite cementation, has been partially preserved. Some secondary porosity is also evident. Most of this porosity is the result of leaching and dissolution of detrital grains but some of the secondary porosity is interpreted to have been produced by grain plucking during thin-section manufacture. Evidence for grain plucking includes oversized pores.

DIAGENESIS

Relative timing of events	Mechanical compaction Authigenic kaolinisation Calcite cementation Dolomitisation
Relative importance of events	

TEXTURAL MATURITY AND INTERPRETATION

Textural maturity	Immature
Interpretation	

MINERALOGICAL CLASSIFICATION AND COMMENTS

Mineralogical classification	Feldspathic litharenite
Comments	

GSWA No. 154823

Well	VINES-1
Sample number	154823
Sample type	
Depth	995.0
Unit	
Facies	Sandstone
Sample quality	The sample is in good condition.
Brief description	Calcite cemented feldspathic litharenite This sample consists of angular to sub-rounded, fine sand sized quartz grains and carbonate, shale and chert rock fragments cemented by a poiklilotopic and finely crystalline calcite cement. Thin, irregular and discontinuous, sub-horizontal solution seams cut through this sample. These seams are filled with medium silt sized quartz supported by illite/sericite clays. Primary and secondary porosity is poor in this sample having been replaced by authigenic cements.

STRUCTURES

Structures	Solution seams Two irregular, sub-horizontal solution seams are evident in this sample, one at the top of the slide and the other in the center. These seams are discontinuous, approximately 0.1mm thick and composed of a concentration of quartz and illite/sericite clays. Quartz grains in these seams are predominantly angular to sub-rounded and coarse silt sized (0.35mm). These grains are supported by a matrix consisting mainly of illite/sericite clay. The dark colouration of the illite/sericite clays is due to the concentration of pyrite and insoluble clay residue with these clays.

TEXTURE

Grain size	Range: Coarse silt (0.035mm) to medium sand (0.35mm) Mode: Fine sand (0.2mm)
Sorting	Well-sorted
Grain morphology	Tabular to sub-rounded
Sediment fabric	Grain display point to concave/convex and moderately sutured grain-grain contacts.

MINERALOGY

Tabulated composition (%)	Detrital components		
	Quartz	Monocrystalline	50
		Polycrystalline	1
	Feldspar	Microcline	Tr
		Albite	3
		Plagioclase	2
		Muscovite	Tr
	Rock Fragments		
	Carbonate	Calcite	5
		Chert	2
		Chalcedony	Tr
		Shale	1
		Volcanics	Tr
		Kaolinite	2
	Accessories	Zircon	Tr
		Tourmaline	Tr
		Biotite	Tr
		Oncoid	Tr

	Authigenic cement Calcite 31 Authigenic silica Tr Chlorite 1 Kaolinite 1 Pyrite Tr Porosity/ Permeability Primary 1 Secondary 1
Detrital components	Quartz Quartz grains range in size from coarse silt (0.035mm) to medium sand (0.35mm) with a mode of fine sand (0.2mm). Quartz grains are well cemented but display point to concave/convex and moderately sutured grain-grain contacts. Feldspar Feldspar grains range in size from very fine sand (0.13mm) to medium sand (0.4mm). Several varieties of feldspar are evident these include microcline, albite and plagioclase. Some grains have undergone partial leaching and dissolution and alteration by authigenic calcite and chlorite cements. Oncoids Trace medium sand sized (0.2mm) sized oncoids are evident in this sample. These grains consist of a concentrically laminated internal quartz grain or colourless phosphate fragment. Some of these grain have been replaced by a micritic cement. Rock fragments *Carbonate* Carbonate clasts are predominantly very fine sand sized (0.1mm) to medium sand sized (0.3mm). Fine sand sized clasts are mainly sub-rounded to rounded. Clast shape may vary though as some of the clasts have been squashed into intergranular pore space. Where clasts occur adjacent they occasionally display minor sutured seam solution at their grain boundaries. The internal constituents of clasts consist of xenotopic matrix of anhedral to subhedral shaped medium crystalline dolomite that displays planar, curved and sutured contacts. The internal fabric of these clasts has commonly been altered by siderite and/or micrite. *Chert* Chert fragments displaying similar grain size to quartz grains are scattered throughout the sample. Chert fragments consist of a mixture of macro and microquartz. *Chalcedony* Traces of chalcedony are scattered throughout this sample. These fragments are approximately medium sand sized (0.4mm). Grains are generally angular and occasionally are broken and display typical chalcedonic texture comprising of radiating fibrous crystals of varying size. *Volcanics* These rock fragments are medium sand sized (0.3mm), sub-angular and consist of large laths of plagioclase feldspar. Grain boundaries are highly irregular and diffuse and some volcanic grains display minor dissolution and dispersion into intergranular pore space. Most volcanic fragments have been partially altered to a mixture of sericite and chlorite which has destroyed their original fabric.

	Shale These fragments are typically coarse sand sized (0.6mm) and angular to sub-rounded in shape. They consist of a mixture of sericite and coarsely crystalline authigenic kaolinite. Kaolinite is interpreted to have replaced sericite in these fragments. Grain boundaries have often been squashed and therefore highly irregular. Some of these squashed grains have been replaced by a fine authigenic chlorite clay. *Kaolinite* Kaolinite occurs as sub-rounded to rounded clasts. These clasts consist of coarsely and finely crystalline accumulation of kaolinite. Most of the clasts have undergone partial compaction resulting in their expansion of the kaolinite into intergranular pore space.
Matrix/ Pseudomatrix	
Authigenic cement	Calcite This sample is partially calcite cemented. Most calcite cement occurs as single crystal poikilotopes or microsparry accumulations of very finely crystalline calcite that fills intergranular pore space and encases clusters of framework grains. The cement forms highly corrosive contacts with surrounding detrital grains and partially replaces portions of framework grains. Silica overgrowths Thin authigenic silica overgrowths are only apparent where triple junctions occur between detrital quartz grains. Irregular compromise boundaries are evident between these grains caused by the interference of individual grain overgrowths.
Porosity/ Permeability	Porosity and permeability in this sample is poor. Most primary and secondary porosity has been filled by compacted detrital grains and poikilotopic calcite cement.

DIAGENESIS

Relative timing of events	Compactional deformation Authigenic silica cementation Primary calcite cementation Sericitisation Kaolinite/chlorite replacement Secondary calcite cementation
Relative importance of events	

TEXTURAL MATURITY AND INTERPRETATION

Textural maturity	Immature
Interpretation	

MINERALOGICAL CLASSIFICATION AND COMMENTS

Mineralogical classification	Feldspathic litharenite
Comments	

GSWA No. 154822

Well	VINES-1
Sample number	154855
Sample type	Core
Depth	985.24
Unit	
Facies	Claystone
Sample quality	The sample is in reasonable condition but has been cracked during thin-section manufacturing.
Brief description	Micritic mudstone This sample is a massive lithic wacke composed predominantly of micritic mud mixed with illite/sericite. Minor quartz and altered shale and carbonate clasts are also scattered throughout. No visual porosity was noted.

STRUCTURES

Structures	Massive

TEXTURE

Grain size	Range: Coarse silt (0.05mm) to medium sand (0.3mm) Mode: Coarse silt
Sorting	Poorly-sorted
Grain morphology	Angular to sub-rounded
Sediment fabric	Matrix supported

MINERALOGY

Tabulated composition (%)	Detrital components		
	Quartz	Monocrystalline	15
		Muscovite	Tr
	Rock fragments		
		Carbonate	Tr
		Shale	1
	Matrix/ Pseudomatrix		
		Carbonate mud	84
	Porosity/ Permeability		
		Primary	Nil
		Secondary	Nil

Detrital components

Quartz

Monocrystalline quartz dominates this sample. Quartz grains range in size from coarse silt (0.05mm) to medium sand (0.3mm) with a mode of coarse silt (0.05mm). Grains are sub-angular to rounded, poorly-sorted and matrix supported.

Mica

Mica flakes display minor preferential alignment sub-vertical to bedding claystone direction.

Rock fragments

Carbonate

Trace medium sand sized (0.2mm) carbonate clasts are evident in this sample. These clasts are generally sub-angular to sub-rounded and have highly corrosive grain boundaries. These clasts are composed of anhedral to subhedral shaped, micro- to medium crystalline dolomite that display planar, curved and sutured contacts. Clasts display varying degrees of dissolution and alteration to micrite.

	Shale Only a rough outline of most shale fragments is preserved. Fragments have almost been completely altered to carbonate mud. The unaltered dark material that is associated with some of these fragments is a mixture of illite/sericite, pyrite and insoluble organic matter.
Matrix/ Pseudomatrix	Carbonate mud A complex mixture of micrite and illite/sericite forms the matrix of this sample. Carbonate mud occurs as a xenotopic fabric of equant, very finely crystalline calcite that has replaced or has been partially replaced by illite/sericite clays. The matrix material forms highly corrosive contacts with surrounding detrital grains. Marginal replacement of these grains by the carbonate mud is often evident.
Authigenic cement	
Porosity/ Permeability	Nil.

DIAGENESIS

Relative timing of events	Sericitisation Illite formation Carbonate mud replacement
Relative importance of events	

TEXTURAL MATURITY AND INTERPRETATION

Textural maturity	Immature
Interpretation	

MINERALOGICAL CLASSIFICATION AND COMMENTS

Mineralogical classification	Micritic mudstone
Comments	SEM or XRD on this sample would aid in the identification of matrix material.

GSWA No. 154821

Well	VINES-1
Sample number	154821
Sample type	Plug
Depth	970.0
Unit	
Facies	Diamictite
Sample quality	The sample is in good condition.
Brief description	Lithic wacke This sample consists coarse silt sized, angular to sub-rounded quartz grains supported in a weakly burrowed carbonate and illite/sericite mud. Visual porosity in this sample is extremely poor. The trace secondary porosity that does exist is interpreted to be due to grain plucking during thin section manufacture.

STRUCTURES

Structures	Burrows A couple of transverse sections of burrows are evident in this section. These burrows were developed parallel to the bedding plane. Burrows are approximately 1.5cm in diameter and filled with medium sand sized (0.25mm) quartz cemented by calcite. Most of the calcite cement occurs as non-equant, porphyrotopic matrix of finely crystalline calcite that fills intergranular pore space and encases quartz grains. The cement forms highly corrosive contacts with surrounding quartz. A partial micritic rim is evident coating the outside of one of the burrows.

TEXTURE

Grain size	Range: Medium silt (0.02mm) to very coarse sand (1.2mm) Mode: Coarse silt (0.04mm)
Sorting	Poorly-sorted
Grain morphology	Angular to sub-rounded
Sediment fabric	Matrix supported. Grains display rare point contacts

MINERALOGY

Tabulated composition (%)	Detrital components		
	Quartz	Monocrystalline	25
		Polycrystalline	Tr
	Feldspar	Albite	Tr
	Rock Fragments		
	Carbonate	Calcite	4
		Chert	1
		Mica	1
		Siltstone	2
		Sandstone	Tr
		Oncoids	Tr
	Accessories	Tourmaline	Tr
		Biotite	Tr
	Matrix/ Pseudomatrix		
	Micritised, illite/sericite mud		65
	Authigenic cement		
		Calcite	2
		Nondular pyrite	Tr
	Porosity/ Permeability		
		Primary	Nil
		Secondary	Tr

Detrital components	Quartz Quartz grains range in size from medium silt (0.02mm) to very coarse sand (1.2mm) with a mode of coarse silt (0.04mm). Coarser grains are scattered throughout the sample and are concentrated in the burrow. These grains tend to be sub-rounded while coarse silt sized grains are typically more angular. Quartz grains are matrix supported but occasional point contacts are evident between grains. Oncoids Trace medium sand sized (0.2mm) sized oncoids are evident in this sample. These grains consist of a concentrically laminated internal quartz grain or colourless phosphate fragment. Rock fragments *Carbonate* Carbonate clasts are predominantly fine sand sized (0.15mm) to medium sand sized. Grain margins are highly corrosive with some of these grains being altered by matrix material. The internal constituents of these clasts consist of patchy xenotopic matrix of anhedral to subhedral shaped finely crystalline and medium crystalline dolomite that displays planar, curved and sutured contacts. Some clasts display partial alteration to micrite and siderite. *Chert* Chert fragments displaying similar grain size to quartz grains are scattered throughout the sample. Only microquartz varieties of chert are evident in this sample. *Siltstone/ Shale* Ghost outlines of relict siltstone or shale fragments are evident in this sample. These fragments are sub-rounded and approximately medium sand sized (0.3mm). The grains have been altered to a sericite/carbonate that resembles the matrix of this rock. Mica flakes within these grains show a preferential sub-vertical orientation along their elongate axis. *Sandstone* Traces of well-cemented sandstone fragments are also evident in this sample. These fragments have also been partially to totally dissolved into the matrix. The sandstone fragments consist of a mixture of moderately sutured coarse silt sized quartz that has been cemented by a poikilotopic calcite cement.
Matrix/ Pseudomatrix	Micrite/illite sericite mud The sample is dominated by a mixture of micritic mud and illite/sericite clays. Micrite occurs as a xenotopic fabric of equant, very finely crystalline calcite mixed with illite/sericite. Trace mica is also scattered throughout this fragment. Mica flakes display a weak preferential orientation possibly parallel to bedding direction.
Authigenic cement	Nodular pyrite Nodular pyrite occurs replacing some grains and matrix material. It generally forms as small isolated nodules but accumulations of nodules into irregularly shaped grains are also evident.
Porosity/ Permeability	Porosity and permeability is poor in this sample. Oversized pores may indicate the trace secondary porosity observed in these samples possibly is the result of grain plucking during thin-section manufacture.

DIAGENESIS

Relative timing of events	Sericite formation Primary calcite replacement Secondary calcite cementation Pyrite formation
Relative importance of events	

TEXTURAL MATURITY AND INTERPRETATION

Textural maturity	Immature
Interpretation	

MINERALOGICAL CLASSIFICATION AND COMMENTS

Mineralogical classification	Lithic wacke
Comments	

GSWA No. 154820

Well	VINES-1
Sample number	154820
Sample type	Plug
Depth	950.0
Unit	
Facies	Sandstone
Sample quality	The sample is in good condition.
Brief description	Quartz arenite Predominantly composed of fine sand sized, monocrystalline, sub-angular to sub-rounded quartz grains. Detrital grains display point to well-sutured grain-grain contacts. Most of the porosity in this sample has been reduced by compactional deformation resulting in the squashing of rock fragments into pore space and calcite and pyrite cementation.

STRUCTURES

Structures	Massive

TEXTURE

Grain size	Range: Coarse silt (0.04mm) to coarse sand (0.7mm)(Mode: Fine sand (0.15mm)
Sorting	Well-sorted
Grain morphology	Sub-angular to sub-rounded
Sediment fabric	Framework grains display point to concave/convex and well-sutured grain-grain contacts.

MINERALOGY

Tabulated composition (%)	Detrital components		
	Quartz	Monocrystalline	75
		Polycrystalline	Tr
	Feldspar	Microcline	1
		Albite	3
		Plagioclase	1
	Rock Fragments		
	Carbonate	Calcite and Siderite	5
		Chert	1
		Volcanics	Tr
		Muscovite	Tr
		Shale	Tr
	Accessories	Zircon	Tr
		Tourmaline	Tr
		Biotite	Tr
	Matrix/ Pseudomatrix		
		Kaolinite	2
	Authigenic cement		
		Calcite	7
		Ferroan calcite	Tr
		Chlorite	1
		Pyrite	1
	Porosity/ Permeability		
		Primary	2
		Secondary	1

Detrital components	Quartz Moderately-sorted, monocrystalline quartz dominates this sample. Quartz grain sizes range coarse silt (0.04mm) to medium sand (0.5mm) with a mode of fine sand (0.15mm). Grains are angular to sub-rounded and display concave/convex to well-sutured grain-grain contacts. Grains often display irregular and diffuse margins due to their partial dissolution and replacement by calcite cement. Some polycrystalline quartz grains are evident in this sample. Feldspar Feldspar grains are predominantly medium sand sized (0.4mm). Several varieties of feldspar are evident these include microcline, albite and plagioclase. Some grains have undergone partial leaching and dissolution and alteration by authigenic calcite and chlorite cements. Muscovite Trace muscovite grains are evident in this sample. These grains have been bent and broken around detrital grains. Rock fragments *Carbonate* Carbonate clasts are predominantly very fine sand sized (0.1mm) but the size of these clasts can vary up to coarse sand (0.7mm). Fine sand sized clasts are mainly sub-rounded to rounded. A larger carbonate clast is evident in this sample. This clast is angular and contains a thin micritic envelope around its margin. Most of the clasts have been broken, dispersed and squashed into intergranular pore space. These clasts display minor sutured seam solution. The internal constituents of clasts consist of xenotopic matrix of anhedral to subhedral shaped medium crystalline dolomite that displays planar, curved and sutured contacts. Some clasts display partial alteration to micrite and siderite. *Siderite clasts* Siderite clasts are predominantly very fine sand sized. These clasts are typically sub-rounded. They consist of an accumulation of very finely crystalline siderite. Grains have very diffuse boundaries and have undergone minor compactional deformation resulting in them being squashed into intergranular pore space *Chert* Chert fragments displaying similar grain size to quartz grains are scattered throughout the sample. Only microquartz varieties of chert are evident in this sample. *Volcanics* The most common volcanic rock fragments are igneous in origin. These rock fragments are of similar size to quartz grains, sub-angular and consist of large laths of plagioclase feldspar grains. Grain boundaries are highly irregular and diffuse and some volcanic grains display minor dissolution and dispersion into intergranular pore space. Most volcanic fragments have been partially altered to a mixture of kaolinite, sericite and chlorite which has destroyed their original fabric. *Shale* These rock fragments are typically medium sand sized and sub-angular to sub-rounded in shape. Deformation and alteration of these fragments is evident. Some of these grains have undergone compactional deformation. Compaction of these grains has resulted in them flowing around adjacent framework grains and into intergranular pore space. Some of the squashed grains display partial alteration to kaolinite.

Matrix/ Pseudomatrix	Kaolinite Kaolinite occurs in a massive pore filling aggregate form. Kaolinite clasts have undergone partial compaction resulting in their expansion into intergranular pore space.
Authigenic cement	Calcite This sample is partially calcite cemented. Most calcite cement occurs as single crystal poikilotopes or microsparry accumulations of very finely crystalline calcite that fills intergranular pore space and encases clusters of framework grains. The cement forms highly corrosive contacts with surrounding detrital grains and partially replaces portions of quartz and feldspar grains. Pyrite Late stage diagenetic pyrite cement occurs in trace amounts filling intergranular pore space.
Porosity/ Permeability	Visual porosity in this sample is poor. Some primary intergranular porosity is preserved but it has mostly been reduced by compactional deformation and calcite and pyrite cementation.

DIAGENESIS

Relative timing of events	Compactional deformation Calcite cementation Pyrite formation
Relative importance of events	

TEXTURAL MATURITY AND INTERPRETATION

Textural maturity	Immature
Interpretation	

MINERALOGICAL CLASSIFICATION AND COMMENTS

Mineralogical classification	Quartz arenite
Comments	

GSWA No. 154819

Well	VINES-1
Sample number	154819
Sample type	Plug
Depth	939.0
Unit	
Facies	Sandstone
Sample quality	The sample is in good condition.
Brief description	Feldspathic litharenite This sample consists predominantly of sub-angular to sub-rounded, very fine sand sized quartz grains and carbonate fragments. Compactional deformation is evident in this sample as most grains are well sutured or have been compacted into intergranular pore space. Framework grains are cemented by poikilotopic and microsparry calcite that has been partially replaced by dolomite. Visual porosity in this sample is poor as most of the porosity has reduced by compaction and filled by late stage calcite cementation.

STRUCTURES

Structures	Massive

TEXTURE

Grain size	Range: Very fine sand (0.07mm) to fine sand (0.2mm) Mode: Very fine sand (0.11mm)
Sorting	Moderately-sorted
Grain morphology	Sub-angular to sub-rounded
Sediment fabric	Grains display concave/convex to well-sutured grain-grain contacts.

MINERALOGY

Tabulated composition (%)	Detrital components		
	Quartz	Monocrystalline	72
		Polycrystalline	Tr
	Feldspar	Microcline	1
		Albite	2
		Plagioclase	1
	Rock Fragments		
	Carbonate	Calcite and Siderite	7
		Chert	2
		Chalcedony	Tr
		Volcanics	1
	Accessories	Zircon	Tr
		Tourmaline	Tr
		Biotite	Tr
	Matrix/ Pseudomatrix		
		Kaolinite	4
	Authigenic cement		
		Calcite	6
		Ferroan calcite	Tr
		Dolomite	1
		Chlorite	1
	Porosity/ Permeability		
		Primary	2
		Secondary	1

Detrital components	Quartz Moderately-sorted, monocrystalline quartz dominates this sample. Quartz grain sizes range from very fine sand (0.07mm) to fine sand (0.2mm) with a mode of very fine sand (0.11mm). Grains are angular to sub-rounded and display concave/convex to well-sutured grain-grain contacts. Grains often display irregular and diffuse margins due to their partial dissolution and replacement by calcite cement. Some polycrystalline quartz grains are evident in this sample. Feldspar Feldspar grains are predominantly fine sand sized (0.15mm). Several varieties of feldspar are evident these include microcline, albite and plagioclase. The degree of preservation of feldspar grains in the sample varies. Smaller grains are typically unaltered while larger grains have been leached and partially replaced by calcite. Rock fragments *Carbonate* Carbonate clasts range in size from very fine sand (0.1mm) to fine sand (0.2mm) size. Clasts are predominantly sub-rounded to rounded but a large percentage of the grains have been broken and dispersed or squashed into intergranular pore space. The internal constituents of clasts consist of xenotopic matrix of anhedral to subhedral shaped medium crystalline dolomite that displays planar, curved and sutured contacts. Some clasts display partial alteration to micrite, siderite and microsparry ferroan calcite. *Chert and chalcedony* Trace detrital chalcedony fragments are located throughout this sample. Grains are generally angular and occasionally are broken and display typical chalcedonic texture comprising of radiating fibrous crystals of varying size. Chert fragments displaying similar grain size to carbonate clasts are scattered throughout the sample. Crystal size varies within grains from micro- to megaquartz. *Volcanics* These rock fragments are of similar size to quartz grains, sub-angular and consist of large laths of plagioclase feldspar grains. Most of these fragments have been partially altered to chlorite which has destroyed their original fabric.
Matrix/ Pseudomatrix	Kaolinite Kaolinite occurs in a massive pore filling aggregate form. Kaolinite clasts have undergone partial compaction resulting in their expansion into intergranular pore space. Kaolinite is gradually being replaced by authigenic calcite cement in this sample.
Authigenic cement	Calcite and dolomite Most of the carbonate cement in this sample occurs as single crystal poikilotopes or microsparry accumulations of very finely crystalline calcite that fills intergranular pore space and encases clusters of framework grains. The cement forms highly corrosive contacts with surrounding detrital grains and partially replaces portions of quartz and feldspar grains. Dolomite occurs as isolated medium crystalline rhombs and small microcrystalline accumulations partially replacing calcite cement.
Porosity/ Permeability	Visual porosity in this sample is poor with most of the porosity being marginally replaced by authigenic cements. The compaction of carbonate clasts and kaolinite into intergranular pore space has also reduced porosity.

DIAGENESIS

Relative timing of events	Mechanical compaction Calcite cementation Siderite and micrite formation Chloritisation
Relative importance of events	

TEXTURAL MATURITY AND INTERPRETATION

Textural maturity	Immature
Interpretation	

MINERALOGICAL CLASSIFICATION AND COMMENTS

Mineralogical classification	Feldspathic litharenite
Comments	

GSWA No. 154817

Well	VINES-1
Sample number	154817
Sample type	Plug
Depth	930.0
Unit	
Facies	Diamictite
Sample quality	Sample is in good condition.
Brief description	Lithic Wacke This sample is dominated by a complex mixture of partially illite/sericite and partially chloritised micritic mud. Quartz occurs as matrix supported angular to sub-rounded, coarse silt sized grains. Sub-horizontal and sub-vertical burrowing is evident in this sample. Sub-horizontal burrows are filled with coarser quartz that has been cemented by a non-equant, porphyrotopic matrix of finely crystalline calcite. Increases in quartz and calcite cementation mark the location of the sub-vertical burrow in this sample. Visual porosity is extremely poor.

STRUCTURES

Structures	Burrows Small burrows are evident in this sample. Burrows have no preferred direction occuring both sub-vertically and sub-horizontally. Two transverse sections of burrows are evident in this section. These burrows possibly were developed parallel to the bedding plane. They are approximately 1 to 1.3mm in diameter and filled with medium sand sized (0.3mm) quartz cemented by calcite, ferroan calcite and siderite. The sample predominantly consists of a non-equant, porphyrotopic matrix of finely crystalline dolomite that fills intergranular pore space and encases quartz grains. The cement forms highly corrosive contacts with surrounding quartz grains and in part has been partially replaced by late stage siderite cementation The sub-vertical burrow is approximately 1mm in diameter. Even though this burrow forms a graduating contact with the surrounding host rock it can be differentiated from the host by an increase in quartz and carbonate cementation. It is composed of approximately 30% coarse silt sized quartz cemented by a xenotopic matrix of very finely crystalline dolomite. This dolomite cement has been partially replaced by siderite and micrite.

TEXTURE

Grain size	Range: Medium silt (0.028mm) to very coarse sand (1.4mm) Mode: Coarse silt (0.035mm)
Sorting	Poorly-sorted
Grain morphology	Angular to sub-rounded
Sediment fabric	Matrix supported but some rare point contacts are evident between detrital grains.

MINERALOGY

Tabulated composition (%)	Detrital components		
	Quartz	Monocrystalline	12
		Polycrystalline	2
	Feldspar	Albite	Tr
		Mica	1
	Rock Fragments		
		Carbonate	Tr
		Chert	3
		Sandstone	4
		Illite/sericite	1
	Accessories	Zircon	Tr
		Tourmaline	Tr
	Matrix/ Pseudomatrix		
		Micritic mud	68
	Authigenic cement		
		Calcite	4
		Ferroan calcite	2
		Chlorite	3
		Siderite	Tr
	Porosity/ Permeability		
		Primary	Nil
		Secondary	Tr

Detrital components

Quartz

Moderately-sorted, monocrystalline quartz dominates this sample. Quartz grain sizes range from medium silt (0.028mm) to very coarse sand (1.4mm) with a mode of coarse silt (0.035mm). Grains are angular to sub-rounded and predominantly matrix supported but occasional point contacts between grains are evident. Grain boundaries appear irregular as they have been marginally replaced by carbonate cements.

Feldspar

Only trace amounts of albite are evident in this sample. These grains are typically very fine sand sized and no evident alteration of these grains is evident.

Illite/sericte

Authigenic illite/sericitic grains are in the form of sub-rounded and squashed grains displaying a similar grain size to quartz grains. Some of these grains display alteration to kaolinite and/or chlorite. Two possible sources for the illitic/sericitic grains are volcanic clasts and/or detrital clay balls.

Rock Fragments

Carbonate clasts

Carbonate clasts range in size from very fine sand (0.1mm) to medium sand (0.3mm) size. Clasts are predominantly sub-rounded to rounded but a large percentage of the grains have been broken and dispersed or squashed into intergranular pore space.

The internal constituents of clasts consist of xenotopic matrix of anhedral to subhedral shaped medium crystalline dolomite that displays planar, curved and sutured contacts.

Chert

Chert fragments displaying similar grain size to carbonate clasts are scattered throughout the sample. These fragments consist predominantly of microquartz.

	Sandstone Sandstone fragments range from coarse sand (0.5mm) to very coarse sand (1.2mm). These fragments are typically composed of a mixture of very fine sand sized (0.08mm) quartz and traces of biotite and mica cemented by chloritised clay, poikilotopic calcite and illite/sericite cement. The cements encase clusters of framework grains and fill intergranular pore space. In some fragments only trace cement is evident with quartz grains display concave/convex and well-sutured grain-grain contacts.
Matrix/ Pseudomatrix	Micritic mud A complex mixture of micritic mud, sericite and chlorite forms the matrix of this sample. Micritic mud occurs as a xenotopic fabric of equant, very finely crystalline calcite that has replaced or has been replaced by illite/sericite and chlorite clays. The matrix material forms highly corrosive contacts with surrounding detrital grains. Marginal replacement of these grains by the carbonate mud is often evident.
Authigenic cement	
Porosity/ Permeability	Visual porosity and permeability is extremely poor in this sample.

DIAGENESIS

Relative timing of events	Carbonate cementation? Illite/sericite formation? Chloritisation? Ferroan calcitisation Dolomitisation Pyrite formation
Relative importance of events	

TEXTURAL MATURITY AND INTERPRETATION

Textural maturity	Immature
Interpretation	

MINERALOGICAL CLASSIFICATION AND COMMENTS

Mineralogical classification	Lithic Wacke
Comments	

GSWA No. 154853

Well	VINES-1
Sample number	154853
Sample type	Core
Depth	763.7
Unit	
Facies	Sandstone
Sample quality	The sample is in good condition
Brief description	Sedarenite This sample consists predominantly of sub-angular to sub-rounded, fine sand sized quartz interbedded with 2-3mm thick sub-horizontal lenses of medium sand sized quartz. The sample has numerous fragments scattered throughout it. These fragments include siltstone, sandstone, shale and carbonate rock fragments. Most fragments display minor compactional deformation and have been partially squashed into pore space. Detrital grains are cemented by massive pore filling chlorite and anhydrite that has been replaced by late stage poikilotopic and microsparry calcite cementation. Visual porosity in this sample is poor.

STRUCTURES

Structures	Quartz-rich beds This sample contains a couple of thin beds composed of medium sand sized quartz grains and rock fragments supported by partially carbonate cemented chlorite matrix. These beds are typically 2-3mm thick and display sharp contacts with the surrounding host rock. It is possible that these beds represent lag deposits or rapidly deposited storm beds.

TEXTURE

Grain size	Range: Coarse silt (0.05mm) to very coarse sand (1.5mm) Mode: Bimodal→ Fine sand (0.15mm) and medium sand (0.45mm)
Sorting	Moderately-sorted
Grain morphology	Sub-angular to sub-rounded
Sediment fabric	Grains display point to concave/convex and moderately sutured grain-grain contacts.

MINERALOGY

Tabulated composition (%)	Detrital components		
	Quartz	Monocrystalline	63
	Feldspar	Microcline	Tr
		Albite	1
		Plagioclase	2
		Muscovite	Tr
	Rock fragments		
		Carbonate	5
		Shale	2
		Chert	2
		Chalcedony	1
		Sandstone	1
		Siltstone	2
		Kaolinite	2
		Volcanic	4
	Accessories	Zircon	Tr
		Tourmaline	Tr
	Authigenic cement		
		Calcite	8
		Ferroan calcite	1

		Chlorite	2
		Siderite	Tr
		Anhydrite	2
		Authigenic silica	1
		Pyrite	Tr
	Porosity/ Permeability		
		Primary	1
		Secondary	Tr

Detrital components

Quartz

Quartz displays a bimodal grain size distribution. The finer sand fraction is concentrated in the host rock. Quartz grains in the host rock are typically fine sand sized (0.15mm). Quartz is poorly sorted and grains occasionally display thin authigenic silica overgrowths. Grains display point to concave/convex and well-sutured grain-grain contacts. Fluid inclusions or vacuoles are evident on most quartz grains. Vacuoles are identified by lines of dark specks that cut across quartz grains.

The larger quartz fraction is contained in the 2-3mm thick, sub-horizontal laminae that cut through this sample. Quartz grains in these lenses have a mode of medium sand (0.45mm). These grains in these lenses are typically sub-angular to sub-rounded and display point to concave/convex to well-sutured grain-grain contacts.

Feldspar

Feldspar grains range from fine sand sized (0.12mm) to medium sand sized (0.4mm). Several varieties of feldspar are evident these include microcline, albite and plagioclase. Some grains have undergone partial leaching resulting in vacuolisation and alteration to kaolinite or partial calcite cementation.

Rock fragments

Shale

These rock fragments range up to very coarse sand (1.5mm) in size. Shale fragments are generally sub-angular in shape. Fragments consist predominantly of a dark brown illite/sericite clay. Grains have undergone compactional deformation and have been squashed into intergranular pore space. Some of the grains have been partially dissolved into intergranular pore space.

Volcanics

These rock fragments range up to pebbles, sub-angular and consist of a mixture of leached and partially altered feldspar laths and augite, undifferentiated black cryptocrystalline matrix and with patchy illite/sericite and chlorite alteration. Volcanic fragments display some deformation and dispersion and have been partially compacted in places into intergranular pore space.

Carbonate

Sub-rounded to rounded carbonate clasts are scattered throughout this sample. Carbonate clasts range up to very coarse sand (1.5mm). These clasts are composed of patchy anhedral to subhedral shaped, finely crystalline dolomite that displays planar, curved and sutured contacts. Micritic alteration is evident in some of these clasts. Most of the micritised clasts consist of equant subhedral to euhedral calcite crystals of microsparite and finer, micrite which have replaced the original very fine to fine calcite. A thin micritic rim is evident on the outside of some of these fragments. Some of the fragments have been squashed into intergranular pore space and display microstylolisation that has a dark brown illite/sericite clay concentrated along them.

Chert

Chert fragments range in size from medium to coarse sand size. These fragments are typically sub-angular to sub-rounded and consist of a patchy

	mixture of macro and microquartz. *Chalcedony* Traces of chalcedony are scattered throughout this sample. These fragments are approximately coarse sand sized (0.7mm). Grains are generally angular and occasionally are broken. These fragments display typical chalcedonic texture comprising of radiating fibrous crystals of varying size. Alteration of these fragments to chert and microsparry calcite is evident in some fragments. *Sandstone* Sandstone fragments range up to granule size (3mm). They are generally-angular to sub-rounded and composed of up to 94% moderately sutured, coarse silt sized (0.05mm) quartz grains, 1% mica, 5% poikilotopic calcite cement and traces of spinel, siderite and pyrite. Advanced pressure solution is evident with grains displaying well-sutured grain-grain contacts. Within the fragment calcite cement encases clusters of framework grains and fills intergranular pore space. Sandstone fragments are often difficult to distinguish from the host rock as calcite cements have overgrown grains. *Kaolinite* Kaolinite occurs as sub-rounded to rounded clasts or balls that occupy intergranular pore space. These clasts consist of coarsely crystalline accumulations of kaolinite. Most of the clasts have undergone partial compaction resulting in their expansion of the kaolinite into intergranular pore space. *Siltstone* Siltstone fragments are typically angular to sub-angular in shape. They consist of coarse silt (0.05mm) and mica supported by an illite/sericite matrix. Most siltstone fragments have been compacted into intergranular pore space.
Matrix/ Pseudo	
Authigenic cement	<u>Calcite and Ferroan calcite</u> Most calcite cement occurs as single crystal poikilotopes or as an equant drusy mosaic of finely crystalline calcite. Calcite cement is particularly evident filling intergranular pore space, replacing leached grains and replacing chlorite and anhydrite cements. It also forms highly corrosive contacts with detrital grains where it marginally replaces these grains. <u>Anhydrite</u> Anhydrite cement occurs in this sample mainly as a massive pore filling poikilotopic cement. Most of the anhydrite in this sample displays a typical blocky appearance. <u>Chlorite</u> Chlorite forms as coarsely crystalline pore filling cement. The cement forms fibrous crusts which line pore space and coat detrital grains. The cement has been partially leached in places and replaced by microsparry calcite accumulations and poikilotopic calcite. <u>Siderite</u> Siderite occurs as microsparry accumulations that marginally replace grains. <u>Silica overgrowths</u> Authigenic silica overgrowths are evident on some quartz grain boundaries. Contacts between adjacent overgrowths are irregular compromise boundaries produced by the mutual interference of individual overgrowths. Overgrowths are defined by pyritic ‘dust rims’ that occur between between the grain and the overgrowth.
Porosity/ Permeability	Visual porosity in this sample is poor. Most of the porosity has been filled by calcite, chlorite and anhydrite cements.

DIAGENESIS

Relative timing of events	Silica overgrowths Isopachous rims Mechanical compaction Chlorite cementation Anhydrite cementation Ferroan and non-ferroan calcite cementation Pyrite cementation
Relative importance of events	

TEXTURAL MATURITY AND INTERPRETATION

Textural maturity	Immature
Interpretation	

MINERALOGICAL CLASSIFICATION AND COMMENTS

Mineralogical classification	Sedarenite
Comments	

GSWA No. 154816

Well	VINES-1
Sample number	154816
Sample type	Plug
Depth	749.0
Unit	
Facies	Conglomerate
Sample quality	The sample is in good condition.
Brief description	Pebble-rich Lithic Wacke This sample consists predominantly of sub-angular to sub-rounded, fine sand sized quartz grains with lesser amounts of carbonate, volcanic and chert rock fragments. Framework grains are well cemented by diagenetic carbonate cements. This cement mixture of poikilotopic and microsparry calcite and siderite that has been partially dolomitised. The cement partially replaces grains and fills intergranular pore space. Visual porosity is poor in this sample.

STRUCTURES

Structures	Massive

TEXTURE

Grain size	Range: Very fine sand (0.1mm) to very coarse sand (1.1mm) Mode: Fine sand (0.13mm)
Sorting	Well-sorted
Grain morphology	Sub-angular to sub-rounded
Sediment fabric	Grains displays point to concave/convex and moderately sutured grain-grain contacts.

MINERALOGY

Tabulated composition (%)	Detrital components		
	Quartz	Monocrystalline	61
		Polycrystalline	1
	Feldspar	Microcline	1
		Albite	2
		Plagioclase	Tr
	Rock Fragments		
	Carbonate	Calcite and Siderite	5
		Siltstone	1
		Chert	2
		Volcanics	2
	Accessories	Zircon	Tr
		Tourmaline	Tr
		Biotite	Tr
	Matrix/ Pseudomatrix		
		Kaolinite	5
	Authigenic cement		
		Calcite	10
		Dolomite	4
		Chlorite	2
		Illite/sericite	3
	Porosity/ Permeability		
		Primary	1
		Secondary	Tr

Detrital components	Quartz Moderately-sorted, monocrystalline quartz dominates this sample. Quartz grain sizes range from very fine sand (0.1mm) to very coarse sand (1.1mm) with a mode of fine sand (0.13mm). Grains are sub-angular to sub-rounded and display point to concave/convex and moderately sutured grain-grain contacts. Grain boundaries appear irregular as they have been marginally replaced by carbonate cements. Trace grains display thick authigenic silica overgrowths. Feldspar The most common feldspars evident in this sample are albite and to a lesser extent microcline. Feldspar grains display a similar grain size to detrital quartz grains. Smaller grains are typically well preserved while larger grains have undergone partial dissolution or are cracked and have undergone vacuolisation and alteration to calcite. Illite/sericte Authigenic illite/sericitic grains are in the form of sub-rounded and squashed grains displaying a similar grain size to quartz grains. These grains have been partially to totally altered to chlorite and have been compacted and deformed. Two possible sources for the illitic/sericitic grains are volcanic clasts and/or detrital clay balls. Rock Fragments *Carbonate clasts* Carbonate clasts range in size from very fine sand (0.1mm) to medium sand (0.3mm) size. Clasts are predominantly sub-rounded to rounded but a large percentage of the grains have been broken and dispersed or squashed into intergranular pore space. The internal constituents of clasts consist of xenotopic matrix of anhedral to subhedral shaped medium crystalline dolomite that displays planar, curved and sutured contacts. *Siderite clasts* Siderite clasts are predominantly medium sand sized. These clasts are typically sub-angular to rounded. They consist of an accumulation of very finely crystalline siderite. Grains have very diffuse boundaries and have undergone minor compactional deformation and as a result have been squashed into intergranular pore space. *Chert* Chert fragments displaying similar grain size to quartz grains are scattered throughout the sample. These fragments consist predominantly of microquartz. *Siltstone* Siltstone fragments are typically angular to sub-angular in shape. They consist of very fine sand (0.12mm), mica and illite/sericite. *Volcanics* The most common volcanic rock fragments are igneous in origin. These rock fragments are of similar size to quartz grains, sub-angular and consist of large laths of plagioclase feldspar grains contained in a cryptocrystalline matrix. Alteration of these clasts to chlorite varies in intensity. Most volcanic rock fragments however only display partial alteration.
Matrix/ Pseudomatrix	Kaolinite Kaolinite occurs as a massive pore filling aggregate form. Kaolinite clasts have undergone partial compaction resulting in their expansion into intergranular pore space. These deformed grains have been partially altered to sericite and chlorite.

Authigenic cement	Calcite and dolomite This sample consists of a mixture of calcite and dolomite cements. Most carbonate cement occurs as single crystal poikilotopes or microsparry accumulations of very finely crystalline calcite that fill intergranular pore space and encase clusters of framework grains. The cement forms highly corrosive contacts with surrounding detrital grains and partially replaces portions of quartz and feldspar grains. Dolomite occurs as isolated rhombs and small microcrystalline accumulations partially replacing calcite cement. Siderite Trace amounts of authigenic siderite are also evident in this sample. Siderite occurs as small individual crystals or microcrystalline accumulations that coat detrital grains and occasionally bridge pore space. These grains form highly corrosive contacts with surrounding grains. Chlorite Chlorite is evident partially replacing illite/sericite in this sample. It forms mainly as a diagenetic clay. Pyrite Late stage diagenetic pyrite cement occurs in trace amounts filling intergranlar pore space.
Porosity/ Permeability	Primary and secondary porosity is poor in this sample as it has been replaced by diagenetic cements.

DIAGENESIS

Relative timing of events	Calcite cementation Siderite cementation Dolomite replacement Chlorite formation Pyrite formation
Relative importance of events	

TEXTURAL MATURITY AND INTERPRETATION

Textural maturity	Immature
Interpretation	

MINERALOGICAL CLASSIFICATION AND COMMENTS

Mineralogical classification	Lithic Wacke
Comments	

GSWA No. 154815

Well	VINES-1
Sample number	154815
Sample type	Plug
Depth	691.0
Unit	
Facies	Sandstone
Sample quality	The sample is in good condition.
Brief description	Lithic wacke This sample is dominated by monocrystalline, angular to sub-angular quartz grains and carbonate and chert rock fragments. Framework grains have been partially cemented by poikilotopic calcite cement. Partial replacement of this sample by diagenetic minerals such as ferroan calcite, dolomite and chlorite is also evident. Primary intergranular porosity is good with much of the pore space in this sample being uncemented.

STRUCTURES

Structures	Very weak lamination defined by the concentration of clean quartz-rich beds.

TEXTURE

Grain size	Range: Coarse silt (0.05mm) to medium sand (0.4mm) Mode: Fine sand (0.14mm)
Sorting	Poorly-sorted
Grain morphology	Angular to sub-rounded
Sediment fabric	Framework grain display point, concave/convex and moderately sutured grain-grain contacts.

MINERALOGY

Tabulated composition (%)	Detrital components		
	Quartz	Monocrystalline	66
		Polycrystalline	1
	Feldspar	Microcline	1
		Albite	2
		Plagioclase	1
	Rock Fragments		
		Carbonate	10
		Siltstone	Tr
		Chert	3
		Volcanics	1
	Accessories	Zircon	Tr
		Tourmaline	Tr
		Biotite	Tr
	Matrix/ Pseudomatrix		
		Kaolinite	2
	Authigenic cement		
		Calcite	5
		Siderite	Tr
		Ferroan calcite	1
		Dolomite	2
		Chlorite	Tr
		Illite/sericite	1
	Porosity/ Permeability		
		Primary	3
		Secondary	1

Detrital components	Quartz Poorly-sorted, monocrystalline quartz dominates this sample. Quartz grain sizes range from coarse silt (0.05mm) to medium sand (0.4mm) with a mode of fine sand (0.14mm). Grains are angular to sub-rounded and display point to concave/convex and moderately sutured grain-grain contacts. Grain boundaries appear irregular as they have been marginally replaced by carbonate cements. No authigenic silica overgrowths are present. Feldspar The most common feldspars evident in this sample are albite and to a lesser extent microcline. Feldspar grains display a similar grain size to detrital quartz grains. Smaller grains are typically well preserved while larger grains have undergone partial dissolution or are cracked and have undergone vacuolisation and alteration to calcite. Illite/sericte Authigenic illite/sericitic grains are in the form of sub-rounded and squashed grains displaying a similar grain size to quartz grains. These grains have been partially to totally altered to chlorite and have been compacted and deformed. Two possible sources for the illitic/sericitic grains are volcanic clasts and/or detrital clay balls. Rock Fragments *Carbonate clasts* Carbonate clasts are typically fine sand sized (0.16mm). Clasts are predominantly sub-rounded to rounded but a large percentage of the grains have been broken and dispersed into intergranular pore space. Grain margins also tend to be highly irregular and diffuse with some secondary carbonate cement growth evident at clast boundaries. The secondary carbonate cement bridges pore space between carbonate clasts and detrital quartz grains. The internal constituents of these clasts consist of xenotopic matrix of anhedral to subhedral shaped medium crystalline dolomite that displays planar, curved and sutured contacts. *Siderite clasts* Siderite clasts are also fine sand sized. These clasts are typically sub-angular to rounded. They consist of an accumulation of very finely crystalline siderite. Grains have very diffuse boundaries. *Siltstone* Siltstone fragments are typically angular to sub-angular in shape. They consist of very fine sand (0.12mm), mica and illite/sericite. *Chert* Chert fragments displaying similar grain size to quartz grains are scattered throughout the sample. Crystal size varies within these fragments is predominantly microquartz. *Volcanics* These rock fragments are of similar size to quartz grains, sub-angular and consist of large laths of plagioclase feldspar grains contained in a cryptocrystalline matrix. Partial phosphate and chlorite alteration of these feldspar and cryptocrystalline matrix is evident.
Matrix/ Pseudomatrix	Kaolinite Kaolinite is evident as finely to coarsely crystalline accumulations filling intergranular pore space.
Authigenic cement	Calcite Most calcite occurs as single crystal poikilotopes that fill intergranular pore

	space and encases clusters of framework grains. The cement forms highly corrosive contacts with surrounding detrital grains and partially replaces portions of quartz and feldspar grains. <u>Siderite</u> Trace amounts of authigenic siderite are also evident in this sample. Siderite occurs as small individual crystals or microcrystalline accumulations that coat detrital grains and occasionally bridge pore space. These grains form highly corrosive contacts with surrounding grains. <u>Dolomite</u> Dolomite occurs as isolated rhombs partially replacing calcite clasts and filling intergranular pore space. <u>Chlorite</u> Chlorite is evident partially replacing illite/sericite in this sample. It forms mainly as a diagenetic clay. <u>Ferroan calcite</u> Traces of ferroan calcite are present in a micro-sparry form filling pore space and partially replacing carbonate clasts. Ferroan calcite displays highly corrosive contacts with the adjacent authigenic and detrital quartz grains.
Porosity/ Permeability	Visual porosity is good in this sample. Primary intergranular porosity although reduced by some calcite cementation has been well preserved. Primary intergranular porosity is interpreted to be the main porosity type evident in this sample. Secondary porosity is evident but has been reduced somewhat by diagenetic cementation.

DIAGENESIS

Relative timing of events	Calcite cementation Siderite cementation Ferroan calcitisation Dolomite replacement Chlorite formation
Relative importance of events	

TEXTURAL MATURITY AND INTERPRETATION

Textural maturity	immature
Interpretation	

MINERALOGICAL CLASSIFICATION AND COMMENTS

Mineralogical classification	Lithic wacke
Comments	

GSWA No. 154814

Well	VINES-1
Sample number	154814
Sample type	Plug
Depth	682.0
Unit	
Facies	Diamictite
Sample quality	Sample is in good condition.
Brief description	Lithic Wacke This sample consists of, angular to sub-rounded coarse silt to sand sized quartz and coarse sand to pebble sized rock fragments supported by a xenotopic matrix of equant, very finely crystalline calcite. The main rock fragments present include chert, carbonate and volcanics. Primary and secondary porosity is poor as most of the porosity has been infilled by the calcite matrix.

STRUCTURES

Structures	Massive

TEXTURE

Grain size	Range: Coarse silt (0.05mm) to pebbles (5mm) Mode: Very fine sand (0.07mm)
Sorting	Poorly-sorted
Grain morphology	Angular to sub-rounded
Sediment fabric	Mainly matrix supported but framework grains do display occasional point, concave/convex and moderately sutured grain-grain contacts.

MINERALOGY

Tabulated composition (%)	Detrital components			
	Quartz	Monocrystalline	15	
		Polycrystalline	4	
	Rock Fragments			
		Carbonate	11	
		Siltstone	1	
		Chert	10	
		Chalcedony	2	
		Volcanics	3	
		Sandstone	2	
		Phosphate	2	
	Accessories	Zircon	Tr	
		Tourmaline	Tr	
		Organic matter	Tr	
	Matrix/ Pseudomatrix			
		Carbonate mud	41	
	Authigenic cement			
		Pyrite	Tr	
		Silica overgrowths		Tr
		Chlorite	Tr	
		Illite/sericite	3	
		Ferroan calcite	2	
		Siderite	3	
	Porosity/ Permeability			
		Primary	1	
		Secondary	Tr	

Detrital components	Quartz Quartz grains range in size from coarse silt (0.05mm) to coarse sand (0.7mm). Smaller quartz grains are typically more angular while larger grains are sub-rounded to rounded. Some grains display thin authigenic silica overgrowths. Rock fragments *Carbonate clasts* Carbonate clasts range in size from very coarse sand (1.5mm) to pebbles (5mm) and display diffuse boundaries that contain thin micritic coatings. Clasts consist of xenotopic texture of anhedral to subhedral shaped dolomite that displays planar, curved and sutured contacts. Most clasts could be termed porphyrotopic in that they consist of patches medium crystalline dolomite in finely crystalline matrix. Micritisation of some carbonate clasts has occurred in this sample. Most of the micritised clasts consist of equant subhedral to euhedral crystals of microsparite and finer micrite which have replaced the original dolomite. In some clasts replacement of peloids by micrite is evident. The micritisation of these peloids is so intense that no internal structure is recognisable. *Chert and chalcedony* Detrital chalcedony fragments are located throughout this sample. These fragments range in size from very coarse sand (1.1mm) to granules (2mm). Grains are generally angular and occasionally are broken and display typical chalcedonic texture comprising of radiating fibrous crystals of varying size. These chalcedonic fragments occasionally have been replaced by a fine microcrystalline chert. Chert fragments displaying similar grain size to detrital chalcedony are scattered throughout the sample. Crystal size varies within grains from micro- to megaquartz. *Sandstone* Sandstone fragments range in size from very coarse sand (1.2mm) to granules (2mm). These fragments are typically composed of a mixture of fine sand sized (0.15mm) quartz cemented by chloritised clay and poikilotopic calcite cement. This cement encases clusters of framework grains and fills intergranular pore space. In some fragments only trace cement is evident with quartz grains display concave/convex and well-sutured grain-grain contacts. *Volcanic* These rock fragments are very coarse sand sized (1.5mm), sub-angular and consist of large laths of plagioclase feldspar grains contained in a cryptocrystalline matrix. Partial phosphate and chlorite alteration of these feldspar and cryptocrystalline matrix is evident. Trace preservation of coaly organic matter is also evident. *Phosphate* Sub-rounded phosphate grains are typically composed of a cryptocrystalline matrix. Grains are occasionally leached and vacuoles have been filled with a mixture of siliceous cement and chlorite. *Siltstone* These rock fragments are typically medium to coarse sand sized and angular to sub-angular in shape. They consist of very fine sand sized (0.12mm) quartz grains, mica and illite/sericite. Mica flakes display some minor preferential alignment.

Matrix/ Pseudomatrix	Micritic mud In this sample a micritic matrix is present between detrital quartz and rock fragments. The matrix has been partially dolomitised in areas.
Authigenic cement	Calcite Late stage calcite occurs predominantly as a cementing agent in sandstone and chert fragments. Secondary calcite forms typically as small microcrystalline grains. Illite/sericte Authigenic illite/sericitic grains are in the form of sub-rounded and squashed grains displaying a similar grain size to quartz grains. These grains have been partially to totally altered to chlorite and have been compacted and deformed. Two possible sources for the illitic/sericitic grains are volcanic clasts and/or detrital clay balls. Siderite Siderite mainly occurs as small microcrystalline accumulations that replace the carbonate mud matrix and marginally replace and coat quartz grains. Ferroan calcite Trace, fabric selective replacement of a siliceous grain by ferroan calcite is evident in this sample. This ferroan calcite occurs as an idiotopic fabric of equant, finely crystalline grains.
Porosity/ Permeability	Porosity is poor in this sample. Almost all of the porosity has been filled by the micritic mud matrix.

DIAGENESIS

Relative timing of events	Authigenic silica overgrowths Calcite cementation Chlorite alteration Dolomite replacement
Relative importance of events	

TEXTURAL MATURITY AND INTERPRETATION

Textural maturity	Immature
Interpretation	

MINERALOGICAL CLASSIFICATION AND COMMENTS

Mineralogical classification	Lithic wacke
Comments	

GSWA No. 154855

Well	VINES-1
Sample number	154855
Sample type	Core
Depth	677.0
Unit	
Facies	Conglomerate
Sample quality	This sample is in good condition.
Brief description	Sedarenite This sample is predominantly composed of cemented sandstone fragments. Carbonate, shale and siltstone fragments are also evident to a lesser degree. Fragments are cemented by a drusy equant calcite cement and massive pore filling calcite. Partial replacement of these grains by dolomite is evident. Visual porosity is poor in this sample.

STRUCTURES

Structures	Massive

TEXTURE

Grain size	Range: Medium silt (0.04mm) to Pebbles (12mm)
Sorting	Poorly-sorted
Grain morphology	Sub-angular to sub-rounded
Sediment fabric	Grains display point to concave/convex and well-sutured grain-grain contacts.

MINERALOGY

Tabulated composition (%)	Detrital components		
	Quartz	Monocrystalline	8
		Polycrystalline	1
	Feldspar	Albite	Tr
		Plagioclase	Tr
	Rock fragments		
		Carbonate	15
		Chert	2
		Kaolinite	3
		Chalcedony	3
		Shale	Tr
		Sandstone	30
		Siltstone	5
		Volcanics	Tr
	Accessories	Zircon	Tr
		Tourmaline	Tr
	Authigenic cement		
		Calcite	8
		Dolomite	3
		Chlorite	5
	Porosity/ Permeability		
		Primary	2
		Secondary	Tr

Detrital components	Quartz Quartz grains range in size from medium sand (0.25mm) to coarse sand (0.6mm) with a mode of medium sand (0.4mm). Grains are angular to sub-rounded and display point to concave/convex and moderately sutured grain-grain contacts. Thin authigenic silica overgrowths are evident on some grains. Overgrowths are defined by a pyritic dust rim. Most quartz grains also contain fluid inclusions or vacuoles. Vacuoles are identified by lines of dark specks that cut across quartz grains. Feldspar Feldspar grains range in size from very fine sand (0.13mm) to coarse sand (0.6mm). Several varieties of feldspar are evident these include microcline, albite and plagioclase. Most of the feldspar grains have undergone partial dissolution or are cracked and have been partially altered. Rock fragments *Carbonate clasts* Carbonate clasts range in size from coarse sand (0.8mm) to pebbles (6mm). The margins of some of the larger grains are coated in a thin micritic rim. Clasts consist of xenotopic texture of anhedral to subhedral shaped very finely to finely crystalline dolomite that displays planar, curved and sutured contacts. In some clasts patchy micritic and ferroan calcite replacement is evident. Most of the micritised clasts consist of equant subhedral to euhedral crystals of microsparite and finer micrite which have replaced the original very fine to fine calcite. Some grains have been cracked and dissolved. One of the fragments has been totally replaced by a planar subhedral matrix of ferroan dolomite. *Ooidal carbonate* Trace ooidal carbonate fragments are evident in this sample. These clasts consist of ooids 0.1 to 0.3mm in size that have been partially recrystallised by a xenotopic matrix of anhedral to subhedral shaped very finely to finely crystalline dolomite that displays planar, curved and sutured contacts. Ooids are micritised making them easily distinguishable from the carbonate host-rock. These fragments have been partially replaced by authigenic cements. *Kaolinite* Kaolinite occurs as sub-rounded to rounded clasts. These clasts consist of coarsely and finely crystalline accumulation of kaolinite. Most of the clasts have undergone partial compaction resulting in their expansion of the kaolinite into intergranular pore space. *Chalcedony* Trace chalcedony fragments are scattered throughout this sample. These fragments range in size from medium (0.2mm) to coarse sand (0.6mm). Grains are generally angular and occasionally are broken and display typical chalcedonic texture comprising of radiating fibrous crystals of varying size. These chalcedonic fragments occasionally have been replaced by a fine microcrystalline chert. *Chert* Chert fragments range in size form medium sand (0.4mm) to pebbles (11mm). Fragments are generally angular to sub-rounded. They are mainly composed of microquartz with patchy megaquartz alteration. Some of the fragments show alteration to chalcedony. Large radiating fibrous crystals are evident replacing the chert.

	Sandstone Sandstone fragments range up to pebble size. These are the most dominant fragments in the sample. They are generally sub-rounded to rounded and composed of fine sand (0.13mm) to medium sand sized (0.2mm) quartz and mica cemented by poikilotopic calcite. Quartz grains are typically well sutured. The degree of calcite cementation is variable between grains. Most fragments have been deformed and squashed into intergranular pore space. *Volcanics* These rock fragments range up to coarse sand to very coarse sand (1.2mm). They are sub-angular and consist of large laths of plagioclase feldspar grains and augite, in a heavily altered cryptocrystalline matrix. Grain boundaries are highly irregular and diffuse and some volcanic grains display minor dissolution and dispersion into intergranular pore space. Most volcanic fragments have been partially altered to a mixture of kaolinite, sericite and chlorite which has destroyed their original fabric and marginally replaced feldspar laths. *Siltstone* These rock fragments are sub-rounded and range in size from fine sand (0.2mm) to granules (3mm). Siltstone fragments are composed of medium silt sized quartz supported in a matrix of illite/sericite. Most fragments have irregularly shaped boundaries as fragments have been squashed and many contain partially corroded margins..
Matrix/ Pseudomatrix	
Authigenic cement	Calcite Calcite cement occurs either partially or totally replacing pore filling anhydrite. Calcite generally occurs as an equant drusy mosaic of very finely to finely crystalline crystals. The cement displays a typical pore-filling characteristic increasing in crystal size towards the pore centre. Chlorite Massive pore filling poikilotopic chlorite cement is evident in this sample. This cement forms sharp contacts with surrounding framework grains. The cement has been partially replaced especially around framework grain boundaries by microsparry calcite and dolomite. Dolomite Dolomite replaces intergranular cements. Large isolated porphyrotopic dolomite crystals are particularly evident replacing chlorite cements.
Porosity/ Permeability	Visual porosity is poor in this sample. Most pore space has been filled by massive chlorite cementation and drusy pore-filling calcite.

DIAGENESIS

Relative timing of events	Chlorite cementation Calcite cementation Dolomitisation
Relative importance of events	

TEXTURAL MATURITY AND INTERPRETATION

Textural maturity	Immature
Interpretation	

MINERALOGICAL CLASSIFICATION AND COMMENTS

Mineralogical classification	Sedarenite
Comments	

GSWA No. 154813

Well	VINES-1
Sample number	154813
Sample type	Core
Depth	675.0
Unit	
Facies	Conglomerate
Sample quality	The sample is in good condition
Brief description	Interbedded quartz arenite and lithic wacke This sample consists predominantly of a quartz-rich lithic wacke in contact with a basal quartz arenite. The contact between the two rock types is sub-horizontal and sharp. The lithic wacke consists of sub-angular to sub-rounded quartz and up to pebble sized rock fragments cemented by poikilotopic and microsparry calcite cements. The quartz arenite consists mainly of well-sutured, fine sand sized quartz grains with minor partially leached and dissolved feldspar. Visual porosity is poor in this sample.

STRUCTURES

Structures	Contact A sharp sub-vertical contact between a well-sutured basal sandstone bed and overlying diamictite is evident. The contact between the two is sharp.

TEXTURE

Grain size	Range: Coarse silt (0.04mm) to pebbles (20mm?) Mode: Fine sand (0.25mm)
Sorting	Sorting is good in the sandstone unit and poor in the diamictite
Grain morphology	Sub-angular to sub-rounded
Sediment fabric	Grains display point to concave/convex and well-sutured grain-grain contacts

MINERALOGY

Tabulated composition (%)	***Diamictite***		
	Detrital components		
	Quartz	Monocrystalline	40
		Polycrystalline	Tr
	Feldspar	Albite	Tr
	Rock Fragments		
		Carbonate	4
		Shale	3
		Chert	2
		Chalcedony	Tr
		Volcanics	1
		Sandstone	2
		Biotite	Tr
		Oncoids	Tr
		Kaolinite	3
		Siltstone	15
	Accessories	Zircon	Tr
		Apatite	Tr
		Tourmaline	Tr
	Authigenic cement		
		Calcite	20
		Pyrite	Tr
		Chlorite	5
		Illite/sericite	5
		Dolomite	Tr

	Porosity/ Permeability		
		Primary	Nil
		Secondary	Tr
	Quartz arenite		
	Detrital components		
	Quartz	Monocrystalline	90
	Feldspar	Albite	1
		Plagioclase	4
	Authigenic cement		
		Silica overgrowths	2
	Porosity/ Permeability		
		Primary	1
		Secondary	Tr
Detrital components	Quartz *Lithic wacke* Quartz grains range in size from coarse silt (0.05mm) to medium sand (0.5mm) with a mode of fine sand (0.25mm). Quartz grains are generally angular to sub-rounded and display point and occasional concave/convex contacts. Marginal replacement of these grains by calcite is evident. Feldspar Heavily leached and vacuolised feldspar grains that have been partially chloritised and seriticised are evident scattered throughout this sample. These grains are of similar size to quartz grains. Rock fragments *Carbonate clasts* Only one carbonate clasts is evident in this sample. This clast is approximately pebble sized (6mm). The clast consists of xenotopic texture of anhedral to subhedral shaped dolomite that displays planar, curved and sutured contacts. Patches of pyrite are evident replacing calcite. The clast contains a thin micritic coating. *Chert and chalcedony* Rare detrital chalcedony fragments are located throughout this sample. These fragments range in size up to coarse sand (0.6mm). Grains are generally angular and occasionally are broken. Grains display typical chalcedonic texture comprising of radiating fibrous crystals of varying size. These chalcedonic fragments occasionally have been replaced by a fine microcrystalline chert. Chert fragments displaying similar grain size to detrital chalcedony are scattered throughout the sample. Crystal size varies within grains from micro- to megaquartz. Some of the grains are heavily leached displaying marginal alteration. *Sandstone* Sandstone fragments range in size from medium sand (0.4mm) to coarse sand (0.7mm). These fragments are typically composed of a mixture of fine sand sized (0.15mm) quartz and trace albite cemented by chloritised clay and calcite. In some fragments only trace cement is evident with quartz grains display concave/convex and well-sutured grain-grain contacts. *Shale* These rock fragments are typically medium to coarse sand sized and angular to sub-angular in shape. Deformation and alteration of these fragments is evident. Some shale fragments have been partially dissolved and dispersed and have been partially altered to kaolinite, sericite and chlorite.		

	Volcanics These rock fragments range up to coarse sand to very coarse sand (1mm). They are sub-angular and consist of large laths of plagioclase feldspar grains in a heavily altered cryptocrystalline matrix. Grain boundaries are highly irregular and diffuse and some volcanic grains display minor dissolution and dispersion into intergranular pore space. Most volcanic fragments have been partially altered to a mixture of kaolinite, sericite and chlorite, which has destroyed their original fabric and replaced feldspar laths. *Siltstone* An irregularly shaped, pebble sized (20mm?) siltstone fragment is evident in this sample. This fragment is vertically oriented. It contains a bimodal quartz grain distribution. The two grain size modes evident are coarse silt (0.5mm) and medium sand sized (0.3mm) quartz. Overall the fragment contains approximately 10% quartz, trace albite, trace augite and approximately 88% calcite cement. Quartz fragments display a minor elongation parallel with the elongate axis of the siltstone fragment. Calcite cement generally forms as single crystal poikilotopes and microsparry accumulations of finely crystalline calcite. The cement forms highly corrosive contacts with surrounding detrital grains. ***Quartz arenite*** Quartz Quartz grains are sub-angular to angular and have a mode of very fine sand (0.26mm). Pressure solution is evident with grains displaying concave/convex to well-sutured grain-grain contacts. Thick authigenic silica overgrowths are evident on most quartz grain boundaries. Feldspar Feldspar grains are of similar size to quartz grains. Most grains are heavily leached and display dissolution on grain boundaries and internal vacuolisation.
Matrix/ Pseudomatrix	
Authigenic cement	Calcite The lithic wacke portion of this slide is calcite cemented. Most calcite cement occurs as single crystal poikilotopes or microsparry accumulations of very finely crystalline calcite that fills intergranular pore space. The cement forms highly corrosive contacts with surrounding detrital grains and partially replaces portions of framework grains. Silica overgrowths Authigenic silica overgrowths are evident on most quartz grain boundaries in the quartz arenite rock type. Contacts between adjacent overgrowths are often irregular compromise boundaries produced by the mutual interference of separate overgrowths.
Porosity/ Permeability	Porosity in this sample is poor. Most of the preserved porosity is evident in the quartz arenite rock type. This porosity is mainly intergranular with minor secondary produced by leaching and dissolution of feldspar grains.

DIAGENESIS

Relative timing of events	Mechanical compaction Authigenic silica growth Carbonate cementation Kaolinite formation Chlorite alteration
Relative importance of events	

TEXTURAL MATURITY AND INTERPRETATION

Textural maturity	Immature
Interpretation	

MINERALOGICAL CLASSIFICATION AND COMMENTS

Mineralogical classification	Interbedded lithic wacke and quartz arenite
Comments	

GSWA No. 154812

Well	VINES-1
Sample number	154812
Sample type	Core
Depth	644.0
Unit	
Facies	Diamictite
Sample quality	Sample is in good condition.
Brief description	Lithic wacke This sample is dominated by carbonate mud. Framework grains include quartz, carbonate clasts and volcanic rock fragments. Visual porosity is negligible.

STRUCTURES

Structures	Massive

TEXTURE

Grain size	Range: Coarse silt (0.04mm) to pebbles (7mm) Mode: Very fine sand (0.07mm)
Sorting	Very-poorly sorted
Grain morphology	Angular to sub-rounded
Sediment fabric	Matrix supported. Grains display occasional point contacts

MINERALOGY

Tabulated composition (%)	Detrital components		
	Quartz	Monocrystalline	10
		Polycrystalline	Tr
	Rock Fragments		
		Carbonate	8
		Shale	1
		Chalcedony	Tr
		Volcanics	15
		Sandstone	Tr
		Lithoclasts	1
		Phosphate	Tr
	Accessories	Zircon	Tr
		Apatite	Tr
		Garnet	Tr
	Matrix/ Pseudomatrix		
		Micrtic mud	63
	Authigenic cement		
		Chlorite	2
		Illite/sericite	Tr
		Haematite	Tr
	Porosity/ Permeability		
		Primary	Nil
		Secondary	Tr

Detrital components	<u>Quartz</u> Quartz grains range in size from coarse silt (0.04mm) to medium sand (0.4mm). Grains are sub-angular to sub-rounded and matrix supported. <u>Rock fragments</u> *Sandstone* Sandstone fragments range up to very coarse sand sized (0.9mm). Fragments are generally sub-rounded and composed of coarse silt sized quartz moderately-sutured mica cemented by microsparry calcite. These fragments have irregular and diffuse margins. *Carbonate* Carbonate clasts range up to granule size. These clasts consist of a xenotopic texture of anhedral to subhedral very finely to finely crystalline dolomite. Patchy alterations to micrite are evident in some clasts. Clasts generally display a sub-angular shape but some grains have been squashed and consequentially are more elongate in shape. *Ooidal limestone* This fragment is pebble sized (6mm) and sub-angular inshape. It is composed of micritised ooids (0.2mm) in diametre. Ooids are surrounded by an equant drusy mosaic of microcrystalline dolomite. Some recrystallised peloids are also evident in these clasts. *Volcanics* *Urtite* These fragments are sub-angular shaped fragment ranging up to granules (3mm) in size. Urtite fragments are generally composed of very coarse sand sized (1mm) nephline flakes that appear brown in plane polarised light. Traces of garnet inclusions and augite are evident in these grains. Minor dissolution and alteration to chlorite is evident. *Amagyoidal basalt* Amagyoidal basalt fragments are typically very coarse sand sized (1.5mm) and sub-angular in shape. These fragments are typically composed of fine calcite and feldspar needles supported by a chlorite and phosphate-rich matrix.
Matrix/ Pseudomatrix	<u>Micritic mud</u> A complex mixture of carbonate mud and illite/sericite forms the matrix of this sample. This mud forms highly corrosive contacts with surrounding grains and in places marginally replaces them.
Authigenic cement	
Porosity/ Permeability	Visual porosity is negligible.

DIAGENESIS

Relative timing of events	Calcite cementation Illite/sericite formation Haematite formation
Relative importance of events	

TEXTURAL MATURITY AND INTERPRETATION

Textural maturity	Immature
Interpretation	

MINERALOGICAL CLASSIFICATION AND COMMENTS

Mineralogical classification	Lithic wacke
Comments	

GSWA No. 154811

Well	VINES-1
Sample number	154811
Sample type	
Depth	617.5
Unit	
Facies	Conglomerate
Sample quality	This sample is in good condition.
Brief description	Sedarenite This sample consists predominantly of carbonate and chert fragments and to lesser extent sandstone, volcanic and dolomite fragments. Carbonate fragments consist of patchy finely and medium crystalline calcite that has been partially micritised and dolomitised. Chert and chalcedony fragments are typically very coarse sand sized and consist of a mixture of micro and megaquartz. This sample is mainly framework supported with most grains displaying only minor compaction. In effect intergranular primary intergranular porosity has been preserved in this sample. Some secondary porosity caused by grain leaching and dissolution is also apparent.

STRUCTURES

Structures	This sample is massive but displays some very minor grain dissolution resulting in stylolitisation between grains is evident.

TEXTURE

Grain size	Range: Medium sand (0.2mm) to pebbles (11mm) Mode: Granules (3mm)
Sorting	Very-poorly sorted
Grain morphology	Angular to sub-rounded
Sediment fabric	Rock fragments display mainly point contacts.

MINERALOGY

Tabulated composition (%)	Detrital components			
	Quartz	Monocrystalline	4	
		Polycrystalline	1	
	Feldspar		1	
	Rock Fragments			
		Carbonate	29	
		Shale	3	
		Chert	17	
		Chalcedony	2	
		Volcanics	10	
		Sandstone	5	
		Lithoclasts	2	
		Phosphate	1	
	Accessories	Zircon	Tr	
		Apatite	Tr	
		Tourmaline	Tr	
		Organic matter	Tr	
	Authigenic cement			
		Calcite	5	
		Pyrite	2	
		Silica overgrowths		Tr
		Chlorite	2	
		Illite/sericite	3	
		Ferroan dolomite	6	
		Siderite	Tr	

	Porosity/ Permeability Primary 5 Secondary 2
Detrital components	Quartz Quartz grains range in size from fine sand (0.13mm) to coarse sand (0.7mm). Quartz mainly occurs as isolated grains but a few accumulations of quartz with triple junctions are evident. Authigenic silica overgrowths occur on most grains. Small siderite accumulations are evident marginally replacing these overgrowths. Feldspar Heavily leached and vacuolised feldspar grains that have been partially chloritised and seriticised are evident scattered throughout this sample. These grains are of similar size to quartz grains. Rock fragments *Carbonate clasts* Carbonate clasts range in size from very coarse sand (1.5mm) to pebbles (11mm) and display diffuse boundaries that contain thin micritic coatings. Clasts consist of xenotopic texture of anhedral to subhedral shaped dolomite that displays planar, curved and sutured contacts. Most clasts could be termed porphyrotopic in that they consist of patches medium crystalline calcite in finely crystalline matrix. Micritisation of some clasts is apparent in this sample. Most of the micritised clasts consist of equant subhedral to euhedral crystals or microsparite. In some clasts patches of finer micrite have replaced the original pseudosparic calcite. Dolmite occurs in varying degrees in all clasts. It occurs as isolated rhombohedral and accumulations replacing original limestone fabric. Trace chert replacement is evident in some carbonate clasts. *Chert and chalcedony* Rare detrital chalcedony fragments are located throughout this sample. These fragments range in size from very coarse sand (1.1mm) to granules (2mm). Grains are generally angular and occasionally are broken. Grains display typical chalcedonic texture comprising of radiating fibrous crystals of varying size. These chalcedonic fragments occasionally have been replaced by a fine microcrystalline chert. Chert fragments displaying similar grain size to detrital chalcedony are scattered throughout the sample. Crystal size varies within grains from micro- to megaquartz. The brownish colouration in some of this chert grains may possibly be the result of Fe staining. *Sandstone* Sandstone fragments range in size from very coarse sand (1.2mm) to granules (3.5mm). These fragments are typically composed of a mixture of fine sand sized (0.15mm) quartz and trace albite cemented by chloritised clay and calcite. In some fragments only trace cement is evident with quartz grains display concave/convex and well-sutured grain-grain contacts. *Shale* These rock fragments are typically medium to coarse sand sized and angular to sub-angular in shape. Deformation and alteration of these fragments is evident. Some shale fragments have been partially seriticised and chloritised. *Lithoclasts* Lithoclasts consist of a mixture of ooids, biclasts and algae that is cemented by a mixture of chert and chlorite. Ooids, bioclasts and algae are undiscernable as they have been recrystallised.

	Volcanic These rock fragments are medium sand sized (0.7mm), sub-angular and consist of small laths of plagioclase feldspar grains contained in a cryptocrystalline matrix. Partial phosphate and chlorite alteration of these fragments is evident. Trace preservation of coaly organic matter is also evident. *Phosphate* Sub-rounded phosphate grains are typically composed of a cryptocrystalline matrix. Grains are occasionally leached and vacuoles have been filled with a mixture of siliceous cement and chlorite.
Matrix/ Pseudomatrix	
Authigenic cement	Calcite Late stage calcite occurs predominantly as a cementing agent in sandstone and chert fragments. Secondary calcite forms typically as small microcrystalline grains. Silica overgrowths Authigenic silica overgrowths are evident on most quartz grain boundaries. In rare cases contacts between adjacent overgrowths are irregular compromise boundaries produced by the mutual interference of individual grain growths. Small siderite grains are evident marginally replacing silica overgrowths on grain margins. Illite/sericte Authigenic illite/sericitic grains are in the form of sub-rounded and squashed grains displaying a similar grain size to quartz grains. These grains have been partially to totally altered to chlorite and have been compacted and deformed. Two possible sources for the illitic/sericitic grains are volcanic clasts and/or detrital clay balls. Ferroan dolomite Ferroan dolomite occurs as isolated rhombs and clasts. Isolated rhombs display varying grains size and may be up to medium sand sized (0.3mm). Clasts consist of a xenotopic mosaic of planar subhedral ferroan dolomite crystals. Dolomite crystal size varies from fine to medium crystalline.
Porosity/ Permeability	Primary intergranular porosity and secondary porosity is good in this sample. The sample is predominantly framework supported and has undergone minor compaction which has resulted in the preservation of original porosity.

DIAGENESIS

Relative timing of events	Calcite formation Neomorphism to micrite Silicification of carbonate to chert Secondary calcitisation Ferroan dolomitisation Chloritisation
Relative importance of events	

TEXTURAL MATURITY AND INTERPRETATION

Textural maturity	Immature
Interpretation	

MINERALOGICAL CLASSIFICATION AND COMMENTS

Mineralogical classification	Sedarenite
Comments	

GSWA No. 154810

Well	VINES-1
Sample number	154810
Sample type	
Depth	608.0
Unit	
Facies	Sandstone
Sample quality	The sample is in good condition.
Brief description	Sedarenite This sample consists of a mixture of subequal carbonate (both limestone and dolomite) and chert. Limestone occurs both as a fine, microsparic matrix that has been partially replaced by chert and as medium to coarse sand sized clasts. These clasts generally consist of a fine pseudospar cement that has often been internally micritised. Illite/sericite and shale clasts which have been partially altered to chlorite are also evident in this sample. Visual porosity in this sample is poor.

STRUCTURES

Structures	Massive

TEXTURE

Grain size	Range: Coarse silt (0.05mm) to very coarse sand (1.8mm) Mode: Fine sand (0.13mm)
Sorting	Very poorly sorted
Grain morphology	Angular to sub-rounded
Sediment fabric	Framework grains display; point, concave/convex and moderately sutured grain-grain contacts.

MINERALOGY

Tabulated composition (%)	Detrital components			
	Quartz	Monocrystalline	11	
		Polycrystalline	2	
	Rock Fragments			
		Carbonate	44	
		Shale	3	
		Chert	2	
		Chalcedony	2	
		Volcanics	4	
	Accessories	Zircon	Tr	
		Apatite	Tr	
		Tourmaline	Tr	
		Chlorite	1	
		Organic matter	Tr	
		Peloids	Tr	
	Authigenic cement			
		Calcite	2	
		Ferroan calcite	1	
		Pyrite	2	
		Silica overgrowths		Tr
		Chlorite	2	
		Illite/sericite	3	
		Chert	15	
		Dolomite	5	
	Porosity/ Permeability			
		Primary	Tr	
		Secondary	Tr	

Detrital components	Quartz Monocrystalline quartz grains range in size from medium sand (0.3mm) to coarse sand (0.6mm) with a mode of medium sand (0.4mm). Grains are sub-angular to rounded, very poorly sorted and display mainly point with occasional concave/convex and moderately sutured grain-grain contacts. Trace polycrystalline quartz grains are also evident. On some quartz grains embayments are evident. Peloids Medium sand sized peloids are evident scattered throughout this sample. These peloids have no preservation of internal structure being heavily micritised. These grains are typically green coloured in plane and cross polarised light. Chlorite Brownish/ green chlorite grains are evident in this sample. These grains are typically medium sand sized (0.4mm) and have been leached and cracked. They also tend to have very diffuse grain margins. Rock fragments *Carbonate* Carbonate in this sample appears patchy as it consists of finer microsparic dolomite matrix and medium sand sized, sub-rounded to rounded carbonate clasts. The carbonate clasts are generally surrounded by a thin micritic rim and are composed of anhedral to subhedral shaped dolomite that displays planar, curved and sutured contacts. The patchiness of this sample indicates that it is neomorphic. Partial micritisation and silicification is evident within the sample. Approximately 15% of the dolomite cement is interpreted to have been replaced by authigenic chert and micritisation of some of the carbonate clasts is also evident. Authigenic chert also displays varying grain size from micro- to megaquartz. Megaquartz replacement tends to occur as patches. Within micritised grains preservation of ghost textures such as peloids are evident. Peloid grain outlines have been preserved by thin micritic envelopes. *Chert and chalcedony* Chert and chalcedony fragments displaying similar grain size to detrital quartz grains are scattered throughout the sample. Chert crystal size varies within grains from micro- to megaquartz. The chalcedony is differentiated from chert grains by its radiating crystal structure. *Volcanic* These rock fragments are medium sand sized (0.7mm), sub-angular and consist of small laths of plagioclase feldspar grains contained in a cryptocrystalline matrix. Partial phosphate and chlorite alteration of these fragments is evident. Trace preservation of coaly organic matter is also evident. *Shale* These rock fragments are typically medium to coarse sand sized and angular to sub-angular in shape. Deformation and alteration of these fragments is evident. Some shale fragments have been partially seriticised and chloritised.
Matrix/ Pseudomatrix	
Authigenic cement	Calcite Late stage calcite cement forms as a cement replacing in part siliceous cements that have replaced original carbonate fabric and intergranular pore space. Secondary calcite forms typically as small microcrystalline grains. Authigenic silica Authigenic silica overgrowths are rare in this sample. Overgrowths tend to be limited to larger quartz grains.

	Illite/sericte Authigenic illite/sericitic grains are in the form of sub-rounded and squashed grains displaying a similar grain size to quartz grains. These grains have been partially to totally altered to chlorite and have been compacted and deformed. Two possible sources for the illitic/sericitic grains are volcanic clasts and/or detrital clay balls. Ferroan calcite Ferroan calcite mainly occurs as a replacement cement. It is predominantly associated with feldspar grains where it partially replaces grains that have been leached and cracked. Ferroan calcite forms highly corrosive contacts with surrounding detrital grains.
Porosity/ Permeability	Visual porosity in this sample is poor. Most of the primary and secondary porosity has been filled by calcite and siliceous cementation.

DIAGENESIS

Relative timing of events	Calcite formation Neomorphism to micrite Silicification of carbonate to chert Secondary calcitisation Chloritisation
Relative importance of events	

TEXTURAL MATURITY AND INTERPRETATION

Textural maturity	Mature
Interpretation	

MINERALOGICAL CLASSIFICATION AND COMMENTS

Mineralogical classification	Sedarenite
Comments	

GSWA No. 154869

Well	VINES-1
Sample number	154869
Sample type	Plug
Depth	598.23
Unit	
Facies	Claystone
Sample quality	The sample is in reasonable condition but has been slightly cracked during thin section manufacture.
Brief description	Lithic wacke This sample is dominated by a matrix of sericite mud cut by irregularly shaped quartz-rich turbidite-like beds. These beds are of varying thickness and orientation and are predominantly composed of partially carbonate cemented very fine sand sized quartz supported in a sericite matrix. Visual porosity in this sample is negligible.

STRUCTURES

Structures	Fining upwards graded laminae Fining upwards beds are irregularly shaped and filled with a mixture of very fine sand sized quartz and partially carbonate cemented illite/sericite mud. These beds can be easily differentiated from the claystone matrix of this sample as the claystone is typically composed of a quartz-free sericitic clay.

TEXTURE

Grain size	Range: Coarse silt (0.05mm) to very fine sand (0.1mm) Mode: Very fine sand (0.07mm)
Sorting	Poorly-sorted
Grain morphology	Sub-angular to sub-rounded
Sediment fabric	Matrix supported

MINERALOGY

Tabulated composition (%)	Detrital components		
	Quartz	Monocrystalline	15
		Muscovite	Tr
	Rock fragments		
		Carbonate	1
		Shale	1
	Matrix/ Pseudomatrix		
		Sericite	80
	Authigenic cements		
		Calcite	3
		Pyrite	Tr
	Porosity/ Permeability		
		Primary	Nil
		Secondary	Nil
Detrital components	Quartz Monocrystalline quartz dominates this sample. Quartz grains range in size from coarse silt (0.05mm) to very fine sand (0.1mm) with a mode of very fine sand (0.07mm). Grains are sub-angular to rounded, poorly-sorted and matrix supported. *Mica* Mica flakes display minor preferential alignment sub-vertical to bedding claystone direction.		

	Rock fragments *Carbonate* Trace medium sand sized (0.2mm) carbonate clasts are evident in this sample. These clasts are generally sub-angular to sub-rounded and have highly corrosive grain boundaries. These clasts are composed of anhedral to subhedral shaped, micro- to medium crystalline dolomite that display planar, curved and sutured contacts. Clasts display varying degrees of dissolution and alteration to carbonate mud.
Matrix/ Pseudomatrix	Sericite This sample is dominated by a partially micritised illite/sericite mud. Carbonate cementation is particularly prevalent in the more quartz-rich areas of the sample.
Authigenic cement	Carbonate Small patches of medium crystalline poikliotopic calcite cement are evident in the quartz-rich beds. This cement fills any intergranular pore space and possibly replaces patches of the sericitic mud. Pyrite Small nodules of pyrite are scattered throughout the sample.
Porosity/ Permeability	Nil

DIAGENESIS

Relative timing of events	Sericitisation Illite formation Carbonate cementation Pyrite formation
Relative importance of events	

TEXTURAL MATURITY AND INTERPRETATION

Textural maturity	Immature
Interpretation	

MINERALOGICAL CLASSIFICATION AND COMMENTS

Mineralogical classification	Lithic wacke
Comments	SEM or XRD on this sample would aid in the identification of matrix material.

GSWA No. 154854

Well	VINES-1
Sample number	154854
Sample type	Core
Depth	559.65
Unit	
Facies	Contact between turbidite and diamictite?
Sample quality	The sample is in good condition.
Brief description	Interbedded Sublitharenite and micritic mudstone This sample consists of a massive siltstone interbedded with a litharenite. The litharenite is composed mainly of poorly-sorted, angular to sub-angular very fine sand sized quartz grains and up to pebble sized carbonate, sandstone, chert, chalcedony and volcanic fragments. All fragments display some form of alteration or grain replacement. The contact between the two rock types is sharp. All of the porosity in this sample is contained within the sublitharenite.

STRUCTURES

Structures	Contact Contact between the turbidite and diamictite sequence is evident. The contact is sharp but irregular.

TEXTURE

Grain size	Range: Coarse silt (0.05mm) to pebbles (10mm) Mode: Very fine sand (0.09mm)
Sorting	Poorly-sorted
Grain morphology	Angular to sub-rounded
Sediment fabric	Grains display point to concave/convex and weakly-sutured grain-grain contacts

MINERALOGY

Tabulated composition (%)	***Sublitharenite***		
	Detrital components		
	Quartz	Monocrystalline	68
	Feldspar	Microcline	Tr
		Albite	Tr
		Plagioclase	Tr
	Rock fragments		
		Carbonate	5
		Chert	5
		Kaolinite	Tr
		Chalcedonic silica	1
		Chalcedony	1
		Shale	1
		Sandstone	3
		Volcanics	5
	Accessories	Zircon	Tr
		Tourmaline	Tr
	Authigenic cement		
		Calcite	3
		Ferroan calcite	1
		Ferroan dolomite	1
		Pyrite	Tr
		Illite/sericite	3
		Chlorite	Tr
	Porosity/ Permeability		
		Primary	2
		Secondary	1

	Micritic mudstone		
	Detrital components		
	Quartz	Monocrystalline	8
		Mica	Tr
	Matrix/Pseudomatrix		
		Micrite	91
	Authigenic cement		
		Pyrite	1
		Micrite	Tr
	Porosity		
		Primary	Nil
		Secondary	Nil
Detrital components	Quartz Quartz grains range in size from coarse silt (0.05mm) to medium sand (0.4mm) with a mode of very fine sand (0.09mm). Grains are angular to sub-rounded and display point to concave/convex and moderately sutured grain-grain contacts. Rock fragments *Carbonate clasts* Carbonate clasts range in size from coarse sand (0.8mm) to pebbles (6mm). The margins of some of the larger grains are coated in a thin micritic rim. Clasts consists of xenotopic texture of anhedral to subhedral shaped very finely to finely crystalline dolomite that displays planar, curved and sutured contacts. In some clasts patchy micritic and ferroan calcite replacement is evident. Most of the micritised clasts consist of equant subhedral to euhedral crystals of microsparite and finer micrite which have replaced the original very fine to fine calcite. Some grains have been cracked and dissolved. One of the fragments has been totally replaced by a planar subhedral matrix of ferroan dolomite. *Ooidal carbonate* Trace ooidal carbonate fragments are evident in this sample. These clasts consist of ooids 0.1 to 0.3mm in size that have been partially recrystallised by a xenotopic matrix of anhedral to subhedral shaped very finely to finely crystalline dolomite that displays planar, curved and sutured contacts. Ooids have a well preserved micritised rim that makes them easily identifiable. Aggrading neomorphism is also apparent in some of these clasts with their centre being replaced by patches of pseudospar. In one of the fragments complete siliceous replacement of the ooids has occurred. *Chalcedony* Trace chalcedony fragments are scattered throughout this sample. These fragments range in size from medium (0.2mm) to coarse sand (0.6mm). Grains are generally angular and occasionally are broken and display typical chalcedonic texture comprising of radiating fibrous crystals of varying size. These chalcedonic fragments occasionally have been replaced by a fine microcrystalline chert. *Chert* Chert fragments range in size from medium sand (0.4mm) to pebbles (11mm). Fragments are generally angular to sub-rounded. They are mainly composed of microquartz with patchy megaquartz alteration. Some of the fragments show alteration to chalcedony. Large radiating fibrous crystals are evident replacing the chert. *Sandstone* Traces of well-cemented sandstone fragments are also evident in this sample. These fragments are typically granular to pebble sized (3-6mm) and angular to sub-angular in shape. They are composed predominantly of well-sutured, coarse		

	silt sized quartz grains and have been partially cemented by a poikilotopic calcite cement. Sandstone fragments have been partially deformed by compactional processes. This has resulted in grain boundaries being difficult to identify. Boundaries are often extremely gradational and have been replaced by the host matrix. *Shale* These rock fragments range from medium sand (0.3mm) to pebble sized (5mm). Grains are sub-angular to sub-rounded in shape. Most shale fragments display some minor chlorite alteration. *Volcanics* These rock fragments range up to coarse sand to very coarse sand (1mm). They are sub-angular and consist of large laths of plagioclase feldspar grains and augite, in a heavily altered cryptocrystalline matrix. Grain boundaries are highly irregular and diffuse and some volcanic grains display minor dissolution and dispersion into intergranular pore space. Most volcanic fragments have been partially altered to a mixture of kaolinite, sericite and chlorite which has destroyed their original fabric and marginally replaced feldspar laths.
Matrix/ Pseudomatrix	Illite/sericite Illite/sericite mainly occurs in the sublitharenite portion of this sample partially filling intergranular pore space. It is the main mineralogical component in the siltstone sequence. It mainly occurs as a massive matrix that displays partial pyrite alteration.
Authigenic cement	Calcite Calcite cement mainly occurs in the sublitharenite portion of this sample as single crystal poikilotopes that replace detrital grains and partially fill intergranular pore space. This cement forms highly corrosive contacts with surrounding detrital grains.
Porosity/ Permeability	Visual porosity is moderate in this sample. All of the porosity observed occurs in the sublitharenite rock type. Most of this porosity is intergranular but some secondary was also observed.

DIAGENESIS

Relative timing of events	Mechanical compaction Calcite cementation Chert replacement Ferroan calcite replacement Ferroan dolomitisation Pyrite formation
Relative importance of events	

TEXTURAL MATURITY AND INTERPRETATION

Textural maturity	Immature
Interpretation	

MINERALOGICAL CLASSIFICATION AND COMMENTS

Mineralogical classification	Interbedded Sublitharenite and micrite mudstone
Comments	

GSWA No. 154808

Well	VINES-1
Sample number	154808
Sample type	Plug
Depth	498.0
Unit	
Facies	Sandstone
Sample quality	The sample is in good condition.
Brief description	Sedarenite This sample is predominantly composed of angular to sub-rounded, medium sand sized quartz grains and to a lesser extent by rock fragments. The main rock fragments evident in this sample are carbonate and siderite clasts, chert, phosphate and volcanics. Framework grains display point to concave/convex and moderately sutured grain-grain contacts. The sample has been partially cemented by fine, microcrystalline calcite cement. Both primary intergranular and secondary porosity is evident in this sample. Secondary porosity is evident where grains have been leached and dissolved.

STRUCTURES

Structures	Massive

TEXTURE

Grain size	Range: Fine sand (0.15mm) to coarse sand (0.9mm) Mode: Medium sand (0.4mm)
Sorting	Moderately-sorted
Grain morphology	Sub-angular to sub-rounded
Sediment fabric	Grains display point to concave/convex and moderately sutured grain-grain contacts.

MINERALOGY

Tabulated composition (%)	Detrital components		
	Quartz	Monocrystalline	65
		Polycrystalline	Tr
	Feldspar	Microcline	Tr
		Albite	3
		Plagioclase	2
	Rock Fragments		
	Carbonate	Calcite	9
		Siderite	2
		Phosphate	1
		Chert	2
		Chalcedony	1
		Volcanics	3
		Kaolinite	1
		Sandstone	Tr
	Accessories	Zircon	Tr
		Tourmaline	Tr
		Spinel	Tr
		Monazite	Tr
		Biotite	Tr
	Authigenic cement		
		Calcite	2
		Ferroan calcite	1
		Pyrite	1

		Silica overgrowths	Tr
		Chlorite	Tr
		Illite/sericite	2
	Porosity/ Permeability		
		Primary	3
		Secondary	2
Detrital components	Quartz Monocrystalline quartz dominates this sample. Quartz grains range in size from fine sand (0.15mm) to coarse sand (0.6mm) with a mode of medium sand (0.4mm). Grains are sub-angular to rounded, well-sorted and display mainly point with occasional concave/convex and moderately sutured grain-grain contacts. Trace polycrystalline quartz grains are also evident. Feldspar Feldspar grains range in size from fine (0.13mm) to medium sand (0.4mm). Several varieties of feldspar are evident these include microcline, albite and plagioclase. The degree of preservation of feldspar grains in the sample varies. Smaller grains are typically unaltered while larger grains have been leached and partially replaced by calcite and chlorite cements. Biotite/chlorite Brownish biotite grains are evident in this sample. These grains are typically medium sand sized (0.4mm) and have been leached and cracked and have undergone partial alteration to chlorite. Authigenic chlorite is particularly evident forming in cracks that have developed in the grain. Rock Fragments *Chert and chalcedony* Chert and chalcedony fragments displaying similar grain size to detrital quartz grains are scattered throughout the sample. Chert crystal size varies within grains from micro- to megaquartz. The chalcedony is differentiated from chert grains by its radiating crystal structure. *Carbonate clasts* Sub-rounded to rounded carbonate clasts are scattered throughout this sample. Carbonate clasts are typically medium sand sized. These clasts are composed of anhedral to subhedral shaped, microcrystalline calcite that display planar, curved and sutured contacts. *Siderite* Smaller, fine sand to medium sand sized siderite clasts are also evident in this sample. These clasts have highly corrosive boundaries and are interpreted as having formed form the alteration of microcrystalline calcite. *Phosphate* Phosphate sediments in this sample are typically brownish-grey clasts of isotropic collophane. Bone fragments can be identified by their characteristic cross-fibrous texture. *Kaolinitic clasts* Kaolinitic clasts occur as sub-rounded grains that have been partially seriticised. Grain margins tend to be soft and grains have been occasionally deformed and squashed into pore space. *Volcanic* These rock fragments are medium sand sized (0.4mm), sub-angular and consist of small laths of plagioclase feldspar grains contained in a cryptocrystalline matrix.		

	The final type of volcanic rock fragment consists of a indiscernible cryptocrystalline matrix. These grains are also display a grain size from medium sand (0.4mm) to coarse sand (0.6mm) and are typically well rounded. *Sandstone* Traces of irregularly shaped sandstone clasts are evident in this sample. These clasts are composed of fine sand sized, sub-rounded quartz grains and clay. Monazite Trace, well rounded, fine sand sized monzonite grains are located within clay-rich laminae. These grains are clear under plane polarised light but display high birefringence colours under cross-polars.
Matrix/ Pseudomatrix	
Authigenic cement	Calcite Most calcite occurs as patchy, microcrysatalline cement that fills intergranular pore space and appears to replace portions of quartz grains and overgrowths. Authigenic silica Authigenic silica overgrowths are apparent on some quartz grains but their extent is limited by the growth thin isopachous chlorite rims on most grains. Illite/sericte Authigenic illite/sericite grains are in the form of sub-rounded and squashed grains displaying a similar grain size to quartz grains. These grains are partially altered and have been compacted into the intergranular pore space where it forms patches encasing clusters of framework grains. Two possible sources for the illitic/sericitic grains are volcanic clasts and/or detrital clay balls. Ferroan calcite Ferroan calcite mainly occurs as a replacement fragment. It is predominantly associated with feldspar grains where it partially replaces grains that have been leached and cracked. Ferroan calcite forms highly corrosive contacts with surrounding detrital grains. Chlorite Chlorite crystals mainly form normal to grain surfaces as isopachous rims on detrital grains. It is also evident partially replacing leached and cracked detrital grains.
Porosity/ Permeability	Primary intergranular porosity is not as prevalent in this sample. Most of the primary porosity has been filled

DIAGENESIS

Relative timing of events	Formation of thin isopachous chlorite rims Calcite formation Ferroan calcite formation Chlorite replacement Pyrite Formation
Relative importance of events	

TEXTURAL MATURITY AND INTERPRETATION

Textural maturity	Immature
Interpretation	

MINERALOGICAL CLASSIFICATION AND COMMENTS

Mineralogical classification	Sedarenite
Comments	

GSWA No. 154807

Well	VINES-1
Sample number	154807
Sample type	
Depth	490.05
Unit	
Facies	Diamictite
Sample quality	The sample is in good condition.
Brief description	Sedarenite This sample consists of a mixture of sub-angular to sub-rounded, coarse silt sized quartz and up to pebble sized volcanic, chert, chalcedony, sandstone, shale and kaolinite fragments. All framework grains have been cemented by a microsparry calcite cement. This cement only partially fills intergranular pore space. Visual porosity is good.

STRUCTURES

Structures	Massive

TEXTURE

Grain size	Range: Coarse silt (0.05mm) to pebbles (6mm) Mode: Bimodal→ Quartz is coarse silt sized (0.07mm) and rock fragments are granule sized (3-4mm)
Sorting	Poorly sorted
Grain morphology	Sub-angular to sub-rounded
Sediment fabric	Grains display predominantly point contacts but occasional concave/convex grain-grain contacts are evident.

MINERALOGY

Tabulated composition (%)	Detrital components		
	Quartz	Monocrystalline	40
		Polycrystalline	Tr
	Feldspar	Microcline	Tr
		Albite	Tr
		Plagioclase	1
	Rock Fragments		
		Carbonate	3
		Phosphate	Tr
		Shale	1
		Volcanics	6
		Sandstone	5
		Siltstone	1
		Glaucophane	Tr
		Organics	Tr
		Glauconite	Tr
	Accessories	Zircon	Tr
		Tourmaline	Tr
		Spinel	Tr
	Authigenic cement		
		Calcite/ Dolomite	39
	Porosity/ Permeability		
		Primary	4
		Secondary	1

Detrital components	Quartz Monocrystalline quartz dominates this sample. Quartz grains range in size from coarse silt (0.05mm) to coarse sand (1.4mm) size with a mode of coarse silt (0.05mm). Grains are sub-angular to rounded, well-sorted and display mainly point with occasional concave/convex and moderately sutured grain-grain contacts. A thin isopachous chlorite rim is evident on some grains. Feldspar Feldspar grains range in size from fine (0.13mm) to medium sand (0.4mm). Several varieties of feldspar are evident these include microcline, albite and plagioclase. Some grains have been cracked and partially dissolved and display alteration to non-ferroan or ferroan calcite. Rock fragments *Shale* These rock fragments range up to coarse sand (0.6mm) in size. Shale fragments are generally sub-angular in shape. Fragments consist predominantly of sericitic clay. Some of these grains have been partially leached resulting in the formation of some secondary porosity. Dolomite and pyrite replacement is evident in some fragments. *Volcanics* These rock fragments range up to very coarse sand (1.2mm), sub-angular and consist of a mixture of leached and partially altered feldspar laths and augite, undifferentiated black cryptocrystalline matrix and with patchy illite/sericite and chlorite alteration. Most of these grains have been partially dissolved, dispersed and altered. *Carbonate* Sub-rounded to rounded carbonate clasts are scattered throughout this sample. Carbonate clasts range up to granule size (3mm). These clasts are composed of patchy anhedral to subhedral shaped, very finely to finely crystalline calcite that display planar, curved and sutured contacts. Micritic alteration is evident in some of these clasts. Most of the micritised clasts consist of equant subhedral to euhedral calcite crystals of microsparite and finer, micrite which have replaced the original very fine to fine calcite. Dolomite and chert replacement of some of these clasts is evident. *Sandstone* Sandstone fragments range up to granule size (3mm). They are generally-angular to sub-rounded and composed of up to 94% moderately sutured, coarse silt sized (0.05mm) quartz grains, 1% mica, 5% poikilotopic calcite cement and traces of augite, siderite and pyrite. Advanced pressure solution is evident with grains displaying well-sutured grain-grain contacts. Within the fragment calcite cement encases clusters of framework grains and fills intergranular pore space. Fragment margins have been partially overgrown by calcite cements giving some grain edges a corrosive appearance. *Siltstone* Siltstone fragments are typically angular to sub-angular in shape. They consist of very fine sand (0.12mm), and mica supported by an illite/sericite matrix. Most siltstone fragments are broken and have expanded into intergranular pore space.
Matrix/ Pseudomatrix	
Authigenic cement	Calcite/Dolomite This sample is partially cemented by calcite and dolomite. Microsparry calcite cement fills intergranular pore space and marginally replaces framework grains. Most of this cement has formed on detrital grain margins and is gradually filling

	intergranular pore space. It has not completely replaced most intergranular pore space, hence the good preservation of porosity. Traces of isolated dolomite rhombs are evident replacing some calcite cements.
Porosity/ Permeability	Porosity is good in this sample. Most of the porosity is preserved intergranular porosity but some secondary porosity developed by the leaching of volcanics and feldspar grains is also evident. Porosity has been preserved as calcite cements have not totally replaced the intergranular pore space.

DIAGENESIS

Relative timing of events	Mechanical compaction Illite/sericite alteration Calcite cementation Pyrite formation
Relative importance of events	

TEXTURAL MATURITY AND INTERPRETATION

Textural maturity	Immature
Interpretation	

MINERALOGICAL CLASSIFICATION AND COMMENTS

Mineralogical classification	Sedarenite
Comments	

GSWA No. 154806

Well	VINES-1
Sample number	154806
Sample type	Plug
Depth	440.05
Unit	
Facies	Sandstone
Sample quality	The sample is in good condition.
Brief description	Sedarenite This sample is predominantly composed of angular to sub-rounded, fine sand sized quartz grains and to a lesser extent by rock fragments. The main rock fragments evident in this sample are carbonate clasts, chert, phosphate and volcanics. Framework grains display point to concave/convex and moderately sutured grain-grain contacts. Minor poikilotopic calcite cementation of detrital grains is evident in this sample. Authigenic silica growth has been limited by thin isopachous chlorite rims on detrital grains. These rims have aided the preservation of primary intergranular porosity in this sample.

STRUCTURES

Structures	Massive

TEXTURE

Grain size	Range: Very fine sand (0.07mm) to coarse sand (1.4mm) Mode: Fine sand (0.14mm)
Sorting	Moderately-sorted
Grain morphology	Angular to sub-rounded
Sediment fabric	Grains display point to concave/convex and moderately sutured grain-grain contacts.

MINERALOGY

Tabulated composition (%)	Detrital components		
	Quartz	Monocrystalline	73
		Polycrystalline	Tr
	Feldspar	Microcline	1
		Albite	2
		Plagioclase	Tr
	Rock Fragments		
		Carbonate	5
		Phosphate	2
		Chert	1
		Volcanics	1
	Accessories	Zircon	Tr
		Tourmaline	Tr
		Spinel	Tr
		Monazite	Tr
	Authigenic cement		
		Calcite	5
		Ferroan calcite	1
		Pyrite	2
		Silica overgrowths	Tr
		Chlorite	1
		Illite/sericite	3
	Porosity/ Permeability		
		Primary	2
		Secondary	1

Detrital components	Quartz Monocrystalline quartz dominates this sample. Quartz grains range in size from very fine sand (0.07mm) to coarse sand (1.4mm) with a mode of fine sand (0.14mm). Grains are sub-angular to rounded, well-sorted and display mainly point with occasional concave/convex and moderately sutured grain-grain contacts. Trace polycrystalline quartz grains are also evident. A thin chlorite coating is evident on most grains. Feldspar Feldspar grains range in size from fine (0.13mm) to medium sand (0.4mm). Several varieties of feldspar are evident these include microcline, albite and plagioclase. The degree of preservation of feldspar grains in the sample varies. Some grains remain intact while others have been leached and partially replaced by ferroan calcite. Authigenic chlorite growth is also evident along cracks that have formed in these grains. Biotite/chlorite Brownish biotite grains are evident in this sample. These grains are typically medium sand sized (0.4mm) and have been leached and cracked and have undergone partial alteration to chlorite. Authigenic chlorite is particularly evident forming in cracks that have developed in the grain. Rock Fragments *Chert* Chert fragments displaying similar grain size to detrital quartz grains are scattered throughout the sample. Chert crystal size varies within grains from micro- to megaquartz. *Carbonate clasts* Sub-rounded to rounded carbonate clasts are scattered throughout this sample. Carbonate clasts are typically medium sand sized. These clasts are composed of anhedral to subhedral shaped, microcrystalline dolomite that displays planar, curved and sutured contacts. Some of the larger carbonate clasts have been subjected to compactional deformation and as a result have been partially squashed and elongated. *Phosphate* Phosphate sediments in this sample are typically brownish-grey clasts of isotropic collophane. Bone fragments can be identified by their characteristic cross-fibrous texture. *Volcanic* A variety of rock fragments are evident in this sample. The most common volcanic rock fragments are igneous in origin. These rock fragments are medium sand sized (0.4mm) , well rounded and consist of small laths of plagioclase feldspar grains contained in a finely crystalline matrix. Heavy leaching causing vacuolisation has resulted in the partial replacement of these grains by ferroan calcite and the development of secondary porosity. The final type of volcanic rock fragment consists of a indiscernible cryptocrystalline matrix. These grains are also display a grain size from medium sand (0.4mm) to coarse sand (0.6mm) and are typically well rounded. Monazite Trace, well rounded, fine sand sized monazite grains are located within clay-rich laminae. These grains are clear under plane polarised light but display high birefringence colours under cross-polars.
Matrix/ Pseudomatrix	

Authigenic cement	Calcite Most calcite occurs as patchy, single crystal poikilotopic cement that fills intergranular pore space and encases clusters of framework grains. Partial replacement of grains with no clay coatings by calcite is evident. Authigenic silica Authigenic silica overgrowths are apparent on some quartz grains. These overgrowths are mostly evident on grains that do not contain isopachous rims. Illite/sericte Authigenic illite/sericitic grains are in the form of sub-rounded and squashed grains displaying a similar grain size to quartz grains. These grains are partially altered and have been compacted into the intergranular pore space where it forms patches encasing clusters of framework grains. Two possible sources for the illitic/sericitic grains are volcanic clasts and/or detrital clay balls. Ferroan calcite Ferroan calcite mainly occurs as a replacement cement. It is predominantly associated with feldspar grains where it partially replaces grains that have been leached and cracked. Ferroan calcite forms highly corrosive contacts with surrounding detrital grains. Chlorite Chlorite crystals mainly form normal to grain surfaces as isopachous rims on detrital grains. It is also evident partially replacing leached and cracked detrital grains.
Porosity/ Permeability	Primary intergranular porosity has been filled by patchy poikilotopic calcite. The preservation of some intergranular porosity may be due to isopachous rims on detrital grains that have heeded the development of authigenic silica overgrowths. Some secondary porosity is also evident caused by the dissolution of detrital grains.

DIAGENESIS

Relative timing of events	Formation of thin isopachous chlorite rims Calcite formation Ferroan calcite formation Chlorite replacement Pyrite formation
Relative importance of events	The formation of isopachous chlorite rims on grains has preserved some of the primary intergranular porosity in this sample.

TEXTURAL MATURITY AND INTERPRETATION

Textural maturity	Immature
Interpretation	

MINERALOGICAL CLASSIFICATION AND COMMENTS

Mineralogical classification	Sedarenite
Comments	

GSWA No. 154852

Well	VINES-1
Sample number	154852
Sample type	Core
Depth	420.1
Unit	
Facies	Sandstone
Sample quality	The sample is in good condition
Brief description	Litharenite This sample consists predominantly of sub-angular to sub-rounded, fine sand quartz grains and carbonate, shale and sandstone rock fragments. The sample is cut by several thin, sub-horizontal, illite-sericite seams. Minor poikilotopic calcite cementation of detrital grains and rock fragments is evident in this sample. Visual porosity is good.

STRUCTURES

Structures	Solution seams This is cut by a series of sub-horizontal, illite/sericite filled solution seams. The seams are irregular, discontinuous and very dispersive in parts. Seams are approximately 0.2mm thick. Their dark colouration can be attributed to insoluble organic compounds and pyrite mixing in with illite/sericite.

TEXTURE

Grain size	Range: Coarse silt (0.05mm) to coarse sand (1mm) Mode: Fine sand (0.2mm)
Sorting	Well-sorted
Grain morphology	Sub-angular to sub-rounded
Sediment fabric	Grains display point to concave/convex and weakly sutured grain-grain contacts.

MINERALOGY

Tabulated composition (%)	Detrital components		
	Quartz	Monocrystalline	72
		Polycrystalline	1
	Feldspar	Microcline	Tr
		Albite	1
		Plagioclase	2
	Rock fragments		
		Carbonate	2
		Chert	Tr
		Kaolinite	1
		Chalcedony	Tr
		Shale	3
		Sandstone	2
		Volcanics	4
	Accessories	Zircon	Tr
		Tourmaline	Tr
		Spinel	Tr
	Authigenic cement		
		Silica overgrowths	1
		Anhydrite	Tr
		Calcite	2
		Pyrite	1
		Illite/sericite	3
		Chlorite	Tr

	Porosity/ Permeability Primary 5 Secondary 1
Detrital components	Quartz Quartz ranges from coarse silt (0.05mm) to coarse sand (0.6mm) with a mode of fine sand (0.2mm). Grains are sub-angular to sub-rounded and generally well sorted. Some grains display thick authigenic silica overgrowths. Grains that do not display authigenic overgrowths are generally have a thin illite/sercite isopachous coating. Fluid inclusions or vacuoles are evident on most quartz grains. Vacuoles are identified by lines of dark specks that cut across quartz grains. Feldspar Feldspar grains range from fine sand sized (0.12mm) to medium sand sized (0.4mm). Several varieties of feldspar are evident these include microcline, albite and plagioclase. Some grains have undergone partial leaching resulting in vacuolisation and alteration to kaolinite or partial calcite cementation. Rock fragments *Carbonate clasts* Carbonate clasts are approximately medium sand sized. These clasts are generally sub- to well rounded and composed of xenotopic matrix of anhedral to subhedral shaped very finely to finely crystalline dolomite that display planar, curved and sutured contacts. Micritic alteration is evident in most of these clasts. Micritised clasts consist of equant subhedral to euhedral calcite crystals of microsparite and finer, micrite which have replaced the original very fine to fine calcite. *Chert* Chert grains are composed of microcrystalline quartz are scattered throughout the sample. These fragments are typically sub-angular to sub-rounded. *Chalcedony* Rare detrital chalcedony fragments are located throughout this sample. These fragments are approximately fine sand sized (0.2mm). Grains are generally sub-rounded and display typical chalcedonic texture comprising of radiating fibrous crystals of varying size. *Shale* These rock fragments are typically medium to coarse sand sized and angular to sub-angular in shape. They are composed of predominantly illite/sericite clay and mica. Mica flakes display a strong preferential orientation parallel with the elongate axis of the shale fragment. *Kaolinite* Kaolinite occurs as sub-rounded to rounded clasts. These clasts consist of coarsely and finely crystalline accumulations of kaolinite. Most of the clasts have undergone partial compaction resulting in their expansion of the kaolinite into intergranular pore space. Compaction of these grains has resulted in them flowing around adjacent framework grains and into intergranular pore space. Dissolution and alteration of these clasts to kaolinite is evident. *Sandstone* Sandstone fragments range up to coarse sand (0.6mm) in size. They are generally angular to sub-rounded and composed of up to 94% moderately sutured, coarse silt sized (0.05mm) quartz grains, 1% mica and 5% poikilotopic calcite cement that has been partially replaced by dolomite. Advanced pressure solution is evident with grains displaying well-sutured grain-grain contacts. Within the fragment calcite cement encases clusters of framework grains and fills intergranular pore space.

	Volcanics These rock fragments range up to coarse sand to very coarse sand (1mm). They are sub-angular and consist of large laths of plagioclase feldspar grains in a heavily altered cryptocrystalline matrix. Grain boundaries are highly irregular and diffuse and some volcanic grains display minor dissolution and dispersion into intergranular pore space. Most volcanic fragments have been partially altered to a mixture of kaolinite, sericite and chlorite which has destroyed their original fabric and replaced feldspar laths.
Matrix/ Pseudomatrix	
Authigenic cement	Silica overgrowths Authigenic silica overgrowths are evident on most quartz grain boundaries. Contacts between adjacent overgrowths are irregular compromise boundaries produced by the mutual interference of individual overgrowths. Trace inclusions are evident on original quartz grain boundaries below authigenic silica overgrowths. Calcite Calcite cement occurs in this sample as mainly as single crystal poikilotopes that replace detrital grains and partially fill intergranular pore space. This cement forms highly corrosive contacts with surrounding detrital grains. Illite/sercite Illite/sericite is mainly concentrated in the thin sub-horizontal solution seams but it is also found dispersed amongst the host rock where it partially fills intergranular pore space and coats detrital grains. Anhydrite Only traces of anhydrite are evident in this sample. The cement mainly occurs replacing leached and dissolved detrital grains.
Porosity/ Permeability	Visual porosity is good in this sample. Minimal cementation and filling of pore space has resulted in a high percentage of the intergranular porosity being preserved.

DIAGENESIS

Relative timing of events	Silica overgrowths Anhydrite cementation Calcite cementation Pyrite formation
Relative importance of events	

TEXTURAL MATURITY AND INTERPRETATION

Textural maturity	Mature
Interpretation	

MINERALOGICAL CLASSIFICATION AND COMMENTS

Mineralogical classification	Litharenite
Comments	

GSWA No. 154851

Well	VINES-1
Sample number	154851
Sample type	Core
Depth	360.2
Unit	
Facies	Rhythmites
Sample quality	The sample is in good condition
Brief description	Lithic Wacke This sample is matrix dominated consisting predominantly of illite/sericite with patchy calcite cementation and chlorite alteration. Quartz grains are typically sub-angular to sub-rounded and medium sand sized. Other constituents include medium sand sized to pebble sized carbonate, siltstone, sandstone and volcanic rock fragments. Visual porosity is poor.

STRUCTURES

Structures	Massive

TEXTURE

Grain size	Range: Coarse silt (0.04mm) to pebbles (6mm) Mode: Very coarse sand (0.7mm)
Sorting	Poorly-sorted
Grain morphology	Angular to sub-rounded
Sediment fabric	Matrix supported but grains display rare point contacts.

MINERALOGY

Tabulated composition (%)	Detrital components		
	Quartz	Monocrystalline	15
		Polycrystalline	Tr
	Feldspar	Albite	Tr
	Rock Fragments	Chert	2
		Sandstone	4
		Chalcedony	4
		Carbonate	5
		Volcanics	4
		Glaucophane	Tr
		Shale	3
	Accessories	Zircon	Tr
		Tourmaline	Tr
	Matrix/Pseudomatrix		
		Carbonate mud	62
	Porosity/ Permeability		
		Primary	1
		Secondary	Tr

Detrital components	Quartz Quartz ranges from coarse silt (0.04mm) coarse sand (0.6mm) with a mode of medium sand (0.5mm). Grains are angular to sub-rounded and are matrix supported. Occasional point contacts are evident between some grains and almost all grains are coated in a thin isopachous clay rim. Feldspar Feldspar grains range in size from very fine sand (0.13mm) to coarse sand (0.6mm). Several varieties of feldspar are evident these include microcline, albite and plagioclase. Most of the feldspar grains have undergone partial dissolution or are cracked and have been partially altered. Rock fragments *Shale* These rock fragments range up to very coarse sand (1.5mm) in size. Shale fragments are generally sub-angular in shape. Fragments consist predominantly of a dark brown illite/sericite clay. Minor chlorite alteration is evident in grains that display some dispersion. *Volcanics* These rock fragments range up to pebbles, sub-angular and consist of a mixture of leached and partially altered feldspar laths and augite, undifferentiated black cryptocrystalline matrix and with patchy illite/sericite and chlorite alteration. The other type of volcanic rock fragment that is abundant in this sample is composed predominantly of small needle shaped fragments in a mixed illite/sericite and black cryptocrystalline matrix. *Carbonate* Sub-rounded to rounded carbonate clasts are scattered throughout this sample. Carbonate clasts range up to granule size (3mm). These clasts are composed of patchy anhedral to subhedral shaped, very finely to finely crystalline dolomite that display planar, curved and sutured contacts. Micritic alteration is evident in some of these clasts. Most of the micritised clasts consist of equant subhedral to euhedral calcite crystals of microsparite and finer, micrite which have replaced the original very fine to fine dolomite. Chert replacement of some of these clasts is evident. *Chert* Chert fragments range in size from medium to coarse sand size. These fragments are typically sub-angular to sub-rounded and consist of a patchy mixture of macro and microquartz. *Chalcedony* Traces of chalcedony are scattered throughout this sample. These fragments are approximately coarse sand sized (0.7mm). Grains are generally angular and occasionally are broken. These fragments display typical chalcedonic texture comprising of radiating fibrous crystals of varying size. Some chalcedonic fragments display alteration to chert. *Sandstone* Sandstone fragments range up to granule size (3mm). They are generally-angular to sub-rounded and composed of up to 94% moderately sutured, coarse silt sized (0.05mm) quartz grains, 1% mica, 5% poikilotopic calcite cement and traces of spinel, siderite and pyrite. Advanced pressure solution is evident with grains displaying well-sutured grain-grain contacts. Within the fragment calcite cement encases clusters of framework grains and fills intergranular pore space.

	Phosphate Phosphate sediments in this sample are typically brownish-grey clasts of isotropic collophane. Bone fragments can be identified by their characteristic cross-fibrous texture.
Matrix/ Pseudomatrix	Illite/sericite This sample is mainly supported by a matrix of illite/sericite that fills intergranular pore space and encases framework grains. Patchy replacement of the matrix by chlorite and microcrystalline calcite cements is evident.
Authigenic cement	
Porosity/ Permeability	Visual porosity is poor in this sample. The porosity that is existent forms mainly by leaching of the matrix and a small amount of it occurs within rock fragments.

DIAGENESIS

Relative timing of events	Illite/sericite Calcite cementation Micritisation Pyrite formation
Relative importance of events	

TEXTURAL MATURITY AND INTERPRETATION

Textural maturity	Immature
Interpretation	

MINERALOGICAL CLASSIFICATION AND COMMENTS

Mineralogical classification	Lithic wacke
Comments	

GSWA No. 154850

Well	VINES-1
Sample number	154850
Sample type	Core
Depth	343.44
Unit	
Facies	Sandstone
Sample quality	The sample is in good condition
Brief description	Structurally contorted lithic wacke and siltstone This sample consist predominantly of a lithic wacke composed of illite/ sericite supported angular to sub-rounded, very fine sand sized quartz grains. Minor volcanic, carbonate, chert, shale and siltstone fragments are also evident in this rock type. A 4-10mm siltstone filled structure occurs cutting sub-vertically through the lithic wacke. This structure is interpreted to be a rapidly deposited sediment flow into a dilated micro-fault or fracture. The siltstone that fills this structure is composed predominantly of a massive sericite clay scattered with minor medium silt sized quartz grains. Almost all of the porosity is interpreted to be secondary in this sample.

STRUCTURES

Structures	Deformation A 4mm to 10mm thick sub-vertical, siltstone filled structure is evident in this slide. The lack of layering in the siltstone suggests that it was deposited rapidly. A sharp contact is evident between the structure and the lithic wacke host rock. A possible explanation for this structure is that it represents a dilated micro-fault or fracture that has been filled rapidly by a siltstone flow. The isolated angular fragment of lithic wacke host rock in the midst of the siltstone may have broken away from the host rock and been redeposited. It is important to note however that there is a possibility that this sample represents a contact between the two rock types as there are conflicting orientations of arrows on the thin-section and stub.

TEXTURE

Grain size	Range: Coarse silt (0.05mm) to very coarse sand (2mm) Mode: Very fine sand (0.08mm)
Sorting	Poorly-sorted
Grain morphology	Angular to sub-rounded
Sediment fabric	Sample is predominantly matrix supported but there are rare point contacts between grains.

MINERALOGY

Tabulated composition (%)	Detrital components		
	Quartz	Monocrystalline	39
		Polycrystalline	1
	Feldspar	Microcline	Tr
		Albite	2
		Plagioclase	1
		Muscovite	Tr
		Glauconite	Tr
		Barite	Tr
	Rock fragments		
		Carbonate	3
		Chert	Tr

		Volcanics	1
		Siltstone	2
		Shale	3
		Phosphate	1
	Accessories		
		Tourmaline	Tr
		Zircon	Tr
	Matrix/ Pseudomatrix		
		Illite/sericite	42
	Authigenic cement		
		Calcite	3
		Pyrite	1
	Porosity/ Permeability		
		Primary	Tr
		Secondary	1
Detrital components	Quartz Quartz ranges from coarse silt (0.05mm) to very coarse sand (2mm) with a mode of very fine sand (0.08mm). Grains are angular to sub-rounded and are matrix supported. Occasional point contacts are evident between some grains and almost all grains are coated in a thin isopachous clay rim. Feldspar Feldspar grains range in size from very fine sand (0.13mm) to coarse sand (0.6mm). Several varieties of feldspar are evident these include microcline, albite and plagioclase. Most of the feldspar grains have undergone partial dissolution or are cracked and have been partial altered to sericite or chlorite. Rock fragments *Shale* These rock fragments are sub-rounded and range in size from medium sand (0.3mm) to very coarse sand (1.4mm). Shale fragments are generally sub-angular to tabular is shape. Most of these fragments display partial leaching and alteration to kaolinite, sericite and chlorite. *Siltstone* These rock fragments are sub-rounded and range in size from fine sand (0.2mm) to very coarse sand (1.4mm). These fragments are heavily altered to illite/sericite and chlorite clays which have been partially replaced by pyrite mineralisation. *Volcanics* These rock fragments range up to very coarse sand (1.2mm), sub-angular and consist of a mixture of leached and partially altered feldspar laths, undifferentiated black cryptocrystalline matrix, augite and chlorite. *Carbonate* Sub-rounded to rounded carbonate clasts are scattered throughout this sample. Carbonate clasts are typically medium sand sized. These clasts are composed of patchy anhedral to subhedral shaped, very finely to finely crystalline dolomite that display planar, curved and sutured contacts. These grain display highly corrosive contacts with surrounding detrital grains. Rare dolomite replacement is evident. *Phosphate* Sub-rounded phosphate grains are typically composed of a cryptocrystalline matrix. Grains are occasionally leached and vacuoles have been filled with a mixture of siliceous cement and chlorite.		

	Chert Chert fragments range in size from medium to coarse sand size. These fragments are typically sub-angular to sub-rounded and consist of a mixture of macro and microquartz. *Chalcedony* Traces of chalcedony are scattered throughout this sample. These fragments are approximately medium sand sized (0.4mm). Grains are generally angular and occasionally are broken and display typical chalcedonic texture comprising radiating fibrous crystals of varying size.
Matrix/ Pseudomatrix	Sericite *Siltstone* Sericite clays form approximately 95% of this rock type. Patchy illitisation and possible alteration to chlorite is also apparent. *Lithic wacke* Illite/sericite occurs as pore filling matrix material in this rock type.
Authigenic cement	Calcite Calcite occurs as coarsely crystalline, poikilotopic grains replacing portions of the illite/sericite matrix and leached grains in the lithic wacke portion of the slide.
Porosity/ Permeability	Most of the porosity is secondary formed by the complete or partial dissolution of detrital grains and possible grain plucking during thin section manufacture.

DIAGENESIS

Relative timing of events	Illite/sericite formation Kaolinite replacement Chloritisation Calcite replacement Pyrite formation
Relative importance of events	

TEXTURAL MATURITY AND INTERPRETATION

Textural maturity	Immature
Interpretation	

MINERALOGICAL CLASSIFICATION AND COMMENTS

Mineralogical classification	85% Lithic wacke 15% Siltstone
Comments	

GSWA No. 154804

Well	VINES-1
Sample number	154804
Sample type	Plug
Depth	327.0
Unit	
Facies	Sandstone
Sample quality	The sample is in good condition.
Brief description	Feldspathic litharenite This sample is dominated by medium grained, sub-rounded to rounded quartz grains and to a lesser extent by feldspar and volcanics. Thin laminae defined by increased clay content cut sub-horizontally across this sample. Although illite/sericite, patchy poikilotopic calcite and ferroan calcite has replaced some of the porosity, primary and secondary visual porosity is still good.

STRUCTURES

Structures	Laminae Thin, discontinuous, sub-horizontal laminae cut across this sample. These laminae are typically 1-2mm thick and defined by a dark colouration caused by an increase in clay content.

TEXTURE

Grain size	Range: Very fine sand (0.1mm) to medium sand (0.45mm) Mode: Medium sand (0.3mm)
Sorting	Well-sorted
Grain morphology	Sub-angular to rounded
Sediment fabric	Detrital grains display predominantly point, with occasional concave/convex grain-grain contacts.

MINERALOGY

Tabulated composition (%)	Detrital components		
	Quartz	Monocrystalline	61
		Polycrystalline	1
	Feldspar	Microcline	2
		Albite	3
		Plagioclase	1
		Chlorite	2
		Biotite	1
		Muscovite	Tr
	Rock Fragments	Volcanic	4
		Chert	2
		Chalcedony	1
		Dolomite	Tr
	Accessories	Zircon	Tr
		Tourmaline	Tr
		Monazite	1
		Spinel	Tr
	Authigenic cement		
		Calcite	3
		Ferroan calcite	2
		Goethite	1
		Illite/sericite	3
		Clay rims	2

	Porosity/ Permeability Primary 3 Secondary 3
Detrital components	Quartz Monocrystalline quartz dominates this sample. Quartz grains range in size from very fine sand (0.1mm) to medium sand (0.45mm) with a mode of medium sand (0.3mm). Grains are sub-angular to rounded, well-sorted and display mainly point with occasional concave/convex grain-grain contacts. Most grains have been coated in a thin film of clay. Feldspar Feldspar grains range in size from fine (0.13mm) to medium sand (0.4mm). Several varieties of feldspar are evident these include microcline, albite and plagioclase. The degree of preservation of feldspar grains in the sample varies. Some grains remain intact while others have been leached and partially replaced by ferroan calcite. Authigenic chlorite growth is also evident along cracks that have formed in these grains. Biotite/chlorite Brownish biotite grains are evident in this sample. These grains are typically medium sand sized (0.4mm) and have been leached and cracked and have undergone partial alteration to chlorite. Authigenic chlorite is particularly evident forming in cracks that have developed in the grain. Rock Fragments *Chert and chalcedony* Chert and chalcedony fragments displaying similar grain size to detrital quartz grains are scattered throughout the sample. Chert crystal size varies within grains from micro- to megaquartz. The chalcedony is differentiated from chert grains by the radiating crystal structure. Monazite Well rounded, fine sand sized monazite grains are located within clay-rich laminae. These grains are clear under plane polarised light but display high birefringence colours under cross-polars. Dolomite Trace sub-rounded dolomite filled lithoclasts are evident scattered around this sample. Volcanic A variety of rock fragments are evident in this sample. These rock fragments are medium sand sized (0.4mm) , well rounded and consist of small laths of plagioclase feldspar grains contained in a finely crystalline matrix. Heavy leaching causing vacuolisation has resulted in the partial replacement of these grains by ferroan calcite and the development of secondary porosity. The final type of volcanic rock fragment consists of a indiscernible cryptocrystalline matrix. These grains also display a grain size from medium sand (0.4mm) to coarse sand (0.6mm) and are typically well rounded.
Matrix/ Pseudomatrix	
Authigenic cement	Illite/sericte Authigenic illite/sericitic grains are in the form of sub-rounded and squashed grains displaying a similar grain size to quartz grains. These grains are partially altered and replaced by ferroan calcite. Two possible sources for the illitic/sericitic grains are volcanic clasts and/or detrital clay balls. A concentration of illite/sericite is evident defining the thin, discontinuous sub-horizontal laminae that cut across this sample. In some areas grain coatings are

	thicker resulting in a bridging of pore space. <u>Goethite</u> Goethite replaces Fe-rich clays that occur in this sample. <u>Calcite</u> Most calcite occurs as patchy, single crystal poikilotopic cement that fills intergranular pore space and encases clusters of framework grains. Partial replacement of grains with no clay coatings by calcite is evident. <u>Ferroan calcite</u> Ferroan calcite mainly occurs as a replacement fragment. It is predominantly associated with illite/sericite grains where it partially to totally replaces these grains. It is also associated with feldspar grains, partially replacing grains that have been leached and cracked.
Porosity/ Permeability	This sample is assumed to have equal amounts of primary intergranular porosity and secondary porosity. Evidence for secondary porosity includes the dissolution of feldspar and volcanic grains, and the occurrence of over-sized pore spaces in the sample.

DIAGENESIS

Relative timing of events	Calcite formation Ferroan calcite formation Chlorite formation Goethite replacement
Relative importance of events	

TEXTURAL MATURITY AND INTERPRETATION

Textural maturity	Immature
Interpretation	

MINERALOGICAL CLASSIFICATION AND COMMENTS

Mineralogical classification	Feldspathic litharenite
Comments	

GSWA No. 154803

Well	VINES-1
Sample number	154803
Sample type	Plug
Depth	309.0
Unit	
Facies	Sandstone
Sample quality	Sample is in good condition.
Brief description	Feldspathic litharenite This sample predominantly of medium sand sized, sub-angular to sub-rounded quartz grains. These grains display varying degrees of silica overgrowth. The occurrence of volcanic fragments and feldspar grains is high. Both of these grains display partial replacement by calcite and illite/sericite. Most of the visual porosity occurs as primary intergranular porosity but the presence of partially dissolved and corroded volcanics and detrital grains indicates there is also good secondary porosity.

STRUCTURES

Structures	Massive

TEXTURE

Grain size	Range: Fine sand (0.13mm) to coarse sand (0.8mm) Mode: Medium sand (0.3mm)
Sorting	Well-sorted
Grain morphology	Sub-angular to sub-rounded
Sediment fabric	Detrital grains display predominantly point with occasional concave/convex and moderately sutured grain-grain contacts.

MINERALOGY

Tabulated composition (%)	Detrital components		
	Quartz	Monocrystalline	71
		Polycrystalline	1
	Feldspar	Microcline	1
		Albite	2
		Plagioclase	1
		Chlorite	1
		Biotite	1
	Rock Fragments	Volcanic	4
		Chert	2
		Chalcedony	1
	Accessories	Zircon	Tr
		Tourmaline	Tr
	Authigenic cement		
		Calcite	3
		Pyrite	1
		Illite/sericite	2
		Authigenic silica	Tr
		Kaolinite	1
	Porosity/ Permeability		
		Primary	5
		Secondary	3

Detrital components	Quartz Monocrystalline quartz dominates this sample. Quartz grains range in size from fine sand (0.13mm) to coarse sand (0.6mm) with a mode of medium sand (0.4mm). Grains are sub-angular to sub-rounded, well-sorted and display mainly point with occasional concave/convex and moderately sutured grain-grain contacts. Feldspar Feldspar grains range in size from fine (0.13mm) to medium sand (0.4mm). Several varieties of feldspar are evident these include microcline, albite and plagioclase. Grains are heavily leached. Replacement of the grains by calcite and illite/sericite is evident. Biotite/chlorite Brownish biotite grains are evident in this sample. These grains are typically medium sand sized (0.4mm) and have been leached and cracked and have undergone partial alteration to chlorite. Authigenic chlorite is particularly evident forming in cracks that have developed in the grain. Traces of sub-rounded, medium sand (0.04mm) sized chlorite grains are also evident in this sample. Rock Fragments *Chert and chalcedony* Chert and chalcedony fragments displaying similar grain size to detrital quartz grains are scattered throughout the sample. Chert crystal size varies within grains from micro- to megaquartz. The chalcedony is differentiated from chert grains by the radiating crystal structure. Volcanic A variety of rock fragments are evident in this sample. The most common volcanic rock fragments are igneous in origin. These rock fragments are typically medium sand (0.4mm) to coarse sand (0.8mm) sized. The grains are well rounded and predominantly composed of quartz and feldspar supported in a matrix of illite/sericite which has been partially chloritised in part. These volcanic fragments display some dissociation and alteration to calcite. The other main volcanic rock fragments consist of small laths of plagioclase feldspar grains contained in a finely crystalline matrix. Heavy leaching causing vacuolisation has resulted in the development of secondary porosity in these grains. The final type of volcanic rock fragment consists of a indiscernible cryptocrystalline matrix. These grains are also display a grain size from medium sand (0.4mm) to coarse sand (0.6mm) and are typically well rounded.
Matrix/ Pseudomatrix	
Authigenic cement	Authigenic silica Authigenic silica overgrowths are apparent on most quartz grains. These overgrowths are of varying thickness but mainly are thin. On grains with thicker overgrowths, pyrite dust rims are evident defining original grain outline. Illite/sericte Authigenic illite/sericitic grains are in the form of sub-rounded and squashed grains displaying a similar grain size to quartz grains. These grains are partially altered and have been compacted into the intergranular pore space. Two possible sources for the illitic/sericitic grains are volcanic clasts and/or detrital clay balls.

	Calcite Most calcite occurs as patchy, single crystal poikilotopic cement that fills intergranular pore space and encases clusters of framework grains. It forms sharp contacts with surrounding detrital grains. Kaolinite Kaolinite occurs mainly replacing illite/sericite clays in volcanic fragments. Pyrite Pyrite is found mainly on grain boundaries where it forms "dust rims" and filling pore space that has not been totally replaced by authigenic silica.
Porosity/ Permeability	Most of the visual porosity in this sample is primary intergranular porosity. Leaching resulting in cracking, dissolution and vacuolisation of some detrital feldspar grains has resulted in the development of secondary porosity.

DIAGENESIS

Relative timing of events	Primary pyrite formation Aughigenic illite/sericite formation Illite/sericite formation Chloritisation
Relative importance of events	

TEXTURAL MATURITY AND INTERPRETATION

Textural maturity	Immature
Interpretation	

MINERALOGICAL CLASSIFICATION AND COMMENTS

Mineralogical classification	Feldspathic litharenite
Comments	

GSWA No. 154849

Well	VINES-1
Sample number	154849
Sample type	Core
Depth	301.65
Unit	
Facies	Pebbly sandstone
Sample quality	The sample is in good condition.
Brief description	Sedarenite A 3mm thick sub-vertical haematite-rich vein surrounded by a 15mm thick altered clay halo cuts through this sample. The clay halo consists predominantly of very fine grained quartz and a greenish clay-rich, sericite/ chlorite matrix. Outside of altered halo the sample consists of very fine quartz, rock fragments and supported by a brown argillaceous matrix that displays some patchy sericite/ chlorite alteration. Visual porosity is moderate in this sample. The majority of the porosity is interpreted to be secondary.

STRUCTURES

Structures	Vertical bleached zone This sample contains a vertical, 3mm thick haematite-rich vein cutting through it. A 15mm bleached and altered halo exits around this vein. Some patchy alteration and bleaching is also evident in the host rock. It is interpreted that this zone possibly initially formed as a vertical micro-fracture or fault. Fluid movement up or down this structure possible resulted in the formation of haematite close to the fracture walls and bleaching and alteration

TEXTURE

Grain size	Range: Very fine sand (0.07mm) to granules (3mm) Mode: Very fine sand (0.16mm)
Sorting	Moderately-sorted
Grain morphology	Sub-angular to sub-rounded
Sediment fabric	Grains display point to concave/convex grain-grain contacts

MINERALOGY

Tabulated composition (%)	Detrital components		
	Quartz	Monocrystalline	55
		Polycrystalline	2
	Feldspar	Microcline	Tr
		Albite	2
		Plagioclase	1
	Rock fragments		
		Chert	2
		Chalcedony	1
		Volcanics	2
		Sandstone	Tr
		Shale	4
		Clay balls	2
		Kaolinite	1
	Accessories		
		Tourmaline	Tr
		Zircon	Tr
		Spinel	Tr
	Matrix/ Pseudomatrix		
		Illite/sericite?	12
		Sericite/chlorite	8
	Authigenic cement		

	Haematite 5 Porosity/ Permeability Primary 1 Secondary 2
Detrital components	Quartz Quartz ranges from very fine sand (0.07mm) to coarse sand (0.55mm) with a mode of very fine sand (0.16mm). Grains are sub-angular to sub-rounded and are matrix supported. Occasional point contacts are evident between some grains and almost all grains are coated in a thin isopachous chlorite clay. Feldspar Feldspar grains range in size from very fine sand (0.13mm) to coarse sand (0.6mm). Grains display a varying array of shapes, from tabular to sub-rounded. Several varieties of feldspar are evident these include microcline, albite and plagioclase. Most of the feldspar grains have undergone some dissolution or are cracked and have been partially altered to sericite or chlorite. Rock fragments *Shale* These rock fragments are angular to sub-angular and range in size from fine sand (0.15mm) to medium sand (0.3mm). Cracking and separation along bedding planes is evident in some shale fragments. Most fragments have been partially deformed and squashed into intergranular pore space and have been altered to a mixed sericite/chlorite composition. Nodular pyrite replacement is also evident in some of these fragments. *Volcanics* These rock fragments range up to very coarse sand (1.2mm) are sub-angular and consist of a mixture of leached and partially altered feldspar laths in an undifferentiated black cryptocrystalline matrix, augite and chlorite. *Chert* Chert fragments range in size from medium to coarse sand size. These fragments are typically sub-angular to sub-rounded and consist of a mixture of macro and microquartz. *Chalcedony* Traces of chalcedony are scattered throughout this sample. These fragments are approximately medium sand sized (0.4mm). Grains are generally angular and occasionally are broken and display typical chalcedonic texture comprising of radiating fibrous crystals of varying size. *Sandstone* Sandstone fragments range up to granules (3mm) size. The fragments are composed of a mixture of sub-angular, very fine sand quartz (0.1mm) and an undifferentiated argillaceous matrix. It is often difficult to distinguish these fragments as they are similar compositionally to the host rock. *Clay balls* These are typically medium to coarse sand sized. They are sub-rounded to rounded and composed of a cryptocrystalline argillaceous matrix. Compactional deformation of these fragments is evident. It is interpreted that these balls were derived directly from the soil profile. *Kaolinite* Kaolinite occurs as sub-rounded to rounded clasts. These clasts consist of coarsely and finely crystalline accumulation of kaolinite. Most of the clasts have undergone partial compaction resulting in their expansion of the kaolinite into intergranular pore space.

Matrix/ Pseudomatrix	The pseudo matrix forms two categories: bleached and unbleached. The bleached or altered portion forms a 15mm wide sub-vertical vein approximately through the centre of the slide. This zone is composed predominantly of sericite and kaolinite that has been altered to chlorite. The chlorite forms thin isopachous rims on some of the detrital quartz grains. A dark argillaceous matrix is evident outside of the main zone of alteration. This matrix is possibly composed of illite/sericite but it is extremely difficult to identify the clay type microscopically. Patchy alteration is also evident in this zone where some of the clay matrix has been altered to sericite and chlorite.
Authigenic cement	Haematite Haematite cement forms mainly in a sub-vertical vein evident in the centre of the slide. It displays varying thickness but is approximately 3mm wide at its thickest point. The cement fills intergranular pore space between grain encases clusters of framework grains. It is interpreted that water flow through a fracture or micro-fault may have been the cause for haematite formation.
Porosity/ Permeability	The porosity of this sample is moderate. Most of the porosity is interpreted to be secondary caused by the partial leaching and dissolution of detrital grains and matrix material form intergranular pore space.

DIAGENESIS

Relative timing of events	Localised haematite cementation Sericitisation Chlorite alteration Pyrite formation
Relative importance of events	

TEXTURAL MATURITY AND INTERPRETATION

Textural maturity	Immature
Interpretation	

MINERALOGICAL CLASSIFICATION AND COMMENTS

Mineralogical classification	Sedarenite
Comments	

GSWA No. 154848

Well	VINES-1
Sample number	154848
Sample type	Core
Depth	301.4
Unit	
Facies	Sandstone
Sample quality	The sample is in good condition.
Brief description	Interbedded litharenite and lithic wacke This slide consist of an interbedded litharenite and lithic wacke. The lithic wacke layer is defined by concentrations of sericitic clay and by two thin, discontinuous haematite laminae bounding the top and the bottom of the bed. Partial alteration of sericite to chlorite is evident in this rock type. The litharenite layer is evident above and below this bed. This layer is predominantly composed of sub-angular to sub-rounded, medium sized quartz supported by a matrix of sericite and partially haematite cemented. Most of the porosity occurs in this rock type. This porosity is interpreted to have been formed by late stage fluid movement leaching intergranular material.

STRUCTURES

Structures	Leached bed A 15mm thick, sub-horizontal clay-rich bed is evident in this sample. It is interpreted that Fe-rich fluid movement through this sample has caused partial haematite cementation of the sandier section and formation of an irregular haematitic crust at the sandstone-claystone contact.

TEXTURE

Grain size	Range: Coarse silt (0.05mm) to coarse sand (0.8mm) Mode: Bimodal → Fine sand (0.15mm) and medium sand (0.3mm)
Sorting	Moderately sorted
Grain morphology	Sub-angular to sub-rounded
Sediment fabric	Grains display point to concave/convex and weakly sutured grain-grain contacts.

MINERALOGY

Tabulated composition (%)	Detrital components		
	Quartz	Monocrystalline	62
		Polycrystalline	3
	Feldspar	Microcline	Tr
		Albite	1
		Plagioclase	1
	Rock fragments		
		Chert	1
		Volcanics	1
		Sandstone	2
		Siltstone	4
		Shale	2
		Symplectite quartz	Tr
	Accessories		
		Tourmaline	Tr
		Zircon	Tr
		Spinel	Tr
	Matrix/ Pseudomatrix		
		Sericite	15

	Authigenic cement Haematite 5 Porosity/ Permeability Primary 2 Secondary 1
Detrital components	Quartz *Lithic wacke* Quartz ranges from very fine sand (0.08mm) to coarse sand (0.5mm) with a mode of fine sand (0.15mm). Grains are angular to sub-rounded and are matrix supported. Quartz grains form highly corrosive contacts with the matrix material. *Litharenite* Quartz ranges from very fine sand (0.1mm) to very coarse sand (0.8mm) with a mode of medium sand (0.3mm). Grains are sub-angular to sub-rounded and display point to concave/convex and weakly sutured grain-grain contacts. A thin isopachous chlorite rim coats some of the quartz grains. Feldspar Feldspar grains range in size from very fine sand (0.13mm) to medium sand (0.3mm). Several varieties of feldspar are evident including microcline, albite and plagioclase. Some grains have undergone partial leaching and dissolution and alteration to authigenic sericite and chlorite clays. Rock fragments *Shale* These rock fragments are sub-rounded and range in size from fine sand (0.2mm) to coarse sand (0.6mm). Deformation and alteration of these fragments is evident. Partial leaching and alteration of these grains to sericite, chlorite and pyrite is evident. *Siltstone* These rock fragments are sub-rounded and range in size from fine sand (0.2mm) to coarse sand (0.6mm). They consist predominantly of medium silt sized quartz grains, mica and sericite. Alteration of some of these clasts to chlorite is evident. A weak preferential sub-vertical orientation of mica flakes to the elongate axis of siltstone fragment is evident in most clasts. *Sandstone* These fragments range up to very coarse sand sized (2mm) and angular to sub-angular in shape. They are composed predominantly of well-sutured, medium silt sized quartz grains and mica supported by a finely crystalline kaolinitic matrix. Partial alteration of kaolinite matrix to sericite and chlorite is evident. *Volcanics* The most common volcanic rock fragments are igneous in origin. These rock fragments are up to 0.7mm in size, sub-angular and consist of an undifferentiated cryptocrystalline matrix. Trace preservation of feldspar laths is evident in some of these fragments. *Symplectite quartz* A symplectite textured grain is evident in the lithic wacke portion of this slide. This grain is sub-rounded and medium sand sized (0.3mm). It consists of a mixture of feldspar and quartz.
Matrix/ Pseudomatrix	Sericite/Chlorite *Lithic wacke* Sericite/ chlorite clays form apoproximately 90% of this rock type. The lithic wacke segment of this slide consists predominantly of sericite matrix that fills intergranular pore space and encases clusters of framework grains. Partial alteration of sericite clays to chlorite is evident.

	Litharenite Sericite and chlorite matrix is patchy in this rock type. In places it may totally fill pore space and encase framework grains but it mainly occurs only partially filling pore space. Thin isopachous chlorite rims are also evident on most detrital quartz grains.
Authigenic cement	Haematite Patchy haematite cementation is evident throughout the litharenite portion of this slide. It mainly occurs filling intergranular pore space and encasing clusters of framework grains. It forms highly corrosive contacts with these grains. It also occurs as two thin (0.2mm), discontinuous sub-horizontal laminae above and below the lithic wacke bed in this slide. The concentration of haematite along the margins of this bed may indicate that fluid flow may have concentrated along the lithic wacke and litharenite contact. The Fe-rich fluid would have settled on this surface as the lithic wacke is relatively impermeable. In effect haematite concentrations would have intensified along this contact causing the production of thin lamiane.
Porosity/ Permeability	There is some preservation of primary porosity in this slide. It is possible that late stage fluid movement has leached matrix material from the sample resulting in the formation of this porosity. If this were the case the porosity would be regarded as secondary. All of the porosity occurs in the litharenite portion of this slide.

DIAGENESIS

Relative timing of events	Sericitisation Chlorite alteration Fluid movement Haematite cementation
Relative importance of events	

TEXTURAL MATURITY AND INTERPRETATION

Textural maturity	Mature
Interpretation	

MINERALOGICAL CLASSIFICATION AND COMMENTS

Mineralogical classification	40 % Lithic Wacke 60% Litharenite
Comments	

GSWA No. 154802

Well	VINES-1
Sample number	154802
Sample type	Plug
Depth	285.0
Unit	
Facies	Sandstone
Sample quality	Sample is in good condition
Brief description	Sedarenite This sample is predominantly composed of medium sand sized, sub-rounded to rounded quartz grains with minor percentages of volcanic rock fragments, chert and chalcedony. Grains typically display point to concave/convex grain-grain contacts. Thin clay coatings are evident on most grains. These coatings have stopped the formation of authigenic silica cementation. Patches of poikilotopic calcite fills intergranular pore space and encases clusters of grains. Thin, sub-horizontal, illite/sericite solution seams cut across the sample. Primary intergranular visual porosity is good. Minor secondary porosity caused by the leaching of grains is also apparent

STRUCTURES

Structures	Seams Thin, sub-horizontal solution seams cut across this sample. These seams are typically 1 to 3 mm thick and are defined by a dark colouration caused by an increase in clay content.

TEXTURE

Grain size	Range: Very fine sand (0.1mm) to coarse sand (0.6mm) Mode: Medium sand (0.3mm)
Sorting	Well-sorted
Grain morphology	Sub-angular to sub-rounded
Sediment fabric	Framework supported. Grains display point to occasional concave/convex grain-grain contacts.

MINERALOGY

Tabulated composition (%)	Detrital components		
	Quartz	Monocrystalline	78
		Polycrystalline	Tr
	Feldspar	Microcline	Tr
		Albite	2
		Plagioclase	Tr
	Rock fragments	Volcanics	3
		Chert	1
		Chalcedony	1
	Accessories	Zircon	Tr
		Tourmaline	Tr
	Authigenic cement		
		Calcite	4
		Illite/sericite	2
		Clay rims	2
		Chlorite	Tr
	Porosity/ Permeability		
		Primary	5
		Secondary	1

Detrital components	Quartz Monocrystalline quartz dominates this sample. Quartz grains range in size from very fine sand (0.1mm) to coarse sand (0.6mm) with a mode of medium sand. Grains are sub-angular to rounded, well-sorted and display mainly point with occasional concave/convex grain-grain contacts. Authigenic overgrowths are not apparent as a thin film of clay coats detrital grains. Feldspar Feldspar grains range in size from fine (0.13mm) to medium sand (0.4mm). Some grains have undergone partial vacuolisation and seritisation. Rock Fragments *Chert and chalcedony* Chert and chalcedony fragments displaying similar grain size to detrital quartz grains are scattered throughout the sample. Chert crystal size varies within grains from micro- to megaquartz. The chalcedony is differentiated from chert grains by the radiating structure of crystals. Volcanic A variety of rock fragments are evident in this sample. These rock fragments are typically medium sand (0.4mm) to coarse sand (0.6mm) sized. The grains are well rounded and predominantly composed of quartz and feldspar supported in a matrix of illite/sericite which has been partially chloritised. The other main volcanic rock fragments consist of small laths of plagioclase feldspar grains contained in a finely crystalline matrix. These grains have been partially altered to chlorite and ferroan calcite. Vacuolisation due to heavy leaching has resulted in the development of secondary porosity in these grains.
Matrix/ Pseudomatrix	
Authigenic cement	Illite/sericte Authigenic illite/sericitic grains are in the form of sub-rounded and squashed grains displaying a similar grain size to quartz grains. These grains are partially altered and have been compacted into the intergranular pore space. Two possible sources for the illitic/sericitic grains are volcanic clasts and/or detrital clay balls. Thin, sub-horizontal seams are defined by the concentration of illite/sericite along them. Illite/sericite in these seams encases grains. In some areas grain coatings are thicker resulting in a bridging of pore space. Clay rims Dead oil and clay have been placed together as they are difficult to distinguish separately. Dead oil/clay typically coats grains in a thin film occasionally bridging pore space. Calcite Most calcite occurs as patchy, single crystal poikilotopic cement that fills intergranular pore space and encases clusters of framework grains. It forms sharp contacts with surrounding detrital grains. Chlorite Traces of sub-rounded chlorite grains are scattered throughout the sample. Chlorite tends to form as a replacement of detrital feldspar grains and authigenic illite/sericite.
Porosity/ Permeability	Primary intergranular porosity is good in these samples. Some secondary porosity is also evident caused by the dissolution of rock fragments.

DIAGENESIS

Relative timing of events	Illite/sericite formation Kaolinite formation Chloritisation
Relative importance of events	The formation of thin films of dead oil/ clay on most detrital grains has resulted in the preservation of primary pore space.

TEXTURAL MATURITY AND INTERPRETATION

Textural maturity	Immature
Interpretation	

MINERALOGICAL CLASSIFICATION AND COMMENTS

Mineralogical classification	Sedarenite
Comments	

GSWA No. 154801

Well	VINES-1
Sample number	154801
Sample type	Plug
Depth	133.2
Unit	Sandstone
Facies	Sanstone
Sample quality	The sample is in excellent condition
Brief description	Volcanic arenite This sample consists predominantly of fine sand sized, sub-rounded to rounded quartz grains, volcanic rock fragments and authigenic illite/sericite clasts and kaolinite. Several types of volcanic fragments are evident. These fragments are well-rounded and of similar size to quartz grains. They are predominantly composed of quartz and feldspar grains supported in matrix of illite/sericite that has been partially chloritised. Other volcanics are difficult to distinguish as they are composed of a cryptocrystalline matrix. Primary and secondary visual porosity is good in this sample.

STRUCTURES

Structures	Massive

TEXTURE

Grain size	Range: Fine sand (0.2mm) to very coarse sand (1.1mm) Mode: Fine sand (0.23mm)
Sorting	Well-sorted
Grain morphology	Sub-angular to rounded
Sediment fabric	Framework grains display point to concave/convex grain-grain contacts.

MINERALOGY

Tabulated composition (%)	Detrital components		
	Quartz	Monocrystalline	78
		Polycrystalline	1
	Feldspar	Albite	Tr
		Microcline	1
		Plagioclase	2
	Rock fragments	Chalcedony	Tr
		Chert	1
	Accessories	Zircon	Tr
		Tourmaline	Tr
		Spinel	Tr
		Volcanic	3
	Authigenic cement		
		Calcite/Ferroan Calcite	1
		Clay rims	1
		Chlorite	1
		Illite/sericite	4
		Kaolinite	2
	Porosity/ Permeability		
		Primary	4
		Secondary	2

Detrital components	<u>Quartz</u> Monocrystalline quartz dominates this sample. Quartz grains range in size from fine sand (0.2mm) to very coarse sand (1.1mm) with a mode of fine sand (0.23mm). Grains are sub-angular to rounded, well-sorted and display mainly point with occasional concave/convex grain-grain contacts. Authigenic overgrowths are not apparent as a thin film of clay and dead oil coats detrital grains. <u>Feldspar</u> Feldspar grains range in size from fine (0.13mm) to medium sand (0.4mm). Grains have undergone partial vacuolisation and seritisation. Grain boundaries are diffuse and corroded. Most of the secondary porosity is the result of partial leaching of feldspar grains. <u>Rock Fragments</u> *Chert and chalcedony* Chert and chalcedony fragments displaying similar grain size to detrital quartz grains are scattered throughout the sample. Chert crystal size varies within grains from micro- to megaquartz. The chalcedony is differentiated from chert grains by its radiating crystal structure. <u>Volcanic</u> A variety of rock fragments are evident in this sample. These rock fragments are typically medium sand (0.4mm) to coarse sand (0.6mm) sized. The grains are well rounded and predominantly composed of quartz and feldspar supported in a matrix of illite/sericite which has been partially chloritised in part. The other main volcanic rock fragments consist of small laths of plagioclase feldspar grains contained in a finely crystalline matrix. These grains have been partially altered to chlorite and ferroan calcite. Vacuolisation due to heavy leaching has resulted in the development of secondary porosity in these grains. The final type of volcanic rock fragment consists of a indiscernible cryptocrystalline matrix. These grains also display a grains size from medium sand (0.4mm) to coarse sand (0.6mm) and are typically well rounded.
Matrix/ Pseudo	
Authigenic cement	<u>Illite/sericte</u> Authigenic illite/sericitic grains are in the form of sub-rounded and squashed grains displaying a similar grain size to quartz grains. These grains are partially altered and have been compacted into the intergranular pore space. Two possible sources for the illitic/sericitic grains are volcanic clasts and/or detrital clay balls. <u>Kaolinite</u> Authigenic kaolinite is evident partially filling intergranular pore space. It is interpreted as having formed from the complete, in situ alteration of detrital grains expanding into adjacent pore space. <u>Clay rims</u> Dead oil and clay have been placed together as they are difficult to distinguish separately. Dead oil/clay typically coats grains in a thin film occasionally bridging pore space. <u>Calcite/Ferroan calcite</u> Calcite and ferroan calcite mainly occurs as an alteration product replacing grains.
Porosity/ Permeability	Porosity is extremely good in this sample. Most of the porosity is primary intergranular porosity but a high degree of secondary porosity is also prevalent. Secondary porosity is the result of leaching and vacuolisation of grains.

DIAGENESIS

Relative timing of events	Illite/sericite formation Kaolinite formation Chloritisation
Relative importance of events	The formation of thin films of dead oil/ clay on most detrital grains has resulted in the preservation of primary pore space.

TEXTURAL MATURITY AND INTERPRETATION

Textural maturity	Immature
Interpretation	

MINERALOGICAL CLASSIFICATION AND COMMENTS

Mineralogical classification	Volcanic arenite
Comments	

GSWA No. 154847

Well	VINES-1
Sample number	154847
Sample type	Core
Depth	104.55
Unit	
Facies	Conglomerate
Sample quality	This sample is in good condition
Brief description	Volcanic arenite This sample consists predominantly of up to pebble sized volcanic fragments with minor sedimentary fragments. All volcanic fragments display some alteration and recrystallisation. Rock fragments are predominantly cemented by coarsly crystalline poikilotopic calcite. However a finely crystalline drusy equant calcite cement does occur in areas. Other cementing agents that occur to a lesser extent include illite/sericite and haematite. It is interpreted that most of the porosity in this sample has been produced by grain plucking during thin-section manufacture.

STRUCTURES

Structures	Massive

TEXTURE

Grain size	Range: Fine sand (0.15mm) to pebbles (6mm)
Sorting	Poorly-sorted
Grain morphology	Sub-angular to sub-rounded
Sediment fabric	Matrix supported but occasional point contacts are evident.

MINERALOGY

Tabulated composition (%)	Detrital components		
	Quartz	Monocrystalline	5
		Polycrystalline	1
	Feldspar		Tr
	Rock Fragments		
		Sandstone	2
		Chert	4
		Myrmekite	1
		Siltstone	3
		Shale	5
		Volcanic	29
		Carbonate clasts	4
	Accessories		
		Sphene	Tr
		Zircon	Tr
		Tourmaline	Tr
		Olivine	Tr
	Authigenic cement		
		Calcite	40
		Haematite	2
		Illite/sericite	3
	Porosity/ Permeability		
		Primary	Tr
		Secondary	1
Detrital components	Quartz Quartz ranges from medium sand (0.3mm) to coarse sand (0.6mm) with a mode of medium sand (0.3mm). No contacts are evident between grains. Grains are cemented by poikilotopic calcite cement.		

	Feldspar Feldspar grains are approximately fine sand sized (0.2mm). Some grains have undergone partial leaching resulting in vacuolisation and alteration to chlorite. Rock fragments *Chert* Chert fragments range in size from medium sand (0.3mm) to granules (2mm). They are typically composed of patchy micro- and macroquartz with minor pyrite alteration. Some minor calcite cementation is also evident replacing some microquartz. Some of the larger chert grains display alteration to chalcedony. *Myrmekite* These fragments range from coarse sand sized (0.6mm) to very coarse sand sized (1.5mm), sub-rounded, and composed of an intergrowth of plagioclase and quartz with a vermicular texture. The quartz typically forms as blebs or veriform shapes within the feldspar. Some of the intergrowths of quartz and feldspar also display a micrographic texture. *Siltstone* Siltstone fragments are irregularly shape and range up to granule sized (3mm). These fragment typically contain approximately 30% coarse silt sized quartz grains and 70% illite/sericite clay. Thin, dark, wispy solution seams are sometimes evident in these clasts. The dark brown colouration of these seams is generated by the accumulation of pyrite and insoluble organic matter with the illite/sericite clays. Where fragments have been partially leached and dissolved authignenic calcite and chlorite growth is evident. *Shale* These rock fragments range up to very coarse sand sized (1mm) and are angular to sub-angular in shape. They are composed predominantly of illite/sericite clay that has been partially chloritised and replaced by iron-oxides. *Sandstone* Traces of well cemented sandstone fragments are also evident in this sample. These fragments are typically granular in size (2-3mm) and angular to sub-angular in shape. They are composed of moderately-sutured very fine sand sized quartz and feldspar grains cemented by poikilotopic calcite that has been partially dolomitised. Quartz grains display thick authigenic silica overgrowths that are defined by "dust rims." Nodular pyrite replacement of some of these clasts is also evident. They are often difficult to distinguish as they have been overgrown by massive pore filling poikilotopic calcite. *Carbonate* Carbonate clasts range up to coarse sand sized (0.8mm). The internal constituents of these clasts consist of non-planar anhedral dolomite that has replaced original calcite. Alteration of some of the carbonate clasts to microquartz is evident. A pebble sized (4mm) boundstone fragment is evident in this sample. This fragment is composed of micritic calcite and dolomite. The fragment displays discontinuous irregularly oriented laminaton. Some faint outlines of recrystallised peloids are evident in these fragments ***Volcanics*** *Altered alkali basalt* The most common volcanic rock fragments are igneous in origin. These rock fragments range up to pebble size (4mm) and are typically sub-angular to sub-rounded. They consist of large laths of plagioclase feldspar grains in an undifferentiated black cryptocrystalline matrix. Grain boundaries are highly irregular and diffuse and some volcanic grains display minor dissolution and

	dispersion into intergranular pore space. Dark crystals are evident in some fragments. These dark brown microphenocrysts are possibly melanite garnet. *Alkali olivine basalt* These fragments range up to pebble sized (4mm) and are typically sub-angular to sub-rounded. They are composed predominantly of clear feldspar laths sub ophitically enclosed by brownish augite laths and opaque pyrite. They commonly display some minor alteration to chlorite. Phenocrysts of finely crystalline calcite in some of the clasts indicate that alteration of olivine has occurred. *Phonolite* These fragments are of similar size to altered alkali basalt fragments. They are sub-angular to sub-rounded and consist of green pyroxene needles surrounded by a semi-opaque cryptocrystalline matrix. Matrix material forms highly corrosive contacts with surrounding calcite cement. *Chlorite* Some chlorite rock fragments are evident in this sample. These fragments are typically of similar size to altered basalt fragments. These fragments possibly originated as volcanic rock fragments that have been completely altered. It is impossible to determine the composition of original fragments due to the degree of alteration. *Microgranite* Fragments of microgranite are also of similar size to altered basalt fragments. These fragments are typically composed of intergrown quartz and alkali feldspar that have a granophyric texture. Trace dolomite replacement of feldspar grains is evident in these fragments. Some of these grains display some microfractures. Microfractures are filled with megaquartz cement. *Undifferentiated volcanics* These volcanic fragments are approximately coarse sand sized (0.9mm). They are sub-angular in shape and composed of a brown cryptocrystalline matrix. Thin micritic rims generally surround these fragments. *Urtite* A coarse grained leucocratic rock fragment consisting predominantly of large nepheline flakes and minor amounts of alkali pyroxene and amphibole. Fragments are typically pebble sized (4mm) and have a brown colouration.
Matrix/ Pseudomatrix	
Authigenic cement	<u>Calcite</u> This sample is predominantly cemented by coarse grained poikilotopic calcite cement that fills intergranular pore space. Patchy, equant drusy finely crystalline calcite cement is also evident. The drusy cement displays typical coarsening outwards into intergranular pore space. <u>Haematite</u> Haematite is generally associated with illite/sericite clays. It forms coating grain boundaries and filling intergranular pore space. The cement is relatively patchy or discontinuous. <u>Sericite/Illite</u> Authigenic sericite/illite mainly occurs replacing and coating rock fragments and filling intergranular pore space. The dark colouration of illite/sericite clays is possibly produced by the mixture of haematite and insoluble organic matter.
Porosity/ Permeability	Some secondary porosity is evident in this sample. Most of this porosity is interpreted to be the result of grain plucking during thin-section manufacture. Evidence for this includes the occurrence of oversized pores.

DIAGENESIS

Relative timing of events	Authigenic silica cementation Illite/sericite formation Calcite cementation Chlorite formation Haematite cementation
Relative importance of events	

TEXTURAL MATURITY AND INTERPRETATION

Textural maturity	Immature
Interpretation	

MINERALOGICAL CLASSIFICATION AND COMMENTS

Mineralogical classification	Volcanic arenite
Comments	

GSWA No. 154846

Well	VINES-1
Sample number	154846
Sample type	Core
Depth	67.8
Unit	
Facies	Conglomerate
Sample quality	Sample is in good condition
Brief description	Volcanic arenite This sample consists predominantly of up to pebble sized volcanic fragments with minor sedimentary fragments. All volcanic fragments display some alteration and recrystallisation. Rock fragments are cemented by a mixture of poikilotopic calcite, illite/sericite, and haematite cements. Only trace secondary porosity is evident in this sample.

STRUCTURES

Structures	Massive

TEXTURE

Grain size	Range: Fine sand (0.15mm) to pebbles (6mm)
Sorting	Poorly-sorted
Grain morphology	Angular to sub-rounded
Sediment fabric	Grains are supported by calcite cement but display occasional point contacts

MINERALOGY

Tabulated composition (%)	Detrital components		
	Quartz	Monocrystalline	8
		Polycrystalline	Tr
	Feldspar		Tr
	Rock Fragments		
		Sandstone	5
		Chalcedony	2
		Chert	2
		Myrmekite	Tr
		Siltstone	4
		Shale	3
		Volcanic	32
		Lithclasts	2
		Pisolitic	1
		Carbonate clasts	2
		Phosphate	1
		Olivine	Tr
	Authigenic cement		
		Calcite	24
		Haematite	5
		Illite/sericite	7
		Silica	1
	Porosity/ Permeability		
		Primary	Tr
		Secondary	Nil

Detrital components	Quartz Quartz ranges from fine sand (0.12mm) to medium sand (0.4mm) with a mode of medium sand (0.3mm). Grains are angular to sub-rounded and moderately sorted. Only trace point contacts are evident between grains. Most of the quartz is supported by a coarsely crystalline poikilotopic cement. Olivine Forms as small vermicular stacks and isolated grains that have been replaced by calcite. Feldspar Feldspar grains are approximately fine sand sized (0.2mm). Some grains have undergone partial leaching resulting in vacuolisation and alteration to chlorite. Rock fragments *Chert* Chert grains are composed of mixture of micro- and megaquartz. These fragments are sub-angular to sub-rounded and range up to very coarse sand in size (1.8mm) *Chalcedony* Rare detrital chalcedony fragments are located throughout this sample. These fragments also range up to coarse sand (0.8mm). Grains are generally angular and occasionally are broken. Grains display typical chalcedonic texture comprising radiating fibrous crystals of varying size. *Lithoclasts* These grains could be termed flint, but due to the truncation of microquartz nodules at the grain boundary they have been termed lithoclasts. Lithoclasts consist of a mixture of concentric microquartz and chalcedonic silica. Microquartz is evident as elongate and round grains varying in size from 0.7mm to 1.1mm. These grains predominantly display single-phase growth but occasional multiphase growth on some grains is evident by differences in colouration between successive phases. Chalcedonic silica is typically located between nodules. It mainly occurs as a radial-fibrous, pore-filing cement. There is a slight increase in chalcedonic crystal grain size towards the centre of pores. *Myrmekite* These grains, sub-rounded and granule sized (2.2mm) and composed of an intergrowth of plagioclase and quartz with a vermicular texture. The quartz typically forms as blebs or vermiform shapes within the feldspar. Some of the intergrowths of quartz and feldspar also display a micrographic texture. *Siltstone* Siltstone fragments are irregularly shaped and range up to granule sized (4mm). These fragment typically contain approximately 30% coarse silt sized quartz grains and 70% illite/sericite clay. Thin, dark, wispy solution seams are sometimes evident in these clasts. The dark brown colouration of these seams is generated by the accumulation of pyrite and insoluble organic matter with the illite/sericite clays. Where fragments have been partially leached and dissolved authigneic calcite growth is evident. *Shale* These rock fragments range up to very coarse sand sized (1mm) and are angular to sub-angular in shape. They are composed predominantly of illite/sericite clay that has been partially chloritised and replaced by iron-oxides.

	Sandstone Traces of well-cemented sandstone fragments are also evident in this sample. These fragments are typically granular in size (2-3mm) and angular to sub-angular in shape. They are composed of well-sutured very fine sand sized quartz grains cemented by poikilotopic calcite that has been partially dolomitised. Nodular pyrite replacement of some of these clasts is also evident. *Carbonate* Carbonate clasts range up to coarse sand sized (0.8mm). The internal constituents of these clasts consist of patchy xenotopic matrix of anhedral to subhedral shaped very finely crystalline dolomite that displays planar, curved and sutured contacts. Some clasts display partial micritisation. Traces of recrystallised blue-green algae are evident in this sample. Longitudinal sections of these filaments have been recrystallised to chert. ***Volcanics*** *Altered alkali basalt* The most common volcanic rock fragments are igneous in origin. These rock fragments range up to pebble size (5mm) and are typically sub-angular to sub-rounded. They consist of large laths of plagioclase feldspar grains in an undifferentiated black cryptocrystalline matrix. Grain boundaries are highly irregular and diffuse and some volcanic grains display minor dissolution and dispersion into intergranular pore space. Dark crystals are evident in some fragments. These dark brown microphenocrysts are possibly melanite garnet. *Alkali olivine basalt* These fragments range up to pebble sized (5mm) and are typically sub-angular to sub-rounded. They are composed predominantly of clear feldspar laths sub-ophitically enclosed by brownish augite laths and opaque pyrite. They commonly display some minor alteration to chlorite. Phenocrysts of finely crystalline calcite in some of the clasts indicate that alteration of olivine has occurred. *Phonolite* These fragments are of similar size to altered alkali basalt fragments. They are sub-angular to sub-rounded and consist of green pyroxene needles surrounded by a semi-opaque cryptocrystalline matrix. Matrix material forms highly corrosive contacts with surrounding calcite cement. *Chlorite* Some chlorite rock fragments are evident in this sample. These fragments are typically of similar size to altered basalt fragments. These fragments possibly originated as volcanic rock fragments that have been completely altered. It is impossible to determine the composition of original fragments due to the degree of alteration. *Microgranite* Fragments of microgranite are also of similar size to altered basalt fragments. These fragments are typically composed of intergrown quartz and alkali feldspar that have a granophyric texture. Trace dolomite replacement of feldspar grains is evident in these fragments. *Undifferentiated volcanics* These volcanic fragments are approximately coarse sand sized (0.9mm). They are sub-angular in shape and composed of a brown cryptocrystalline matrix. Thin micritic rims generally surround these fragments. *Pisolites* These fragments are typically sub-rounded to rounded and composed of iron-oxide (haematite?) and small olivine fragments.

Matrix/ Pseudomatrix	
Authigenic cement	Calcite Most calcite occurs as patchy, single crystal poikilotopic cement that fills intergranular pore space and encases clusters of framework grains. It is evident mainly filling pore space between rock fragments. Microsparry accumulations of calcite are also apparent in this sample. The calcite is typically very finely crystalline and cements detrital components within rock fragments. Haematite Haematite is generally associated with illite/sericite clays. It forms coating grain boundaries and filling intergranular pore space. The cement is relatively patchy or discontinuous. Silica overgrowths Authigenic silica overgrowths are evident on some quartz grain boundaries. They are generally 0.01mm thick and defined by haematitic dust rims that occur between the grain boundary and the overgrowth. Sericite/Illite Authigenic sericite/illite mainly occurs replacing and coating rock fragments and filling intergranular pore space. The dark colouration of illite/sericite clays is possibly produced by the mixture of haematite and insoluble organic matter.
Porosity/ Permeability	Only trace secondary porosity is evident in this sample. This porosity has been produced by the partial leaching and dissolution of detrital grains.

DIAGENESIS

Relative timing of events	Authigenic silica cementation Illite/sericite formation Calcite cementation Chlorite formation Haematite cementation
Relative importance of events	

TEXTURAL MATURITY AND INTERPRETATION

Textural maturity	Immature
Interpretation	

MINERALOGICAL CLASSIFICATION AND COMMENTS

Mineralogical classification	Volcanic arenite
Comments	

GSWA No. 154466

Well	EMPRESS 1A
Sample number	154466
Sample type	
Depth	1060.05
Unit	
Facies	Sandstone
Sample quality	The sample is in good condition.
Brief description	Quartz arenite This sample is a massive quartz arenite. Quartz grains range in size from very fine sand to coarse sand with a mode of medium sand. Grains are sub-rounded to rounded and display concave/convex to moderately sutured grain-grain contacts. Thin, authigenic silica overgrowths are evident on some detrital grains. Intergranular porosity has been partially occluded by poikilotopic calcite, ferroan calcite and dolomite.

STRUCTURES

Structures	Massive

TEXTURE

Grain size	Range: Very fine sand (0.1mm) to coarse sand (0.8mm) Mode: Medium sand (0.4mm)
Sorting	Well-sorted
Grain morphology	Sub-rounded to rounded
Sediment fabric	Grains display concave/convex to well-sutured grain-grain contacts.

MINERALOGY

Tabulated composition (%)	Detrital components		
	Quartz	Monocrystalline	83
		Polycrystalline	Tr
	Feldspar		2
	Rock fragments		
		Carbonate	3
		Chert	1
		Sandstone	Tr
		Kaolinite	Tr
	Authigenic cements		
		Calcite	4
		Pyrite	Tr
		Ferroan calcite	2
		Silica overgrowths	Tr
		Dolomite	1
	Porosity/ Permeability		
		Primary	3
		Secondary	1
Detrital components	Quartz Quartz grains range in size from very fine sand (0.1mm) to coarse sand (0.8mm) with a mode of medium sand (0.4mm). Grains are sub-rounded to rounded and display concave/convex to well-sutured contacts. Vacuoles or fluid inclusions are evident in most grains. These inclusions are defined as dark specks. Thin authigenic silica overgrowths are evident on most grains. Feldspar Feldspar grains are approximately fine sand sized (0.2mm). Some grains have undergone partial leaching resulting in vacuolisation and alteration to chlorite.		

	Rock fragments *Carbonate* Sub-rounded to rounded carbonate clasts are scattered throughout this sample. Carbonate clasts range up to medium sand sized (0.3mm). These clasts are composed of patchy anhedral to subhedral shaped, very finely to finely crystalline dolomite that display planar, curved and sutured contacts. Micritic alteration is evident in some of these clasts. Most of the micritised clasts consist of equant subhedral to euhedral crystals of microsparite and finer, micrite which have replaced the original very fine to fine dolomite. Chert replacement and ferroan calcite of some of these clasts is evident. *Kaolinite* Kaolinite occurs as sub-rounded to rounded clasts. These clasts consist of coarsely and finely crystalline accumulation of kaolinite. Most of the clasts have undergone partial compaction resulting in their expansion of the kaolinite into intergranular pore space.
Matrix/ Pseudomatrix	
Authigenic cement	Calcite Calcite mainly forms as poikilotopic cement that fills intergranular pore space and replaces or overgrows detrital grains. It forms highly corrosive contacts with surrounding framework grains in some areas. Pyrite Pyrite forms infilling intergranular pore space. It is particularly prevalant in sections that have an intense concentration of clay. Silica overgrowths Trace authigenic silica overgrowths are evident on some quartz grain boundaries. Most of these overgrowths are very thin but occasionally thicker growths are produced at triple junctions between adjacent overgrowths. At these points are irregular compromise boundaries are produced by the mutual interference of individual overgrowths. Overgrowths have been marginally replaced by single, poikilotopic calcite cement and dolomite. Ferroan calcite Ferroan calcite occurs as microsparry accumulations that fill intergranular pore space and marginally replace framework grains. This cement forms highly corrosive contacts with surrounding detrital grains. Dolomite Dolomite occurs as isolated rhombs and microsparry accumulations that marginally replace pore filling cements.
Porosity/ Permeability	There is good preservation of primary integranular porosity in this sample.

DIAGENESIS

Relative timing of events	Authigenic silica cementation Calcite cementation Ferroan calcite formation Dolomite formation Pyrite formation
Relative importance of events	

TEXTURAL MATURITY AND INTERPRETATION

Textural maturity	Immature
Interpretation	

MINERALOGICAL CLASSIFICATION AND COMMENTS

Mineralogical classification	Quartz arenite
Comments	

GSWA No. 154465

Well	EMPRESS 1A
Sample number	154465
Sample type	Core
Depth	319.0m
Unit	
Facies	Sandstone
Sample quality	The sample is in good condition.
Brief description	Quartz arenite This sample is a weakly laminated quartz arenite. Lamination is defined by the alternation of fine and coarse quartz grains. Quartz is generally sub-angular to well-rounded and display point to concave/convex grain-grain contacts. Thin illite/sericite clay coatings are evident on most detrital grains. Porosity is good but it has been partially filled by poikilotopic calcite.

STRUCTURES

Structures	Weak lamination defined by the alternation of finer and coarser quartz grains.

TEXTURE

Grain size	Range: Fine silt (0.1mm) coarse sand (0.7mm) Mode: Bimodal→very fine sand (0.1mm) and medium sand (0.4mm)
Sorting	Well-sorted
Grain morphology	Sub-angular to sub-rounded
Sediment fabric	Grains display point to concave/convex grain-grain contacts.

MINERALOGY

Tabulated composition (%)	Detrital components		
	Quartz	Monocrystalline	82
		Polycrystalline	1
		Muscovite	Tr
	Feldspar		3
	Rock fragments		
		Carbonate	Tr
		Chert	Tr
	Authigenic cements		
		Calcite	4
		Pyrite	2
		Illite/Sericite	4
	Porosity/ Permeability		
		Primary	3
		Secondary	1
Detrital components	Quartz This sample contains a bimodal grains size distribution. The coarser fraction with a mode of medium sand (0.4mm) is concentrated along thin irregular, discontinuous laminae. The finer fraction is concentrated in the host rock. This fraction has a mode of very fine sand (0.1mm). Quartz grains are generally sub-angular to sub-rounded and display point to concave/convex grain-grain contacts. No authigenic silica overgrowths are evident on grains as overgrowths have been impeded by thick clay coatings evident on detrital grain boundaries. Feldspar Feldspar grains are approximately fine sand sized (0.2mm). Some grains have undergone partial leaching resulting in vacuolisation and alteration to chlorite.		

	Rock fragments *Carbonate* Sub-rounded to rounded carbonate clasts are scattered throughout this sample. Carbonate clasts range up to medium sand sized (0.3mm). These clasts are composed of patchy anhedral to subhedral shaped, very finely to finely crystalline dolomite that display planar, curved and sutured contacts. Micritic alteration is evident in some of these clasts. Most of the micritised clasts consist of equant subhedral to euhedral crystals of microsparite and finer, micrite which have replaced the original very fine to fine dolomite. Chert replacement and ferroan calcite of some of these clasts is evident. *Chert* Chert fragments range in size up to medium sand size. These fragments are typically sub-angular to sub-rounded and consist of a patchy mixture of macro and microquartz.
Matrix/ Pseudomatrix	
Authigenic cement	Calcite Calcite mainly forms as poikilotopic cement that fills intergranular pore space and replaces or overgrows detrital grains. It forms highly corrosive contacts with surrounding framework grains in some areas. Pyrite Pyrite forms infilling intergranular pore space. It is particularly prevalant in sections that have an intense concentration of clay. Illite/sericite Illite/sericite generally forms as isopachous rims on detrital grains. Occasionally individual grain coatings are thick enough to totally bridge pore space and fill intergranular pore space.
Porosity/ Permeability	There is a good preservation of primary porosity in this sample even though some calcite cementation has occurred. Preservation of primary porosity is principally due to isopachous coatings on grains that have decreased the thickness of overgrowths and cements. Some secondary porosity has been produced by the dissolution of feldspars.

DIAGENESIS

Relative timing of events	Isopachous clay coatings Mechanical compaction Calcite cementation Pyrite formation
Relative importance of events	

TEXTURAL MATURITY AND INTERPRETATION

Textural maturity	Immature
Interpretation	

MINERALOGICAL CLASSIFICATION AND COMMENTS

Mineralogical classification	Quartz arenite
Comments	

DIAGENESIS

Relative timing of events	Anhydrite cementation Calcite cementation
Relative importance of events	

MINERALOGICAL CLASSIFICATION AND COMMENTS

Mineralogical classification	Siltstone
Comments	SEM or XRD on this sample would aid in the identification of matrix material.

APPENDIX B (Reflective light descriptions)

Brief description have been supplied identifying sulphides in the following samples.

Polished Section 154862

Sulphides in this polished section are all circular aggregates of anhedral grains of galena or individual anhedral galena grains.

Polished section 154856

Subhedral pyrite grains ranging from 2-50μm form a semi-massive replacement vein, which includes pyrite in fractured quartz or carbonate clasts, and on corroded margins of clasts. Pyrite is also finely disseminated throughout the host rock.

Minor coarse sphalerite aggregates 50-150μm are developed interstitially to coarse quartz clasts and is broadly localised in a narrow corridor in the vein centre. Minor pyrite is contained within sphalerite grains. A second phase of fine-grained, semi-massive sphalerite has replaced part of a carbonate clast and contains abundant disseminated euhedral pyrite. This sphalerite phase is interpreted to be later than the disseminated pyrite.

Polished section 154860

Coarse (200μm) subhedral chalcopyrite is sparsely intergrown with carbonate. Very fine to fine (2-25μm) anhedral sphalerite is disseminated in the carbonate-haematite laminated band at the base of the thin section.

APPENDIX C (Photomicrographs)

See Photo Library on CD for all photomicrographs

Sample 154867 (1983.0m) PPL
Feldspathic wacke. Sample displays coarse silt to fine sand sized, sub-angular to sub-rounded quartz grains with point to concave/convex and moderately sutured grain contacts. A bent muscovite grain is located at C1-D1. Patchy microsparry to poikilotopic calcite cement is evident filling intergranular pore space.

Sample 154867 (1983.0m) XPL
Feldspathic wacke. Poikilotopic and microsparry calcite cement is evident filling intergranular pore space and marginally replacing detrital grains (eg D5). The cement forms highly corrosive contacts with surrounding detrital grains.

Sample 154844 (1902.0) XPL
Massive Quartz arenite. Grains display concave/convex and moderately sutured grain-grain contacts. An authigenic silica overgrowth is visible (B4). Microsparry and poikilotopic calcite is well developed, filling intergranular pore space. Replacement of this cement is evident at D2.

Sample 154844 (1902.0) XPL

Quartz arenite. Angular to sub-rounded quartz grains have moderately sutured or concave/convex contacts. Vacuoles or fluid inclusions are evident in the quartz grain in D5. A dolomite clast is evident at H3. Dolomite in this clast forms a xenotopic matrix of planar subhedral and euhedral grain contacts. Outlines of micritised peloids are evident in this clast. The intergranular pore space has been filled by a mixture of poikilotopic calcite (eg E4) and dolomite. Visual porosity is poor.

Sample 154843 (1815.0m) PPL

Quartz arenite. Framework grains are mainly angular to sub-rounded quartz clasts, with minor siltstone (F5), kaolinite (I3), feldspar (D6) and carbonate (J5). Visible porosity is good with silica overgrowths (B1) and calcite and dolomite cement limited to grain contacts. Dissolution of a feldspar grain resulting in secondary porosity is evident in C6.

Sample 154843 (1815.0m) XPL

Quartz arenite. Quartz grains are angular to sub-angular and display moderately to well-sutured grain-grain contacts. Fragmented carbonate clasts are evident at A1-A6. This clast has been partially compacted. Poikilotopic and microsparry calcite is evident filling intregranular pore space. Visual porosity is poor.

Sample 154842 (1713.0m) PPL

Quartz arenite. The sample is generally massive, consisting of moderately well sorted clasts of quartz, feldspar. Minor haematite is flattened on grain margins (E1). Quartz grains contain abundant fluid inclusions (H6 and I4). Minor silica overgrowth cementation is evident on some quartz grains (G6). Pore space has been partially filled by microsparry calcite cement. Porosity is moderate and the occurrence of oversized pores (D4) may indicate that the majority of this porosity is secondary.

Sample 154842 (1713.0m) XPL

Quartz arenite. Quartz grains are angular to sub-angular in shape and display concave/convex to moderately sutured grain-grain contacts. Authigenic silica overgrowths are evident on some quartz grain boundaries. Pore space has been partially filled by a poikilitopic calcite cement that has been partially dolomitised (E2-G2). This cement forms highly corrosive contacts with surrounding framework grains.

Sample 154866 (1665.6m) PPL

Sandstone. Quartz grains display a variation in grain size from coarse silt to medium sand. Grains range in shape from angular to sub-rounded and display point to concave/convex grain-grain contacts. Quartz grains contain abundant vacuoles and fluid inclusions. An algal fragment is evident in H4 with a micritic coating. Trace intergranular porosity is evident in blue.

Sample 154866 (1665.6m) XPL
The field of view is dominated by a clast of radiating chalcedony crystals that has been partially replaced by poikilotopic calcite and ferroan calcite. Detrital kaolinite is evident in A1-B3 bounded by poikilotopic calcite. Visual porosity in this sample is poor.

Sample 154841 (1656.0m) PPL

Quartz arenite. Clasts range from coarse silt to coarse sand and are sub-angular to sub-rounded with sutured or concave/convex grain contacts. The sample contains several micritised carbonate clasts with one illustrating partial aggrading neomorphism (D2). Additional dolomite cement is developed on framework grain margins and partially replaces silica overgrowths (F6). Visual porosity is poor with most intergranular pore space being filled by cement.

Sample 154841 (1656.0m) XPL
Quartz grains display mainly point contacts. Quartz grain margins are corrosive as they are being partially overgrown by calcite cement. A carbonate clast is evident in H1. Visual porosity is poor.

Sample 154865 (1569.1m) XPL
Mudstone or dismicrite. Matrix consists of a micritised peloidal mud. Secondary anhydrite has infilled most of the primary vugular porosity (I6). Visual porosity is extremely poor.

Sample 154865 (1569.1m) XPL
Sample consists of micrtitised peloidal mud. Displacive anhydrite cement is evident in the centre of this photomicrograph. The incorporation of small patches of carbonate mud in the centre of the anhydrite may indicate that the anhydrite cement has replaced this mud. Late stage calcite cement can be seen radiating from the edge of peloids. This cement is partially replacing anhydrite cements. Apart from some minor secondary porosity caused by the leaching of anhydrite cements, overall porosity is poor.

Sample 154864 (1537.05m) XPL
Sample consists predominantly of micritic mud. Porosity is poor. Trace anhydrite cementation is evident in H1.

Sample 154863 (1478.95m) PPL
Argillaceous siltstone (upwards to right). Fining upward graded bedding is evident with hummocky bed surfaces. Coarse silt to fine sand sized, angular to sub-rounded quartz grains are bound within an illite/sericite matrix. Discontinuity of clay horizons from soft sediment deformation is apparent in this sample. Trace visible porosity.

Sample 154838 (1473.95m) PPL

The sample is poorly sorted and consists of angular to sub-rounded clasts and coarse silt sized, angular quartz. Clasts include detrital fine crystalline carbonate with patchy micritisation, and chert. The framework grains are supported in a matrix of illite/sericite which has minor calcite and dolomite replacement.

Sample 154837 (1469.0m) PPL

Lithic wacke. This poorly-sorted , matrix-supported sample, consists of angular to sub-rounded grains of coarse silt sized quartz. The matrix comprises of a complex mixture of micrite, illite/sericite and silt. No visible porosity is evident in this sample.

Sample 154837 (1469.0m) XPL
Detailed view of the carbonate mud and illite/sericite. The mud is partially overgrowing the detrital quartz grain in the upper left of this photomicrograph. Visible porosity is extremely poor.

Sample 154862 (1465.65m) PPL
This sample consists predominantly of partially dolomitised micritic mud. Displacive anhydrite (clear) is evident growing within the micritic mud. Visual porosity is negligible.

Sample 154861 (1463.2m) PPL
Graded siltstone (way up to left). Graded bedding of medium to coarse silt defines persistent laminations. Clasts are predominantly quartz and are matrix supported in illite/sericite. Notable chlorite alteration bands are developed in the upper limits of the clay-rich horizons. Visual porosity is poor.

Sample 154861 (1463.2m) XPL
Siltstone. Graded bedding is shown here by the silt-sized, quartz clast-bearing laminae and the clay-rich laminae. Anhydrite commonly develops in fractures in the clay rich laminae or has grown early as displasive crystals. The illite/sericite matrix in the siltstone has resulted in negligible porosity.

Sample 154835 (1458.53m) PPL
Argillaceous siltstone (upwards to left). Graded laminations are disrupted throughout the sample due to intense bioturbation. Clasts are sub-angular to sub-rounded and generally matrix supported with occasional point contacts. No porosity is evident in this sample.

Sample 154835 (1458.53m) XPL

This sample consists of a mixed micrite and illite/sericite matrix that has been partially dolomitised. This mud forms highly corrosive contacts with surrounding detrital grains. Quartz grains are predominantly matrix supported but do display occasional point contacts. Some anhydrite cementation is evident at F1. Visual porosity is extremely poor.

Sample 154834 (1410.0m) PPL
Angular to sub-rounded quartz dominates this sample. These grains display point to concave/convex grain-grain contacts. Sorting is good with lamination defined by subtle changes in quartz grain size. Visual porosity is poor as most of the intergranular pore space is cemented by anhydrite.

Sample 154834 (1410.0m) XPL
Massive pore filling anhydrite is apparent in this view. Patchy replacement of anhydrite by calcite is evident (G2,B2). There is a weak, subhorizontal preferential alignment of quartz grains. Some trace secondary porosity is evident in this sample (eg F2) where anhydrite cements have been partially leached.

Sample 154860 (1395.95m) XPL
Displacive anhydrite growth is evident between F6 and J3. Several generations of anhydrite growth are possibly evident. The surrounding groundmass is composed of a partially dolomitised micritic mud. A 2mm thick sub-horizontal dolomite-rich bed is evident cutting across the top of this photomicrograph. Visual porosity is negligible.

Sample 154859 (1383.7m) PPL

This sample is composed of a poorly sorted matrix consisting of a complex mixture of illite/sericite and micritic mud and coarse silt sized quartz. A thin vein is evident cutting across this photomicrograph. This structure is predominantly composed of anhydrite but some replacement by microcrystalline calcite is evident at B6. Visual porosity is poor.

Sample 154858 (1372.95m) PPL

Quartz grains are sub-angular to sub-rounded and display point contacts. Very thin authigenic silica on a quartz grain is visible at E6. Microsparry siderite accumulation is located at A4-D4, F6 and F2/3. Intergranular pore space is mainly filled by anhydrite. Trace secondary porosity has developed as a result of leaching of anhydrite (eg E5).

Sample 154858 (1372.95m) XPL

Coarse sand-sized clasts of quartz, carbonate and an oncoid display predominantly point to convex/concave grain contacts. Some grains display sutured contacts elsewhere. The oncoid at E2-H1 displays micritisation especially at the grain margin. Trace authigenic silica is evident in C3-D3 Coarse anhydrite is developed as a cement on and between corroded margins of clasts. Visual porosity in this photomicrograph is poor.

Sample 154833 (1325.1m) PPL
Quartz grains and clasts are sub-angular to sub-rounded and generally display point or concave/convex grain-grain contacts. Clast lithologies include quartz, carbonate, and chalcedony and the matrix is mainly micritic mud with trace anhydrite cements. Visual porosity is extremely poor.

Sample 154833 (1325.1m) XPL

This sample is dominated by sub-angular to sub-rounded quartz and feldspar grains and rock fragments. Partial leaching of a dissolution of a feldspar grain is evident in F5. The intergranular pore space is filled by a mixture of poikilotopic calcite, microsparry calcite and dolomite. These cements form highly corrosive contacts with surrounding detrital grains partially overgrowing grain margins. Anhydrite cement is evident in E2. This cement is being partially replaced by carbonate cement. Some secondary pore space is evident within the anhydrite caused by the partial dissolution and leaching of the cement.

Sample 154857 (1227.95m) XPL
Quartz grains demonstrate sutured, concave/convex and point contacts in this view. An embayed quartz grain is evident at E3. Carbonate clast fragments are present at J6, I2 and A1-H1. Detrital grains are supported in a complex mixture of micritic mud and illite/sericite that has been partially dolomitised. Visual porosity is poor.

Sample 154857 (1227.95m) XPL
This photomicrograph display the micritised peloidal mud that dominates this sample. Detrital grains are dominantly matrix supported but display point to concave/convex contacts. Porosity is extremely poor.

Sample 154830 (1215.0m) PPL

Quartz grains are dominantly sub-rounded to well-rounded and display point to concave/convex contacts. Porosity is reduced in this sample due to the development of silica overgrowths, anhydrite cement filling intergranular space. Abundant nodular pyrite is evident at A5. A partially dolomitised siltstone clast is evident at C2.

Sample 154830 (1215.0m) XPL

This sample is dominated by polycrystalline and monocrystalline quartz, feldspar (H6), siltstone (B2), and carbonate clasts. Detrital grains and carbonate clasts are sub-angular to sub-rounded. Grain contacts are either point or concave/convex. Intergranular pore space is occupied by early anhydrite that has been replaced by drusy mosaic of calcite (D4) cement. Only trace porosity is evident in this sample.

Sample 154829 (1212.0m) PPL

This sample is massive and consists of poorly-sorted angular to sub-rounded quartz grains and clasts supported in a matrix consisting predominantly of illite/sericite. Visual porosity is extremely poor.

Sample 154829 (1212.0m) XPL

The sample is poorly sorted. Clasts and detrital grains range from 0.05mm to >2.0mm. The sample is composed of angular to sub-rounded grains of quartz, feldspar, and lithic fragments including oncoids that contain some incorporation of detrital quartz grains (B3). No visual porosity is evident in this photomicrograph as the pore space is completely filled by illite/sericite clays.

Sample 154828 (1100.15m) PPL

This sample is dominated by angular to sub-rounded clasts of quartz, sandstone, siltstone and chalcedony. Clasts are supported by matrix consisting of a mixture of micritic mud and illite/sericite. The sample is massive and poorly sorted with no visible porosity.

Sample 154828 (1100.15m) XPL
Microsparry calcite and dolomite is evident replacing a leached feldspar grain at C3. The sample is dominated by a mixture of micritic mud and illite/sericite which forms highly corrosive contacts with surrounding detrital grains. A single olivine crystal is evident in D6.

Sample 154856 (1076.65m) PPL

A large broken micritsed dolomite grain is evident cutting across this sample. It is surrounded by an authigenic cement consisting predominantly of medium crystalline dolomite. Pyrite (black) is evident marginally replacing coarser dolomite grains. Visual porosity is negligible.

Sample 154856 (1076.65m) XPL

Contact between authigenic medium crystalline dolomite and pyrite cement is evident between J6 and A2. Dolomite crystals display a xenotopic matrix of anhedral to subhedral shaped medium crystalline dolomite that displays planar, curved and sutured contacts. Dolomite cements marginally replace sub-rounded quartz grains. Authigenic pyrite (black) is evident replacing matrix and authigenic cements. Pyrite displays corrosive contacts with surrounding detrital grains. Visual porosity has been filled by authigenic cements.

Sample 154827 (1070.0m) PPL

This sample is dominated by sub-rounded quartz grains and chert, carbonate and siltstone rock fragments. Sutured and concave/convex grain contacts are well illustrated with several grains showing authigenic silica overgrowths (E4, I3). Calcite is locally developed on grain margins. The calcite cement partially replaces these grains and fills intergranular pore space. Intergranular porosity is poor in this sample.

Sample 154827 (1070.0m) XPL

This sample is dominated by angular to sub-rounded quartz that displays mainly sutured contacts. The degree of suturing between grains is variable. An authigenic silica overgrowth is shown on a quartz grain at F6 and a sandstone clast with aligned internal mica flakes is located at C4. Remaining intergranular space is filled by poikilotopic calcite cement that marginally replaces grains and fills intergranular pore space. This cement has been partially replaced by dolomite.

Sample 154826 (1062.0m) PPL
Sedarenite. This very poorly sorted sample consists of quartz, feldspar, carbonate, and chalcedony which display point to concave/convex grain-grain contacts. Chlorite and calcite form an extensive poikilotopic cement near B3. Large grain at F6 is clay ball, possibly volcanic in origin. Some trace porosity is evident in this sample.

Sample 154826 (1062.0m) XPL

Micritic calcite rimming a carbonate grain is evident between A3 and I1. The carbonate clast predominantly consists of an interlocking mosaic of anhedral dolomite crystals. A late stage of fbrous calcite growth is evident growing from the micritic surface into pore space. Quartz grains are generally medium sand sized, sub-rounded to rounded and display point contacts. A sandstone clast is also present (F6-J6). Visual porosity is poor.

Sample 154825 (1050.0m) PPL
Laminated quartz arenite. Subtle lamination can be detected by the variation in quartz grain size. Framework grains consist of mainly quartz, with some feldspar, muscovite, carbonate, chert and kaolinite (I3? brown). Grain contacts vary from point, concave/convex, to sutured. Visual porosity is good.

Sample 154825 (1050.0m) XPL

This sample consists predominantly of sub-angular to sub-rounded quartz grains and trace feldspar (J6). Framework grains display predominantly point to concave/ convex grain-grain contacts. Pore space has been filled by a partially dolomitised poikilotopic and microsparry calcite cement.

Sample 154824 (1000.1m) PPL
Quartz, and feldspar grains here show variable angularity. Kaolinite clasts are evident in D6 and B5. These clasts have been compacted and subsequently have expanded into intergranular pore space. Intergranular pore space is filled by partially dolomitised poikilotopic calcite cement.

Sample 154824 (1000.1m) XPL

This sample consists of predominantly of sub-angular to sub-rounded quartz grains and feldspar and carbonate and siltstone rock fragments. Detrital grain and rock fragments predominantly display point, to concave/convex and sutured grain contacts. The cement is predominantly calcite with minor ferroan calcite/dolomite. Visual porosity is poor.

Sample 154823 (995.0m) XPL

Framework grains are tabular to well rounded and display concave/convex to sutured contacts. Framework grains include sub-angular to sub-rounded quartz, feldspar and carbonate. Calcite is pervasively developed as a poikilotopic and microsparry intergranular cement. Visual porosity is poor.

Sample 154821 (970.0m) PPL
Sample is dominated by angular to sub-rounded, matrix supported quartz grains which are poorly sorted. The lower right of this photomicrograph displays a structure interpreted to possibly represent a burrow that has been partially calcite cemented (G6-J4). Visual porosity is poor.

Sample 154821 (970.0m) XPL
A large oncoid grain consisting of a large quartz grain dominates this photomicrograph. An irregular micritic rim is evident surrounding this grain. The remainder of the sample consists of angular to sub-angular, coarse silt sized quartz supported in a complex matrix consisting of illite/sericite and peloidal micritic mud. Visual porosity is extremely poor.

Sample 154820 (950.0m) PPL

This sample is dominated by sub-angular to sub-rounded quartz grains and rock fragments The sample is well-sorted and grains display point to concave/convex and moderately sutured grain-grain contacts. The sample is massive and contains minor porosity due to cementation of small poikilotopic calcite (D3). Shale clasts are evident in C4. These clasts have been compacted and subsequently have expanded into intergranular pore space flowing between detrital grains.

Sample 154820 (950.0m) XPL

The sample is dominated by sub-angular to sub-rounded, quartz grains displaying point to concave/convex contacts. A large microcline grain is evident at G2. Sub-rounded carbonate clasts are scattered throughout this photomicrograph (C3, B5). These clasts consist of an anhedral dolomite crystals. An elongated kaolinite clast is evident at C2. Porosity in this sample is poor as the pore space has been partially infilled by microsparry calcite and dolomite and traces of anhydrite.

Sample 154819 (939.0m) XPL

This sample is moderately well sorted, comprising of quartz, feldspar, carbonate, chert (I3), biotite clasts and kaolinite (B2). Grain contacts are commonly sutured or concave/convex. Poikilotopic calcite cement is evident encasing framework grains and filling intergranular pore space (E6). Visual porosity is poor.

Sample 154819 (939.0m) XPL

This sample is predominantly composed of angular to sub-rounded quartz grains displaying point, concave/convex and moderately sutured grain-grain contacts. Traces of carbonate clasts are evident in this sample at D6 and D4. These clasts consist predominantly of a xenotopic matrix of subhedral and anhedral dolomite. Pore space has been filled by poikilotoipic calcite cement (ie E5 and G5) and trace anhydrite (F6). Visual porosity is poor.

Sample 154817 (930.0m) PPL

This sample consists predominantly of angular to sub-angular quartz, chalcedony (A1) and carbonate fragments supported in a complex mixture of peloidal micritic mud and illite/sericite. The fine grained groundmass displays patchy alteration to chlorite. A carbonate clast is evident at C4. This clast is composed of a xenotopic matrix of anhedral to sub-hedral dolomite. A thin, wispy illite/sericite filled stylolite is evident under this clast. Visual porosity is poor.

Sample 154817 (930.0m) XPL
An example of calcite cement locally developed and contrasting illite/sericite and peloidal micrite mud matrix. A thick authigenic silica overgrowth is evident on the grain at B2. The calcite cemented structure in the left hand side of this photomicrograph is interpreted to be a remnant burrow (F6-A1). Visual porosity is extremely poor.

Sample 154853 (763.7m) PPL

The framework grains include rounded clasts of siltstone, angular to sub-rounded quartz and feldspar (B4) clasts. Grain contacts are point, concave/convex and weakly sutured with authigenic silica overgrowths not uncommon. Block anhydrite (I2), micritic siderite (C3), and calcite/ferroan calcite (F1) and dolomite are present as cement. Visible porosity is poor.

Sample 154853 (763.7m) PPL

Sedarenite. Coarse sand sized fragments of angular to sub-rounded quartz, chalcedony (E6) (containing folds?), carbonate grains (B5, and volcanic rock (J3) comprise the framework grains in this view. Note feldspar grains in an altered, cryptocrystalline groundmass of the volcanic rock. Grain contacts vary from point, concave/convex, and sutured, with some grains showing coaxial flattening. Authigenic silica is present on the margin of a quartz grain (G4). Chlorite (A4) and calcite (G6) form authigenic cement in this sample. Partial dissolution of volcanic fragments has resulted in the occurrence of trace secondary porosity in this sample.

Sample 154816 (749.0m) PPL

This sample consists of sub-angular to sub-rounded quartz and feldspar with traces of chert, volcanics (B1) and peloidal carbonate clasts (H2). Framework grains display point to concave/convex and moderately sutured grain-grain contacts. Calcite forms the majority of cement, however locally developed chlorite (B2) and dolomite is present. Visual porosity is poor.

Sample 154816 (749.0m) XPL

This sample is dominated by angular to sub-rounded quartz grains with traces of albite (A2) and rock fragments. These grains display point to moderately sutured grain-grain contacts. Carbonate clasts are evident scattered throughout (ie G4). These clasts have been flattened and compacted into intergranular pore space. Visual porosity is poor as most of the sample is cemented by microsparry and poikilotopic calcite cements.

Sample 154815 (691.0m) PPL

Primary intergranular porosity has been preserved in this sample with microcrystalline chlorite and calcite cements confined to thin coatings on grains (H3). Framework grains include quartz, feldspar, chert, kaolinite (D/E4) and carbonate. Carbonate clasts are predominantly composed of anhedral to subhedral dolomite.

Sample 154815 (691.0m) XPL

This sample is dominated by angular to sub-angular quartz grains in point, concave/convex and sutured grain contacts. Other framework grains include feldspar, carbonate clasts and chert. Framework grains are cemented by poikilotopic calcite and minor dolomite. The sample is poorly sorted and has moderate visible porosity.

Sample 154814 (682.0m) PPL

This sample consists predominantly of a complex illite/sericite and micrite matrix. Framework grains are dominated by sub-angular to sub-rounded quartz with trace shale fragments (G6), volcanics (G3) and carbonate clasts (D2). A cryptocrystalline volcanic is evident in C6. Visual porosity is poor.

Sample 154814 (682.0m) XPL

The sample is poorly sorted and consists of angular to sub-rounded quartz grains and carbonate, chalcedony, siltstone, and kaolinite fragments. Silica overgrowths are evident at E2. The matrix is composed of carbonate mud, with authigenic cements including, illite/sericite, chalcedony (ie B2) and late stage calcite. Primary and secondary porosity is poor.

Sample 154855 (677.0m) PPL

The sample comprises variable sized clasts of volcanic rock fragments, quartz, ooidal carbonate (I6), siltstone, sandstone, carbonate, and chert. Grain margins are either well-sutured or in point contact. The volcanic rock fragment in the lower left of the photomicrograph consists of brownish feldspar laths, greenish augite and pyrite. Visual porosity is good.

Sample 154855 (677.0m) PPL
Rock fragments in this view include volcanic rock (J2), and chalcedonic quartz (B4) that displays anhydrite grains developed as an early cement. A mosaic of equant dolomite is rimmed and overgrown by microsparry calcite (B/C1) and is inter-grown with microcrystalline quartz and coarse chlorite (G4) to form a variably extensive cement. Muscovite clast at H2/3.

Sample 154813 (675.0m) PPL

This sample consists of angular to sub-rounded clasts and quartz grains. Framework grains mainly display concave/convex or sutured grain contacts. Dominant clasts include, carbonate, volcanic rock, sandstone, chert, and siltstone. The large clast at D3 is a cryptocrystalline volcanic fragment that displays some alteration to chalcedony. Intergranular porosity is poor.

Sample 154813 (675.0m) XPL

Quartz grains and clasts are predominantly sub-angular to sub-rounded and poorly sorted. Clasts present include chert (D6) and biotite. The clasts generally display point or concave/convex contacts and are enclosed in a microsparry or poikilotopic calcite matrix with chlorite locally developed. The cements form highly corrosive contacts with surrounding detrital grains. A chert fragment composed of microcrystalline quartz is evident in E6.

Sample 154812 (644.0m) PPL

An ooidal limestone fragment is evident at C6. This fragment is composed of micritised ooids surrounded by equant drusy dolomite. The volcanic fragment in the right two-thirds of the view shows nepheline phenocrysts with trace augite. Pressure solution seam is evident between the two clast where compaction has caused the fluidisation and relocation of interstitial matrial. The matrix between the framework grains consists of quartz-feldspar clasts in an illite/sericite and micritic mud cement. Visual porosity is poor.

Sample 154812 (644.0m) PPL

The clasts are supported in a matrix of carbonate mud and are angular to sub-rounded. Several grains in this view show point contacts and include amygdaloidal basalt (G6), and other altered volcanic fragments. Most of these volcanic fragments have been heavily altered and a thin micritic rim is evident coating these grains.

Sample 154811 (617.5m) PPL

This sample consists predominantly of altered volcanic fragments. Volcanic fragments are composed of brownish feldspar grains and augite supported in a heavily altered cryptocrystalline matrix. The fragments display mainly point contacts. Intergranular pore space is filled principally by chlorite (G6) with some minor dolomite cementation (G6). Visual porosity is poor.

Sample 154810 (608.0m) XPL

Clasts show sub-angular to sub-rounded morphology. A thick authigenic silica overgrowth is evident at E6. The carbonate clast at J6 to E2 is mainly composed of a xenotopic matrix of subhedral to anhedral dolomite that has been partially micritised. A large poikilotopic calcite grain is evident to the right of the dolomite clast. A sandstone frament is evident at D2. This fragment consists predominantly of well-sutured quartz and mica. Visual porosity is poor in this sample.

Sample 154869 (598.23m) PPL

This sample is predominantly composed by a partially micritised illite/sericite mud with only trace porosity. An accumulation of quartz grains is evident in the left of this photomicrograph. These grains are typically sub-angular to sub-rounded and matrix supported but occasional point contacts are visible.

Sample 154854 (559.65m) PPL

Clasts are sub-angular to sub-rounded and poorly sorted. Clast types include sandstone, chert, volcanics (H6) and carbonate (D5). Grain contacts are mainly point contacts. Compaction is minimal in this sample and subsequently there has been good preservation of intergranular porosity. Some poikilotopic calcite is evident at I3, patchily filling pore space. A partially dissolved feldspar grain is evident at I6.

Sample 154854 (559.65m) XPL

This sample consists predominantly of moderately sutured rock fragments and minor quartz. A dolomitised carbonate fragment is evident from E3 to J6. This fragment displays some dissociation resulting in the formation of some secondary porosity (black). To the left of this fragment is a large chert fragment. This fragment is mainly composed of microquartz with patches of macroquartz. Calcite cement is well developed in the intergranular voids. This cement has been partially replaced by ankerite (G1). Visual porosity is very good in this sample.

Sample 154808 (498.0m) PPL

Clasts are sub-angular to sub-rounded and moderately sorted. Grain contacts are concave/convex or moderately sutured. The sample consists predominantly of sub-rounded quartz, chert, volcanic fragments (I5) and sandstone (C3). Authigenic silica overgrowths are present on some quartz grains (A5), and patch microcrystalline calcite forms a cement that has marginally replaced some grain margins. Visible porosity is good. Some secondary porosity is developed through the partial dissolution of volcanic fragments (J6).

Sample 154808 (498.0m) XPL

Clasts have concave/convex or sutured contacts. The sample is dominated by sub-angular quartz, and kaolinite, illite/sericite (C1) and carbonate (H6) rock fragments. Poikilotopic calcite is developed in intergranular pore space (ie I2). Minor dissolution of a feldspar grain is evident in C2.

Sample 154807 (490.05m) PPL

Clasts are sub-angular to sub-rounded and display point or concave/convex grain contacts. Framework grains that dominate this sample are sub-angular quartz and volcanics (B2). The volcanic fragments at B2 consist of feldspar laths supported in an altered cryptocrystalline matrix. Framework grains are supported by a complex mixture of illite/sericite and micritic mud. The matrix has been partially replaced by large dolomite rhombs (C4). Visual porosity is poor.

Sample 154806 (440.05m) PPL

The sample consists of sub-angular to sub-rounded quartz and feldspar grains and carbonate, phosphate (H5, E4/5), volcanic and chert rock fragments. Grain contacts are either concave/convex or sutured. Trace porosity is evident in this sample even though some porosity has been replaced by pyrite and calcite cements.

Sample 154806 (440.05m) XPL

This sample is dominated by sub-angular to sub-rounded quartz grains. An albite grain is evident at E3. Some of these grains as in E4 display partial dissolution and alteration. A compacted carbonate grain is evident at F2. This grain is composed predominantly of sutured sub-hedral and anhedral dolomite crystals. Pore space has been filled by a poikilotopic calcite cement and trace anhydrite. Visual porosity is poor.

Sample 154852 (420.1m) PPL

This sample consists of sub-angular to sub-rounded, coarse silt sized to fine sand sized quartz and feldspar. Other framework grains include carbonate clasts (H4).and shale fragments. A partially altered and dissolved feldspar grain is evident at C2. Intergranular porosity has been partially filled by dark illite/sericite mud (ie E5). Trace porosity is evident in this sample.

Sample 154852 (420.1m) XPL
Sample consists predominantly of sub-angular to sub-rounded quartz grains supported in a matrix primarily composed of illite/sericite. Dissolution and alteration of a feldspar grain is evident at G3. Altered grains have been partially replaced by poikilotopic calcite cement. Visual porosity is poor.

Sample 154851 (360.2m) PPL

The sample is dominated by sub-rounded to sub-angular quartz grains that display point contact or concave/convex contact with other grains. The matrix consists of micritic mud that displays intensive concentrations near framework grains. Trace pyrite is evident at G4 and unidentified organics are evident at E2. Visual porosity is good even though isolated dolomite rhombs are evident partially filling this porosity.

Sample 154850 (343.44m) PPL

This sample is dominated by sub-angular to sub-rounded quartz and feldspar grains. These grains display point to concave/convex grain-grain contacts. A partially dissolved chalcedony fragment is evident at H2. Volcanic fragments (D6) display partial alteration to a cryptocrystalline matrix. Framework grains are supported by a matrix consisting predominantly of illite/sericite with minor micritic alteration. Visual porosity is moderate.

Sample 154850 (343.44m) XPL

Sub-rounded to rounded quartz and feldspar grains dominate this sample. These grains are supported in a matrix consisting predominantly of illite/sericite that has been partially micritised. A partially altered volcanic fragment is evident in I5. A leached and marginally altered feldspar grain is evident in this rock fragment. Visual porosity is poor.

Sample 154804 (327.0m) PPL

Framework grains are sub-angular to sub-rounded and display mainly point contacts. A thin isopacous clay rim is evident on the outside of quartz grains.. This view shows one of many laminae in the sample with increased clay-illite/sericite and silt sized quartz content. Visual porosity is excellent. Clay rims have hindered the development of secondary cements and compaction in this sample is minimal.

Sample 154804 (327.0m) XPL

This sample consists predominantly of sub-rounded quartz grains, feldspar and carbonate and volcanic rock fragments. Detrital grains are all coated in a thick isopachous clay. Partial alteration and replacement of a feldspar grain by dolomite is evident at G4. The carbonate clast at H2 is composed of a xenotopic matrix of anhedral to subhedral dolomite. Pore space in this photomicrograph has been cemented by poikilotopic calcite (ie I4) that displays trace replacement by isolated dolomite rhombs (G5).

Sample 154803 (309.0m) PPL

The sample is well sorted and consists predominantly of sub-angular to sub-rounded quartz grains that display point, concave/convex and sutured grain contacts. Thin authigenic overgrowths are evident on some quartz grain boundaries. Replacement of a calcite grain by pyrite is evident at I2. A fractured and partially deformed illite/sericite grain is evident at F3. Other rock fragments evident in this sample include carbonate (J2) and volcanic G-J6. This sample has excellent intergranular porosity.

Sample 154803 (309.0m) PPL

Sample is dominated by sub-rounded quartz grains and feldspars. Quartz grains display thick authigenic silica overgrowths with triple junctions produced by the mutual interference of individual grain growths. An altered and partialy dissolved feldspar grain is evident at F3. A volcanic fragment displaying similar characteristics is evident at C2. Pore space has been partially replaced in J3 by anhydrite and calcite cements. Visual porosity is good in this sample (ie D5).

Sample 154849 (301.65m) PPL

This sample is dominated by sub-angular to sub-rounded quartz grains that display point, concave/convex and weakly sutured grain-grain contacts. Intergranular pore space is filled with illite/sericite matrix. An altered volcanic fragment is evident at B1. Trace Mica is evident scattered throughout this sample. The angular grain at E4 may be a shark tooth? composed of phosphate. Visual porosity is moderate.

Sample 154848 (301.4m) PPL

This sample is composed of coarse silt to medium sand sized, sub-angular to sub-rounded quartz grains. These grains have been cemented by a dark haematitic cement. Trace porosity is evident.

Sample 154848 (301.4m) PPL

This sample comprises predominantly sub-angular to sub-rounded quartz grains that display point, concave/convex and moderately sutured grain-grain contacts. This isopachous chlorite rims are evident coating detrital grains. A partially compacted dolomite clast is evident at D4. Pore space has been partially filled by haematite and calcite cements. Visual porosity is poor.

Sample 154802 (285.0m) PPL

This sample is dominated by sub-rounded quartz grains that display mainly point to concave/convex contacts. Other framework grains include carbonate (G4) and volcanic fragments (I2 and B2). Detrital grains are coated in a thin isopachous clay coating. Trace hamatite cementation is evident filling intergranular pore space. Porosity is good even though pore space has been partially infilled by authigenic chlorite.

Sample 154802 (285.0m) XPL

A large polycrystalline quartz grain is evident in the centre of this sample. This grains displays predominantly point contacts with surrounding sub-angular quartz grains and the chert fragment at B5. A poikilotopic calcite grain is evident filling pore space at I5. This clay coatings are evident on some framework grains (ie C2). Visual porosity is poor.

Sample 154801 (133.2m)

Quartz grains are sub-angular to sub-rounded and display point or concave/convex grain contacts. Vacuoles or fluid inclusions are evident in most detrital grains. An altered biotite grain is evident at F2. Detrital grains are coated in a thin illite/sericite mud. This mud is also evident partially filling intergranular pore space. The brown grain in the centre of the quartz grain in E4 is possibly spinel. Visual porosity is poor.

Sample 154847 (104.55m) PPL

Clasts are predominantly volcanic origin with the clast B6-E1 showing relic plagioclase outlines, secondary chlorite and a cryptocrystalline matrix. The coarse dolomitic clast (H3) shows former calcite in patches (pink) and encloses olivine grains (H5). This is probably an intensely altered ultramafic precursor. Poikilotopic calcite infills intergranular pore space.

Sample 154846 (67.8m) PPL

Most clasts show a rim of haematite cement. Grain boundaries are generally sutured or concave/convex. Framework grains include quartz and varied volcanic rock fragments. Possible spinifex textures in the grain located at H2. Euhedral calcite and poikilotopic calcite is developed as a cement (F5). Trace porosity is evident.

Sample 154846 (67.8m) XPL
This sample is dominated by altered volcanic rock fragments. Pore space between fragments is filled by poikilotopic calcite that displays highly corrosive contacts with surrounding grains (ie J6 to E2).

Sample 154465 (319.0m) PPL

This sample consists predominantly of sub-rounded quartz grains that display point to concave/convex grain-grain contacts. An altered feldspar (albite) grain is evident at I2. A thin isopachous clay coating is evident coating most framework grains. The dolomite clast in the bottom of this photomicrograph displays some pyritic alteration. Intergranular pore space has been partially filled by poikilotopic calcite, illite/sericite and dolomite cements (C2). Visual porosity is moderate.

Sample 154466 (1060.05m) PPL

This sample consists predominantly of bimodally sized quartz grains that define an irregular lamination. Laminae containg the finer quartz fraction have been selectively compacted. Grains are predominantly sub-rounded to rounded and display point to concave/convex grain-grain contacts. Shale fragements and chlorite cements are scattered throughout this sample filling intergranular pore space. Visual porosity is good.

APPENDIX D (Summary Table of mineralogy)

| | | Framework Grains | | |

| | | |

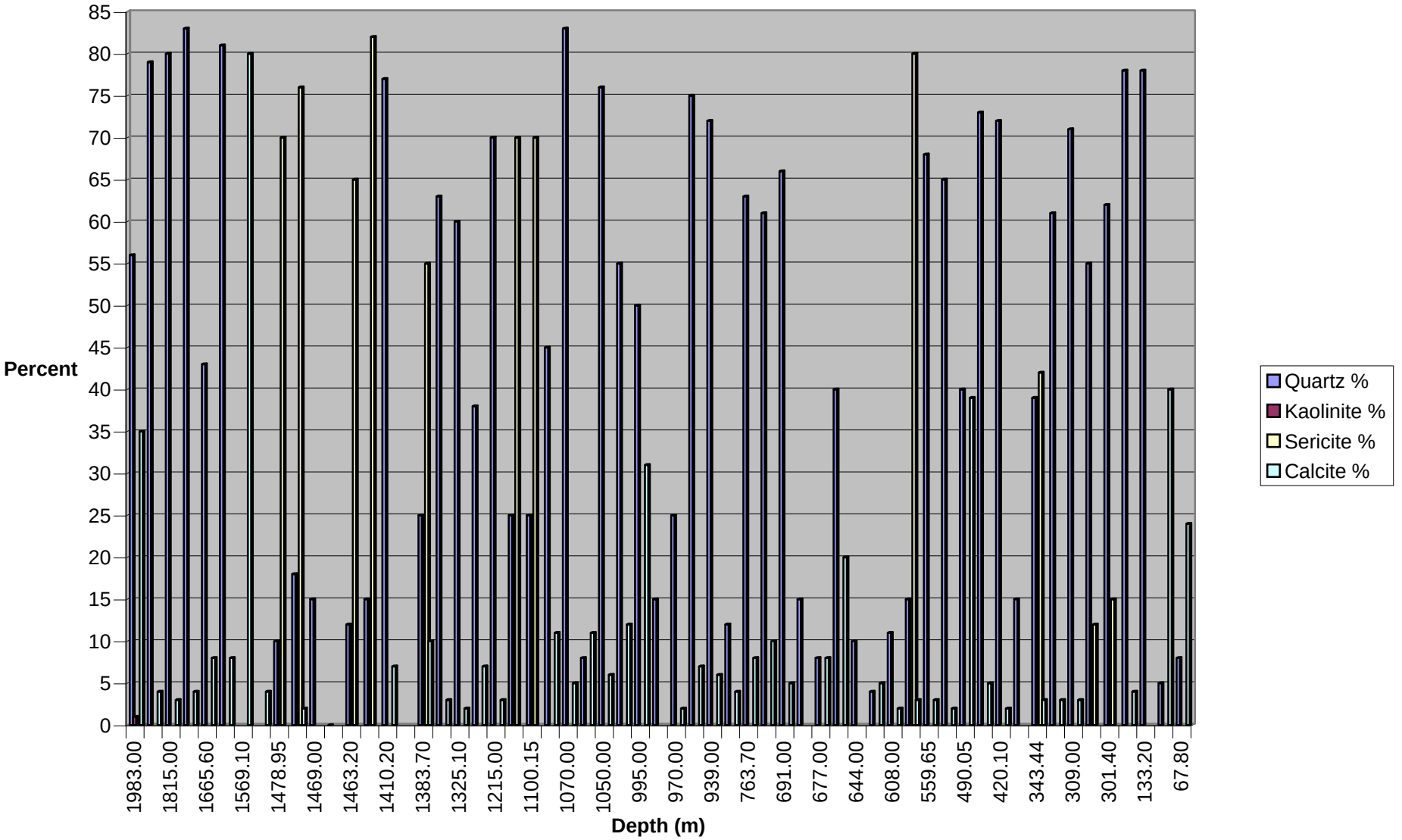
Percent
85
80
75
70
65
60
55
50
45
40
35
30
25
20
15
10
5
0
1983.00
1815.00
1665.60
1569.10
1478.95
1469.00
1463.20
1410.20
1383.70
1325.10
1215.00
1100.15
1070.00
1050.00
995.00
970.00
939.00
763.70
691.00
677.00
644.00
608.00
559.65
490.05
420.10
343.44
309.00
301.40
133.20
67.80
Depth (m)
Quartz %
Kaolinite %
Sericite %
Calcite %

Appendix 3

Palynology of samples from Vines 1

by K. Grey

Introduction

Palynological studies were carried out on 62 conventional core samples from Vines 1 (Table 3.1). This report presents only preliminary results because of the complex nature of the biota. All samples appear to show extensive reworking and redeposition, and further investigation is needed to determine the age and provenance of the various fossils recovered. As discussed below, Vines 1 contains a mixed assemblage that includes four components. At present, none of the components appear to be in situ. Components 1 and 2 are probably the result of contamination. Components 3 and 4 are not well preserved, and it is probable that both are reworked from older sediments. Consequently, no direct determination of depositional age is possible although some limits are imposed by the species identified. As discussed below, they denote only the age of the sedimentary rocks in the provenance area, not the age of the Vines 1 core itself.

Samples were processed by Laola Pty Ltd using a modified preparation technique for Proterozoic samples, which eliminates harsh and vigorous treatments that might fragment large or delicate specimens (Grey, 1998, 1999a). It became apparent as sample logging progressed that this processing technique may have introduced a bias in favour of Component 4 (the mid-Neoproterozoic component) of the mixed assemblage. In particular, oxidation by nitric acid, required to remove high levels of surface encrustation by pyrite framboids, may have eliminated, or at least partially destroyed features of younger, less robust specimens. So far, one sample has been reprepared to exclude oxidation and it yielded a higher proportion of Component 3 specimens, which were better preserved than in other, more oxidized preparations.

Maturity was determined using the thermal alteration index (TAI; see Traverse, 1988, p. 431–435, Pl. 1). The index was devised for Phanerozoic spores and pollen and needs to be applied with caution to Proterozoic samples, since the colour variation shown by Proterozoic acritarchs and other biogenic material may be slightly different and is not well calibrated. In spite of the limitations, the colour of Proterozoic biogenic matter is still a useful guide to maturity, and is mostly consistent with results obtained using organic geochemistry.

Slides will be placed in the Geological Survey of Western Australia Petroleum Exploration Relinquishment Collection (PERC) on completion of the current studies.

Palynological observations

The yield of palynomorphs varied throughout the section examined. The fragmented nature of many specimens indicates extensive reworking; a result entirely consistent with the lithology, which is mostly diamictitic in the upper part and mostly turbiditic below 1632.0 m. A very high-energy regime is indicated throughout, which is essentially inimical to palynomorph preservation. In many samples only the more robust taxa seem to have survived erosion and transportation, and even these are represented by small fragments that fortunately preserve a distinctive morphology. None of the components are considered to be in situ (i.e. contemporaneous with the time of deposition).

Table 3.1. Sample details and distribution of palynomorph components in Vines 1

GSWA No.	*Depth (m)*	*Comments*	*Contaminants*	
			Plant material	*Pollen grains*
154878	64.56	barren	–	–
155082	66.40	barren	–	–
154879	69.37	barren	–	–
155083	88.80	barren	–	–
155168	311.25	barren	–	–
155084	335.50	barren	–	–
155085	355.00	palynomorphs present	x	–
155086	372.80	palynomorphs present	x	–
155142	398.75	palynomorphs present	–	–
155087	409.00	no identifiable palynomorphs	x	–
155101	434.10	palynomorphs present	–	–
155088	477.00	barren	–	–
155169	520.60	palynomorphs abundant	–	–
155102	556.10	no identifiable palynomorphs	x	–
155089	586.20	barren	–	–
155090	605.70	barren	–	–
155103	694.75	palynomorphs present	x	–
155091	723.45 – 723.50	no identifiable palynomorphs	–	–
155104	723.50	palynomorphs present	x	x
155105	799.50	palynomorphs present	–	–
155106	828.10	no identifiable palynomorphs	–	–
155107	836.70	barren	–	–
155108	977.70	palynomorphs abundant	x	–
155109	987.20	palynomorphs abundant	x	–
155110	1 068.80	barren	x	–
155092	1 068.95	palynomorphs abundant	x	–
155111	1 116.50	palynomorphs present	–	–
155093	1 138.82	palynomorphs present	–	–
155094	1 139.73 – 1 139.79	barren	–	–
155095	1 149.05 – 1 149.09	palynomorphs present	x	–
155112	1 320.90	palynomorphs present	–	–
155113	1 422.15	palynomorphs present	–	–
155096	1 464.08 – 1 464.13	no identifiable palynomorphs	x	x
155098	1 478.93 – 1 479.05	barren	–	–
155116	1 571.40	palynomorphs present	–	–
155117	1 654.50	palynomorphs present	–	–
155118	1 672.40	palynomorphs present	–	–
155119	1 679.70	palynomorphs abundant	–	–
155120	1 685.35	palynomorphs abundant	x	–
155121	1 709.00	palynomorphs abundant	x	x
155122	1 739.80	palynomorphs abundant	x	x
155123	1 747.55	palynomorphs abundant	–	–
155124	1 774.20	palynomorphs present	–	–
155125	1 823.60	palynomorphs present	–	–
155143	1 840.50	palynomorphs abundant	–	–
155126	1 861.55	palynomorphs present	–	–
155127	1 897.20	palynomorphs present	–	–
155128	1 906.30	palynomorphs present	–	–
155129	1 918.95	palynomorphs present	–	–
155130	1 928.75	palynomorphs abundant	–	–
155131	1 940.10	palynomorphs abundant	–	–
155132	1 946.70	palynomorphs present	–	–
155133	1 960.10	palynomorphs present	–	–
155134	1 970.00	palynomorphs abundant	–	–
155135	1 975.45	palynomorphs present	x	–
155136	1 986.80	palynomorphs abundant	x	x
155137	1 992.60	palynomorphs present	–	–
155138	1 999.20	palynomorphs abundant	x	x
155139	2 002.45	palynomorphs present	x	–
155140	2 007.95	palynomorphs present	–	–
155170	2 012.95	barren	–	–
155171	2 015.20	barren	–	–
155141	2 017.50	palynomorphs present	–	–

Organic material is absent or sparse in the diamictite-dominated section, but increases significantly in the turbidite-dominated section. Most samples contain a high percentage of unidentifiable amorphous fragments of organic material. Some of these appear to be degraded mat material, but there is also a large component that is probably derived from degraded acritarch vesicles. Mostly, the degree of fragmentation decreases downhole, and there is a corresponding increase in the number of more delicate specimens. Preservation of recognizable palynomorphs is universally poor throughout the drillhole. Nearly all specimens recorded above 1632.0 m are either highly fragmented, badly corroded, or both. Those below this depth are somewhat better preserved, and several whole specimens of large (c. 100–200 µm diameter) acritarchs are present. Smaller, spherical acritarchs (c. 30 µm in diameter) are present in nearly all samples from the turbidite interval, but are either less common or absent in the diamictite interval.

The taxonomic composition of the assemblage shows little variation throughout the drillhole. Four components have been recognized.

Component 1

This is the youngest component in terms of the palynomorphs present, and consists of extant pollen grains that are probably a result of airborne contamination. They can be readily distinguished, not only by their morphology but also by their low degree of thermal maturity. Some slides contain as many as 20 grains and therefore steps are being taken to monitor and reduce the degree of airborne pollen contamination in future preparations. A species of *Pinus* predominates, and since the vegetation near the drillsite comprises Australian native sandplain species, the most likely source is windborne pollen from pine plantations around the Perth area during laboratory preparation.

Component 2

Component 2 comprises plant fragments that show a low degree of thermal maturity. The fragments appear to be contaminants, but are common in several samples, and in one case, survived ultrasonic cleaning prior to sample dissolution. The origins of this material and probable source of contamination are currently being investigated, but it is thought that it may have been introduced in the drilling mud. Based on the pale colour and the complex tissue structure, the material appears to be recent in origin. A Devonian or younger age is possible, based on the presence of vascular tissue, but the low thermal maturity is inconsistent with an early or middle Phanerozoic age. In addition, if the plant material was derived from a nearby land mass, the samples might also be expected to contain abundant spores of the same age. However, no spores were recovered.

Component 3

Component 3 consists of thin-walled occasionally ornamented acritarchs of uncertain age. The acritarchs are usually lighter in colour than those deemed to belong to Component 4, indicating a lower thermal maturity. In unoxidized kerogen mounts they have a TAI of about 2+, whereas those of Component 4 have values of 3 or more. The relatively lower thermal maturity suggests that Component 3 is younger than Component 4.

Component 3 specimens are typically much smaller than those of Component 4. Most are about 30 µm in diameter, whereas the smallest taxa in Component 4 usually have a diameter of about 50 µm, and the larger, more robust species range from about 100 to >250 µm in diameter. Many specimens assigned to Component 3 are ruptured

or badly corroded, and they may have large holes caused by the dissolution of pyrite framboids from nitric used acid during the oxidation process. However, some appear to have openings that have a consistent shape and structure, and these may be archeopyles (excystment structures).

Component 3 is poorly represented in samples from the diamictite-dominated interval, but forms a significant percentage in some samples below 1660.0 m, comprising up to 40% of identifiable specimens. In other samples the percentage is much lower, sometimes <10%. However, because of the preparation techniques used, the small quantity may reflect the degree of nitric acid oxidation rather than the actual percentage of the assemblage. Examination of the taphonomy and mode of preservation indicates that the palynomorphs are reworked, although they are typically better preserved than Component 4. The age of the sedimentation in Vines 1 therefore probably post-dates the age of Component 3. Species identification and attempts to provide better age constraints for Component 3 continue, but as discussed below, a latest Neoproterozoic – earliest Cambrian age for the palynomorphs seems most likely.

Component 4

The fourth component includes palynomorphs diagnostic of a mid-Neoproterozoic age (mid- to late Cryogenian; c. 750 to 700 Ma) belonging to 'Assemblage 2' of Grey and Cotter (1996). It is comparable with an assemblage recorded in other Officer Basin drillholes (Zang, 1995a,b; Grey, 1995a,b, 1999b, 2000; Grey and Cotter, 1996; Grey and Stevens, 1997; Cotter, 1997, 1999; Hill et al., 2000). Specimens forming this component are mostly darker than those of Component 3, and in unoxidized kerogen mounts have a TAI of 3 to 3+, and up to 4 near the base of the drillhole.

Many samples above 1632.0 m contain only a few fragments of robust acritarch species, together with badly degraded filaments. Other types of palynomorph, such as leiospheres and coenobial aggregates are uncommon. The number of whole specimens and the size of fragments increases in the turbiditic interval below 1632.0 m, and there is a marked increase in the number of leiospheres and coenobial aggregates.

The most distinctive palynomorphs belong to two species of large wrinkled acritarch, *Cerebrosphaera buickii* and *C. ananguae*. Fragments of the large, thick-walled, smooth-surfaced acritarch *Chuaria circularis* are found in some samples. Also present are fragments and rare whole specimens of leiospheres belonging to the species *Leiosphaeridia crassa, L. jacutica, L. minutissima,* and *L. tenuissima.* Colonial clusters of *Synsphaeridium* sp. and species of *Satka*, both commonly showing signs of fragmentation, are present in certain samples. Fragments of colonies of *Myxococcoides cantabrigiensis* and *Ostiana microcystis* are rarer. Many samples contain poorly preserved filaments, mostly belonging to species of *Siphonophycus*.

Biostratigraphy

Biostratigraphic analysis of Vines 1 is difficult because of the degree of reworking and level of contamination. A preliminary assessment of the age and significance of each of the components is presented here, and comparisons are made with selected drillholes in an effort to provide some constraints on the age of the Vines 1 succession.

Many of the Neoproterozoic taxa observed, particularly those assigned to Component 4, are long ranging conservative species. In Australia, as elsewhere in the world (Knoll, 1996), age determination is handicapped by gaps in the biochronological record. The late Cryogenian (Sturtian Epoch, latest Riphean, between about 750 and

600 Ma), Marinoan glacial (c. 600 Ma), and latest Neoproterozoic – earliest Cambrian (c. 545 Ma) successions are poorly documented, and so there are few descriptions available for comparison. However, assemblages in between these intervals, and both younger and older than them, are well documented from the Officer and Amadeus Basins and the Adelaide Rift Complex (Damassa and Knoll, 1986; Zang and Walter, 1989, 1992; Zang, 1991, 1994, 1995a,b, 1997; Zang and McKirdy, 1994; Grey 1995a,b, 1998, 1999b; Grey and Cotter, 1996; Gravestock et al., 1997; Grey and Stevens, 1997; Cotter, 1997, 1999, Hill et al., 2000). Diagnostic species of certain better documented intervals have not been recognized, thereby providing some restrictions on timeframes.

Components 1 and 2

Components 1 and 2 are here treated as contaminants, although it is difficult to explain the abundance of plant tissue throughout the succession. At present, the most likely source for this material seems to be the drilling mud, although investigations so far have failed to confirm this.

Component 3

Component 3 is considered to be of latest Neoproterozoic – earliest Cambrian age. This is because well-developed archeopyles do not seem to have been reliably recorded earlier than this, and distinctive acritarchs found in younger and older palynofloras are absent. To date, a single specimen with processes of a type associated with the Ediacarian complex acanthomorph-dominated palynoflora (ECAP) of Grey (1998) has been observed, suggesting that Component 3 might postdate the main ECAP development.

The age of the ECAP is Neoproterozoic III, and it is restricted to c. 565–590 Ma in Australia (Walter et al., 2000). The ECAP is equivalent to the Volhyn–Redkino biochron of northern Europe (Vidal and Moczydlowska-Vidal, 1997) and the Doushantuo biota of China (Yin and Li, 1978; Awramik et al., 1985; Yin, L., 1985a,b, 1991; Yin, C., 1990; Yin and Gao, 1996). Vidal and Moczydlowska-Vidal (1997) estimated a restricted time span of less than 50 m.y. for this distinctive palynoflora, before most species became extinct.

Very few assemblages have been described from the post-ECAP, latest Neoproterozoic – earliest Cambrian of Australia (or elsewhere in the world). In many successions there is a hiatus in sedimentation, and even where continuous sedimentation might have taken place, lithologies are mostly unsuitable for palynological preservation. An impoverished palynoflora of simple leiospheres has been noted (Damassa and Knoll, 1986; Zang and Walter, 1992; Zang *in* Gravestock et al., 1997; Grey, 1998), but never properly documented.

Both latest Neoproterozoic – earliest Cambrian and Cambrian biostratigraphy have been investigated in more detail in northern Europe, where a zonal scheme for the Early Cambrian has been erected (Moczydlowska, 1991). As in the European succession, only a few species are present in Component 3, and they are mainly simple leiospheres, although a few with more complex features have been observed.

Preliminary comparisons indicate that the Component 3 palynomorphs may correspond to species recorded from the Kotlin – (lower) Rovno biota of the Lublin Slope, East European Platform (Vidal and Moczydlowska-Vidal, 1997). The Kotlin–Rovno palynoflora is a depauperate (substantially reduced intensity), late Vendian to earliest Cambrian microbiota that is estimated to be c. <551 Ma in age, and which straddles the Proterozoic–Cambrian boundary. Component 3 therefore possibly indicates a latest Neoproterozoic – earliest Cambrian age.

None of the small (10–50 µm in diameter) spiny acritarchs belonging to genera such as *Skiagia* have been recognized. Consequently, it seems unlikely that the component is as young as the *Asteridium tornatum – Comasphaeridium velvetum* Acritarch zone recognized just above the base of the Cambrian in northern Europe (Moczydlowska, 1991). Because most Cambrian and younger successions contain distinctive species, none of which have been identified in Vines 1, an age younger than earliest Cambrian for Component 3 is very unlikely.

Depauperate assemblages of simple forms are also associated with both the Sturtian and Marinoan glaciations, although these intervals are very poorly documented (Vidal and Moczydlowska-Vidal, 1997). The simple leiosphere *Leiosphaeridia crassa* is usually present in significant numbers in both glacial intervals, whereas *L. crassa* forms only a small percentage of the assemblage in Vines 1 samples. None of the more restricted taxa recorded from glacial intervals have been observed in Vines 1. In addition, the presence of possible archeopyles suggests that correlation with either glacial interval is less likely than with a latest Neoproterozoic one.

Component 4

Limited age control for Component 4, the Neoproterozoic component, is provided by the known ranges of certain species. The assemblage is characterized by the presence of *Cerebrosphaera buickii*, *C. ananguae*, and *Chuaria circularis.*

Cerebrosphaera buickii has so far only been recorded from the younger part of Supersequence 1 in Australia (Grey and Cotter, 1996; Cotter, 1999; Hill et al., 2000) and the Svanbergfjellet Formation of Spitsbergen (Butterfield et al., 1994). In the western Officer Basin, it first appears in the middle Hussar Formation and then ranges through the Kanpa and Steptoe Formations. In the northern Adelaide Rift Complex, it has been recorded in the middle Burra Group (Hill et al., 2000), which is probably similar in age to the upper Hussar Formation. It is usually a dominant species throughout this interval; however, the upper extent of its range has not been determined. It was not recorded from the Steptoe Formation in Kanpa 1A (Cotter, 1999), although it is present in the lower Steptoe Formation in Empress 1A (Grey, 1999b). It may range into the Sturtian Epoch, but has not been found in samples above the Marinoan glaciation. In Spitsbergen the species is present in the Svanbergfjellet Formation in 'pre-Vendian' (older than c. 600 Ma) rocks (Butterfield et al., 1994).

Cerebrosphaera ananguae is another robust form that differs from *C. buickii* in having coarser, broader intertwining folds (Cotter, 1999), and which has a similar stratigraphic distribution to *C. buickii*. Neither of these taxa have been recorded from the Alinya Formation in Giles 1 in the eastern Officer Basin (Zang, 1995a), nor in the Browne Formation and its lateral equivalents in the western Officer Basin. From the available data, these two species appear to be restricted to the younger part of Supersequence 1, but may extend into Supersequence 2, for which only limited data is available. Many of the other species associated with *Cerebrosphaera* have been found in the Browne Formation and reported from even older rocks around the world, but *Cerebrosphaera* itself appears diagnostic of rocks younger than about 770 Ma.

Chuaria circularis, another robust species, is present in small numbers throughout the section studied. According to Talyzina (2000), it ranges from the early Neoproterozoic (late Riphean) and predates the Varanger (=Marinoan) glacial event. Some records suggest that it might range into the Cambrian (Haines, 1998), but none of these records have been confirmed. In particular, reports of *C. circularis* in rocks younger than the Marinoan glaciation are difficult to substantiate. Damassa and Knoll

(1986) and Grey (1998) reported *Chuaria* cf. *C. circularis* from the Arcoona Quartzite Member (Tent Hill Formation), an equivalent of the ABC Range Quartzite of the Adelaide Rift Complex, but the relationship of this form to the species sensu stricto, is not clear. Structures described by Zang (1997) as poorly preserved megascopic *Chuaria* and associated *Tawuia* from the ABC Range Quartzite and Wonoka Formations, appear to be carbonaceous flakes of uncertain affinity. However, despite a few anomalous records, the majority of records of *C. circularis* are confined to pre-Marinoan successions.

In Australia, various species of filamentous bacteria, in particular *Siphonophycus* spp., and acritarchs, particularly *Satka colonialica* and *Leiosphaeridia* spp., were previously recorded from the early to mid-Cryogenian. They were particularly noted in the Browne, Skates Hills, Hussar, Kanpa, and Steptoe Formations, and the Tarcunyah Group of the western Officer Basin (Grey and Cotter, 1996; Grey and Stevens, 1997; Cotter, 1997, 1999; Grey 1999b), the Alinya Formation of the eastern Officer Basin (Zang, 1995a), and the Bitter Springs Formation in the Amadeus Basin (Zang and Walter, 1992). Most of these species range from the late Mesoproterozoic to early or mid-Neoproterozoic (mid- to late Riphean), as documented in Russian, northern European, and Canadian successions. However, several key species that are restricted to the latest Mesoproterozoic and earliest Neoproterozoic, such as *Valeria lophostriata* and *Trachyhystrichosphaera aimika*, have not been observed in any of the Vines 1 samples, so the age of Component 4 is probably younger than early Neoproterozoic, and therefore younger than 850 Ma (Knoll, 1996).

From the above assessment of species ranges, many of the reworked palynomorphs in Component 4 must have been derived from the middle Hussar Formation or younger rocks. Most of the longer ranging species were probably also derived from that source. However, because of their long-ranging stratigraphic distribution, there remains a possibility that some palynomorphs were reworked from the Browne Formation or its lateral equivalents, giving rise to a mixture of lower and upper Supersequence 1 assemblages.

Component 4 does not appear to be younger than the Marinoan glaciation because no typical ECAP species, common from c. 580 Ma to shortly before the beginning of the Cambrian (Zang and Walter, 1992; Gravestock et al., 1997; Grey, 1998), were observed. This indicates that the Vines 1 assemblage does not contain a component equivalent in age to the upper Ungoolya Group of the eastern Officer Basin (Morton, 1997).

Leiosphaeridia crassa is present throughout Vines 1 and supports the interpretation that the assemblage is pre-Marinoan in age. *L. crassa* is a common species in early and middle Neoproterozoic rocks, but is rarely dominant, except for a short time after the Marinoan glaciation (c. 600 Ma) where it forms more than 80% of the taxa recorded (Damassa and Knoll, 1986; Grey, 1998). It is very rare thereafter.

Component 4 palynomorphs are present in both the diamictite- and turbidite-dominated sections of Vines 1. Several species in this component indicate derivation from rocks of middle Hussar Formation or younger rocks, but probably no younger than the Marinoan glacigenic succession. At present, the upper age range of many 'Assemblage 2' species remains uncertain because of limited study of this part of the succession (Grey, 1995a; Grey and Cotter, 1996; Grey and Stevens, 1997; Cotter, 1999; Hill et al., 2000). However, very few 'Assemblage 2' species are known from rocks as young as the middle of Supersequence 3 (Ediacarian), and none of the distinctive ECAP process-bearing species have been recognized in Vines 1. A latest Supersequence 1, or possible Supersequence 2 age is the most probable for Component 4 of the Vines 1 assemblage.

Discussion

The significance of the Vines 1 assemblage is best determined through comparison with selected drillholes in the Officer Basin and Adelaide Rift Complex. These drillholes provide information on other diamictite units and on the potential provenance of reworked Vines 1 palynomorphs. Assigning a definitive palynological age to rocks in Vines 1 is not feasible because of the extensive reworking throughout the succession.

Comparison with Empress 1 and 1A assemblages

Although Vines 1 contains many species also observed in Empress 1A drillcore (Stevens and Apak, 1999) within the middle Hussar to Steptoe Formations, and a few forms ranging down into the Browne Formation (Grey, 1999b), the main difference is the mode of preservation. Most specimens in Empress 1A are whole and show little evidence of degradation. By contrast, nearly all specimens in Vines 1 are badly corroded and highly fragmented. Nevertheless, Component 4 of the Vines assemblage is very similar in composition to the *Cerebrosphaera*-dominated assemblage in Empress 1A, and a provenance from upper Supersequence 1 rocks, similar to those in Empress 1A, is indicated.

Diamictites in Vines 1 and Empress 1A show interesting contrasts. Empress 1A samples, with one exception, are almost entirely devoid of organic material and contain no identifiable palynomorphs (K. Grey, unpublished data). Only a single sample, from silty mudstone at 462.1 m, yielded fragments of amorphous organic material and sparse palynomorphs. The palynomorphs comprise a single specimen of *Leiosphaeridia minutissima*, two specimens of *Synsphaeridium* spp. (all long ranging taxa), and one fragment each of *C. buickii* and *C. ananguae.* This contrasts with Vines 1, in which organic debris and identifiable palynomorphs, while never abundant, are more common.

The diamictite unit in Empress 1A was assigned to the ?Lupton Formation, and interpreted as Marinoan in age because of the presence of a cap dolomite, and limited carbon isotope and stromatolite correlations (Grey et al., 1999; Walter and Hill, 1999). Despite the presence of fragments of the two species of *Cerebrosphaera* in both drillholes, there is nothing to suggest that the successions are of the same age, only that they were derived from a similar source.

Comparison with other western Officer Basin assemblages

No wells or drillholes in the western Officer Basin other than Empress 1A and possibly Talbot 5 have penetrated known Neoproterozoic diamictite, although the *Cerebrosphaera* assemblage is well represented in several wells (Cotter, 1999). A poorly documented leiosphere-dominated assemblage (‘Assemblage 4’ of Grey and Cotter, 1996) has been recorded from sidewall cores between 900 and 1000 m in Yowalga 3. Further investigation of the Yowalga 3 samples is required to determine whether there are any similarities between ‘Assemblage 4’ and Component 3 of Vines 1. Current data suggest that the taxa are not really similar, but a detailed comparison is needed to confirm this.

Comparison with Birksgate 1 assemblages, eastern Officer Basin

Birksgate 1 in South Australia is the closest well to Vines 1, but penetrates a very different succession. Palynological studies indicate that the base of Birksgate 1 most probably lies in the Alinya Formation and is of Supersequence 1 age (Grey, 1999c). The middle part of the well most probably coincides with the Dey Dey Mudstone, Karlaya Limestone, and Tanana Formation, and is therefore of middle Supersequence 3

age. This interpretation differs considerably from previously published interpretations, and indicates that some re-interpretation of well-logs and seismic line correlations (in particular the AGSO Deep Seismic Line 93AGS.01) is warranted. *Cerebrosphaera buickii* was not recorded from Birksgate 1. It appears that Vines 1 and Birksgate 1 have little in common stratigraphically or palynologically.

Comparison with Nicholson 2

A recently examined assemblage from Nicholson 2, which penetrated the Chambers Bluff Tillite along the northern margin of the eastern Officer Basin, contains an assemblage interpreted as uppermost Supersequence 1 or lowermost Supersequence 2 (Grey, 2000). The presence of partially fragmented *C. buickii* indicates that it is younger than the deposition of the middle Hussar Formation, and the lack of ECAP species suggests that it is unlikely to be as young as the Marinoan glaciation. Although there is a possibility that 'Assemblage 2' fossils are present in the Chambers Bluff Tillite as a consequence of reworking, the good preservation of many of the specimens reduces this possibility. While not entirely diagnostic, the assemblage is consistent with a late Cryogenian age (c. 770–650 Ma), and supports a probable Sturtian age for the Chambers Bluff Tillite. However, Sturtian successions require more study to confirm the nature of palynomorph assemblages in this period. Samples from Blinman 2, which penetrated Sturtian-age diamictites in the Adelaide Rift Complex, were barren (K. Grey, unpublished data).

Preservation in Nicholson 2 is mostly better than in much of the upper part of Vines 1, although many specimens are fragmented. However, no Component 3 acritarchs were noted, which suggests that the diamictites in Nicholson 2 and Vines 1 do not correlate, and that the Vines 1 succession is younger than the Chambers Bluff Tillite.

Environment

Environmental interpretation is difficult because of the extensive reworking. Deposition of the original sedimentary rocks probably took place in a shelfal to open marine area, although the presence of filaments and some degraded mat fragments indicates the probable proximity of a benthic microbial community in a near-shore environment. Most of the palynomorphs suffered severe fragmentation and corrosion during subsequent erosion and transportation.

Maturity

Maturity was determined using TAI (Traverse, 1988). Palynomorphs from Vines 1 show mixed levels of maturity, which probably relates only to the maturity of the rocks from which they were derived. A TAI of 2+ to 3 (within the oil generation window) was common for simple leiospheres considered part of Component 3, whereas those from Component 4 showed maturities of 3 to 3+. There is a slight, but regular increase downhole, with samples near TD showing maximum values of 4, which could represent a later overprint.

Conclusions

Palynological evidence is inconclusive with respect to the age of successions in Vines 1. The assemblage contains elements of 'Assemblage 2' of Grey and Cotter (1996), here referred to as Component 4. This component was previously recorded from the youngest

Supersequence 1 rocks of the western Officer Basin (Hussar, Kanpa, and Steptoe Formations), and possibly extends into rocks of Sturtian glaciation age in Nicholson 2 in the eastern Officer Basin. Species most indicative of a mid- to late Cryogenian age are *Cerebrosphaera buickii* and *Chuaria circularis*, but the fragmented and corroded nature of the mid-Neoproterozoic specimens, together with the presence of a younger, possibly latest Neoproterozoic – earliest Cambrian component (Component 3), indicates that most palynomorphs were derived during extensive reworking of exposed sedimentary rocks. Deposition of the Vines 1 succession therefore took place at a time when mid-Cryogenian and latest Neoproterozoic – earliest Cambrian rocks were exposed and subject to rapid erosion. No depositional age can be determined from the palynomorph assemblage, although a maximum age of latest Neoproterozoic – earliest Cambrian seems probable. It is unlikely that the succession is much younger than earliest Cambrian because no later Cambrian forms have been recognized. Likewise, no mid-'Neoproterozoic III' palynomorphs have been recognized, inferring that deposition was younger than this.

Acknowledgments

This study relied heavily on material and data from South Australia made available by Primary Industry and Resources of South Australia (PIRSA) and M. R. Walter and P. Gorjan of Macquarie University. Thanks to Nick and Carolyn Eyles who sampled Nicholson 2. Contamination levels were assessed with the help of J. Backhouse. Palynological preparation was carried out by Laola Pty Ltd.

List of taxa cited

Asteridium tornatum (Volkova 1968) Moczydlowska 1991

Cerebrosphaera buickii Butterfield 1994 *in* Butterfield, Knoll, and Swett, 1994

Cerebrosphaera ananguae Cotter 1999

Chuaria circularis Walcott 1899; emend. Vidal and Ford 1985

Comasphaeridium velvetum Moczydlowska 1988

Leiosphaeridia Eisenack 1958, emend. Downie and Sarjeant 1963

Leiosphaeridia crassa (Naumova) emend. Mikhailova and Jankauskas *in* Jankauskas, 1989

Leiosphaeridia jacutica (Timofeev 1966) Mikhailova and Jankauskas 1989 *in* Jankauskas et al., 1989

Leiosphaeridia minutissima (Naumova 1949) emend. Jankauskas 1989 *in* Jankauskas et al., 1989

Leiosphaeridia tenuissima Eisenack 1958

Myxococcoides cantabrigiensis Knoll 1982

Ostiana microcystis Hermann 1976

Pinus Linnaeus 1753

Satka Jankauskas 1979

Satka colonialica Jankauskas 1979

Skiagia Downie 1982

Siphonophycus Schopf 1968 emend. Knoll, Swett, and Mark 1991

Synsphaeridium Eisenack 1965

Tawuia Hofmann *in* Hofmann and Aitken 1979

Trachyhystrichosphaera aimika German 1976 emend. Butterfield, Knoll, and Swett, 1994

Valeria lophostriata (Jankauskas) Jankauskas 1982

References

AWRAMIK, S. M., McMENAMIN, D. S., YIN CHONGYU, ZHAO ZIQIANG, DING QIXIU, and ZHANG SHUSEN, 1985, Prokaryotic and eukaryotic microfossils from a Proterozoic/Phanerozoic transition in China: Nature, v. 315, no. 6021, p. 655–658.

BUTTERFIELD, N. J., KNOLL, A. H., and SWETT, K., 1994, Paleobiology of the Neoproterozoic Svanbergfjellet Formation, Spitsbergen: Fossils and Strata, no. 34, p. 1–84.

COTTER, K. L., 1997, Neoproterozoic microfossils from the Officer Basin, Western Australia: Alcheringa, v. 21, p. 247–270.

COTTER, K. L., 1999, Microfossils from Neoproterozoic Supersequence 1 of the Officer Basin: Western Australia: Alcheringa, v. 23, p. 63–86.

DAMASSA, S. P., and KNOLL, A. H., 1986, Micropalaeontology of the late Proterozoic Arcoona Quartzite Member of the Tent Hill Formation, Stuart Shelf, South Australia: Alcheringa, v. 10, p. 417–430.

GRAVESTOCK, D. I., MORTON, J. G. G., and ZANG, W-L., 1997, Biostratigraphy and correlation, *in* Petroleum geology of South Australia, Volume 3: Officer Basin *edited by* J. G. G. MORTON and J. F. DREXEL: South Australia Department of Mines and Energy Resources, Report Book 97/19, p. 87–97.

GREY, K., 1995a, Officer Basin drillholes — review of Neoproterozoic palynological data: Western Australia Geological Survey, Palaeontology Report 1995/11 (unpublished).

GREY, K., 1995b, Savory Basin drillholes TWB 1, 2, 6, 9 (Trainor water bores) palynology and thermal maturation: Western Australia Geological Survey, Palaeontology Report 1995/20 (unpublished).

GREY, K., 1998, Ediacarian acritarchs of Australia: Macquarie University, PhD thesis (unpublished).

GREY, K., 1999a, A modified palynological preparation technique for the extraction of large Neoproterozoic acanthomorph acritarchs and other acid insoluble microfossils: Western Australia Geological Survey, Record 1999/10, 23p.

GREY, K., 1999b, Appendix 7: Proterozoic palynology of samples from Empress 1A, *in* GSWA Empress 1 and 1A well completion report, Yowalga Sub-basin, Officer Basin, Western Australia *compiled by* M. K. STEVENS and S. N. APAK: Western Australia Geological Survey, Record 1999/4, p. 68–69.

GREY, K., 1999c, Palynology of samples from Continental Oil Birksgate 1 (OEL 28), Officer Basin, South Australia: Western Australia Geological Survey, Palaeontology Report 1999/02 (unpublished).

GREY, K., 2000, Palynology of samples from Comalco Nicholson 2, Officer Basin, South Australia: Western Australia Geological Survey, Palaeontology Report 2000/01 (unpublished).

GREY, K., and COTTER, K. L., 1996, Palynology in the search for Proterozoic hydrocarbons: Western Australia Geological Survey, Annual Review 1995–96, p. 70–80.

GREY, K., and STEVENS, M. K., 1997, Neoproterozoic palynomorphs from the Savory Sub-basin, Officer Basin, and their relevance to petroleum and mineral exploration: Western Australia Geological Survey, Annual Review 1996–97, p. 49–54.

GREY, K., APAK, S. N., EYLES, C., EYLES, N., STEVENS, M. K., and CARLSEN, G. M., 1999, Neoproterozoic glacigene successions, western Officer Basin, Western Australia: Western Australia Geological Survey, Annual Review 1998–99, p. 74–80.

HAINES, P. W., 1998, *Chuaria* Walcott, 1899 in the lower Wessel Group, Arafura Basin, northern Australia: Alcheringa, v. 22, p. 1–8.

HILL, A. C., COTTER, K. L., and GREY, K., 2000, Mid-Neoproterozoic biostratigraphy and isotope stratigraphy in Australia: Precambrian Research, v. 100, p. 283–300.

KNOLL, A. H., 1996, Chapter 4, Archaean and Proterozoic palaeontology, *in* Palynology: principles and applications *edited by* J. JANSONIUS and D. C. McGREGOR: American Association of Stratigraphic Palynologists Foundation, Salt Lake City, Publishers Press, v. 1, p. 51–80.

MOCZYDLOWSKA, M., 1991, Acritarch biostratigraphy of the Lower Cambrian and the Precambrian–Cambrian boundary in southeastern Poland: Fossils and Strata, no. 29, p. 1–127.

MORTON, J. G. G., 1997, Lithostratigraphy and environments of deposition, *in* The petroleum geology of South Australia, Volume 3: Officer Basin *edited by* J. G. G. MORTON and J. F. DREXEL: South Australia Department of Mines and Energy Resources, Report Book 97/19, p. 47–86.

STEVENS, M. K., and APAK, S. N., (compilers), 1999, Empress 1 and 1A Well Completion Report, Yowalga Sub-basin, Officer Basin, Western Australia: Western Australia Geological Survey, Record 1999/4, 110p.

TALYZINA, N. M., 2000, Ultrastructure and morphology of *Chuaria circularis* (Walcott, 1899) Vidal and Ford (1985) from the Neoproterozoic Visingsö Group, Sweden: Precambrian Research, v. 102, p. 123–134.

TRAVERSE, A., 1988, Palaeopalynology: Boston, Unwin Hyman, 600p.

VIDAL, G., and MOCZYDLOWSKA-VIDAL, M., 1997, Biodiversity, speciation, and extinction trends of Proterozoic and Cambrian phytoplankton: Paleobiology, v. 23, p. 230–246.

WALTER, M. R., and HILL, A. C., 1999, Carbon isotope stratigraphy of Empress 1/1A, Supersequence 1, Western Officer Basin: Western Australia Geological Survey, Statutory petroleum exploration report, S20424 A8 (unpublished).

WALTER, M. R., VEEVERS, J. J., CALVER, C. R., GORJAN, P., and HILL, A. C., 2000, Dating the 840–544 Ma Neoproterozoic interval by isotopes of strontium, carbon, and sulfur in seawater, and some interpretative models: Precambrian Research, v. 100, p. 371–433.

YIN CHONGYU, 1990, Spinose acritarchs from the Doushantuo Formation in the Yangtze Gorges and its geological significance: Acta Micropalaeontologica Sinica, v. 7, p. 265–270 (in Chinese with English summary).

YIN CHONGYU, and GAO LINZHI, 1996, The early evolution of the acanthomorphic acritarchs in China and their biostratigraphical implication: Acta Geologica Sinica, v. 9, p. 193–206.

YIN LEIMING, 1985a, Microfossils of the Doushantuo Formation in the Yantze Gorge district, western Hubei: Palaeontologia Cathayana, v. 2, p. 229–249 (in Chinese with English summary).

YIN LEIMING, 1985b, Microfossils from the Precambrian rocks of the Daihongyu Formation of Jixian, North China: Acta Palaeontologica Sinica, v. 24, p. 111–115 (in Chinese with English summary).

YIN LEIMING, 1991, Ecological history of Doushantuo period in Yangtze Gorge district, S. China, *in* Palaeoecology of China, 1 *edited by* JIN YU-GAN, WANG JUN-GENG, and XU SHAN-HONG: Nanjing, Nanjing University Press, p. 1–9.

YIN LEIMING, and LI ZAIPING, 1978, Precambrian microfloras of Southwest China, with reference to their stratigraphic significance: Memoirs of Nanjing Institute of Geology and Palaeontology, Academia Sinica, v. 10, p. 41–102 (in Chinese with English summary).

ZANG, W-L., 1991, Late Proterozoic and Cambrian acritarchs, *in* Geological and geophysical studies in the Amadeus Basin, central Australia *edited by* R. J. KORSCH and J. M. KENNARD: Australia BMR, Bulletin 236, p. 99–100.

ZANG, W-L., 1994, Review of Neoproterozoic and Early Palaeozoic acritarch biostratigraphy in Australia: Petroleum Exploration Society of Australia (PESA) Journal, v. 22, p. 101–106.

ZANG, W-L., 1995a, Early Neoproterozoic sequence stratigraphy and acritarch biostratigraphy, eastern Officer Basin, South Australia: Precambrian Research, v. 74, p. 119–175.

ZANG, W-L., 1995b, Neoproterozoic depositional sequences and tectonics, eastern Officer Basin, South Australia: South Australia Department of Mines and Energy, Report Book 95/21, 100p.

ZANG, W-L., 1997, Megascopic carbonaceous *Chuaria* and *Tawuia* from the late Neoproterozoic in South Australia: Mines and Energy of South Australia (MESA) Journal, v. 4, p. 37–41.

ZANG, W-L., and McKIRDY, D. M., 1994, Microfossils and molecular fossils from the Neoproterozoic Alinya Formation — a possible new source rock in the eastern Officer Basin: Petroleum Exploration Society of Australia (PESA) Journal, v. 22, p. 89–90.

ZANG, W-L., and WALTER, M. R., 1989, Latest Proterozoic plankton from the Amadeus Basin in central Australia, Nature, v. 337, no. 6208, p. 642–645.

ZANG, W-L., and WALTER, M. R., 1992, Late Proterozoic and Early Cambrian microfossils and biostratigraphy, Amadeus Basin, central Australia: Association of Australasian Palaeontologists, Memoir 12, p. 1–132.

Appendix 4

Palaeomagnetic study of Vines 1

by S. A. Pisarevsky
(Tectonics Special Research Centre, University of Western Australia)

Sixty-nine core plugs were drilled from 45 oriented HQ- and NQ-size core samples over the following depth intervals: 748–811 m, 935–1066 m, 1186–1188 m, 1256.03 – 1256.09 m, 1339–1340 m, 1361–1366 m, 1390–1400 m, 1418–1421 m, 1424.8 – 1424.92 m, 1487–1490 m, 1536–1550 m, and 1640–2015 m.

Vines 1 is a vertical drillhole and hence there is uncertainty as to the azimuthal orientation of the core. A three-arm dipmeter was acquired and the core was approximately oriented azimuthally by comparing visible bedding or cross-bedding with the interpreted dips from the dipmeter log. Thermal demagnetization was the main sample preparation procedure.

Samples from depths >1900 m show only unstable remanence, and therefore are not discussed below. The remaining samples yielded scattered, but distinct, mostly haematite-bearing remanence. Most samples also possess a near-vertical 'drilling' component of remanence, which was usually removed during the thermal demagnetization. The mean direction of the stable magnetization is statistically the same between ~750 and 1900 m; declination = 200°, inclination = -18.2° (negative inclinations point upwards). The number of samples and cylinders are 45 and 69, respectively. The precision parameter (k) = 3.2 and the radii of the circle of confidence (a_{95}) = 14.3°. The poor statistics are caused mostly by the method of orientation. Both polarities are present, but the shallow upward south-southwest direction is dominant.

The corresponding palaeomagnetic pole of 49.3°N, 159.4°E (dp/dm = 7.7/14.9) is close to a group of well defined 540–610 Ma Australian poles (Table 4.1). There are no known younger Australian palaeomagnetic poles close to this group (e.g. McElhinny and McFadden, 2000; table 6.14). This probably means that the section between 750 and 1900 m was magnetized in latest Neoproterozoic – earliest Cambrian.

Table 4.1. Australian late Neoproterozoic – earliest Cambrian palaeomagnetic poles

Rock unit	*Age (Ma)*	*Plat (°N)*	*Plon (°E)*	*dp (°)*	*dm (°)*	*References*
Elatina Formation	600	52.4	167.1	3.7	7.4	Schmidt and Williams, 1995
Elatina Formation	600	38.9	185.6	6.7	13	Sohl et al., 1999
Yaltipena Formation	610	44.2	172.7	5.9	11.4	Sohl et al., 1999
Vines Formation	?	49.3	159.4	7.7	14.9	This study
Todd River Dolomite	540	43.2	159.9	4.5	7.7	Kirschvink, 1978
Upper Arumbera Sandstone	545	46.6	152.8	2.6	4.6	Kirschvink, 1978
Albany Belt dykes	560	37.8	166.9	11.7	11.7	Harris and Li, 1995

NOTES: Plat: palaeolatitude
Plon: palaeolongitude
dp and dm: semi-axes of oval of confidence

References

HARRIS, L. B., and LI, Z. X., 1995, Palaeomagnetic dating and tectonic significance of dolerite intrusions in the Albany Mobile Belt, Western Australia: Earth and Planetary Science Letters, v. 131, p. 143–164.

KIRSCHVINK, J. L., 1978, The Precambrian–Cambrian boundary problem: palaeomagnetic directions from the Amadeus Basin, Central Australia: Earth and Planetary Science Letters, v. 40, p. 91–100.

McELHINNY, M. W., and McFADDEN, P. L., 2000, Palaeomagnetism: continents and oceans: Academic Press, San Diego, 382p.

SCHMIDT, P. W., and WILLIAMS, G. E., 1995, The Neoproterozoic climatic paradox: equatorial palaeolatitude for Marinoan glaciation near sea level in South Australia: Earth and Planetary Science Letters, v. 134, p. 107–124.

SOHL, L. E., CHRISTIE-BLICK, N., and KENT, D. V., 1999, Palaeomagnetic polarity reversals in Marinoan (ca. 600 Ma) glacial deposits of Australia: implications for the duration of low-latitude glaciation in Neoproterozoic time: Geological Society of America Bulletin, v. 111, p. 1120–1139.

Appendix 5

Gravity modelling of the Waigen area

by K. A. Blundell

The Waigen gravity survey (Geoterrex–Dighem Pty Ltd, 1998) was commissioned by the Geological Survey of Western Australia in 1998 as a precursor to the drilling of Vines 1. The survey was chosen, using existing regional gravity data, to cover a structurally interesting area marginal to the Musgrave Complex (Fig. 5.1). The survey area includes the southern margin of the Musgrave Complex, the northwestern margin of the Waigen Sub-basin, and the shelf formed by the northern extent of the Neale Arch. The objective of the survey was to provide detailed gravity data from which lineament information and basin modelling could identify structurally simple areas with a relatively thin (<2000 m), but complete, Neoproterozoic–Palaeozoic section.

Qualitative interpretation of the new gravity data (Blundell, 1999) reveals a dominantly west-northwesterly oriented structural trend, as indicated by large vertical gradients in the gravity field. These are attributed to compressional structures caused by the Petermann Ranges Orogeny. A subordinate northerly to northeasterly structural trend is represented by the offset and truncation of the vertical gradient anomalies and is attributed to the southerly movement of the Musgrave Complex along northeasterly trending accommodation faults during Cambrian to post-Miocene tectonism.

Due to the lack of geological constraint on gravity modelling (no drillhole, well, or seismic data, and limited outcrop), depth-to-basement analysis of aeromagnetic data was carried out in order to gain an appreciation of the thickness of sedimentary rocks in the sub-basin. Euler deconvolution and Phillip's depth solutions provided an approximate depth to basement for the areas southwest of the survey area. This depth was used to produce a depth-to-basement map over the survey area using the gravity data and a constant density slab model (Shevchenko and Iasky, 1997).

A model traverse was chosen to pass through the proposed Vines 1 well site and cross the west-northwesterly striking structural trend (Fig. 5.1). Although the first vertical derivative of Bouguer gravity reveals a number of west-northwesterly oriented lineaments, only the three major inflections in the Bouguer gravity were modelled in order to keep the model relatively simple. These inflections are attributed to thrust faults. The depth-to-basement map was used as a starting point for the sedimentary thickness.

Densities and thicknesses for the sedimentary succession were derived from lithology and density logs of selected wells in other parts of the Officer Basin. For the purpose of the model, the sedimentary succession was divided into five density layers as illustrated in Table 5.1. Using these layers, along with an approximate total sedimentary thickness and some limited constraints from the surface geology, an initial model was created (Fig. 5.2). The final thicknesses of the units and the amount of displacement along the thrusts were governed by interactively adjusting the model such that the model response matched the Bouguer gravity response. The thicknesses of all the density layers was kept constant, apart from the 2.45 g/cm^3 layer, which was modelled as a thicker succession under the gravity low. The only plausible way to model the major inflection in the Bouguer gravity to the north of the main thrust (the southern margin of the Musgrave Complex as mapped using aeromagnetic data), was to have a considerable overthrust of the Musgrave Complex above the lower density sedimentary rocks.

It should be stressed that, with such limited constraints, the non-uniqueness of gravity modelling means that the initial model is one of infinitely many variations, and is

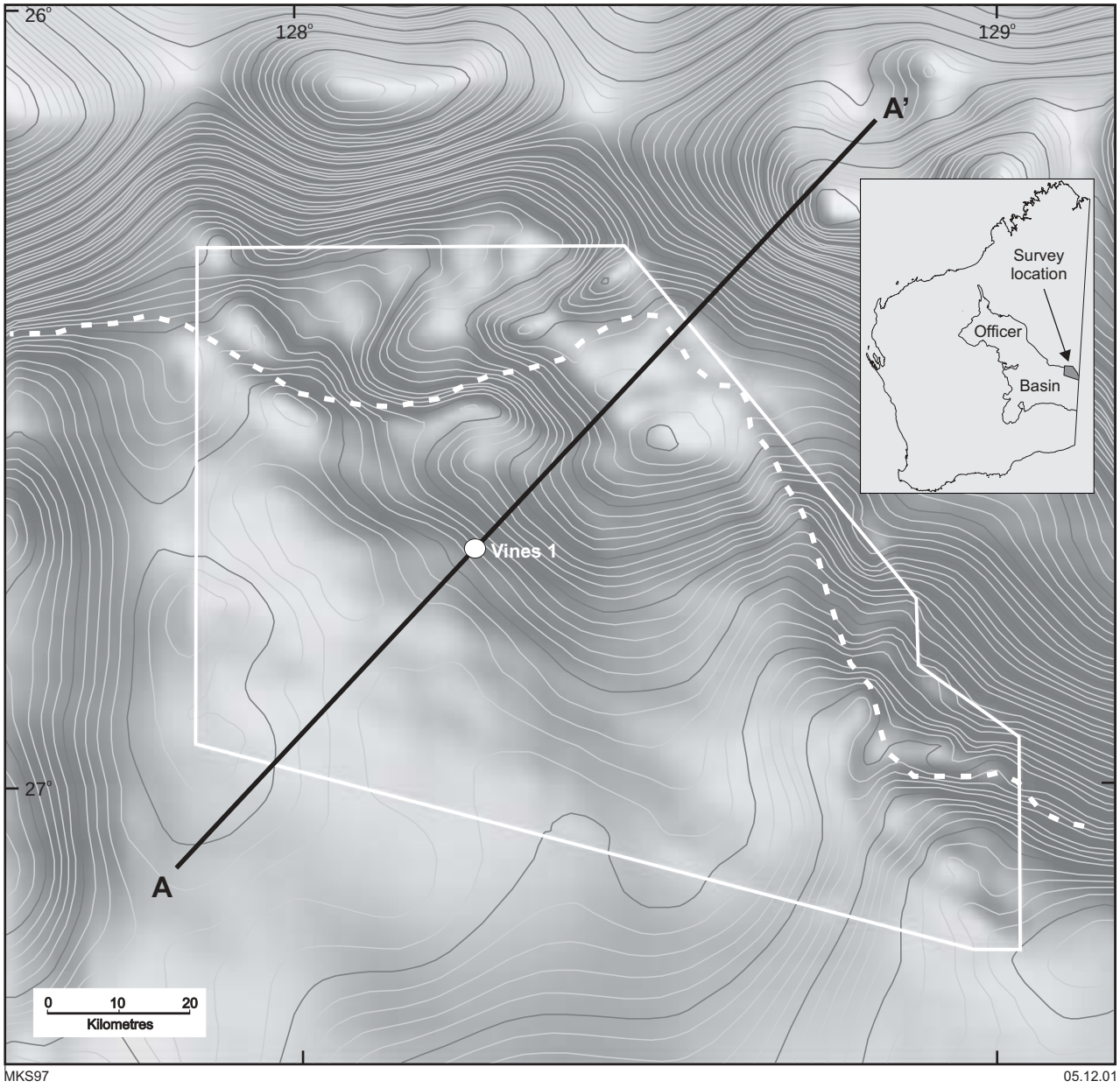

Figure 5.1. Bouguer gravity image of the Waigen gravity survey data combined with regional gravity data, showing the model cross-section (A–A') and the location of Vines 1. The polygon represents the extent of the new survey and the dashed white line represents the southern margin of the Musgrave Complex. Sun angle is from the northeast and contours range from –1200 to 700 μm/sec^2 (interval = 20 μm/sec^2)

Table 5.1. Formation thicknesses and densities used for gravity modelling

Formation	*Estimated thickness (m)*	*Average density (g/cm³)*	*Model layer (g/cm³)*
Cainozoic cover	0–100	2.20	
Paterson Formation	50–200	2.10	2.20
Lennis/Wanna Formations	120–200	2.30	
Table Hill Volcanics	100	2.80	2.80
Unnamed unit 4B	30–100	2.20	
Unnamed unit 4A	100–400	2.45	
Lupton Formation	150–400	2.50	2.45
Kanpa Formation	400	2.45	
Hussar Formation	400	2.50	
Browne Formation	1 000	2.25	2.25
Lefroy Formation	300	2.80	2.65
Townsend Quartzite	400	2.60	
Basement	–	2.70	2.70
Total thickness	**3 050 – 4 000**		

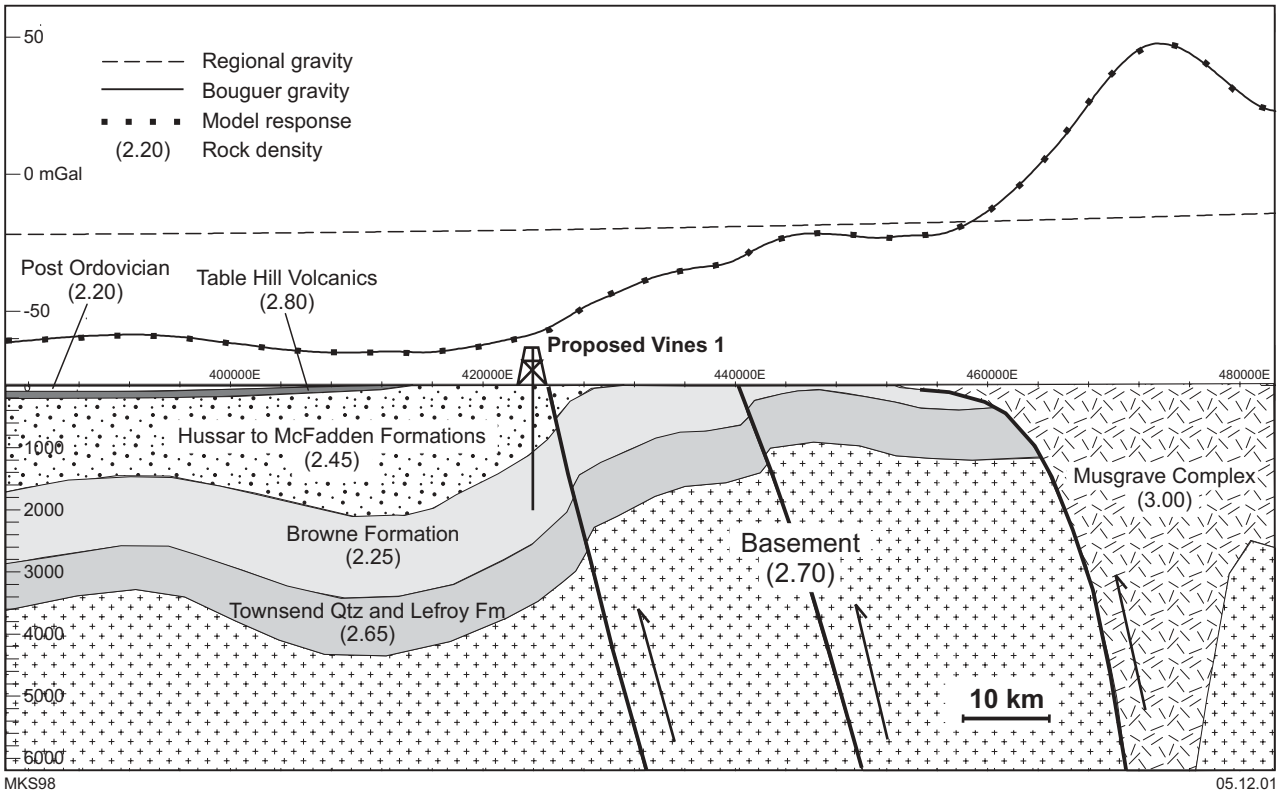

Figure 5.2. Initial gravity model (after Blundell, 1999). The location and proposed depth of Vines 1 is shown to illustrate the expected geology. V/H = 7.5

intended only as a schematic of the possible geology. Also, variations in geology along strike will affect the accuracy of the model due to its 2½ dimensionality (i.e. the model assumes infinite strike extent).

Based on the initial model and lineament interpretation, as well as access and groundwater issues, Vines 1 was drilled just south of the southernmost modelled thrust. This ensured that no complex structure was intersected. It was also hoped that, despite the assumptions made in the modelling, within 2000 m the drillhole would intersect all of the upper units of Supersequence 1B and penetrate at least the upper part of the Browne Formation (lower Supersequence 1B).

Vines 1 (drilled to 2017.5 m) revealed a markedly different stratigraphy than that proposed in the initial model. Although the thickness and density of the upper unnamed units (Units 6, 5, and the upper part of Unit 4) approximates the model (363 m of 2.25 g/cm^3), the density and thickness of the ?Neoproterozoic to Early Cambrian strata was vastly underestimated. A 1269 m-thick unit of dominantly diamictite was intersected from 363 to 1632 m, of which the first 262 m has a density of 2.65 g/cm^3. The remainder increased in density with depth. Overall an average of 2.70 g/cm^3 has been estimated for this interval, which includes the lower part of Unit 4 and all of Units 3 and 2. Beneath Unit 2, 386 m of Unit 1 was intersected. This unit has a density of 2.75 g/cm^3, which is greater than most strata in the Officer Basin.

Consequently, a revised gravity model was derived incorporating the new data. The increase in density of the upper part of the model could be compensated for in a number of ways:

1. altering the regional field
2. increasing the density of basement
3. decreasing the density of the underlying sedimentary succession
4. increasing the thickness of the underlying sedimentary succession.

The regional field had been established by analysing regional gravity profiles and filtering the gridded regional gravity data, so was considered to be relatively accurate. Increasing the density of basement is a reasonable option, but without any evidence for dense basement, a granitic gneiss composition has to be assumed. Decreasing the density of the underlying sedimentary rocks is geologically implausible, since the modelled density of the Browne Formation already took into consideration a large proportion of salt. The pressure of the overlying, relatively dense succession would certainly produce diapirism if the density of the Browne Formation was lowered (increased salt content).

The confidence in the depth-to-basement interpretation was low, due to the low reliability of the Euler deconvolution depth estimates and the assumptions used in the constant density slab interpolation of those estimates. An error of up to 50% can be expected for this method, meaning that an estimated depth to basement of 4000 m may be out by as much as 2000 m. Hence, a depth to basement of 6000 m is not unreasonable for the model and allows for an increase in the thickness of the underlying succession — namely the low-density Browne Formation. Diapirism is again a problem under this scenario due to the relatively dense succession overlying such a thick salt-rich unit. Therefore, some doming of salt in the Browne Formation was incorporated into the new model by laterally varying the thickness and density of the Browne Formation (2.25 g/cm^3 in the thickest section and 2.60 g/cm^3 where the salt has migrated away). This effectively removes the syncline in the south of the original model since the gravity low can be attributed to a salt ridge.

The increase in density of the Hussar and Kanpa Formations and the salt-reduced Browne Formation near the Musgrave Complex requires that these units be overthrust

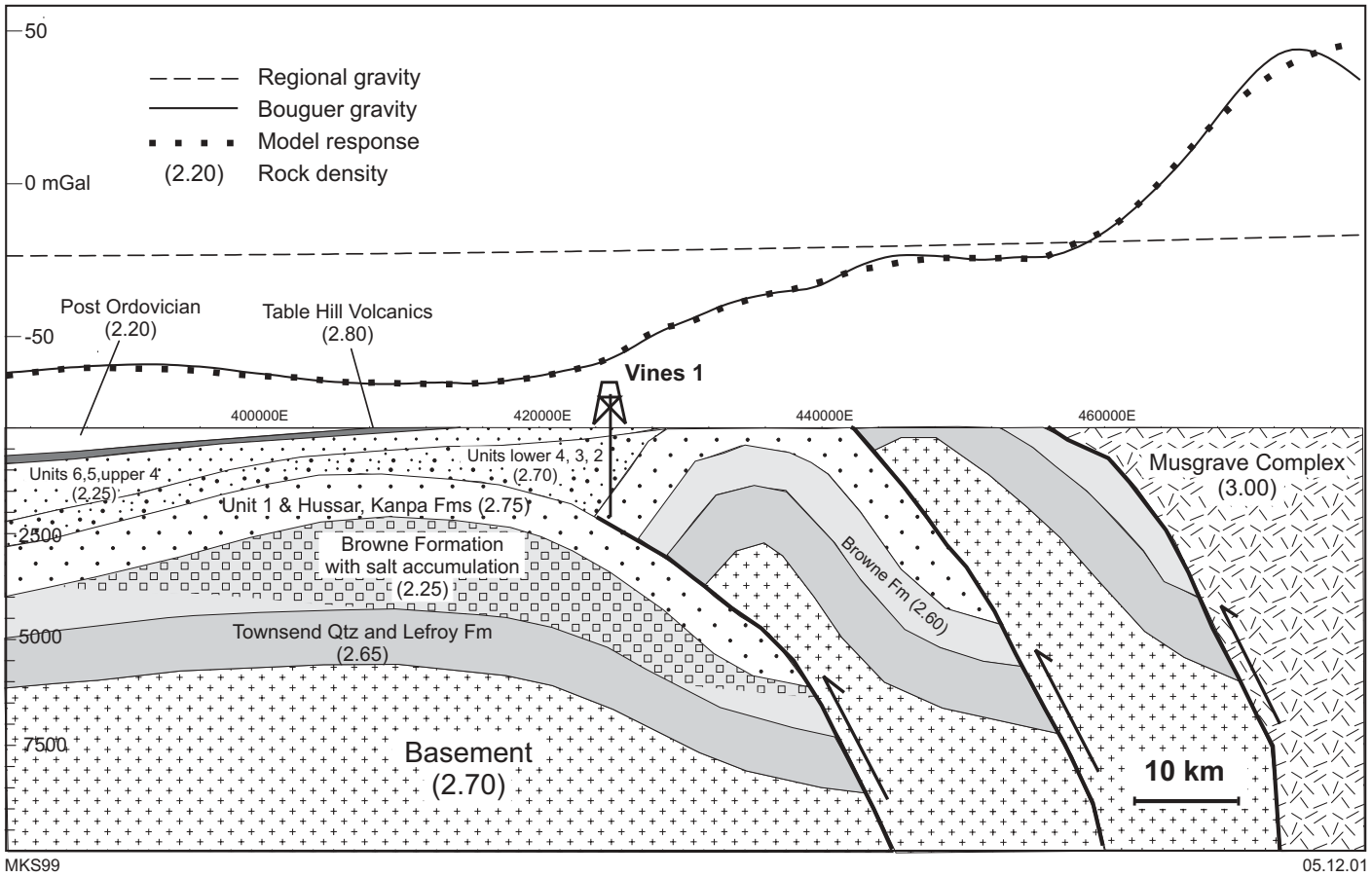

Figure 5.3. Revised gravity model based on log density information from Vines 1. V/H = 4

to a greater extent in order to match the large inflection in the Bouguer gravity. The same overthrust geometry is required to produce a matching model response for the other main inflections in the Bouguer gravity. Hence, the revised model (Fig. 5.3) is more complex and shows a markedly different structural style than the initial model, with a thicker sedimentary succession, major overthrusting, and salt migration.

Again it should be stressed that the constraints on the model are extremely limited, and because of the non-uniqueness of potential fields and the inherent assumption used in 2½-dimensional modelling, the revised model should only be considered as one approximation of the many possible geological systems that could produce this Bouguer gravity response. The marked difference between the initial and revised models, as a result of information from one stratigraphic test, has already shown the importance of constraining factors in gravity modelling. Hence, further drilling and ultimately the acquisition of a seismic traverse in the area is needed before a reasonable degree of confidence can be placed on a gravity model.

References

BLUNDELL, K. A., 1999, Waigen gravity survey — the contribution of semi-detailed gravity data to the stratigraphic and structural interpretation of the Waigen Sub-basin, Officer Basin: Western Australia Geological Survey, Record 1999/8, 33p.

GEOTERREX–DIGHEM PTY LTD, 1998, Operation and processing report for the Waigen Sub-basin Gravity Survey: Western Australia Geological Survey, Statutory petroleum exploration report, S10401 A1 (unpublished).

SHEVCHENKO, S. I., and IASKY, R. P., 1997, Calculating depth to basement from magnetic and gravity data, with an example from the western Officer Basin: Western Australia Geological Survey, Annual Review 1996–97, p. 69–75.

Appendix 6

PGA CONSULTANTS PTY LTD

VINES-1

Post-petrographic SEM and XRD reports for Vines 1

JOHN SONEGO

Suite 6, 6 Richardson St,
West Perth, Perth, W.A.
Ph: (08) 9226 3590
Email: jst@highway1.com.au

CONTENTS

1. INTRODUCTION 4
2. AIMS 4
3. SEM METHOD 4
4. SUMMARY 4

LIST OF APPENDICIES

APPENDIX A (SEM IMAGES) 7
PLATE 1A 8
PLATE 1B 8
PLATE 1C 8
PLATE 2A 9
PLATE 2B 9
PLATE 2C 9
PLATE 2D 9
PLATE 2E 9
PLATE 3A 10
PLATE 3B 10
PLATE 3C 10
PLATE 3D 10
PLATE 3E 10
PLATE 3F 10
PLATE 3G 11
PLATE 4A 11
PLATE 4B 11
PLATE 4C 11
PLATE 4D 11
PLATE 5A 12
PLATE 5B 12
PLATE 5C 12
PLATE 5D 12
PLATE 6A 13
PLATE 6B 13
PLATE 6C 13
PLATE 7A 13
PLATE 7B 13
PLATE 7C 14
PLATE 7D 14

APPENDIX B (XRD ANALYSIS) 15

1. INTRODUCTION

SEM images of 9 samples from Vines 1 are presented in this report. These samples are listed in Table 1.

Table 1. List of samples provided for SEM and XRD analysis.

Sample No	Depth (m)	Analysis
154801	133.20	SEM
154802	285.00	SEM
154869	598.23	SEM/XRD
154812	644.00	SEM/XRD
154814	682.00	SEM/XRD
154817	930.00	SEM/XRD
154871	985.25	SEM
154828	1100.15	SEM
154838	1473.95	SEM

Four of the samples, 154869 (598.23m), 154812 (644m), 154814 (682m) and 154817 (930m) were primarily analysed for seal capacity. These samples were analysed both by SEM and XRD. Splits of these samples were sent to Dr Ray Chang at the XRD Laboratory at the University of Western Australia for qualitative XRD clay analysis. A brief analytical report by Dr Ray Chang is provided in Appendix B of this report.

2. AIMS

The initial aims for SEM and XRD work were as follows;

1) Determine the nature of isopachous rims within samples 154801 (133.2m) and 154802 (285m) and whether they contain bituminous coatings.
2) Determine the composition and packing relationships of clays within all samples.
3) Investigate the seal capacity of four samples 154869 (598.23m), 154812 (644m), 154814 (682m) and 154817 (930m).
4) To observe and record in samples 154869 (598.23m), 154812 (644m), 154814 (682m) and 154817 (930m) any microfracturing and microporosity.
5) Identify and record any zircons (particularly xenotime) within samples.
6) Through XRD analysis provide a qualitative compositional analysis of clays within selected samples.

3. SEM METHOD

All SEM work was completed at the Curtin University of Technology Electron Microscopy Centre over two sessions using the Phillips XL-30 Secondary Detector. Samples were manually broken and mounted onto stubs. Stubs were vacuum pumped and carbon coated. Image quality in this report varies due to quality of the coated surface and the quality of samples. Charging may be apparent on some grain surfaces. In most samples clay structure is highly disorganised making imaging extremely difficult. Images ranging between 200μm and 5μm have been provided for most samples. Images were mainly taken as Secondary Electron Micrographs to show textural relationships between detrital grains and matrix components. Back scattered imaging was used to help in the identification of zircons and other high reflectivity minerals.

4. SUMMARY

Apart from samples 154801 (133.2m) and 154802 (285m) most samples consisted of a mixture of detrital grains and highly disorganised authigenic clays and dolomite. SEM imaging of samples 154801 and 154802 indicates that the isopachous rims originally considered in petrographic work to be bituminous are in fact clays. There is a possibility however that in sample 154802 (285m) grain coatings may still contain a mixture of clay and bitumen. Preparation of samples for SEM imaging

included drying the samples and then vaccuum pumping them. This may have resulted in the extraction of any bitumen trapped within clay rims.

Two types of grain coating are evident in samples 154801 and 154802. In sample 154801 clays coat detrital grains with an orientation parallel with grain surfaces. The clay coating on grains in this sample is inferred to be "inherited," in that it formed on framework grains prior to their deposition. These rims tend to vary in thickness and rough textural appearance. The formation of clay rims on detrital grains has resulted in the preservation of intergranular porosity. Only traces of bridging resulting in the partial occlusion of pore space are evident in this sample.

In sample 154802 (285m) the isopachous rim is inferred to be authigenic. This coating is interpreted to have formed during early diagenesis. The rim in this sample is composed predominantly of illite occurring tangential to the grain surface. Generally the thickness of the illite coat is uniform however some bridging is evident at grain contacts. Traces of chlorite are evident growing within the illite clays.

Samples 154869 (598.23m), 154812 (644m), 154814 (682m) and 154817 (930m) were investigated through XRD and SEM analysis. XRD analysis (Appendix B) indicates that all 4 samples are compositionally similar. Apart from slight variations in the percentages all samples consisted predominantly of quartz, dolomite, microcline and albite with small amounts of kaolinite, illite and swelling chlorite. Trace amounts of haematite and pyrite are also evident (Appendix B). SEM images of these sample show them to be mainly "dirty" samples composed of a detrital and authigenic matrix compacted around detrital grains. The matrix component of these samples is composed predominantly of kaolinite/ sericite that rarely contains an ordered, stacked appearance. Most of the kaolinite/sericite occur as highly disordered and partially corroded pseudohexagonal crystals. The disordering and displacement of the clays in these samples is due to the growth of late stage microcrystalline dolomite. Dolomite crystals range from 2 to 10μm in size. Thin, wispy illite terminations are evident marginally overgrowing kaolinite/sericite crystals. Illitic clays occasionally bridge pore space.

Small microfractures are evident in samples 154814 (682m), 154817 (930m) and 154871 (983.24m). These microfractures tend to be multi-directional displaying both sub-vertical and sub-horizontal orientations. In sample 154817, microfractures have an irregular stylolitic appearance (PLATE 4A). Most microfractures tend to be discontinuous and small with most not reaching more than 150μm in length. It is proposed that these microfractures have no effect on the sealing capacity of these units. It is important to note also that some of the microfractures seen in SEM micrographs may have been induced during sample preparation. Microporosity within these samples is also poor. The lack of ordering of clays and the development of late stage dolomite and illite cements have destroyed most interlayer porosity in the clays. Remnant micropores tend to be small (2 to 10μm in diameter) and isolated. The lack of microfractures and micorpores suggests that these samples would have excellent sealing capacity.

Two samples, 154828 (1100.15m) and 154838 (1478.95m) were analysed from the lower part of the well and therefore were more prone to diagenetic effects. These samples consisted predominantly of a complex mixture of randomly oriented kaolinite/sericite clays. The disordering of the clays as in the samples above, is caused by the late stage expansion of microcrystalline dolomite into pore space. Thin, wispy terminations of illite are evident marginally overgrowing kaolinite/sericite clays and detrital grains. Microporosity within these samples is extremely poor with most micropores ranging between 1 and 4μm in diameter.

Samples were imaged by back scattering in an attempt to find any zircons that may have assisted in the dating of these samples. Unfortunately back scattered images failed to provide any zircons for analysis. All high reflectivity minerals under back scattered imaging were probed. Probing identified only two main minerals, barite and illmenite? (i.e. Figures 1 & 2). Barite crystals are evident in all samples except 154801 (133.2m) and 154802 (285m). These crystals range in size from 1 to 10μm in diameter. Barite crystals typically form blocking micropores. The occurrence of barite in samples 154869 (598.23m), 154812 (644m), 154814 (682m) and 154817 (930m) has therefore aided in the reduction of microporosity and an increase in the overall seal capacity. Illmenite crystals tend to occur as elongate laths embedded within the matrix of these samples.

In summary samples used in this study were poor for SEM analysis. The disordering of clays and the destruction of primary fabrics made mineral identification and imaging difficult. However the aims were still able to be addressed effectively. It is recommended however that sample 154802 (285m) be analysed geochemically as there still may be a possibility of encountering bitumen within the trapped within grain coatings.

APPENDIX A (SEM IMAGES)

See Photo Library on this CD for Plates 1–7

PLATE 1

PLATE 1A

Sample 154801 (133.2m)
200μm

Low magnification SEM of framework grains coated by an isopachous clay rim. Clays display an orientation parallel with grain surfaces. Clay coatings are ragged with coating thickness varying considerably. Bridging of pore space between framework grains is evident at A. Locally, faint outlines of illitic fibers can be recognised. Intergranular porosity is good in this sample.

PLATE 1B

Sample 154801 (133.2m)
200μm
Low magnification SEM. Sample consists of framework grains coated in an isopachous clay rim. Clays are generally oriented parallel to the framework grain surface. Trace illite growth is evident on grain boundaries. Kaolinite and sericite clays are evident filling pore and marginally overgrowing detrital grains at A. High reflectivity mineral (B) is barite.

PLATE 1C

Sample 154802 (285m)
50μm
High magnification SEM. Detrital grains are coated in a thin illitic clay. Illite is evident oriented tangential to grain surface. It occurs as a secondary cement following quartz overgrowth cementation. Evidence of pre-illite quartz overgrowth formation is evident at A. Illitic clays generally terminate in intergranular pore space but occasionally they can be seen to bridge across pore space. Isolated outlines of small euhedral chlorite crystals are evident growing within illite clay rims.

PLATE 2

PLATE 2A

Sample 154869 (598.23m)
200µm
Low magnification SEM. Overview image of sample displays only trace microporosity making it an effective sealing rock type.

PLATE 2B

Sample 154869 (598.23m)
10µm
High magnification SEM of a "dirty" sample showing detrital and authigenic matrix compacted around detrital grains. Matrix content consists of a mixture of kaolinite and illite clays. Clays have been marginally displaced by late stage dolomite growth (i.e. B). At A, a large feldspar grain is evident. This grain has been partially leached and replaced in part by illite and chlorite clays. Thin authigenic silica overgrowths are evident on some detrital quartz grains (i.e. C). Visual microporosity in this sample is poor.

PLATE 2C

Sample 154812 (644m)
20µm
High magnification SEM. Sample consists predominantly of sub-rounded quartz grains that have been overgrown by authigenic quartz. Intergranular pore space is filled by a mixture of dolomite and kaolinite with thin, wispy overgrowths of illite. Microporosity is poor. Micropores range from 2 to 10µm in diameter. Traces of barite (high reflectivity) are scattered throughout the sample.

PLATE 2D

Sample 154812 (644m)
50µm
High magnification SEM. Imprint of feldspar grain removed during sample preparation is evident at A. The surrounding matrix consists predominantly of microcrystalline dolomite rhombs and thin wispy illite terminations. Small (5 to 10µm in size) pseudohexagonal outlines of kaolinite are also evident scattered throughout the matrix. Some microfracturing is evident in this sample but it is inferred to have been developed during sample preparation. Traces of barite (high reflectivity) are scattered throughout the sample.

PLATE 2E

Sample 154812 (644m)
20µm
High magnification SEM. Vermicular kaolinite stacks are evident at A. Ordering of the clays is rare, most of the sample consists of highly disorganised clays. An interlocking mosaic of microcrystalline dolomite rhombs are evident at C. Late stage dolomite growth is the cause of most of the disordering of pore filling clays within the sample. At B a large, sub-rounded detrital quartz grain is evident. Early quartz overgrowth cementation is present on the grain surface. Traces of barite (high reflectivity) are evident scattered throughout the sample. Existent microporosity in this sample is interpreted to be due to plucking during sample preparation.

PLATE 3

PLATE 3A

Sample 154814 (682m)
200µm
Low magnification SEM. Sample is in reasonable condition, however grain plucking during sample manufacture is evident at A, B and C. At this magnification no microporosity is apparent. In effect it is predicted that this sample would contain good sealing capacity.

PLATE 3B

Sample 15414 (682m)
5µm
High magnification SEM of matrix component. Sample consists predominantly of randomly oriented clays and small euhedral dolomite crystals. Sericitic clays are occasionally evident by their vermicular stacking pattern. Thin, wispy terminations of illite are evident at A, partially coating authigenic clays. Trace microporosity is evident mainly between clay sheets.

PLATE 3C

Sample 154814 (682m)
20µm
High magnification back scattered image displaying a large 10µm mineral in the centre which was identified by microprobing as barite (Figure 1). The barite crystal has been partially dissolved and marginally overgrown by authigenic clay matrix. The matrix is dominated by corroded pseudohexagonal crystals of kaolinite, sericite and thin wispy overgrowths of illite. Visual microporosity is poor.

PLATE 3D

Sample 154814 (682m)
50µm
High magnification back scattered image. Spectra (Figure 2) indicates that the large elongate lath at the centre of micrograph is possibly illmenite. This grain is supported in a matrix consisting of sheet-like illite and small euhedral dolomite rhombs. Illitic clays are evident overgrowing the illmenite crystal at B. A small microfracture is evident at C. This microfracture is thin and discontinuous and would have no effect on the sealing capacity of this sample. Micopores range from 2 to 10µm in diameter. Overgrowth cementation is evident on the illmenite crystal at D.

PLATE 3E

Sample 154814 (682m)
50µm
High magnification SEM of a “dirty” sample showing detrital and authigenic matrix compacted around detrital grains. Matrix content consists of a mixture of disorganised (kaolinite and sericite) clays and microcrystalline dolomite. Grain plucking during sample manufacture is evident within this sample (i.e. A). Small microfractures are also evident propogating sub-horizontally throughout this sample. Microfractures are inferred to be in situ and form an irregular, discontinuous, anastomosing network. A large illmenite? lath is evident at C. Traces of barite (high reflectivity) are scattered throughout the sample.

PLATE 3F

Sample 154814 (682m)
50µm
High magnification back scattered image displaying an barite crystal (A) and an elongate Fe-rich (illmenite?) lath (B).

PLATE 3G

Sample 154814 (682m)
20μm
High magnification SEM. A large micropore approximately 40μm in diameter is evident at A. Small wispy terminations of illite are evident protruding from pore margins and into pore space. A small, discontinuous localised fracture is evident at B. Clays within the matrix are highly disorganised and difficult to distinguish. XRD analysis indicates that this sample is dominated by dolomite with minor illite and kaolinite. Well-developed microporosity is evident scattered throughout this sample. Micropore sizes range from 2 to 8μm in diameter.

PLATE 4

PLATE 4A

Sample 154817 (930m)
500μm
Low magnification SEM. Overview image of sample showing distinctive sub-horizontal microfracturing. These microfractures appear stylolitic. High reflectivity mineral at A is barite.

PLATE 4B

Sample 154817 (930m)
20μm
High magnification SEM of a dirty sample showing detrital and authigenic matrix compacted around detrital quartz grains. Clays are highly disorganised and difficult to distinguish. XRD analysis indicates that this sample is dominated by dolomite, chlorite, illite and kaolinite. Clays form a thin isopachous rim on detrital grains (A). Thin, wispy Illitic clays display a weak sub-vertical preferential alignment. A small discontinuous microfracture is evident propogating parallel to clay direction. Visual microporosity in this sample is negligible.

PLATE 4C

Sample 154817 (930m)
20μm
High magnification back scattered image of an elongate Fe-rich (illmenite?) crystal embedded in a matrix composed predominantly of dolomite, chlinochlore, illite and kaolinite (inferred through XRD). Clays within the matrix are highly disorganised.

PLATE 4D

Sample 154817 (930m)
50μm
High magnification SEM displaying microfracturing within the sample. Fractures are multi-directional. Grain plucking is evident at A. Quartz grain at B is being marginally overgrown by authigenic clays. The intergranular pore space consists of a mixture of dolomite and kaolinite overgrown by thin, wispy terminations of illite. Visual microporosity is poor in this sample.

PLATE 5

PLATE 5A

Sample 154871 (985.24m)
100µm
Overview low magnification SEM. Sample consists of a mixture of sub-rounded quartz supported in a "dirty" matrix consisting of a mixture of detrital and authigenic clays. Matrix clays consist predominantly of kaolinite/sericite and thin, wispy terminations of illite. Clays are highly disorganised due the late stage growth of displacive microcrystalline dolomite. Visual microporosity in this sample is extremely poor.

PLATE 5B

Sample 154871 (985.24m)
50µm
Low magnification SEM. Image contains a large sub-angular quartz grain at its centre which is surrounded by a matrix consisting predominantly of an interlocking mosaic of small 2 to 5µm euhedral dolomite crystals. Trace clays evident within the matrix are highly disorganised. Thin, wisps of illite are occasionally evident overgrowing detrital grain margins and authigenic dolomite. Early authigenic silica overgrowths are evident coating detrital quartz grains. High reflectivity mineral 5µm in size is barite. Visual microporosity is poor.

PLATE 5C

Sample 154871 (985.24m)
50µm
High magnification SEM of "dirty" sample showing detrital and authigenic matrix compacted around detrital grains. Matrix is composed predominantly of an interlocking mosaic of small 2 to 5µm euhedral dolomite crystals and traces of kaolinite/sericite. Matrix and detrital grains have been partially overgrown by late stage illite. Barite (high reflectivity) grains are randomly scattered throughout the sample. Visual microporosity is poor.

PLATE 5D

Sample 154871 (983.24m)
50µm
High magnification SEM. Large quartz grain at A display early quartz overgrowth cementation. Matrix consists of a mixture of small 2 to 5µm euhedral dolomite crystals and traces of kaolinite/sericite and chlorite. Small sub-vertical microfractures are evident in this sample. It is inferred that these microfractures were formed during sample preparation. Visual microporosity is poor.

PLATE 6

PLATE 6A

Sample 154828 (1100.15m)
20µm
High magnification SEM. Pore space is filled by predominately kaolinite/sericite with minor wisps of illite/sericite. The disordered nature of pore filling material may be due to late stage cementation of dolomite. Occasional corroded outlines of finely crystalline pseudohexagonal kaolinite are evident. Traces of barite (high reflectivity mineral) are evident. Some microfracturing is evident in this sample but fractures are inferred to have been generated during sample preparation. Visual microporosity is poor. Micopores that are evident range from 2 to 4µm in diameter.

PLATE 6B

Sample 154828 (1100.15m)
5µm
High magnification SEM of matrix material. The sample is dominated by corroded pseudohexagonal outlines of kaolinite and sericite. Clays are randomly oriented. Thin wispy, terminations of illite are evident partially overgrowing corroded kaolinite and sericite crystals. Well-developed microporosity is evident in this sample. Micropores range from 2 to 5µm in diameter.

PLATE 6C

Sample 154828 (1100.15m)
20µm
High magnification SEM. Solitary quartz is evident in the right hand side of this image. Pore filling material is predominately composed of a disordered and complex mixture of microcrystalline dolomite and thin wispy illite terminations. Visual microporosity in this sample is poor. Rare micropores that are evident in this sample range from 1 to 4µm in diameter.

PLATE 7

PLATE 7A

Sample 154838 (1473.95m)
10µm
High magnification SEM. This sample consists of a complex mixture of randomly oriented clays. It is predominantly composed of finely crystalline pseudohexagonal kaolinite and sericite. Clay margins are difficult to distinguish as they have been broken, corroded and altered. Thin wispy terminations of illite are evident overgrowing clays and projecting into adjacent pore space. The relationship of illite to surrounding matrix classifies it as being late in the diagenetic sequence. Occasionally wisps of illite from individual grains join and bridge pore space. Only trace microporosity is evident in this sample. Traces of barite (high reflectivity) are evident at A.

PLATE 7B

Sample 154838 (1473.95m)
10µm
High magnification SEM. Sample is dominated by detrital quartz grains displaying thick illite wisps radiating from grain margins which overgrow and replace kaolinite/sericite clays. The matrix component consists of corroded pseudohexagonal outlines of kaolinite and sericite and small isolated euhedral dolomite rhombs. Traces of barite (high reflectivity mineral) are present scattered throughout the sample. Barite grains are approximately 1 to 2µm in size. Visual micorporosity is poor.

PLATE 7C

Sample 154838 (1473.95m)
5μm
High magnification SEM of clay matrix. Clay matrix consists of randomly oriented sericite and illite. Pseudohexagonal outlines of authigenic kaolinite crystals are also present (A). Illite wisps generally terminate in pore space but occasionally growths from individual grains coalesce and bridge pore space. Microporosity in this sample is abundant but poor in quality. Most pores are extremely poor ranging between 1 and 4μm, and exist only within interlayered clays.

PLATE 7D

Sample 154838 (1473.95m)
20μm
High magnification back scattered image. High reflectivity mineral at A is barite. The matrix consists of a complex mixture of detrital quartz grains and authigenic clays, mainly illite, kaolinite and sericite. Visual microporosity is poor.

APPENDIX B (XRD ANALYSIS)

X-ray Analytical & Research Laboratory

c/o Department of Geology and Geophysics
The University of Western Australia
Nedlands, W.A. 6907

Telephone: (08) 9380 2694
Facsimile: (08) 9380 1037
E-mail: rchang@geol.uwa.edu.au

DATE: 20th October, 2000
REFERENCE No.: 201320

REPORT ON: QUALITATIVE X-RAY DIFFRACTION ANALYSIS

FOR: PGA Consultants Pty Ltd
PO Box 637
West Perth, W.A. 6872

PREPARED BY:

for Ray Chang B.Sc. (Nuclear Engineering)
Ph.D. (Solid State Physics)
Dip. Metallurgy
Dip. Gemmology

Note: While all reasonable care is used in all work produced by this Laboratory, this Laboratory does not represent that this work is suitable in respect of any particular use or function. Accordingly, this Laboratory accepts no liability in respect of any use or reliance upon such work unless specially acknowledged in writing.

REQUEST

Four clay samples as listed in Table 1 were submitted for qualitative X-ray diffraction (XRD) clay analysis.

Table 1. Sample information

Lab No	Sample Name
201320	Vines 1 598.23M
201321	Vines 1 644M
201322	Vines 1 682M
201323	Vines 1 930M

SAMPLE PREPARATION

All of the submitted samples were firstly crushed with an impact ring mill, then pulverized in a McCrone micronizing mill to homogenize the samples and reduce particle sizes. Randomly orientated specimens were prepared for qualitative XRD analysis by pressing the pulverized samples onto aluminium specimen holders making disks of depth 2mm and diameter 27mm.

Clay fraction of the submitted samples were extracted using sedimentation method. For clay identification XRD measurements, preferred orientation specimens were prepared by air-drying some slurries of the clay fraction of the submitted samples onto ceramic specimen holders at room temperature. After the initial XRD measurements, the original specimens were firstly saturated with ethylene glycol and then heated at 110°C and 500°C sequentially. XRD measurements were carried out after each of the above mentioned treatments.

X-RAY DIFFRACTOMETRY

All of the X-ray powder diffraction patterns were recorded at room temperature using a Philips PW1700 automatic diffractometer. X-rays generated from a copper x-ray tube operated at 45kV and 40mA were diffracted by a graphite monochromator for the production of monochromatic radiation. Both pulse-height discriminator and automatic diverging slits were used. The specimen was scanned at 0.5° per minute for 2θ range from 2° to 70°.

Positions and intensities of the diffraction lines were calculated using an on-line computer. Diffraction results were searched through 32,000 reference patterns of minerals and inorganic compounds which are stored in the memory of the computer.

RESULTS AND INTERPRETATION

Results from the XRD automatic computer Search/Match process are shown in the attached figures with vertical scales as diffraction intensities and horizontal scales as diffraction angles (2θ). Bar diagrams of identified phases are plotted together with the XRD pattern of the sample measured for comparison.

Diffraction patterns of the clay fraction of each sample after each treatment, i.e. "ORIGINAL", "GLYCOLAT", "110°C" and "500°C" have been plotted on the same graph for comparison of the effects of those treatments. The shift of peak positions below 10° of 2θ after the glycolation treatment, which indicates the existence of smectite in those samples.

The disappearance of a diffraction peak at approximately 12° of 2θ after the specimen was heated at 500°C indicates the existence of kaolinite in the specimen.

Table 2 summarizes the results of quantitative XRD clay analysis.

Sample	Remarks
Vines 1 598.23M	Mainly quartz, dolomite, microcline and albite; with small amounts of kaolinite, illite and swelling chlorite. Trace amounts of hematite and pyrite were probably also present. Dolomite content in this sample is the lowest among the four samples.
Vines 1 644M	Containing phases similar to Vines 1 598.23M. Dolomite content in this sample is the highest among the four samples.
Vines 1 682M	Containing phases similar to Vines 1 598.23M. Quartz content in this sample is the highest among the four samples.
Vines 1 930M	Containing phases similar to Vines 1 598.23M.

Sample identification: VINES 1 20-Oct-2000 9:30

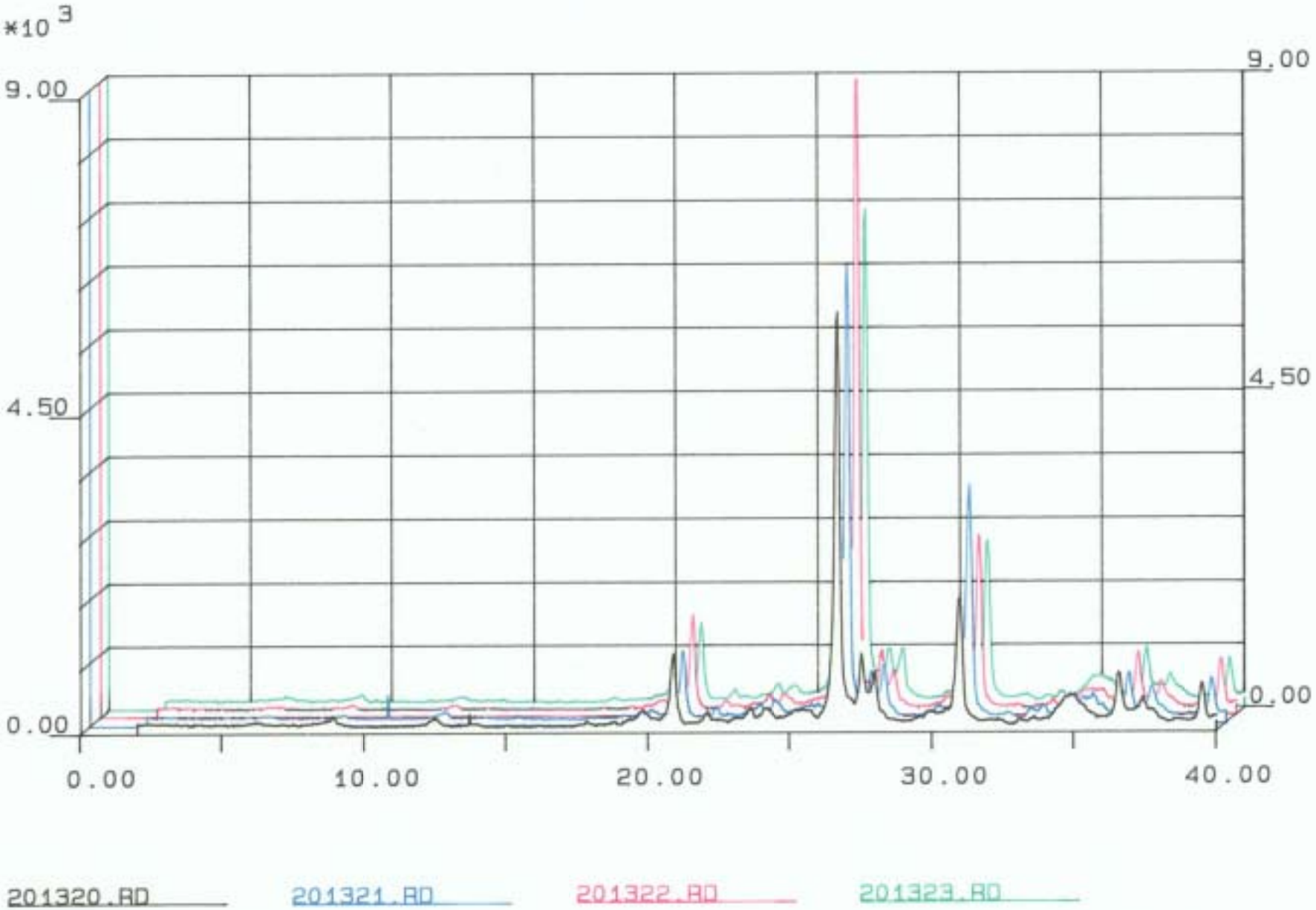

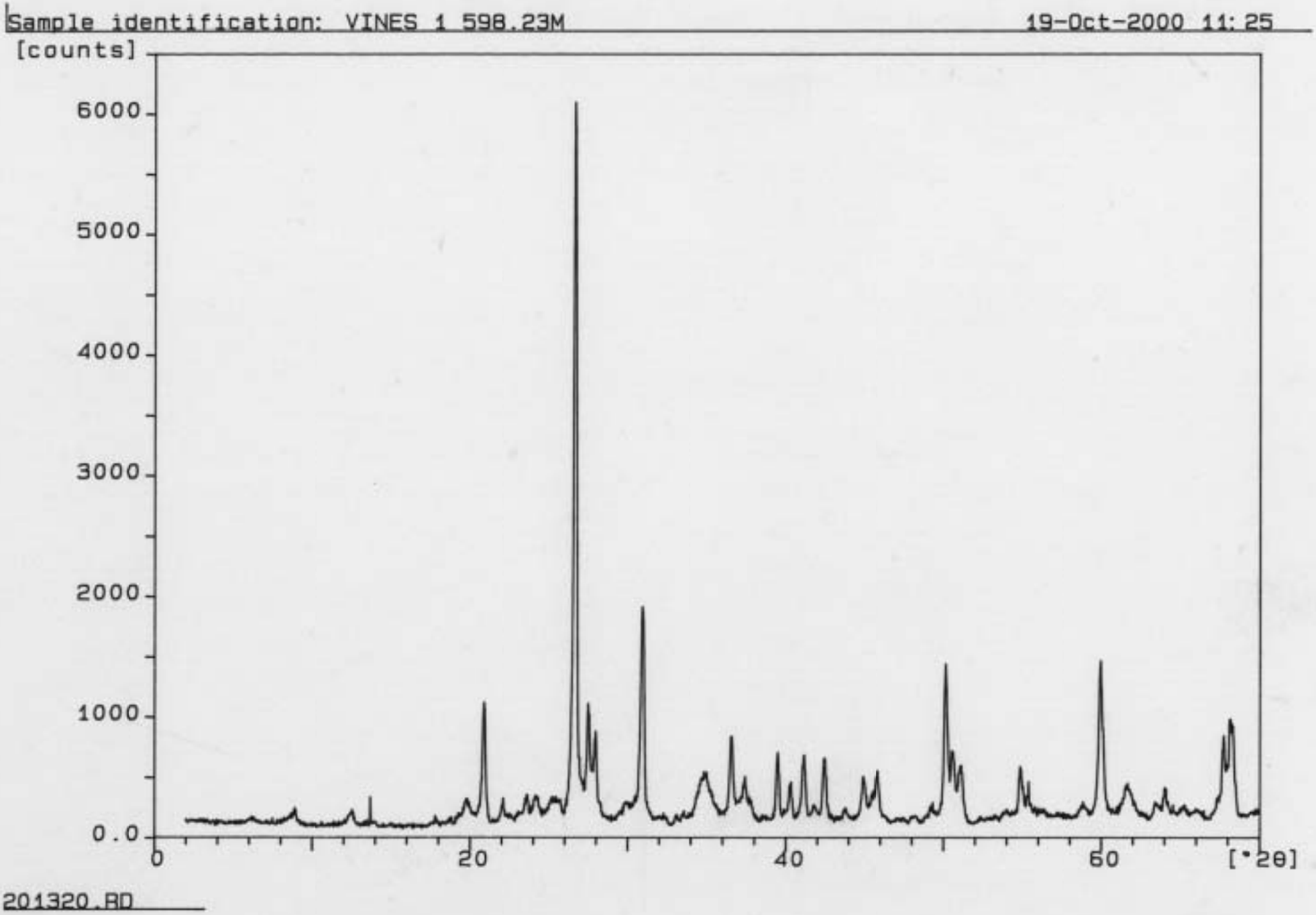
Sample identification: VINES 1 598.23M
19-Oct-2000 11:25
[counts]
6000
5000
4000
3000
2000
1000
0.0
0
20
40
60
[°2θ]
201320.RD

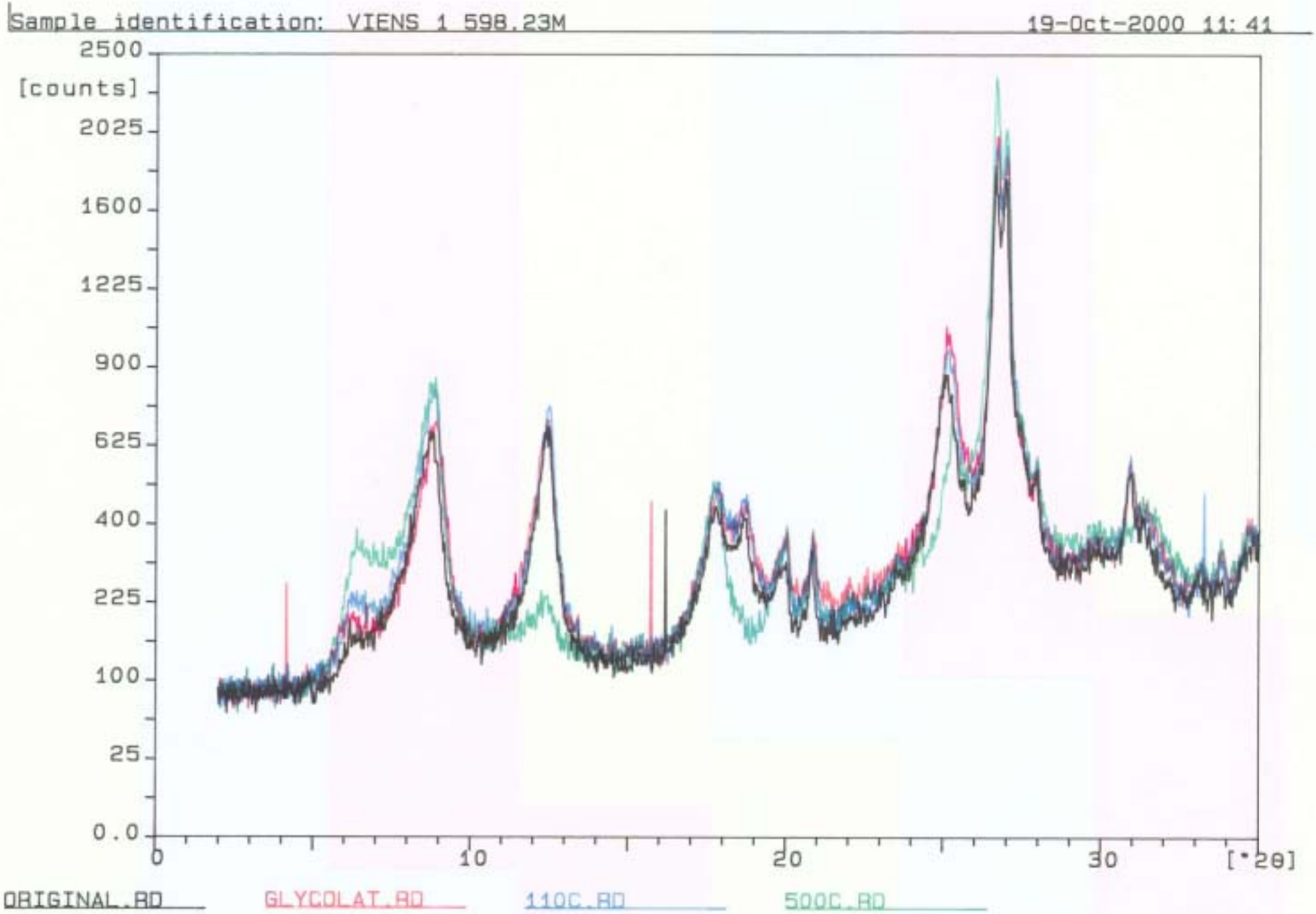
Sample identification: VIENS 1 598.23M
19-Oct-2000 11:41
2500
[counts]
2025
1600
1225
900
625
400
225
100
25
0.0
0
10
20
30
[°2θ]
ORIGINAL.RD
GLYCOLAT.RD
110C.RD
500C.RD

Sample ident.: VINES 1 598.23M 19-Oct-2000 15:52

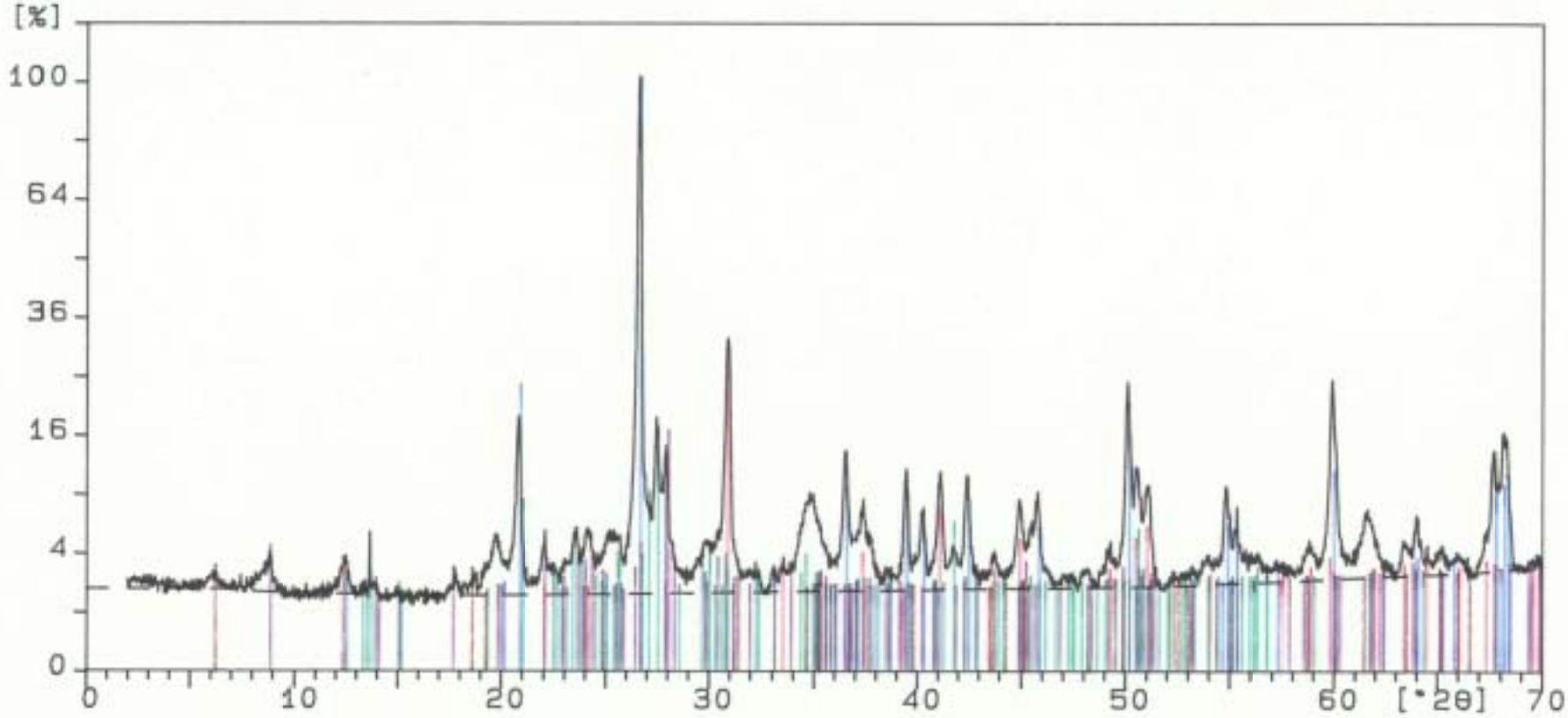

201320

33-1161	Quartz, syn	SiO2
36-0426	Dolomite	CaMg(CO3)2
19-0932	Microcline, intermediat	KAlSi3O8
41-1480	Albite, calcian, ordere	(Na,Ca)Al(Si,Al)3O8
29-0853	Clinochlore-1\ITM#I#I#b	Mg5Al(Si3Al)O10(OH)8
29-1488	Kaolinite-1\ITMd\RG	Al2Si2O5(OH)4
33-0664	Hematite, syn	Fe2O3
42-1340	Pyrite	FeS2
26-0911	Illite-2\ITM#1\RG	(K,H3O)Al2Si3AlO10(OH)

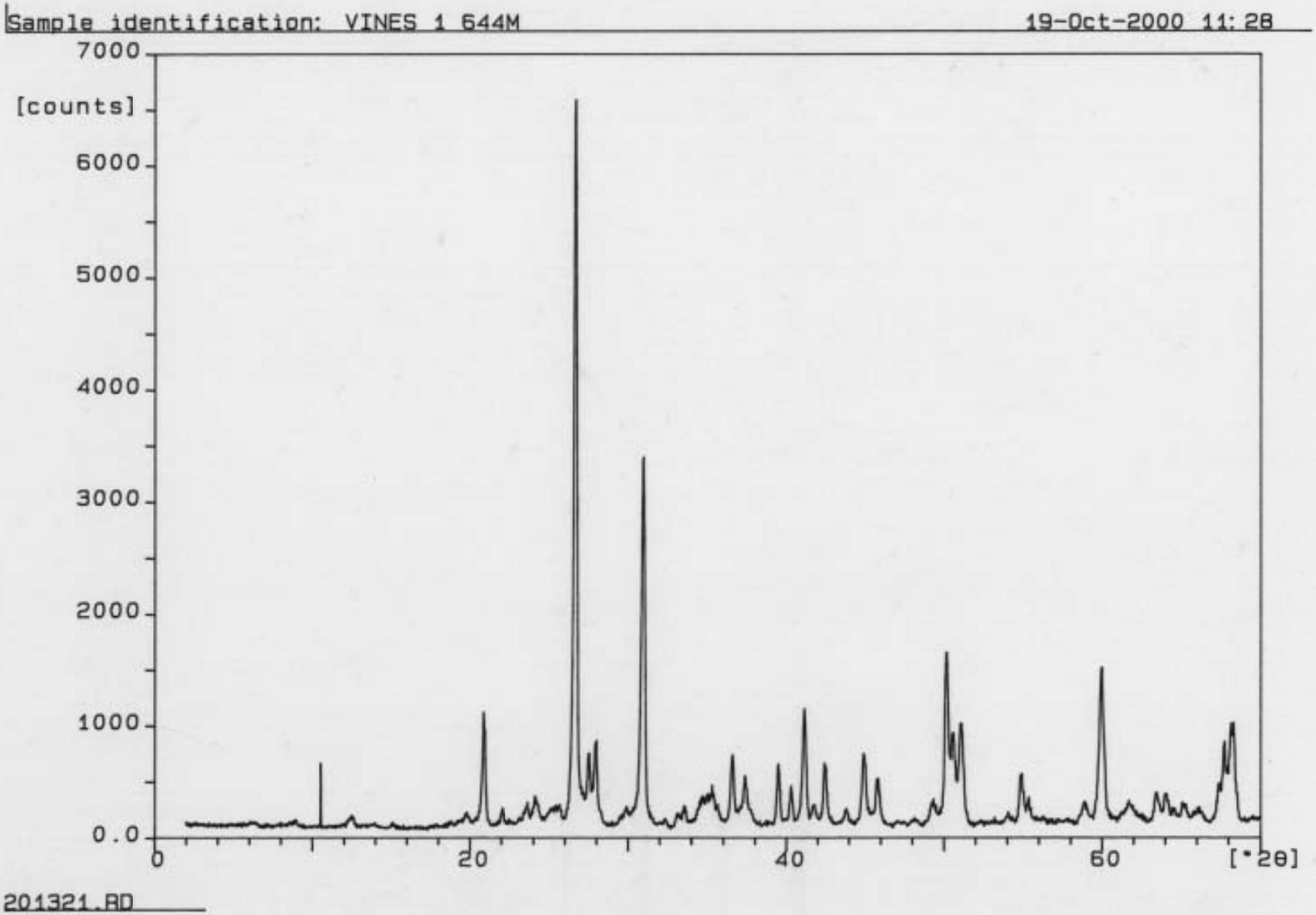
Sample identification: VINES 1 644M
19-Oct-2000 11:28
7000
[counts]
6000
5000
4000
3000
2000
1000
0.0
0
20
40
60
[°2θ]
201321.RD

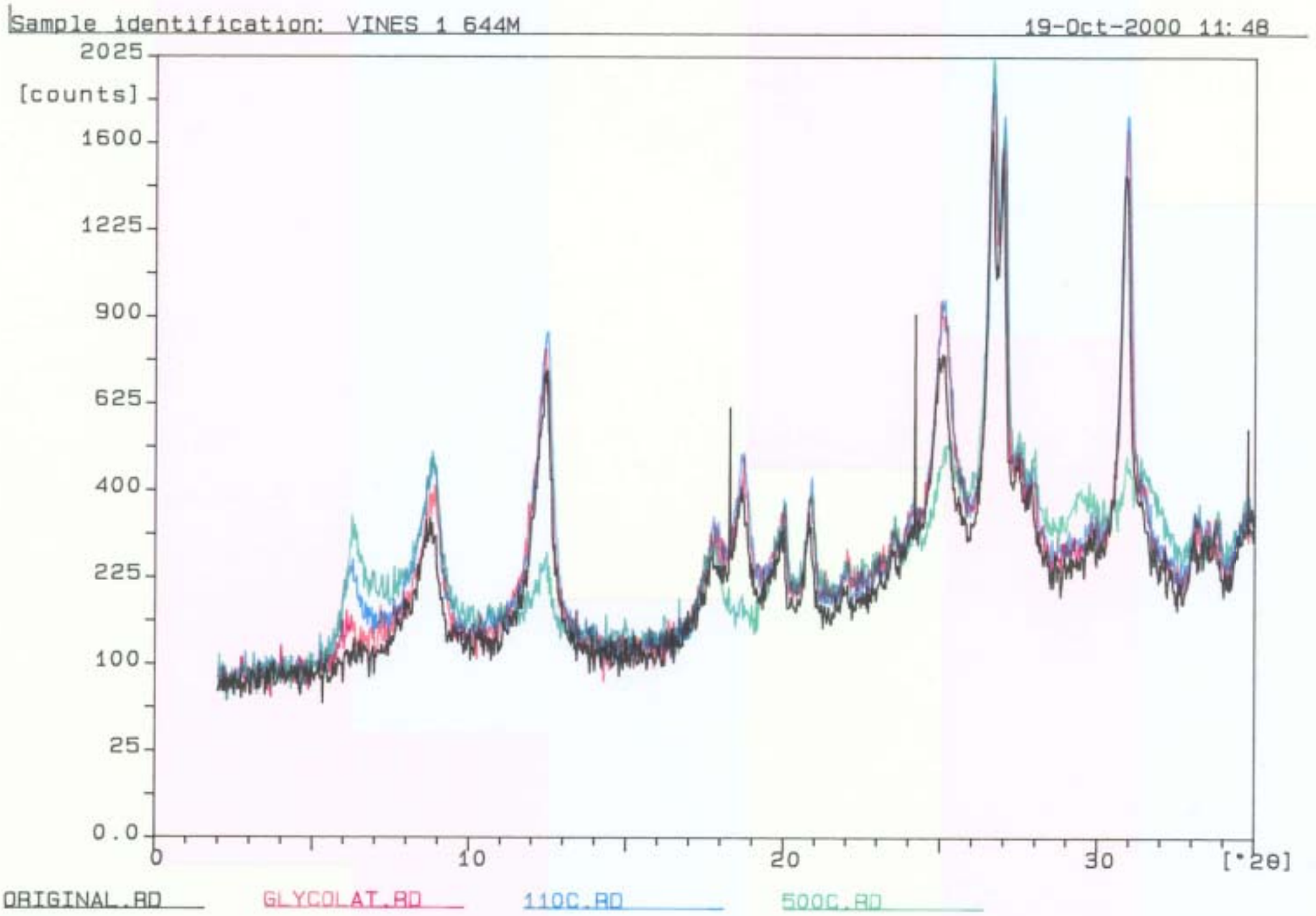
Sample identification: VINES 1 644M
19-Oct-2000 11:48
2025
[counts]
1600
1225
900
625
400
225
100
25
0.0
0
10
20
30
[°2θ]
ORIGINAL.RD
GLYCOLAT.RD
110C.RD
500C.RD

Sample ident.: VINES 1 644M 19-Oct-2000 16:02

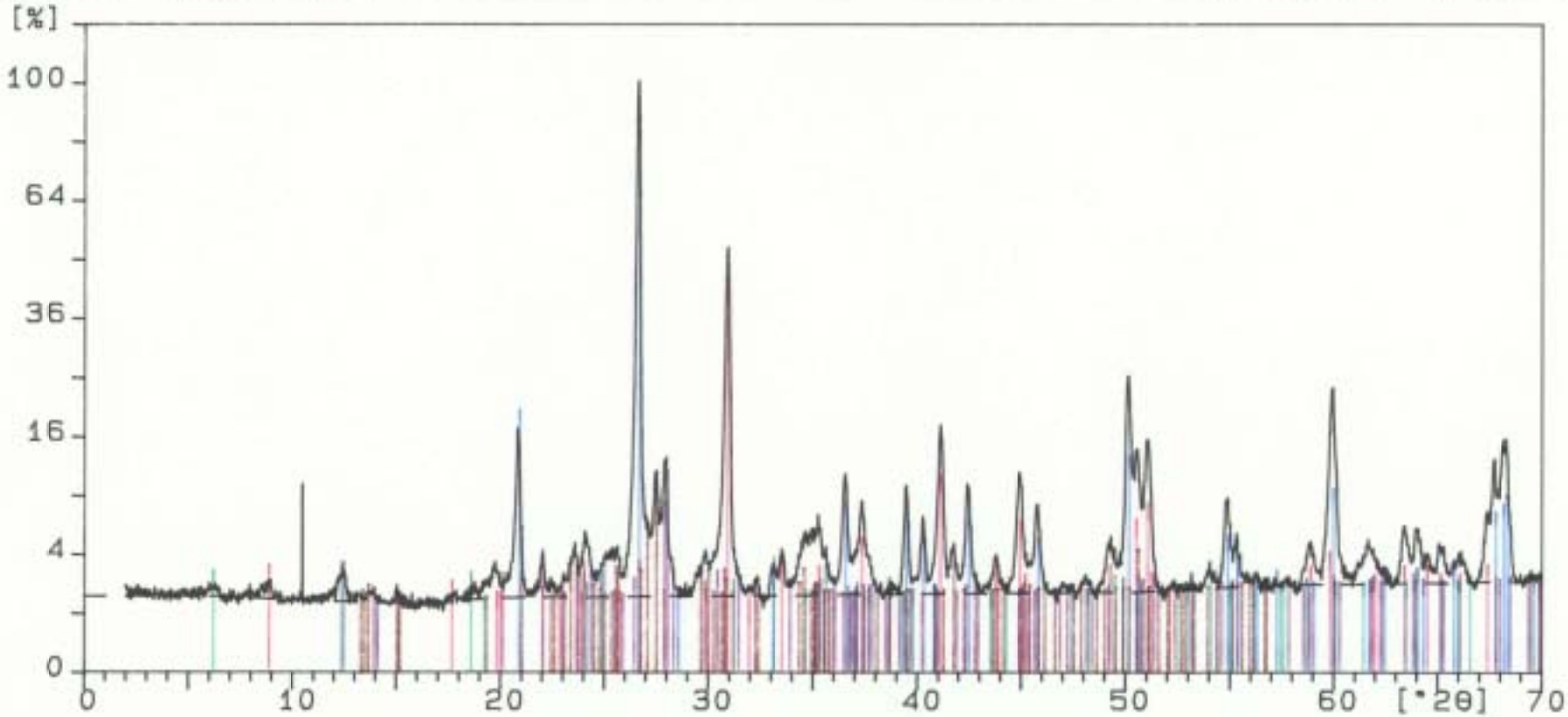

201321

33-1161	Quartz, syn	SiO2
36-0426	Dolomite	CaMg(CO3)2
33-0664	Hematite, syn	Fe2O3
41-1480	Albite, calcian, ordere	(Na,Ca)Al(Si,Al)3O8
19-0932	Microcline, intermediat	KAlSi3O8
42-1340	Pyrite	FeS2
26-0911	Illite-2\ITM#1\RG	(K,H3O)Al2Si3AlO10(OH)
29-0853	Clinochlore-1\ITM#I#I#b	Mg5Al(Si3Al)O10(OH)8
29-1488	Kaolinite-1\ITMd\RG	Al2Si2O5(OH)4

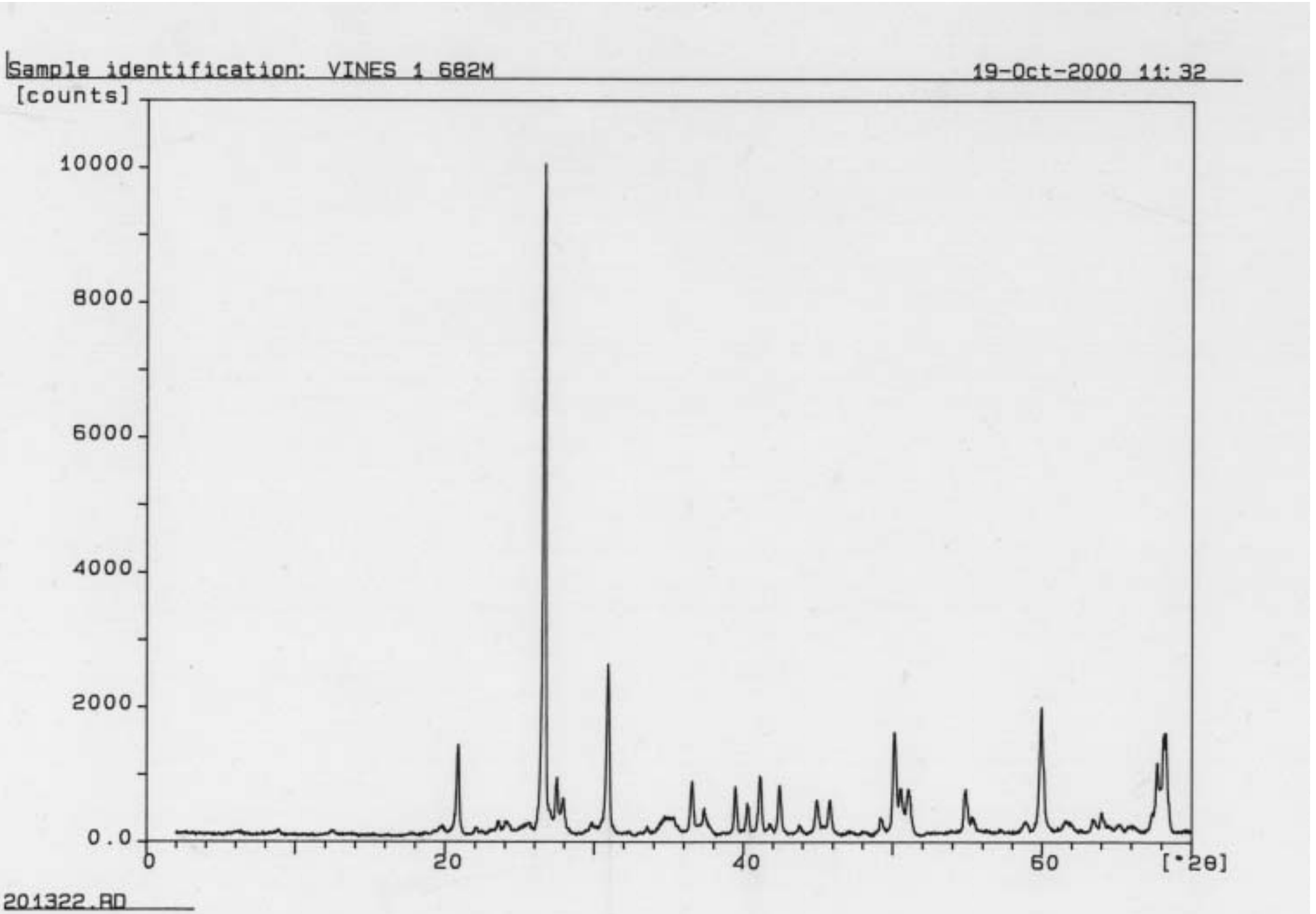
Sample identification: VINES 1 682M
19-Oct-2000 11:32
[counts]
10000
8000
6000
4000
2000
0.0
0
20
40
60
[°2θ]
201322.RD

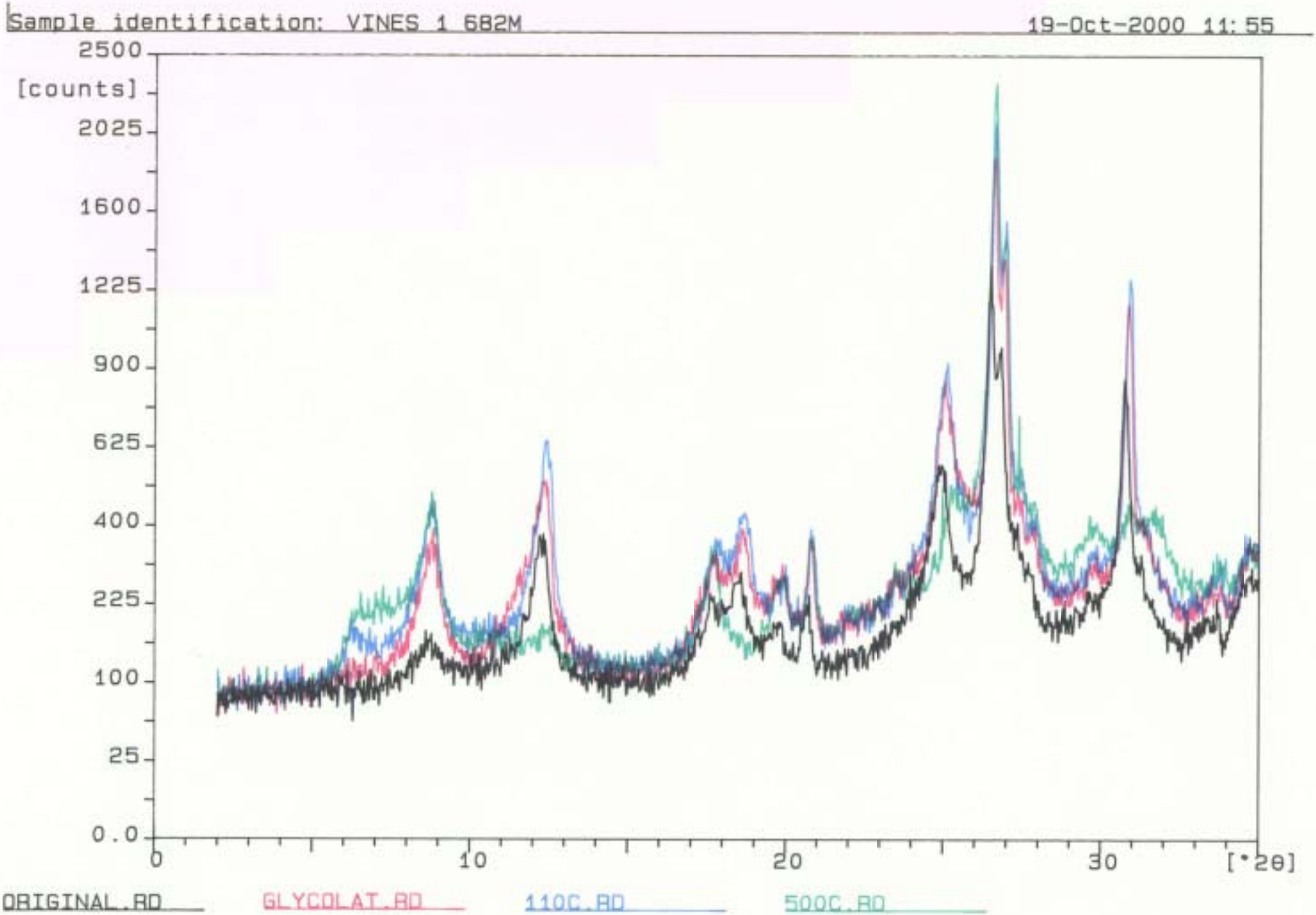
Sample identification: VINES 1 682M
19-Oct-2000 11:55
2500
[counts]
2025
1600
1225
900
625
400
225
100
25
0.0
0
10
20
30
[°2θ]
ORIGINAL.RD
GLYCOLAT.RD
110C.RD
500C.RD

Sample ident.: VINES 1 682M 19-Oct-2000 16:12

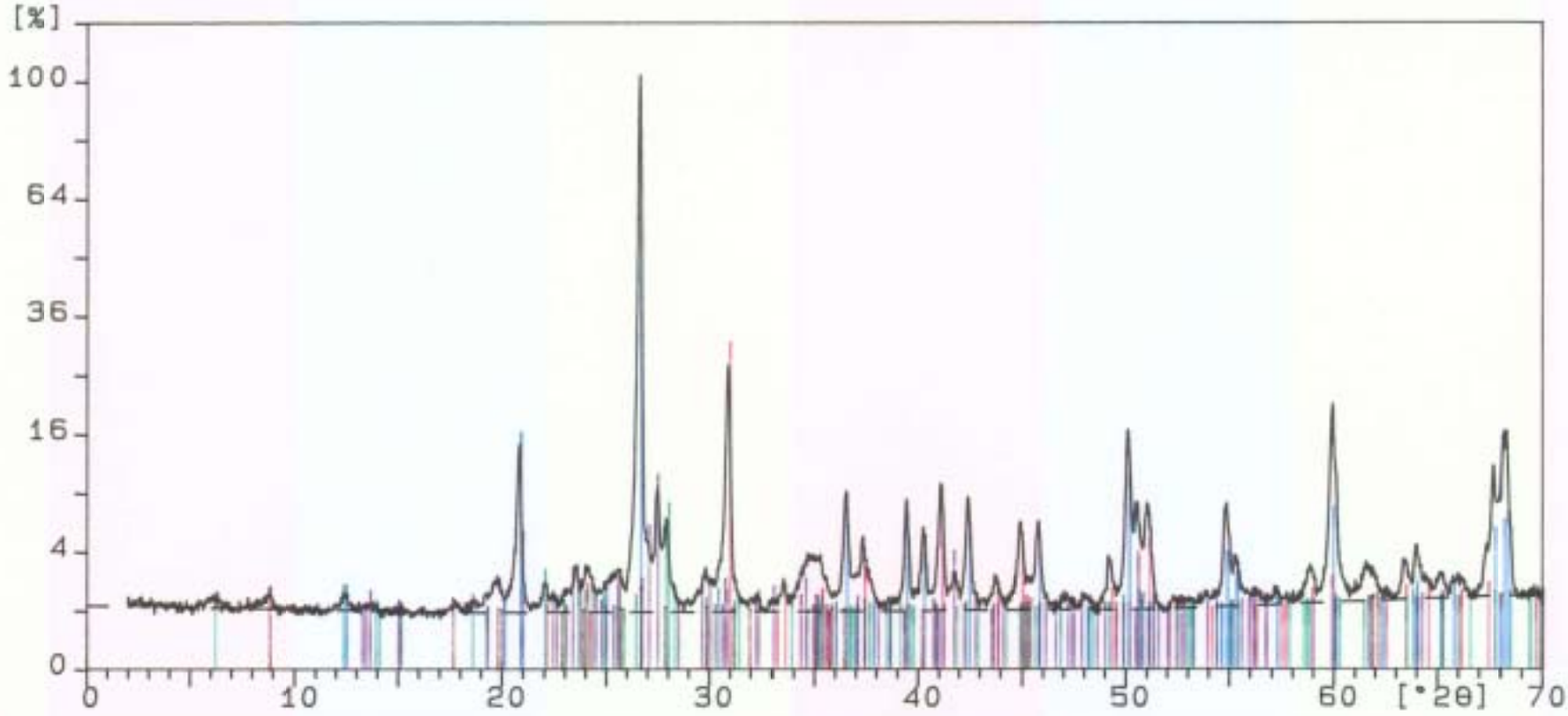

201322

33-1161	Quartz, syn	SiO2
36-0426	Dolomite	CaMg(CO3)2
41-1480	Albite, calcian, ordere	(Na,Ca)Al(Si,Al)3O8
19-0932	Microcline, intermediat	KAlSi3O8
26-0911	Illite-2\ITM#1\RG	(K,H3O)Al2Si3AlO10(OH)
29-1488	Kaolinite-1\ITMd\RG	Al2Si2O5(OH)4
33-0664	Hematite, syn	Fe2O3
29-0853	Clinochlore-1\ITM#I#I#b	Mg5Al(Si3Al)O10(OH)8
42-1340	Pyrite	FeS2

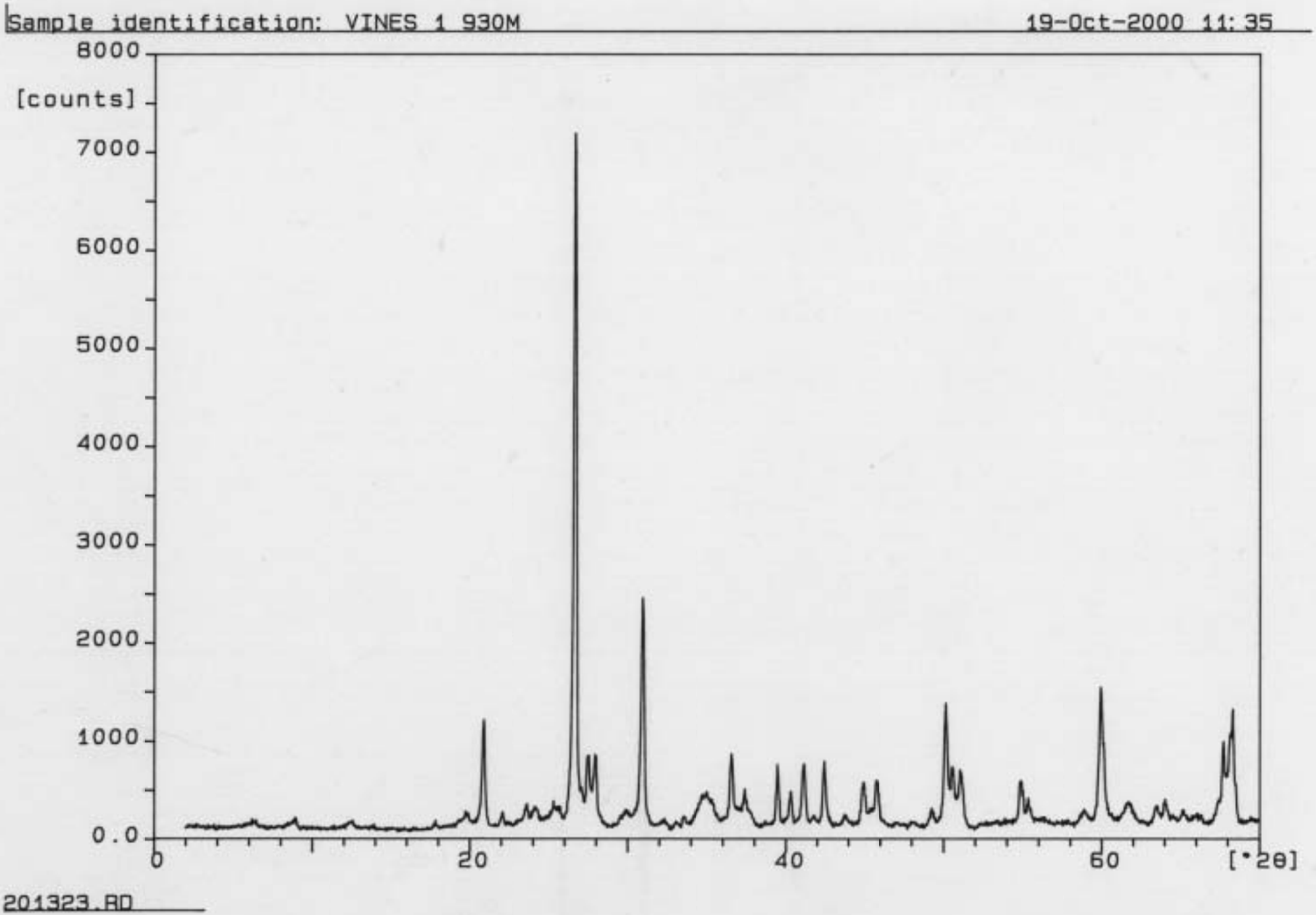
Sample identification: VINES 1 930M
19-Oct-2000 11:35
8000
[counts]
7000
6000
5000
4000
3000
2000
1000
0.0
0
20
40
60
[°2θ]
201323.RD

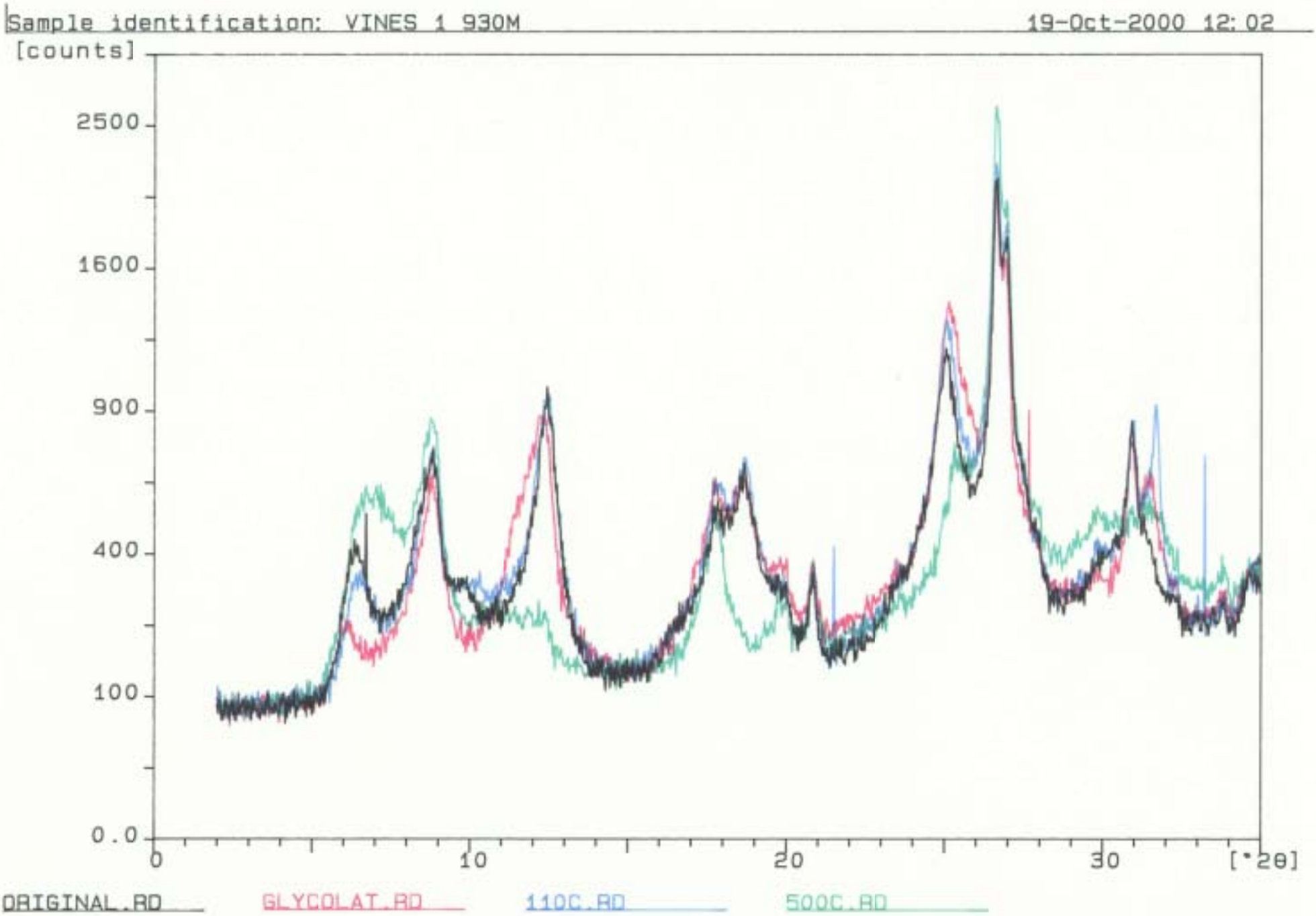
Sample identification: VINES 1 930M
19-Oct-2000 12:02
[counts]
2500
1600
900
400
100
0.0
0
10
20
30
[°2θ]
ORIGINAL.RD
GLYCOLAT.RD
110C.RD
500C.RD

Sample ident.: VINES 1 930M 19-Oct-2000 16:22

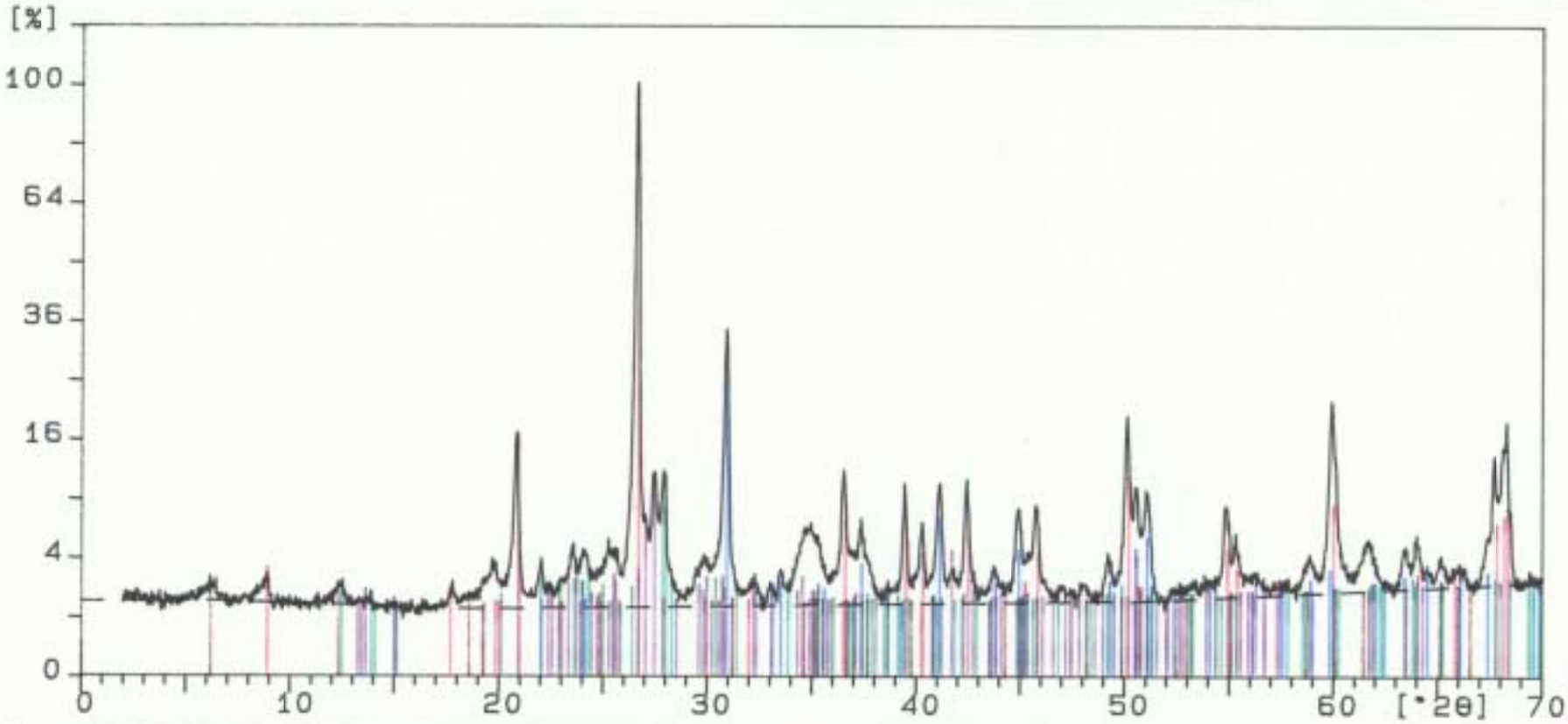

201323

36-0426	Dolomite	CaMg(CO3)2
33-1161	Quartz, syn	SiO2
41-1480	Albite, calcian, ordere	(Na,Ca)Al(Si,Al)3O8
19-0932	Microcline, intermediat	KAlSi3O8
29-0853	Clinochlore-1\ITM#I#I#b	Mg5Al(Si3Al)O10(OH)8
33-0664	Hematite, syn	Fe2O3
26-0911	Illite-2\ITM#1\RG	(K,H3O)Al2Si3AlO10(OH)
29-1488	Kaolinite-1\ITMd\RG	Al2Si2O5(OH)4
42-1340	Pyrite	FeS2

Appendix 6

PGA CONSULTANTS PTY LTD

VINES-1

Post-petrographic SEM and XRD reports for Vines 1

JOHN SONEGO

Suite 6, 6 Richardson St,
West Perth, Perth, W.A.
Ph: (08) 9226 3590
Email: jst@highway1.com.au

CONTENTS

1. INTRODUCTION 4
2. AIMS 4
3. SEM METHOD 4
4. SUMMARY 4

LIST OF APPENDICIES

APPENDIX A (SEM IMAGES) 7
PLATE 1A 8
PLATE 1B 8
PLATE 1C 8
PLATE 2A 9
PLATE 2B 9
PLATE 2C 9
PLATE 2D 9
PLATE 2E 9
PLATE 3A 10
PLATE 3B 10
PLATE 3C 10
PLATE 3D 10
PLATE 3E 10
PLATE 3F 10
PLATE 3G 11
PLATE 4A 11
PLATE 4B 11
PLATE 4C 11
PLATE 4D 11
PLATE 5A 12
PLATE 5B 12
PLATE 5C 12
PLATE 5D 12
PLATE 6A 13
PLATE 6B 13
PLATE 6C 13
PLATE 7A 13
PLATE 7B 13
PLATE 7C 14
PLATE 7D 14

APPENDIX B (XRD ANALYSIS) 15

1. INTRODUCTION

SEM images of 9 samples from Vines 1 are presented in this report. These samples are listed in Table 1.

Table 1. List of samples provided for SEM and XRD analysis.

Sample No	Depth (m)	Analysis
154801	133.20	SEM
154802	285.00	SEM
154869	598.23	SEM/XRD
154812	644.00	SEM/XRD
154814	682.00	SEM/XRD
154817	930.00	SEM/XRD
154871	985.25	SEM
154828	1100.15	SEM
154838	1473.95	SEM

Four of the samples, 154869 (598.23m), 154812 (644m), 154814 (682m) and 154817 (930m) were primarily analysed for seal capacity. These samples were analysed both by SEM and XRD. Splits of these samples were sent to Dr Ray Chang at the XRD Laboratory at the University of Western Australia for qualitative XRD clay analysis. A brief analytical report by Dr Ray Chang is provided in Appendix B of this report.

2. AIMS

The initial aims for SEM and XRD work were as follows;

1) Determine the nature of isopachous rims within samples 154801 (133.2m) and 154802 (285m) and whether they contain bituminous coatings.
2) Determine the composition and packing relationships of clays within all samples.
3) Investigate the seal capacity of four samples 154869 (598.23m), 154812 (644m), 154814 (682m) and 154817 (930m).
4) To observe and record in samples 154869 (598.23m), 154812 (644m), 154814 (682m) and 154817 (930m) any microfracturing and microporosity.
5) Identify and record any zircons (particularly xenotime) within samples.
6) Through XRD analysis provide a qualitative compositional analysis of clays within selected samples.

3. SEM METHOD

All SEM work was completed at the Curtin University of Technology Electron Microscopy Centre over two sessions using the Phillips XL-30 Secondary Detector. Samples were manually broken and mounted onto stubs. Stubs were vacuum pumped and carbon coated. Image quality in this report varies due to quality of the coated surface and the quality of samples. Charging may be apparent on some grain surfaces. In most samples clay structure is highly disorganised making imaging extremely difficult. Images ranging between 200μm and 5μm have been provided for most samples. Images were mainly taken as Secondary Electron Micrographs to show textural relationships between detrital grains and matrix components. Back scattered imaging was used to help in the identification of zircons and other high reflectivity minerals.

4. SUMMARY

Apart from samples 154801 (133.2m) and 154802 (285m) most samples consisted of a mixture of detrital grains and highly disorganised authigenic clays and dolomite. SEM imaging of samples 154801 and 154802 indicates that the isopachous rims originally considered in petrographic work to be bituminous are in fact clays. There is a possibility however that in sample 154802 (285m) grain coatings may still contain a mixture of clay and bitumen. Preparation of samples for SEM imaging

included drying the samples and then vaccuum pumping them. This may have resulted in the extraction of any bitumen trapped within clay rims.

Two types of grain coating are evident in samples 154801 and 154802. In sample 154801 clays coat detrital grains with an orientation parallel with grain surfaces. The clay coating on grains in this sample is inferred to be "inherited," in that it formed on framework grains prior to their deposition. These rims tend to vary in thickness and rough textural appearance. The formation of clay rims on detrital grains has resulted in the preservation of intergranular porosity. Only traces of bridging resulting in the partial occlusion of pore space are evident in this sample.

In sample 154802 (285m) the isopachous rim is inferred to be authigenic. This coating is interpreted to have formed during early diagenesis. The rim in this sample is composed predominantly of illite occurring tangential to the grain surface. Generally the thickness of the illite coat is uniform however some bridging is evident at grain contacts. Traces of chlorite are evident growing within the illite clays.

Samples 154869 (598.23m), 154812 (644m), 154814 (682m) and 154817 (930m) were investigated through XRD and SEM analysis. XRD analysis (Appendix B) indicates that all 4 samples are compositionally similar. Apart from slight variations in the percentages all samples consisted predominantly of quartz, dolomite, microcline and albite with small amounts of kaolinite, illite and swelling chlorite. Trace amounts of haematite and pyrite are also evident (Appendix B). SEM images of these sample show them to be mainly "dirty" samples composed of a detrital and authigenic matrix compacted around detrital grains. The matrix component of these samples is composed predominantly of kaolinite/ sericite that rarely contains an ordered, stacked appearance. Most of the kaolinite/sericite occur as highly disordered and partially corroded pseudohexagonal crystals. The disordering and displacement of the clays in these samples is due to the growth of late stage microcrystalline dolomite. Dolomite crystals range from 2 to 10μm in size. Thin, wispy illite terminations are evident marginally overgrowing kaolinite/sericite crystals. Illitic clays occasionally bridge pore space.

Small microfractures are evident in samples 154814 (682m), 154817 (930m) and 154871 (983.24m). These microfractures tend to be multi-directional displaying both sub-vertical and sub-horizontal orientations. In sample 154817, microfractures have an irregular stylolitic appearance (PLATE 4A). Most microfractures tend to be discontinuous and small with most not reaching more than 150μm in length. It is proposed that these microfractures have no effect on the sealing capacity of these units. It is important to note also that some of the microfractures seen in SEM micrographs may have been induced during sample preparation. Microporosity within these samples is also poor. The lack of ordering of clays and the development of late stage dolomite and illite cements have destroyed most interlayer porosity in the clays. Remnant micropores tend to be small (2 to 10μm in diameter) and isolated. The lack of microfractures and micorpores suggests that these samples would have excellent sealing capacity.

Two samples, 154828 (1100.15m) and 154838 (1478.95m) were analysed from the lower part of the well and therefore were more prone to diagenetic effects. These samples consisted predominantly of a complex mixture of randomly oriented kaolinite/sericite clays. The disordering of the clays as in the samples above, is caused by the late stage expansion of microcrystalline dolomite into pore space. Thin, wispy terminations of illite are evident marginally overgrowing kaolinite/sericite clays and detrital grains. Microporosity within these samples is extremely poor with most micropores ranging between 1 and 4μm in diameter.

Samples were imaged by back scattering in an attempt to find any zircons that may have assisted in the dating of these samples. Unfortunately back scattered images failed to provide any zircons for analysis. All high reflectivity minerals under back scattered imaging were probed. Probing identified only two main minerals, barite and illmenite? (i.e. Figures 1 & 2). Barite crystals are evident in all samples except 154801 (133.2m) and 154802 (285m). These crystals range in size from 1 to 10μm in diameter. Barite crystals typically form blocking micropores. The occurrence of barite in samples 154869 (598.23m), 154812 (644m), 154814 (682m) and 154817 (930m) has therefore aided in the reduction of microporosity and an increase in the overall seal capacity. Illmenite crystals tend to occur as elongate laths embedded within the matrix of these samples.

In summary samples used in this study were poor for SEM analysis. The disordering of clays and the destruction of primary fabrics made mineral identification and imaging difficult. However the aims were still able to be addressed effectively. It is recommended however that sample 154802 (285m) be analysed geochemically as there still may be a possibility of encountering bitumen within the trapped within grain coatings.

APPENDIX A (SEM IMAGES)

See Photo Library on this CD for Plates 1–7

PLATE 1

PLATE 1A

Sample 154801 (133.2m)
200μm

Low magnification SEM of framework grains coated by an isopachous clay rim. Clays display an orientation parallel with grain surfaces. Clay coatings are ragged with coating thickness varying considerably. Bridging of pore space between framework grains is evident at A. Locally, faint outlines of illitic fibers can be recognised. Intergranular porosity is good in this sample.

PLATE 1B

Sample 154801 (133.2m)
200μm
Low magnification SEM. Sample consists of framework grains coated in an isopachous clay rim. Clays are generally oriented parallel to the framework grain surface. Trace illite growth is evident on grain boundaries. Kaolinite and sericite clays are evident filling pore and marginally overgrowing detrital grains at A. High reflectivity mineral (B) is barite.

PLATE 1C

Sample 154802 (285m)
50μm
High magnification SEM. Detrital grains are coated in a thin illitic clay. Illite is evident oriented tangential to grain surface. It occurs as a secondary cement following quartz overgrowth cementation. Evidence of pre-illite quartz overgrowth formation is evident at A. Illitic clays generally terminate in intergranular pore space but occasionally they can be seen to bridge across pore space. Isolated outlines of small euhedral chlorite crystals are evident growing within illite clay rims.

PLATE 2

PLATE 2A

Sample 154869 (598.23m)
200µm
Low magnification SEM. Overview image of sample displays only trace microporosity making it an effective sealing rock type.

PLATE 2B

Sample 154869 (598.23m)
10µm
High magnification SEM of a "dirty" sample showing detrital and authigenic matrix compacted around detrital grains. Matrix content consists of a mixture of kaolinite and illite clays. Clays have been marginally displaced by late stage dolomite growth (i.e. B). At A, a large feldspar grain is evident. This grain has been partially leached and replaced in part by illite and chlorite clays. Thin authigenic silica overgrowths are evident on some detrital quartz grains (i.e. C). Visual microporosity in this sample is poor.

PLATE 2C

Sample 154812 (644m)
20µm
High magnification SEM. Sample consists predominantly of sub-rounded quartz grains that have been overgrown by authigenic quartz. Intergranular pore space is filled by a mixture of dolomite and kaolinite with thin, wispy overgrowths of illite. Microporosity is poor. Micropores range from 2 to 10µm in diameter. Traces of barite (high reflectivity) are scattered throughout the sample.

PLATE 2D

Sample 154812 (644m)
50µm
High magnification SEM. Imprint of feldspar grain removed during sample preparation is evident at A. The surrounding matrix consists predominantly of microcrystalline dolomite rhombs and thin wispy illite terminations. Small (5 to 10µm in size) pseudohexagonal outlines of kaolinite are also evident scattered throughout the matrix. Some microfracturing is evident in this sample but it is inferred to have been developed during sample preparation. Traces of barite (high reflectivity) are scattered throughout the sample.

PLATE 2E

Sample 154812 (644m)
20µm
High magnification SEM. Vermicular kaolinite stacks are evident at A. Ordering of the clays is rare, most of the sample consists of highly disorganised clays. An interlocking mosaic of microcrystalline dolomite rhombs are evident at C. Late stage dolomite growth is the cause of most of the disordering of pore filling clays within the sample. At B a large, sub-rounded detrital quartz grain is evident. Early quartz overgrowth cementation is present on the grain surface. Traces of barite (high reflectivity) are evident scattered throughout the sample. Existent microporosity in this sample is interpreted to be due to plucking during sample preparation.

PLATE 3

PLATE 3A

Sample 154814 (682m)
200µm
Low magnification SEM. Sample is in reasonable condition, however grain plucking during sample manufacture is evident at A, B and C. At this magnification no microporosity is apparent. In effect it is predicted that this sample would contain good sealing capacity.

PLATE 3B

Sample 15414 (682m)
5µm
High magnification SEM of matrix component. Sample consists predominantly of randomly oriented clays and small euhedral dolomite crystals. Sericitic clays are occasionally evident by their vermicular stacking pattern. Thin, wispy terminations of illite are evident at A, partially coating authigenic clays. Trace microporosity is evident mainly between clay sheets.

PLATE 3C

Sample 154814 (682m)
20µm
High magnification back scattered image displaying a large 10µm mineral in the centre which was identified by microprobing as barite (Figure 1). The barite crystal has been partially dissolved and marginally overgrown by authigenic clay matrix. The matrix is dominated by corroded pseudohexagonal crystals of kaolinite, sericite and thin wispy overgrowths of illite. Visual microporosity is poor.

PLATE 3D

Sample 154814 (682m)
50µm
High magnification back scattered image. Spectra (Figure 2) indicates that the large elongate lath at the centre of micrograph is possibly illmenite. This grain is supported in a matrix consisting of sheet-like illite and small euhedral dolomite rhombs. Illitic clays are evident overgrowing the illmenite crystal at B. A small microfracture is evident at C. This microfracture is thin and discontinuous and would have no effect on the sealing capacity of this sample. Micopores range from 2 to 10µm in diameter. Overgrowth cementation is evident on the illmenite crystal at D.

PLATE 3E

Sample 154814 (682m)
50µm
High magnification SEM of a “dirty” sample showing detrital and authigenic matrix compacted around detrital grains. Matrix content consists of a mixture of disorganised (kaolinite and sericite) clays and microcrystalline dolomite. Grain plucking during sample manufacture is evident within this sample (i.e. A). Small microfractures are also evident propogating sub-horizontally throughout this sample. Microfractures are inferred to be in situ and form an irregular, discontinuous, anastomosing network. A large illmenite? lath is evident at C. Traces of barite (high reflectivity) are scattered throughout the sample.

PLATE 3F

Sample 154814 (682m)
50µm
High magnification back scattered image displaying an barite crystal (A) and an elongate Fe-rich (illmenite?) lath (B).

PLATE 3G

Sample 154814 (682m)
20μm
High magnification SEM. A large micropore approximately 40μm in diameter is evident at A. Small wispy terminations of illite are evident protruding from pore margins and into pore space. A small, discontinuous localised fracture is evident at B. Clays within the matrix are highly disorganised and difficult to distinguish. XRD analysis indicates that this sample is dominated by dolomite with minor illite and kaolinite. Well-developed microporosity is evident scattered throughout this sample. Micropore sizes range from 2 to 8μm in diameter.

PLATE 4

PLATE 4A

Sample 154817 (930m)
500μm
Low magnification SEM. Overview image of sample showing distinctive sub-horizontal microfracturing. These microfractures appear stylolitic. High reflectivity mineral at A is barite.

PLATE 4B

Sample 154817 (930m)
20μm
High magnification SEM of a dirty sample showing detrital and authigenic matrix compacted around detrital quartz grains. Clays are highly disorganised and difficult to distinguish. XRD analysis indicates that this sample is dominated by dolomite, chlorite, illite and kaolinite. Clays form a thin isopachous rim on detrital grains (A). Thin, wispy Illitic clays display a weak sub-vertical preferential alignment. A small discontinuous microfracture is evident propogating parallel to clay direction. Visual microporosity in this sample is negligible.

PLATE 4C

Sample 154817 (930m)
20μm
High magnification back scattered image of an elongate Fe-rich (illmenite?) crystal embedded in a matrix composed predominantly of dolomite, chlinochlore, illite and kaolinite (inferred through XRD). Clays within the matrix are highly disorganised.

PLATE 4D

Sample 154817 (930m)
50μm
High magnification SEM displaying microfracturing within the sample. Fractures are multi-directional. Grain plucking is evident at A. Quartz grain at B is being marginally overgrown by authigenic clays. The intergranular pore space consists of a mixture of dolomite and kaolinite overgrown by thin, wispy terminations of illite. Visual microporosity is poor in this sample.

PLATE 5

PLATE 5A

Sample 154871 (985.24m)
100µm
Overview low magnification SEM. Sample consists of a mixture of sub-rounded quartz supported in a "dirty" matrix consisting of a mixture of detrital and authigenic clays. Matrix clays consist predominantly of kaolinite/sericite and thin, wispy terminations of illite. Clays are highly disorganised due the late stage growth of displacive microcrystalline dolomite. Visual microporosity in this sample is extremely poor.

PLATE 5B

Sample 154871 (985.24m)
50µm
Low magnification SEM. Image contains a large sub-angular quartz grain at its centre which is surrounded by a matrix consisting predominantly of an interlocking mosaic of small 2 to 5µm euhedral dolomite crystals. Trace clays evident within the matrix are highly disorganised. Thin, wisps of illite are occasionally evident overgrowing detrital grain margins and authigenic dolomite. Early authigenic silica overgrowths are evident coating detrital quartz grains. High reflectivity mineral 5µm in size is barite. Visual microporosity is poor.

PLATE 5C

Sample 154871 (985.24m)
50µm
High magnification SEM of "dirty" sample showing detrital and authigenic matrix compacted around detrital grains. Matrix is composed predominantly of an interlocking mosaic of small 2 to 5µm euhedral dolomite crystals and traces of kaolinite/sericite. Matrix and detrital grains have been partially overgrown by late stage illite. Barite (high reflectivity) grains are randomly scattered throughout the sample. Visual microporosity is poor.

PLATE 5D

Sample 154871 (983.24m)
50µm
High magnification SEM. Large quartz grain at A display early quartz overgrowth cementation. Matrix consists of a mixture of small 2 to 5µm euhedral dolomite crystals and traces of kaolinite/sericite and chlorite. Small sub-vertical microfractures are evident in this sample. It is inferred that these microfractures were formed during sample preparation. Visual microporosity is poor.

PLATE 6

PLATE 6A

Sample 154828 (1100.15m)
20µm
High magnification SEM. Pore space is filled by predominately kaolinite/sericite with minor wisps of illite/sericite. The disordered nature of pore filling material may be due to late stage cementation of dolomite. Occasional corroded outlines of finely crystalline pseudohexagonal kaolinite are evident. Traces of barite (high reflectivity mineral) are evident. Some microfracturing is evident in this sample but fractures are inferred to have been generated during sample preparation. Visual microporosity is poor. Micopores that are evident range from 2 to 4µm in diameter.

PLATE 6B

Sample 154828 (1100.15m)
5µm
High magnification SEM of matrix material. The sample is dominated by corroded pseudohexagonal outlines of kaolinite and sericite. Clays are randomly oriented. Thin wispy, terminations of illite are evident partially overgrowing corroded kaolinite and sericite crystals. Well-developed microporosity is evident in this sample. Micropores range from 2 to 5µm in diameter.

PLATE 6C

Sample 154828 (1100.15m)
20µm
High magnification SEM. Solitary quartz is evident in the right hand side of this image. Pore filling material is predominately composed of a disordered and complex mixture of microcrystalline dolomite and thin wispy illite terminations. Visual microporosity in this sample is poor. Rare micropores that are evident in this sample range from 1 to 4µm in diameter.

PLATE 7

PLATE 7A

Sample 154838 (1473.95m)
10µm
High magnification SEM. This sample consists of a complex mixture of randomly oriented clays. It is predominantly composed of finely crystalline pseudohexagonal kaolinite and sericite. Clay margins are difficult to distinguish as they have been broken, corroded and altered. Thin wispy terminations of illite are evident overgrowing clays and projecting into adjacent pore space. The relationship of illite to surrounding matrix classifies it as being late in the diagenetic sequence. Occasionally wisps of illite from individual grains join and bridge pore space. Only trace microporosity is evident in this sample. Traces of barite (high reflectivity) are evident at A.

PLATE 7B

Sample 154838 (1473.95m)
10µm
High magnification SEM. Sample is dominated by detrital quartz grains displaying thick illite wisps radiating from grain margins which overgrow and replace kaolinite/sericite clays. The matrix component consists of corroded pseudohexagonal outlines of kaolinite and sericite and small isolated euhedral dolomite rhombs. Traces of barite (high reflectivity mineral) are present scattered throughout the sample. Barite grains are approximately 1 to 2µm in size. Visual micorporosity is poor.

PLATE 7C

Sample 154838 (1473.95m)
5μm
High magnification SEM of clay matrix. Clay matrix consists of randomly oriented sericite and illite. Pseudohexagonal outlines of authigenic kaolinite crystals are also present (A). Illite wisps generally terminate in pore space but occasionally growths from individual grains coalesce and bridge pore space. Microporosity in this sample is abundant but poor in quality. Most pores are extremely poor ranging between 1 and 4μm, and exist only within interlayered clays.

PLATE 7D

Sample 154838 (1473.95m)
20μm
High magnification back scattered image. High reflectivity mineral at A is barite. The matrix consists of a complex mixture of detrital quartz grains and authigenic clays, mainly illite, kaolinite and sericite. Visual microporosity is poor.

APPENDIX B (XRD ANALYSIS)

X-ray Analytical & Research Laboratory

c/o Department of Geology and Geophysics
The University of Western Australia
Nedlands, W.A. 6907

Telephone: (08) 9380 2694
Facsimile: (08) 9380 1037
E-mail: rchang@geol.uwa.edu.au

DATE: 20th October, 2000
REFERENCE No.: 201320

REPORT ON: QUALITATIVE X-RAY DIFFRACTION ANALYSIS

FOR: PGA Consultants Pty Ltd
PO Box 637
West Perth, W.A. 6872

PREPARED BY:

for Ray Chang B.Sc. (Nuclear Engineering)
Ph.D. (Solid State Physics)
Dip. Metallurgy
Dip. Gemmology

Note: While all reasonable care is used in all work produced by this Laboratory, this Laboratory does not represent that this work is suitable in respect of any particular use or function. Accordingly, this Laboratory accepts no liability in respect of any use or reliance upon such work unless specially acknowledged in writing.

REQUEST

Four clay samples as listed in Table 1 were submitted for qualitative X-ray diffraction (XRD) clay analysis.

Table 1. Sample information

Lab No	Sample Name
201320	Vines 1 598.23M
201321	Vines 1 644M
201322	Vines 1 682M
201323	Vines 1 930M

SAMPLE PREPARATION

All of the submitted samples were firstly crushed with an impact ring mill, then pulverized in a McCrone micronizing mill to homogenize the samples and reduce particle sizes. Randomly orientated specimens were prepared for qualitative XRD analysis by pressing the pulverized samples onto aluminium specimen holders making disks of depth 2mm and diameter 27mm.

Clay fraction of the submitted samples were extracted using sedimentation method. For clay identification XRD measurements, preferred orientation specimens were prepared by air-drying some slurries of the clay fraction of the submitted samples onto ceramic specimen holders at room temperature. After the initial XRD measurements, the original specimens were firstly saturated with ethylene glycol and then heated at 110°C and 500°C sequentially. XRD measurements were carried out after each of the above mentioned treatments.

X-RAY DIFFRACTOMETRY

All of the X-ray powder diffraction patterns were recorded at room temperature using a Philips PW1700 automatic diffractometer. X-rays generated from a copper x-ray tube operated at 45kV and 40mA were diffracted by a graphite monochromator for the production of monochromatic radiation. Both pulse-height discriminator and automatic diverging slits were used. The specimen was scanned at 0.5° per minute for 2θ range from 2° to 70°.

Positions and intensities of the diffraction lines were calculated using an on-line computer. Diffraction results were searched through 32,000 reference patterns of minerals and inorganic compounds which are stored in the memory of the computer.

RESULTS AND INTERPRETATION

Results from the XRD automatic computer Search/Match process are shown in the attached figures with vertical scales as diffraction intensities and horizontal scales as diffraction angles (2θ). Bar diagrams of identified phases are plotted together with the XRD pattern of the sample measured for comparison.

Diffraction patterns of the clay fraction of each sample after each treatment, i.e. "ORIGINAL", "GLYCOLAT", "110°C" and "500°C" have been plotted on the same graph for comparison of the effects of those treatments. The shift of peak positions below 10° of 2θ after the glycolation treatment, which indicates the existence of smectite in those samples.

The disappearance of a diffraction peak at approximately 12° of 2θ after the specimen was heated at 500°C indicates the existence of kaolinite in the specimen.

Table 2 summarizes the results of quantitative XRD clay analysis.

Sample	Remarks
Vines 1 598.23M	Mainly quartz, dolomite, microcline and albite; with small amounts of kaolinite, illite and swelling chlorite. Trace amounts of hematite and pyrite were probably also present. Dolomite content in this sample is the lowest among the four samples.
Vines 1 644M	Containing phases similar to Vines 1 598.23M. Dolomite content in this sample is the highest among the four samples.
Vines 1 682M	Containing phases similar to Vines 1 598.23M. Quartz content in this sample is the highest among the four samples.
Vines 1 930M	Containing phases similar to Vines 1 598.23M.

Sample identification: VINES 1 20-Oct-2000 9:30

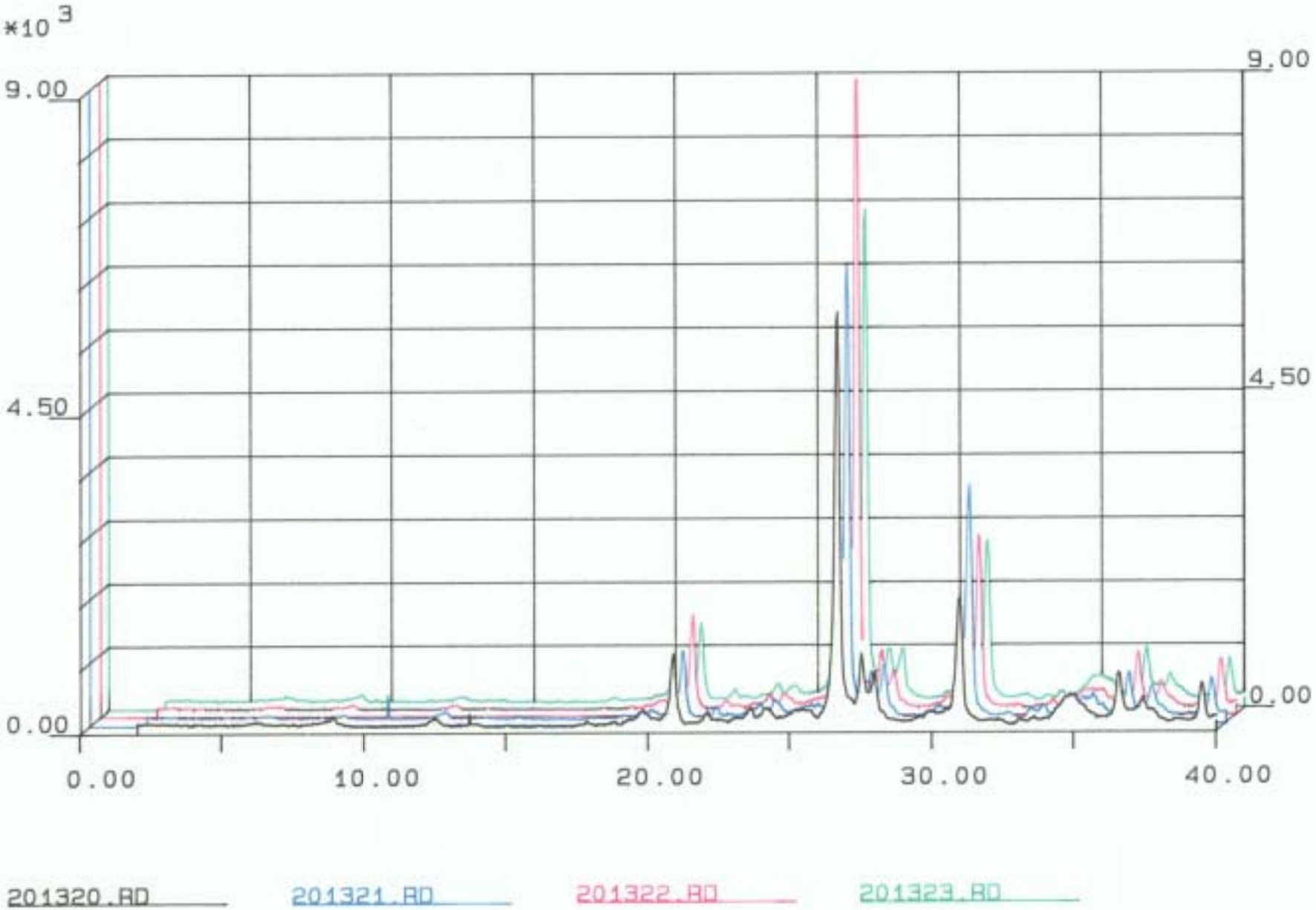

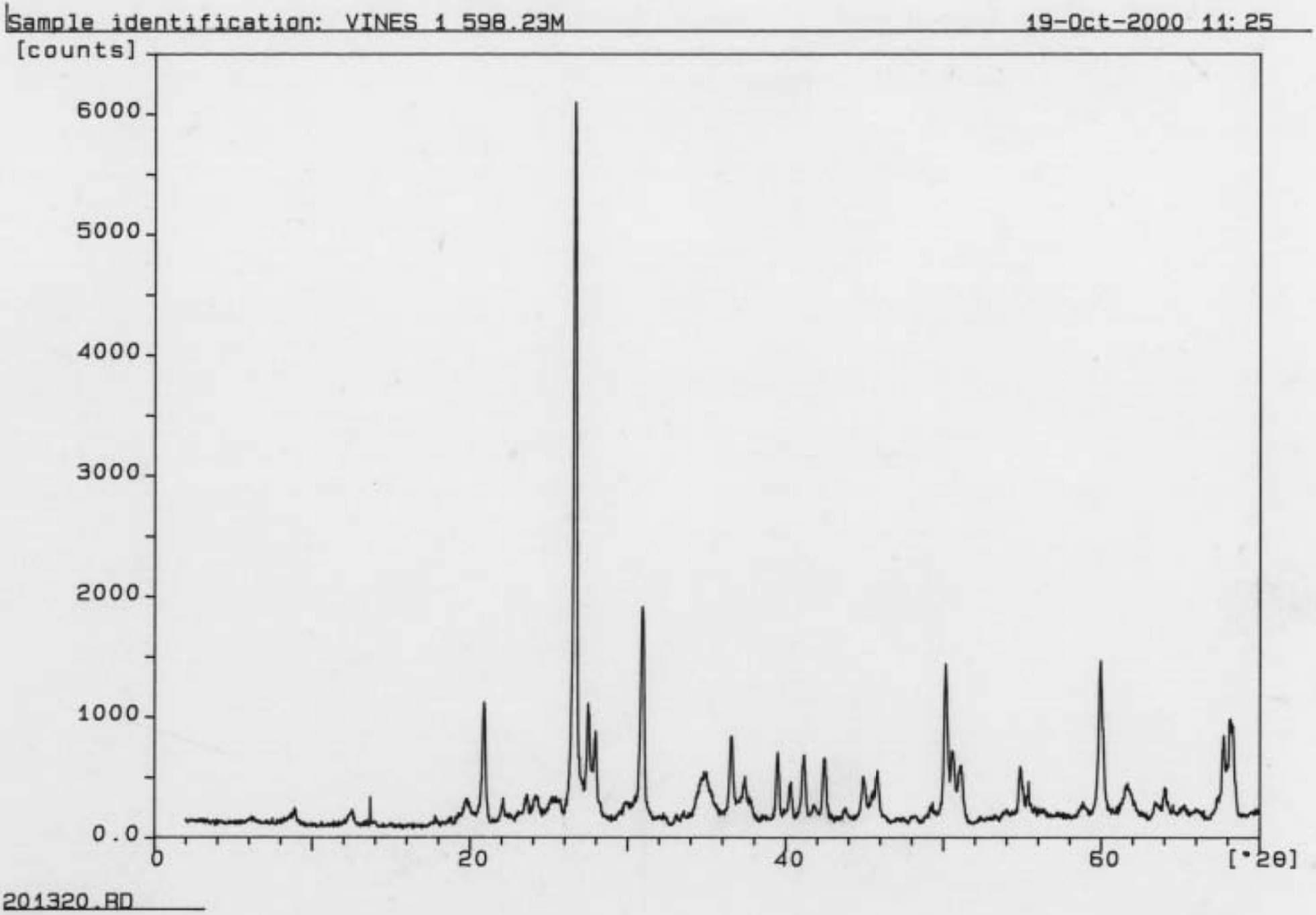
Sample identification: VINES 1 598.23M
19-Oct-2000 11:25
[counts]
6000
5000
4000
3000
2000
1000
0.0
0
20
40
60
[°2θ]
201320.RD

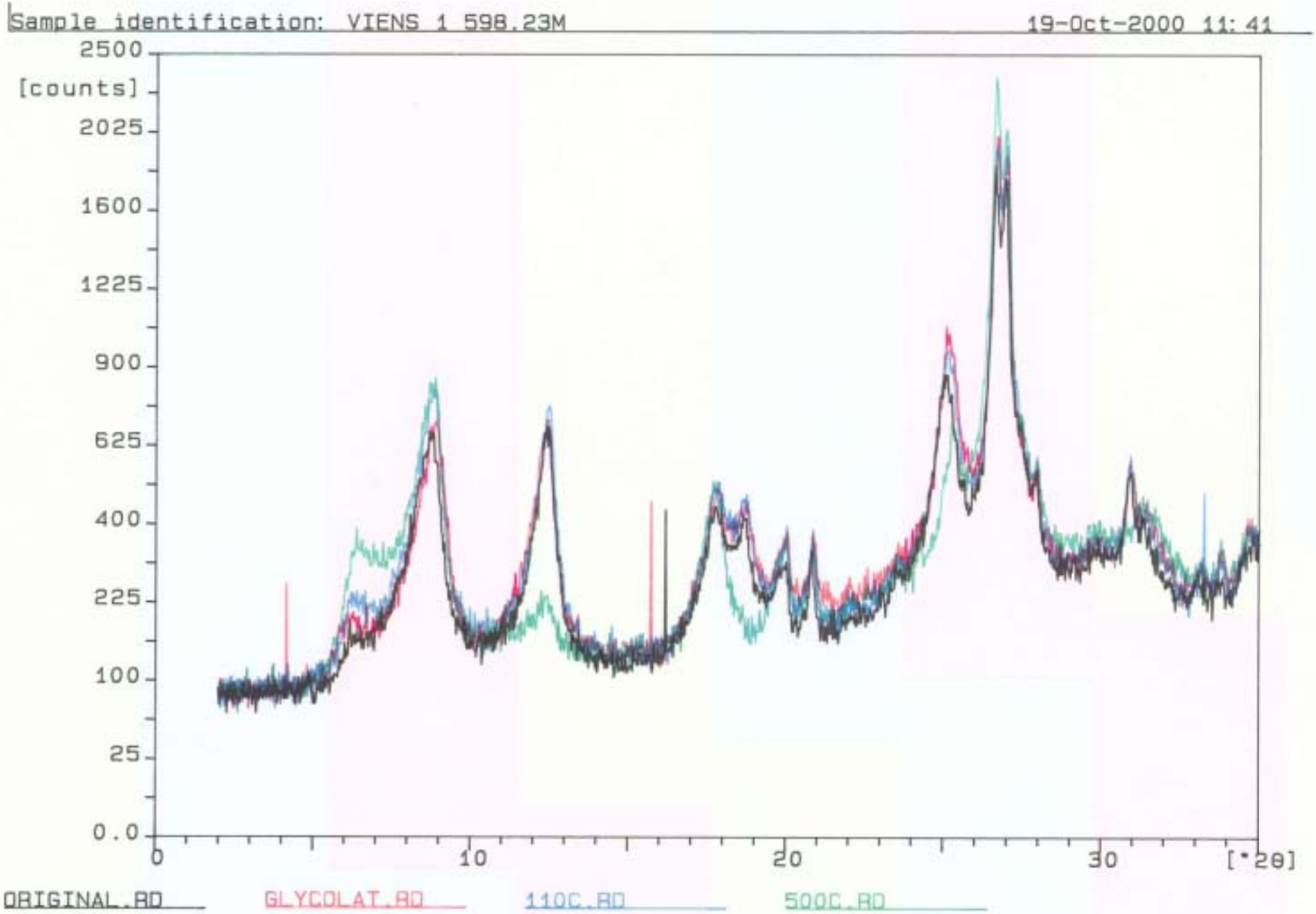
Sample identification: VIENS 1 598.23M
19-Oct-2000 11:41
2500
[counts]
2025
1600
1225
900
625
400
225
100
25
0.0
0
10
20
30
[°2θ]
ORIGINAL.RD
GLYCOLAT.RD
110C.RD
500C.RD

Sample ident.: VINES 1 598.23M 19-Oct-2000 15:52

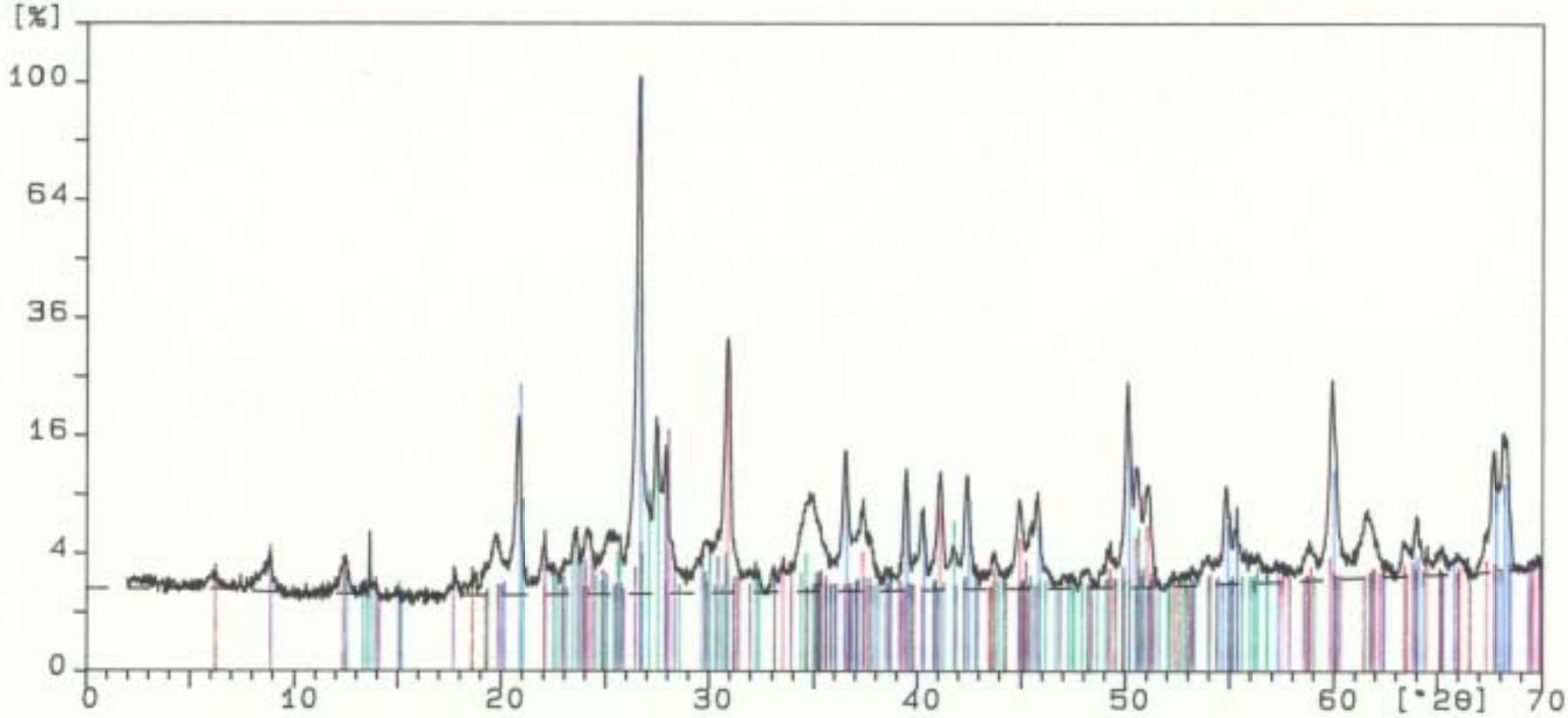

201320

33-1161	Quartz, syn	SiO2
36-0426	Dolomite	CaMg(CO3)2
19-0932	Microcline, intermediat	KAlSi3O8
41-1480	Albite, calcian, ordere	(Na,Ca)Al(Si,Al)3O8
29-0853	Clinochlore-1\ITM#I#I#b	Mg5Al(Si3Al)O10(OH)8
29-1488	Kaolinite-1\ITMd\RG	Al2Si2O5(OH)4
33-0664	Hematite, syn	Fe2O3
42-1340	Pyrite	FeS2
26-0911	Illite-2\ITM#1\RG	(K,H3O)Al2Si3AlO10(OH)

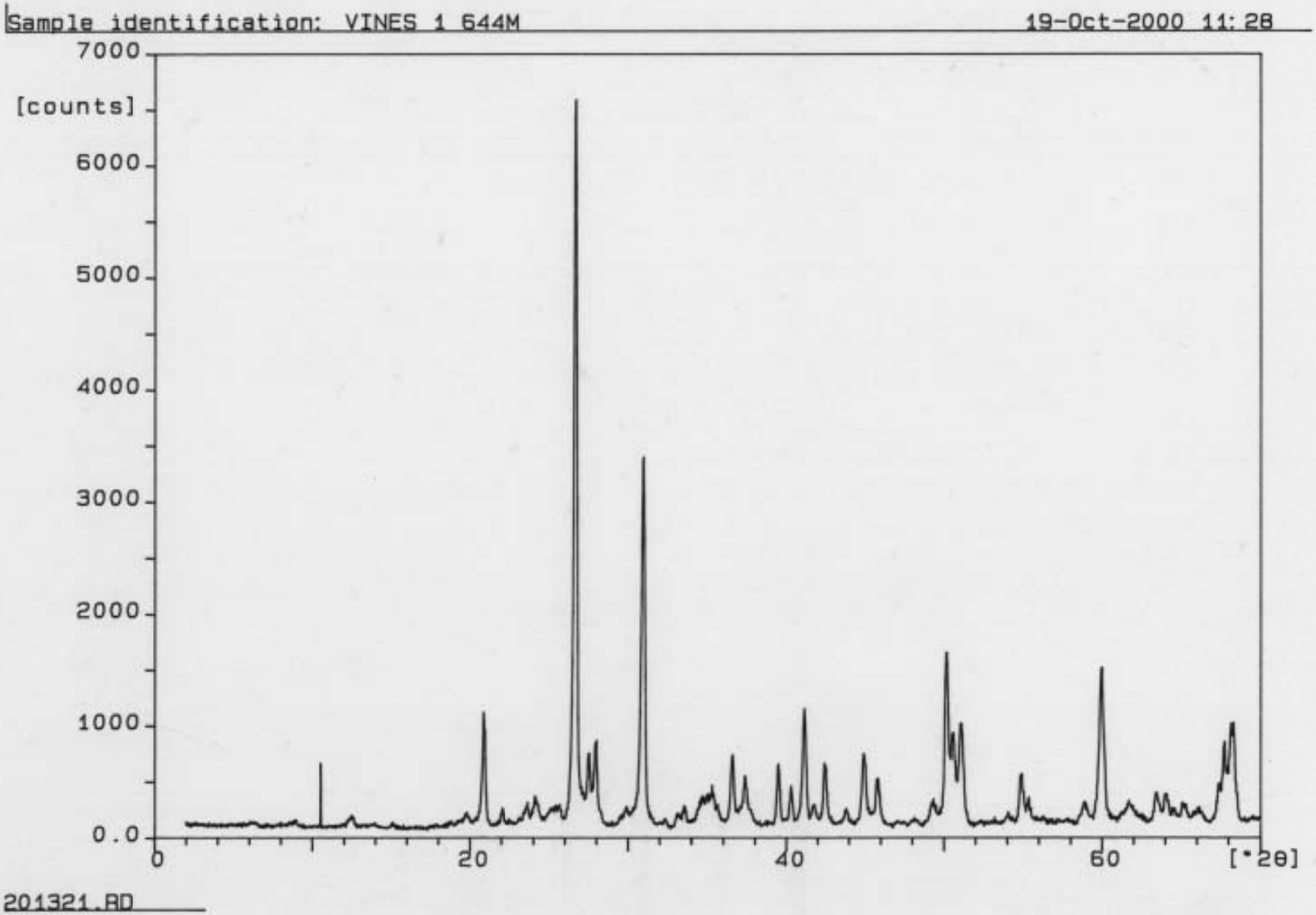
Sample identification: VINES 1 644M
19-Oct-2000 11:28
7000
[counts]
6000
5000
4000
3000
2000
1000
0.0
0
20
40
60
[°2θ]
201321.RD

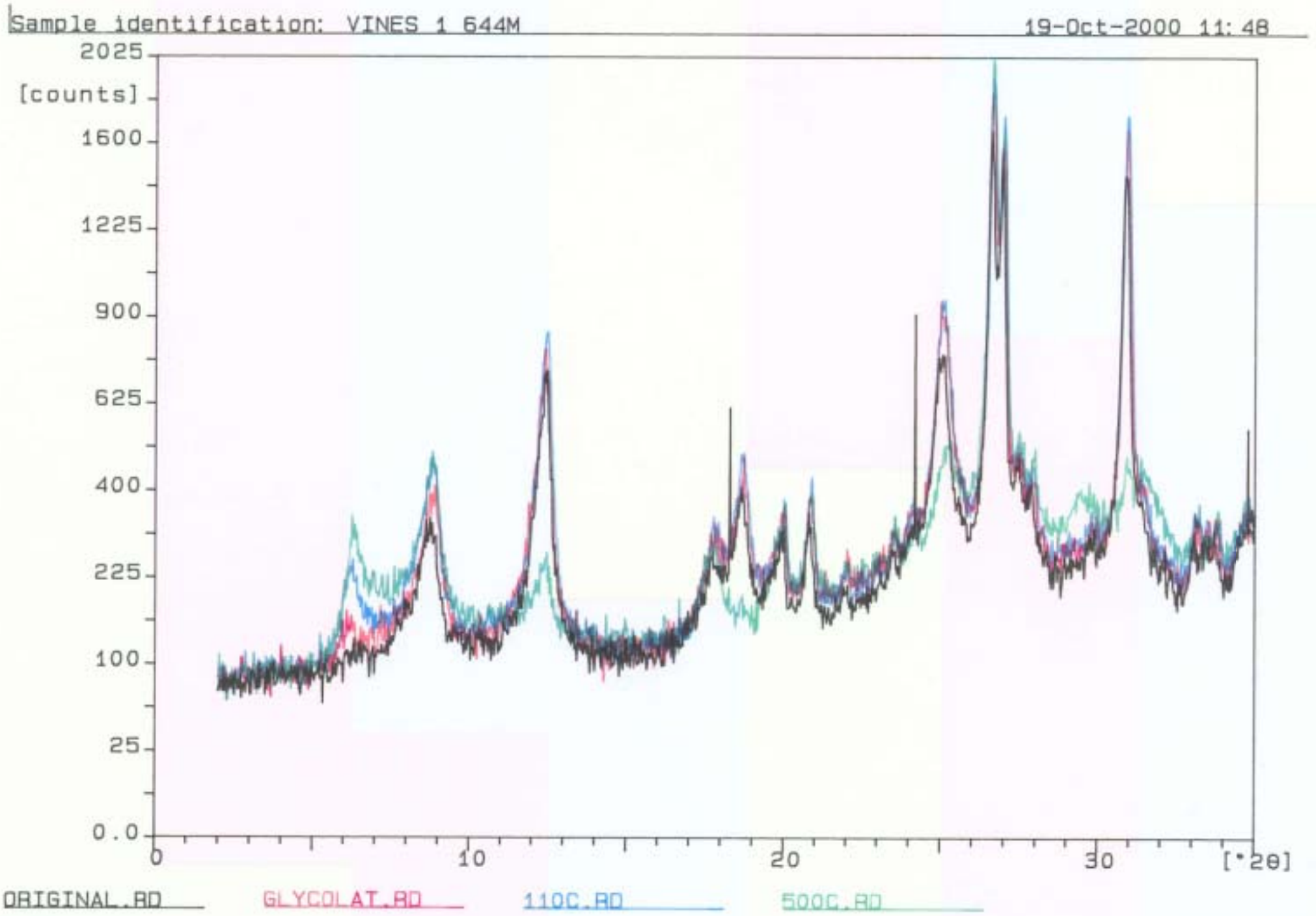
Sample identification: VINES 1 644M
19-Oct-2000 11:48
2025
[counts]
1600
1225
900
625
400
225
100
25
0.0
0
10
20
30
[°2θ]
ORIGINAL.RD
GLYCOLAT.RD
110C.RD
500C.RD

Sample ident.: VINES 1 644M 19-Oct-2000 16:02

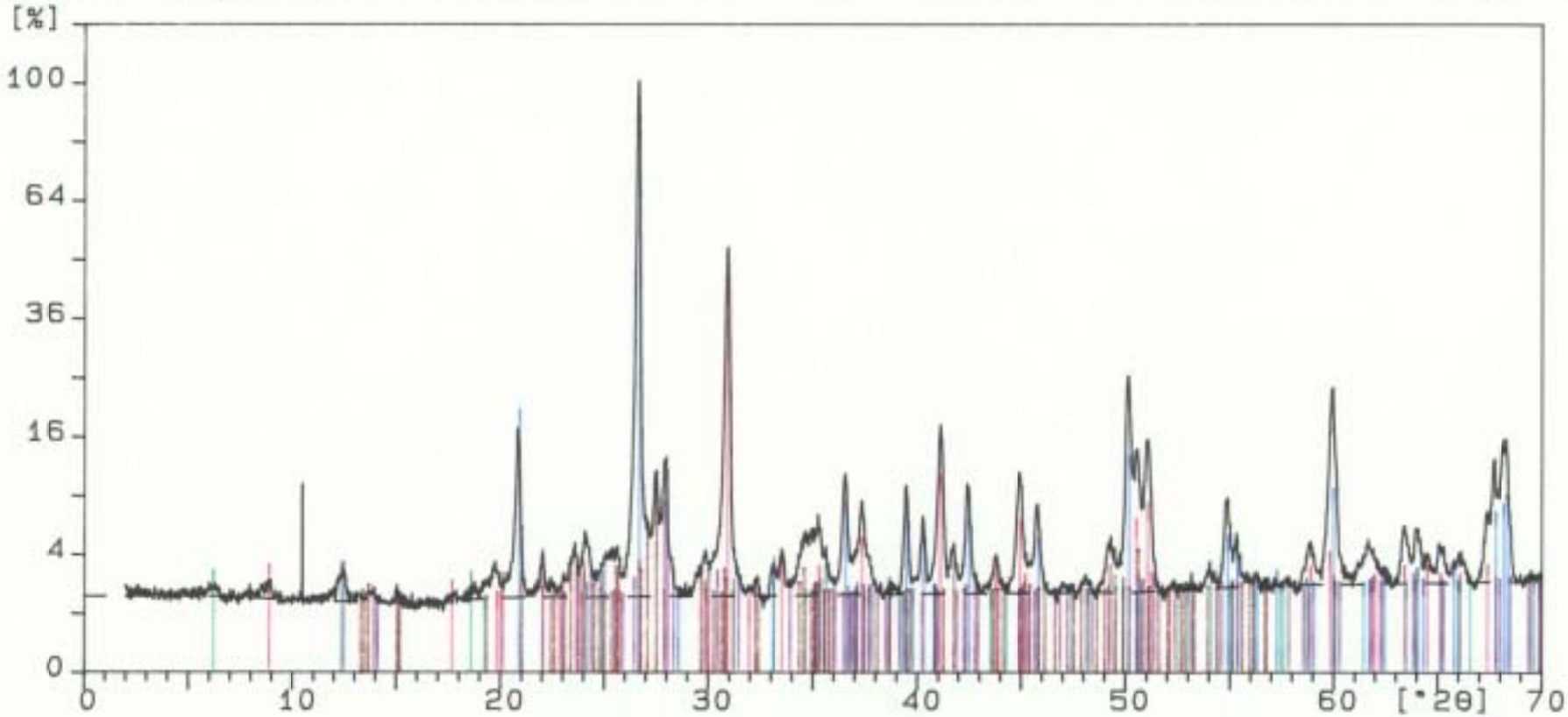

201321

33-1161	Quartz, syn	SiO2
36-0426	Dolomite	CaMg(CO3)2
33-0664	Hematite, syn	Fe2O3
41-1480	Albite, calcian, ordere	(Na,Ca)Al(Si,Al)3O8
19-0932	Microcline, intermediat	KAlSi3O8
42-1340	Pyrite	FeS2
26-0911	Illite-2\ITM#1\RG	(K,H3O)Al2Si3AlO10(OH)
29-0853	Clinochlore-1\ITM#I#I#b	Mg5Al(Si3Al)O10(OH)8
29-1488	Kaolinite-1\ITMd\RG	Al2Si2O5(OH)4

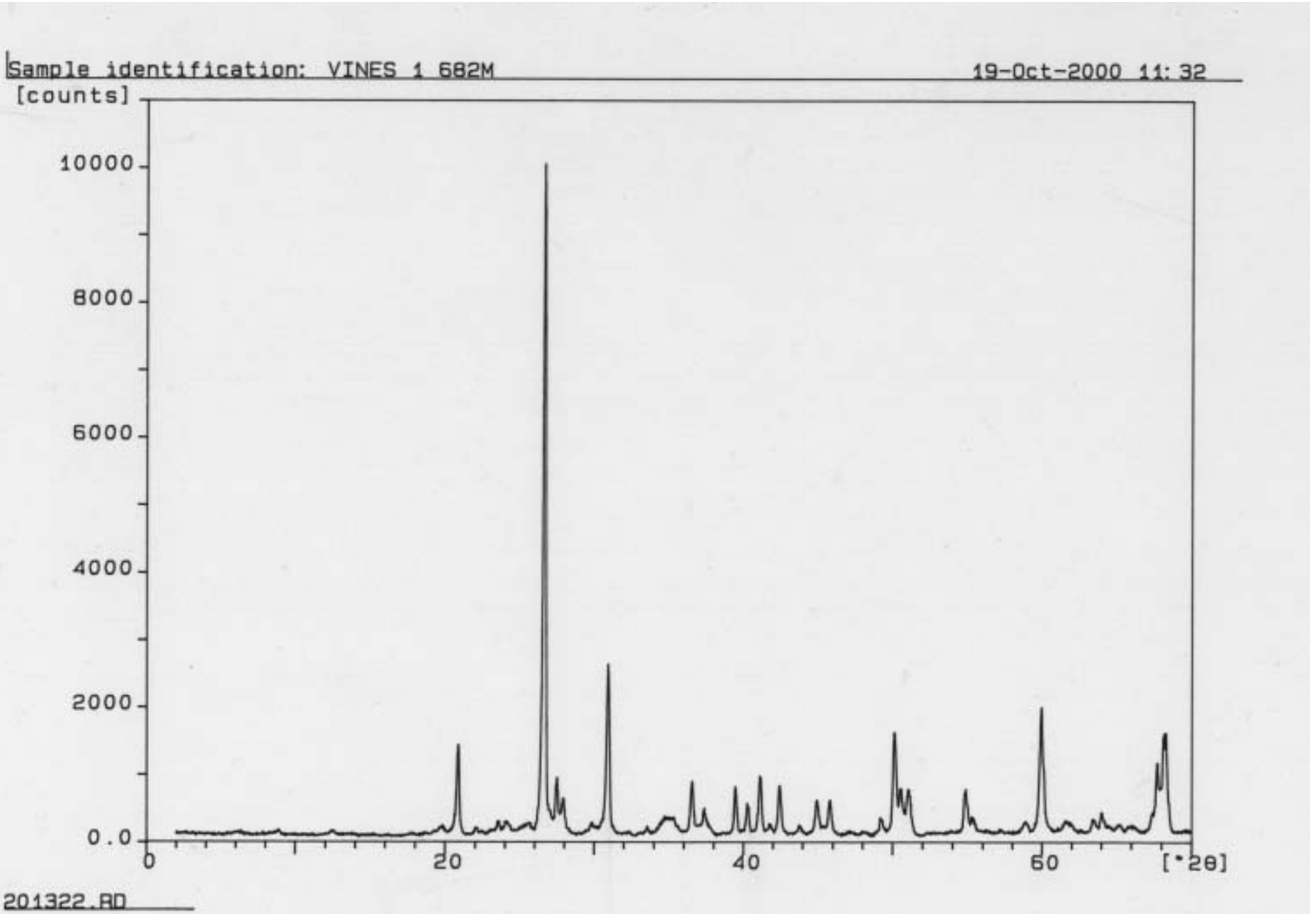
Sample identification: VINES 1 682M
19-Oct-2000 11:32
[counts]
10000
8000
6000
4000
2000
0.0
0
20
40
60
[°2θ]
201322.RD

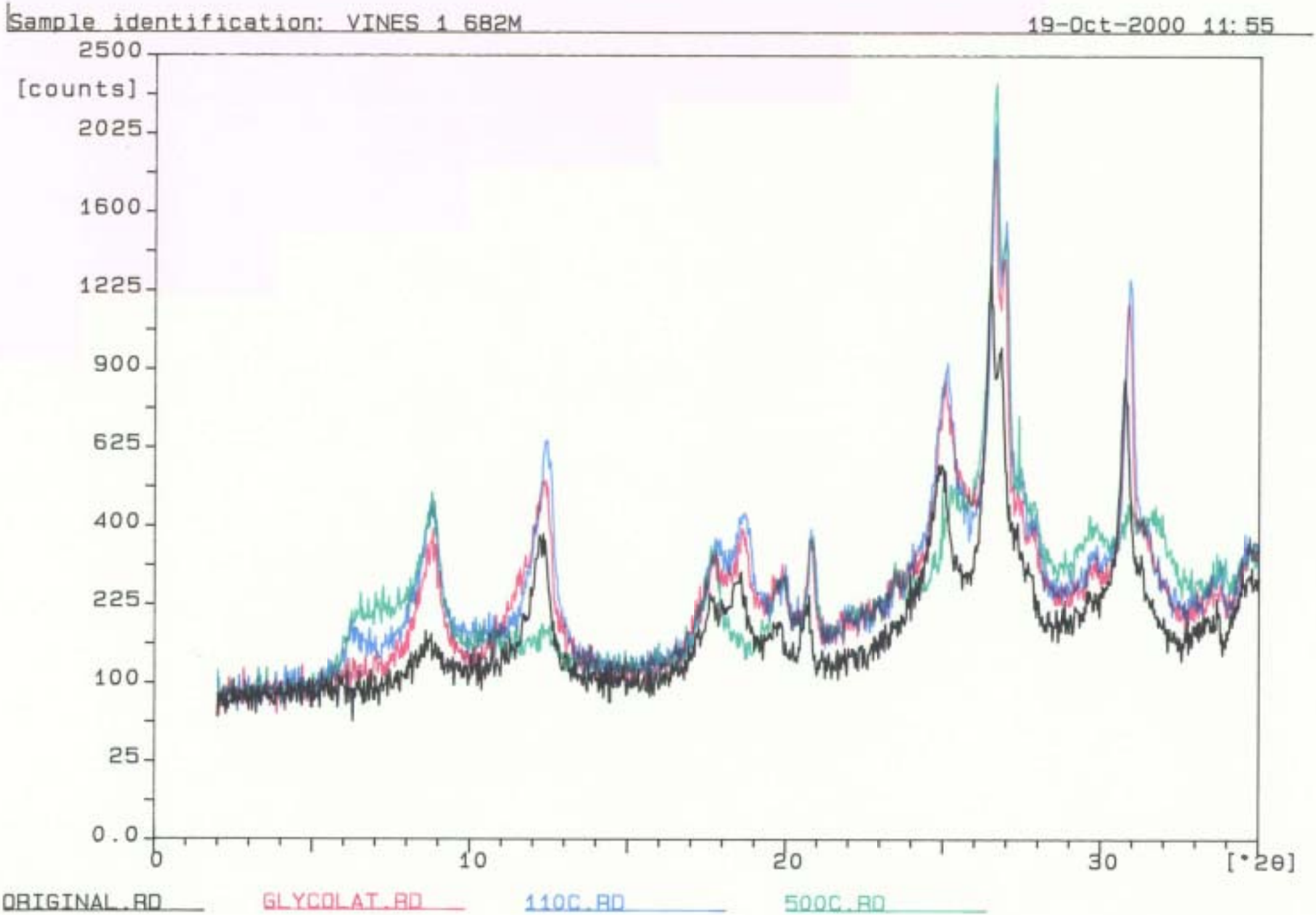
Sample identification: VINES 1 682M
19-Oct-2000 11:55
2500
[counts]
2025
1600
1225
900
625
400
225
100
25
0.0
0
10
20
30
[°2θ]
ORIGINAL.RD
GLYCOLAT.RD
110C.RD
500C.RD

Sample ident.: VINES 1 682M 19-Oct-2000 16:12

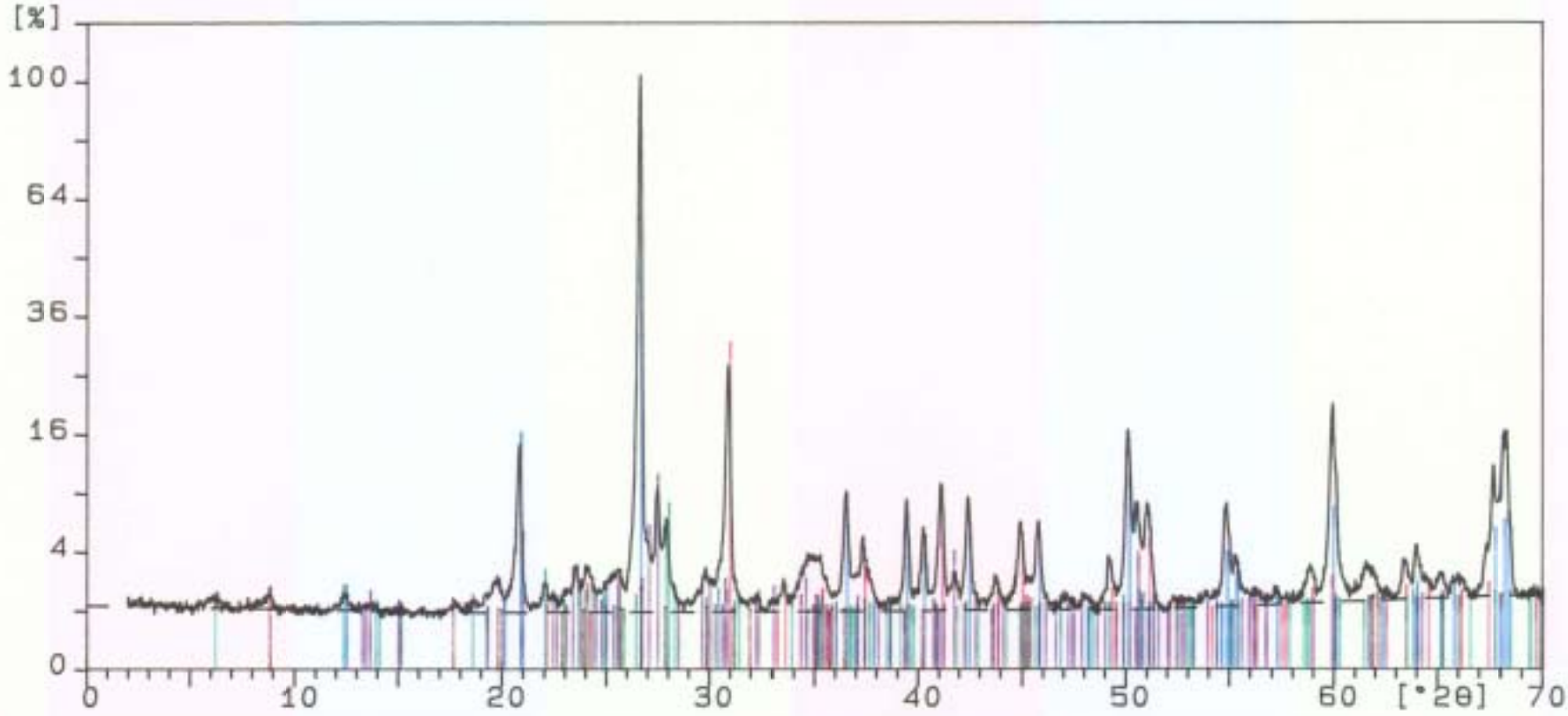

201322

33-1161	Quartz, syn	SiO2
36-0426	Dolomite	CaMg(CO3)2
41-1480	Albite, calcian, ordere	(Na,Ca)Al(Si,Al)3O8
19-0932	Microcline, intermediat	KAlSi3O8
26-0911	Illite-2\ITM#1\RG	(K,H3O)Al2Si3AlO10(OH)
29-1488	Kaolinite-1\ITMd\RG	Al2Si2O5(OH)4
33-0664	Hematite, syn	Fe2O3
29-0853	Clinochlore-1\ITM#I#I#b	Mg5Al(Si3Al)O10(OH)8
42-1340	Pyrite	FeS2

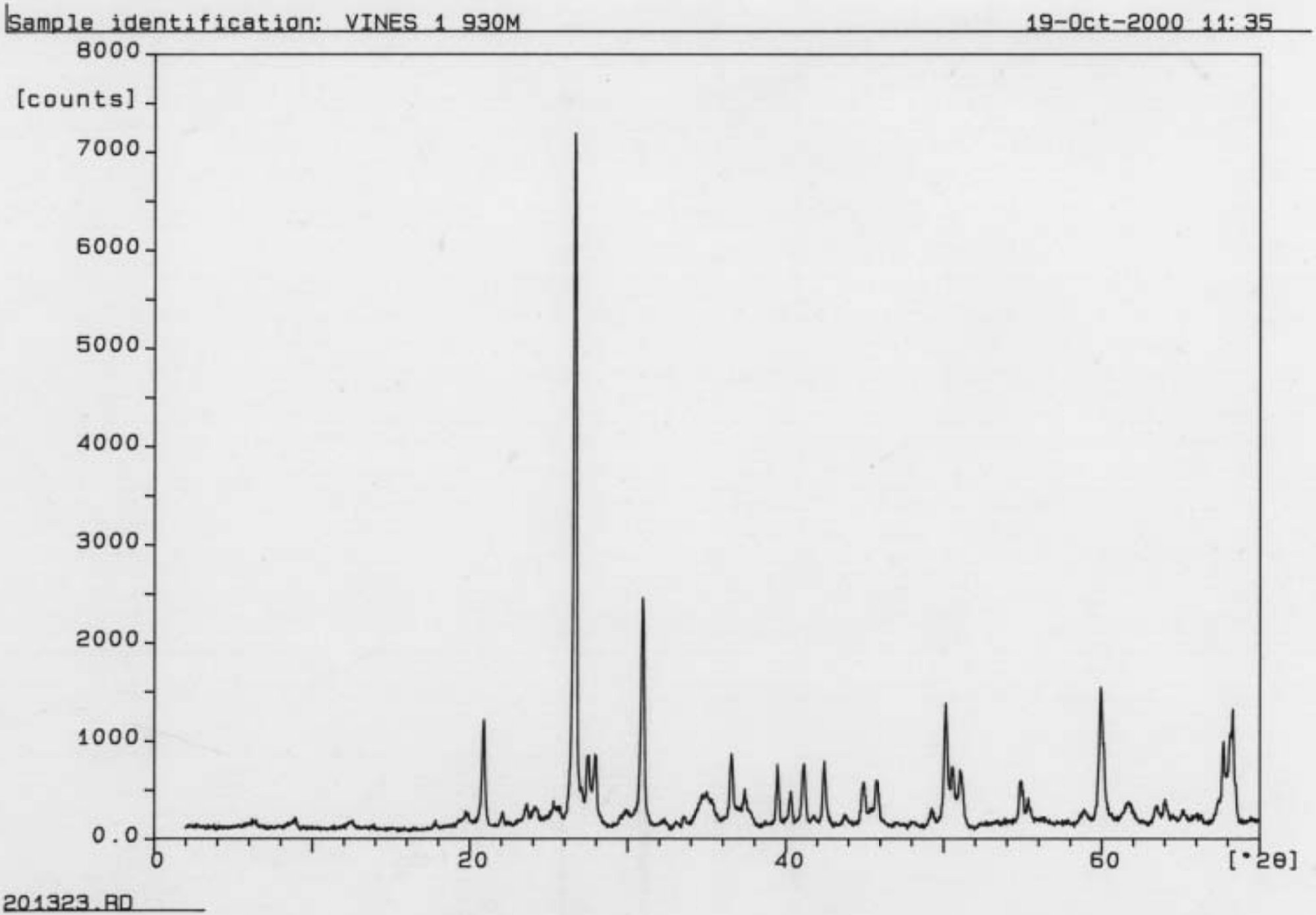
Sample identification: VINES 1 930M
19-Oct-2000 11:35
8000
[counts]
7000
6000
5000
4000
3000
2000
1000
0.0
0
20
40
60
[°2θ]
201323.RD

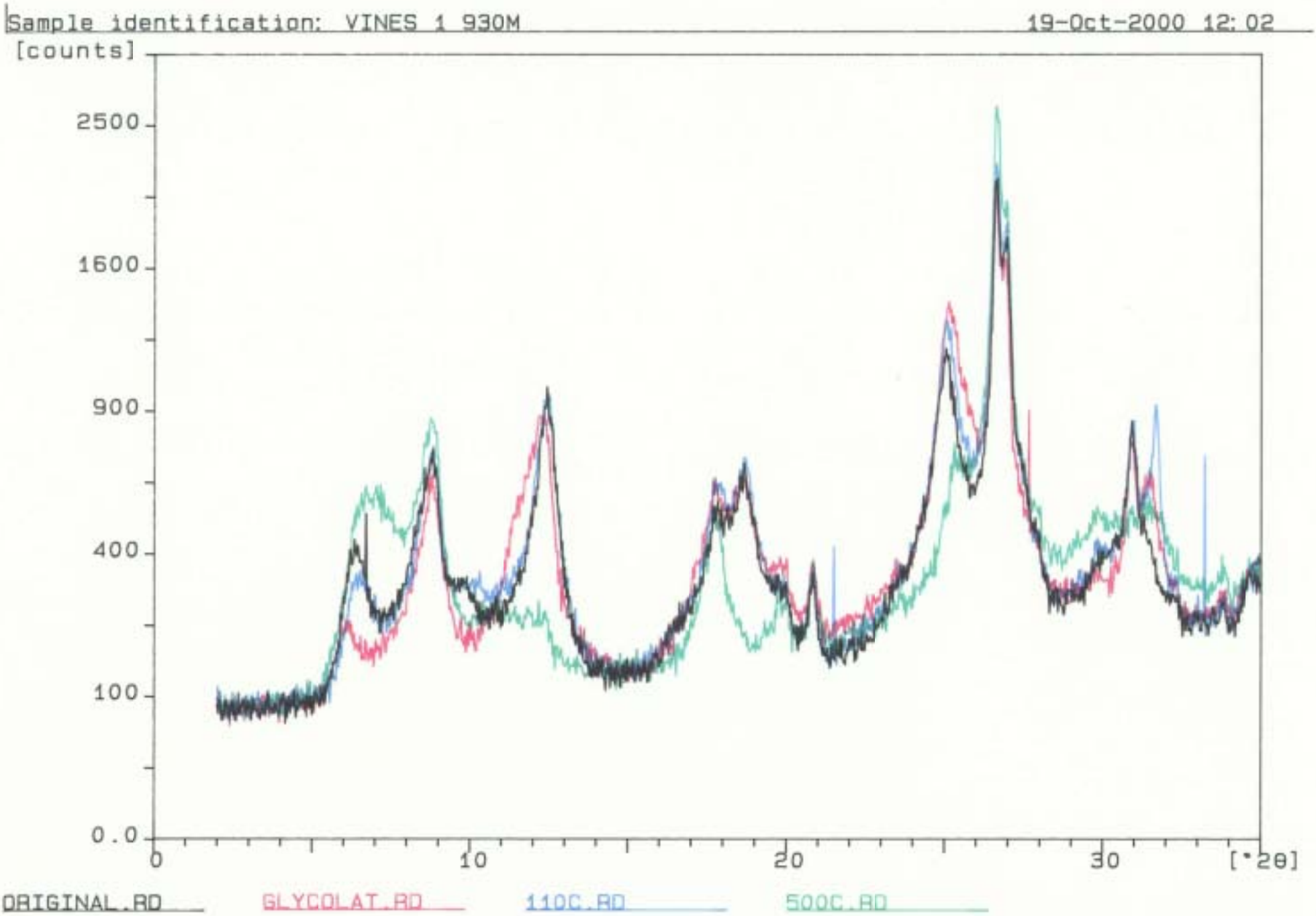
Sample identification: VINES 1 930M
19-Oct-2000 12:02
[counts]
2500
1600
900
400
100
0.0
0
10
20
30
[°2θ]
ORIGINAL.RD
GLYCOLAT.RD
110C.RD
500C.RD

Sample ident.: VINES 1 930M 19-Oct-2000 16:22

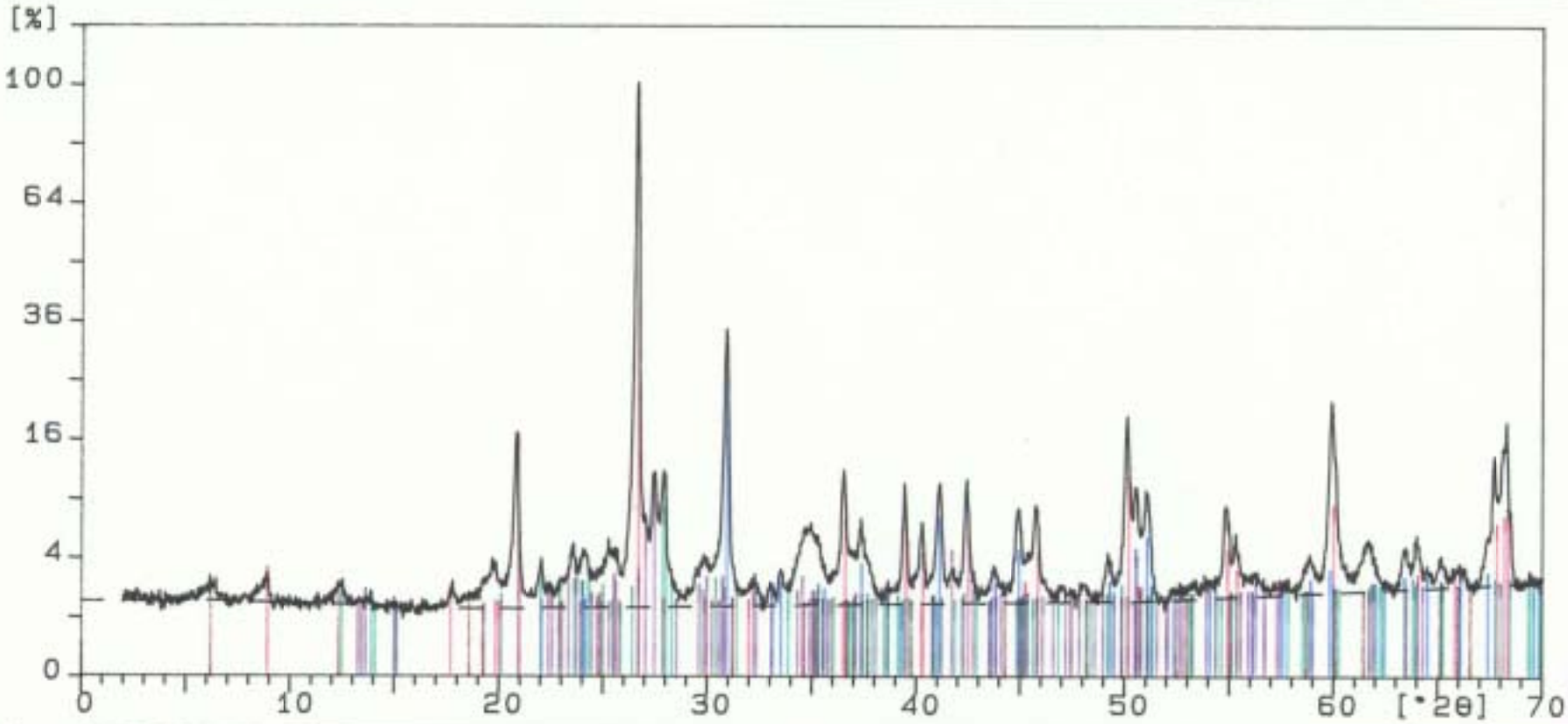

201323

36-0426	Dolomite	CaMg(CO3)2
33-1161	Quartz, syn	SiO2
41-1480	Albite, calcian, ordere	(Na,Ca)Al(Si,Al)3O8
19-0932	Microcline, intermediat	KAlSi3O8
29-0853	Clinochlore-1\ITM#I#I#b	Mg5Al(Si3Al)O10(OH)8
33-0664	Hematite, syn	Fe2O3
26-0911	Illite-2\ITM#1\RG	(K,H3O)Al2Si3AlO10(OH)
29-1488	Kaolinite-1\ITMd\RG	Al2Si2O5(OH)4
42-1340	Pyrite	FeS2

Appendix 7

Petroleum geochemistry

by K. A. R. Ghori

Introduction

To evaluate hydrocarbon generating potential and thermal maturity of rocks in stratigraphic drillhole Vines 1, fifty-six core samples from all likely source-rock lithologies between 355.0 and 2017.5 m total depth (TD) were collected. Total organic carbon (TOC) and Rock-Eval pyrolysis were undertaken to evaluate organic richness and hydrocarbon generating potential of rocks, and organic petrology and Rock-Eval parameter T_{max} were used to assess the level of thermal maturity. Total organic carbon and Rock-Eval pyrolysis analytical work was carried out by Geotechnical Services Pty Ltd (GEOTECH) and organic petrology was done by Keiraville Konsultants Pty Ltd. The number and type of geochemical analyses carried out are summarized in Table 7.1.

Source-rock potential

The TOC analysis indicated that all the samples are very lean in organic content, with the highest TOC value being 0.36%. Thus, all are classified as non-source-rock samples. The usual minimum organic richness limit for a source rock in favourable conditions is considered to be 0.5% TOC, while good source rocks typically contain over 1% TOC. Despite their low TOC content, ten samples were analysed by Rock-Eval pyrolysis to quantify the hydrocarbon-generating potential and evaluate thermal maturity. The highest potential yield from Rock-Eval pyrolysis was 0.37 mg/g $S_1 + S_2$ with a hydrogen index value of 231, which confirmed that the analysed samples are non-source rocks; good source rocks typically yield over 5 mg/g $S_1 + S_2$. The TOC and Rock-Eval pyrolysis data are summarized in Table 7.2.

Source-rock maturity

Organic petrology and Rock-Eval pyrolysis have been used to assess thermal maturation in Vines 1.

Organic petrology

Lamalginite and bitumen reflectance data can provide maturity levels for rocks older than Devonian (Crick et al., 1988). The reflectance values of lamalginite are more reliable for moderate to high maturation levels (Cook, 1995). Thucholitic bitumen (solid

Table 7.1. Geochemical analyses carried out on core samples from Vines 1

Analysis type	*Samples*	*Purpose*	*Analyst*
Total organic carbon (TOC)	56	Source potential	Geotech
Rock-Eval pyrolysis	10	Source potential	Geotech
Organic petrology	10	Source maturity	Keiraville Konsultants

Table 7.2. TOC and Rock-Eval pyrolysis data of core samples from Vines 1

GSWA no.	*Depth (m)*	*T_{max} (°C)*	*TOC (%)*	*S_1*	*S_2*	*S_3*	*$S_1 + S_2$*	*S_2/S_3*	*PI*	*HI*	*OI*
155085	355.00	–	0.11	–	–	–	–	–	–	–	–
155086	372.80	–	0.13	–	–	–	–	–	–	–	–
155142	398.75	–	0.36	0.03	0.17	0.26	0.20	0.65	0.15	47	72
155087	409.00	–	0.07	–	–	–	–	–	–	–	–
155101	434.10	–	0.05	–	–	–	–	–	–	–	–
155088	477.00	–	0.06	–	–	–	–	–	–	–	–
155102	556.10	–	0.10	–	–	–	–	–	–	–	–
155089	586.20	–	0.05	–	–	–	–	–	–	–	–
155090	605.70	–	0.13	–	–	–	–	–	–	–	–
155103	694.75	–	0.14	–	–	–	–	–	–	–	–
155091	723.45	–	0.10	–	–	–	–	–	–	–	–
155104	723.50	–	0.09	–	–	–	–	–	–	–	–
155105	799.50	–	0.06	–	–	–	–	–	–	–	–
155106	828.10	–	0.09	–	–	–	–	–	–	–	–
155107	836.70	–	0.08	–	–	–	–	–	–	–	–
155108	977.70	–	0.09	–	–	–	–	–	–	–	–
155109	987.20	–	0.10	–	–	–	–	–	–	–	–
155110	1 068.80	–	0.13	–	–	–	–	–	–	–	–
155092	1 068.95	–	0.19	–	–	–	–	–	–	–	–
155111	1 116.50	–	0.08	–	–	–	–	–	–	–	–
155093	1 138.82	–	0.12	–	–	–	–	–	–	–	–
155094	1 139.73 – 1 139.79	–	0.11	–	–	–	–	–	–	–	–
155095	1 149.05 – 1 149.09	–	0.11	–	–	–	–	–	–	–	–
155112	1 320.90	–	0.11	–	–	–	–	–	–	–	–
155113	1 422.15	–	0.04	–	–	–	–	–	–	–	–
155096	1 464.08 – 1 464.13	–	0.06	–	–	–	–	–	–	–	–
155098	1 478.93 – 1 479.05	–	0.05	–	–	–	–	–	–	–	–
155114	1 496.58 – 1 496.66	–	0.07	–	–	0.02	–	–	–	–	29
155115	1 496.58 – 1 496.66	–	0.18	–	–	–	–	–	–	–	–
155116	1 571.40	–	0.09	–	–	–	–	–	–	–	–
155117	1 654.50	–	0.16	–	–	–	–	–	–	–	–
155118	1 672.40	–	0.20	–	–	–	–	–	–	–	–
155119	1 679.70	447	0.16	0.00	0.37	0.03	0.37	12.33	0.00	231	19
155120	1 685.35	–	0.20	–	–	–	–	–	–	–	–
155121	1 709.00	–	0.16	–	–	–	–	–	–	–	–
155122	1 739.80	–	0.16	–	–	–	–	–	–	–	–
155123	1 747.55	–	0.18	–	–	–	–	–	–	–	–
155124	1 774.20	–	0.13	–	–	–	–	–	–	–	–
155125	1 823.60	–	0.06	0.00	0.18	0.16	0.18	1.13	0.00	300	267
155143	1 840.50	–	0.21	–	–	–	–	–	–	–	–
155126	1 861.55	479	0.16	0.01	0.29	0.02	0.30	14.50	0.03	181	13
155127	1 897.20	–	0.23	–	–	–	–	–	–	–	–
155128	1 906.30	474	0.18	0.00	0.20	0.07	0.20	2.86	0.00	111	39
155129	1 918.95	–	0.23	0.00	0.16	0.09	0.16	1.78	0.00	70	39
155130	1 928.75	465	0.24	0.00	0.35	0.02	0.35	17.50	0.00	146	8
155131	1 940.10	479	0.24	0.01	0.20	0.14	0.21	1.43	0.05	83	58
155132	1 946.70	–	0.21	–	–	–	–	–	–	–	–
155133	1 960.10	–	0.16	–	–	–	–	–	–	–	–
155134	1 970.00	469	0.16	0.00	0.22	0.07	0.22	3.14	0.00	138	44
155135	1 975.45	–	0.22	–	–	–	–	–	–	–	–
155136	1 986.80	–	0.18	–	–	–	–	–	–	–	–
155137	1 992.60	–	0.13	–	–	–	–	–	–	–	–
155138	1 999.20	–	0.18	–	–	–	–	–	–	–	–
155139	2 002.45	–	0.08	–	–	–	–	–	–	–	–
155140	2 007.95	–	0.07	–	–	–	–	–	–	–	–
155141	2 017.50	–	0.07	–	–	–	–	–	–	–	–

NOTES: TOC: total organic carbon
S_1: volatile hydrocarbons (HC)
S_3: organic carbon dioxide
PI: production index
OI: oxygen index
T_{max}: temperature of maximum pyrolytic yield (S_2)
S_2: HC generating potential
$S_1 + S_2$: potential yield
HI: hydrogen index

Table 7.3. Organic petrological data for core samples from Vines 1

Depth (m)	*Maceral*	*Mean (%Ro)*	*Minimum (%Ro)*	*Maximum (%Ro)*	*Number of readings*	*Description including liptinite fluorescence characteristics*
355.00	–	?1.00	–	?1.00	1	Liptinite appears to be absent. Claystone. DOM rare, ?'V' material referable to vitrinite, inertinite, and liptinite absent. The 'V' population is probably analogous to non-fluorescing lamalginite, but is present as a rounded body and could represent bitumen. Mineral fluorescence dominantly absent but weak dull orange patches present. Small fluorescing objects are present, but all were assessed as being above the polished surface and as being contaminants. Iron oxides sparse. Pyrite abundant
398.75	NFL FL	– 0.32	– 0.28	– 0.36	– 2	Whole rock: common lamalginite dull orange, altering to bright orange on irradiation for about 15 minutes. Claystone. DOM common, L>I, V absent. Liptinite common, material resembling inertinite rare, vitrinite absent. The lamalginite is present as elongate layers. These layers are diffuse and have not, for the most part, taken a polish. The layers are complex and this complexity shows more clearly after alteration. The matrix showed contraction during grinding and polishing. The claystone is probably lacustrine in origin. Mineral fluorescence pervasive, very weak dull orange to absent. Pyrite common
398.75	NFL FL	0.75 0.31	0.66 0.20	0.88 0.54	20 20	Organic matter concentrate: major lamalginite fluorescence not apparent initially, but the lower reflectance population develops weak dull orange fluorescence on prolonged irradiation. A higher reflectance population is present and consists of thicker entities that are easier to measure. Inertinite is also present, but may be a contaminant from the drilling mud as some structures appear to be related to those higher plants. Lamalginite comprises about 40 to 60% of the sample, the lower reflectance component being about ten times more abundant than the higher reflectance component. The thickness of the layers within the organic matter concentrate is probably in part an artifact of the demineralization procedure. Botanical structures are obscure but mostly confirm the impression of lamellar material gained from examination of the whole rock sample. Pyrite major Within the whole rock sample, most of the lamalginite has not taken a polish. However, it does show weak dull orange fluorescence. In the organic matter concentrate, the lamalginite has taken a good polish but most does not show fluorescence when initially examined. After some hours, positive alteration took place to yield fluorescence similar to that seen in the whole rock sample after about 10 minutes alteration The section can be assessed as late mature, with a vitrinite reflectance equivalent estimated at about 1.1%
694.75	NFL FL	0.97 0.28	0.85 0.13	1.19 0.43	5 5	Rare lamalginite dull orange. Claystone, mostly silty and interbedded with thin layers of siltstone. DOM rare, L> indeterminate. Liptinite rare, vitrinite and inertinite absent but one high indeterminate by highly reflecting field could be referred inertinite. The lamalginite is present in both fluorescing and non-fluorescing forms. It is derived from cyst-like forms rather than extensive lamellae. Mineral fluorescence dominantly absent but weak dull orange patches present. Pyrite common
1 068.95	NFL FL Bit	0.85 0.43 0.87	0.82 0.32 –	0.88 0.57 –	3 7 1	Rare lamalginite dull orange to very dull orange and non-fluorescing. Claystone very fine grained but with some silty layers. DOM rare, L>bitumen. Liptinite rare, vitrinite and inertinite absent but one high indeterminate by high reflecting field could be referred to inertinite. The lamalginite is present in both fluorescing and non-fluorescing forms. It is derived from cyst-like forms rather than extensive lamellae. One grain of probably bitumen, R 0.87%, is present. Mineral fluorescence dominantly absent but weak dull orange patches present

Table 7.3. (continued)

Depth (m)	*Maceral*	*Mean (%Ro)*	*Minimum (%Ro)*	*Maximum (%Ro)*	*Number of readings*	*Description including liptinite fluorescence characteristics*
1 672.40	NFL FL Bit	1.03 0.47 1.08	0.88 0.32 0.99	1.22 0.63 1.24	6 11 3	Sparse lamalginite orange to dull orange, very dull orange and non-fluorescing. Claystone fine grained, silty. DOM L>bitumen. Liptinite sparse, bitumen rare, vitrinite and inertinite absent. The lamalginite is present in both fluorescing and non-fluorescing forms. It is derived from cyst-like forms rather than extensive lamellae. Mineral fluorescence pervasive very weak dull brown. Pyrite abundant
1 897.20	NFL FL	1.16 0.64	0.98 –	1.56 –	5 1	Rare lamalginite largely non-fluorescing but two reflectance populations were distinguished. Claystone. DOM rare L only. Liptinite rare, vitrinite and inertinite absent. Mineral fluorescence mostly absent. Pyrite abundant
1 940.10	NFL FL Bit	1.18 0.60 1.38	1.05 – –	1.35 – –	5 1 1	Rare lamalginite almost entirely non-fluorescing but two reflectance populations were distinguished. Claystone. DOM rare L>bitumen. Liptinite and bitumen rare, vitrinite and inertinite absent. Mineral fluorescence absent. Pyrite abundant
1 975.45	NFL	1.15	1.05	1.31	4	Rare lamalginite possibly entirely non-fluorescing, some orange entities could be lamalginite or fluorescing grains of micas Silty claystone>siltstone. DOM rare L only. Liptinite rare, vitrinite and inertinite absent. Mineral fluorescence largely absent, but some very small orange lenses that could be minerals or liptinite. The reflectance of the non-fluorescing lamalginite suggests that they are more likely to be minerals. Pyrite common to abundant
1 999.20	NFL FL	1.16 0.29	1.10 –	1.44 –	5 1	Rare lamalginite mostly non-fluorescing but rare lenses show very weak dull orange fluorescence. Claystone, silty with some siltstone intercalations. DOM rare L only. Liptinite rare, vitrinite and inertinite absent. DOM confined to the finer claystone layers. Mineral fluorescence largely absent. Pyrite common to abundant

NOTES: DOM: dispersed organic matter
L: liptinite
V: vitrinite
I: inertinite
NFL: non-fluorescing lamalginite
FL: fluorescing lamalginite
Bit: bitumen

The equivalent vitrinite reflectance at the top of the section appears be in the range 0.8 to 0.9%. Deeper in the section there is a rise in the reflectance of the non-fluorescing lamalginite and a decrease in the amount of fluorescing lamalginite, and a shift towards the red end of the spectrum. The equivalent vitrinite reflectance at the base of the section sampled is assessed as 1.15%

Maturation estimates from the lamalginite reflectances are typically confirmed by the bitumen reflectances. The origin of the very rare, high reflecting grains is not known.
Mineral fluorescence is weak throughout, possibly related to the mostly low abundance of organic matter within the section. Some structures within the finer clastics could be burrows or dewatering structures. Since it is unlikely that burrowing organism were present, dewatering appears to be the more probable origin

bitumen), which encases radioactive minerals, show that reflectance values on the outer rim are very similar to those of the co-existing vitrinite. Fluorescing lamalginite becomes non-fluorescing at higher levels of maturation, and both forms can be present in a single sample.

Ten samples between 355.0 and 1999.2 m were subjected to reflectance and fluorescence intensity measurements on fluorescing and non-fluorescing lamalginite and thucholitic bitumen. The basic analytical data from Keiraville Konsultants are summarized in Table 7.3 and Figure 7.1. The analysed section is assessed as late mature for oil generation. Equivalent vitrinite reflectance at the top of the section is between 0.8 and 0.9%, and at the base of the section is 1.15%. Although the analysed section is 1644.2 m thick, the maturity increase is very low without an obvious maturity break. However, there is an increase in reflectance of the non-fluorescing lamalginite and a decrease in the amount of fluorescing lamalginite. The maturity estimates from the lamalginite reflectances are similar to the bitumen reflectances and these reflectance values suggest that the analysed section is not overmature

Rock-Eval pyrolysis

The paramater T_{max} is a maturation parameter (in °C) at which the pyrolytic yield of hydrocarbons (from a rock sample) reaches its maximum. Production index (PI) is also a maturation parameter; the ratio of already generated hydrocarbon (S_1) to potential hydrocarbon (S_2). Six T_{max} and eight PI values were obtained from Rock-Eval pyrolysis (Table 7.2). The T_{max} and PI values can not be considered reliable due to very low values of TOC, S_1, and S_2. However, the T_{max} values range from 447 to 479°C, which suggest that the section is from late mature to overmature for oil generation and, to some extent, support the maturity indicated by organic petrology. Figure 7.2 summarizes the petroleum source potential of rocks in Vines 1.

Present-day temperature

The present-day temperature is available from the maximum bottom hole temperature (BHT) measured in the following wireline log suites: dual laterolog – SP – compensated sonic, density – gamma ray – caliper – compensated neutron, dipmeter – gamma ray – caliper, and cement-bond log. The first two log suites were run on 31 August 1999, after 20 hours and 10 minutes and 28 hours and 50 minutes since mud circulation time, respectively, and recorded a maximum temperature of 67°C. The last two log suites were run on 2 September 1999, but time since circulation was not recorded. Although these logs were run at different times since mud circulation, the same BHT was recorded. The minimum-recorded and estimated geothermal gradients in Vines 1 are 2.1°C/100 m and 2.4°C/100 m, respectively, using 25°C as surface temperature and an arbitrary factor of plus 10% for estimated equilibrium temperature. Table 7.4 summarizes the temperature data.

Hydrocarbon show

Petrography of a core sample from 285.0 m suggested bitumen coating on grains. The sample was analysed by gas chromatography and a total extract of 59.3 ppm was obtained from 38.8 g of rock sample. The chromatogram from whole extract GC–MS (gas chromatography – mass spectrometry; m/z 57) indicates the presence of hydrocarbons. Because the sample is too lean in organic content, the traces of hydrocarbons require further geochemical and petrological analyses to confirm it is a true hydrocarbon show.

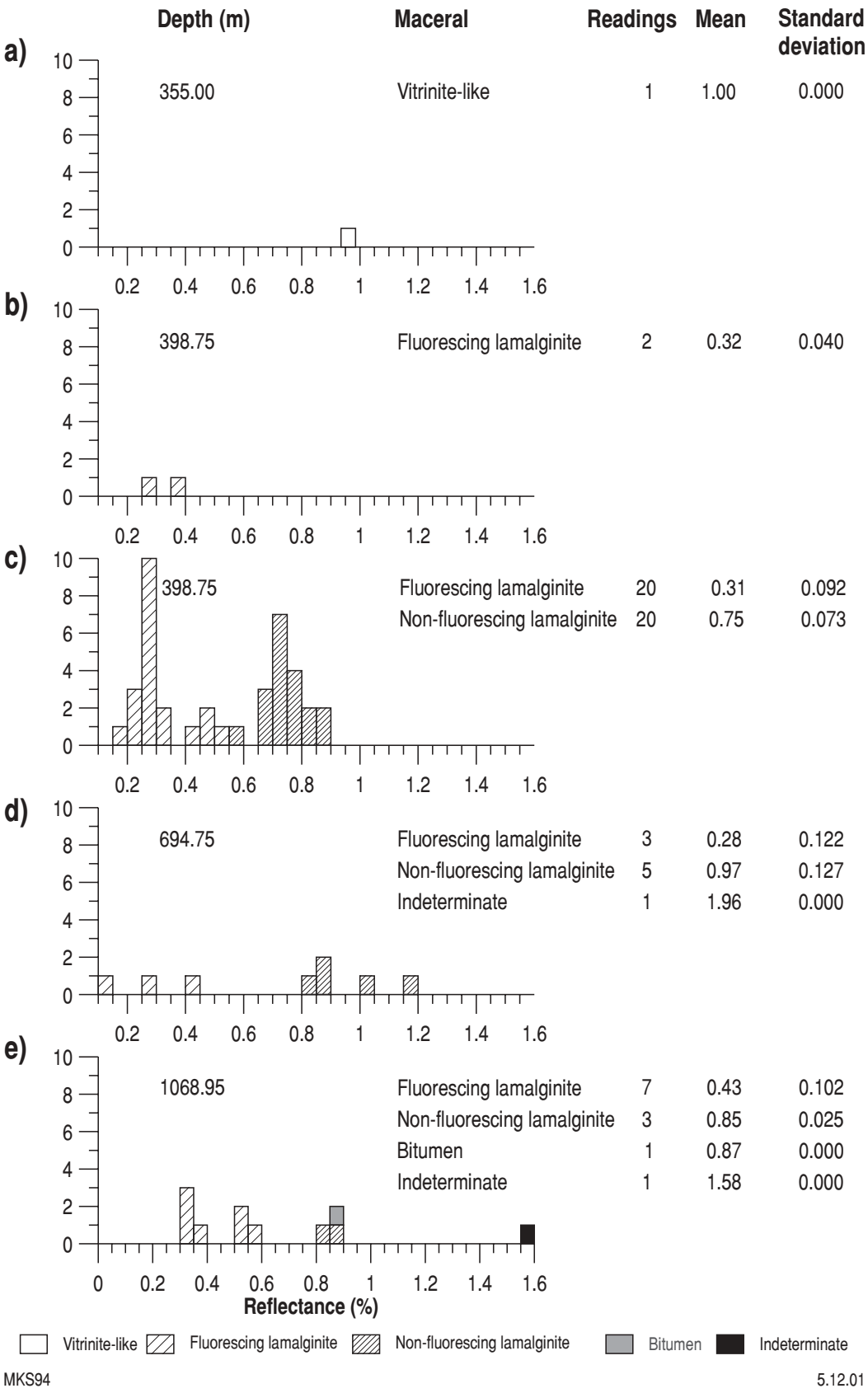

Figure 7.1. Percent reflectance histograms for core samples from Vines 1: a) 355.00 m; b) 398.75 m; c) 398.75 m (organic concentrate); d) 694.75 m; e) 1068.95 m; f) 1672.40 m; g) 1897.20 m; h) 1940.10 m; i) 1975.65 m; j) 1999.20 m

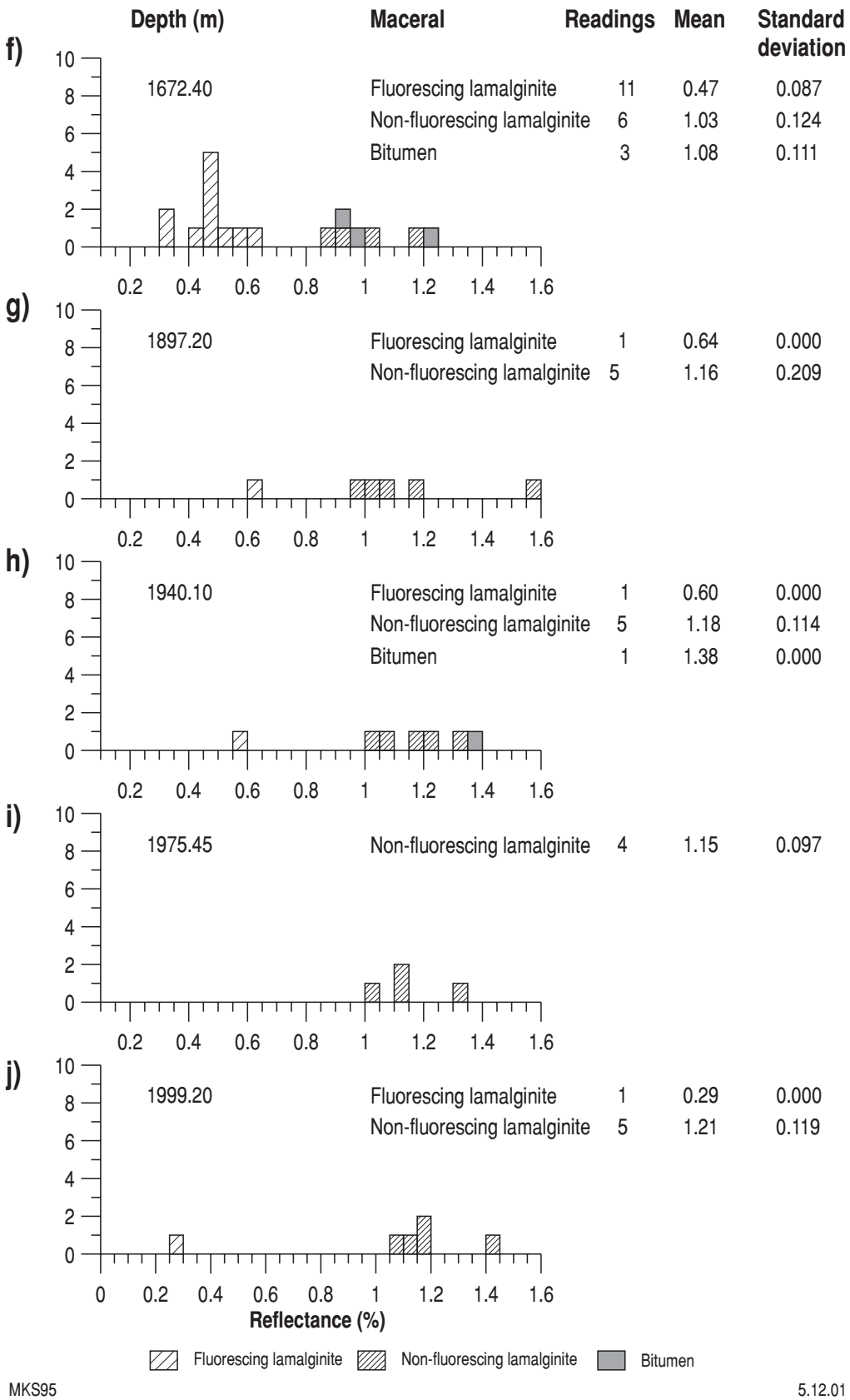

Figure 1. (continued)

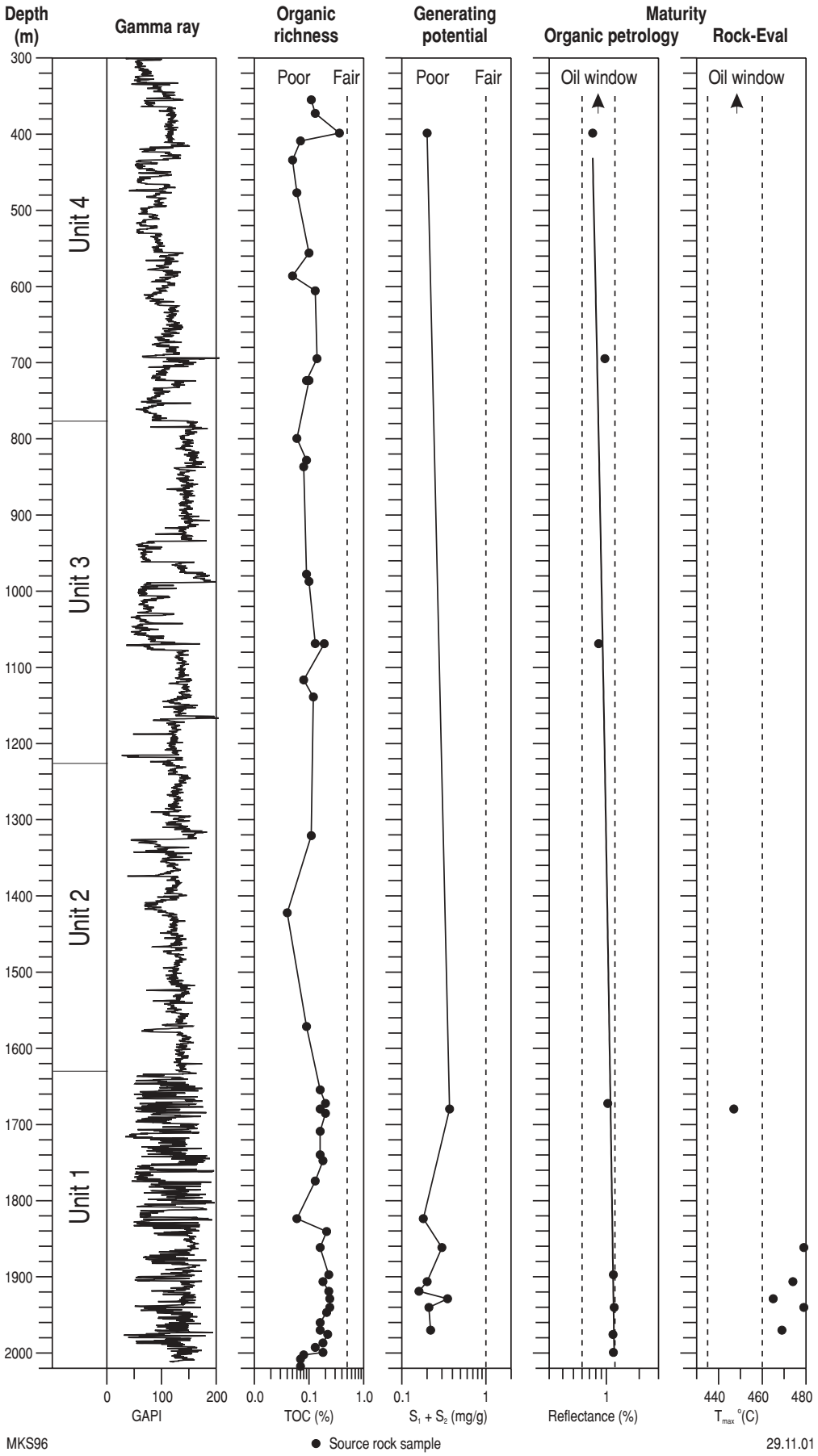

Figure 7.2. Plot of organic richness, generating potential, and thermal maturity, versus depth and gamma ray, illustrating petroleum source potential of rocks in Vines 1

Table 7.4. Present-day subsurface temperature data in Vines 1

Depth (m)	*Recorded (°C)*	*Estimated (°C)*	*Surface (°C)*	*Gradient (°C/100 m)*	*Log*	*Date*	*Time since circulation (h/min)*
2 018.5	67.0	73.7	25	2.4	Density–gamma–caliper, compensated neutron – sonic	31/8/99	28h 50 min
2 018.5	67.0	73.7	25	2.4	Dipmeter	2/9/99	56 h+
2 018.5	67.0	73.7	25	2.4	Dual laterolog – SP	31/8/99	20 h 10 min

NOTES: Depth: measured from ground level, 472 m above permanent datum (AMSL)
GL: ground level; elevation above permanent datum: 0.0 m

Conclusions

The TOC determination (56 samples), Rock-Eval pyrolysis (10 samples), and organic petrology (10 samples) of core samples between 355.0 and 2017.5 m TD in Vines 1, suggest that the analysed samples are non-source rocks and at late mature stages of the oil generative window. The highest value measured for TOC is 0.36% and the highest potential yield from Rock-Eval pyrolysis is 0.37 mg/g $S_1 + S_2$, which confirm that the analysed samples are non-source rocks. The recorded and estimated present-day geothermal gradient is 2.1°C/100 m and 2.4°C/100 m, respectively.

References

COOK, A. C., 1995, Report on source rock type, maturation levels, thermal history and hydrocarbon occurrence in suites of samples from four wells in the Officer Basin, W.A; Keiraville Konsultants Pty Ltd: Western Australia Geological Survey, Statutory petroleum exploration report, S31319 A1 (unpublished).

CRICK, I. H., BOREHAM, C. J., COOK, A. C., and POWELL, T. G., 1988, Petroleum geology and geochemistry of the Middle Proterozoic McArthur Basin, Northern Australia II: assessment of source rock potential: American Association of Petroleum Geologists, Bulletin, v. 72, p. 1495–1514.

Appendix 8

Log analysis

by M. K. Stevens

Wireline log acquisition and quality

Vines 1 was logged by Reeves Wireline Services. The dual laterolog, compensated sonic, SP, caliper, density, and 3-arm-dipmeter logs were acquired from about 2018 m to the casing shoe at 625 m. The gamma-ray log and compensated neutron log were acquired in open hole from about 2018 m to 625 m and in cased hole from 625 m to the surface. A cement-bond log and gamma-ray log were acquired in casing from 0 to 620 m. All logs are considered good quality, with the hole mostly being close to in-gauge. The dipmeter appears to give invalid dips where mud has probably temporarily stuck to one of the pads, such as at 1734–1750 m. Note that all depths quoted are log depths.

Log analysis

Log analysis to determine porosity and water saturation was conducted using Petrolog software (Crocker Data Processing).

Log analysis parameters are listed in Table 8.1. All sandstones with significant porosity are interpreted as 100% water saturated. The zone of the gas show at approximately 1482 m has about 1% calculated porosity, which confirms the visual assessment of the core at the wellsite. The results of the log analysis are presented graphically in Plate 1. A decrease in porosity with increasing depth is evident from the log analysis results, and calculated porosities are mostly similar to the measured porosities where open hole logs are available below 625 m. Above 625 m only the gamma-ray and neutron logs are available, and calculated porosities are similar to or less than measured porosities.

A significant change in formation water salinity is interpreted from the SP response between 1060 and 1070 m. The SP has a negative shift in non-shaley beds below this zone, indicating that formation water is more saline than the drilling-mud filtrate. Above this interval a positive SP shift in non-shaley beds indicates that formation water is less saline than the drilling-mud filtrate. As this SP response is consistent throughout the open-hole logged section, a significant sealing horizon is indicated at about 1060 m, and it is inferred that this seal is of regional extent.

Acknowledgements

Robert Charlebois of Crocker Data Processing is thanked for assisting with the log analysis.

Table 8.1. Log analysis zone input parameters for Vines 1

Vines Formation (unit)	*6*	*5,4*	*4,3*	*3*	*2,1*	*1*
Zone no.	*1*	*2*	*3*	*4*	*5*	*6*
Top depth (m)	45.0	124.7	626.7	1068.3	1228.5	1742.1
Bottom depth (m)	124.5	626.5	1068.3	1228.5	1741.9	2011.1
No logs	DT RHOB	DT RHOB	–	–	–	–
Rw @ FT	–	–	0.599	0.053	0.044	0.051
Rw ppm	–	–	6 586	90 000	100 000	75 327
RHOMA	2.65	2.65	2.65	2.65	2.65	2.65
Tma	55.5	55.5	55.5	60.0	50.0	60.0
Sonic option	Wylie	Wylie	Wylie	Wylie	Wylie	Wylie
No clay	–	SP RT N	SP MN SD	SP	SP	SP
GR clean	45	25	33	26	25	21
GR clay	140	113	112	108	106	122
R clay	–	–	26.6	21.3	14.6	20.1
$RHOB_{clay}$	–	–	2.720	2.730	2.760	2.780
$PHIN_{clay}$	0.200	0.200	0.200	0.150	0.210	0.140
t_{clay}	–	–	78.8	70.8	79.1	71.0
M_{clay}	–	–	0.648	0.692	0.632	0.671
N_{clay}	–	–	0.470	0.497	0.457	0.489
$PHIN_{2.2}$	0.235	0.221	0.200	0.235	0.266	0.244
$t_{2.2}$	–	–	90.0	90.0	90.0	90.0
PHImax	0.397	0.319	0.207	0.119	0.093	0.101

NOTES:

Abbreviation	**Definition**	**Units**	**Data Source**
GR clay	100% clay formation gamma-ray cut-off	API	Petrolog user specification
GR clean	Clay-free gamma-ray cut-off	API	Petrolog user specification
M_{clay}	$(t_{fluid}-t_{clay})/(RHOB_{clay}-RHO_f)$		Petrolog crossplots
MN	MN crossplot		Petrolog crossplots
N_{clay}	$(PHIN_{fluid}-PHIN_{clay})/(RHOB_{clay}-RHO_{fluid})$		Petrolog crossplots
No clay	Switch for undesired clay indicators		Petrolog user specification
PHImax	Crossplot-limited maximum porosity	fraction	Petrolog user specification
PHImaxcalc	Calculated maximum effective porosity	fraction	Petrolog calculation
$PHIN_{clay}$	Clay neutron value	fraction	Petrolog crossplots
$PHIN_{fluid}$	Fluid neutron value	fraction	Petrolog calculation
PHIN	Clean point on density–neutron crossplot		Petrolog crossplots
RHG	Raymer–Hunt–Gardner porosity equation		Petrolog user specification
$RHOB_{clay}$	Clay density	g/cm^3	Petrolog crossplots
RHO_{fluid}	Fluid density	g/cm^3	Petrolog calculation
RHOMA	Rock solids density	g/cm^3	Core analysis (CoreLab, 1997)
SD	Sonic–density crossplot		Petrolog crossplots
Sonic option	Sonic porosity equation		Petrolog user specification
t_{clay}	Clay transit time	us/ft	Petrolog crossplots
$t_{2.2}$	Clean point on density–sonic crossplot		Petrolog crossplots
t_{fluid}	Formation fluid transit time	us/ft	Petrolog calculation
Tma	Average formation transit time	us/ft	Petrolog user specification

Appendix 9

VINES-1
ROUTINE CORE ANALYSIS
REPORT

PROFESSIONAL OPINION

Prepared for:

Geological Survey
Department of Minerals and Energy

October 2000

Geotechnical Services Pty Ltd shall not be responsible or liable for the results of any actions taken on the basis of the information contained in this study, nor for any errors or omissions in it.

1. SAMPLE PREPARATION

A total of 49 horizontal plug samples, suitable for poroperm measurements were cut from selected depths. Where possible, larger diameter (3.81cm), in preference to the smaller diameter (2.54cm) plugs were cut using tap water.

The samples were cleaned by hot solvent extraction, using toluene followed by methanol in a Soxhlet apparatus to remove residual hydrocarbons and salts, respectively.

Extracted plug samples were dried at 115^{o}C in a top-ventilated, fan-forced convectional oven until constant weights were achieved. Samples were allowed to cool to room temperature in an evacuated desiccator prior to carrying out poroperm measurements.

2. POROSITY, PERMEABILITY AND GRAIN DENSITY MEASUREMENTS

Helium porosities were determined at ambient and at overburden pressure of 2000 psi, as requested.

Ambient helium porosities were measured in a matrix cup using a Coberly-Stevens porosimeter. Pore volumes were calculated from Boyle's Law (i.e. $P_1V_1 = P_2V_2$) and expressed as a fraction of the bulk volume

$$\phi = (V_p/BV) \times 100$$

where ϕ = porosity (%)

V_p = pore volume (cm^3)

BV = bulk volume (cm^3)

Bulk volumes were determined by the mercury displacement technique using a customised digital displacement pump. Grain densities were then calculated from the expression

$$GD = w/GV$$

$$= w/(BV - V_p)$$

where GD = grain density ($g\ cm^{-3}$)

w = weight of sample (g)

GV = grain volume (cm^3)

Helium porosities at overburden pressure of 2000 psi were conducted in a core holder. Porosities were calculated using the expression

$$\phi_{OB} = V_{p(OB)}/[BV\ (V_{p(amb)} - V_{p(OB)})] \times 100$$

where ϕ_{OB} = overburden porosity (%)

$V_{p(amb)}$ = pore volume at ambient conditions (cm^3)

$V_{p(OB)}$ = pore volume at overburden conditions (cm^3)

BV = bulk volume at ambient conditions (cm^3)

Calculated ambient and overburden porosities and grain density values for the plugs are presented in Table 1.

2.1 Permeability measurements

Air permeabilities were determined at ambient (800 psi) and at overburden pressure (2000psi) and were calculated using Darcy's equation

$$k_g = (\mu Q_b P_b L)/(A \delta p P_m)$$

where k_g = gas permeability (darcies)

μ = gas viscosity (cp)

Q_b = atmospheric gas flow rate ($cm^{-3}\ s^{-1}$)

P_b = base or atmospheric pressure (atm)

δ_p = differential pressure (atm)

P_m = mean sample gas pressure (atm)

L = length of sample (cm)

A = cross sectional area of sample (cm^2)

Ambient and overburden permeabilities are presented in Table 1.

3. MINI-PROBE PERMEAMETRY

A total of 327 mini-probe permeametry measurements were performed at *ca.* 2cm intervals along the unslabbed surface of the core. Test locations were carefully selected so as to exclude visible fractures, where possible. All measurements were carried out using a FPP300 steady state field probe. Mini-probe permeametry data are presented in Table 2.

4. DISCUSSION

Higher permeability interval is concentrated in the shallow section of the core up to a depth of 327m. The plug permeabilities in this interval ranged from 95 mD to 928 mD. With a few exceptions, e.g. at 617.5m

(plug permeability is 72 mD), the permeabilities below 327m dropped off dramatically, ranging from a few millidarcies to less than 0.01 millidarcy.

The permeabilities measured are consistent with the lithology of the core. In general, relatively higher permeabilities are associated with fine-medium grained sandstones and lower permeabilities are associated with very well cemented, very fine/silty sandstones or shale.

Some of the plugs e.g. 985.24m (permeabilities at 800 psi and 2000 psi are 0.44 mD and 0.1 mD respectively), exhibit large differences between ambient and overburden permeabilities. This is attributed to the presence of micro and/hairline fractures, which close up when overburden pressure is applied to the samples, resulting in a much lower permeability. Due to the age of the core, the shaly sections have become very friable and are prone to fractures when handled. Therefore, no further attempts were made to obtain another set of replacement plugs to cover for those which are defective.

Some of the plugs, e.g. 999.65m (mini-probe and ambient plug permeability values are 0.17mD and 4.2mD respectively) exhibit permeability values higher than expected as compared to their mini-probe permeametry values. This could be due to a number of factors

i) infiltration of drilling mud into the pore throats, which impedes airflow and result in lower permeabilities measured using the mini-probe permeameter.

ii) the plugs have been solvent extracted with toluene and methanol to remove residual hydrocarbons and salts respectively, and thus would offer a less tortuous pathway for the air to flow through. Consequently they yield a relatively higher permeability values as compared to the mini-probe permeametry values.

Table 1

POROPERM/GRAIN DENSITY DATA AT 800 and 2000 psi

GEOTECH

Company: DEPARTMENT OF MINERALS AND ENERGY (WESTERN AUSTRALIA) Date: 25-Oct-00
Well: VINES-1 File No: CA-0061

GSWA No	Core Depth (m)	Plug Depth (m)	Plug Diameter (cm)	Porosity (%) 800 psi	Porosity (%) 2000 psi	Grain Density (gm/cc)	Permeability (mD) 800 psi	Permeability (mD) 2000 psi	Remarks
154801	133.13-133.30	133.15	3.81	23.4	22.4	2.65	105	95	
154845	179.00-179.20	179.05	3.81	28.7	27.6	2.66	844	818	
154802	284.96-285.10	285.00	3.81	24.9	24.0	2.67	344	333	
154803	308.90-309.10	309.00	3.81	24.3	23.3	2.67	954	928	
154804	326.85-327.40	327.00	3.81	23.1	22.2	2.68	193	185	
154877	402.30-402.39	402.30	PNR	NA	NA	NA	NA	NA	
154868	402.90-403.00	402.90	PNR	NA	NA	NA	NA	NA	
154805	404.18-404.26	404.22	PNR	NA	NA	NA	NA	NA	
154806	443.96-441.11	440.05	3.81	18.4	17.6	2.70	0.56	0.49	
154807	490.00-490.19	490.05	3.81	6.3	5.8	2.74	<0.01	NP	
154808	497.87-498.04	498.00	3.81	21.6	20.9	2.68	6.8	6.3	
154809	597.96-598.12	598.00	PNR	NA	NA	NA	NA	NA	
154869	598.2-598.34	598.23	2.54	12.1	10.9	2.77	<0.01	NP	
154810	607.81-608.11	608.00	3.81	7.5	6.6	2.75	<0.01	NP	
154811	617.41-617.58	617.50	3.81	11.5	10.7	2.73	101	72	
154812	643.86-644.08	644.00	2.54	4.9	4.5	2.76	<0.01	NP	
154813	674.86-675.06	675.00	2.54	5.9	4.8	2.72	<0.01	NP	
154814	681.88-682.20	682.00	2.54	4.9	4.0	2.74	<0.01	NP	
154815	690.89-691.12	691.00	2.54	10.4	8.9	2.70	0.04	0.03	
154816	748.99-749.17	749.00	2.54	10.3	9.1	2.70	0.03	0.02	
154817	929.93-930.14	930.00	2.54	5.7	4.7	2.74	0.03	<0.01	
154870	931.75-931.86	931.80	PNR	NA	NA	NA	NA	NA	

PNR = Plug not recovered from core (ie failed) NA = Data not available NP = Not performed

Table 1

POROPERM/GRAIN DENSITY DATA AT 800 and 2000 psi

Company: DEPARTMENT OF MINERALS AND ENERGY (WESTERN AUSTRALIA) Date: 25-Oct-00
Well: VINES-1 File No: CA-0061

GSWA No	Core Depth (m)	Plug Depth (m)	Plug Diameter (cm)	Porosity (%) 800 psi	Porosity (%) 2000 psi	Grain Density (gm/cc)	Permeability (mD) 800 psi	Permeability (mD) 2000 psi	Remarks
154818	931.93-932.03	932.00	PNR	NA	NA	NA	NA	NA	
154819	938.87-939.09	939.00	2.54	12.7	11.4	2.72	0.04	0.02	
154820	949.73-950.06	950.00	2.54	14.8	13.4	2.70	0.06	0.04	
154821	969.84-970.13	970.00	2.54	4.3	3.3	2.73	<0.01	NP	
154871	985.15-985.34	985.24	2.54	6.4	5.3	2.77	0.44	0.1	Visible Hairline Fracture
CORE TRAY		985.40	2.54	3.3	2.6	2.71	0.08	0.03	Visible Hairline Fracture
154822	986.00-986.10	986.05	PNR	NA	NA	NA	NA	NA	
CORE TRAY		991.15	2.54	8.1	7.7	2.71	0.04	0.02	
CORE TRAY		991.75	2.54	8.3	7.5	2.74	0.06	<0.01	Microfracture
CORE TRAY		994.85	2.54	7.4	7.0	2.71	0.03	0.02	
154823	994.96-995.34	995.00	2.54	8.7	8.1	2.71	0.02	<0.01	
CORE TRAY		996.05	2.54	5.9	5.4	2.70	0.08	0.02	Hairline and microfractures
CORE TRAY		997.05	2.54	18.4	17.7	2.69	51	48	
CORE TRAY		999.65	2.54	16.2	15.6	2.69	4.2	3.8	
154824	1000.00-1000.25	1000.10	2.54	11.2	10.5	2.70	0.27	0.2	
154825	1049.95-1050.05	1050.00	2.54	16.1	15.3	2.68	0.06	0.04	
154826	1061.85-1062.13	1062.00	2.54	5.1	4.2	2.71	0.02	<0.01	
154827	1069.90-1070.23	1070.00	2.54	4.5	3.4	2.71	0.02	0.01	
154828	1100.10-1100.32	1100.15	2.54	6.9	5.5	2.77	<0.01	NP	
154829	1211.99-1212.15	1212.00	2.54	5.7	4.5	2.77	NA	NA	Fracture
154830	1214.90-1215.19	1215.00	2.54	2.0	1.7	2.75	0.02	<0.01	
154872	1311.10-1311.25	1311.10	PNR	NA	NA	NA	NA	NA	

PNR = Plug not recovered from core (ie failed) NA = Data not available NP = Not performed

Table 1

POROPERM/GRAIN DENSITY DATA AT 800 and 2000 psi

Company: DEPARTMENT OF MINERALS AND ENERGY (WESTERN AUSTRALIA) Date: 25-Oct-00
Well: VINES-1 File No: CA-0061

GSWA No	Core Depth (m)	Plug Depth (m)	Plug Diameter (cm)	Porosity (%) 800 psi	Porosity (%) 2000 psi	Grain Density (gm/cc)	Permeability (mD) 800 psi	Permeability (mD) 2000 psi	Remarks
154831	1311.84-1311.99	1312.00	PNR	NA	NA	NA	NA	NA	
154832	1319.28-1319.39	1319.35	PNR	NA	NA	NA	NA	NA	
CORE TRAY		1323.97	2.54	6.6	NP	2.76	<0.01	NP	Fracture
154833	1325.04-1325.31	1325.10	2.54	3.1	2.7	2.74	<0.01	NP	
CORE TRAY		1326.30	2.54	3.8	3.0	2.74	<0.01	NP	
CORE TRAY		1330.10	2.54	5.7	5.2	2.73	<0.01	NP	
CORE TRAY		1331.50	2.54	5.6	4.9	2.72	<0.01	NP	
154834	1410.10-1410.36	1410.20	2.54	3.0	2.7	2.77	<0.01	NP	
154841	1655.77-1656.01	1656.00	2.54	3.2	2.9	2.70	<0.01	NP	
154835	1458.60-1458.73	1458.70	2.54	4.8	4.1	2.76	0.04	0.01	
154836	1464.57-1464.68	1464.60	PNR	NA	NA	NA	NA	NA	
154873	1465.50-1465.60	1465.50	PNR	NA	NA	NA	NA	NA	
154837	1468.97-1496.23	1469.00	2.54	7.5	NA	2.79	NA	NA	Plug Failed after ambient porosity
154874	1472.95-1473.05	1472.98	2.54	6.9	5.9	2.79	NA	NA	Length too short to perfrom perm
154838	1473.89-1474.01	1473.95	PNR	NA	NA	NA	NA	NA	
154839	1477.99-1478.10	1478.00	PNR	NA	NA	NA	NA	NA	
154875	1478.70-1478.81	1478.70	PNR	NA	NA	NA	NA	NA	
154840	1481.95-1482.06	1482.00	PNR	NA	NA	NA	NA	NA	
154876	1484.25-1484.44	1484.30	PNR	NA	NA	NA	NA	NA	
154842	1712.90-1713.16	1713.00	2.54	5.5	4.9	2.68	0.01	<0.01	
154843	1814.93-1815.20	1815.00	2.54	5.0	4.0	2.70	<0.01	NP	
154844	1901.88-1902.15	1902.00	2.54	2.7	2.4	2.71	<0.01	NP	

PNR = Plug not recovered from core (ie failed) NA = Data not available NP = Not performed

Table 2

MINI-PROBE PERMEAMETER MEASUREMENTS

Company: DEPARTMENT OF MINERALS AND ENERGY (WESTERN AUSTRALIA)
Well: VINES-1 Date: 25-Oct-00
Date 25.10.00 File No: CA-0061

Depth (m)	Permeability (mD)		Depth (m)	Permeability (mD)		Depth (m)	Permeability (mD)
122.55	50		133.50	128		993.35	0.06
122.90	48		133.68	80		993.55	0.03
123.20	52		133.83	79		993.75	0.03
123.40	49		134.03	239		994.25	0.01
124.35	64		134.20	94		994.45	0.01
125.15	104		134.39	40		994.65	0.04
125.30	189		134.60	42		994.85	0.06
125.53	252		134.87	157		995.26	0.06
125.73	60		135.03	29		995.45	0.04
125.95	21		984.51	0.01		995.62	0.01
126.10	42		984.70	<0.01		995.85	<0.01
126.30	110		984.90	<0.01		995.85	<0.01
126.50	103		985.10	<0.01		996.05	<0.01
126.75	120		985.40	<0.01		996.25	<0.01
126.91	276		985.58	<0.01		996.45	<0.01
127.10	74		985.79	<0.01		996.65	0.05
127.30	97		986.20	0.01		996.85	0.13
127.50	87		986.40	0.01		997.05	0.18
127.75	286		988.10	<0.01		997.25	0.15
127.92	56		988.30	0.02		997.45	0.16
128.10	67		988.50	0.01		997.65	0.07
128.30	66		988.68	0.02		997.85	0.12
128.50	130		988.88	0.02		998.05	0.11
128.65	114		988.95	0.01		998.25	0.12
128.85	50		989.15	0.02		998.45	0.12
129.12	273		989.35	0.03		998.65	0.08
129.30	209		989.55	0.03		998.85	0.13
129.43	161		989.75	0.04		999.05	0.13
129.66	207		989.95	0.04		999.25	0.14
129.94	187		990.15	0.06		999.45	0.16
130.10	211		990.35	0.04		999.65	0.17
130.35	234		990.55	0.05		999.85	0.16
130.55	291		990.75	0.03		1000.30	0.08
130.78	290		990.95	0.05		1000.50	0.06
130.90	110		991.15	0.08		1000.70	0.15
131.25	108		991.33	0.04		1000.90	0.11
131.40	248		991.55	0.03		1001.10	0.14
131.60	162		991.75	<0.01		1001.30	0.11
131.75	208		991.95	0.06		1001.50	0.10
131.95	92		992.15	0.06		1001.70	0.06
132.20	64		992.35	0.04		1001.90	0.07
132.40	287		992.55	0.06		1002.10	0.08
132.62	350		992.75	0.08		1002.30	0.12
132.80	207		992.95	0.06		1318.30	0.03
133.00	224		993.15	0.02		1318.50	0.01

Table 2

MINI-PROBE PERMEAMETER MEASUREMENTS

Company: DEPARTMENT OF MINERALS AND ENERGY (WESTERN AUSTRALIA)
Well: VINES-1 Date: 25-Oct-00
Date 25.10.00 File No: CA-0061

1318.68	<0.01		1329.10	0.01		1466.25	0.06
1318.90	0.02		1329.30	0.01		1466.44	<0.01
1319.10	0.02		1329.50	0.01		1466.63	0.06
1319.42	0.01		1329.70	0.01		1466.83	0.03
1319.64	0.02		1329.90	0.01		1467.05	0.06
1319.82	0.02		1330.10	0.03		1467.25	0.07
1320.04	0.02		1330.30	0.01		1467.47	0.06
1320.22	0.02		1330.50	0.01		1467.67	0.06
1320.45	0.01		1330.70	0.01		1467.87	0.01
1320.60	0.01		1330.90	0.01		1468.07	0.03
1321.02	0.02		1331.06	0.03		1468.34	0.06
1321.20	0.02		1331.30	0.01		1468.65	0.02
1321.61	<0.01		1331.50	<0.01		1468.85	<0.01
1321.81	0.03		1331.70	0.01		1469.30	<0.01
1322.00	0.01		1331.90	0.01		1469.60	<0.01
1322.22	<0.01		1459.58	0.04		1469.88	0.02
1322.40	0.01		1459.78	0.01		1470.09	0.03
1322.80	0.04		1459.96	0.04		1470.28	0.03
1323.00	0.05		1460.18	0.01		1470.38	<0.01
1323.17	<0.01		1460.39	0.01		1470.65	0.04
1323.37	0.00		1460.58	0.04		1470.83	<0.01
1323.60	0.02		1460.77	<0.01		1471.03	<0.01
1323.76	0.01		1460.95	<0.01		1471.23	<0.01
1323.97	<0.01		1461.15	0.05		1471.53	<0.01
1324.17	0.07		1461.40	0.07		1471.71	0.01
1324.48	0.04		1461.57	<0.01		1471.92	<0.01
1324.60	0.01		1461.77	0.04		1472.17	0.05
1324.82	0.04		1461.97	0.07		1472.35	<0.01
1325.33	0.04		1462.17	0.06		1472.52	0.04
1325.50	0.01		1462.40	0.05		1472.71	0.01
1325.70	0.01		1462.68	0.06		1472.91	0.05
1325.90	0.01		1462.87	0.02		1473.14	0.07
1326.10	0.02		1463.18	<0.01		1473.31	0.02
1326.30	0.04		1463.26	0.05		1473.51	<0.01
1326.50	0.01		1463.44	0.02		1473.71	<0.01
1326.70	0.03		1463.64	<0.01		1473.88	0.01
1326.90	0.02		1463.86	<0.01		1474.11	<0.01
1327.10	0.01		1464.22	0.04		1474.30	<0.01
1327.30	<0.01		1464.43	0.04		1474.50	<0.01
1327.50	0.03		1464.63	0.06		1474.70	<0.01
1327.70	<0.01		1464.83	<0.01		1474.90	<0.01
1327.87	0.01		1465.05	0.02		1475.21	0.01
1328.08	0.01		1465.24	<0.01		1475.40	0.09
1328.30	0.01		1465.43	0.03		1475.57	0.05
1328.50	<0.01		1465.68	0.01		1475.74	<0.01
1328.69	0.01		1465.87	<0.01		1475.92	0.02
1328.91	0.01		1466.07	0.06		1476.12	0.03

Table 2

MINI-PROBE PERMEAMETER MEASUREMENTS

Company: DEPARTMENT OF MINERALS AND ENERGY (WESTERN AUSTRALIA)
Well: VINES-1 Date: 25-Oct-00
Date 25.10.00 File No: CA-0061

1476.41	<0.01		1486.32	0.03			
1476.61	<0.01		1486.50	0.01			
1476.82	<0.01		1486.68	0.02			
1477.06	0.04		1486.86	0.03			
1477.25	<0.01						
1477.46	0.02						
1477.66	<0.01						
1477.89	0.03						
1478.08	<0.01						
1478.27	<0.01						
1478.47	0.02						
1478.68	<0.01						
1478.88	<0.01						
1479.11	<0.01						
1479.31	<0.01						
1479.52	0.06						
1479.72	<0.01						
1479.91	<0.01						
1480.12	0.05						
1480.33	<0.01						
1480.51	0.05						
1480.68	0.03						
1480.90	0.05						
1481.16	0.07						
1481.30	<0.01						
1481.50	0.05						
1481.71	0.06						
1481.90	0.07						
1482.16	0.04						
1482.39	0.04						
1482.56	0.02						
1482.91	0.06						
1483.11	0.04						
1483.34	<0.01						
1483.52	<0.01						
1483.71	<0.01						
1483.90	<0.01						
1484.20	0.04						
1484.50	0.01						
1484.72	<0.01						
1484.90	0.07						
1485.08	0.06						
1485.30	0.01						
1485.50	<0.01						
1485.70	0.01						
1485.90	0.05						
1486.11	0.05						

Appendix 10

VINES-1
SEAL CAPACITY
STUDY

PROFESSIONAL OPINION

Prepared by:
Khiam Ooi

Prepared for:
Mark Stevens
Department of Minerals and Energy

October 2000

Geotechnical Services Pty Ltd shall not be responsible or liable for the results of any actions taken on the basis of the information contained in this study, nor for any errors or omissions in it.

Seal Capacity Study on core plugs from Vines-1

Laboratory procedure and discussion of data

Four one-inch diameter core plugs, 598.23m, 644.00m, 682.00m and 930.00m which had undergone routine helium injection porosity and air permeability measurements were selected for seal capacity determination.

The samples were dried at approximately 115°C before they were individually loaded into the Micrometrics AutoPore Mercury Porosimeter. The samples were evacuated to less than 50 microns vacuum and then mercury was injected at incremental pressures ranging from 1.64 to 60,000 psia. The amount of mercury injected after equilibration at each pressure point was recorded automatically using a 30 second monitoring cycle.

Closure pressures were determined from the point of inflection on a plot of mercury intrusion (as a percentage of the sample bulk volume) against intrusion pressure. Pressure versus mercury intrusion data were then used to construct a plot of pore space occupied by mercury (%) versus capillary pressure or a “drainage” curve.

Hydrocarbon heights (h) were calculated from the capillary pressures ($Pc_{oil\text{-}brine}$) using the expression

$$Pc_{oil\text{-}brine} = h\,(\rho_{brine} - \rho_{oil}) \times 0.433$$

$$h\,(\text{ft}) = Pc_{oil\text{-}brine} / (\rho_{brine} - \rho_{oil}) \times 0.433$$

where Pc_{brine} = brine density (1.110 g cm^{-3})

Pc_{oil} = oil density (0.85 g cm^{-3})

Pc_{gas} = gas density (0.20 g cm^{-3})

Height above free water h (ft)

$$h\,(\text{oil-brine}) = 0.728 \times Pc_{air\text{-}mercury}$$

$$h\,(\text{gas-brine}) = 0.345 \times Pc_{air\text{-}mercury}$$

The table on the next page shows calculated oil and gas heights (i.e. sealing capacities) for 10 % mercury saturation. Studies undertaken by Schowalter (1979) indicated that the non-water phase saturation needed to establish a connected filament and hence breakthrough across the length of a sample ranged from 4.5 to 17% or an average of 10%.

Calculated hydrocarbon column heights

Sample (metre)	MICP Porosity (%)	Calculated MICP Perm (md)	Grain density (g/cc)	Capillary Pressure (psia)	Oil column held (feet)	Gas column held (feet)
598.23	5.95	0.00007	2.683	18798	13685	6485
644.00	5.60	0.00006	3.174	20662	15042	7129
682.00	2.48	0.00003	2.680	16457	11981	5678
930.00	2.84	0.00003	2.685	16622	12101	5734

As expected, all the samples tested exhibit excellent sealing capacities. However care should be taken when interpreting seal capacity data. In the laboratory when examining microscale seals on small samples, macrofractures such as fractures, faults, lateral and vertical variations in lithology are not accounted for.

Two types of seal have been defined: those that fail by capillary leakage (membrane seals) and those whose capillary entry pressures are so high that seal fracture preferentially occurs by fracturing and/or wedging open of faults (hydraulic seals). Stratigraphic units identified as having the capillary properties of seals need to be examined carefully prior to sampling for lithological uniformity. If the unit changes areally, it is important to measure the capillary properties of the weak “link”, that is the least effective seal. The thickness of the seal should also be considered. A unit containing a thin shale, say a few inches thick can theoretically trap a large column height of hydrocarbons, but the chance that the unit will not contain a fracture or some other migration pathway is slim. Ductility can be important as well; brittle rocks will tend to fracture rather than flow under regional stress.

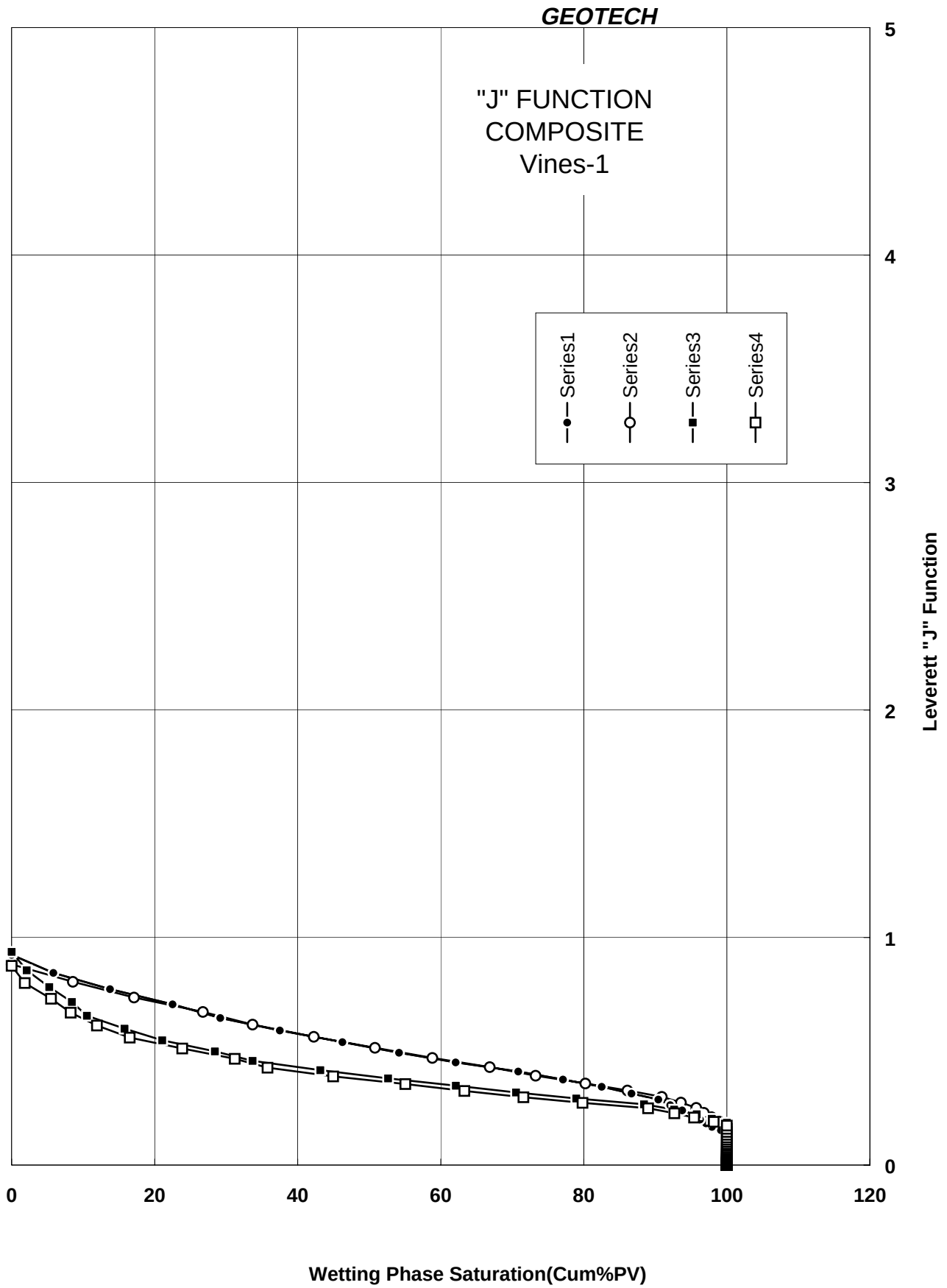
GEOTECH
"J" FUNCTION
COMPOSITE
Vines-1
Series1
Series2
Series3
Series4
5
4
3
2
1
0
Leverett "J" Function
0
20
40
60
80
100
120
Wetting Phase Saturation(Cum%PV)

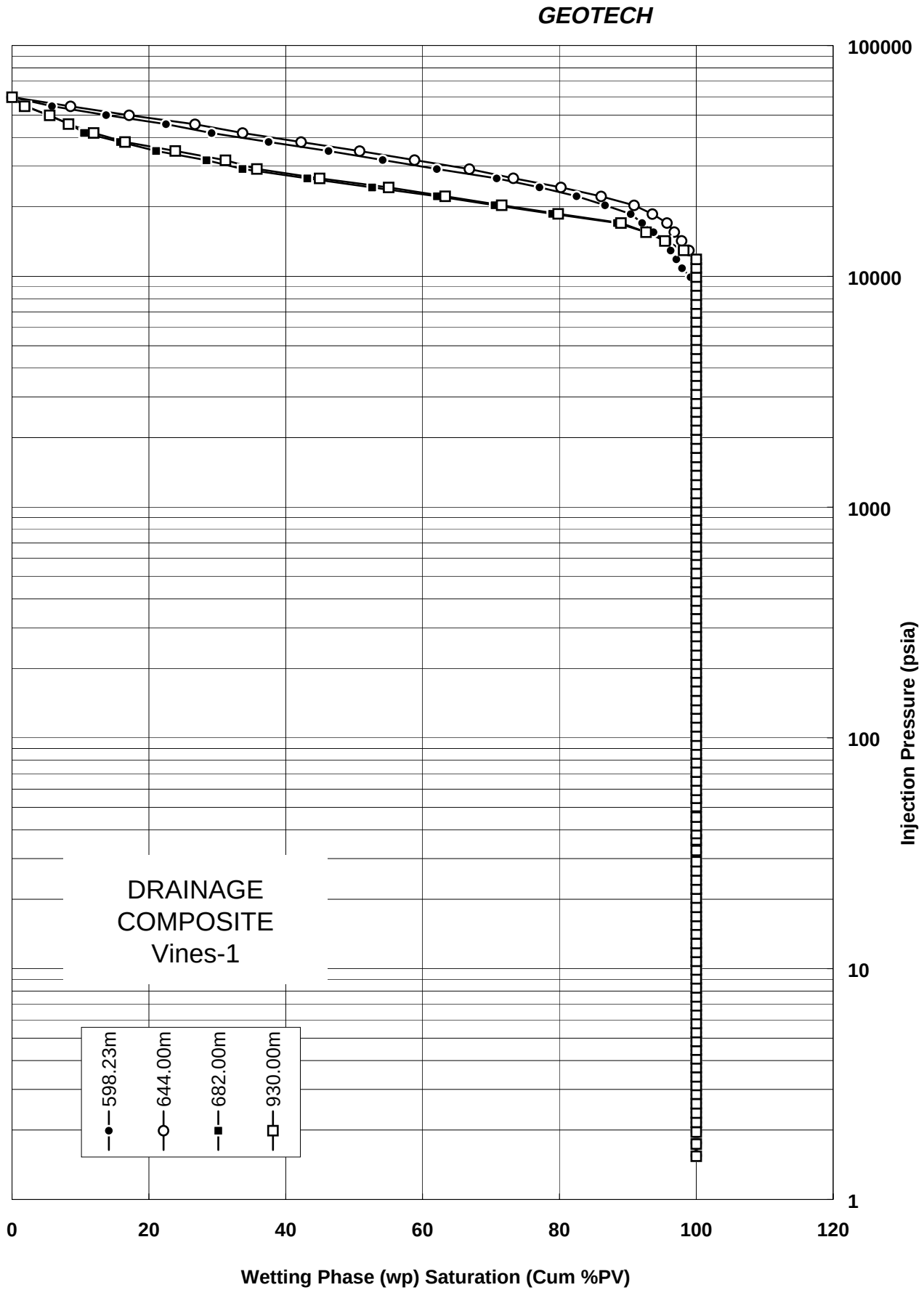
GEOTECH
100000
10000
1000
100
10
1
Injection Pressure (psia)
0
20
40
60
80
100
120
Wetting Phase (wp) Saturation (Cum %PV)
DRAINAGE
COMPOSITE
Vines-1
598.23m
644.00m
682.00m
930.00m

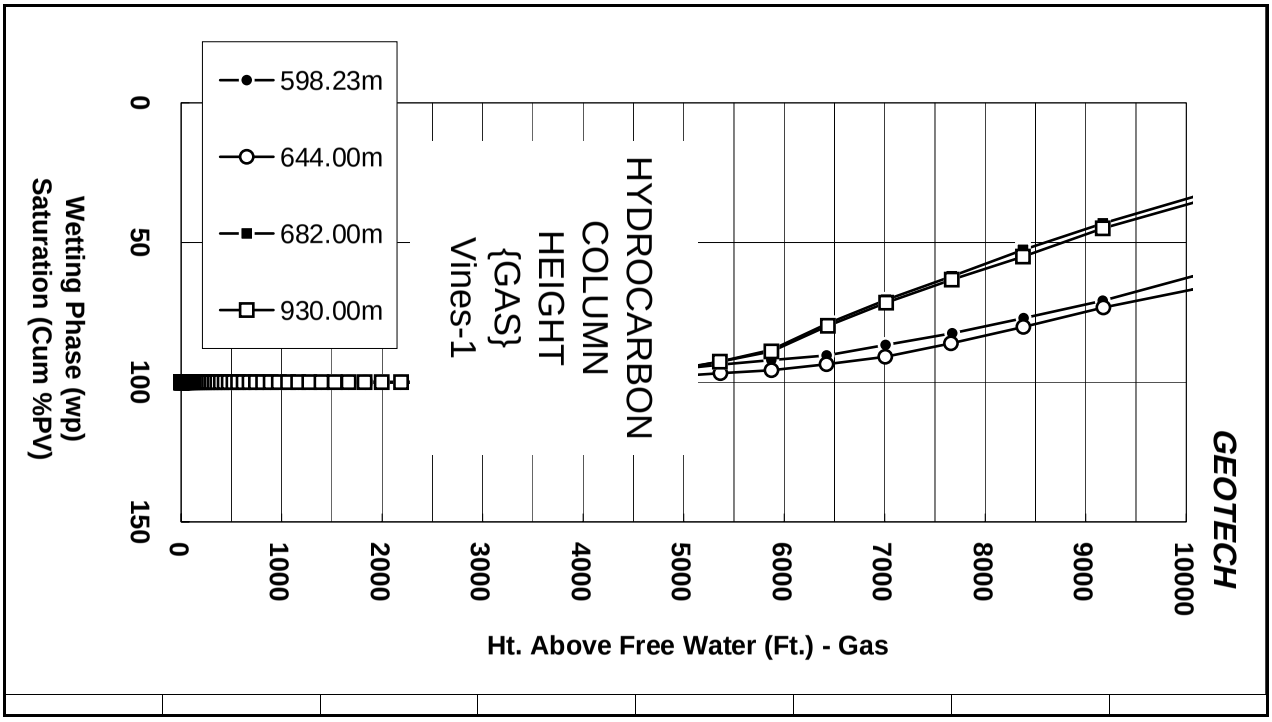
598.23m
644.00m
682.00m
930.00m
HYDROCARBON COLUMN HEIGHT {GAS} Vines-1
Wetting Phase (wp) Saturation (Cum %PV)
0
50
100
150
0
1000
2000
3000
4000
5000
6000
7000
8000
9000
10000
Ht. Above Free Water (Ft.) - Gas
GEOTECH

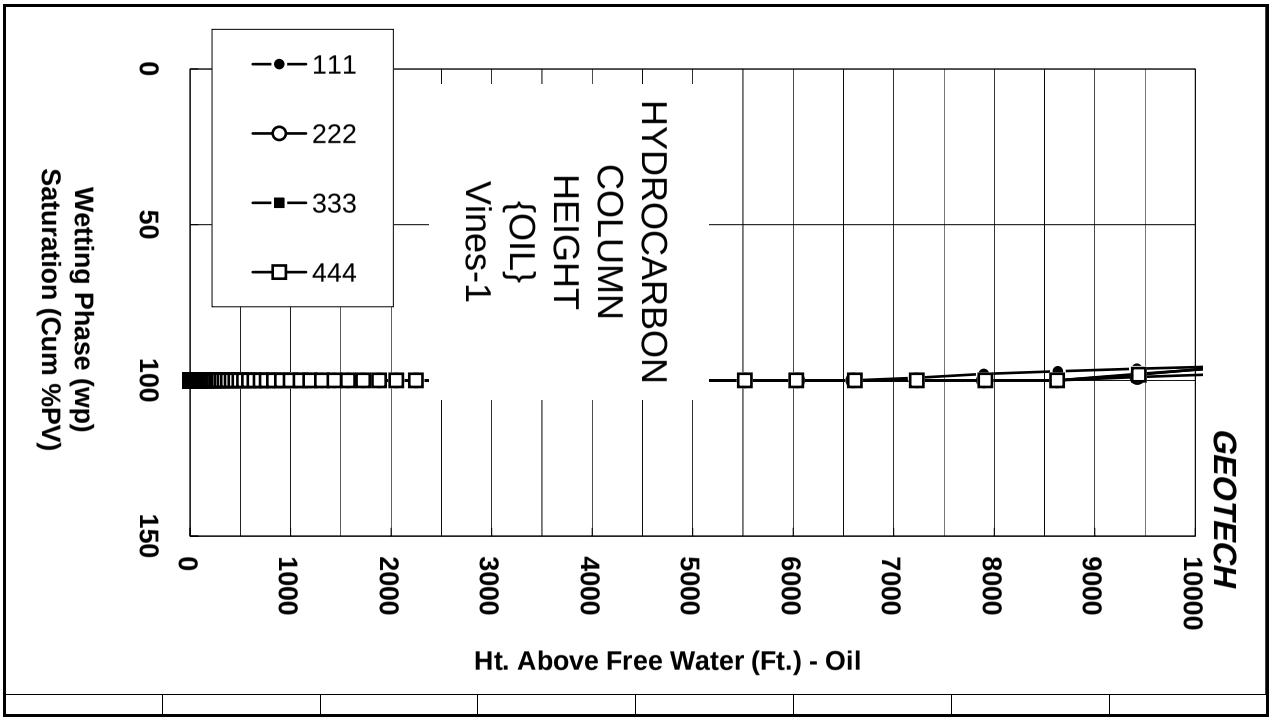
111
222
333
444
HYDROCARBON COLUMN HEIGHT
{OIL}
Vines-1
Wetting Phase (wp) Saturation (Cum %PV)
0
50
100
150
0
1000
2000
3000
4000
5000
6000
7000
8000
9000
10000
Ht. Above Free Water (Ft.) - Oil
GEOTECH

Int Pres psia	Pore Dia microns	Inc Int mL/gm	Cum Int mL/gm	Cum Int %PV(bc)	Cum Int %BV	Inc Int %PV(ac)
1.54	138.1692	0	0	0	0	0
1.74	122.3784	0	0	0.081	0	0
1.97	108.0395	0.0002	0.0002	0.7958	0.049616	0
2.17	98.356	0.0003	0.0005	1.793	0.124039	0
2.38	89.4748	0	0.0005	1.793	0.124039	0
2.62	81.5105	0	0.0005	1.793	0.124039	0
2.85	74.8903	0.0002	0.0007	2.5672	0.173655	0
3.12	68.4083	0	0.0007	2.7386	0.173655	0
3.4	62.6619	0	0.0007	2.7386	0.173655	0
3.71	57.5555	0	0.0007	2.7386	0.173655	0
4.06	52.5447	0	0.0007	2.7386	0.173655	0
4.43	48.1438	0	0.0007	2.7386	0.173655	0
4.84	44.0839	0	0.0007	2.7386	0.173655	0
5.29	40.3221	0	0.0007	2.7386	0.173655	0
5.79	36.8221	0	0.0007	2.7386	0.173655	0
6.34	33.6665	0	0.0007	2.7386	0.173655	0
6.91	30.8792	0	0.0007	2.7386	0.173655	0
7.55	28.2572	0	0.0007	2.7386	0.173655	0
8.27	25.7876	0	0.0007	2.7386	0.173655	0
9.04	23.597	0	0.0007	2.7386	0.173655	0
9.87	21.6149	0	0.0007	2.7386	0.173655	0
10.77	19.8091	0	0.0007	2.7386	0.173655	0
11.78	18.1122	0	0.0007	2.7386	0.173655	0
12.87	16.5789	0	0.0007	2.7386	0.173655	0
14.16	15.0682	0	0.0007	2.7386	0.173655	0
15.45	13.8083	0	0.0008	2.8355	0.198462	0
16.86	12.6554	0	0.0008	2.8355	0.198462	0
18.45	11.5622	0.0001	0.0009	3.3225	0.22327	0
20.24	10.5406	0	0.0009	3.3225	0.22327	0
22.12	9.6455	0	0.0009	3.3225	0.22327	0
24.22	8.808	0	0.0009	3.3225	0.22327	0
26.52	8.0429	0.0001	0.001	3.5638	0.248078	0
29.15	7.3179	0.0001	0.001	3.8493	0.248078	0
31.85	6.6977	0	0.001	3.8493	0.248078	0
34.81	6.1286	0	0.001	3.8493	0.248078	0
38.07	5.6034	0.0001	0.0011	4.1644	0.272886	0
41.57	5.1314	0	0.0011	4.1644	0.272886	0
45.51	4.6876	0	0.0011	4.1644	0.272886	0
50.1	4.2575	0	0.0011	4.1644	0.272886	0

54.48	3.9159	0	0.0011	4.1644	0.272886	0
59.41	3.5909	0	0.0011	4.1644	0.272886	0
65.4	3.2618	0	0.0011	4.1644	0.272886	0
71.36	2.9894	0	0.0011	4.1644	0.272886	0
77.98	2.7357	0	0.0011	4.1644	0.272886	0
84.94	2.5116	0.0001	0.0012	4.4951	0.297694	0
93.19	2.2891	0.0001	0.0013	4.9433	0.322501	0
102.14	2.0885	0	0.0013	4.9433	0.322501	0
111.8	1.9081	0.0001	0.0014	5.1594	0.347309	0
121.48	1.756	0.0001	0.0015	5.7128	0.372117	0
133.56	1.5972	0	0.0015	5.7128	0.372117	0
145.47	1.4664	0	0.0015	5.7128	0.372117	0
160.12	1.3322	0	0.0015	5.7128	0.372117	0
175.55	1.2152	0	0.0015	5.7128	0.372117	0
191.74	1.1125	0	0.0015	5.7128	0.372117	0
208.2	1.0246	0	0.0015	5.7128	0.372117	0
228.57	0.9333	0	0.0015	5.7128	0.372117	0
250.22	0.8525	0.0002	0.0017	6.4404	0.421733	0
274.77	0.7764	0	0.0017	6.4404	0.421733	0
298.94	0.7136	0	0.0017	6.4404	0.421733	0
330.18	0.6461	0	0.0017	6.4404	0.421733	0
357.87	0.5961	0	0.0017	6.4404	0.421733	0
394.17	0.5412	0	0.0017	6.4404	0.421733	0
429.9	0.4962	0	0.0017	6.4404	0.421733	0
470.11	0.4538	0	0.0017	6.4404	0.421733	0
522.88	0.408	0	0.0017	6.4404	0.421733	0
563.52	0.3786	0	0.0017	6.4404	0.421733	0
615.42	0.3466	0	0.0017	6.4404	0.421733	0
673.25	0.3169	0	0.0017	6.4404	0.421733	0
734.14	0.2906	0	0.0017	6.4404	0.421733	0
802.58	0.2658	0	0.0017	6.4404	0.421733	0
877.13	0.2432	0	0.0017	6.4404	0.421733	0
965	0.2211	0	0.0017	6.4404	0.421733	0
1045.98	0.2039	0	0.0017	6.4404	0.421733	0
1145.74	0.1862	0	0.0017	6.4404	0.421733	0
1254.03	0.1701	0	0.0017	6.4404	0.421733	0
1377.41	0.1549	0	0.0017	6.4404	0.421733	0
1504.64	0.1418	0	0.0017	6.4404	0.421733	0
1643.93	0.1298	0	0.0017	6.4431	0.421733	0
1801.69	0.1184	0.0001	0.0018	6.6844	0.44654	0
1974.56	0.108	0.0001	0.0019	7.0132	0.471348	0
2150.96	0.0992	0.0001	0.002	7.2511	0.496156	0

2360.78	0.0904	0.0001	0.0021	7.7763	0.520964	0
2583.13	0.0826	0.0001	0.0022	8.2256	0.545772	0
2823.63	0.0755	0.0001	0.0023	8.5494	0.570579	0
3095.8	0.0689	0	0.0023	8.5494	0.570579	0
3373.69	0.0632	0	0.0023	8.5494	0.570579	0
3697.21	0.0577	0.0001	0.0024	8.7939	0.595387	0
4046.42	0.0527	0.0001	0.0025	9.2802	0.620195	0
4422.06	0.0482	0.0001	0.0026	9.5202	0.645003	0
4832.14	0.0441	0.0001	0.0026	9.7245	0.645003	0
5288.95	0.0403	0.0001	0.0027	9.9271	0.669811	0
5787.77	0.0369	0.0001	0.0028	10.2508	0.694618	0
6347.16	0.0336	0	0.0028	10.2508	0.694618	0
6937.09	0.0308	0.0001	0.0028	10.4533	0.694618	0
7579.07	0.0281	0.0001	0.0029	10.859	0.719426	0
8290.46	0.0257	0.0001	0.0031	11.3446	0.769042	0
9059.69	0.0235	0.0001	0.0031	11.5883	0.769042	0
9915.67	0.0215	0.0002	0.0033	12.2768	0.818657	0.83333333
10846.83	0.0197	0.0003	0.0036	13.3304	0.893081	1.25
11858.97	0.018	0.0002	0.0038	14.0194	0.942696	0.83333333
12938.58	0.0165	0.0002	0.004	14.6272	0.992312	0.83333333
14241.83	0.015	0.0003	0.0042	15.6807	1.041928	0.83333333
15535.43	0.0137	0.0004	0.0046	16.9773	1.141159	1.66666667
17019.89	0.0125	0.0004	0.005	18.435	1.24039	1.66666667
18614.24	0.0115	0.0004	0.0054	20.016	1.339621	1.66666667
20316.54	0.0105	0.0009	0.0063	23.2174	1.562891	3.75
22238.6	0.0096	0.0011	0.0073	27.1081	1.810969	4.16666667
24297.54	0.0088	0.0013	0.0086	31.7262	2.133471	5.41666667
26578.17	0.008	0.0015	0.0101	37.2366	2.505588	6.25
29171.09	0.0073	0.0021	0.0122	45.0159	3.026552	8.75
31914.39	0.0067	0.0019	0.0141	52.1051	3.4979	7.91666667
34919.89	0.0061	0.0019	0.016	58.9546	3.969248	7.91666667
38222.28	0.0056	0.0021	0.0181	66.8262	4.490212	8.75
41765.66	0.0051	0.002	0.0201	74.1524	4.986368	8.33333333
45648.37	0.0047	0.0016	0.0217	79.9786	5.383292	6.66666667
49966.76	0.0043	0.0022	0.0238	88.0111	5.904256	8.75
54587.85	0.0039	0.0018	0.0257	94.8074	6.375604	7.91666667
59710.2	0.0036	0.0014	0.0271	100	6.722914	5.83333333

Cum Int %PV(ac)	Pore Rad microns	W.P. Sat %PV(ac)	Lev "J" Funct.	G/B Pc psia	G/O Pc psia	O/B Pc psia	Ht FWL,ft G/B
0	69.0846	100	0.000	0.20944	0.1001	0.12628	0.5313
0	61.1892	100	0.000	0.23664	0.1131	0.14268	0.6003
0	54.01975	100	0.000	0.26792	0.12805	0.16154	0.67965
0	49.178	100	0.000	0.29512	0.14105	0.17794	0.74865
0	44.7374	100	0.000	0.32368	0.1547	0.19516	0.8211
0	40.75525	100	0.000	0.35632	0.1703	0.21484	0.9039
0	37.44515	100	0.000	0.3876	0.18525	0.2337	0.98325
0	34.20415	100	0.000	0.42432	0.2028	0.25584	1.0764
0	31.33095	100	0.000	0.4624	0.221	0.2788	1.173
0	28.77775	100	0.000	0.50456	0.24115	0.30422	1.27995
0	26.27235	100	0.000	0.55216	0.2639	0.33292	1.4007
0	24.0719	100	0.000	0.60248	0.28795	0.36326	1.52835
0	22.04195	100	0.000	0.65824	0.3146	0.39688	1.6698
0	20.16105	100	0.000	0.71944	0.34385	0.43378	1.82505
0	18.41105	100	0.000	0.78744	0.37635	0.47478	1.99755
0	16.83325	100	0.000	0.86224	0.4121	0.51988	2.1873
0	15.4396	100	0.000	0.93976	0.44915	0.56662	2.38395
0	14.1286	100	0.000	1.0268	0.49075	0.6191	2.60475
0	12.8938	100	0.000	1.12472	0.53755	0.67814	2.85315
0	11.7985	100	0.000	1.22944	0.5876	0.74128	3.1188
0	10.80745	100	0.000	1.34232	0.64155	0.80934	3.40515
0	9.90455	100	0.000	1.46472	0.70005	0.88314	3.71565
0	9.0561	100	0.000	1.60208	0.7657	0.96596	4.0641
0	8.28945	100	0.000	1.75032	0.83655	1.05534	4.44015
0	7.5341	100	0.000	1.92576	0.9204	1.16112	4.8852
0	6.90415	100	0.000	2.1012	1.00425	1.2669	5.33025
0	6.3277	100	0.000	2.29296	1.0959	1.38252	5.8167
0	5.7811	100	0.000	2.5092	1.19925	1.5129	6.36525
0	5.2703	100	0.000	2.75264	1.3156	1.65968	6.9828
0	4.82275	100	0.000	3.00832	1.4378	1.81384	7.6314
0	4.404	100	0.000	3.29392	1.5743	1.98604	8.3559
0	4.02145	100	0.000	3.60672	1.7238	2.17464	9.1494
0	3.65895	100	0.000	3.9644	1.89475	2.3903	10.05675
0	3.34885	100	0.000	4.3316	2.07025	2.6117	10.98825
0	3.0643	100	0.001	4.73416	2.26265	2.85442	12.00945
0	2.8017	100	0.001	5.17752	2.47455	3.12174	13.13415
0	2.5657	100	0.001	5.65352	2.70205	3.40874	14.34165
0	2.3438	100	0.001	6.18936	2.95815	3.73182	15.70095
0	2.12875	100	0.001	6.8136	3.2565	4.1082	17.2845

0	1.95795	100	0.001	7.40928	3.5412	4.46736	18.7956
0	1.79545	100	0.001	8.07976	3.86165	4.87162	20.49645
0	1.6309	100	0.001	8.8944	4.251	5.3628	22.563
0	1.4947	100	0.001	9.70496	4.6384	5.85152	24.6192
0	1.36785	100	0.001	10.60528	5.0687	6.39436	26.9031
0	1.2558	100	0.001	11.55184	5.5211	6.96508	29.3043
0	1.14455	100	0.001	12.67384	6.05735	7.64158	32.15055
0	1.04425	100	0.002	13.89104	6.6391	8.37548	35.2383
0	0.95405	100	0.002	15.2048	7.267	9.1676	38.571
0	0.878	100	0.002	16.52128	7.8962	9.96136	41.9106
0	0.7986	100	0.002	18.16416	8.6814	10.95192	46.0782
0	0.7332	100	0.002	19.78392	9.45555	11.92854	50.18715
0	0.6661	100	0.002	21.77632	10.4078	13.12984	55.2414
0	0.6076	100	0.003	23.8748	11.41075	14.3951	60.56475
0	0.55625	100	0.003	26.07664	12.4631	15.72268	66.1503
0	0.5123	100	0.003	28.3152	13.533	17.0724	71.829
0	0.46665	100	0.004	31.08552	14.85705	18.74274	78.85665
0	0.42625	100	0.004	34.02992	16.2643	20.51804	86.3259
0	0.3882	100	0.004	37.36872	17.86005	22.53114	94.79565
0	0.3568	100	0.005	40.65584	19.4311	24.51308	103.1343
0	0.32305	100	0.005	44.90448	21.4617	27.07476	113.9121
0	0.29805	100	0.006	48.67032	23.26155	29.34534	123.4652
0	0.2706	100	0.006	53.60712	25.62105	32.32194	135.9887
0	0.2481	100	0.007	58.4664	27.9435	35.2518	148.3155
0	0.2269	100	0.007	63.93496	30.55715	38.54902	162.188
0	0.204	100	0.008	71.11168	33.9872	42.87616	180.3936
0	0.1893	100	0.009	76.63872	36.6288	46.20864	194.4144
0	0.1733	100	0.010	83.69712	40.0023	50.46444	212.3199
0	0.15845	100	0.010	91.562	43.76125	55.2065	232.2713
0	0.1453	100	0.011	99.84304	47.7191	60.19948	253.2783
0	0.1329	100	0.012	109.1509	52.1677	65.81156	276.8901
0	0.1216	100	0.014	119.2897	57.01345	71.92466	302.6099
0	0.11055	100	0.015	131.24	62.725	79.13	332.925
0	0.10195	100	0.016	142.2533	67.9887	85.77036	360.8631
0	0.0931	100	0.018	155.8206	74.4731	93.95068	395.2803
0	0.08505	100	0.019	170.5481	81.51195	102.8305	432.6404
0	0.07745	100	0.021	187.3278	89.53165	112.9476	475.2065
0	0.0709	100	0.023	204.631	97.8016	123.3805	519.1008
0	0.0649	100	0.025	223.5745	106.8555	134.8023	567.1559
0	0.0592	100	0.028	245.0298	117.1099	147.7386	621.5831
0	0.054	100	0.031	268.5402	128.3464	161.9139	681.2232
0	0.0496	100	0.033	292.5306	139.8124	176.3787	742.0812

0	0.0452	100	0.037	321.0661	153.4507	193.584	814.4691
0	0.0413	100	0.040	351.3057	167.9035	211.8167	891.1799
0	0.03775	100	0.044	384.0137	183.536	231.5377	974.1524
0	0.03445	100	0.048	421.0288	201.227	253.8556	1068.051
0	0.0316	100	0.052	458.8218	219.2899	276.6426	1163.923
0	0.02885	100	0.057	502.8206	240.3187	303.1712	1275.537
0	0.02635	100	0.063	550.3131	263.0173	331.8064	1396.015
0	0.0241	100	0.068	601.4002	287.4339	362.6089	1525.611
0	0.02205	100	0.075	657.171	314.0891	396.2355	1667.088
0	0.02015	100	0.082	719.2972	343.7818	433.6939	1824.688
0	0.01845	100	0.090	787.1367	376.2051	474.5971	1996.781
0	0.0168	100	0.098	863.2138	412.5654	520.4671	2189.77
0	0.0154	100	0.107	943.4442	450.9109	568.8414	2393.296
0	0.01405	100	0.117	1030.754	492.6396	621.4837	2614.779
0	0.01285	100	0.128	1127.503	538.8799	679.8177	2860.209
0	0.01175	100	0.140	1232.118	588.8799	742.8946	3125.593
0.833333	0.01075	99.16667	0.153	1348.531	644.5186	813.0849	3420.906
2.083333	0.00985	97.91667	0.168	1475.169	705.044	889.4401	3742.156
2.916667	0.009	97.08333	0.184	1612.82	770.8331	972.4355	4091.345
3.75	0.00825	96.25	0.200	1759.647	841.0077	1060.964	4463.81
4.583333	0.0075	95.41667	0.220	1936.889	925.719	1167.83	4913.431
6.25	0.00685	93.75	0.240	2112.818	1009.803	1273.905	5359.723
7.916667	0.00625	92.08333	0.263	2314.705	1106.293	1395.631	5871.862
9.583333	0.00575	90.41667	0.288	2531.537	1209.926	1526.368	6421.913
13.33333	0.00525	86.66667	0.314	2763.049	1320.575	1665.956	7009.206
17.5	0.0048	82.5	0.344	3024.45	1445.509	1823.565	7672.317
22.91667	0.0044	77.08333	0.376	3304.465	1579.34	1992.398	8382.651
29.16667	0.004	70.83333	0.411	3614.631	1727.581	2179.41	9169.469
37.91667	0.00365	62.08333	0.452	3967.268	1896.121	2392.029	10064.03
45.83333	0.00335	54.16667	0.494	4340.357	2074.435	2616.98	11010.46
53.75	0.00305	46.25	0.540	4749.105	2269.793	2863.431	12047.36
62.5	0.0028	37.5	0.592	5198.23	2484.448	3134.227	13186.69
70.83333	0.00255	29.16667	0.646	5680.13	2714.768	3424.784	14409.15
77.5	0.00235	22.5	0.707	6208.178	2967.144	3743.166	15748.69
86.25	0.00215	13.75	0.773	6795.479	3247.839	4097.274	17238.53
94.16667	0.00195	5.833333	0.845	7423.948	3548.21	4476.204	18832.81
100	0.0018	0	0.924	8120.587	3881.163	4896.236	20600.02

Ht FWL,ft O/B	Swanson's Sb/Pc(ac)
1.12112	-0.4993778
1.26672	-0.441978
1.43416	-0.365191
1.57976	-0.2972363
1.73264	-0.2710096
1.90736	-0.2461843
2.0748	-0.2089078
2.27136	-0.1908292
2.4752	-0.1751139
2.70088	-0.1604817
2.95568	-0.1466471
3.22504	-0.1343989
3.52352	-0.1230139
3.85112	-0.1125496
4.21512	-0.1028303
4.61552	-0.0939097
5.03048	-0.0861631
5.4964	-0.0788592
6.02056	-0.0719936
6.58112	-0.0658614
7.18536	-0.0603229
7.84056	-0.055282
8.57584	-0.0505422
9.36936	-0.0462616
10.30848	-0.0420471
11.2476	-0.0369307
12.27408	-0.0338422
13.4316	-0.0295811
14.73472	-0.026965
16.10336	-0.0246732
17.63216	-0.0225339
19.30656	-0.0196442
21.2212	-0.0178718
23.1868	-0.0163568
25.34168	-0.0149659
27.71496	-0.0130327
30.26296	-0.0119354
33.13128	-0.0109021
36.4728	-0.0099033

39.66144	-0.0091071
43.25048	-0.0083514
47.6112	-0.0075865
51.95008	-0.0069529
56.76944	-0.0063626
61.83632	-0.0055492
67.84232	-0.0047917
74.35792	-0.0043718
81.3904	-0.0037722
88.43744	-0.0032674
97.23168	-0.0029719
105.9022	-0.0027286
116.5674	-0.0024789
127.8004	-0.002261
139.5867	-0.0020701
151.5696	-0.0019065
166.399	-0.0017366
182.1602	-0.001388
200.0326	-0.001264
217.6283	-0.0011618
240.371	-0.0010519
260.5294	-0.0009705
286.9558	-0.0008811
312.9672	-0.0008079
342.2401	-0.0007388
380.6566	-0.0006642
410.2426	-0.0006163
448.0258	-0.0005643
490.126	-0.0005159
534.4539	-0.0004731
584.2782	-0.0004327
638.5506	-0.000396
702.52	-0.0003599
761.4734	-0.000332
834.0987	-0.0003031
912.9338	-0.000277
1002.754	-0.0002521
1095.378	-0.0002308
1196.781	-0.0002113
1311.63	-0.000179
1437.48	-0.0001508
1565.899	-0.0001269

1718.648	-0.0001051
1880.519	-8.643E-05
2055.603	-7.029E-05
2253.742	-6.411E-05
2456.046	-5.883E-05
2691.569	-4.697E-05
2945.794	-3.678E-05
3219.26	-2.805E-05
3517.798	-2.567E-05
3850.356	-1.876E-05
4213.497	-1.286E-05
4620.732	-1.173E-05
5050.202	-1.073E-05
5517.563	-6.546E-06
6035.455	0
6595.454	0
7218.608	5.0038E-06
7896.492	1.1436E-05
8633.33	1.4643E-05
9419.286	1.7256E-05
10368.05	1.9161E-05
11309.79	2.3953E-05
12390.48	2.7694E-05
13551.17	3.0653E-05
14790.44	3.9074E-05
16189.7	4.6852E-05
17688.61	5.6155E-05
19348.91	6.5337E-05
21236.55	7.7389E-05
23233.68	8.5506E-05
25421.68	9.1644E-05
27825.82	9.7356E-05
30405.4	0.00010098
33232.01	0.00010108
36375.8	0.00010277
39739.95	0.00010271
43469.03	9.9713E-05
	0.00010277

AIR|MERCURY CAPILLARY PRESSURE DATA : BY GEOTECH

Spl @ 598.23m Vines-1

Bulk Volume = 4.8517cc
Closure @ 9060. psia
Pore Volume = 0.2889cc
Porosity = 5.95%
Median Pore Aperture = 0.0064 microns (dia.)

Injection Pressure (psia)	Pore Diameter (microns)	Hg (nwp) Saturation cum%PV	100-Hg(wp) Saturation cum%PV	Leverett "J" Function	Gas/Brine Pc (psia)	Gas/Oil Pc (psia)	Oil/Brine Pc (psia)	Ht. Above Free Water (ft.) Gas/Brine	Ht. Above Free Water (ft.) Oil/Brine
1.54	138.17	0.0	100.0	0.00	0.21	0.10	0.13	0.5	1.1
1.74	122.38	0.0	100.0	0.00	0.24	0.11	0.14	0.6	1.3
1.97	108.04	0.0	100.0	0.00	0.27	0.13	0.16	0.7	1.4
2.17	98.36	0.0	100.0	0.00	0.30	0.14	0.18	0.7	1.6
2.38	89.47	0.0	100.0	0.00	0.32	0.15	0.20	0.8	1.7
2.62	81.51	0.0	100.0	0.00	0.36	0.17	0.21	0.9	1.9
2.85	74.89	0.0	100.0	0.00	0.39	0.19	0.23	1.0	2.1
3.12	68.41	0.0	100.0	0.00	0.42	0.20	0.26	1.1	2.3
3.40	62.66	0.0	100.0	0.00	0.46	0.22	0.28	1.2	2.5
3.71	57.56	0.0	100.0	0.00	0.50	0.24	0.30	1.3	2.7
4.06	52.54	0.0	100.0	0.00	0.55	0.26	0.33	1.4	3.0
4.43	48.14	0.0	100.0	0.00	0.60	0.29	0.36	1.5	3.2
4.84	44.08	0.0	100.0	0.00	0.66	0.31	0.40	1.7	3.5
5.29	40.32	0.0	100.0	0.00	0.72	0.34	0.43	1.8	3.9
5.79	36.82	0.0	100.0	0.00	0.79	0.38	0.47	2.0	4.2
6.34	33.67	0.0	100.0	0.00	0.86	0.41	0.52	2.2	4.6
6.91	30.88	0.0	100.0	0.00	0.94	0.45	0.57	2.4	5.0
7.55	28.26	0.0	100.0	0.00	1.03	0.49	0.62	2.6	5.5
8.27	25.79	0.0	100.0	0.00	1.12	0.54	0.68	2.9	6.0
9.04	23.60	0.0	100.0	0.00	1.23	0.59	0.74	3.1	6.6
9.87	21.61	0.0	100.0	0.00	1.34	0.64	0.81	3.4	7.2
10.77	19.81	0.0	100.0	0.00	1.46	0.70	0.88	3.7	7.8
11.78	18.11	0.0	100.0	0.00	1.60	0.77	0.97	4.1	8.6
12.87	16.58	0.0	100.0	0.00	1.75	0.84	1.06	4.4	9.4
14.16	15.07	0.0	100.0	0.00	1.93	0.92	1.16	4.9	10.3
15.45	13.81	0.0	100.0	0.00	2.10	1.00	1.27	5.3	11.2
16.86	12.66	0.0	100.0	0.00	2.29	1.10	1.38	5.8	12.3
18.45	11.56	0.0	100.0	0.00	2.51	1.20	1.51	6.4	13.4
20.24	10.54	0.0	100.0	0.00	2.75	1.32	1.66	7.0	14.7
22.12	9.646	0.0	100.0	0.00	3.01	1.44	1.81	7.6	16.1
24.22	8.808	0.0	100.0	0.00	3.29	1.57	1.99	8.4	17.6
26.52	8.043	0.0	100.0	0.00	3.61	1.72	2.17	9.1	19.3
29.15	7.318	0.0	100.0	0.00	3.96	1.89	2.39	10.1	21.2
31.85	6.698	0.0	100.0	0.00	4.33	2.07	2.61	11.0	23.2
34.81	6.129	0.0	100.0	0.00	4.73	2.26	2.85	12.0	25.3

AIR|MERCURY CAPILLARY PRESSURE DATA : BY GEOTECH

Spl @ 598.23m Vines-1

Injection Pressure (psia)	Pore Diameter (microns)	Hg (nwp) Saturation cum%PV	100-Hg(wp) Saturation cum%PV	Leverett "J" Function	Gas/Brine Pc (psia)	Gas/Oil Pc (psia)	Oil/Brine Pc (psia)	Ht. Above Free Water (ft.) Gas/Brine	Ht. Above Free Water (ft.) Oil/Brine
38.07	5.603	0.0	100.0	0.00	5.18	2.47	3.12	13.1	27.7
41.57	5.131	0.0	100.0	0.00	5.65	2.70	3.41	14.3	30.3
45.51	4.688	0.0	100.0	0.00	6.19	2.96	3.73	15.7	33.1
50.10	4.258	0.0	100.0	0.00	6.81	3.26	4.11	17.3	36.5
54.48	3.916	0.0	100.0	0.00	7.41	3.54	4.47	18.8	39.7
59.41	3.591	0.0	100.0	0.00	8.08	3.86	4.87	20.5	43.3
65.40	3.262	0.0	100.0	0.00	8.89	4.25	5.36	22.6	47.6
71.36	2.989	0.0	100.0	0.00	9.7	4.64	5.85	24.6	52.0
77.98	2.736	0.0	100.0	0.00	10.6	5.07	6.39	26.9	56.8
84.94	2.512	0.0	100.0	0.00	11.6	5.52	6.97	29.3	61.8
93.19	2.289	0.0	100.0	0.00	12.7	6.06	7.64	32.2	67.8
102.14	2.089	0.0	100.0	0.00	13.9	6.64	8.38	35.2	74.4
111.80	1.908	0.0	100.0	0.00	15.2	7.27	9.17	38.6	81.4
121.48	1.756	0.0	100.0	0.00	16.5	7.90	9.96	41.9	88.4
133.56	1.597	0.0	100.0	0.00	18.2	8.68	10.95	46.1	97.2
145.47	1.466	0.0	100.0	0.00	19.8	9.46	11.93	50.2	105.9
160.12	1.332	0.0	100.0	0.00	21.8	10.41	13.1	55.2	116.6
175.55	1.215	0.0	100.0	0.00	23.9	11.41	14.4	60.6	128
191.74	1.113	0.0	100.0	0.00	26.1	12.46	15.7	66.2	140
208.20	1.025	0.0	100.0	0.00	28.3	13.5	17.1	71.8	152
228.57	0.933	0.0	100.0	0.00	31.1	14.9	18.7	78.9	166
250.22	0.853	0.0	100.0	0.00	34.0	16.3	20.5	86.3	182
274.77	0.776	0.0	100.0	0.00	37.4	17.9	22.5	95	200
298.94	0.714	0.0	100.0	0.00	40.7	19.4	24.5	103	218
330.18	0.646	0.0	100.0	0.01	44.9	21.5	27.1	114	240
357.87	0.596	0.0	100.0	0.01	48.7	23.3	29.3	123	261
394.17	0.541	0.0	100.0	0.01	53.6	25.6	32.3	136	287
429.90	0.496	0.0	100.0	0.01	58.5	27.9	35.3	148	313
470.11	0.454	0.0	100.0	0.01	63.9	30.6	38.5	162	342
522.88	0.408	0.0	100.0	0.01	71.1	34.0	42.9	180	381
563.52	0.379	0.0	100.0	0.01	76.6	36.6	46.2	194	410
615.42	0.347	0.0	100.0	0.01	83.7	40.0	50.5	212	448
673.25	0.317	0.0	100.0	0.01	91.6	43.8	55.2	232	490
734.14	0.291	0.0	100.0	0.01	99.8	47.7	60.2	253	534
802.58	0.266	0.0	100.0	0.01	109.2	52.2	65.8	277	584
877.13	0.243	0.0	100.0	0.01	119.3	57.0	71.9	303	639
965.00	0.221	0.0	100.0	0.01	131.2	62.7	79.1	333	703
1045.98	0.204	0.0	100.0	0.02	142.3	68.0	85.8	361	761
1145.74	0.186	0.0	100.0	0.02	155.8	74.5	94.0	395	834
1254.03	0.170	0.0	100.0	0.02	170.5	81.5	102.8	433	913
1377.41	0.155	0.0	100.0	0.02	187.3	89.5	112.9	475	1003
1504.64	0.142	0.0	100.0	0.02	204.6	97.8	123.4	519	1095
1643.93	0.130	0.0	100.0	0.03	223.6	106.9	134.8	567	1197

AIR|MERCURY CAPILLARY PRESSURE DATA : BY GEOTECH

Spl @ 598.23m Vines-1

Injection Pressure (psia)	Pore Diameter (microns)	Hg (nwp) Saturation cum%PV	100-Hg(wp) Saturation cum%PV	Leverett "J" Function	Gas/Brine Pc (psia)	Gas/Oil Pc (psia)	Oil/Brine Pc (psia)	Ht. Above Free Water (ft.) Gas/Brine	Ht. Above Free Water (ft.) Oil/Brine
1801.69	0.118	0.0	100.0	0.03	245.0	117.1	147.7	622	1312
1974.56	0.108	0.0	100.0	0.03	268.5	128.3	161.9	681	1437
2150.96	0.0992	0.0	100.0	0.03	292.5	139.8	176.4	742	1566
2360.78	0.0904	0.0	100.0	0.04	321.1	153.5	193.6	814	1719
2583.13	0.0826	0.0	100.0	0.04	351.3	167.9	211.8	891	1881
2823.63	0.0755	0.0	100.0	0.04	384.0	183.5	231.5	974	2056
3095.80	0.0689	0.0	100.0	0.05	421.0	201.2	253.9	1068	2254
3373.69	0.0632	0.0	100.0	0.05	458.8	219.3	276.6	1164	2456
3697.21	0.0577	0.0	100.0	0.06	502.8	240.3	303.2	1276	2692
4046.42	0.0527	0.0	100.0	0.06	550.3	263.0	331.8	1396	2946
4422.06	0.0482	0.0	100.0	0.07	601.4	287.4	362.6	1526	3219
4832.14	0.0441	0.0	100.0	0.07	657.2	314.1	396.2	1667	3518
5288.95	0.0403	0.0	100.0	0.08	719.3	343.8	433.7	1825	3850
5787.77	0.0369	0.0	100.0	0.09	787.1	376.2	474.6	1997	4213
6347.16	0.0336	0.0	100.0	0.10	863.2	412.6	520.5	2190	4621
6937.09	0.0308	0.0	100.0	0.11	943	450.9	568.8	2393	5050
7579.07	0.0281	0.0	100.0	0.12	1031	492.6	621.5	2615	5518
8290.46	0.0257	0.0	100.0	0.13	1128	538.9	679.8	2860	6035
9059.69	0.0235	0.0	100.0	0.14	1232	588.9	742.9	3126	6595
9915.67	0.0215	0.8	99.2	0.15	1349	644.5	813.1	3421	7219
10846.83	0.0197	2.1	97.9	0.17	1475	705.0	889.4	3742	7896
11858.97	0.0180	2.9	97.1	0.18	1613	770.8	972.4	4091	8633
12938.58	0.0165	3.8	96.3	0.20	1760	841.0	1061.0	4464	9419
14241.83	0.0150	4.6	95.4	0.22	1937	925.7	1167.8	4913	10368
15535.43	0.0137	6.3	93.8	0.24	2113	1009.8	1274	5360	11310
17019.89	0.0125	7.9	92.1	0.26	2315	1106.3	1396	5872	12390
18614.24	0.0115	9.6	90.4	0.29	2532	1209.9	1526	6422	13551
20316.54	0.0105	13.3	86.7	0.31	2763	1321	1666	7009	14790
22238.60	0.0096	17.5	82.5	0.34	3024	1446	1824	7672	16190
24297.54	0.0088	22.9	77.1	0.38	3304	1579	1992	8383	17689
26578.17	0.0080	29.2	70.8	0.41	3615	1728	2179	9169	19349
29171.09	0.0073	37.9	62.1	0.45	3967	1896	2392	10064	21237
31914.39	0.0067	45.8	54.2	0.49	4340	2074	2617	11010	23234
34919.89	0.0061	53.8	46.3	0.54	4749	2270	2863	12047	25422
38222.28	0.0056	62.5	37.5	0.59	5198	2484	3134	13187	27826
41765.66	0.0051	70.8	29.2	0.65	5680	2715	3425	14409	30405
45648.37	0.0047	77.5	22.5	0.71	6208	2967	3743	15749	33232
49966.76	0.0043	86.3	13.8	0.77	6795	3248	4097	17239	36376
54587.85	0.0039	94.2	5.8	0.84	7424	3548	4476	18833	39740
59710.20	0.0036	100.0	0.0	0.92	8121	3881	4896	20600	43469

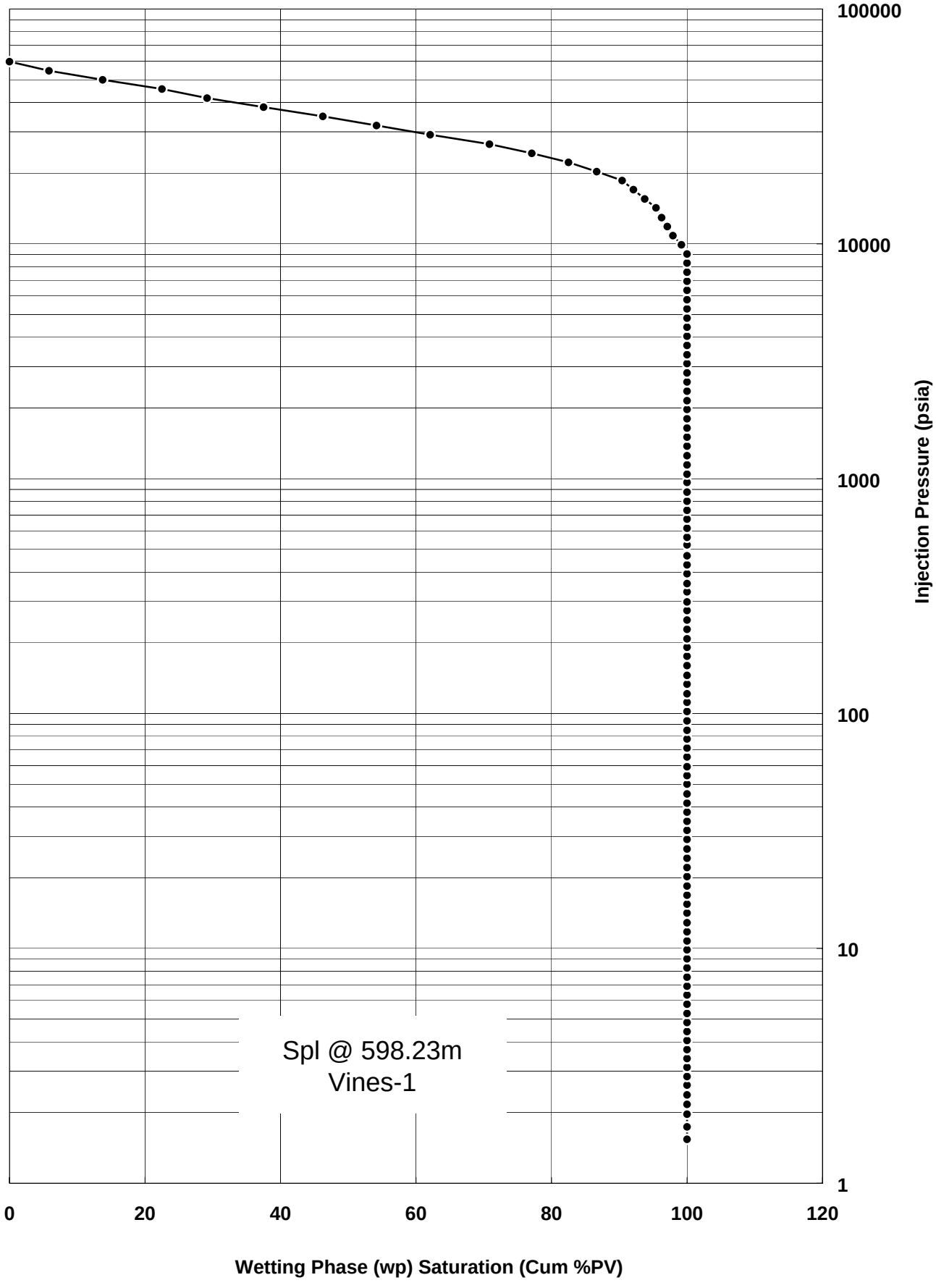
100000
10000
1000
100
10
1
Injection Pressure (psia)
0
20
40
60
80
100
120
Wetting Phase (wp) Saturation (Cum %PV)
Spl @ 598.23m
Vines-1

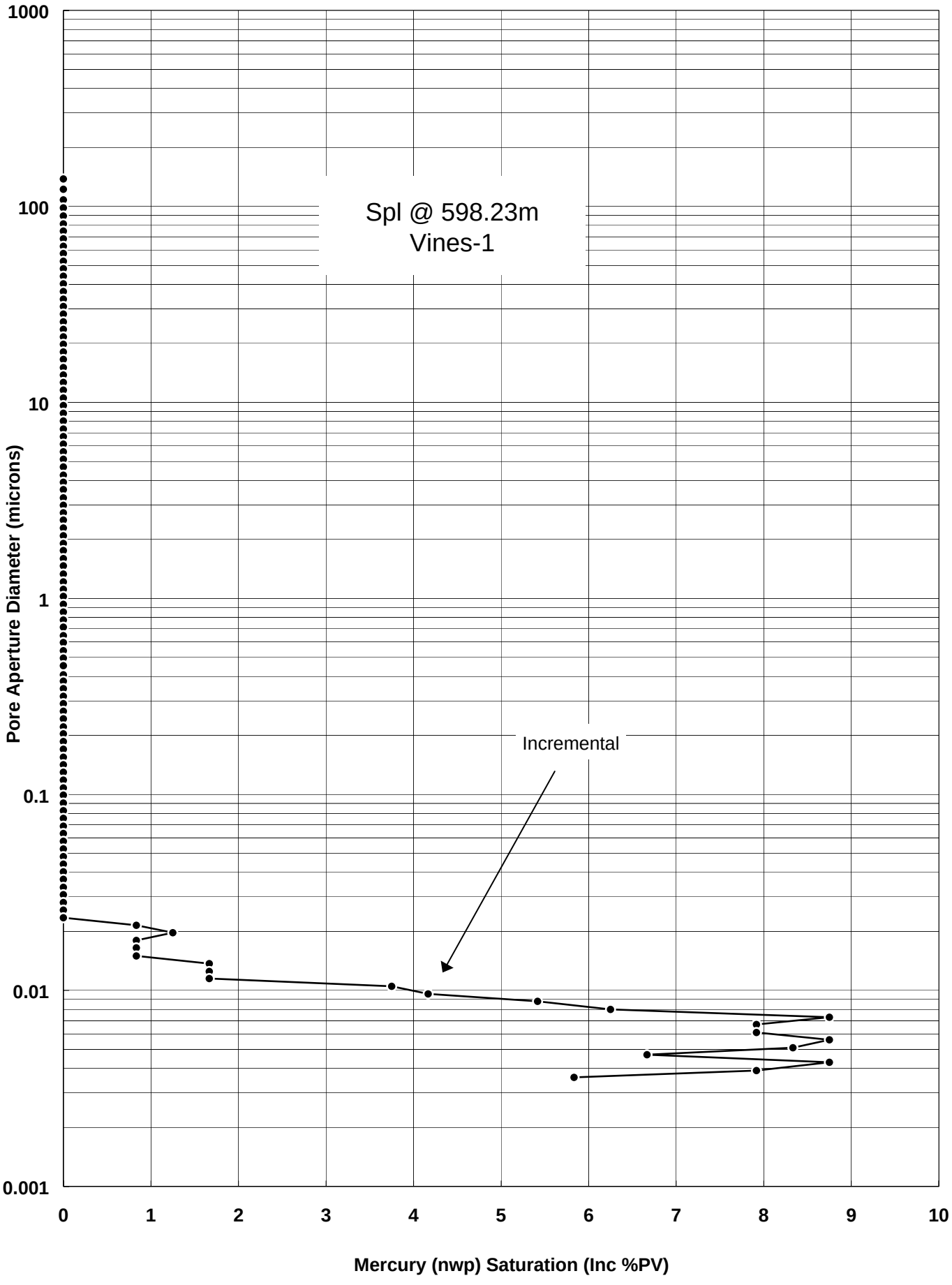
Spl @ 598.23m
Vines-1
Incremental
Pore Aperture Diameter (microns)
1000
100
10
1
0.1
0.01
0.001
0
1
2
3
4
5
6
7
8
9
10
Mercury (nwp) Saturation (Inc %PV)

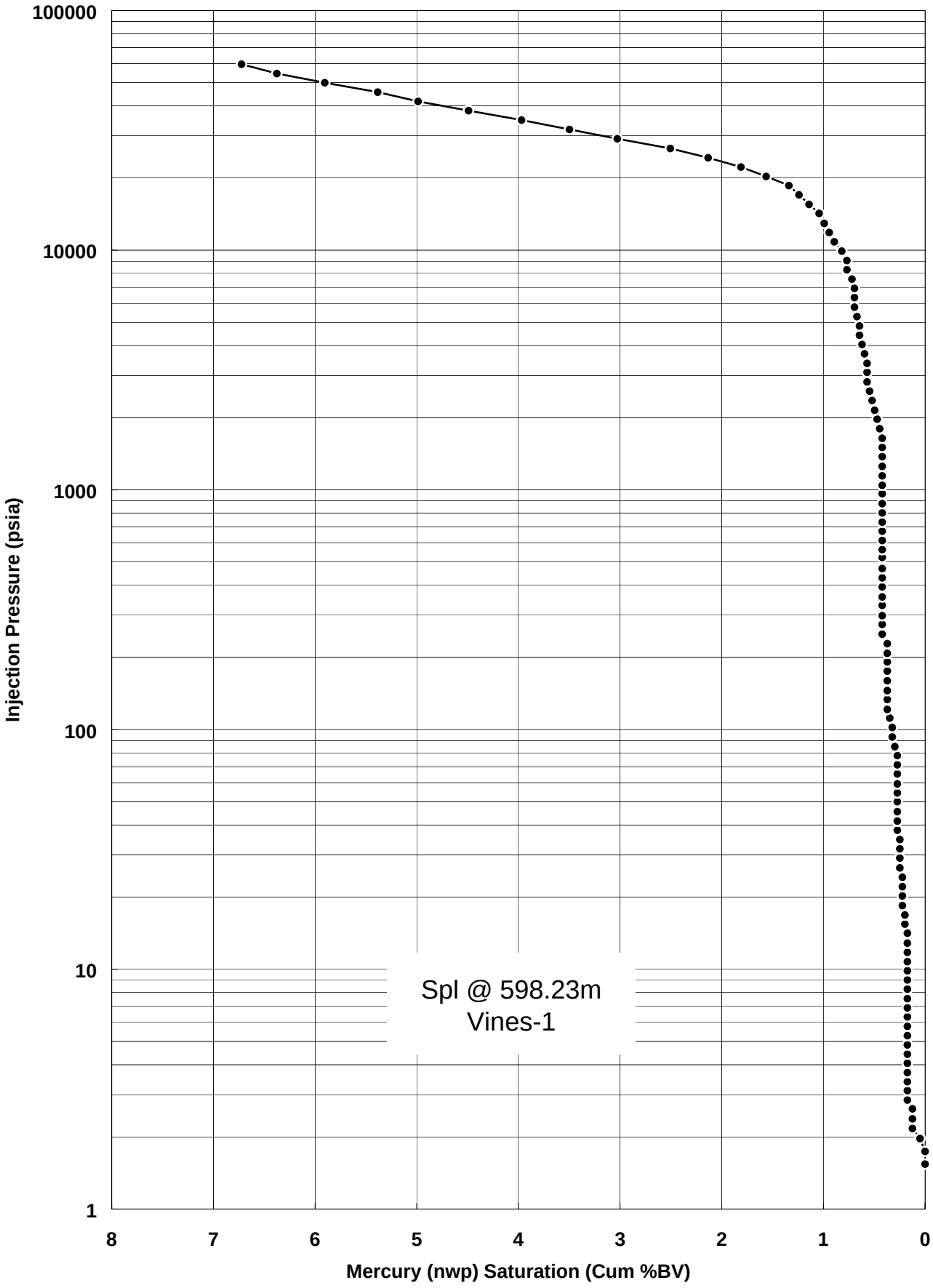
100000
10000
1000
100
10
1
Injection Pressure (psia)
8
7
6
5
4
3
2
1
0
Mercury (nwp) Saturation (Cum %BV)
Spl @ 598.23m
Vines-1

Int Pres psia	Pore Dia microns	Inc Int mL/gm	Cum Int mL/gm	Cum Int %PV(bc)	Cum Int %BV
1.55	137.454	0	0	0	0
1.76	121.1502	0	0	0.2175	0
1.97	108.4809	0.0001	0.0001	0.4859	0.029963228
2.16	98.7216	0	0.0001	0.5404	0.029963228
2.39	89.2343	0	0.0001	0.6199	0.029963228
2.62	81.4605	0	0.0001	0.6199	0.029963228
2.85	74.7218	0.0001	0.0002	0.8905	0.059926456
3.11	68.585	0	0.0002	0.8905	0.059926456
3.4	62.6619	0	0.0002	0.8905	0.059926456
3.72	57.2824	0	0.0002	0.9444	0.059926456
4.06	52.524	0	0.0002	0.9444	0.059926456
4.44	48.0393	0	0.0002	1.1084	0.059926456
4.86	43.9089	0	0.0003	1.2168	0.089889685
5.29	40.2976	0	0.0003	1.2429	0.089889685
5.8	36.7915	0	0.0003	1.2432	0.089889685
6.32	33.7349	0	0.0003	1.2699	0.089889685
6.9	30.908	0	0.0003	1.324	0.089889685
7.55	28.2392	0	0.0003	1.3781	0.089889685
8.27	25.7977	0	0.0003	1.3781	0.089889685
9.02	23.6391	0	0.0003	1.4057	0.089889685
9.88	21.5974	0	0.0003	1.5131	0.089889685
10.77	19.8032	0	0.0004	1.729	0.119852913
11.78	18.1147	0	0.0004	1.7293	0.119852913
12.86	16.5831	0	0.0004	1.7293	0.119852913
14.16	15.0682	0	0.0004	1.8103	0.119852913
15.46	13.794	0	0.0004	1.8103	0.119852913
16.84	12.6663	0	0.0004	1.8644	0.119852913
18.45	11.5642	0	0.0004	1.8914	0.119852913
20.23	10.544	0	0.0004	1.8914	0.119852913
22.12	9.6441	0	0.0004	1.9724	0.119852913
24.23	8.8051	0	0.0004	2.1075	0.119852913
26.53	8.041	0	0.0005	2.3243	0.149816141
29.1	7.3295	0.0001	0.0005	2.5908	0.149816141
32	6.667	0	0.0006	2.7049	0.179779369
34.89	6.1143	0	0.0006	2.7263	0.179779369
37.97	5.6176	0	0.0006	2.7501	0.179779369
41.52	5.1373	0	0.0006	2.7903	0.179779369
45.49	4.6892	0	0.0006	2.9181	0.179779369
49.65	4.2962	0	0.0006	2.9452	0.179779369
54.28	3.93	0	0.0006	2.9669	0.179779369
59.55	3.5824	0.0001	0.0007	3.2662	0.209742598
64.95	3.2846	0	0.0007	3.2662	0.209742598
71	3.0043	0	0.0007	3.2662	0.209742598

77.69	2.746	0	0.0007	3.2694	0.209742598
85.25	2.5023	0	0.0007	3.2694	0.209742598
93.22	2.2884	0	0.0007	3.2963	0.209742598
101.69	2.0979	0	0.0007	3.4307	0.209742598
112.1	1.903	0	0.0007	3.4307	0.209742598
121.48	1.7561	0	0.0007	3.4307	0.209742598
133.77	1.5947	0	0.0007	3.4601	0.209742598
147.34	1.4478	0	0.0008	3.6798	0.239705826
159.36	1.3386	0	0.0008	3.7016	0.239705826
175.78	1.2136	0	0.0008	3.7016	0.239705826
191.14	1.1161	0	0.0008	3.7016	0.239705826
208.25	1.0244	0	0.0008	3.782	0.239705826
228.67	0.9329	0	0.0008	3.7828	0.239705826
250.19	0.8526	0	0.0008	3.9449	0.239705826
273.18	0.7809	0	0.0008	3.9449	0.239705826
302.2	0.7059	0	0.0008	3.9449	0.239705826
330.31	0.6458	0	0.0008	3.9989	0.239705826
360.01	0.5925	0	0.0008	3.9989	0.239705826
392.03	0.5442	0	0.0008	4.0227	0.239705826
430.34	0.4957	0	0.0008	4.0253	0.239705826
468.14	0.4557	0	0.0008	4.053	0.239705826
519.13	0.4109	0	0.0008	4.053	0.239705826
567.17	0.3761	0	0.0009	4.2421	0.269669054
615.84	0.3464	0	0.0009	4.2421	0.269669054
669.99	0.3184	0	0.0009	4.2669	0.269669054
739.07	0.2886	0	0.0009	4.2669	0.269669054
802.37	0.2659	0	0.0009	4.2669	0.269669054
877.88	0.243	0	0.0009	4.3229	0.269669054
962.86	0.2216	0	0.0009	4.4314	0.269669054
1047.37	0.2037	0	0.0009	4.5393	0.269669054
1149.22	0.1856	0	0.0009	4.5393	0.269669054
1254.77	0.17	0	0.001	4.6474	0.299632282
1376.23	0.155	0	0.001	4.7555	0.299632282
1506.52	0.1416	0	0.001	4.7555	0.299632282
1648.06	0.1294	0	0.001	4.7555	0.299632282
1802.29	0.1184	0	0.001	4.7825	0.299632282
1973.07	0.1081	0	0.001	4.9714	0.299632282
2154.45	0.099	0.0001	0.0011	5.2418	0.329595511
2363.62	0.0903	0	0.0011	5.2419	0.329595511
2583.56	0.0826	0	0.0011	5.4304	0.329595511
2820.05	0.0756	0	0.0012	5.512	0.359558739
3085.69	0.0691	0	0.0012	5.6471	0.359558739
3383.52	0.063	0	0.0012	5.8625	0.359558739
3692.79	0.0578	0	0.0013	5.9987	0.389521967
4043.97	0.0528	0	0.0013	6.2145	0.389521967
4425.42	0.0482	0.0001	0.0014	6.5387	0.419485195
4837.83	0.0441	0	0.0014	6.7279	0.419485195

5312.86	0.0402	0	0.0015	6.9441	0.449448423
5795.38	0.0368	0.0001	0.0015	7.3223	0.449448423
6337.45	0.0337	0.0001	0.0016	7.5655	0.479411652
6925.45	0.0308	0.0001	0.0016	7.863	0.479411652
7582.86	0.0281	0.0001	0.0017	8.1603	0.50937488
8298.1	0.0257	0.0001	0.0018	8.5655	0.539338108
9063.46	0.0235	0.0001	0.0019	9.1596	0.569301336
9934.87	0.0215	0.0001	0.002	9.565	0.599264565
10848.67	0.0197	0.0001	0.0021	10.0791	0.629227793
11845.39	0.018	0.0001	0.0022	10.6998	0.659191021
12946.2	0.0165	0.0002	0.0024	11.5104	0.719117477
14245.58	0.015	0.0002	0.0026	12.5097	0.779043934
15552.67	0.0137	0.0002	0.0028	13.5629	0.83897039
17025.57	0.0125	0.0002	0.003	14.5096	0.898896847
18612.2	0.0115	0.0003	0.0034	16.1308	1.01874976
20306.76	0.0105	0.0005	0.0039	18.6207	1.168565901
22201.79	0.0096	0.0009	0.0048	23.1572	1.438234955
24289.61	0.0088	0.001	0.0059	28.1557	1.767830465
26597.17	0.008	0.0013	0.0072	34.5576	2.157352432
29155.38	0.0073	0.0012	0.0084	40.2867	2.516911171
31890.93	0.0067	0.0015	0.0099	47.3918	2.966359595
34900.23	0.0061	0.0015	0.0114	54.7406	3.415808018
38183.3	0.0056	0.0015	0.013	62.0109	3.89521967
41801.81	0.0051	0.0016	0.0146	69.6298	4.374631321
45576.51	0.0047	0.0013	0.0159	76.0057	4.764153288
49867.84	0.0043	0.0018	0.0177	84.7604	5.303491396
54546.71	0.0039	0.0016	0.0193	92.2441	5.782903048
59730.66	0.0036	0.0016	0.0209	100	6.2623147

Inc Int %PV(ac)	Cum Int %PV(ac)	Pore Rad microns	W.P. Sat %PV(ac)	Lev "J" Funct.	G/B Pc psia
0	0	68.727	100	2.29E-05	0.2108
0	0	60.5751	100	2.6E-05	0.23936
0	0	54.24045	100	2.91E-05	0.26792
0	0	49.3608	100	3.19E-05	0.29376
0	0	44.61715	100	3.53E-05	0.32504
0	0	40.73025	100	3.87E-05	0.35632
0	0	37.3609	100	4.21E-05	0.3876
0	0	34.2925	100	4.59E-05	0.42296
0	0	31.33095	100	5.02E-05	0.4624
0	0	28.6412	100	5.49E-05	0.50592
0	0	26.262	100	6E-05	0.55216
0	0	24.01965	100	6.56E-05	0.60384
0	0	21.95445	100	7.18E-05	0.66096
0	0	20.1488	100	7.81E-05	0.71944
0	0	18.39575	100	8.57E-05	0.7888
0	0	16.86745	100	9.34E-05	0.85952
0	0	15.454	100	0.000102	0.9384
0	0	14.1196	100	0.000112	1.0268
0	0	12.89885	100	0.000122	1.12472
0	0	11.81955	100	0.000133	1.22672
0	0	10.7987	100	0.000146	1.34368
0	0	9.9016	100	0.000159	1.46472
0	0	9.05735	100	0.000174	1.60208
0	0	8.29155	100	0.00019	1.74896
0	0	7.5341	100	0.000209	1.92576
0	0	6.897	100	0.000228	2.10256
0	0	6.33315	100	0.000249	2.29024
0	0	5.7821	100	0.000273	2.5092
0	0	5.272	100	0.000299	2.75128
0	0	4.82205	100	0.000327	3.00832
0	0	4.40255	100	0.000358	3.29528
0	0	4.0205	100	0.000392	3.60808
0	0	3.66475	100	0.00043	3.9576
0	0	3.3335	100	0.000473	4.352
0	0	3.05715	100	0.000515	4.74504
0	0	2.8088	100	0.000561	5.16392
0	0	2.56865	100	0.000613	5.64672
0	0	2.3446	100	0.000672	6.18664
0	0	2.1481	100	0.000733	6.7524
0	0	1.965	100	0.000802	7.38208
0	0	1.7912	100	0.00088	8.0988
0	0	1.6423	100	0.000959	8.8332
0	0	1.50215	100	0.001049	9.656

0	0	1.373	100	0.001148	10.56584
0	0	1.25115	100	0.001259	11.594
0	0	1.1442	100	0.001377	12.67792
0	0	1.04895	100	0.001502	13.82984
0	0	0.9515	100	0.001656	15.2456
0	0	0.87805	100	0.001794	16.52128
0	0	0.79735	100	0.001976	18.19272
0	0	0.7239	100	0.002176	20.03824
0	0	0.6693	100	0.002354	21.67296
0	0	0.6068	100	0.002596	23.90608
0	0	0.55805	100	0.002823	25.99504
0	0	0.5122	100	0.003076	28.322
0	0	0.46645	100	0.003378	31.09912
0	0	0.4263	100	0.003695	34.02584
0	0	0.39045	100	0.004035	37.15248
0	0	0.35295	100	0.004464	41.0992
0	0	0.3229	100	0.004879	44.92216
0	0	0.29625	100	0.005318	48.96136
0	0	0.2721	100	0.005791	53.31608
0	0	0.24785	100	0.006356	58.52624
0	0	0.22785	100	0.006915	63.66704
0	0	0.20545	100	0.007668	70.60168
0	0	0.18805	100	0.008377	77.13512
0	0	0.1732	100	0.009096	83.75424
0	0	0.1592	100	0.009896	91.11864
0	0	0.1443	100	0.010917	100.5135
0	0	0.13295	100	0.011852	109.1223
0	0	0.1215	100	0.012967	119.3917
0	0	0.1108	100	0.014222	130.949
0	0	0.10185	100	0.01547	142.4423
0	0	0.0928	100	0.016975	156.2939
0	0	0.085	100	0.018534	170.6487
0	0	0.0775	100	0.020328	187.1673
0	0	0.0708	100	0.022252	204.8867
0	0	0.0647	100	0.024343	224.1362
0	0	0.0592	100	0.026621	245.1114
0	0	0.05405	100	0.029143	268.3375
0	0	0.0495	100	0.031823	293.0052
0	0	0.04515	100	0.034912	321.4523
0	0	0.0413	100	0.038161	351.3642
0	0	0.0378	100	0.041654	383.5268
0	0	0.03455	100	0.045578	419.6538
0	0	0.0315	100	0.049977	460.1587
0	0	0.0289	100	0.054545	502.2194
0	0	0.0264	100	0.059732	549.9799
0	0	0.0241	100	0.065366	601.8571
0	0	0.02205	100	0.071458	657.9449

0	0	0.0201	100	0.078474	722.549
0	0	0.0184	100	0.085601	788.1717
0	0	0.01685	100	0.093608	861.8932
0	0	0.0154	100	0.102293	941.8612
0	0	0.01405	100	0.112004	1031.269
0	0	0.01285	100	0.122568	1128.542
0	0	0.01175	100	0.133873	1232.631
0	0	0.01075	100	0.146744	1351.142
0	0	0.00985	100	0.160242	1475.419
0	0	0.009	100	0.174964	1610.973
1.069518717	1.069518717	0.00825	98.93048128	0.191223	1760.683
1.069518717	2.139037433	0.0075	97.86096257	0.210416	1937.399
1.069518717	3.20855615	0.00685	96.79144385	0.229723	2115.163
1.069518717	4.278074866	0.00625	95.72192513	0.251478	2315.478
2.139037433	6.417112299	0.00575	93.5828877	0.274914	2531.259
2.673796791	9.090909091	0.00525	90.90909091	0.299944	2761.719
4.812834225	13.90374332	0.0048	86.09625668	0.327934	3019.443
5.882352941	19.78609626	0.0044	80.21390374	0.358773	3303.387
6.951871658	26.73796791	0.004	73.26203209	0.392857	3617.215
6.417112299	33.15508021	0.00365	66.84491979	0.430643	3965.132
8.021390374	41.17647059	0.00335	58.82352941	0.471049	4337.166
8.021390374	49.19786096	0.00305	50.80213904	0.515498	4746.431
8.556149733	57.7540107	0.0028	42.2459893	0.563991	5192.929
8.556149733	66.31016043	0.00255	33.68983957	0.617439	5685.046
6.951871658	73.26203209	0.00235	26.73796791	0.673193	6198.405
9.625668449	82.88770053	0.00215	17.11229947	0.736579	6782.026
8.556149733	91.44385027	0.00195	8.556149733	0.805689	7418.353
8.556149733	100	0.0018	0	0.882259	8123.37

G/O Pc psia	O/B Pc psia	Ht FWL,ft G/B	Ht FWL,ft O/B	Swanson's Sb/Pc(ac)
0.10075	0.1271	0.53475	1.1284	-0.42528453
0.1144	0.14432	0.6072	1.28128	-0.37454035
0.12805	0.16154	0.67965	1.43416	-0.31940497
0.1404	0.17712	0.7452	1.57248	-0.29130916
0.15535	0.19598	0.82455	1.73992	-0.26327523
0.1703	0.21484	0.9039	1.90736	-0.24016328
0.18525	0.2337	0.98325	2.0748	-0.21026827
0.20215	0.25502	1.07295	2.26408	-0.19268957
0.221	0.2788	1.173	2.4752	-0.17625428
0.2418	0.30504	1.2834	2.70816	-0.16109262
0.2639	0.33292	1.4007	2.95568	-0.14760211
0.2886	0.36408	1.5318	3.23232	-0.1349695
0.3159	0.39852	1.6767	3.53808	-0.11714019
0.34385	0.43378	1.82505	3.85112	-0.1076184
0.377	0.4756	2.001	4.2224	-0.0981554
0.4108	0.51824	2.1804	4.60096	-0.09007933
0.4485	0.5658	2.3805	5.0232	-0.08250744
0.49075	0.6191	2.60475	5.4964	-0.07540415
0.53755	0.67814	2.85315	6.02056	-0.06883934
0.5863	0.73964	3.1119	6.56656	-0.06311545
0.6422	0.81016	3.4086	7.19264	-0.05762159
0.70005	0.88314	3.71565	7.84056	-0.05007782
0.7657	0.96596	4.0641	8.57584	-0.04578422
0.8359	1.05452	4.4367	9.36208	-0.0419392
0.9204	1.16112	4.8852	10.30848	-0.03808885
1.0049	1.26772	5.3337	11.25488	-0.03488604
1.0946	1.38088	5.8098	12.25952	-0.0320272
1.19925	1.5129	6.36525	13.4316	-0.02923242
1.31495	1.65886	6.97935	14.72744	-0.02666031
1.4378	1.81384	7.6314	16.10336	-0.02438237
1.57495	1.98686	8.35935	17.63944	-0.0222591
1.72445	2.17546	9.15285	19.31384	-0.01919996
1.8915	2.3862	10.0395	21.1848	-0.01750429
2.08	2.624	11.04	23.296	-0.01498161
2.26785	2.86098	12.03705	25.39992	-0.01374066
2.46805	3.11354	13.09965	27.64216	-0.01262606
2.6988	3.40464	14.3244	30.22656	-0.01154652
2.95685	3.73018	15.69405	33.11672	-0.01053884
3.22725	4.0713	17.12925	36.1452	-0.00965582
3.5282	4.45096	18.7266	39.51584	-0.0088322
3.87075	4.8831	20.54475	43.3524	-0.00754741
4.22175	5.3259	22.40775	47.2836	-0.00691991
4.615	5.822	24.495	51.688	-0.00633026

5.04985	6.37058	26.80305	56.55832	-0.00578515
5.54125	6.9905	29.41125	62.062	-0.00527212
6.0593	7.64404	32.1609	67.86416	-0.00482137
6.60985	8.33858	35.08305	74.03032	-0.00441979
7.2865	9.1922	38.6745	81.6088	-0.00400935
7.8962	9.96136	41.9106	88.43744	-0.00369977
8.69505	10.96914	46.15065	97.38456	-0.00335986
9.5771	12.08188	50.8323	107.2635	-0.00284706
10.3584	13.06752	54.9792	116.0141	-0.00263231
11.4257	14.41396	60.6441	127.9678	-0.00238642
12.4241	15.67348	65.9433	139.1499	-0.00219465
13.53625	17.0765	71.84625	151.606	-0.00201433
14.86355	18.75094	78.89115	166.4718	-0.00183446
16.26235	20.51558	86.31555	182.1383	-0.00167667
17.7567	22.40076	94.2471	198.875	-0.00153556
19.643	24.7804	104.259	220.0016	-0.0013881
21.47015	27.08542	113.957	240.4657	-0.00126997
23.40065	29.52082	124.2035	262.0873	-0.0011652
25.48195	32.14646	135.2504	285.3978	-0.00107003
27.9721	35.28788	148.4673	313.2875	-0.00097478
30.4291	38.38748	161.5083	340.8059	-0.00089607
33.74345	42.56866	179.0999	377.9266	-0.00080805
36.86605	46.50794	195.6737	412.8998	-0.00068678
40.0296	50.49888	212.4648	448.3315	-0.00063251
43.54935	54.93918	231.1466	487.7527	-0.00058138
48.03955	60.60374	254.9792	538.043	-0.00052704
52.15405	65.79434	276.8177	584.1254	-0.00048546
57.0622	71.98616	302.8686	639.0966	-0.00044371
62.5859	78.95452	332.1867	700.9621	-0.00040455
68.07905	85.88434	361.3427	762.4854	-0.0003719
74.6993	94.23604	396.4809	836.6322	-0.00033894
81.56005	102.8911	432.8957	913.4726	-0.00028655
89.45495	112.8509	474.7994	1001.895	-0.00026126
97.9238	123.5346	519.7494	1096.747	-0.00023867
107.1239	135.1409	568.5807	1199.788	-0.00021817
117.1489	147.7878	621.7901	1312.067	-0.0001995
128.2496	161.7917	680.7092	1436.395	-0.00018223
140.0393	176.6649	743.2853	1568.44	-0.00015298
153.6353	193.8168	815.4489	1720.715	-0.00013945
167.9314	211.8519	891.3282	1880.832	-0.00012757
183.3033	231.2441	972.9173	2052.996	-0.00010625
200.5699	253.0266	1064.563	2246.382	-9.7104E-05
219.9288	277.4486	1167.314	2463.203	-8.8556E-05
240.0314	302.8088	1274.013	2688.351	-7.3026E-05
262.8581	331.6055	1395.17	2944.01	-6.6684E-05
287.6523	362.8844	1526.77	3221.706	-5.4166E-05
314.459	396.7021	1669.051	3521.94	-4.9548E-05

345.3359	435.6545	1832.937	3867.762	-3.9478E-05
376.6997	475.2212	1999.406	4219.037	-3.6191E-05
411.9343	519.6709	2186.42	4613.664	-2.8368E-05
450.1543	567.8869	2389.28	5041.728	-2.5959E-05
492.8859	621.7945	2616.087	5520.322	-1.9757E-05
539.3765	680.4442	2862.845	6041.017	-1.4443E-05
589.1249	743.2037	3126.894	6598.199	-9.9178E-06
645.7666	814.6593	3427.53	7232.585	-6.0319E-06
705.1636	889.5909	3742.791	7897.832	-2.7619E-06
769.9504	971.322	4086.66	8623.444	0
841.503	1061.588	4466.439	9424.834	4.6289E-06
925.9627	1168.138	4914.725	10370.78	8.4133E-06
1010.924	1275.319	5365.671	11322.34	1.1559E-05
1106.662	1396.097	5873.822	12394.61	1.4079E-05
1209.793	1526.2	6421.209	13549.68	1.9318E-05
1319.939	1665.154	7005.832	14783.32	2.5084E-05
1443.116	1820.547	7659.618	16162.9	3.5089E-05
1578.825	1991.748	8379.915	17682.84	4.5643E-05
1728.816	2180.968	9176.024	19362.74	5.6328E-05
1895.1	2390.741	10058.61	21225.12	6.3718E-05
2072.91	2615.056	11002.37	23216.6	7.2346E-05
2268.515	2861.819	12040.58	25407.37	7.8986E-05
2481.915	3131.031	13173.24	27797.44	8.475E-05
2717.118	3427.748	14421.62	30431.72	8.8882E-05
2962.473	3737.274	15723.9	33179.7	9.0067E-05
3241.41	4089.163	17204.4	36303.79	9.3132E-05
3545.536	4472.83	18818.61	39710	9.3933E-05
3882.493	4897.914	20607.08	43483.92	9.3806E-05
				9.3933E-05

AIR\MERCURY CAPILLARY PRESSURE DATA : BY GEOTECH

Spl @ 644.00m Vines-1

Bulk Volume = 7.8049cc
Closure @ 11845. psia
Pore Volume = 0.4373cc
Porosity = 5.60%
Median Pore Aperture = 0.0061 microns (dia.)

Injection Pressure (psia)	Pore Diameter (microns)	Hg (nwp) Saturation cum%PV	100-Hg(wp) Saturation cum%PV	Leverett "J" Function	Gas/Brine Pc (psia)	Gas/Oil Pc (psia)	Oil/Brine Pc (psia)	Ht. Above Free Water (ft.) Gas/Brine	Ht. Above Free Water (ft.) Oil/Brine
1.55	137.45	0.0	100.0	0.00	0.21	0.10	0.13	0.5	1.1
1.76	121.15	0.0	100.0	0.00	0.24	0.11	0.14	0.6	1.3
1.97	108.48	0.0	100.0	0.00	0.27	0.13	0.16	0.7	1.4
2.16	98.72	0.0	100.0	0.00	0.29	0.14	0.18	0.7	1.6
2.39	89.23	0.0	100.0	0.00	0.33	0.16	0.20	0.8	1.7
2.62	81.46	0.0	100.0	0.00	0.36	0.17	0.21	0.9	1.9
2.85	74.72	0.0	100.0	0.00	0.39	0.19	0.23	1.0	2.1
3.11	68.59	0.0	100.0	0.00	0.42	0.20	0.26	1.1	2.3
3.40	62.66	0.0	100.0	0.00	0.46	0.22	0.28	1.2	2.5
3.72	57.28	0.0	100.0	0.00	0.51	0.24	0.31	1.3	2.7
4.06	52.52	0.0	100.0	0.00	0.55	0.26	0.33	1.4	3.0
4.44	48.04	0.0	100.0	0.00	0.60	0.29	0.36	1.5	3.2
4.86	43.91	0.0	100.0	0.00	0.66	0.32	0.40	1.7	3.5
5.29	40.30	0.0	100.0	0.00	0.72	0.34	0.43	1.8	3.9
5.80	36.79	0.0	100.0	0.00	0.79	0.38	0.48	2.0	4.2
6.32	33.73	0.0	100.0	0.00	0.86	0.41	0.52	2.2	4.6
6.90	30.91	0.0	100.0	0.00	0.94	0.45	0.57	2.4	5.0
7.55	28.24	0.0	100.0	0.00	1.03	0.49	0.62	2.6	5.5
8.27	25.80	0.0	100.0	0.00	1.12	0.54	0.68	2.9	6.0
9.02	23.64	0.0	100.0	0.00	1.23	0.59	0.74	3.1	6.6
9.88	21.60	0.0	100.0	0.00	1.34	0.64	0.81	3.4	7.2
10.77	19.80	0.0	100.0	0.00	1.46	0.70	0.88	3.7	7.8
11.78	18.11	0.0	100.0	0.00	1.60	0.77	0.97	4.1	8.6
12.86	16.58	0.0	100.0	0.00	1.75	0.84	1.05	4.4	9.4
14.16	15.07	0.0	100.0	0.00	1.93	0.92	1.16	4.9	10.3
15.46	13.79	0.0	100.0	0.00	2.10	1.00	1.27	5.3	11.3
16.84	12.67	0.0	100.0	0.00	2.29	1.09	1.38	5.8	12.3
18.45	11.56	0.0	100.0	0.00	2.51	1.20	1.51	6.4	13.4
20.23	10.54	0.0	100.0	0.00	2.75	1.31	1.66	7.0	14.7
22.12	9.644	0.0	100.0	0.00	3.01	1.44	1.81	7.6	16.1
24.23	8.805	0.0	100.0	0.00	3.30	1.57	1.99	8.4	17.6
26.53	8.041	0.0	100.0	0.00	3.61	1.72	2.18	9.2	19.3
29.10	7.330	0.0	100.0	0.00	3.96	1.89	2.39	10.0	21.2
32.00	6.667	0.0	100.0	0.00	4.35	2.08	2.62	11.0	23.3
34.89	6.114	0.0	100.0	0.00	4.75	2.27	2.86	12.0	25.4

AIR\MERCURY CAPILLARY PRESSURE DATA : BY GEOTECH

Spl @ 644.00m Vines-1

Injection Pressure (psia)	Pore Diameter (microns)	Hg (nwp) Saturation cum%PV	100-Hg(wp) Saturation cum%PV	Leverett "J" Function	Gas/Brine Pc (psia)	Gas/Oil Pc (psia)	Oil/Brine Pc (psia)	Ht. Above Free Water (ft.) Gas/Brine	Ht. Above Free Water (ft.) Oil/Brine
37.97	5.618	0.0	100.0	0.00	5.16	2.47	3.11	13.1	27.6
41.52	5.137	0.0	100.0	0.00	5.65	2.70	3.40	14.3	30.2
45.49	4.689	0.0	100.0	0.00	6.19	2.96	3.73	15.7	33.1
49.65	4.296	0.0	100.0	0.00	6.75	3.23	4.07	17.1	36.1
54.28	3.930	0.0	100.0	0.00	7.38	3.53	4.45	18.7	39.5
59.55	3.582	0.0	100.0	0.00	8.10	3.87	4.88	20.5	43.4
64.95	3.285	0.0	100.0	0.00	8.83	4.22	5.33	22.4	47.3
71.00	3.004	0.0	100.0	0.00	9.66	4.62	5.82	24.5	51.7
77.69	2.746	0.0	100.0	0.00	10.57	5.05	6.37	26.8	56.6
85.25	2.502	0.0	100.0	0.00	11.59	5.54	6.99	29.4	62.1
93.22	2.288	0.0	100.0	0.00	12.68	6.06	7.64	32.2	67.9
101.69	2.098	0.0	100.0	0.00	13.83	6.61	8.34	35.1	74.0
112.10	1.903	0.0	100.0	0.00	15.25	7.29	9.19	38.7	81.6
121.48	1.756	0.0	100.0	0.00	16.52	7.90	9.96	41.9	88.4
133.77	1.595	0.0	100.0	0.00	18.19	8.70	10.97	46.2	97.4
147.34	1.448	0.0	100.0	0.00	20.04	9.58	12.08	50.8	107.3
159.36	1.339	0.0	100.0	0.00	21.67	10.36	13.07	55.0	116.0
175.78	1.214	0.0	100.0	0.00	23.91	11.43	14.41	60.6	128
191.14	1.116	0.0	100.0	0.00	26.00	12.42	15.67	65.9	139
208.25	1.024	0.0	100.0	0.00	28.32	13.54	17.08	71.8	152
228.67	0.933	0.0	100.0	0.00	31.10	14.86	18.75	78.9	166
250.19	0.853	0.0	100.0	0.00	34.03	16.26	20.52	86.3	182
273.18	0.781	0.0	100.0	0.00	37.15	17.76	22.40	94	199
302.20	0.706	0.0	100.0	0.00	41.10	19.64	24.78	104	220
330.31	0.646	0.0	100.0	0.00	44.92	21.47	27.09	114	240
360.01	0.593	0.0	100.0	0.01	48.96	23.40	29.52	124	262
392.03	0.544	0.0	100.0	0.01	53.32	25.48	32.15	135	285
430.34	0.496	0.0	100.0	0.01	58.53	27.97	35.29	148	313
468.14	0.456	0.0	100.0	0.01	63.67	30.43	38.39	162	341
519.13	0.411	0.0	100.0	0.01	70.60	33.74	42.57	179	378
567.17	0.376	0.0	100.0	0.01	77.14	36.87	46.51	196	413
615.84	0.346	0.0	100.0	0.01	83.75	40.03	50.50	212	448
669.99	0.318	0.0	100.0	0.01	91.12	43.55	54.94	231	488
739.07	0.289	0.0	100.0	0.01	100.51	48.04	60.60	255	538
802.37	0.266	0.0	100.0	0.01	109.12	52.15	65.79	277	584
877.88	0.243	0.0	100.0	0.01	119.39	57.06	71.99	303	639
962.86	0.222	0.0	100.0	0.01	130.95	62.59	78.95	332	701
1047.37	0.204	0.0	100.0	0.02	142.44	68.08	85.88	361	762
1149.22	0.186	0.0	100.0	0.02	156.29	74.70	94.24	396	837
1254.77	0.170	0.0	100.0	0.02	170.65	81.56	102.89	433	913
1376.23	0.155	0.0	100.0	0.02	187.17	89.45	112.85	475	1002
1506.52	0.142	0.0	100.0	0.02	204.89	97.92	123.53	520	1097
1648.06	0.129	0.0	100.0	0.02	224.14	107.12	135.14	569	1200

AIR\MERCURY CAPILLARY PRESSURE DATA : BY GEOTECH

Spl @ 644.00m Vines-1

Injection Pressure (psia)	Pore Diameter (microns)	Hg (nwp) Saturation cum%PV	100-Hg(wp) Saturation cum%PV	Leverett "J" Function	Gas/Brine Pc (psia)	Gas/Oil Pc (psia)	Oil/Brine Pc (psia)	Ht. Above Free Water (ft.) Gas/Brine	Ht. Above Free Water (ft.) Oil/Brine
1802.29	0.118	0.0	100.0	0.03	245.11	117.15	147.79	622	1312
1973.07	0.108	0.0	100.0	0.03	268.34	128.25	161.79	681	1436
2154.45	0.0990	0.0	100.0	0.03	293.01	140.04	176.66	743	1568
2363.62	0.0903	0.0	100.0	0.03	321.45	153.64	193.82	815	1721
2583.56	0.0826	0.0	100.0	0.04	351.36	167.93	211.85	891	1881
2820.05	0.0756	0.0	100.0	0.04	383.53	183.30	231.24	973	2053
3085.69	0.0691	0.0	100.0	0.05	419.65	200.57	253.03	1065	2246
3383.52	0.0630	0.0	100.0	0.05	460.16	219.93	277.45	1167	2463
3692.79	0.0578	0.0	100.0	0.05	502.22	240.03	302.81	1274	2688
4043.97	0.0528	0.0	100.0	0.06	549.98	262.86	331.61	1395	2944
4425.42	0.0482	0.0	100.0	0.07	601.86	287.65	362.88	1527	3222
4837.83	0.0441	0.0	100.0	0.07	657.94	314.46	396.70	1669	3522
5312.86	0.0402	0.0	100.0	0.08	722.55	345.34	435.65	1833	3868
5795.38	0.0368	0.0	100.0	0.09	788.17	376.70	475.22	1999	4219
6337.45	0.0337	0.0	100.0	0.09	861.89	411.93	519.67	2186	4614
6925.45	0.0308	0.0	100.0	0.10	941.86	450.15	567.89	2389	5042
7582.86	0.0281	0.0	100.0	0.11	1031.27	492.89	621.79	2616	5520
8298.10	0.0257	0.0	100.0	0.12	1128.54	539.38	680.44	2863	6041
9063.46	0.0235	0.0	100.0	0.13	1232.63	589.12	743.20	3127	6598
9934.87	0.0215	0.0	100.0	0.15	1351.14	645.77	814.66	3428	7233
10848.67	0.0197	0.0	100.0	0.16	1475.42	705.16	889.59	3743	7898
11845.39	0.0180	0.0	100.0	0.17	1610.97	769.95	971.32	4087	8623
12946.20	0.0165	1.1	98.9	0.19	1760.68	841.50	1061.59	4466	9425
14245.58	0.0150	2.1	97.9	0.21	1937.40	925.96	1168.14	4915	10371
15552.67	0.0137	3.2	96.8	0.23	2115.16	1010.92	1275.32	5366	11322
17025.57	0.0125	4.3	95.7	0.25	2315.48	1106.66	1396.10	5874	12395
18612.20	0.0115	6.4	93.6	0.27	2531.26	1209.79	1526.20	6421	13550
20306.76	0.0105	9.1	90.9	0.30	2761.72	1319.94	1665.15	7006	14783
22201.79	0.0096	13.9	86.1	0.33	3019.44	1443.12	1820.55	7660	16163
24289.61	0.0088	19.8	80.2	0.36	3303.39	1578.82	1991.75	8380	17683
26597.17	0.0080	26.7	73.3	0.39	3617.22	1728.82	2180.97	9176	19363
29155.38	0.0073	33.2	66.8	0.43	3965.13	1895.10	2390.74	10059	21225
31890.93	0.0067	41.2	58.8	0.47	4337.17	2072.91	2615.06	11002	23217
34900.23	0.0061	49.2	50.8	0.52	4746.43	2268.51	2861.82	12041	25407
38183.30	0.0056	57.8	42.2	0.56	5192.93	2481.91	3131.03	13173	27797
41801.81	0.0051	66.3	33.7	0.62	5685.05	2717.12	3427.75	14422	30432
45576.51	0.0047	73.3	26.7	0.67	6198.41	2962.47	3737.27	15724	33180
49867.84	0.0043	82.9	17.1	0.74	6782.03	3241.41	4089.16	17204	36304
54546.71	0.0039	91.4	8.6	0.81	7418.35	3545.54	4472.83	18819	39710
59730.66	0.0036	100.0	0.0	0.88	8123.37	3882.49	4897.91	20607	43484

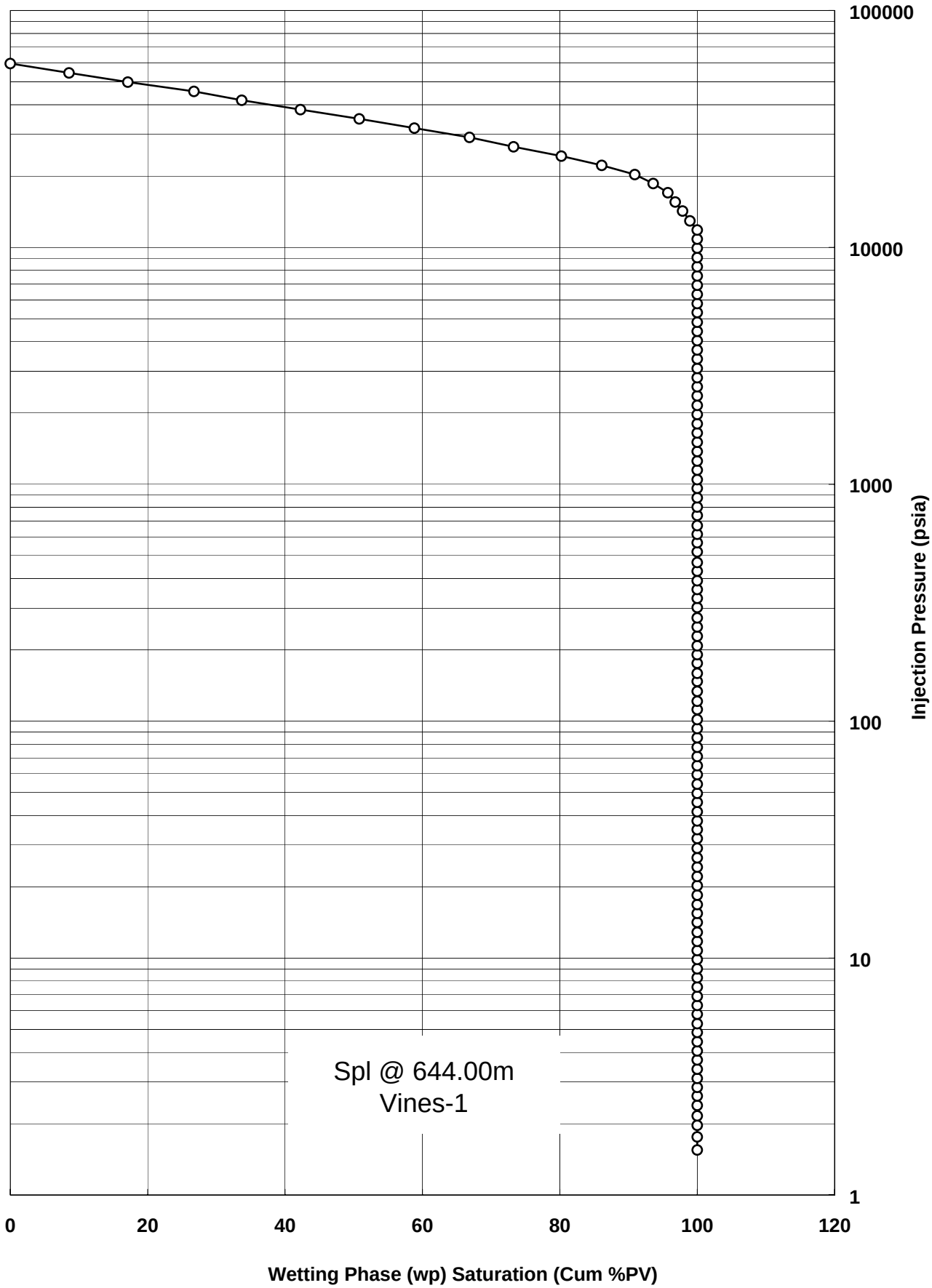
100000
10000
1000
100
10
1
Injection Pressure (psia)
0
20
40
60
80
100
120
Wetting Phase (wp) Saturation (Cum %PV)
Spl @ 644.00m
Vines-1

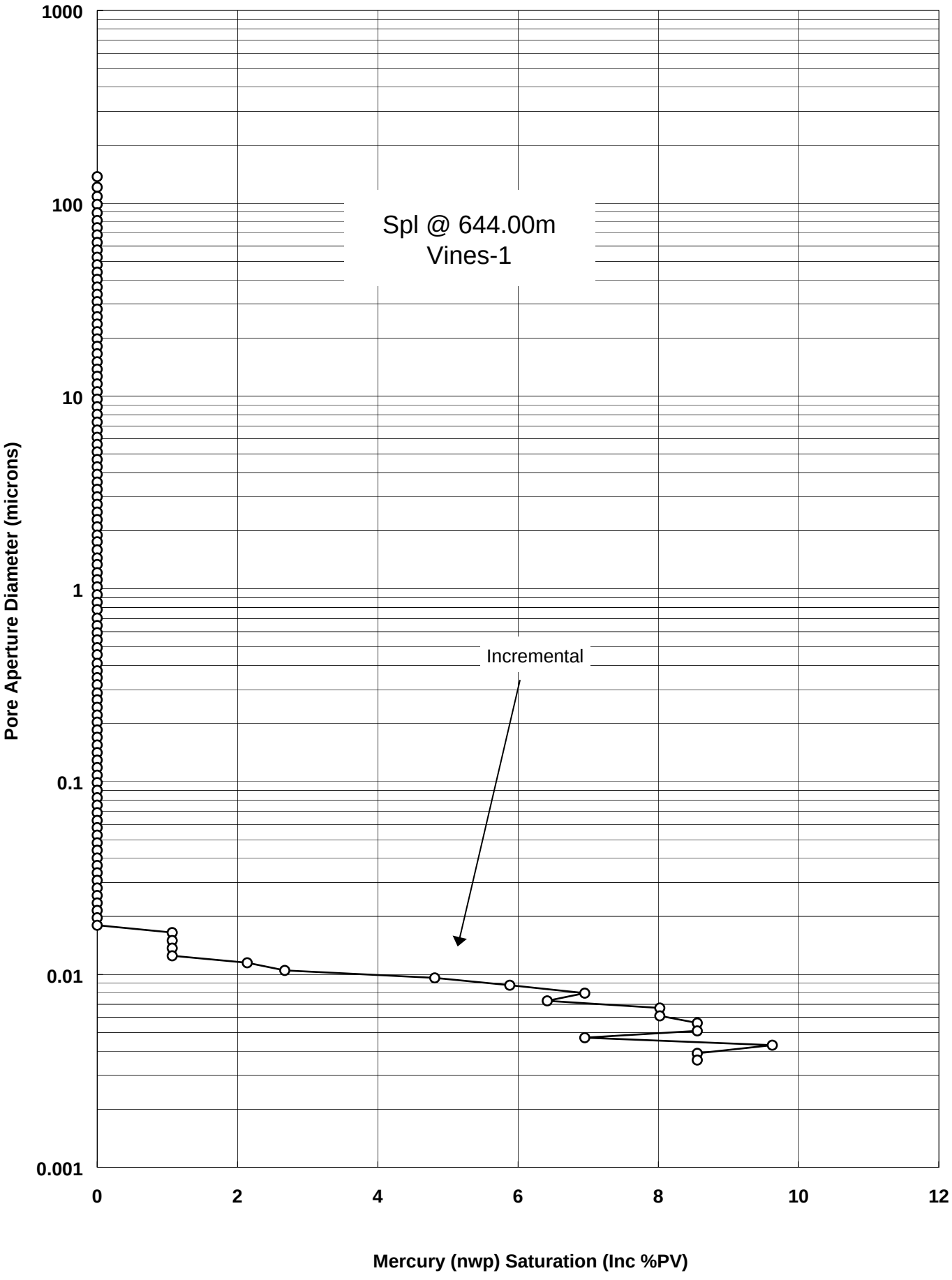
Spl @ 644.00m
Vines-1
Incremental
Pore Aperture Diameter (microns)
1000
100
10
1
0.1
0.01
0.001
0
2
4
6
8
10
12
Mercury (nwp) Saturation (Inc %PV)

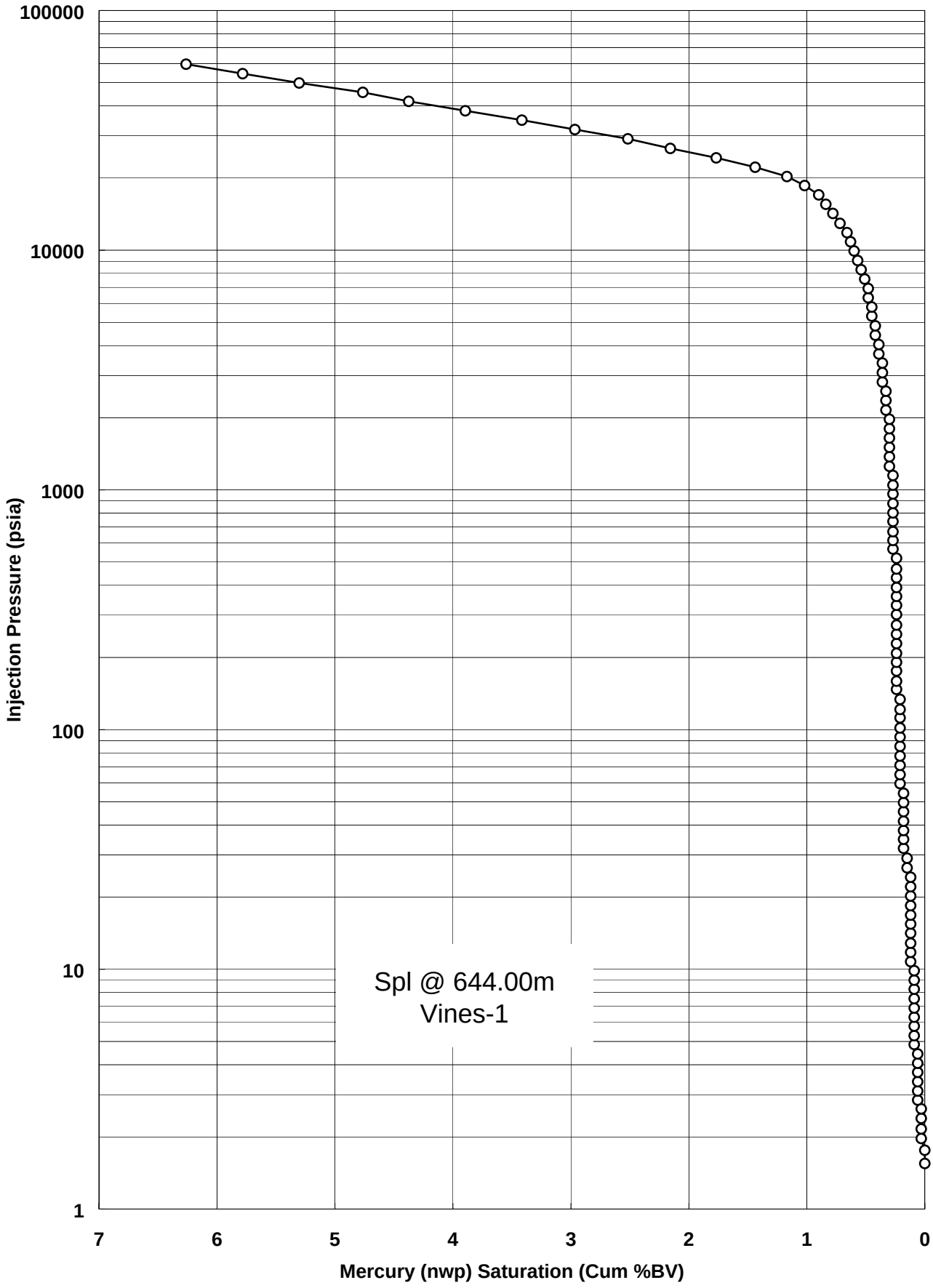
100000
10000
1000
100
10
1
Injection Pressure (psia)
7
6
5
4
3
2
1
0
Mercury (nwp) Saturation (Cum %BV)
Spl @ 644.00m
Vines-1

Int Pres psia	Pore Dia microns	Inc Int mL/gm	Cum Int mL/gm	Cum Int %PV(bc)	Cum Int %BV
1.54	138.3131	0	0	0	0
1.74	122.3784	0.0001	0.0001	0.957	0.026129792
1.96	108.8365	0.0002	0.0003	2.938	0.078389377
2.16	98.575	0.0001	0.0004	3.5321	0.104519169
2.37	89.9597	0	0.0004	3.5321	0.104519169
2.6	82.0139	0	0.0004	3.5321	0.104519169
2.86	74.6797	0	0.0004	3.71	0.104519169
3.12	68.3731	0.0001	0.0005	4.4668	0.130648961
3.4	62.6915	0.0001	0.0006	4.9275	0.156778753
3.73	57.2577	0.0001	0.0007	5.8483	0.182908546
4.07	52.4203	0	0.0007	5.8483	0.182908546
4.44	48.0915	0	0.0007	5.8483	0.182908546
4.84	44.0839	0	0.0007	5.8483	0.182908546
5.29	40.3588	0	0.0007	5.8483	0.182908546
5.79	36.8426	0	0.0007	5.8483	0.182908546
6.33	33.7007	0	0.0007	6.1378	0.182908546
6.91	30.8936	0	0.0007	6.1378	0.182908546
7.55	28.2572	0	0.0007	6.1378	0.182908546
8.26	25.8378	0	0.0007	6.1378	0.182908546
9.04	23.597	0	0.0007	6.1378	0.182908546
9.88	21.5938	0	0.0007	6.1378	0.182908546
10.77	19.8003	0	0.0007	6.1378	0.182908546
11.77	18.127	0	0.0007	6.1378	0.182908546
12.86	16.5851	0	0.0007	6.1378	0.182908546
14.17	15.0528	0	0.0007	6.1378	0.182908546
15.45	13.8054	0	0.0007	6.1378	0.182908546
16.84	12.6663	0	0.0007	6.2536	0.182908546
18.45	11.5632	0	0.0007	6.2536	0.182908546
20.24	10.5398	0	0.0007	6.2536	0.182908546
22.13	9.6413	0	0.0007	6.2536	0.182908546
24.22	8.8086	0	0.0007	6.2536	0.182908546
26.53	8.0405	0	0.0008	6.4272	0.209038338
29.12	7.3262	0	0.0008	6.4272	0.209038338
32.59	6.5462	0	0.0008	6.4272	0.209038338
36.19	5.8952	0	0.0008	6.4272	0.209038338
38.6	5.527	0	0.0008	6.4272	0.209038338
41.7	5.1159	0	0.0008	6.4272	0.209038338
45.44	4.6946	0	0.0008	6.4272	0.209038338
50.48	4.2256	0	0.0008	6.4272	0.209038338
54.82	3.8913	0	0.0008	6.4272	0.209038338
59.32	3.5961	0	0.0008	6.4272	0.209038338
65.15	3.2742	0	0.0008	6.4272	0.209038338
71.14	2.9985	0	0.0008	6.4272	0.209038338

78.1	2.7314	0	0.0008	6.4272	0.209038338
85.22	2.5033	0	0.0008	6.4272	0.209038338
93.19	2.2892	0	0.0008	6.4272	0.209038338
101.83	2.0949	0	0.0008	6.4272	0.209038338
111.81	1.908	0	0.0008	6.4272	0.209038338
122.17	1.7461	0	0.0008	6.4272	0.209038338
133.48	1.5982	0	0.0008	6.4272	0.209038338
145.3	1.4681	0	0.0008	6.4272	0.209038338
159.7	1.3358	0	0.0008	6.4272	0.209038338
175.36	1.2165	0	0.0008	6.4272	0.209038338
191.06	1.1165	0	0.0008	6.4272	0.209038338
208.84	1.0215	0	0.0008	6.4272	0.209038338
228.48	0.9337	0	0.0008	6.4272	0.209038338
250.73	0.8508	0	0.0008	6.4272	0.209038338
275.11	0.7754	0	0.0008	6.5349	0.209038338
301.94	0.7065	0	0.0008	6.5349	0.209038338
328.87	0.6486	0	0.0008	6.5349	0.209038338
360.99	0.5909	0	0.0008	6.5439	0.209038338
392.14	0.544	0	0.0008	6.5439	0.209038338
431.22	0.4947	0	0.0008	6.5439	0.209038338
471.34	0.4526	0	0.0008	6.5955	0.209038338
516.08	0.4134	0	0.0008	6.5955	0.209038338
567.81	0.3757	0	0.0008	6.5955	0.209038338
619.22	0.3445	0	0.0008	6.5955	0.209038338
673.2	0.3169	0	0.0008	6.6615	0.209038338
737.46	0.2893	0	0.0008	7.0064	0.209038338
804.78	0.2651	0	0.0008	7.0064	0.209038338
878.68	0.2428	0	0.0008	7.0064	0.209038338
963.18	0.2215	0	0.0008	7.0064	0.209038338
1046.08	0.2039	0	0.0008	7.255	0.209038338
1146.01	0.1861	0	0.0009	7.5254	0.23516813
1255.26	0.1699	0	0.0009	7.7591	0.23516813
1373.18	0.1553	0	0.0009	8.1069	0.23516813
1508.61	0.1414	0	0.0009	8.1069	0.23516813
1642.28	0.1299	0	0.0009	8.1069	0.23516813
1801.65	0.1184	0	0.001	8.5119	0.261297922
1972.59	0.1081	0.0001	0.0011	9.0908	0.287427715
2157.66	0.0989	0	0.0011	9.3225	0.287427715
2365.71	0.0902	0	0.0011	9.5541	0.287427715
2582.6	0.0826	0.0001	0.0012	10.249	0.313557507
2817.64	0.0757	0	0.0012	10.5385	0.313557507
3086.39	0.0691	0	0.0013	10.8857	0.339687299
3376.31	0.0632	0	0.0013	11.2331	0.339687299
3696.03	0.0577	0.0001	0.0014	11.6961	0.365817091
4047.69	0.0527	0.0001	0.0015	12.5068	0.391946884
4432.19	0.0481	0	0.0015	12.565	0.391946884
4830.01	0.0442	0	0.0015	12.7968	0.391946884

5290.55	0.0403	0.0001	0.0016	13.3758	0.418076676
5785.85	0.0369	0	0.0016	13.7757	0.418076676
6343.25	0.0336	0.0001	0.0017	14.6479	0.444206468
6933.18	0.0308	0	0.0017	14.7012	0.444206468
7580.95	0.0281	0	0.0017	14.8813	0.444206468
8284.63	0.0257	0.0001	0.0018	15.692	0.47033626
9084.7	0.0235	0.0001	0.0019	16.4447	0.496466053
9931.04	0.0215	0.0001	0.002	17.1974	0.522595845
10867.98	0.0196	0.0001	0.0021	18.1818	0.548725637
11849.28	0.018	0.0001	0.0022	19.1083	0.574855429
12965.51	0.0165	0.0002	0.0024	20.7851	0.627115014
14235.98	0.015	0.0002	0.0026	22.4079	0.679374598
15537.29	0.0137	0.0003	0.0029	24.6671	0.757763975
17023.67	0.0125	0.0004	0.0033	27.9097	0.862283144
18652.67	0.0114	0.0009	0.0042	35.607	1.097451274
20331.8	0.0105	0.0008	0.005	42.5023	1.306489612
22224.93	0.0096	0.0009	0.0058	49.7991	1.51552795
24278.08	0.0088	0.0009	0.0067	57.2088	1.750696081
26579.91	0.008	0.0009	0.0076	65.258	1.985864211
29186.36	0.0073	0.0009	0.0085	73.1308	2.221032341
31846.81	0.0067	0.0005	0.009	77.0155	2.351681302
34942.96	0.0061	0.0007	0.0097	82.9184	2.534589848
38208.78	0.0056	0.0005	0.0102	87.5536	2.665238809
41817.77	0.0051	0.0004	0.0107	91.2565	2.79588777
45683.18	0.0047	0.0003	0.0109	93.5727	2.848147355
49857.06	0.0043	0.0002	0.0112	95.7006	2.926536732
54561.11	0.0039	0.0003	0.0115	98.3787	3.004926108
59722.07	0.0036	0.0002	0.0117	100	3.057185693

Inc Int %PV(ac)	Cum Int %PV(ac)	Pore Rad microns	W.P. Sat %PV(ac)	Lev "J" Funct.	G/B Pc psia
0	0	69.15655	100	2.42E-05	0.20944
0	0	61.1892	100	2.73E-05	0.23664
0	0	54.41825	100	3.08E-05	0.26656
0	0	49.2875	100	3.39E-05	0.29376
0	0	44.97985	100	3.72E-05	0.32232
0	0	41.00695	100	4.08E-05	0.3536
0	0	37.33985	100	4.49E-05	0.38896
0	0	34.18655	100	4.9E-05	0.42432
0	0	31.34575	100	5.34E-05	0.4624
0	0	28.62885	100	5.85E-05	0.50728
0	0	26.21015	100	6.39E-05	0.55352
0	0	24.04575	100	6.97E-05	0.60384
0	0	22.04195	100	7.6E-05	0.65824
0	0	20.1794	100	8.3E-05	0.71944
0	0	18.4213	100	9.09E-05	0.78744
0	0	16.85035	100	9.93E-05	0.86088
0	0	15.4468	100	0.000108	0.93976
0	0	14.1286	100	0.000118	1.0268
0	0	12.9189	100	0.00013	1.12336
0	0	11.7985	100	0.000142	1.22944
0	0	10.7969	100	0.000155	1.34368
0	0	9.90015	100	0.000169	1.46472
0	0	9.0635	100	0.000185	1.60072
0	0	8.29255	100	0.000202	1.74896
0	0	7.5264	100	0.000222	1.92712
0	0	6.9027	100	0.000242	2.1012
0	0	6.33315	100	0.000264	2.29024
0	0	5.7816	100	0.00029	2.5092
0	0	5.2699	100	0.000318	2.75264
0	0	4.82065	100	0.000347	3.00968
0	0	4.4043	100	0.00038	3.29392
0	0	4.02025	100	0.000416	3.60808
0	0	3.6631	100	0.000457	3.96032
0	0	3.2731	100	0.000511	4.43224
0	0	2.9476	100	0.000568	4.92184
0	0	2.7635	100	0.000606	5.2496
0	0	2.55795	100	0.000654	5.6712
0	0	2.3473	100	0.000713	6.17984
0	0	2.1128	100	0.000792	6.86528
0	0	1.94565	100	0.00086	7.45552
0	0	1.79805	100	0.000931	8.06752
0	0	1.6371	100	0.001023	8.8604
0	0	1.49925	100	0.001117	9.67504

0	0	1.3657	100	0.001226	10.6216
0	0	1.25165	100	0.001337	11.58992
0	0	1.1446	100	0.001463	12.67384
0	0	1.04745	100	0.001598	13.84888
0	0	0.954	100	0.001755	15.20616
0	0	0.87305	100	0.001917	16.61512
0	0	0.7991	100	0.002095	18.15328
0	0	0.73405	100	0.00228	19.7608
0	0	0.6679	100	0.002506	21.7192
0	0	0.60825	100	0.002752	23.84896
0	0	0.55825	100	0.002999	25.98416
0	0	0.51075	100	0.003278	28.40224
0	0	0.46685	100	0.003586	31.07328
0	0	0.4254	100	0.003935	34.09928
0	0	0.3877	100	0.004318	37.41496
0	0	0.35325	100	0.004739	41.06384
0	0	0.3243	100	0.005162	44.72632
0	0	0.29545	100	0.005666	49.09464
0	0	0.272	100	0.006155	53.33104
0	0	0.24735	100	0.006768	58.64592
0	0	0.2263	100	0.007398	64.10224
0	0	0.2067	100	0.0081	70.18688
0	0	0.18785	100	0.008912	77.22216
0	0	0.17225	100	0.009718	84.21392
0	0	0.15845	100	0.010566	91.5552
0	0	0.14465	100	0.011574	100.2946
0	0	0.13255	100	0.012631	109.4501
0	0	0.1214	100	0.013791	119.5005
0	0	0.11075	100	0.015117	130.9925
0	0	0.10195	100	0.016418	142.2669
0	0	0.09305	100	0.017986	155.8574
0	0	0.08495	100	0.019701	170.7154
0	0	0.07765	100	0.021552	186.7525
0	0	0.0707	100	0.023677	205.171
0	0	0.06495	100	0.025775	223.3501
0	0	0.0592	100	0.028276	245.0244
0	0	0.05405	100	0.030959	268.2722
0	0	0.04945	100	0.033864	293.4418
0	0	0.0451	100	0.037129	321.7366
0	0	0.0413	100	0.040533	351.2336
0	0	0.03785	100	0.044222	383.199
0	0	0.03455	100	0.04844	419.749
0	0	0.0316	100	0.05299	459.1782
0	0	0.02885	100	0.058008	502.6601
0	0	0.02635	100	0.063527	550.4858
0	0	0.02405	100	0.069562	602.7778
0	0	0.0221	100	0.075805	656.8814

0	0	0.02015	100	0.083033	719.5148
0	0	0.01845	100	0.090807	786.8756
0	0	0.0168	100	0.099555	862.682
0	0	0.0154	100	0.108814	942.9125
0	0	0.01405	100	0.11898	1031.009
0	0	0.01285	100	0.130024	1126.71
0	0	0.01175	100	0.142581	1235.519
0	0	0.01075	100	0.155864	1350.621
0	0	0.0098	100	0.170569	1478.045
0	0	0.009	100	0.18597	1611.502
2.105263158	2.105263158	0.00825	97.89473684	0.203489	1763.309
2.105263158	4.210526316	0.0075	95.78947368	0.223429	1936.093
3.157894737	7.368421053	0.00685	92.63157895	0.243853	2113.071
4.210526316	11.57894737	0.00625	88.42105263	0.267181	2315.219
9.473684211	21.05263158	0.0057	78.94736842	0.292747	2536.763
8.421052632	29.47368421	0.00525	70.52631579	0.319101	2765.125
8.421052632	37.89473684	0.0048	62.10526316	0.348813	3022.59
9.473684211	47.36842105	0.0044	52.63157895	0.381036	3301.819
9.473684211	56.84210526	0.004	43.15789474	0.417163	3614.868
9.473684211	66.31578947	0.00365	33.68421053	0.45807	3969.345
5.263157895	71.57894737	0.00335	28.42105263	0.499825	4331.166
7.368421053	78.94736842	0.00305	21.05263158	0.548418	4752.243
5.263157895	84.21052632	0.0028	15.78947368	0.599674	5196.394
5.263157895	89.47368421	0.00255	10.52631579	0.656316	5687.217
2.105263158	91.57894737	0.00235	8.421052632	0.716982	6212.912
3.157894737	94.73684211	0.00215	5.263157895	0.78249	6780.56
3.157894737	97.89473684	0.00195	2.105263158	0.856318	7420.311
2.105263158	100	0.0018	0	0.937318	8122.202

G/O Pc psia	O/B Pc psia	Ht FWL,ft G/B	Ht FWL,ft O/B	Swanson's Sb/Pc(ac)
0.1001	0.12628	0.5313	1.12112	-0.37328275
0.1131	0.14268	0.6003	1.26672	-0.31535956
0.1274	0.16072	0.6762	1.42688	-0.25329901
0.1404	0.17712	0.7452	1.57248	-0.21774827
0.15405	0.19434	0.81765	1.72536	-0.19845412
0.169	0.2132	0.897	1.8928	-0.18089856
0.1859	0.23452	0.9867	2.08208	-0.16445324
0.2028	0.25584	1.0764	2.27136	-0.14237387
0.221	0.2788	1.173	2.4752	-0.12296373
0.24245	0.30586	1.28685	2.71544	-0.10507959
0.26455	0.33374	1.40415	2.96296	-0.09630145
0.2886	0.36408	1.5318	3.23232	-0.08827633
0.3146	0.39688	1.6698	3.52352	-0.08098076
0.34385	0.43378	1.82505	3.85112	-0.07409204
0.37635	0.47478	1.99755	4.21512	-0.06769376
0.41145	0.51906	2.18385	4.60824	-0.06191894
0.44915	0.56662	2.38395	5.03048	-0.05672169
0.49075	0.6191	2.60475	5.4964	-0.05191349
0.5369	0.67732	2.8497	6.01328	-0.0474512
0.5876	0.74128	3.1188	6.58112	-0.04335696
0.6422	0.81016	3.4086	7.19264	-0.03967074
0.70005	0.88314	3.71565	7.84056	-0.03639247
0.76505	0.96514	4.06065	8.56856	-0.0333005
0.8359	1.05452	4.4367	9.36208	-0.03047798
0.92105	1.16194	4.88865	10.31576	-0.02766033
1.00425	1.2669	5.33025	11.2476	-0.02536873
1.0946	1.38088	5.8098	12.25952	-0.02327476
1.19925	1.5129	6.36525	13.4316	-0.02124373
1.3156	1.65968	6.9828	14.73472	-0.01936496
1.43845	1.81466	7.63485	16.11064	-0.01771111
1.5743	1.98604	8.3559	17.63216	-0.01618278
1.72445	2.17546	9.15285	19.31384	-0.01378881
1.8928	2.38784	10.0464	21.19936	-0.0125624
2.11835	2.67238	11.24355	23.72552	-0.01122483
2.35235	2.96758	12.48555	26.34632	-0.01010824
2.509	3.1652	13.317	28.1008	-0.00947713
2.7105	3.4194	14.3865	30.3576	-0.00877259
2.9536	3.72608	15.6768	33.08032	-0.00805055
3.2812	4.13936	17.4156	36.74944	-0.00724677
3.5633	4.49524	18.9129	39.90896	-0.00667306
3.8558	4.86424	20.4654	43.18496	-0.00616684
4.23475	5.3423	22.47675	47.4292	-0.005615
4.6241	5.83348	24.5433	51.78992	-0.00514221

5.0765	6.4042	26.9445	56.8568	-0.00468396
5.5393	6.98804	29.4009	62.04016	-0.00429262
6.05735	7.64158	32.15055	67.84232	-0.0039255
6.61895	8.35006	35.13135	74.13224	-0.00359243
7.26765	9.16842	38.57445	81.39768	-0.00327177
7.94105	10.01794	42.14865	88.93976	-0.00299433
8.6762	10.94536	46.0506	97.17344	-0.00274061
9.4445	11.9146	50.1285	105.7784	-0.00251767
10.3805	13.0954	55.0965	116.2616	-0.00229065
11.3984	14.37952	60.4992	127.6621	-0.00208609
12.4189	15.66692	65.9157	139.0917	-0.00191467
13.5746	17.12488	72.0498	152.0355	-0.00175166
14.8512	18.73536	78.8256	166.3334	-0.00160109
16.29745	20.55986	86.50185	182.5314	-0.00145901
17.88215	22.55902	94.91295	200.2801	-0.00132971
19.6261	24.75908	104.1693	219.8123	-0.00121156
21.37655	26.96734	113.4602	239.4174	-0.00111235
23.46435	29.60118	124.5416	262.8007	-0.00101337
25.4891	32.15548	135.2883	285.4779	-0.00093287
28.0293	35.36004	148.7709	313.9282	-0.00084833
30.6371	38.64988	162.6123	343.1355	-0.00077612
33.5452	42.31856	178.0476	375.7062	-0.00070884
36.90765	46.56042	195.8945	413.3657	-0.00064426
40.2493	50.77604	213.6309	450.7922	-0.00059077
43.758	55.2024	232.254	490.0896	-0.0005434
47.9349	60.47172	254.4237	536.8709	-0.00049605
52.3107	65.99196	277.6491	585.8798	-0.00045456
57.1142	72.05176	303.1446	639.679	-0.00041633
62.6067	78.98076	332.2971	701.195	-0.0003798
67.9952	85.77856	360.8976	761.5462	-0.0003497
74.49065	93.97282	395.3735	834.2953	-0.00029641
81.5919	102.9313	433.0647	913.8293	-0.00027061
89.2567	112.6008	473.7471	999.675	-0.00024737
98.05965	123.706	520.4705	1098.268	-0.00022517
106.7482	134.667	566.5866	1195.58	-0.00020684
117.1073	147.7353	621.5693	1311.601	-0.00017404
128.2184	161.7524	680.5436	1436.046	-0.00014571
140.2479	176.9281	744.3927	1570.776	-0.00013321
153.7712	193.9882	816.17	1722.237	-0.0001215
167.869	211.7732	890.997	1880.133	-0.00010118
183.1466	231.0465	972.0858	2051.242	-9.2736E-05
200.6154	253.084	1064.805	2246.892	-7.6195E-05
219.4602	276.8574	1164.827	2457.954	-6.9652E-05
240.242	303.0745	1275.13	2690.71	-5.6558E-05
263.0999	331.9106	1396.453	2946.718	-4.5188E-05
288.0924	363.4396	1529.106	3226.634	-4.1268E-05
313.9507	396.0608	1666.353	3516.247	-3.7869E-05

343.8858	433.8251	1825.24	3851.52	-2.9634E-05
376.0803	474.4397	1996.118	4212.099	-2.7097E-05
412.3113	520.1465	2188.421	4617.886	-2.0597E-05
450.6567	568.5208	2391.947	5047.355	-1.8844E-05
492.7618	621.6379	2615.428	5518.932	-1.7234E-05
538.501	679.3397	2858.197	6031.211	-1.2616E-05
590.5055	744.9454	3134.222	6613.662	-8.6287E-06
645.5176	814.3453	3426.209	7229.797	-5.2622E-06
706.4187	891.1744	3749.453	7911.889	-2.4043E-06
770.2032	971.641	4088.002	8626.276	0
842.7582	1063.172	4473.101	9438.891	4.0307E-06
925.3387	1167.35	4911.413	10363.79	7.3419E-06
1009.924	1274.058	5360.365	11311.15	1.1772E-05
1106.539	1395.941	5873.166	12393.23	1.6884E-05
1212.424	1529.519	6435.171	13579.14	2.8017E-05
1321.567	1667.208	7014.471	14801.55	3.5985E-05
1444.62	1822.444	7667.601	16179.75	4.2325E-05
1578.075	1990.803	8375.938	17674.44	4.8432E-05
1727.694	2179.553	9170.069	19350.17	5.3086E-05
1897.113	2393.282	10069.29	21247.67	5.6402E-05
2070.043	2611.438	10987.15	23184.48	5.5793E-05
2271.292	2865.323	12055.32	25438.47	5.6084E-05
2483.571	3133.12	13182.03	27815.99	5.471E-05
2718.155	3429.057	14427.13	30443.34	5.3112E-05
2969.407	3746.021	15760.7	33257.36	4.9762E-05
3240.709	4088.279	17200.69	36295.94	4.7168E-05
3546.472	4474.011	18823.58	39720.49	4.4539E-05
3881.935	4897.21	20604.11	43477.67	4.1565E-05
				5.6402E-05

AIR\|MERCURY CAPILLARY PRESSURE DATA : BY GEOTECH

Spl @ 682.00m Vines-1

Bulk Volume = 7.4704cc
Closure @ 11849. psia
Pore Volume = 0.1854cc
Porosity = 2.48%
Median Pore Aperture = 0.0086 microns (dia.)

Injection Pressure (psia)	Pore Diameter (microns)	Hg (nwp) Saturation cum%PV	100-Hg(wp) Saturation cum%PV	Leverett "J" Function	Gas/Brine Pc (psia)	Gas/Oil Pc (psia)	Oil/Brine Pc (psia)	Ht. Above Free Water (ft.) Gas/Brine	Ht. Above Free Water (ft.) Oil/Brine
1.54	138.31	0.0	100.0	0.00	0.21	0.10	0.13	0.5	1.1
1.74	122.38	0.0	100.0	0.00	0.24	0.11	0.14	0.6	1.3
1.96	108.84	0.0	100.0	0.00	0.27	0.13	0.16	0.7	1.4
2.16	98.58	0.0	100.0	0.00	0.29	0.14	0.18	0.7	1.6
2.37	89.96	0.0	100.0	0.00	0.32	0.15	0.19	0.8	1.7
2.60	82.01	0.0	100.0	0.00	0.35	0.17	0.21	0.9	1.9
2.86	74.68	0.0	100.0	0.00	0.39	0.19	0.23	1.0	2.1
3.12	68.37	0.0	100.0	0.00	0.42	0.20	0.26	1.1	2.3
3.40	62.69	0.0	100.0	0.00	0.46	0.22	0.28	1.2	2.5
3.73	57.26	0.0	100.0	0.00	0.51	0.24	0.31	1.3	2.7
4.07	52.42	0.0	100.0	0.00	0.55	0.26	0.33	1.4	3.0
4.44	48.09	0.0	100.0	0.00	0.60	0.29	0.36	1.5	3.2
4.84	44.08	0.0	100.0	0.00	0.66	0.31	0.40	1.7	3.5
5.29	40.36	0.0	100.0	0.00	0.72	0.34	0.43	1.8	3.9
5.79	36.84	0.0	100.0	0.00	0.79	0.38	0.47	2.0	4.2
6.33	33.70	0.0	100.0	0.00	0.86	0.41	0.52	2.2	4.6
6.91	30.89	0.0	100.0	0.00	0.94	0.45	0.57	2.4	5.0
7.55	28.26	0.0	100.0	0.00	1.03	0.49	0.62	2.6	5.5
8.26	25.84	0.0	100.0	0.00	1.12	0.54	0.68	2.8	6.0
9.04	23.60	0.0	100.0	0.00	1.23	0.59	0.74	3.1	6.6
9.88	21.59	0.0	100.0	0.00	1.34	0.64	0.81	3.4	7.2
10.77	19.80	0.0	100.0	0.00	1.46	0.70	0.88	3.7	7.8
11.77	18.13	0.0	100.0	0.00	1.60	0.77	0.97	4.1	8.6
12.86	16.59	0.0	100.0	0.00	1.75	0.84	1.05	4.4	9.4
14.17	15.05	0.0	100.0	0.00	1.93	0.92	1.16	4.9	10.3
15.45	13.81	0.0	100.0	0.00	2.10	1.00	1.27	5.3	11.2
16.84	12.67	0.0	100.0	0.00	2.29	1.09	1.38	5.8	12.3
18.45	11.56	0.0	100.0	0.00	2.51	1.20	1.51	6.4	13.4
20.24	10.54	0.0	100.0	0.00	2.75	1.32	1.66	7.0	14.7
22.13	9.641	0.0	100.0	0.00	3.01	1.44	1.81	7.6	16.1
24.22	8.809	0.0	100.0	0.00	3.29	1.57	1.99	8.4	17.6
26.53	8.041	0.0	100.0	0.00	3.61	1.72	2.18	9.2	19.3
29.12	7.326	0.0	100.0	0.00	3.96	1.89	2.39	10.0	21.2
32.59	6.546	0.0	100.0	0.00	4.43	2.12	2.67	11.2	23.7
36.19	5.895	0.0	100.0	0.00	4.92	2.35	2.97	12.5	26.3

AIR\MERCURY CAPILLARY PRESSURE DATA : BY GEOTECH

Spl @ 682.00m Vines-1

Injection Pressure (psia)	Pore Diameter (microns)	Hg (nwp) Saturation cum%PV	100-Hg(wp) Saturation cum%PV	Leverett "J" Function	Gas/Brine Pc (psia)	Gas/Oil Pc (psia)	Oil/Brine Pc (psia)	Ht. Above Free Water (ft.) Gas/Brine	Ht. Above Free Water (ft.) Oil/Brine
38.60	5.527	0.0	100.0	0.00	5.25	2.51	3.17	13.3	28.1
41.70	5.116	0.0	100.0	0.00	5.67	2.71	3.42	14.4	30.4
45.44	4.695	0.0	100.0	0.00	6.18	2.95	3.73	15.7	33.1
50.48	4.226	0.0	100.0	0.00	6.87	3.28	4.14	17.4	36.7
54.82	3.891	0.0	100.0	0.00	7.46	3.56	4.50	18.9	39.9
59.32	3.596	0.0	100.0	0.00	8.07	3.86	4.86	20.5	43.2
65.15	3.274	0.0	100.0	0.00	8.86	4.23	5.34	22.5	47.4
71.14	2.999	0.0	100.0	0.00	9.68	4.62	5.83	24.5	51.8
78.10	2.731	0.0	100.0	0.00	10.62	5.08	6.40	26.9	56.9
85.22	2.503	0.0	100.0	0.00	11.59	5.54	6.99	29.4	62.0
93.19	2.289	0.0	100.0	0.00	12.67	6.06	7.64	32.2	67.8
101.83	2.095	0.0	100.0	0.00	13.85	6.62	8.35	35.1	74.1
111.81	1.908	0.0	100.0	0.00	15.21	7.27	9.17	38.6	81.4
122.17	1.746	0.0	100.0	0.00	16.62	7.94	10.02	42.1	88.9
133.48	1.598	0.0	100.0	0.00	18.15	8.68	10.95	46.1	97.2
145.30	1.468	0.0	100.0	0.00	19.76	9.44	11.91	50.1	105.8
159.70	1.336	0.0	100.0	0.00	21.72	10.38	13.10	55.1	116.3
175.36	1.217	0.0	100.0	0.00	23.85	11.40	14.38	60.5	128
191.06	1.117	0.0	100.0	0.00	25.98	12.42	15.67	65.9	139
208.84	1.022	0.0	100.0	0.00	28.40	13.57	17.12	72.0	152
228.48	0.934	0.0	100.0	0.00	31.07	14.85	18.74	78.8	166
250.73	0.851	0.0	100.0	0.00	34.10	16.30	20.56	86.5	183
275.11	0.775	0.0	100.0	0.00	37.41	17.88	22.56	95	200
301.94	0.707	0.0	100.0	0.00	41.06	19.63	24.76	104	220
328.87	0.649	0.0	100.0	0.01	44.73	21.38	26.97	113	239
360.99	0.591	0.0	100.0	0.01	49.09	23.46	29.60	125	263
392.14	0.544	0.0	100.0	0.01	53.33	25.49	32.16	135	285
431.22	0.495	0.0	100.0	0.01	58.65	28.03	35.36	149	314
471.34	0.453	0.0	100.0	0.01	64.10	30.64	38.65	163	343
516.08	0.413	0.0	100.0	0.01	70.19	33.55	42.32	178	376
567.81	0.376	0.0	100.0	0.01	77.22	36.91	46.56	196	413
619.22	0.345	0.0	100.0	0.01	84.21	40.25	50.78	214	451
673.20	0.317	0.0	100.0	0.01	91.56	43.76	55.20	232	490
737.46	0.289	0.0	100.0	0.01	100.29	47.93	60.47	254	537
804.78	0.265	0.0	100.0	0.01	109.45	52.31	65.99	278	586
878.68	0.243	0.0	100.0	0.01	119.50	57.11	72.05	303	640
963.18	0.222	0.0	100.0	0.02	130.99	62.61	78.98	332	701
1046.08	0.204	0.0	100.0	0.02	142.27	68.00	85.78	361	762
1146.01	0.186	0.0	100.0	0.02	155.86	74.49	93.97	395	834
1255.26	0.170	0.0	100.0	0.02	170.72	81.59	102.93	433	914
1373.18	0.155	0.0	100.0	0.02	186.75	89.26	112.60	474	1000
1508.61	0.141	0.0	100.0	0.02	205.17	98.06	123.71	520	1098
1642.28	0.130	0.0	100.0	0.03	223.35	106.75	134.67	567	1196

AIR\MERCURY CAPILLARY PRESSURE DATA : BY GEOTECH

Spl @ 682.00m Vines-1

Injection Pressure (psia)	Pore Diameter (microns)	Hg (nwp) Saturation cum%PV	100-Hg(wp) Saturation cum%PV	Leverett "J" Function	Gas/Brine Pc (psia)	Gas/Oil Pc (psia)	Oil/Brine Pc (psia)	Ht. Above Free Water (ft.) Gas/Brine	Ht. Above Free Water (ft.) Oil/Brine
1801.65	0.118	0.0	100.0	0.03	245.02	117.11	147.74	622	1312
1972.59	0.108	0.0	100.0	0.03	268.27	128.22	161.75	681	1436
2157.66	0.0989	0.0	100.0	0.03	293.44	140.25	176.93	744	1571
2365.71	0.0902	0.0	100.0	0.04	321.74	153.77	193.99	816	1722
2582.60	0.0826	0.0	100.0	0.04	351.23	167.87	211.77	891	1880
2817.64	0.0757	0.0	100.0	0.04	383.20	183.15	231.05	972	2051
3086.39	0.0691	0.0	100.0	0.05	419.75	200.62	253.08	1065	2247
3376.31	0.0632	0.0	100.0	0.05	459.18	219.46	276.86	1165	2458
3696.03	0.0577	0.0	100.0	0.06	502.66	240.24	303.07	1275	2691
4047.69	0.0527	0.0	100.0	0.06	550.49	263.10	331.91	1396	2947
4432.19	0.0481	0.0	100.0	0.07	602.78	288.09	363.44	1529	3227
4830.01	0.0442	0.0	100.0	0.08	656.88	313.95	396.06	1666	3516
5290.55	0.0403	0.0	100.0	0.08	719.51	343.89	433.83	1825	3852
5785.85	0.0369	0.0	100.0	0.09	786.88	376.08	474.44	1996	4212
6343.25	0.0336	0.0	100.0	0.10	862.68	412.31	520.15	2188	4618
6933.18	0.0308	0.0	100.0	0.11	942.91	450.66	568.52	2392	5047
7580.95	0.0281	0.0	100.0	0.12	1031.01	492.76	621.64	2615	5519
8284.63	0.0257	0.0	100.0	0.13	1126.71	538.50	679.34	2858	6031
9084.70	0.0235	0.0	100.0	0.14	1235.52	590.51	744.95	3134	6614
9931.04	0.0215	0.0	100.0	0.16	1350.62	645.52	814.35	3426	7230
10867.98	0.0196	0.0	100.0	0.17	1478.05	706.42	891.17	3749	7912
11849.28	0.0180	0.0	100.0	0.19	1611.50	770.20	971.64	4088	8626
12965.51	0.0165	2.1	97.9	0.20	1763.31	842.76	1063.17	4473	9439
14235.98	0.0150	4.2	95.8	0.22	1936.09	925.34	1167.35	4911	10364
15537.29	0.0137	7.4	92.6	0.24	2113.07	1009.92	1274.06	5360	11311
17023.67	0.0125	11.6	88.4	0.27	2315.22	1106.54	1395.94	5873	12393
18652.67	0.0114	21.1	78.9	0.29	2536.76	1212.42	1529.52	6435	13579
20331.80	0.0105	29.5	70.5	0.32	2765.12	1321.57	1667.21	7014	14802
22224.93	0.0096	37.9	62.1	0.35	3022.59	1444.62	1822.44	7668	16180
24278.08	0.0088	47.4	52.6	0.38	3301.82	1578.08	1990.80	8376	17674
26579.91	0.0080	56.8	43.2	0.42	3614.87	1727.69	2179.55	9170	19350
29186.36	0.0073	66.3	33.7	0.46	3969.34	1897.11	2393.28	10069	21248
31846.81	0.0067	71.6	28.4	0.50	4331.17	2070.04	2611.44	10987	23184
34942.96	0.0061	78.9	21.1	0.55	4752.24	2271.29	2865.32	12055	25438
38208.78	0.0056	84.2	15.8	0.60	5196.39	2483.57	3133.12	13182	27816
41817.77	0.0051	89.5	10.5	0.66	5687.22	2718.16	3429.06	14427	30443
45683.18	0.0047	91.6	8.4	0.72	6212.91	2969.41	3746.02	15761	33257
49857.06	0.0043	94.7	5.3	0.78	6780.56	3240.71	4088.28	17201	36296
54561.11	0.0039	97.9	2.1	0.86	7420.31	3546.47	4474.01	18824	39720
59722.07	0.0036	100.0	0.0	0.94	8122.20	3881.93	4897.21	20604	43478

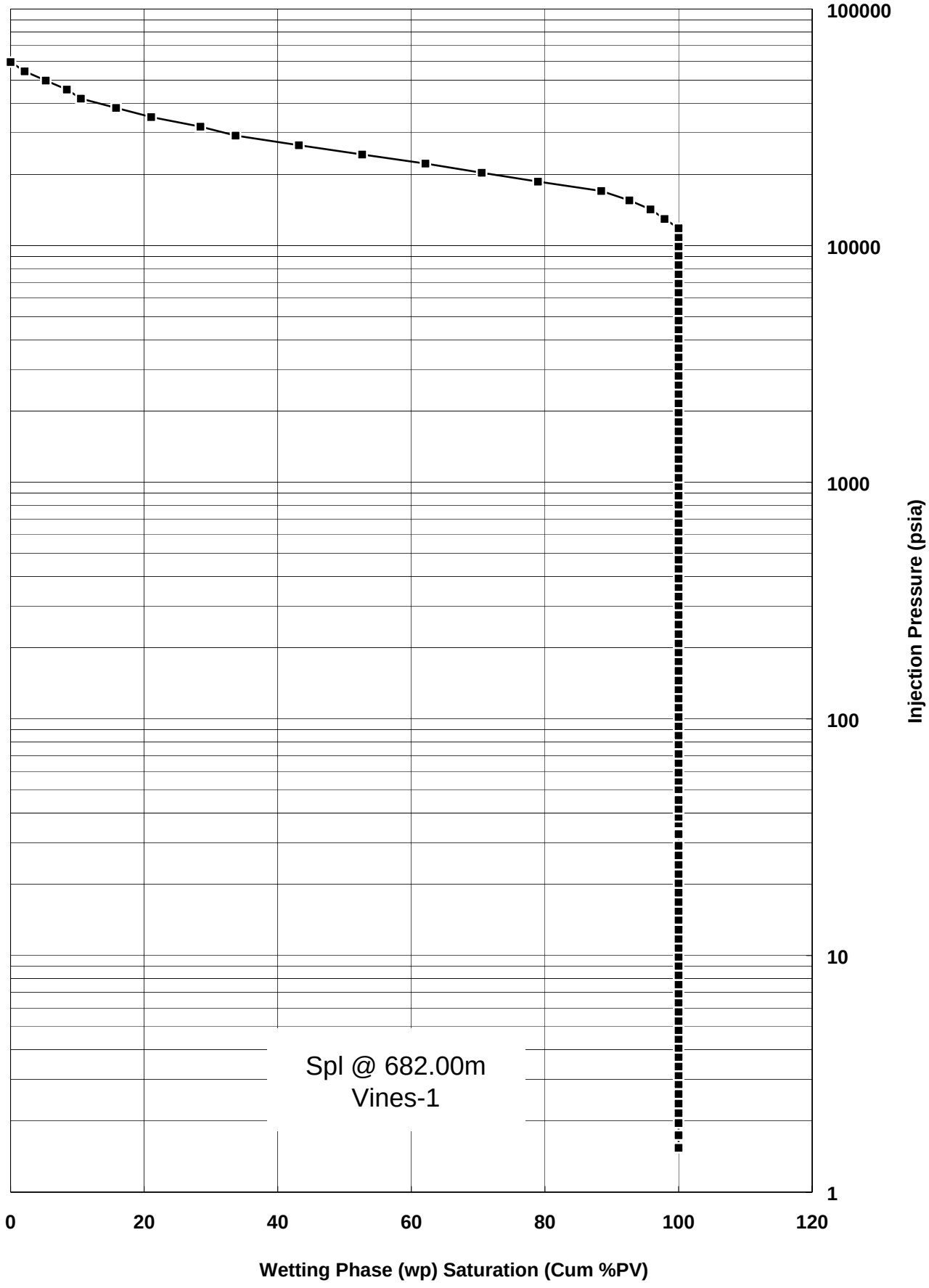
100000
10000
1000
100
10
1
Injection Pressure (psia)
0
20
40
60
80
100
120
Wetting Phase (wp) Saturation (Cum %PV)
Spl @ 682.00m
Vines-1

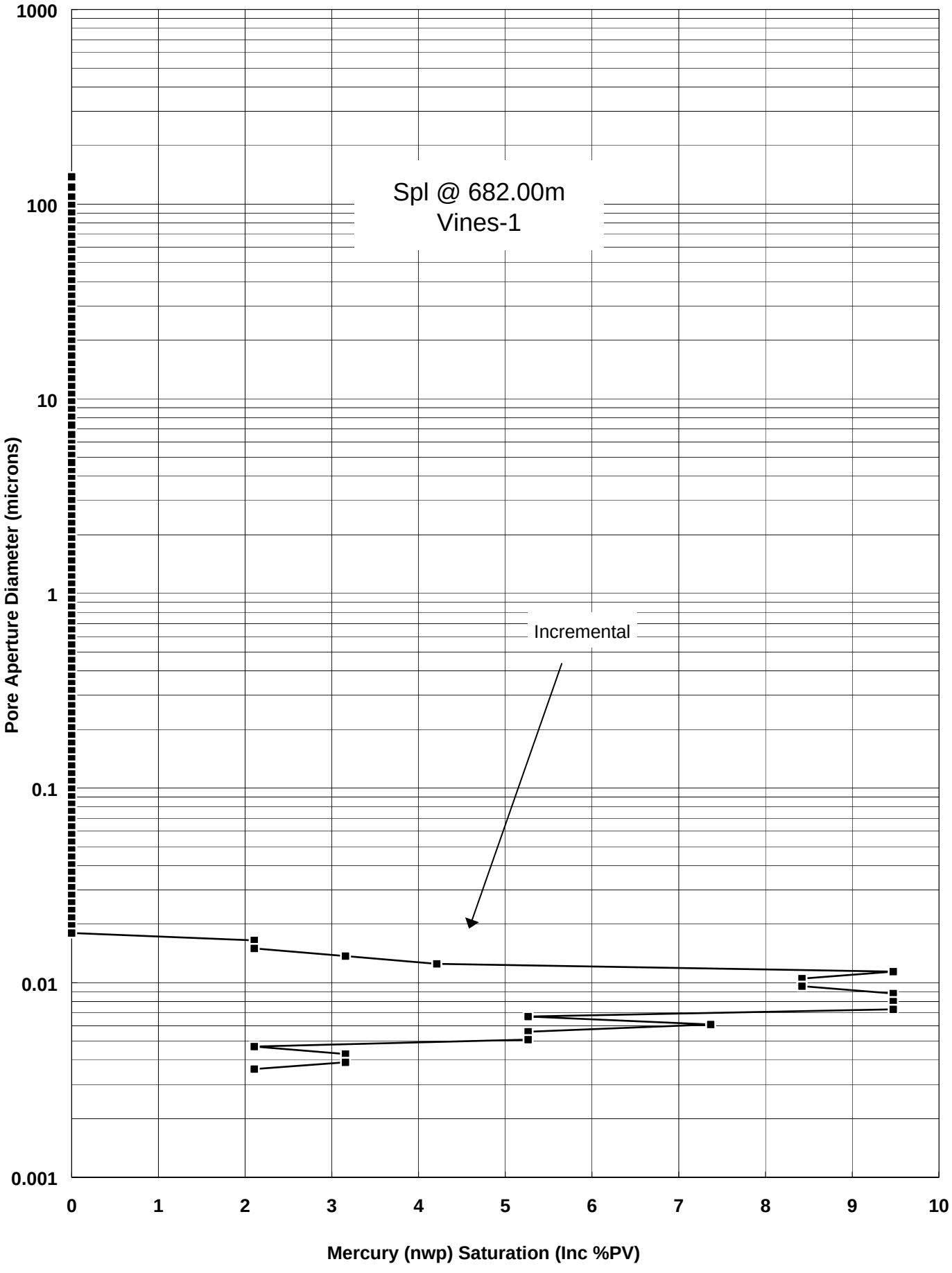
Spl @ 682.00m
Vines-1
Incremental
Pore Aperture Diameter (microns)
1000
100
10
1
0.1
0.01
0.001
0
1
2
3
4
5
6
7
8
9
10
Mercury (nwp) Saturation (Inc %PV)

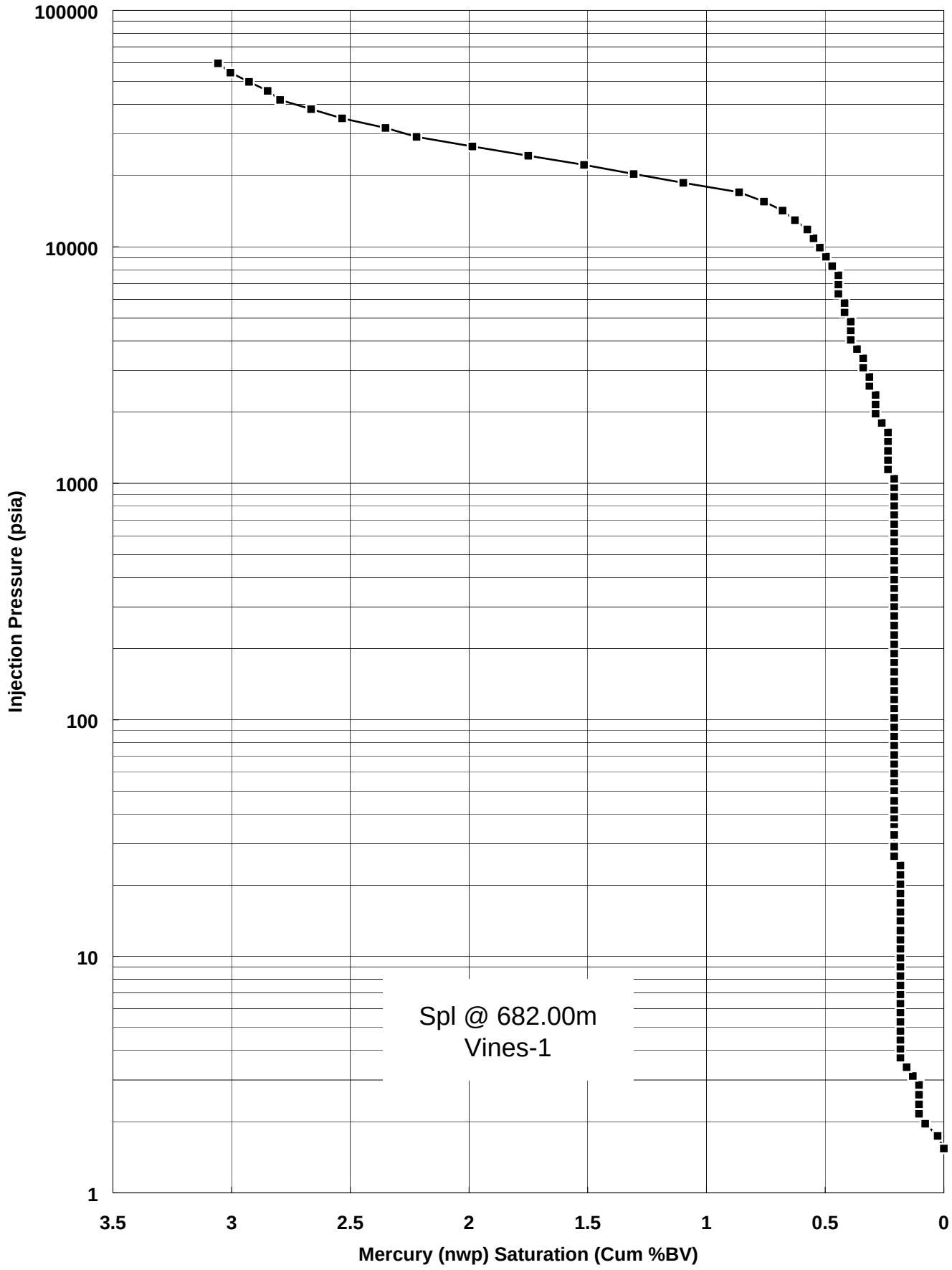
100000
10000
1000
100
10
1
Injection Pressure (psia)
3.5
3
2.5
2
1.5
1
0.5
0
Mercury (nwp) Saturation (Cum %BV)
Spl @ 682.00m
Vines-1

Int Pres psia	Pore Dia microns	Inc Int mL/gm	Cum Int mL/gm	Cum Int %PV(bc)	Cum Int %BV
1.54	138.3131	0	0	0	0
1.74	122.3784	0.0002	0.0002	1.1034	0.052155757
1.96	108.8365	0.0002	0.0004	2.6197	0.104311513
2.16	98.575	0.0001	0.0005	3.3065	0.130389392
2.37	89.9597	0.0001	0.0006	4.0214	0.15646727
2.6	82.0139	0.0001	0.0006	4.6917	0.15646727
2.86	74.6797	0	0.0007	5.0051	0.182545148
3.12	68.3731	0.0002	0.0009	6.3896	0.234700905
3.4	62.6915	0	0.0009	6.4343	0.234700905
3.73	57.2577	0	0.0009	6.6577	0.234700905
4.07	52.4203	0	0.001	6.9252	0.260778783
4.44	48.0915	0	0.001	7.1046	0.260778783
4.84	44.0839	0	0.001	7.1939	0.260778783
5.29	40.3588	0	0.001	7.2833	0.260778783
5.79	36.8426	0	0.001	7.5071	0.260778783
6.33	33.7007	0	0.0011	7.7301	0.286856661
6.91	30.8936	0.0001	0.0011	8.1323	0.286856661
7.55	28.2572	0	0.0011	8.1323	0.286856661
8.26	25.8378	0	0.0011	8.2663	0.286856661
9.04	23.597	0	0.0011	8.2663	0.286856661
9.88	21.5938	0	0.0011	8.2663	0.286856661
10.77	19.8003	0	0.0011	8.2663	0.286856661
11.77	18.127	0	0.0011	8.2663	0.286856661
12.86	16.5851	0	0.0012	8.4004	0.31293454
14.17	15.0528	0	0.0012	8.5346	0.31293454
15.45	13.8054	0	0.0012	8.5797	0.31293454
16.84	12.6663	0	0.0012	8.5797	0.31293454
18.45	11.5632	0	0.0012	8.6684	0.31293454
20.24	10.5398	0	0.0012	8.9364	0.31293454
22.13	9.6413	0	0.0012	8.9812	0.31293454
24.22	8.8086	0	0.0012	8.9819	0.31293454
26.53	8.0405	0	0.0013	9.0708	0.339012418
29.07	7.3395	0	0.0013	9.0708	0.339012418
32.53	6.5569	0	0.0013	9.0708	0.339012418
36.13	5.9038	0	0.0013	9.16	0.339012418
38.54	5.5346	0	0.0013	9.16	0.339012418
41.64	5.1226	0	0.0013	9.2901	0.339012418
45.39	4.7001	0	0.0013	9.2901	0.339012418
50.43	4.2299	0	0.0013	9.294	0.339012418
54.77	3.895	0	0.0013	9.4281	0.339012418
59.27	3.5993	0	0.0013	9.4281	0.339012418
65.1	3.2769	0	0.0013	9.4281	0.339012418
71.09	3.0007	0	0.0013	9.4283	0.339012418

78.05	2.7333	0	0.0013	9.6481	0.339012418
85.16	2.5049	0	0.0013	9.6481	0.339012418
93.13	2.2905	0	0.0013	9.6481	0.339012418
101.78	2.096	0	0.0014	9.8353	0.365090296
111.75	1.9089	0	0.0014	10.0536	0.365090296
122.11	1.7469	0	0.0014	10.0536	0.365090296
133.42	1.5988	0	0.0014	10.0536	0.365090296
145.25	1.4687	0	0.0014	10.0536	0.365090296
159.64	1.3363	0	0.0014	10.0536	0.365090296
175.31	1.2169	0	0.0014	10.0536	0.365090296
191	1.1169	0	0.0014	10.0536	0.365090296
208.79	1.0217	0	0.0014	10.0536	0.365090296
228.42	0.9339	0	0.0014	10.143	0.365090296
250.67	0.851	0	0.0014	10.4555	0.365090296
275.06	0.7756	0	0.0014	10.4573	0.365090296
301.89	0.7066	0	0.0014	10.4573	0.365090296
328.82	0.6488	0	0.0015	10.5891	0.391168175
360.94	0.591	0	0.0015	10.6805	0.391168175
392.09	0.5441	0	0.0015	10.7226	0.391168175
431.17	0.4948	0	0.0015	10.7676	0.391168175
471.28	0.4526	0	0.0015	10.9037	0.391168175
516.02	0.4134	0	0.0016	11.2592	0.417246053
567.75	0.3757	0	0.0016	11.2592	0.417246053
619.16	0.3445	0	0.0016	11.2592	0.417246053
673.14	0.3169	0	0.0016	11.4388	0.417246053
737.4	0.2893	0	0.0016	11.5274	0.417246053
804.72	0.2651	0	0.0016	11.5751	0.417246053
878.62	0.2428	0	0.0016	11.5751	0.417246053
963.13	0.2215	0	0.0016	11.7081	0.417246053
1046.02	0.2039	0	0.0016	11.7869	0.417246053
1145.95	0.1862	0	0.0016	11.8774	0.417246053
1255.2	0.17	0	0.0017	11.9303	0.443323931
1373.12	0.1554	0	0.0017	12.0165	0.443323931
1508.56	0.1414	0	0.0017	12.1984	0.443323931
1642.22	0.1299	0	0.0017	12.2859	0.443323931
1801.59	0.1184	0	0.0017	12.5112	0.443323931
1972.53	0.1081	0	0.0018	12.8667	0.46940181
2157.61	0.0989	0	0.0018	12.8688	0.46940181
2365.66	0.0902	0	0.0018	13.0883	0.46940181
2582.55	0.0826	0	0.0018	13.2244	0.46940181
2817.59	0.0757	0	0.0018	13.3155	0.46940181
3086.34	0.0691	0.0001	0.0019	13.7161	0.495479688
3376.26	0.0632	0	0.0019	13.941	0.495479688
3695.98	0.0577	0	0.002	14.1632	0.521557566
4047.63	0.0527	0	0.002	14.4748	0.521557566
4432.14	0.0481	0.0001	0.0021	15.0529	0.547635445
4829.95	0.0442	0.0001	0.0021	15.4567	0.547635445

5290.49	0.0403	0.0001	0.0022	15.9954	0.573713323
5785.79	0.0369	0	0.0022	15.9954	0.573713323
6343.19	0.0336	0.0001	0.0023	16.4433	0.599791201
6933.12	0.0308	0	0.0023	16.7113	0.599791201
7580.89	0.0281	0.0001	0.0024	17.2029	0.625869079
8284.57	0.0257	0.0001	0.0025	17.9547	0.651946958
9084.64	0.0235	0.0001	0.0026	18.6763	0.678024836
9930.98	0.0215	0.0001	0.0027	19.3022	0.704102714
10867.92	0.0196	0.0001	0.0028	20.2407	0.730180593
11849.21	0.018	0.0001	0.0029	21.0434	0.756258471
12965.45	0.0165	0.0002	0.0031	22.6567	0.808414228
14235.91	0.015	0.0002	0.0034	24.3074	0.886647863
15537.22	0.0137	0.0003	0.0037	26.4079	0.964881497
17023.59	0.0125	0.0005	0.0041	29.6654	1.069193011
18652.58	0.0114	0.001	0.0051	36.8186	1.329971794
20331.7	0.0105	0.0009	0.006	43.3869	1.564672699
22224.82	0.0096	0.0009	0.0069	49.9109	1.799373603
24277.96	0.0088	0.0009	0.0078	56.2108	2.034074508
26579.78	0.008	0.0011	0.0089	64.0751	2.32093117
29186.2	0.0073	0.0011	0.0099	71.7603	2.581709953
31846.66	0.0067	0.0005	0.0104	75.3351	2.712099344
34942.79	0.0061	0.0008	0.0112	81.0567	2.920722371
38208.59	0.0056	0.0007	0.012	86.4656	3.129345397
41817.57	0.0051	0.0005	0.0125	90.1273	3.259734789
45682.97	0.0047	0.0004	0.0129	93.1212	3.364046302
49856.84	0.0043	0.0004	0.0132	95.7511	3.442279937
54560.87	0.0039	0.0004	0.0136	98.5255	3.54659145
59721.84	0.0036	0.0002	0.0138	100	3.598747207

Inc Int %PV(ac)	Cum Int %PV(ac)	Pore Rad microns	W.P. Sat %PV(ac)	Lev "J" Funct.	G/B Pc psia
0	0	69.15655	100	2.26E-05	0.20944
0	0	61.1892	100	2.55E-05	0.23664
0	0	54.41825	100	2.87E-05	0.26656
0	0	49.2875	100	3.17E-05	0.29376
0	0	44.97985	100	3.48E-05	0.32232
0	0	41.00695	100	3.81E-05	0.3536
0	0	37.33985	100	4.19E-05	0.38896
0	0	34.18655	100	4.58E-05	0.42432
0	0	31.34575	100	4.99E-05	0.4624
0	0	28.62885	100	5.47E-05	0.50728
0	0	26.21015	100	5.97E-05	0.55352
0	0	24.04575	100	6.51E-05	0.60384
0	0	22.04195	100	7.1E-05	0.65824
0	0	20.1794	100	7.76E-05	0.71944
0	0	18.4213	100	8.49E-05	0.78744
0	0	16.85035	100	9.28E-05	0.86088
0	0	15.4468	100	0.000101	0.93976
0	0	14.1286	100	0.000111	1.0268
0	0	12.9189	100	0.000121	1.12336
0	0	11.7985	100	0.000133	1.22944
0	0	10.7969	100	0.000145	1.34368
0	0	9.90015	100	0.000158	1.46472
0	0	9.0635	100	0.000173	1.60072
0	0	8.29255	100	0.000189	1.74896
0	0	7.5264	100	0.000208	1.92712
0	0	6.9027	100	0.000227	2.1012
0	0	6.33315	100	0.000247	2.29024
0	0	5.7816	100	0.000271	2.5092
0	0	5.2699	100	0.000297	2.75264
0	0	4.82065	100	0.000325	3.00968
0	0	4.4043	100	0.000355	3.29392
0	0	4.02025	100	0.000389	3.60808
0	0	3.66975	100	0.000426	3.95352
0	0	3.27845	100	0.000477	4.42408
0	0	2.9519	100	0.00053	4.91368
0	0	2.7673	100	0.000565	5.24144
0	0	2.5613	100	0.000611	5.66304
0	0	2.35005	100	0.000666	6.17304
0	0	2.11495	100	0.00074	6.85848
0	0	1.9475	100	0.000803	7.44872
0	0	1.79965	100	0.000869	8.06072
0	0	1.63845	100	0.000955	8.8536
0	0	1.50035	100	0.001043	9.66824

0	0	1.36665	100	0.001145	10.6148
0	0	1.25245	100	0.001249	11.58176
0	0	1.14525	100	0.001366	12.66568
0	0	1.048	100	0.001493	13.84208
0	0	0.95445	100	0.001639	15.198
0	0	0.87345	100	0.001791	16.60696
0	0	0.7994	100	0.001957	18.14512
0	0	0.73435	100	0.00213	19.754
0	0	0.66815	100	0.002341	21.71104
0	0	0.60845	100	0.002571	23.84216
0	0	0.55845	100	0.002801	25.976
0	0	0.51085	100	0.003062	28.39544
0	0	0.46695	100	0.00335	31.06512
0	0	0.4255	100	0.003676	34.09112
0	0	0.3878	100	0.004034	37.40816
0	0	0.3533	100	0.004428	41.05704
0	0	0.3244	100	0.004823	44.71952
0	0	0.2955	100	0.005294	49.08784
0	0	0.27205	100	0.00575	53.32424
0	0	0.2474	100	0.006324	58.63912
0	0	0.2263	100	0.006912	64.09408
0	0	0.2067	100	0.007568	70.17872
0	0	0.18785	100	0.008327	77.214
0	0	0.17225	100	0.009081	84.20576
0	0	0.15845	100	0.009872	91.54704
0	0	0.14465	100	0.010815	100.2864
0	0	0.13255	100	0.011802	109.4419
0	0	0.1214	100	0.012886	119.4923
0	0	0.11075	100	0.014125	130.9857
0	0	0.10195	100	0.015341	142.2587
0	0	0.0931	100	0.016807	155.8492
0	0	0.085	100	0.018409	170.7072
0	0	0.0777	100	0.020139	186.7443
0	0	0.0707	100	0.022125	205.1642
0	0	0.06495	100	0.024085	223.3419
0	0	0.0592	100	0.026423	245.0162
0	0	0.05405	100	0.02893	268.2641
0	0	0.04945	100	0.031644	293.435
0	0	0.0451	100	0.034695	321.7298
0	0	0.0413	100	0.037876	351.2268
0	0	0.03785	100	0.041323	383.1922
0	0	0.03455	100	0.045265	419.7422
0	0	0.0316	100	0.049517	459.1714
0	0	0.02885	100	0.054206	502.6533
0	0	0.02635	100	0.059363	550.4777
0	0	0.02405	100	0.065003	602.771
0	0	0.0221	100	0.070837	656.8732

0	0	0.02015	100	0.077592	719.5066
0	0	0.01845	100	0.084856	786.8674
0	0	0.0168	100	0.093031	862.6738
0	0	0.0154	100	0.101683	942.9043
0	0	0.01405	100	0.111183	1031.001
0	0	0.01285	100	0.121503	1126.702
0	0	0.01175	100	0.133237	1235.511
0	0	0.01075	100	0.14565	1350.613
0	0	0.0098	100	0.159391	1478.037
0	0	0.009	100	0.173783	1611.493
1.834862385	1.834862385	0.00825	98.16513761	0.190154	1763.301
2.752293578	4.587155963	0.0075	95.41284404	0.208787	1936.084
2.752293578	7.339449541	0.00685	92.66055046	0.227873	2113.062
3.669724771	11.00917431	0.00625	88.99082569	0.249672	2315.208
9.174311927	20.18348624	0.0057	79.81651376	0.273563	2536.751
8.256880734	28.44036697	0.00525	71.55963303	0.29819	2765.111
8.256880734	36.69724771	0.0048	63.30275229	0.325954	3022.576
8.256880734	44.95412844	0.0044	55.04587156	0.356066	3301.803
10.09174312	55.04587156	0.004	44.95412844	0.389825	3614.85
9.174311927	64.22018349	0.00365	35.77981651	0.428052	3969.323
4.587155963	68.80733945	0.00335	31.19266055	0.467071	4331.146
7.339449541	76.14678899	0.00305	23.85321101	0.512479	4752.219
7.339449541	83.48623853	0.0028	16.51376147	0.560376	5196.368
4.587155963	88.0733945	0.00255	11.9266055	0.613306	5687.19
3.669724771	91.74311927	0.00235	8.256880734	0.669997	6212.884
2.752293578	94.49541284	0.00215	5.504587156	0.731212	6780.53
3.669724771	98.16513761	0.00195	1.834862385	0.800203	7420.278
1.834862385	100	0.0018	0	0.875895	8122.17

G/O Pc psia	O/B Pc psia	Ht FWL,ft G/B	Ht FWL,ft O/B	Swanson's Sb/Pc(ac)
0.1001	0.12628	0.5313	1.12112	-0.4910769
0.1131	0.14268	0.6003	1.26672	-0.4046567
0.1274	0.16072	0.6762	1.42688	-0.332626
0.1404	0.17712	0.7452	1.57248	-0.2897542
0.15405	0.19434	0.81765	1.72536	-0.2530765
0.169	0.2132	0.897	1.8928	-0.2306889
0.1859	0.23452	0.9867	2.08208	-0.2005991
0.2028	0.25584	1.0764	2.27136	-0.1671659
0.221	0.2788	1.173	2.4752	-0.1533993
0.24245	0.30586	1.28685	2.71544	-0.1398278
0.26455	0.33374	1.40415	2.96296	-0.1217395
0.2886	0.36408	1.5318	3.23232	-0.1115945
0.3146	0.39688	1.6698	3.52352	-0.1023718
0.34385	0.43378	1.82505	3.85112	-0.0936635
0.37635	0.47478	1.99755	4.21512	-0.0855751
0.41145	0.51906	2.18385	4.60824	-0.0741551
0.44915	0.56662	2.38395	5.03048	-0.0679308
0.49075	0.6191	2.60475	5.4964	-0.0621724
0.5369	0.67732	2.8497	6.01328	-0.0568283
0.5876	0.74128	3.1188	6.58112	-0.051925
0.6422	0.81016	3.4086	7.19264	-0.0475103
0.70005	0.88314	3.71565	7.84056	-0.0435842
0.76505	0.96514	4.06065	8.56856	-0.0398812
0.8359	1.05452	4.4367	9.36208	-0.0344731
0.92105	1.16194	4.88865	10.31576	-0.0312861
1.00425	1.2669	5.33025	11.2476	-0.0286941
1.0946	1.38088	5.8098	12.25952	-0.0263256
1.19925	1.5129	6.36525	13.4316	-0.0240284
1.3156	1.65968	6.9828	14.73472	-0.0219034
1.43845	1.81466	7.63485	16.11064	-0.0200327
1.5743	1.98604	8.3559	17.63216	-0.018304
1.72445	2.17546	9.15285	19.31384	-0.0157273
1.88955	2.38374	10.02915	21.16296	-0.0143531
2.11445	2.66746	11.22285	23.68184	-0.0128265
2.34845	2.96266	12.46485	26.30264	-0.0115485
2.5051	3.16028	13.2963	28.05712	-0.0108263
2.7066	3.41448	14.3658	30.31392	-0.0100203
2.95035	3.72198	15.65955	33.04392	-0.0091925
3.27795	4.13526	17.39835	36.71304	-0.0082738
3.56005	4.49114	18.89565	39.87256	-0.0076181
3.85255	4.86014	20.44815	43.14856	-0.0070398
4.2315	5.3382	22.4595	47.3928	-0.0064093
4.62085	5.82938	24.52605	51.75352	-0.0058693

5.07325	6.4001	26.92725	56.8204	-0.0053459
5.5354	6.98312	29.3802	61.99648	-0.0048996
6.05345	7.63666	32.12985	67.79864	-0.0044803
6.6157	8.34596	35.1141	74.09584	-0.0038433
7.26375	9.1635	38.55375	81.354	-0.0035004
7.93715	10.01302	42.12795	88.89608	-0.0032034
8.6723	10.94044	46.0299	97.12976	-0.0029319
9.44125	11.9105	50.11125	105.742	-0.0026931
10.3766	13.09048	55.0758	116.2179	-0.0024503
11.39515	14.37542	60.48195	127.6257	-0.0022313
12.415	15.662	65.895	139.048	-0.002048
13.57135	17.12078	72.03255	151.9991	-0.0018735
14.8473	18.73044	78.8049	166.2898	-0.0017125
16.29355	20.55494	86.48115	182.4878	-0.0015605
17.8789	22.55492	94.8957	200.2437	-0.0014221
19.62285	24.75498	104.1521	219.7759	-0.0012957
21.3733	26.96324	113.4429	239.381	-0.0011103
23.4611	29.59708	124.5243	262.7643	-0.0010115
25.48585	32.15138	135.2711	285.4415	-0.0009311
28.02605	35.35594	148.7537	313.8918	-0.0008467
30.6332	38.64496	162.5916	343.0918	-0.0007747
33.5413	42.31364	178.0269	375.6626	-0.000657
36.90375	46.5555	195.8738	413.322	-0.0005971
40.2454	50.77112	213.6102	450.7485	-0.0005475
43.7541	55.19748	232.2333	490.0459	-0.0005036
47.931	60.4668	254.403	536.8272	-0.0004597
52.3068	65.98704	277.6284	585.8362	-0.0004213
57.1103	72.04684	303.1239	639.6354	-0.0003858
62.60345	78.97666	332.2799	701.1586	-0.000352
67.9913	85.77364	360.8769	761.5026	-0.0003241
74.48675	93.9679	395.3528	834.2516	-0.0002958
81.588	102.9264	433.044	913.7856	-0.0002493
89.2528	112.5958	473.7264	999.6314	-0.0002279
98.0564	123.7019	520.4532	1098.232	-0.0002074
106.7443	134.662	566.5659	1195.536	-0.0001906
117.1034	147.7304	621.5486	1311.558	-0.0001737
128.2145	161.7475	680.5229	1436.002	-0.0001454
140.2447	176.924	744.3755	1570.74	-0.000133
153.7679	193.9841	816.1527	1722.2	-0.0001213
167.8658	211.7691	890.9798	1880.096	-0.0001111
183.1434	231.0424	972.0686	2051.206	-0.0001018
200.6121	253.0799	1064.787	2246.856	-8.449E-05
219.4569	276.8533	1164.81	2457.917	-7.724E-05
240.2387	303.0704	1275.113	2690.673	-6.35E-05
263.096	331.9057	1396.432	2946.675	-5.798E-05
288.0891	363.4355	1529.088	3226.598	-4.707E-05
313.9468	396.0559	1666.333	3516.204	-4.319E-05

343.8819	433.8202	1825.219	3851.477	-3.45E-05
376.0764	474.4348	1996.098	4212.055	-3.155E-05
412.3074	520.1416	2188.401	4617.842	-2.467E-05
450.6528	568.5158	2391.926	5047.311	-2.257E-05
492.7579	621.633	2615.407	5518.888	-1.72E-05
538.4971	679.3347	2858.177	6031.167	-1.259E-05
590.5016	744.9405	3134.201	6613.618	-8.612E-06
645.5137	814.3404	3426.188	7229.753	-5.252E-06
706.4148	891.1694	3749.432	7911.846	-2.4E-06
770.1987	971.6352	4087.977	8626.225	0
842.7543	1063.167	4473.08	9438.848	4.0227E-06
925.3342	1167.345	4911.389	10363.74	9.1592E-06
1009.919	1274.052	5360.341	11311.1	1.3427E-05
1106.533	1395.934	5873.139	12393.17	1.8382E-05
1212.418	1529.512	6435.14	13579.08	3.0758E-05
1321.561	1667.199	7014.437	14801.48	3.9761E-05
1444.613	1822.435	7667.563	16179.67	4.6935E-05
1578.067	1990.793	8375.896	17674.35	5.2633E-05
1727.686	2179.542	9170.024	19350.08	5.8867E-05
1897.103	2393.268	10069.24	21247.55	6.2545E-05
2070.033	2611.426	10987.1	23184.37	6.1414E-05
2271.281	2865.309	12055.26	25438.35	6.1943E-05
2483.558	3133.104	13181.96	27815.85	6.2109E-05
2718.142	3429.041	14427.06	30443.19	5.9867E-05
2969.393	3746.004	15760.62	33257.2	5.7084E-05
3240.695	4088.261	17200.61	36295.78	5.3875E-05
3546.457	4473.991	18823.5	39720.31	5.1142E-05
3881.92	4897.191	20604.03	43477.5	4.7595E-05
				6.2545E-05

AIR\MERCURY CAPILLARY PRESSURE DATA : BY GEOTECH

Spl @ 930.00m Vines-1

Bulk Volume = 8.1897cc
Closure @ 11849. psia
Pore Volume = 0.2328cc
Porosity = 2.84%
Median Pore Aperture = 0.0084 microns (dia.)

Injection Pressure (psia)	Pore Diameter (microns)	Hg (nwp) Saturation cum%PV	100-Hg(wp) Saturation cum%PV	Leverett "J" Function	Gas/Brine Pc (psia)	Gas/Oil Pc (psia)	Oil/Brine Pc (psia)	Ht. Above Free Water (ft.) Gas/Brine	Ht. Above Free Water (ft.) Oil/Brine
1.54	138.31	0.0	100.0	0.00	0.21	0.10	0.13	0.5	1.1
1.74	122.38	0.0	100.0	0.00	0.24	0.11	0.14	0.6	1.3
1.96	108.84	0.0	100.0	0.00	0.27	0.13	0.16	0.7	1.4
2.16	98.58	0.0	100.0	0.00	0.29	0.14	0.18	0.7	1.6
2.37	89.96	0.0	100.0	0.00	0.32	0.15	0.19	0.8	1.7
2.60	82.01	0.0	100.0	0.00	0.35	0.17	0.21	0.9	1.9
2.86	74.68	0.0	100.0	0.00	0.39	0.19	0.23	1.0	2.1
3.12	68.37	0.0	100.0	0.00	0.42	0.20	0.26	1.1	2.3
3.40	62.69	0.0	100.0	0.00	0.46	0.22	0.28	1.2	2.5
3.73	57.26	0.0	100.0	0.00	0.51	0.24	0.31	1.3	2.7
4.07	52.42	0.0	100.0	0.00	0.55	0.26	0.33	1.4	3.0
4.44	48.09	0.0	100.0	0.00	0.60	0.29	0.36	1.5	3.2
4.84	44.08	0.0	100.0	0.00	0.66	0.31	0.40	1.7	3.5
5.29	40.36	0.0	100.0	0.00	0.72	0.34	0.43	1.8	3.9
5.79	36.84	0.0	100.0	0.00	0.79	0.38	0.47	2.0	4.2
6.33	33.70	0.0	100.0	0.00	0.86	0.41	0.52	2.2	4.6
6.91	30.89	0.0	100.0	0.00	0.94	0.45	0.57	2.4	5.0
7.55	28.26	0.0	100.0	0.00	1.03	0.49	0.62	2.6	5.5
8.26	25.84	0.0	100.0	0.00	1.12	0.54	0.68	2.8	6.0
9.04	23.60	0.0	100.0	0.00	1.23	0.59	0.74	3.1	6.6
9.88	21.59	0.0	100.0	0.00	1.34	0.64	0.81	3.4	7.2
10.77	19.80	0.0	100.0	0.00	1.46	0.70	0.88	3.7	7.8
11.77	18.13	0.0	100.0	0.00	1.60	0.77	0.97	4.1	8.6
12.86	16.59	0.0	100.0	0.00	1.75	0.84	1.05	4.4	9.4
14.17	15.05	0.0	100.0	0.00	1.93	0.92	1.16	4.9	10.3
15.45	13.81	0.0	100.0	0.00	2.10	1.00	1.27	5.3	11.2
16.84	12.67	0.0	100.0	0.00	2.29	1.09	1.38	5.8	12.3
18.45	11.56	0.0	100.0	0.00	2.51	1.20	1.51	6.4	13.4
20.24	10.54	0.0	100.0	0.00	2.75	1.32	1.66	7.0	14.7
22.13	9.641	0.0	100.0	0.00	3.01	1.44	1.81	7.6	16.1
24.22	8.809	0.0	100.0	0.00	3.29	1.57	1.99	8.4	17.6
26.53	8.041	0.0	100.0	0.00	3.61	1.72	2.18	9.2	19.3
29.07	7.340	0.0	100.0	0.00	3.95	1.89	2.38	10.0	21.2
32.53	6.557	0.0	100.0	0.00	4.42	2.11	2.67	11.2	23.7
36.13	5.904	0.0	100.0	0.00	4.91	2.35	2.96	12.5	26.3

AIR\MERCURY CAPILLARY PRESSURE DATA : BY GEOTECH

Spl @ 930.00m Vines-1

Injection Pressure (psia)	Pore Diameter (microns)	Hg (nwp) Saturation cum%PV	100-Hg(wp) Saturation cum%PV	Leverett "J" Function	Gas/Brine Pc (psia)	Gas/Oil Pc (psia)	Oil/Brine Pc (psia)	Ht. Above Free Water (ft.) Gas/Brine	Ht. Above Free Water (ft.) Oil/Brine
38.54	5.535	0.0	100.0	0.00	5.24	2.51	3.16	13.3	28.1
41.64	5.123	0.0	100.0	0.00	5.66	2.71	3.41	14.4	30.3
45.39	4.700	0.0	100.0	0.00	6.17	2.95	3.72	15.7	33.0
50.43	4.230	0.0	100.0	0.00	6.86	3.28	4.14	17.4	36.7
54.77	3.895	0.0	100.0	0.00	7.45	3.56	4.49	18.9	39.9
59.27	3.599	0.0	100.0	0.00	8.06	3.85	4.86	20.4	43.1
65.10	3.277	0.0	100.0	0.00	8.85	4.23	5.34	22.5	47.4
71.09	3.001	0.0	100.0	0.00	9.67	4.62	5.83	24.5	51.8
78.05	2.733	0.0	100.0	0.00	10.61	5.07	6.40	26.9	56.8
85.16	2.505	0.0	100.0	0.00	11.58	5.54	6.98	29.4	62.0
93.13	2.291	0.0	100.0	0.00	12.67	6.05	7.64	32.1	67.8
101.78	2.096	0.0	100.0	0.00	13.84	6.62	8.35	35.1	74.1
111.75	1.909	0.0	100.0	0.00	15.20	7.26	9.16	38.6	81.4
122.11	1.747	0.0	100.0	0.00	16.61	7.94	10.01	42.1	88.9
133.42	1.599	0.0	100.0	0.00	18.15	8.67	10.94	46.0	97.1
145.25	1.469	0.0	100.0	0.00	19.75	9.44	11.91	50.1	105.7
159.64	1.336	0.0	100.0	0.00	21.71	10.38	13.09	55.1	116.2
175.31	1.217	0.0	100.0	0.00	23.84	11.40	14.38	60.5	128
191.00	1.117	0.0	100.0	0.00	25.98	12.42	15.66	65.9	139
208.79	1.022	0.0	100.0	0.00	28.40	13.57	17.12	72.0	152
228.42	0.934	0.0	100.0	0.00	31.07	14.85	18.73	78.8	166
250.67	0.851	0.0	100.0	0.00	34.09	16.29	20.55	86.5	182
275.06	0.776	0.0	100.0	0.00	37.41	17.88	22.55	95	200
301.89	0.707	0.0	100.0	0.00	41.06	19.62	24.75	104	220
328.82	0.649	0.0	100.0	0.00	44.72	21.37	26.96	113	239
360.94	0.591	0.0	100.0	0.01	49.09	23.46	29.60	125	263
392.09	0.544	0.0	100.0	0.01	53.32	25.49	32.15	135	285
431.17	0.495	0.0	100.0	0.01	58.64	28.03	35.36	149	314
471.28	0.453	0.0	100.0	0.01	64.09	30.63	38.64	163	343
516.02	0.413	0.0	100.0	0.01	70.18	33.54	42.31	178	376
567.75	0.376	0.0	100.0	0.01	77.21	36.90	46.56	196	413
619.16	0.345	0.0	100.0	0.01	84.21	40.25	50.77	214	451
673.14	0.317	0.0	100.0	0.01	91.55	43.75	55.20	232	490
737.40	0.289	0.0	100.0	0.01	100.29	47.93	60.47	254	537
804.72	0.265	0.0	100.0	0.01	109.44	52.31	65.99	278	586
878.62	0.243	0.0	100.0	0.01	119.49	57.11	72.05	303	640
963.13	0.222	0.0	100.0	0.01	130.99	62.60	78.98	332	701
1046.02	0.204	0.0	100.0	0.02	142.26	67.99	85.77	361	762
1145.95	0.186	0.0	100.0	0.02	155.85	74.49	93.97	395	834
1255.20	0.170	0.0	100.0	0.02	170.71	81.59	102.93	433	914
1373.12	0.155	0.0	100.0	0.02	186.74	89.25	112.60	474	1000
1508.56	0.141	0.0	100.0	0.02	205.16	98.06	123.70	520	1098
1642.22	0.130	0.0	100.0	0.02	223.34	106.74	134.66	567	1196

AIR\MERCURY CAPILLARY PRESSURE DATA : BY GEOTECH

Spl @ 930.00m Vines-1

Injection Pressure (psia)	Pore Diameter (microns)	Hg (nwp) Saturation cum%PV	100-Hg(wp) Saturation cum%PV	Leverett "J" Function	Gas/Brine Pc (psia)	Gas/Oil Pc (psia)	Oil/Brine Pc (psia)	Ht. Above Free Water (ft.) Gas/Brine	Ht. Above Free Water (ft.) Oil/Brine
1801.59	0.118	0.0	100.0	0.03	245.02	117.10	147.73	622	1312
1972.53	0.108	0.0	100.0	0.03	268.26	128.21	161.75	681	1436
2157.61	0.0989	0.0	100.0	0.03	293.43	140.24	176.92	744	1571
2365.66	0.0902	0.0	100.0	0.03	321.73	153.77	193.98	816	1722
2582.55	0.0826	0.0	100.0	0.04	351.23	167.87	211.77	891	1880
2817.59	0.0757	0.0	100.0	0.04	383.19	183.14	231.04	972	2051
3086.34	0.0691	0.0	100.0	0.05	419.74	200.61	253.08	1065	2247
3376.26	0.0632	0.0	100.0	0.05	459.17	219.46	276.85	1165	2458
3695.98	0.0577	0.0	100.0	0.05	502.65	240.24	303.07	1275	2691
4047.63	0.0527	0.0	100.0	0.06	550.48	263.10	331.91	1396	2947
4432.14	0.0481	0.0	100.0	0.07	602.77	288.09	363.44	1529	3227
4829.95	0.0442	0.0	100.0	0.07	656.87	313.95	396.06	1666	3516
5290.49	0.0403	0.0	100.0	0.08	719.51	343.88	433.82	1825	3851
5785.79	0.0369	0.0	100.0	0.08	786.87	376.08	474.43	1996	4212
6343.19	0.0336	0.0	100.0	0.09	862.67	412.31	520.14	2188	4618
6933.12	0.0308	0.0	100.0	0.10	942.90	450.65	568.52	2392	5047
7580.89	0.0281	0.0	100.0	0.11	1031.00	492.76	621.63	2615	5519
8284.57	0.0257	0.0	100.0	0.12	1126.70	538.50	679.33	2858	6031
9084.64	0.0235	0.0	100.0	0.13	1235.51	590.50	744.94	3134	6614
9930.98	0.0215	0.0	100.0	0.15	1350.61	645.51	814.34	3426	7230
10867.92	0.0196	0.0	100.0	0.16	1478.04	706.41	891.17	3749	7912
11849.21	0.0180	0.0	100.0	0.17	1611.49	770.20	971.64	4088	8626
12965.45	0.0165	1.8	98.2	0.19	1763.30	842.75	1063.17	4473	9439
14235.91	0.0150	4.6	95.4	0.21	1936.08	925.33	1167.34	4911	10364
15537.22	0.0137	7.3	92.7	0.23	2113.06	1009.92	1274.05	5360	11311
17023.59	0.0125	11.0	89.0	0.25	2315.21	1106.53	1395.93	5873	12393
18652.58	0.0114	20.2	79.8	0.27	2536.75	1212.42	1529.51	6435	13579
20331.70	0.0105	28.4	71.6	0.30	2765.11	1321.56	1667.20	7014	14801
22224.82	0.0096	36.7	63.3	0.33	3022.58	1444.61	1822.44	7668	16180
24277.96	0.0088	45.0	55.0	0.36	3301.80	1578.07	1990.79	8376	17674
26579.78	0.0080	55.0	45.0	0.39	3614.85	1727.69	2179.54	9170	19350
29186.20	0.0073	64.2	35.8	0.43	3969.32	1897.10	2393.27	10069	21248
31846.66	0.0067	68.8	31.2	0.47	4331.15	2070.03	2611.43	10987	23184
34942.79	0.0061	76.1	23.9	0.51	4752.22	2271.28	2865.31	12055	25438
38208.59	0.0056	83.5	16.5	0.56	5196.37	2483.56	3133.10	13182	27816
41817.57	0.0051	88.1	11.9	0.61	5687.19	2718.14	3429.04	14427	30443
45682.97	0.0047	91.7	8.3	0.67	6212.88	2969.39	3746.00	15761	33257
49856.84	0.0043	94.5	5.5	0.73	6780.53	3240.69	4088.26	17201	36296
54560.87	0.0039	98.2	1.8	0.80	7420.28	3546.46	4473.99	18824	39720
59721.84	0.0036	100.0	0.0	0.88	8122.17	3881.92	4897.19	20604	43477

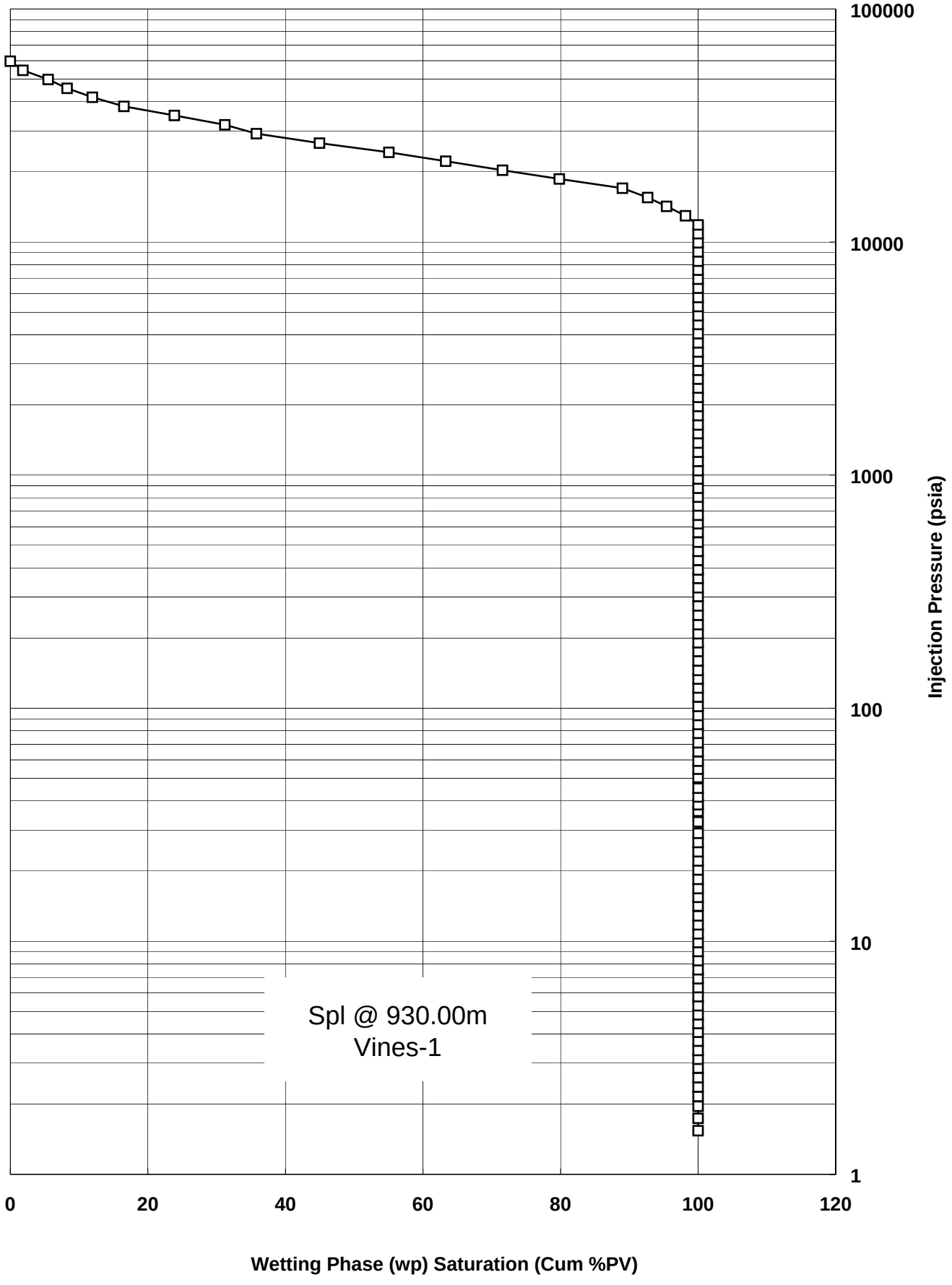
100000
10000
1000
100
10
1
Injection Pressure (psia)
0
20
40
60
80
100
120
Wetting Phase (wp) Saturation (Cum %PV)
Spl @ 930.00m
Vines-1

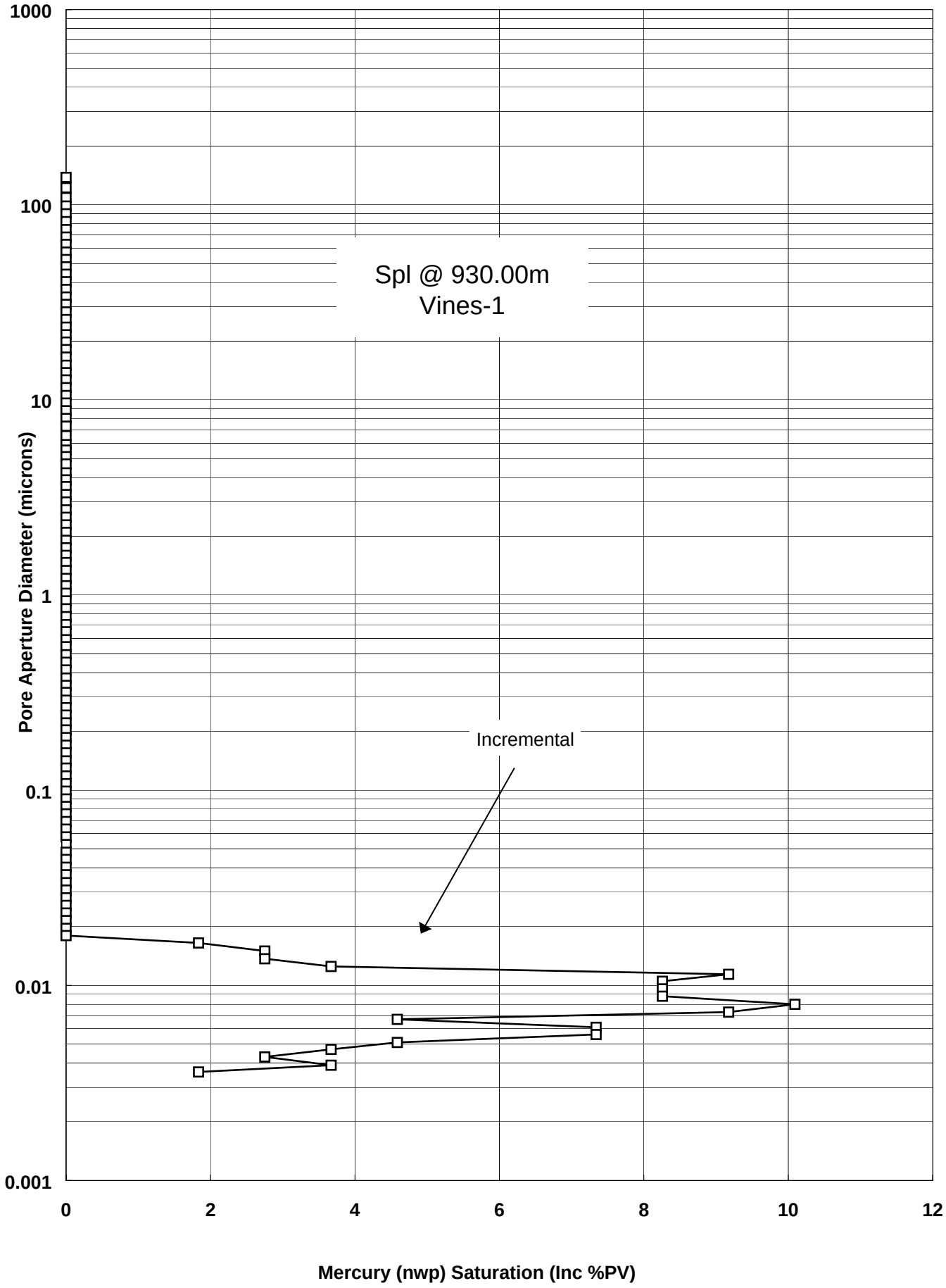
Spl @ 930.00m
Vines-1
Incremental
Pore Aperture Diameter (microns)
1000
100
10
1
0.1
0.01
0.001
0
2
4
6
8
10
12
Mercury (nwp) Saturation (Inc %PV)

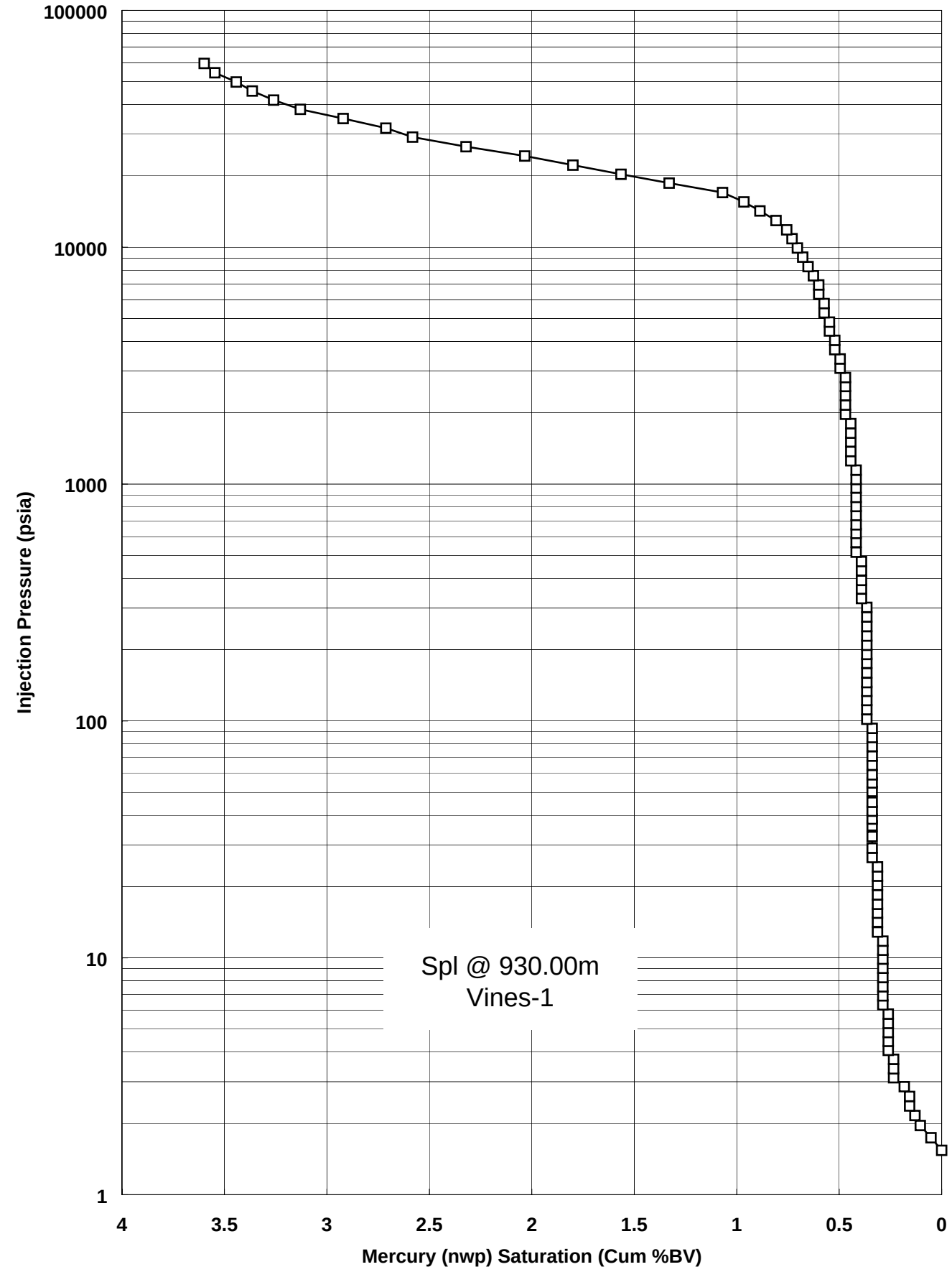
100000
10000
1000
100
10
1
Injection Pressure (psia)
4
3.5
3
2.5
2
1.5
1
0.5
0
Mercury (nwp) Saturation (Cum %BV)
Spl @ 930.00m
Vines-1

Appendix 11

Chemical analysis of drillcore from Vines 1 to assess potential for base metals

by I. Ruddock

Seven drillcore samples were collected from diamictite and siltstone intervals in Vines 1 to test the potential for sedimentary hosted base-metal mineralization. The samples were analysed for the following nine elements: Ag, As, Ba, Co, Cu, Mn, P, Pb, and Zn.

Core samples were obtained as 2.0 m intervals of edge-slabbed HQ core (aproximately 1 cm edge slices). Sampled intervals were selected to provide a spot check of zones that had the most likely mineral potential; those intervals where minor sulfides or evaporitic minerals were observed.

Sample preparation and analysis was undertaken by Genalysis Laboratory Services in Maddington, W.A.. Crushing and pulverising were carried out using a jaw crusher and a chrome steel ring grinder. Sample dissolution was by digestion in a multi-acid mixture of hydrofluoric, hydrochloric, nitric, and perchloric acids. Sample solutions were analysed by inductively coupled plasma optical-emssion spectrography.

Sample analyses are shown in Table 11.1. Results from the core sampling are not encouraging for base metal potential.

Table 11.1. Drillcore analyses

Depth (m)	*Ag*	*As*	*Ba*	*Co*	*Cu*	*Mn*	*P*	*Pb*	*Zn*
				Parts per million					
618.0 – 620.0	x	x	1 261	12	20	906	588	52	88
1 068.0 – 1 070.0	x	6	408	11	24	315	462	43	63
1 380.0 – 1 382.0	x	x	411	14	25	566	518	19	65
1 396.0 – 1 398.0	x	x	259	14	24	798	472	30	67
1 443.0 – 1 445.0	x	11	339	16	24	506	524	22	65
1 632.0 – 1 634.0	x	8	412	7	12	432	280	19	41
2 014.0 – 2 016.0	x	8	386	18	33	468	588	28	78
Detection limit	2	5	2	2	1	1	20	5	1

NOTES: 'x' denotes result that is less than detection limit

Appendix 12

Well index sheet

ORGANIZATION: Geological Survey of Western Australia
WELL: Vines 1
SPUDDED: 4 July 1999
COMPLETED: 8 August 1999
TD: 2017.5 m
STATUS: Plugged and abandoned

BASIN: Officer Basin

ELEV. GL: 472 m AHD (differential GPS)
LAT: 26°42'04.87"S; **LONG:** 128°15'07.72"E
EASTING: 425605; **NORTHING:** 7046424
ZONE: GDA94 Zone 52

STATUTORY PETROLEUM EXPLORATION REPORT NO: S20623
TYPE: Stratigraphic

FORMATION	TOPS (m)		LITHOLOGICAL SUMMARY
	DRILL	SUBSEA	
Unit 6	4	+468	Sandstone, conglomerate
Unit 5	124.7	+347.3	Sandstone, conglomerate, claystone
Unit 4	301.5	+170.5	Sandstone, diamictite, claystone
Unit 3	779.2	-307.2	Diamictite, sandstone, siltstone, claystone
Unit 2	1228.5	-756.5	Siltstone, diamictite, sandstone
Unit 1	1632	-1160	Sandstone, siltstone, diamictite
Total depth	**2017.5**	**-1545.5**	

CORES	Fully cored:	PQ: 44.5 – 625 m	(99.7% recovery)
		HQ: 625 – 1741.5 m	(100% recovery)
		NQ: 1741.5 – 2017.5 m	(100% recovery)
LOGS	Dual laterolog, compensated sonic, SP, gamma ray, caliper		625–2018 m
	Density, compensated neutron, gamma ray, caliper		0–2018 m
	Dipmeter, gamma ray, caliper		625–2011 m
	Cement bond, gamma ray		0–620 m
CASING	177.8 mm 7"	44.5 m	
	122.6 mm PF	624 m	
	96.1 mm HQ	1741.5 m (HQ rods as temporary casing)	

GSWA RECORD 2001/16 Plate 1

Department of Mineral and Petroleum Resources

GSWA Vines 1

Geological Survey of Western Australia

GSWA Vines 1

Composite well log

Scale 1:500

Operator: Geological Survey of WA
Well name: Vines 1
Alias:
Basin: Officer
Region: Yilgarn Craft
Field:
Discovery well:
Status: Dry
Purpose: Stratigraphic
Type: Vertical
Datum elevation: 0 m
Ground elevation: 0 m
Total depth driller: 1,000.00 m
Total depth logger: 1,000.00 m
Spud date: 1 Jan 2000
Completion date: 1 Jan 2000
Run number: One

Logged interval: 0.00 m to 1,000.00 m

Run	Logged interval	Hole size
One	0.00 m to 1,000.00 m	152.4 mm

Casing	Shoe depth	Hole size
Conductor	0.00 m	152.4 mm
Surface	0.00 m	152.4 mm
Intermediate	0.00 m	152.4 mm
Production	0.00 m	152.4 mm
Liner	0.00 m	152.4 mm

Mud type	Mud weight	Viscosity	Fluid loss
Water	1.00 g/cm³	1 cP	0 mL

Bit run	Bit size	Bit type	Interval
One	152.4 mm	Tricone	0.00 m to 1,000.00 m

Tool	Serial number	Interval
Gamma ray	GR-001	0.00 m to 1,000.00 m
Density	DEN-001	0.00 m to 1,000.00 m
Neutron	NEU-001	0.00 m to 1,000.00 m
Resistivity	RES-001	0.00 m to 1,000.00 m
Sonic	SON-001	0.00 m to 1,000.00 m
Caliper	CAL-001	0.00 m to 1,000.00 m
Temperature	TEMP-001	0.00 m to 1,000.00 m

Recorded by: Schlumberger
Witnessed by: GSWA
Processed by: GSWA
Depth reference: Ground level
Log datum: Ground level
Permanent datum: Ground level
Elevation of kelly bushing: 0 m above ground level
Elevation of derrick floor: 0 m above ground level
Elevation of ground level: 0 m
Elevation of mean sea level: 0 m
Elevation of rotary table: 0 m above ground level
Elevation of drill floor: 0 m above ground level
Elevation of casing flange: 0 m above ground level
Elevation of tubing head: 0 m above ground level
Elevation of christmas tree: 0 m above ground level
Elevation of wellhead: 0 m above ground level
Elevation of blowout preventer: 0 m above ground level
Elevation of rig floor: 0 m above ground level
Elevation of rig substructure: 0 m above ground level
Elevation of rig derrick: 0 m above ground level
Elevation of rig crown block: 0 m above ground level
Elevation of rig traveling block: 0 m above ground level
Elevation of rig swivel: 0 m above ground level
Elevation of rig kelly: 0 m above ground level
Elevation of rig drawworks: 0 m above ground level
Elevation of rig mud pump: 0 m above ground level
Elevation of rig shale shaker: 0 m above ground level
Elevation of rig desander: 0 m above ground level
Elevation of rig desilter: 0 m above ground level
Elevation of rig mud cleaner: 0 m above ground level
Elevation of rig centrifuge: 0 m above ground level
Elevation of rig degasser: 0 m above ground level
Elevation of rig mud tank: 0 m above ground level
Elevation of rig trip tank: 0 m above ground level
Elevation of rig pill pit: 0 m above ground level
Elevation of rig reserve pit: 0 m above ground level
Elevation of rig flare pit: 0 m above ground level
Elevation of rig burn pit: 0 m above ground level
Elevation of rig waste pit: 0 m above ground level
Elevation of rig sump pit: 0 m above ground level
Elevation of rig cellar: 0 m above ground level
Elevation of rig rathole: 0 m above ground level
Elevation of rig mousehole: 0 m above ground level
Elevation of rig doghouse: 0 m above ground level
Elevation of rig toolpusher's office: 0 m above ground level
Elevation of rig crew quarters: 0 m above ground level
Elevation of rig galley: 0 m above ground level
Elevation of rig radio room: 0 m above ground level
Elevation of rig helideck: 0 m above ground level
Elevation of rig emergency shelter: 0 m above ground level
Elevation of rig lifeboat station: 0 m above ground level
Elevation of rig muster point: 0 m above ground level
Elevation of rig assembly point: 0 m above ground level
Elevation of rig evacuation route: 0 m above ground level
Elevation of rig escape route: 0 m above ground level
Elevation of rig fire extinguisher: 0 m above ground level
Elevation of rig fire hose: 0 m above ground level
Elevation of rig fire alarm: 0 m above ground level
Elevation of rig gas detector: 0 m above ground level
Elevation of rig H2S detector: 0 m above ground level
Elevation of rig CO2 detector: 0 m above ground level
Elevation of rig LEL detector: 0 m above ground level
Elevation of rig oxygen detector: 0 m above ground level
Elevation of rig radiation detector: 0 m above ground level
Elevation of rig noise detector: 0 m above ground level
Elevation of rig vibration detector: 0 m above ground level
Elevation of rig temperature detector: 0 m above ground level
Elevation of rig pressure detector: 0 m above ground level
Elevation of rig flow detector: 0 m above ground level
Elevation of rig level detector: 0 m above ground level
Elevation of rig weight detector: 0 m above ground level
Elevation of rig speed detector: 0 m above ground level
Elevation of rig position detector: 0 m above ground level
Elevation of rig motion detector: 0 m above ground level
Elevation of rig sound detector: 0 m above ground level
Elevation of rig light detector: 0 m above ground level
Elevation of rig camera: 0 m above ground level
Elevation of rig video recorder: 0 m above ground level
Elevation of rig data logger: 0 m above ground level
Elevation of rig computer: 0 m above ground level
Elevation of rig software: 0 m above ground level
Elevation of rig hardware: 0 m above ground level
Elevation of rig network: 0 m above ground level
Elevation of rig server: 0 m above ground level
Elevation of rig client: 0 m above ground level
Elevation of rig printer: 0 m above ground level
Elevation of rig plotter: 0 m above ground level
Elevation of rig scanner: 0 m above ground level
Elevation of rig modem: 0 m above ground level
Elevation of rig router: 0 m above ground level
Elevation of rig switch: 0 m above ground level
Elevation of rig firewall: 0 m above ground level
Elevation of rig antivirus: 0 m above ground level
Elevation of rig backup: 0 m above ground level
Elevation of rig restore: 0 m above ground level
Elevation of rig archive: 0 m above ground level
Elevation of rig retrieve: 0 m above ground level
Elevation of rig delete: 0 m above ground level
Elevation of rig format: 0 m above ground level
Elevation of rig partition: 0 m above ground level
Elevation of rig mount: 0 m above ground level
Elevation of rig unmount: 0 m above ground level
Elevation of rig share: 0 m above ground level
Elevation of rig permission: 0 m above ground level
Elevation of rig user: 0 m above ground level
Elevation of rig group: 0 m above ground level
Elevation of rig password: 0 m above ground level
Elevation of rig encryption: 0 m above ground level
Elevation of rig decryption: 0 m above ground level
Elevation of rig key: 0 m above ground level
Elevation of rig certificate: 0 m above ground level
Elevation of rig authority: 0 m above ground level
Elevation of rig signature: 0 m above ground level
Elevation of rig hash: 0 m above ground level
Elevation of rig checksum: 0 m above ground level
Elevation of rig backup: 0 m above ground level
Elevation of rig restore: 0 m above ground level
Elevation of rig archive: 0 m above ground level
Elevation of rig retrieve: 0 m above ground level
Elevation of rig delete: 0 m above ground level
Elevation of rig format: 0 m above ground level
Elevation of rig partition: 0 m above ground level
Elevation of rig mount: 0 m above ground level
Elevation of rig unmount: 0 m above ground level
Elevation of rig share: 0 m above ground level
Elevation of rig permission: 0 m above ground level
Elevation of rig user: 0 m above ground level
Elevation of rig group: 0 m above ground level
Elevation of rig password: 0 m above ground level
Elevation of rig encryption: 0 m above ground level
Elevation of rig decryption: 0 m above ground level
Elevation of rig key: 0 m above ground level
Elevation of rig certificate: 0 m above ground level
Elevation of rig authority: 0 m above ground level
Elevation of rig signature: 0 m above ground level
Elevation of rig hash: 0 m above ground level
Elevation of rig checksum: 0 m above ground level

Notes:
1. Depths are measured from the rotary table (RT) unless otherwise stated.
2. All logs were run in a single run unless otherwise stated.
3. Casing and hole sizes are nominal.
4. Mud properties are typical values.
5. Bit runs are numbered sequentially.
6. Tool serial numbers are fictitious.
7. Logged intervals may not be continuous.
8. Elevations are relative to ground level.
9. Permanent datum is the reference for all depths.
10. Log datum is the reference for all depths.
11. Depth reference is the reference for all depths.
12. Elevations are relative to mean sea level.
13. Elevations are relative to the rotary table.
14. Elevations are relative to the kelly bushing.
15. Elevations are relative to the drill floor.
16. Elevations are relative to the casing flange.
17. Elevations are relative to the tubing head.
18. Elevations are relative to the christmas tree.
19. Elevations are relative to the wellhead.
20. Elevations are relative to the blowout preventer.
21. Elevations are relative to the rig floor.
22. Elevations are relative to the rig substructure.
23. Elevations are relative to the rig derrick.
24. Elevations are relative to the rig crown block.
25. Elevations are relative to the rig traveling block.
26. Elevations are relative to the rig swivel.
27. Elevations are relative to the rig kelly.
28. Elevations are relative to the rig drawworks.
29. Elevations are relative to the rig mud pump.
30. Elevations are relative to the rig shale shaker.
31. Elevations are relative to the rig desander.
32. Elevations are relative to the rig desilter.
33. Elevations are relative to the rig mud cleaner.
34. Elevations are relative to the rig centrifuge.
35. Elevations are relative to the rig degasser.
36. Elevations are relative to the rig mud tank.
37. Elevations are relative to the rig trip tank.
38. Elevations are relative to the rig pill pit.
39. Elevations are relative to the rig reserve pit.
40. Elevations are relative to the rig flare pit.
41. Elevations are relative to the rig burn pit.
42. Elevations are relative to the rig waste pit.
43. Elevations are relative to the rig sump pit.
44. Elevations are relative to the rig cellar.
45. Elevations are relative to the rig rathole.
46. Elevations are relative to the rig mousehole.
47. Elevations are relative to the rig doghouse.
48. Elevations are relative to the rig toolpusher's office.
49. Elevations are relative to the rig crew quarters.
50. Elevations are relative to the rig galley.
51. Elevations are relative to the rig radio room.
52. Elevations are relative to the rig helideck.
53. Elevations are relative to the rig emergency shelter.
54. Elevations are relative to the rig lifeboat station.
55. Elevations are relative to the rig muster point.
56. Elevations are relative to the rig assembly point.
57. Elevations are relative to the rig evacuation route.
58. Elevations are relative to the rig escape route.
59. Elevations are relative to the rig fire extinguisher.
60. Elevations are relative to the rig fire hose.
61. Elevations are relative to the rig fire alarm.
62. Elevations are relative to the rig gas detector.
63. Elevations are relative to the rig H2S detector.
64. Elevations are relative to the rig CO2 detector.
65. Elevations are relative to the rig LEL detector.
66. Elevations are relative to the rig oxygen detector.
67. Elevations are relative to the rig radiation detector.
68. Elevations are relative to the rig noise detector.
69. Elevations are relative to the rig vibration detector.
70. Elevations are relative to the rig temperature detector.
71. Elevations are relative to the rig pressure detector.
72. Elevations are relative to the rig flow detector.
73. Elevations are relative to the rig level detector.
74. Elevations are relative to the rig weight detector.
75. Elevations are relative to the rig speed detector.
76. Elevations are relative to the rig position detector.
77. Elevations are relative to the rig motion detector.
78. Elevations are relative to the rig sound detector.
79. Elevations are relative to the rig light detector.
80. Elevations are relative to the rig camera.
81. Elevations are relative to the rig video recorder.
82. Elevations are relative to the rig data logger.
83. Elevations are relative to the rig computer.
84. Elevations are relative to the rig software.
85. Elevations are relative to the rig hardware.
86. Elevations are relative to the rig network.
87. Elevations are relative to the rig server.
88. Elevations are relative to the rig client.
89. Elevations are relative to the rig printer.
90. Elevations are relative to the rig plotter.
91. Elevations are relative to the rig scanner.
92. Elevations are relative to the rig modem.
93. Elevations are relative to the rig router.
94. Elevations are relative to the rig switch.
95. Elevations are relative to the rig firewall.
96. Elevations are relative to the rig antivirus.
97. Elevations are relative to the rig backup.
98. Elevations are relative to the rig restore.
99. Elevations are relative to the rig archive.
100. Elevations are relative to the rig retrieve.
101. Elevations are relative to the rig delete.
102. Elevations are relative to the rig format.
103. Elevations are relative to the rig partition.
104. Elevations are relative to the rig mount.
105. Elevations are relative to the rig unmount.
106. Elevations are relative to the rig share.
107. Elevations are relative to the rig permission.
108. Elevations are relative to the rig user.
109. Elevations are relative to the rig group.
110. Elevations are relative to the rig password.
111. Elevations are relative to the rig encryption.
112. Elevations are relative to the rig decryption.
113. Elevations are relative to the rig key.
114. Elevations are relative to the rig certificate.
115. Elevations are relative to the rig authority.
116. Elevations are relative to the rig signature.
117. Elevations are relative to the rig hash.
118. Elevations are relative to the rig checksum.
119. Elevations are relative to the rig backup.
120. Elevations are relative to the rig restore.
121. Elevations are relative to the rig archive.
122. Elevations are relative to the rig retrieve.
123. Elevations are relative to the rig delete.
124. Elevations are relative to the rig format.
125. Elevations are relative to the rig partition.
126. Elevations are relative to the rig mount.
127. Elevations are relative to the rig unmount.
128. Elevations are relative to the rig share.
129. Elevations are relative to the rig permission.
130. Elevations are relative to the rig user.
131. Elevations are relative to the rig group.
132. Elevations are relative to the rig password.
133. Elevations are relative to the rig encryption.
134. Elevations are relative to the rig decryption.
135. Elevations are relative to the rig key.
136. Elevations are relative to the rig certificate.
137. Elevations are relative to the rig authority.
138. Elevations are relative to the rig signature.
139. Elevations are relative to the rig hash.
140. Elevations are relative to the rig checksum.
141. Elevations are relative to the rig backup.
142. Elevations are relative to the rig restore.
143. Elevations are relative to the rig archive.
144. Elevations are relative to the rig retrieve.
145. Elevations are relative to the rig delete.
146. Elevations are relative to the rig format.
147. Elevations are relative to the rig partition.
148. Elevations are relative to the rig mount.
149. Elevations are relative to the rig unmount.
150. Elevations are relative to the rig share.
151. Elevations are relative to the rig permission.
152. Elevations are relative to the rig user.
153. Elevations are relative to the rig group.
154. Elevations are relative to the rig password.
155. Elevations are relative to the rig encryption.
156. Elevations are relative to the rig decryption.
157. Elevations are relative to the rig key.
158. Elevations are relative to the rig certificate.
159. Elevations are relative to the rig authority.
160. Elevations are relative to the rig signature.
161. Elevations are relative to the rig hash.
162. Elevations are relative to the rig checksum.
163. Elevations are relative to the rig backup.
164. Elevations are relative to the rig restore.
165. Elevations are relative to the rig archive.
166. Elevations are relative to the rig retrieve.
167. Elevations are relative to the rig delete.
168. Elevations are relative to the rig format.
169. Elevations are relative to the rig partition.
170. Elevations are relative to the rig mount.
171. Elevations are relative to the rig unmount.
172. Elevations are relative to the rig share.
173. Elevations are relative to the rig permission.
174. Elevations are relative to the rig user.
175. Elevations are relative to the rig group.
176. Elevations are relative to the rig password.
177. Elevations are relative to the rig encryption.
178. Elevations are relative to the rig decryption.
179. Elevations are relative to the rig key.
180. Elevations are relative to the rig certificate.
181. Elevations are relative to the rig authority.
182. Elevations are relative to the rig signature.
183. Elevations are relative to the rig hash.
184. Elevations are relative to the rig checksum.
185. Elevations are relative to the rig backup.
186. Elevations are relative to the rig restore.
187. Elevations are relative to the rig archive.
188. Elevations are relative to the rig retrieve.
189. Elevations are relative to the rig delete.
190. Elevations are relative to the rig format.
191. Elevations are relative to the rig partition.
192. Elevations are relative to the rig mount.
193. Elevations are relative to the rig unmount.
194. Elevations are relative to the rig share.
195. Elevations are relative to the rig permission.
196. Elevations are relative to the rig user.
197. Elevations are relative to the rig group.
198. Elevations are relative to the rig password.
199. Elevations are relative to the rig encryption.
200. Elevations are relative to the rig decryption.
201. Elevations are relative to the rig key.
202. Elevations are relative to the rig certificate.
203. Elevations are relative to the rig authority.
204. Elevations are relative to the rig signature.
205. Elevations are relative to the rig hash.
206. Elevations are relative to the rig checksum.
207. Elevations are relative to the rig backup.
208. Elevations are relative to the rig restore.
209. Elevations are relative to the rig archive.
210. Elevations are relative to the rig retrieve.
211. Elevations are relative to the rig delete.
212. Elevations are relative to the rig format.
213. Elevations are relative to the rig partition.
214. Elevations are relative to the rig mount.
215. Elevations are relative to the rig unmount.
216. Elevations are relative to the rig share.
217. Elevations are relative to the rig permission.
218. Elevations are relative to the rig user.
219. Elevations are relative to the rig group.
220. Elevations are relative to the rig password.
221. Elevations are relative to the rig encryption.
222. Elevations are relative to the rig decryption.
223. Elevations are relative to the rig key.
224. Elevations are relative to the rig certificate.
225. Elevations are relative to the rig authority.
226. Elevations are relative to the rig signature.
227. Elevations are relative to the rig hash.
228. Elevations are relative to the rig checksum.
229. Elevations are relative to the rig backup.
230. Elevations are relative to the rig restore.
231. Elevations are relative to the rig archive.
232. Elevations are relative to the rig retrieve.
233. Elevations are relative to the rig delete.
234. Elevations are relative to the rig format.
235. Elevations are relative to the rig partition.
236. Elevations are relative to the rig mount.
237. Elevations are relative to the rig unmount.
238. Elevations are relative to the rig share.
239. Elevations are relative to the rig permission.
240. Elevations are relative to the rig user.
241. Elevations are relative to the rig group.
242. Elevations are relative to the rig password.
243. Elevations are relative to the rig encryption.
244. Elevations are relative to the rig decryption.
245. Elevations are relative to the rig key.
246. Elevations are relative to the rig certificate.
247. Elevations are relative to the rig authority.
248. Elevations are relative to the rig signature.
249. Elevations are relative to the rig hash.
250. Elevations are relative to the rig checksum.
251. Elevations are relative to the rig backup.
252. Elevations are relative to the rig restore.
253. Elevations are relative to the rig archive.
254. Elevations are relative to the rig retrieve.
255. Elevations are relative to the rig delete.
256. Elevations are relative to the rig format.
257. Elevations are relative to the rig partition.
258. Elevations are relative to the rig mount.
259. Elevations are relative to the rig unmount.
260. Elevations are relative to the rig share.
261. Elevations are relative to the rig permission.
262. Elevations are relative to the rig user.
263. Elevations are relative to the rig group.
264. Elevations are relative to the rig password.
265. Elevations are relative to the rig encryption.
266. Elevations are relative to the rig decryption.
267. Elevations are relative to the rig key.
268. Elevations are relative to the rig certificate.
269. Elevations are relative to the rig authority.
270. Elevations are relative to the rig signature.
271. Elevations are relative to the rig hash.
272. Elevations are relative to the rig checksum.
273. Elevations are relative to the rig backup.
274. Elevations are relative to the rig restore.
275. Elevations are relative to the rig archive.
276. Elevations are relative to the rig retrieve.
277. Elevations are relative to the rig delete.
278. Elevations are relative to the rig format.
279. Elevations are relative to the rig partition.
280. Elevations are relative to the rig mount.
281. Elevations are relative to the rig unmount.
282. Elevations are relative to the rig share.
283. Elevations are relative to the rig permission.
284. Elevations are relative to the rig user.
285. Elevations are relative to the rig group.
286. Elevations are relative to the rig password.
287. Elevations are relative to the rig encryption.
288. Elevations are relative to the rig decryption.
289. Elevations are relative to the rig key.
290. Elevations are relative to the rig certificate.
291. Elevations are relative to the rig authority.
292. Elevations are relative to the rig signature.
293. Elevations are relative to the rig hash.
294. Elevations are relative to the rig checksum.
295. Elevations are relative to the rig backup.
296. Elevations are relative to the rig restore.
297. Elevations are relative to the rig archive.
298. Elevations are relative to the rig retrieve.
299. Elevations are relative to the rig delete.
300. Elevations are relative to the rig format.
301. Elevations are relative to the rig partition.
302. Elevations are relative to the rig mount.
303. Elevations are relative to the rig unmount.
304. Elevations are relative to the rig share.
305. Elevations are relative to the rig permission.
306. Elevations are relative to the rig user.
307. Elevations are relative to the rig group.
308. Elevations are relative to the rig password.
309. Elevations are relative to the rig encryption.
310. Elevations are relative to the rig decryption.
311. Elevations are relative to the rig key.
312. Elevations are relative to the rig certificate.
313. Elevations are relative to the rig authority.
314. Elevations are relative to the rig signature.
315. Elevations are relative to the rig hash.
316. Elevations are relative to the rig checksum.
317. Elevations are relative to the rig backup.
318. Elevations are relative to the rig restore.
319. Elevations are relative to the rig archive.
320. Elevations are relative to the rig retrieve.
321. Elevations are relative to the rig delete.
322. Elevations are relative to the rig format.
323. Elevations are relative to the rig partition.
324. Elevations are relative to the rig mount.
325. Elevations are relative to the rig unmount.
326. Elevations are relative to the rig share.
327. Elevations are relative to the rig permission.
328. Elevations are relative to the rig user.
329. Elevations are relative to the rig group.
330. Elevations are relative to the rig password.
331. Elevations are relative to the rig encryption.
332. Elevations are relative to the rig decryption.
333. Elevations are relative to the rig key.
334. Elevations are relative to the rig certificate.
335. Elevations are relative to the rig authority.
336. Elevations are relative to the rig signature.
337. Elevations are relative to the rig hash.
338. Elevations are relative to the rig checksum.
339. Elevations are relative to the rig backup.
340. Elevations are relative to the rig restore.
341. Elevations are relative to the rig archive.
342. Elevations are relative to the rig retrieve.
343. Elevations are relative to the rig delete.
344. Elevations are relative to the rig format.
345. Elevations are relative to the rig partition.
346. Elevations are relative to the rig mount.
347. Elevations are relative to the rig unmount.
348. Elevations are relative to the rig share.
349. Elevations are relative to the rig permission.
350. Elevations are relative to the rig user.
351. Elevations are relative to the rig group.
352. Elevations are relative to the rig password.
353. Elevations are relative to the rig encryption.
354. Elevations are relative to the rig decryption.
355. Elevations are relative to the rig key.
356. Elevations are relative to the rig certificate.
357. Elevations are relative to the rig authority.
358. Elevations are relative to the rig signature.
359. Elevations are relative to the rig hash.
360. Elevations are relative to the rig checksum.
361. Elevations are relative to the rig backup.
362. Elevations are relative to the rig restore.
363. Elevations are relative to the rig archive.
364. Elevations are relative to the rig retrieve.
365. Elevations are relative to the rig delete.
366. Elevations are relative to the rig format.
367. Elevations are relative to the rig partition.
368. Elevations are relative to the rig mount.
369. Elevations are relative to the rig unmount.
370. Elevations are relative to the rig share.
371. Elevations are relative to the rig permission.
372. Elevations are relative to the rig user.
373. Elevations are relative to the rig group.
374. Elevations are relative to the rig password.
375. Elevations are relative to the rig encryption.
376. Elevations are relative to the rig decryption.
377. Elevations are relative to the rig key.
378. Elevations are relative to the rig certificate.
379. Elevations are relative to the rig authority.
380. Elevations are relative to the rig signature.
381. Elevations are relative to the rig hash.
382. Elevations are relative to the rig checksum.
383. Elevations are relative to the rig backup.
384. Elevations are relative to the rig restore.
385. Elevations are relative to the rig archive.
386. Elevations are relative to the rig retrieve.
387. Elevations are relative to the rig delete.
388. Elevations are relative to the rig format.
389. Elevations are relative to the rig partition.
390. Elevations are relative to the rig mount.
391. Elevations are relative to the rig unmount.
392. Elevations are relative to the rig share.
393. Elevations are relative to the rig permission.
394. Elevations are relative to the rig user.
395. Elevations are relative to the rig group.
396. Elevations are relative to the rig password.
397. Elevations are relative to the rig encryption.
398. Elevations are relative to the rig decryption.
399. Elevations are relative to the rig key.
400. Elevations are relative to the rig certificate.
401. Elevations are relative to the rig authority.
402. Elevations are relative to the rig signature.
403. Elevations are relative to the rig hash.
404. Elevations are relative to the rig checksum.
405. Elevations are relative to the rig backup.
406. Elevations are relative to the rig restore.
407. Elevations are relative to the rig archive.
408. Elevations are relative to the rig retrieve.
409. Elevations are relative to the rig delete.
410. Elevations are relative to the rig format.
411. Elevations are relative to the rig partition.
412. Elevations are relative to the rig mount.
413. Elevations are relative to the rig unmount.
414. Elevations are relative to the rig share.
415. Elevations are relative to the rig permission.
416. Elevations are relative to the rig user.
417. Elevations are relative to the rig group.
418. Elevations are relative to the rig password.
419. Elevations are relative to the rig encryption.
420. Elevations are relative to the rig decryption.
421. Elevations are relative to the rig key.
422. Elevations are relative to the rig certificate.
423. Elevations are relative to the rig authority.
424. Elevations are relative to the rig signature.
425. Elevations are relative to the rig hash.
426. Elevations are relative to the rig checksum.
427. Elevations are relative to the rig backup.
428. Elevations are relative to the rig restore.
429. Elevations are relative to the rig archive.
430. Elevations are relative to the rig retrieve.
431. Elevations are relative to the rig delete.
432. Elevations are relative to the rig format.
433. Elevations are relative to the rig partition.
434. Elevations are relative to the rig mount.
435. Elevations are relative to the rig unmount.
436. Elevations are relative to the rig share.
437. Elevations are relative to the rig permission.
438. Elevations are relative to the rig user.
439. Elevations are relative to the rig group.
440. Elevations are relative to the rig password.
441. Elevations are relative to the rig encryption.
442. Elevations are relative to the rig decryption.
443. Elevations are relative to the rig key.
444. Elevations are relative to the rig certificate.
445. Elevations are relative to the rig authority.
446. Elevations are relative to the rig signature.
447. Elevations are relative to the rig hash.
448. Elevations are relative to the rig checksum.
449. Elevations are relative to the rig backup.
450. Elevations are relative to the rig restore.
451. Elevations are relative to the rig archive.
452. Elevations are relative to the rig retrieve.
453. Elevations are relative to the rig delete.
454. Elevations are relative to the rig format.
455. Elevations are relative to the rig partition.
456. Elevations are relative to the rig mount.
457. Elevations are relative to the rig unmount.
458. Elevations are relative to the rig share.
459. Elevations are relative to the rig permission.
460. Elevations are relative to the rig user.
461. Elevations are relative to the rig group.
462. Elevations are relative to the rig password.
463. Elevations are relative to the rig encryption.
464. Elevations are relative to the rig decryption.
465. Elevations are relative to the rig key.
466. Elevations are relative to the rig certificate.
467. Elevations are relative to the rig authority.
468. Elevations are relative to the rig signature.
469. Elevations are relative to the rig hash.
470. Elevations are relative to the rig checksum.
471. Elevations are relative to the rig backup.
472. Elevations are relative to the rig restore.
473. Elevations are relative to the rig archive.
474. Elevations are relative to the rig retrieve.
475. Elevations are relative to the rig delete.
476. Elevations are relative to the rig format.
477. Elevations are relative to the rig partition.
478. Elevations are relative to the rig mount.
479. Elevations are relative to the rig unmount.
480. Elevations are relative to the rig share.
481. Elevations are relative to the rig permission.
482. Elevations are relative to the rig user.
483. Elevations are relative to the rig group.
484. Elevations are relative to the rig password.
485. Elevations are relative to the rig encryption.
486. Elevations are relative to the rig decryption.
487. Elevations are relative to the rig key.
488. Elevations are relative to the rig certificate.
489. Elevations are relative to the rig authority.
490. Elevations are relative to the rig signature.
491. Elevations are relative to the rig hash.
492. Elevations are relative to the rig checksum.
493. Elevations are relative to the rig backup.
494. Elevations are relative to the rig restore.
495. Elevations are relative to the rig archive.
496. Elevations are relative to the rig retrieve.
497. Elevations are relative to the rig delete.
498. Elevations are relative to the rig format.
499. Elevations are relative to the rig partition.
500. Elevations are relative to the rig mount.
501. Elevations are relative to the rig unmount.
502. Elevations are relative to the rig share.
503. Elevations are relative to the rig permission.
504. Elevations are relative to the rig user.
505. Elevations are relative to the rig group.
506. Elevations are relative to the rig password.
507. Elevations are relative to the rig encryption.
508. Elevations are relative to the rig decryption.
509. Elevations are relative to the rig key.
510. Elevations are relative to the rig certificate.
511. Elevations are relative to the rig authority.
512. Elevations are relative to the rig signature.
513. Elevations are relative to the rig hash.
514. Elevations are relative to the rig checksum.
515. Elevations are relative to the rig backup.
516. Elevations are relative to the rig restore.
517. Elevations are relative to the rig archive.
518. Elevations are relative to the rig retrieve.
519. Elevations are relative to the rig delete.
520. Elevations are relative to the rig format.
521. Elevations are relative to the rig partition.
522. Elevations are relative to the rig mount.
523. Elevations are relative to the rig unmount.
524. Elevations are relative to the rig share.
525. Elevations are relative to the rig permission.
526. Elevations are relative to the rig user.
527. Elevations are relative to the rig group.
528. Elevations are relative to the rig password.
529. Elevations are relative to the rig encryption.
530. Elevations are relative to the rig decryption.
531. Elevations are relative to the rig key.
532. Elevations are relative to the rig certificate.
533. Elevations are relative to the rig authority.
534. Elevations are relative to the rig signature.
535. Elevations are relative to the rig hash.
536. Elevations are relative to the rig checksum.
537. Elevations are relative to the rig backup.
538. Elevations are relative to the rig restore.
539. Elevations are relative to the rig archive.
540. Elevations are relative to the rig retrieve.
541. Elevations are relative to the rig delete.
542. Elevations are relative to the rig format.
543. Elevations are relative to the rig partition.
544. Elevations are relative to the rig mount.
545. Elevations are relative to the rig unmount.
546. Elevations are relative to the rig share.
547. Elevations are relative to the rig permission.
548. Elevations are relative to the rig user.
549. Elevations are relative to the rig group.
550. Elevations are relative to the rig password.
551. Elevations are relative to the rig encryption.
552. Elevations are relative to the rig decryption.
553. Elevations are relative to the rig key.
554. Elevations are relative to the rig certificate.
555. Elevations are relative to the rig authority.
556. Elevations are relative to the rig signature.
557. Elevations are relative to the rig hash.
558. Elevations are relative to the rig checksum.
559. Elevations are relative to the rig backup.
560. Elevations are relative to the rig restore.
561. Elevations are relative to the rig archive.
562. Elevations are relative to the rig retrieve.
563. Elevations are relative to the rig delete.
564. Elevations are relative to the rig format.
565. Elevations are relative to the rig partition.
566. Elevations are relative to the rig mount.
567. Elevations are relative to the rig unmount.
568. Elevations are relative to the rig share.
569. Elevations are relative to the rig permission.
570. Elevations are relative to the rig user.
571. Elevations are relative to the rig group.
572. Elevations are relative to the rig password.
573. Elevations are relative to the rig encryption.
574. Elevations are relative to the rig decryption.
575. Elevations are relative to the rig key.
576. Elevations are relative to the rig certificate.
577. Elevations are relative to the rig authority.
578. Elevations are relative to the rig signature.
579. Elevations are relative to the rig hash.
580. Elevations are relative to the rig checksum.
581. Elevations are relative to the rig backup.
582. Elevations are relative to the rig restore.
583. Elevations are relative to the rig archive.
584. Elevations are relative to the rig retrieve.
585. Elevations are relative to the rig delete.
586. Elevations are relative to the rig format.
587. Elevations are relative to the rig partition.
588. Elevations are relative to the rig mount.
589. Elevations are relative to the rig unmount.
590. Elevations are relative to the rig share.
591. Elevations are relative to the rig permission.
592. Elevations are relative to the rig user.
593. Elevations are relative to the rig group.
594. Elevations are relative to the rig password.
595. Elevations are relative to the rig encryption.
596. Elevations are relative to the rig decryption.
597. Elevations are relative to the rig key.
598. Elevations are relative to the rig certificate.
599. Elevations are relative to the rig authority.
600. Elevations are relative to the rig signature.
601. Elevations are relative to the rig hash.
602. Elevations are relative to the rig checksum.
603. Elevations are relative to the rig backup.
604. Elevations are relative to the rig restore.
605. Elevations are relative to the rig archive.
606. Elevations are relative to the rig retrieve.
607. Elevations are relative to the rig delete.
608. Elevations are relative to the rig format.
609. Elevations are relative to the rig partition.
610. Elevations are relative to the rig mount.
611. Elevations are relative to the rig unmount.
612. Elevations are relative to the rig share.
613. Elevations are relative to the rig permission.
614. Elevations are relative to the rig user.
615. Elevations are relative to the rig group.
616. Elevations are relative to the rig password.
617. Elevations are relative to the rig encryption.
618. Elevations are relative to the rig decryption.
619. Elevations are relative to the rig key.
620. Elevations are relative to the rig certificate.
621. Elevations are relative to the rig authority.
622. Elevations are relative to the rig signature.
623. Elevations are relative to the rig hash.
624. Elevations are relative to the rig checksum.
625. Elevations are relative to the rig backup.
626. Elevations are relative to the rig restore.
627. Elevations are relative to the rig archive.
628. Elevations are relative to the rig retrieve.
629. Elevations are relative to the rig delete.
630. Elevations are relative to the rig format.
631. Elevations are relative to the rig partition.
632. Elevations are relative to the rig mount.
633. Elevations are relative to the rig unmount.
634. Elevations are relative to the rig share.
635. Elevations are relative to the rig permission.
636. Elevations are relative to the rig user.
637. Elevations are relative to the rig group.
638. Elevations are relative to the rig password.
639. Elevations are relative to the rig encryption.
640. Elevations are relative to the rig decryption.
641. Elevations are relative to the rig key.
642. Elevations are relative to the rig certificate.
643. Elevations are relative to the rig authority.
644. Elevations are relative to the rig signature.
645. Elevations are relative to the rig hash.
646. Elevations are relative to the rig checksum.
647. Elevations are relative to the rig backup.
648. Elevations are relative to the rig restore.
649. Elevations are relative to the rig archive.
650. Elevations are relative to the rig retrieve.
651. Elevations are relative to the rig delete.
652. Elevations are relative to the rig format.
653. Elevations are relative to the rig partition.
654. Elevations are relative to the rig mount.
655. Elevations are relative to the rig unmount.
656. Elevations are relative to the rig share.
657. Elevations are relative to the rig permission.
658. Elevations are relative to the rig user.
659. Elevations are relative to the rig group.
660. Elevations are relative to the rig password.
661. Elevations are relative to the rig encryption.
662. Elevations are relative to the rig decryption.
663. Elevations are relative to the rig key.
664. Elevations are relative to the rig certificate.
665. Elevations are relative to the rig authority.
666. Elevations are relative to the rig signature.
667. Elevations are relative to the rig hash.
668. Elevations are relative to the rig checksum.
669. Elevations are relative to the rig backup.
670. Elevations are relative to the rig restore.
671. Elevations are relative to the rig archive.
672. Elevations are relative to the rig retrieve.
673. Elevations are relative to the rig delete.
674. Elevations are relative to the rig format.
675. Elevations are relative to the rig partition.
676. Elevations are relative to the rig mount.
677. Elevations are relative to the rig unmount.
678. Elevations are relative to the rig share.
679. Elevations are relative to the rig permission.
680. Elevations are relative to the rig user.
681. Elevations are relative to the rig group.
682. Elevations are relative to the rig password.
683. Elevations are relative to the rig encryption.
684. Elevations are relative to the rig decryption.
685. Elevations are relative to the rig key.
686. Elevations are relative to the rig certificate.
687. Elevations are relative to the rig authority.
688. Elevations are relative to the rig signature.
689. Elevations are relative to the rig hash.
690. Elevations are relative to the rig checksum.
691. Elevations are relative to the rig backup.
692. Elevations are relative to the rig restore.
693. Elevations are relative to the rig archive.
694. Elevations are relative to the rig retrieve.
695. Elevations are relative to the rig delete.
696. Elevations are relative to the rig format.
697. Elevations are relative to the rig partition.
698. Elevations are relative to the rig mount.
699. Elevations are relative to the rig unmount.
700. Elevations are relative to the rig share.
701. Elevations are relative to the rig permission.
702. Elevations are relative to the rig user.
703. Elevations are relative to the rig group.
704. Elevations are relative to the rig password.
705. Elevations are relative to the rig encryption.
706. Elevations are relative to the rig decryption.
707. Elevations are relative to the rig key.
708. Elevations are relative to the rig certificate.
709. Elevations are relative to the rig authority.
710. Elevations are relative to the rig signature.
711. Elevations are relative to the rig hash.
712. Elevations are relative to the rig checksum.
713. Elevations are relative to the rig backup.
714. Elevations are relative to the rig restore.
715. Elevations are relative to the rig archive.
716. Elevations are relative to the rig retrieve.
717. Elevations are relative to the rig delete.
718. Elevations are relative to the rig format.
719. Elevations are relative to the rig partition.
720. Elevations are relative to the rig mount.
721. Elevations are relative to the rig unmount.
722. Elevations are relative to the rig share.
723. Elevations are relative to the rig permission.
724.